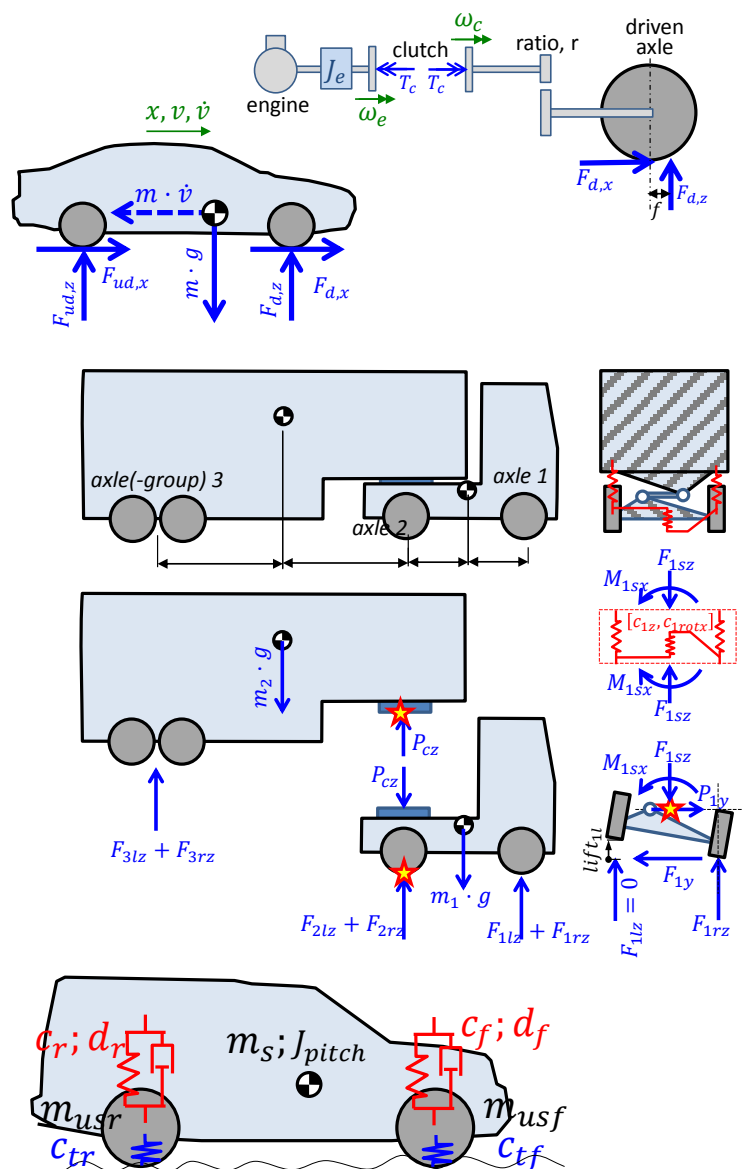# CHALMERS

Vehicle Dynamics
Compendium for course MMF062

Preface 2016

This edition has various changes and additions. Some of these are: Chapter 1: Control engineering, Chapter 2: Tyre models, Driver models, Chapter 3: Propulsion systems, Varying road pitch, Non-reactive truck suspensions, Chapter 4: Track-ability, Articulated vehicles, and Cambering vehicles.

Thanks to Cornelia Lex (TU Graz), Fredrik Bruzelius (VTI), Niklas Fröjd, Anders Hedman, Kristoffer Tagesson, Peter Nilsson, Sixten Berglund (Volvo GTT), Tobias Brandin, Edo Drenth, Mats Jonasson (VCC), Mathias Lidberg, Artem Kusachov, Anton Albinsson, Manjurul Islam, Pär Pettersson, Ola Benderius (Chalmers), Mats Sabelström, and Roland Svensson among others.

Bengt Jacobson, Göteborg, October 2016

Preface 2015

This edition has various changes and additions. Some of these are: brush model with parabolic pressure distribution, typical numerical data for heavy vehicle, added "**2.3.1 Tyre** ", "**4.5.3.2 (Example of) Explicit form** model", more about tyre relaxation, introduction of neutral steering point, introduction of steady state roll-over wheel lift diagram. Thanks to Anton Albinsson, Edo Drenth (VCC), Gunnar Olsson (LeanNova), Manjurul Islam, Mathias Lidberg, Mats Jonasson (VCC), Niklas Fröjd (Volvo GTT), Ola Benderius, Pär Pettersson, and Zuzana Nedelkova among other.

Bengt Jacobson, Göteborg, 2015

Preface 2014

This edition has various small changes and additions. The largest changes are: Function definitions added and major update of section **1.3**, **3.1.1**, **4.1.1**, **5.1.1**.

Thanks to Lars Almefelt from Chalmers, Jan Andersson from VCC, Kristoffer Tagesson from Volvo GTT and Gunnar Olsson from Leannova and Karthik Venkataraman. *Bengt Jacobson, Göteborg, 2014*

Preface 2013

This edition has various small changes and additions. The largest additions were in: Functional architecture, Smaller vehicles, Roll-over, Pendulum effect in lateral load transfer and Step steer.

Thanks to Gunnar Olsson from LeanNova, Mathias Lidberg, Marco Dozza, Andrew Dawkes from Chalmers, Erik Coelingh from Volvo Cars, Fredrik Bruzelius from VTI, Edo Drenth from Modelon, Mats Sabelström, Martin Petersson and Leo Laine from Volvo GTT. *Bengt Jacobson, Göteborg, 2013*

Preface 2012

A major revision is done. The material is renamed from "Lecture notes" to "Compendium". Among the changes it is worth mentioning: 1) the chapters about longitudinal, lateral and vertical are more organised around design for vehicle functions, 2) a common notation list is added, 3) brush tyre model added, 4) more organised and detailed about different load transfer models, and 5) road spectral density roughness model is added.

Thanks to Adithya Arikere, John Aurell, Andrew Dawkes, Edo Drenth, Mathias Lidberg, Peter Nilsson, Gunnar Olsson, Mats Sabelström, Ulrich Sander, Simone Sebben, Kristoffer Tagesson, Alexey Vdovin and Derong Yang for review reading. *Bengt Jacobson, Göteborg, 2012*

Preface 2011

Material on heavy vehicles is added with help from John Aurell. Coordinate system is changed from SAE to ISO. Minor additions and changes are also done. *Bengt Jacobson, Göteborg, 2011*

Preface 2007

This document was developed as a result of the reorganization of the Automotive Engineering Master's Programme at Chalmers in 2007. The course content has been modified in response to the redistribution of vehicle dynamics and power train education.

These lecture notes are based on the original documents developed by Dr Bengt Jacobson. The text and examples have been reformatted and edited but the author is indebted to the contribution of Dr Jacobson.

Rob Thomson, Gothenburg, 2007

Cover: Left column, from top: Improved low speed manoeuvring by actively steered converter dolly, Driving event in course TME102 Vehicle Dynamics Advanced, and Vehicle state estimation by camera on ego vehicle. Right column: Figures from written examinations 2016.

This compendium is also available as pdf file at http://pingpong.chalmers.se/public/courseId/7244/lang-en/publicPage.do.

Contents

1 INTRODUCTION

1.1 Definition of Vehicle Dynamics

Vehicle Dynamics is the engineering subject about vehicle motion in relevant user operations. It is an applied subject, applied on a certain group of products, namely vehicles. Vehicle Dynamics always uses theories and methods from Mechanical engineering, but often also from Control/Signal engineering and Human behavioural science.

1.2 About this compendium

This compendium is intended for first-time-studies studies of vehicle dynamics. At Chalmers University of Technology this is in the course "MMF062 Vehicle Dynamics". The compendium covers more than actually included in the course; both in terms of subsystem designs, which not necessarily has to be fully understood in order to learn the vehicle level; and in terms of some teasers for more advanced studies of vehicle dynamics. Therefore, the compendium can also be useful in general vehicle engineering courses, e.g. in the Chalmers course "TME121 Engineering of Automotive Systems"; and as an introduction to more advance courses, which at Chalmers is the course "TME102 Vehicle Dynamics Advanced".

The overall objective of the compendium is to contribute to education of automotive engineers with good skills to design for, and verify, requirements on complete vehicle level functions, regarding vehicle dynamics or motion.

The compendium focus on road vehicles, primarily passenger cars and commercial vehicles. Smaller road vehicles, such as bicycles and single-person cars, are only very briefly addressed. It should be mentioned that there exist a lot of ground-vehicle types not covered at all, such as: off-road/construction vehicles, tracked vehicles, horse wagons, hovercrafts or railway vehicles.

The vehicle can be seen as a component (or sub-system) in a superior transport system, consisting of vehicles with drivers, other road users and roads with wind and weather. A vehicle is also, in itself, a system, within which many components (or sub-systems) interact. In order to approach the vehicle dynamics in a structured way, the course is divided into the following parts:

- **Longitudinal** dynamics (also introducing subsystems for propulsion and braking)
- **Lateral** dynamics (also introducing subsystems for steering)
- **Vertical** dynamics (also introducing subsystems for suspension)

These 3 parts are found as chapters 3-**5**, and the goal is that the compendium should lead all the way to "functions". Functions are needed for requirement setting, design and verification. The overall order within the compendium is that models/methods/tools needed to understand each function are placed before the functions.

It is important to qualitatively understand the characteristics of the vehicle's sub-systems and, from this, learn how to quantitatively predict and analyse the vehicle's behaviour. These skills support the overall goal of engineering design for desired attributes and functions, see Section 1.3.

The reader of this compendium is assumed to have knowledge of mathematics and mechanics, to the level of a Bachelor of Engineering degree. Previous knowledge in dynamic systems, e.g. from Control Engineering courses, is often useful. There are no prerequisites on previous knowledge in automotive engineering, because basic vehicle components (or sub-systems) are presented to the necessary level of detail. This could be considered as unnecessary repetition for some readers. References and suggestions for further reading are provided and readers are directed to these sources of information for a deeper understanding of a specific topic.

1.3 Automotive engineering

This section is about a larger area than Vehicle Dynamics. It is about the context where Vehicle Dynamics is mainly applied.

OEM means Original Equipment Manufacturer and is, within the automotive industry, used for a vehicle manufacturer. OEM status is a legal identification in some countries.

In the automotive industry, the word Supplier means supplier to an OEM. There are Tier1 suppliers, Tier2 suppliers, etc. A Tier1 supplies directly to an OEM. A Tier2 supplies to a Tier1 and so on. Primarily, suppliers supply parts and systems to the OEMs, but suppliers can also supply competence, i.e. consultant services.

From an engineering view it is easy to think that an OEM only does Product Development and Manufacturing. But it is good to remember that there is also Purchasing, Marketing & Sales, After Sales, etc. However, Product Development is the main area where the vehicles are designed. It is typically divided into Powertrain, Chassis, Body, Electrical and Vehicle Engineering. Vehicle Dynamics competence is mainly needed in Chassis, Powertrain and Vehicle Engineering.

On supplier side, Vehicle Dynamics competence is mainly needed for system suppliers that supplies propulsion, brake, steering and suspension systems.

Except for OEMs and suppliers, Vehicle Dynamics competence is also needed at some governmental legislation and testing as well as research institutes.

There are engineering associations for automotive engineering. FISITA (Fédération Internationale des Sociétés d'Ingénieurs des Techniques de l' Automobile, www.fisita.com) is the umbrella organisation for the national automotive societies around the world. Examples of national societies are IMechE (United Kingdom), JSAE (Japan), SAE (USA), SAE-C (Kina), SATL (Finland), SIA (France), SVEA (Sweden, www.sveafordon.com) and VDI FVT (Germany). There is a European level association also, EAEC.

1.4 Attributes and Functions

Development of a vehicle is driven by requirements which come from:

- Use case based needs of the customer/users
- Legislation from the authorities and Rating from consumer organisation, and
- Engineering constraints from the manufacturer's platform/architecture on which is it to certain vehicle should be built.

One way of organising most of those, in particular the first ones, is to define **Attributes** and **Functions**. The terms are not strictly defined and may vary between vehicle manufacturers and over time. With this said, it is assumed that the reader understand that the following is an approximate and simplified description.

In this compendium, both attributes and functions implicitly concern the **complete vehicle**; not the sub-systems within the vehicles and not the superior level of the transportation system with several vehicles in a road infrastructure.

Attributes and Functions are used to establish processes and structures for requirement setting and verification within a vehicle engineering organisation. Such processes and structures are important to enable a good overall design of such a complex product as a vehicle intended for mass production at affordable cost for the customers/users. Figure 1-1 tries to give an overview, with reference to the well-known V-process, how a vehicle program generally is organised. The figure is idealized in many ways. First, one have more levels of functions and subsystems. Secondly, it is difficult to keep such a clean hierarchical order between functions and subsystems. Thirdly and most conceptually difficult, is

the fact that each subsystem gets requirements from many functions as showed by the dashed lines; this makes the complexity explode.
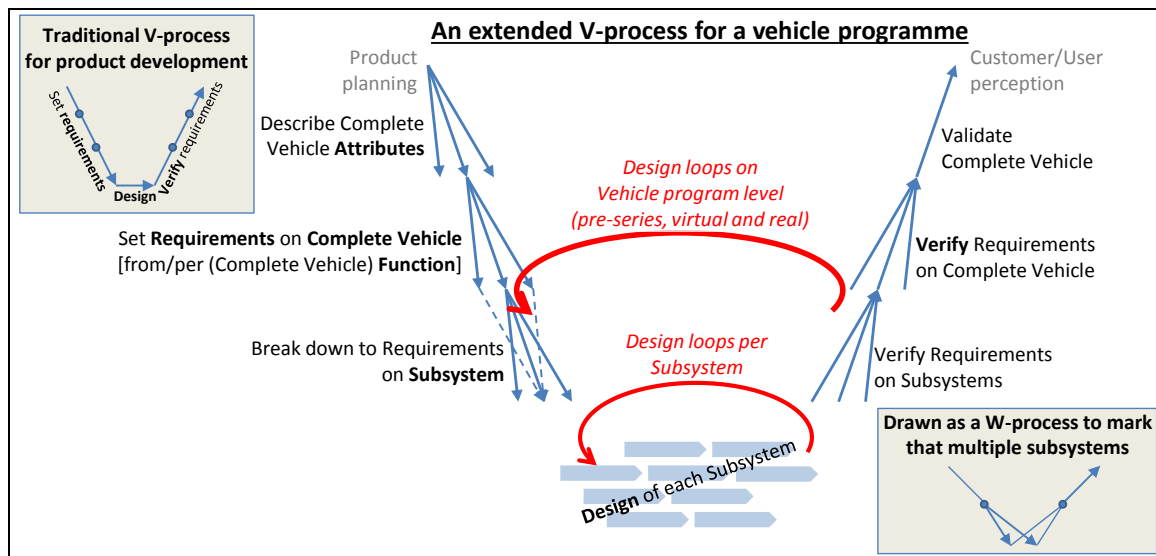
Figure 1-1: V-process applied to a vehicle program. Note that it becomes a W-process, since multiple subsystems..

1.4.1 Attributes

An attribute is a high-level aspect of how the user of the vehicle perceives the vehicle. Attributes which are especially relevant for Vehicle Dynamics are listed in Table 1.1. The table is much generalised and the attributes in it would typically need to be decomposed into more attributes when used in the engineering organisation of an OEM. Also, not mentioned in the table, are attributes which are less specific for vehicle dynamics, such as **Affordability** (low cost for user), **Quality** (functions sustained over vehicle lifetime), **Styling** (appearance, mainly visual), etc.

Attributes can be seen as one way to categorise or group functions, especially useful for an OEM organisation and vehicle development programs. Functions can, in turn, be seen as one way to group requirements. **Legal** requirements are often, but not always, possible to trace back to primarily one specific attribute. Requirements arising from OEM-internal **platform and architecture constraints** are often more difficult to trace in that way. Hence, legal and platform/architecture can be seen as two "attribute-like requirement containers", beside the other user-derived attributes.

Table 1.1: Attributes

↓Attribute	Description↓
Transport Efficiency	This attribute means to maximize output from and minimize costs for transportation. Transport output can be measured in $person \cdot km, ton \cdot km$ or $m^3 \cdot km$. The costs are mainly energy costs and time, but also wear of vehicle parts influence. The attribute is most important for commercial vehicles, but becomes increasingly important also for passenger vehicles. The attribute is mainly addressing long-term vehicle usage pattern, typically 10 min to 10 hours. There are different ways to define such usages, e.g. (Urban / Highway / Mixed) driving cycles. So far, the attribute is mainly required and assessed by the vehicle customers/users.
	The attribute can also be seen to include "Environmental Efficiency", which means low usage of natural resources (mainly energy) and low pollution, per performed transport task. This is to a large extent required and assessed by society/legislation.
Safety	Minimizing risk of property damages, personal injuries and fatalities both in vehicle and outside, while performing the transportation. This attribute is to a large extent required and assessed by society/legislation. In some markets, mainly developed countries, it is also important for vehicle customers/users.

Driving Experience	How the driver experiences driving, from relaxed transport driving (comfort) to active driving (sensation). Driving Experience contains sub-attributes as: • **Driveability, Handling and Road-holding** describes how the vehicle responds to inputs from driver and disturbances, and how driver gets feedback from vehicle motion e.g. through steering feel. (It can be noted that same response aspects are similarly important for a "virtual driver", i.e. a control algorithm doing some automatic/autonomous control.) Driveability often refers to longitudinal (acceleration, braking gear shifting). Handling and Road-holding often refer to lateral manoeuvres. • **Performance** describes how the vehicle can perform at the limits of its capabilities; acceleration, deceleration or cornering. Most often, it refers to longitudinal limitations due to propulsion and brake systems limitations. • **Ride comfort**. Ride comfort often refers to vibrations and harshness of the occupants' motion, primarily vertical but secondly longitudinal. So, V and H in NVH (=Noise, Vibration and Harshness) is included. If expanding to "comfort" it would include also N (noise) and compartment air conditioning, but these sub-attributes are less related to vehicle dynamics. • **Comfort and trust by automated driving** is a new emerging sub-attribute. This attribute is to a large extent required and assessed by the vehicle customers/users, both through own experience but to a large extent indirectly via assessments by experts, e.g. in motor journals.

1.4.2   Functions

A function supplies certain functionality to the customer/user of the vehicle. A function is more specific than an attribute, which is needed to set (quantitative) requirements, see Section 1.4.3. The (complete vehicle) function does not primarily stipulate any specific subsystem. However, the realisation of a function, in one particular vehicle programme, normally only engages a limited subset of all subsystems. So, the function will there pose requirements on that subsystem. Hence, it is easy to mix up whether a function origins from an attribute or a subsystem. One way to categorise functions is to let each function belong to the subsystem which it mainly implies requirements on rather than the source attribute. Categorizing functions by subsystems tends to lead to "carry-over" function realisations from previous vehicle program, which can be good enough in many cases. Categorizing functions by source attribute facilitates more novel function realisations, which can be motivated in other cases.

The word "function" has appeared very frequently lately along with development of electrically controlled systems. The function "Accelerator pedal driving" in Section 3.5.2.1 has always been there, but when the design of it changed from mechanical cable and cam to electronic communication and algorithms (during 1990's) it became much more visible as a function, sometimes referred to as "electronic throttle". The point is that the main function was there all the time, but the design was changed. The change of design enabled, or was motivated by, improvement of some sub-functions, e.g. idle speed control which works better in a wider range of engine and ambient temperature.

At some places, the compendium emphasizes the functions by adding an **asterisk "*"** in section heading and a "**Function definition**" in the following typographic form:

> *Function definition:* **{The Function}** *is the* {Measure} … *for* {Fixed Conditions} *and certain* {Parameterized Conditions}.

The {*Measure*} should be one unambiguously defined measure (such as time, velocity or force) of something the vehicle does. The {*Measure*} is ideally a continuous, objective and scalar physical quantity, subjected for setting a requirement on. The {*Fixed Conditions*} should be unambiguously defined and quantified conditions for the vehicle and its surroundings. The keyword "*certain*" identifies the {*Parameterized Conditions*}, which need to be fixed to certain (particular) numerical values before using the Function definition for requirement setting. A requirement can be: *"{Measure} shall be =, ≈, > or < {value*unit}"*, see more in Section 1.4.3.

Since the term "Function" is defined very broadly in the compendium, these definitions become very different. One type of Function definition can be seen in beginning of Section "3.2.4 Top speed", which includes a well-defined measure. Another type of Function definition is found in Section "3.5.2.3 Anti-

lock Braking System, ABS" and "4.3.3 Under-, Neutral- and Over-steering". Here, the definitions are more on free-text format, and an exact measure is not so well defined.

The compendium defines functions on complete vehicle level, i.e. not cascaded to requirements on specific sub-systems.

1.4.2.1 Organise functionality in functions

There is, of course, no physically correct or incorrect way to organise the total package of functionality in a vehicle into a finite list or tree structure of a finite number of functions. However, defining separate functions is very helpful when organising a combined hardware and software development process within a vehicle programme or when inheriting functionality between vehicle programmes. Some examples of categorisation of functions are:

- Functions assigned to the **(sub-)system** which the function mainly belong (purchase wise or technically). Such categories can be, e.g., Brake functions and Steering functions.
- Functions sorted in **"Customer** functions**"** and **"Support** functions**"**. Support functions are typically used by many customer functions, see Section "1.5.10.1 Reference architecture of vehicle functionality".
- Functions sorted in whether they are realized solely **mechanically** or if realization involve **electronics**.
- Functions sorted in **Standard** and **Option** in the product to end customer.
- **Seeing** vs **Blind** functions, differentiated by whether the function acts on observed environment to the vehicle or only on subject vehicle own states.
- **Dynamic** vs **Driver-informing** functions, differentiated by whether the function actuates vehicle motion or only inform/warn driver.

1.4.3 Requirements

A requirement shall be possible to verify as pass or fail. A requirement on complete vehicle level is typically formulated as: *"The vehicle shall {measure} {< or > or =} {number} {unit}. {Conditions}"*. Examples:

- The vehicle shall accelerate from 50 to 100 km/h on level road in <5 s when acceleration pedal is fully applied.
- The vehicle shall decelerate from 100 to 0 km/h on level road in <35 m when brake pedal is fully applied, without locking any rear wheel.
- The vehicle shall turn with outermost wheel edge on a diameter <11m when turning with full-lock steering at low speed.
- The vehicle shall have a characteristic speed of 70 km/h (±10 km/h) on level ground and high-friction road conditions and any recommended tyres.
- The vehicle shall give a weighted RMS-value of vertical seat accelerations <1.5 m/s^2 when driving on road with class B according to ISO 8608 in 100 km/h.
- The vehicle shall keep its body above a 0.1 m high peaky two-sided bump when passing the bump in 50 km/h.

In order to limit the amount of text and diagrams in the requirements it is useful to refer to ISO and OEM specific standards. Also, it is often good to include the purpose in a use case, when documenting the requirement.

The above listed requirements stipulate the function of the vehicle, which is the main approach in this compendium. Alternatively, a requirement can stipulate the design of the vehicle, such as "The vehicle shall weigh <1600 kg" or "The vehicle shall have a wheel base of 2.5 m". The first type (above listed) can be called *Performance based requirement*. The latter type can be called *Design based requirement* or *Prescriptive requirement* and such are rather "means" than "functions", when seen in a function vs

mean hierarchy. It is typically desired that legal requirements are Performance based, else they would limit the technology development in society.

1.4.4 Models, methods and tools

The attributes, functions and requirements are top level entities in vehicle development process. But in order to define/formulate them, design for them and verify them, the engineers need knowledge in terms of models, methods and tools.

As mentioned above, some sections in the compendium have an asterisk "*" in the section heading, to mark that they explains a function, which can be subject for complete vehicle requirement setting. The remaining section, without an asterisk "*", are there to give the necessary knowledge to understand the function. It is the intention that the necessary knowledge for a certain function appears before that function section. One example is that the Sections "3.2.1 Propulsion System", "3.2.2 Traction diagram" and "3.2.3 Driving Resistance" are placed before Section "3.2.4 Top speed *".

The functions only appear in Chapter 3, Chapter 4 and Chapter **5**.

1.5 Technical References

This section introduces notations. The section also covers some basic disciplines, methods and tools. Parts of this section probably repeat some of the reader's previous education.

1.5.1 Engineering

Engineering Design or Engineering (in Swedish "Ingenjörsvetenskap", in German "Ingenieurwissenschaften"), is not the same as Analysis, Inverse analysis and (Nature) Science, see Figure 1-2. In education, it is often easiest to do Analysis (or Inverse Analysis). However, in a product based subject, such as Vehicle Dynamics, it is important to keep in mind that the ultimate use of the knowledge is engineering, which is to propose and motivate the design and actual numerical values of design parameters of a product. The distinction between Analysis and Inverse Analysis can only be made if there is a natural direction (input or output) of interface signals.

1.5.2 Modelling, drawing and mathematics

1.5.2.1 Modelling stages

For the analysis in Figure 1-2, modelling is needed to derive a model. A model is a representation of something during a certain event or course of events, such as the model of the motion of a car during acceleration from stand-still to 100 km/h. Models are always based on assumptions, approximations and simplifications. However, when using models as a tool for solving a particular problem, the models at least have to be able to reproduce the problem one is trying to solve. Also, models for engineering have to reflect design changes (e.g. changed parameters or input signals) in a representative way, so that new designs can be proposed which solve/reduce the problem. Too advanced models tend to be a disadvantage, since they require and produce a lot of data.

The modelling focused in vehicle dynamics (and many related areas) has no well-established name, but some alternative names are: *functional models*, one-dimensional models, system models, DAE-model, ODE-models, etc. Functional models are typically multi-domain type, involving mechanics, hydraulics, pneumatics, electric, control algorithms, etc. Functional models typically lumps or discretises possible continuous parts of the system. Examples of modelling methods which are very seldom directly used for functional models are: Finite Elements, Computational Fluid Dynamics, CAD geometry models, etc.
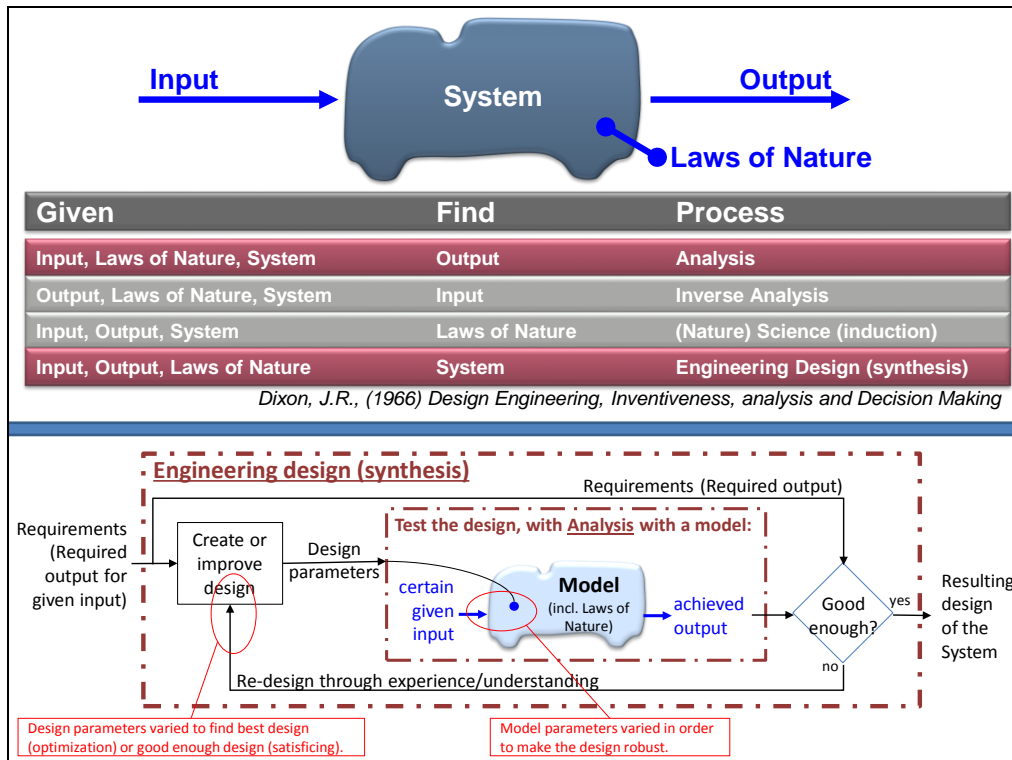
Figure 1-2: Upper: Distinction between Engineering and its neighbouring activities. Picture from Stefan Edlund, Volvo Trucks. Lower: How Analysis can be used as a sub-process in Engineering design.

One can identify the modelling in different stages in the overall process of engineering:

- **Engineering design task**, which describes which design decisions (<u>design parameters</u>) for the system (an existing product or a concept/drawing) that is to be found. Also, <u>requirements</u> on how the output of the system should react on certain input have to be identified. See Figure 1-2.
- **Design & verification plan** is formulated to decide <u>what to test</u> including its <u>inputs and outputs</u>. Also, a plan for <u>how to evaluate</u> the outputs with respect to the requirements.
  <small>Note: Here one can decide for either real tests or virtual tests=computations. Below written for virtual tests.</small>
- **Physical model**, in <u>sketches (or thoughts & words</u>, but sketches are really recommended!). It clarifies assumptions for different parts of the system, e.g. rigid/elastic and inertial/massless. How to model here should be based on what physical phenomena is needed to be captured and what physical variations (e.g. which design parameters) are intended for simulations with the model.
- **Mathematical model** (or *Declarative* model), in <u>equations</u>. Basically, it is about finding exactly the right number of equations; equally many as unknown variables. Here, the assumptions are transformed into equations. For dynamic systems, the equations form a "DAE" (Differential-Algebraic system of Equations). It is seldom necessary to introduce derivatives with respect to other independent variables, such as positions, i.e. one does seldom need PDE (Partial Differential Equations). The general form of a DAE:

    $$\boldsymbol{f_z}(\dot{\boldsymbol{z}}, \boldsymbol{z}, t) = \boldsymbol{0};$$

  where $\boldsymbol{z}$ are the (dependent) variables and t is time (independent variable).
  The mathematical model is complete only if there are equally many (independent) equations in f_z as there are variables in z.
  Note that the DAE is generally on implicit form with respect to calculating the state derivatives, as opposed to explicit form below. Note also that it is not only a question of finding suitable equations, but also to decide *parameterisation*, which is how parameters relate to each other. The parameterisation has to reflect a "fair" comparison between different design parameters, which often requires a lot of experience of the product and the full set of requirements on the

vehicle.

Also, *selection of output variables* is important so that output variables are enough to evaluate the requirements on the system. Selecting more might drive unnecessary complex models.

- **Explicit form model** (or *Imperative* model) is the equations rearranged to an explicit form (algorithm) to calculate the state derivatives. You probably recognize this from solving "ODE" (Ordinary Differential Equations) or "IVP" (Initial Value Problems). The general form is:

  $\dot{x} = f_x(x, u, t);\ y = g(x, u, t);\ u = u(t);$

  where x is the state variables, u is the input variables, and y the output variables. In the mathematical model, there was no distinction between different dependent variables in z. However, in the explicit model, each variables in z can be identified as belonging to either of x, y or u.

  In linear cases, the State Space Form can be used:

  $\dot{x} = A(t) \cdot x + B(t) \cdot u(t);\ \ y = C(t) \cdot x + D(t) \cdot u(t);$ where A, B, C, D are matrices.

- **Computation**. Several methods can be used, e.g.:

  - *Closed form solution*, $[x, y] = f_t(t);$, can be derived for some mathematical/explicit form models, sometimes called "Analytic models". Examples of such are linear models with inputs $u(t)$ expressed as a simple time functions, such as step functions or harmonic functions.

  - *Simulation* (e.g. Initial value problem, IVP or End value problem, EVP). There are many advanced pre-programmed integration methods and tools which one can rely on without knowing the details. It is often enough to know that the concept is similar to the simplest of them, "Euler forward", in which the state variables are updated in each time step, Δt, as follows:

    $\dot{x}_{now} = f(x(t_{now}), u(t_{now}), t_{now});$
    $x(t_{now} + \Delta t) = x(t_{now}) + \Delta t \cdot \dot{x}_{now};$

    Note: With a linear model and certain $u(t)$, it is also possible to find explicit solutions in time, especially if constant coefficients.

  - *System characterisation,* e.g. for studies of stationary oscillation excitation, eigen-modes, eigen-frequencies, step response, stability, etc.

  - *Optimization*. Either optimizing a finite number of defined design parameters or time trajectories. During optimization (also if trial-and-error optimization), some parameters are varied and could therefore potentially be called variables, but the name *Design parameters* are suggested, as opposed to *Design variables*.

  - *(Linearization*. The model can be linearized and brought to next step, for use in control design with control design methods, which often requires linear models.)

- **Evaluation and Redesign** (or Analysis and Synthesis) of the result from the computation. Verify requirements. Understand and interpret to real world. Includes also validity judgement of the model.

- **Propose design**, meaning a concrete proposal of design, such as a numerical design parameter value, drawing/control algorithm, …

In this process description, we can identify 3 modelling steps with 3 different kinds of models: Physical model, Mathematical model and Explicit form model. The compendium spends most effort on the first 2 of those.

It can be noted that the process assumes physical modelling. As opposite to this, one can think of formulating a mathematical model without having a physical model in mind. An example of such mathematical model is a neural network model. Without a physical model, the parameters is generally not interpretable to real design parameters, sometimes their units can even be unknown. For vehicle design the vehicle model has to be physical, so that its real-world design parameters can be identified,

but a driver model can be useful also without strict physical model, since the driver is not to be designed.

The bullet list above assumes only continuous dynamics, as opposed to also including **discrete dynamics**. Discrete dynamics modelling can be used for computational efficient models of, e.g., ideal dry friction or ideal backlash. The way the states evolve over time differs between continuous and discrete dynamics: Continuous states, x_c, are updated in every time step using an derivative approximation, e.g. $\dot{x}_c = (x_c(t + \Delta t) - x_c)/\Delta t$;. Discrete states, x_d, are updated only at the time instants (not time step!) when one of the transition conditions, h, becomes true. These time instants are called events. When a system includes both types (hybrid dynamics) the states evolve as follows:

$$x_c(t + \Delta t) = x_c + \Delta t \cdot \dot{x}_c = x_c + \Delta t \cdot f_c(x_c, x_d, u(t), t); \text{ and}$$
$$when\ h(x_c(t), x_d(t), u(t), t) > 0\ then\ x_d(t^+) = f_d(x_c(t), x_d(t), u(t), t);.$$

Some continuous state variables can also be reinitialized ($x_c(t^+) = \cdots$) in some events, e.g. motivated by impact dynamics. There is a risk that the numerical solution gets stuck in undesired high frequency switching of discrete states which is called chattering. Chattering can be caused by the computational method, but is very often also due to inconsistent physical modelling. Discrete dynamics is not as well established in most basic engineering education as continuous dynamics. A special type of discrete dynamics is time events, where $h = h(t)$;. Time events often appears when modelling the sampling in digitally computed control algorithms.

1.5.2.2   Variables, constants and parameters

A **variable** is something that varies in time. **Constants** and **parameters** are not varying. A parameter does not change during an experiment with the model, but can be changed between subsequent experiments. A constant does not even change between experiments. Typical constant is pi or gravity. Typical parameter is vehicle mass or road friction co-efficient.

A variable can be used as (continuous) **state variable**, which means that it is given initial values and then updated through integration along the time interval studied. Which variables to use as state variables is **not** strictly defined by the physical (or mathematical) model. For mechanical systems, one often uses positions and velocities of (inertial) bodies as state variables, but it is quite possible and sometimes preferable, to use forces in compliances (springs) and velocities of bodies as state variables. With mass/spring system as simple example, the two alternatives becomes [$\dot{v} = F/m$; $F = c \cdot x$; $\dot{x} = v$;] and [$\dot{v} = F/m$; $\dot{F} = c \cdot v$; $x = F/c$;], respectively. The latter alternative is especially relevant when position is not of interest; then the last equation can be omitted. It is also often easier to express steady state initial conditions for a pre-tensioned system. One can see the second alternative as if the states are the variables which represents the two energy forms kinetic and potential energy, respectively, see Lagrange mechanics in Section 1.5.3.1.

1.5.2.3   Causality

Systems can be modelled with **Natural causality**. For mechanical systems, this is when forces on the masses (or motion of the compliance's ends) are prescribed as functions of time. Then the velocities of the masses (or forces of the compliances) become state variables and have to be solved through time integration. The opposite is called **Inverse dynamics** and means that velocities of masses (or forces of compliances) are prescribed. For instance, the velocity of a mass can be prescribed and then the required forces on the mass can be calculated through time differentiation of the prescribed velocity. Cf. Analysis and Inverse Analysis in Figure 1-2.

1.5.2.4   Model validity

A model always has it validity borders, so it will always be possible to simulate it in an operation where it is not valid. Whether a model for engineering is valid or not, or good or bad, is often a question about if the influence of the intended design parameter on the measure is correct enough. Since one often don't know exactly how the model is going to be used, it can be a good habit to include a boolean auxiliary variable for validity. One clear reason to set the validity false is when the physical model assumptions are not met, such as if a wheel lifts from ground during simulation (assuming

equations to handle wheel lift is not included). In other cases it can be more of an engineering judgement on what threshold to set the validity false. Then, if validity have been false during a tiny fraction of the whole simulation, it is again a judgement whether to disqualify the simulation result or not.

1.5.2.5 Drawing

Drawing is a very important tool for understanding and explaining. Very often, the drawing contains free body diagrams, see Section 1.5.3.1, but also other diagrams are useful. Beyond normal drawing rules for engineering drawings, it is also important to draw motion and forces. The notation for this is proposed in Figure 1-3.
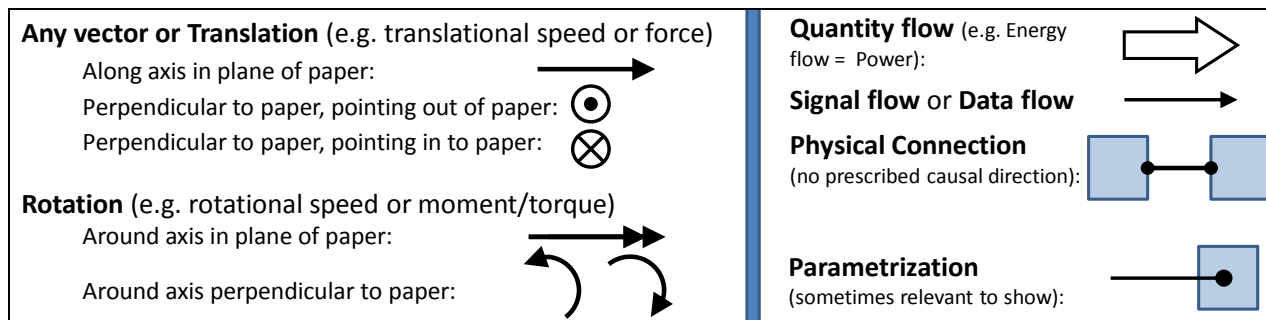
Figure 1-3: Arrow like notation. <u>Left</u>: For motion and forces in drawings. <u>Right</u>: Other

It is often necessary to include more than just speeds and forces in the drawings. In vehicle dynamics these could be: power flow and signal flows. These are often natural to draw as arrows

When connecting components with signal flow, the resulting diagram is a *data flow diagram*. Physical components and physical connections can be included in such diagram, and if arrows between them it would represent data flow or causality. Physical components can also be connected by "Physical connections", which does not have a direction, see Section 1.5.2.5.1. It should be noted that a *(computation) flow charts* and *(discrete) state diagram* represents a quite different type of diagram, even if they may look similar; here an arrow between two blocks represents a transition from one (discrete) state, or operation mode, to another.

1.5.2.5.1 <u>Physical connections</u>

When connecting physical components in a data flow diagram with "Physical connections", there can be two main concepts:

- Connecting in "nodes", see Figure 3-2. Here, each node have typically potential and flow variables (velocities and forces in Mechanical systems). And there are only two components connected to each node. The node variables appears in both components' equations.
- Connecting with "connections between connectors", see Figure 3-12. Here, the same variables are defined in connectors at the components. A connection can be made with lines between the connectors at the components, possibly connecting more than two components. The equations in each component is formulated in the connector's variables. The connection itself generates these equations: "Potential variables in all components are equal" and "Sum of flow variables to all components are zero".

The first is often the easiest (least number of equations and variables) for small models with a fixed topology. The latter is a more systematic which easier handles larger models and models with varying topology. The latter is supported in the standard modelling language Modelica, see Section 1.5.7.5 and http://www.xogeny.com/.

1.5.2.6 Notation conventions

Generally, a variable is denoted x or $x(t)$, where t is the independent variable time. In contexts where one means that variable's value at a certain time instant, t_0, it can be denoted $x(t_0)$. In contexts where

one want to mark that the variable's time history over a time interval (infinitely many values over an infinite or finite time interval) is referred to, it can be denoted $\boldsymbol{x}(\cdot)$.

Differentiation (of x) with respect to time (t): $\frac{dx}{dt} = \dot{x} = der(x)$.

Vectors exist of two kinds: **Geometrical vector** (or physical vector, or spatial vector), denoted by $\vec{v}$, and **mathematical vector**, denoted $[v_x; v_y]$. The geometrical vector is the true vector, while the mathematical is a representation of it, in a certain coordinate system. Matrices are denoted with brackets, e.g. [A]. Row vectors are denoted with parentheses, e.g. (a).

Parentheses shall be used to avoid ambiguity, e.g. $(a/b) \cdot c$ or $a/(b \cdot c)$, not $a/b \cdot c$.

Multiplication symbol (* or ·) shall be used to avoid ambiguity, e.g. $a \cdot bx$, not abx (assuming bx is one variable, not two). Stringent use of multiplication symbol enables use of variables with more than one token, cf. programming. Stringent use of multiplication symbol reduces the risk of ambiguity when using operators, e.g. it shows the difference between $f(x)$ and $f \cdot (x)$.

An **interval** has a notation with double dots. Example: Interval between a and b is denoted $a..b$.

An **explanation**, between two consecutively following steps in a derivation of equations is written within {} brackets. Example: $x + y = \{a + b = b + a\} = y + x$ or $x + y = 7 \Rightarrow \{a + b = b + a\} \Rightarrow y + x = 7$.

An **inverse function** is denoted with -1 as superscript, e.g. $y = f(x); \Leftrightarrow x = f^{-1}(y)$.

Fourier and Laplace **transforms** of function $f(t)$ are denoted $\mathcal{F}(f(t))$ and $\mathcal{L}(f(t))$, respectively.

1.5.2.7 Notation list

Table 1.2 shows notation of parameters, variables and subscripts used in this compendium. The intention of this compendium is to follow International Standards (ISO8855), but deviations from this is sometimes used, especially motivated by conflicts with areas not covered by (ISO8855). Some alternative notations are also shown, to prepare the reader for other frequently used notation in other literature.

The list does not show the order of subscripting. For example, it does not show whether longitudinal (x) force (F) on rear axle (r) should be denoted F_{rx} or F_{xr}. The intention in this compendium is to order subscript with the physical vehicle part (here rear axle) as first subscript and the specification (longitudinal, x) as second, leading to F_{rx}. If there is also further detailed specifications, such as coordinate system, e.g. wheel coordinate (w), it will be the third subscript, leading to F_{rxw}.

INTRODUCTION

Table 1.2: Notation

Categorization			Notation				
			Recommended		Alternatives		
Engineering	Sub category	Subject for notation	in code	by hand		Unit	Description / Note
1. General	Basic	(Shaft) Torque	T	T	M	Nm	
1. General	Basic	Coefficient of friction	mu	μ	mue, muh	1=N/N	
1. General	Basic	Damping coefficient	d	d	c,k,D	N/(m/s) or Nm/(rad/s)	
1. General	Basic	Density	roh	ρ			
1. General	Basic	Efficiency	eta	η		1=W/W	Ratio between useful/output power and used/input power
1. General	Basic	Energy	E	E	W	Nm=J	
1. General	Basic	Force	F	F	f	N	
1. General	Basic	Gravity	g	g		m/s^2	9.80665 average on Earth
1. General	Basic	Height	h	h	H		
1. General	Basic	Imaginary unit	j	j	i	-	j*j=-1
1. General	Basic	Mass	m	m	M	kg	
1. General	Basic	Mass moment of inertia	J	J	I	kg*m^2	Subscript can be given to denote around which axis
1. General	Basic	Moment (of forces)	M	M	T	Nm	Not for shaft torque
1. General	Basic	Power	P	P		W=Nm/s=J/s	
1. General	Basic	Ratio	r	r	u, i (ISO8855)	Nm/(Nm) or (rad/s)/(rad/s)	Ratio between input and output rotational speed, or output and input torque, in a transmission
1. General	Basic	Rotational speed	w	ω	ω	rad/s	
1. General	Basic	Shear stress	tau	τ		N/m^2	
1. General	Basic	Stiffness coefficient	c	c	C, k, K	N/m or Nm/rad	
1. General	Basic	Strain	eps	ε		m/m	
1. General	Basic	Translational speed	v	v	V	m/s	
1. General	Basic	Wave length	lambda	λ		m	
1. General	Basic	Width	W	W	w	m	Can be track width, vehicle width, tyre width, ...
1. General	Dynamics	(Time) Frequency	f	f		1/s=periods/s	
1. General	Dynamics	Angular (time) frequency	w	ω	ω	rad/s	
1. General	Dynamics	Angular spatial frequency	W	Ω		rad/m	
1. General	Dynamics	Dependent variables in a dynamic system	z	z		<various>	Both state variables and output variables
1. General	Dynamics	Input variables in a dynamic system	u	u		<various>	
1. General	Dynamics	Mean Square value	MS	MS			
1. General	Dynamics	Output variables in a dynamic system	y	y		<various>	
1. General	Dynamics	Power spectral density	G	Φ	PSD		
1. General	Dynamics	Root Mean Square value	RMS	RMS			
1. General	Dynamics	Spacial frequency as radians per travelled distance	W	Ω		rad/m	
1. General	Dynamics	Spatial frequency	fs	f_s		1/m=periods/m	
1. General	Dynamics	States variables in a dynamic system	x	x		<various>	
1. General	Dynamics	Time	t	t	τ, T	s	The independent variable in a dynamic system
1. General	Operators	Transfer function	H	H		<not applicable>	
2. Vehicle	1. General	Air resistance coefficient	cd	c_d	Cd	1	
2. Vehicle	1. General	Cornering stiffness or lateral tyre stiffness	Cy	C_y	C_α	N/rad or N/1	$dF_y/d\alpha = dF_y/ds_y$ at $\alpha = s_y = 0$
2. Vehicle	1. General	Longitudinal tyre stiffness	Cx	C_x		N/1	df_{yw}/ds_x at $s_x=0$

| Categorization | | | Notation | | | | |
Engineering	Sub category	Subject for notation	Recommended in code	Recommended by hand	Alternatives	Unit	Description / Note
2. Vehicle	1. General	Mass	m	m	M	kg	
2. Vehicle	1. General	Rolling resistance coefficient	f	f		1=N/N	
2. Vehicle	1. General	Track width	W	W		m	
2. Vehicle	1. General	Tyre stiffness	C	C	c	N/1	dF/ds at $s=0$
2. Vehicle	1. General	Understeer gradient	Ku	K_u	Kus, kus, U (ISO8855)	N/(N/rad) = rad/(m/s^2)	
2. Vehicle	1. General	Vehicle side slip angle	b	β	β	rad	If no subscript, undefined or CoG
2. Vehicle	1. General	Wheel base	L	L	l, lf+lr, WB	m	
2. Vehicle	1. General	Wheel radius	R	R	r, Rw	m	
2. Vehicle	2. Road	Curvature	kappa	κ	roh, ρ	rad/m=1/m	road or path
2. Vehicle	2. Road	Curve radius	R	R	r, roh, ρ	m	road or path
2. Vehicle	2. Road	Road bank angle	pxr	φ_{xr}			Positive when right side of ground is lower than left side ground
2. Vehicle	2. Road	Road inclination angle	pyr	φ_{yr}		rad	Positive downhill
2. Vehicle	2. Road	Vertical Position of road	zr	z_r	z, Z	m	
2. Vehicle	3. Motion	Vehicle acceleration, in interial system	ax, ay, az	a_x, a_y, a_z		m/(s*s)	decomposed in vehicle coordinates direction
2. Vehicle	3. Motion	Vehicle acceleration, in vehicle system	dervx, dervy, dervz	$\dot{v}_x, \dot{v}_y, \dot{v}_z$	der(vx), der(vy), der(vz)	m/(s*s)	decomposed in vehicle coordinates direction
2. Vehicle	3. Motion	Vehicle position	x,y,z	x, y, z	r=[rx,ry,rz] or [X,Y,Z]	m	Often refering to Center of Gravity, CoG
2. Vehicle	3. Motion	Vehicle velocity, in interial system	vx,vy,vz	v_x, v_y, v_z	u,v,w	m/s	decomposed in vehicle coordinates direction
2. Vehicle	4. Forces	Forces and moments on vehicle	Fx, Fy, Fz, Mx, My, Mz	$F_x, F_y, F_z, M_x, M_y, M_z$		[N, N, N, Nm, Nm, Nm]	From ground, air, towed units, colliding objects, etc. May appear also as reduced, e.g. for in road plane: F=[Fx, Fy, Mz]
2. Vehicle	4. Forces	Forces on one wheel, axle or side from ground	Fix,Fiy,Fiz	F_{ix}, F_{iy}, F_{iz}	lowercase f	N	Subscript "i" is placeholder for particular wheel, axle or side. May appear also extended with moments: [Fx, Fy, Fz, Mx, My, Mz]
2. Vehicle	4. Forces	Forces on one wheel, axle or side from ground	Fixv, Fiyv,Fizv	$F_{ixv}, F_{iyv}, F_{izv}$	lowercase f	N	in vehicle coordinate system
2. Vehicle	4. Forces	Forces on one wheel, axle or side from ground	Fixw,Fiyw,Fizw	$F_{ixw}, F_{iyw}, F_{izw}$	lowercase f	N	in wheel coordinate system
2. Vehicle	5. Angles	Camber angle	g	g	gamma, γ	rad	Sign convention might be positive when either of "rotated as wheel roll angle" or "leaning outward vs vehicle body".
2. Vehicle	5. Angles	Low speed or Ackermann speed steering wheel angle	dswA	δ_{swA}		rad	The angle required for a certain vehicle path curvature at low speeds
2. Vehicle	5. Angles	Euler rotations		ψ, θ, φ		rad	Order: yaw, pitch, roll
2. Vehicle	5. Angles	Roll, pitch, yaw angle	px, py, pz	$\varphi_x, \varphi_y, \varphi_z$	φ, θ, ψ	rad	Angles, not rotations. Roll and Pitch normally small
2. Vehicle	5. Angles	Roll, pitch, yaw angular velocities	wx, wy, wz	$\omega_x, \omega_y, \omega_z$	$[\dot{\varphi}, \dot{\theta}, \dot{\psi}], [\dot{\varphi}, \dot{\theta}, \Omega]$	rad/s	
2. Vehicle	5. Angles	Steering angle	d	δ	delta	rad	May refer to steering wheel, road wheel or axle
2. Vehicle	5. Angles	Steering angle of road wheels	drw	δ_{rw}	RWA	rad	Normally an average of angles on front axle

INTRODUCTION

Categorization			Notation				
			Recommended		Alternatives		
Engineering	Sub category	Subject for notation	in code	by hand		Unit	Description / Note
2. Vehicle	5. Angles	Steering angle of steering wheel	dsw	δ_{sw}	SWA	rad	
2. Vehicle	6. Slip	Tyre (lateral) slip angle	a	α	alpha	rad	a=arctan(sy)
2. Vehicle	6. Slip	Tyre lateral slip	sy	s_y		1=(m/s)/(m/s)	sy=tan(a)
2. Vehicle	6. Slip	Tyre longitudinal slip	sx	s_x	$\kappa, -\kappa$	1=(m/s)/(m/s)	
2. Vehicle	6. Slip	Tyre slip	s	s		1=(m/s)/(m/s)	
2. Vehicle	7. Subscript	axle	a	a		<not applicable>	used e.g. as Ca=cornering stiffness for any axle
2. Vehicle	7. Subscript	centre of gravity	CoG	CoG	COG, cog, CG, cg	<not applicable>	
2. Vehicle	7. Subscript	front	f	f	F, 1	<not applicable>	Often used as double subscript, e.g. fr=front right
2. Vehicle	7. Subscript	inner	i	i		<not applicable>	Often means with respect to curve
2. Vehicle	7. Subscript	left	l	l	L	<not applicable>	Often used as double subscript, e.g. fl=front left
2. Vehicle	7. Subscript	outer	o	o		<not applicable>	Often means with respect to curve
2. Vehicle	7. Subscript	rear	r	r	R, 2	<not applicable>	Often used as double subscript, e.g. fr=rear right
2. Vehicle	7. Subscript	road	r	r		<not applicable>	
2. Vehicle	7. Subscript	road wheel	rw	rw	RW	<not applicable>	E.g. drw=road wheel steering angle
2. Vehicle	7. Subscript	sprung mass	s	s		<not applicable>	
2. Vehicle	7. Subscript	steering wheel	sw	sw	SW, H (ISO8855)	<not applicable>	E.g. dsw=steering wheel angle
2. Vehicle	7. Subscript	unsprung mass	u	u	us	<not applicable>	
2. Vehicle	7. Subscript	vehicle	v	v		<not applicable>	used e.g. as F1v to denote wheel force on wheel 1 in vehicle coordinates
2. Vehicle	7. Subscript	wheel	w	w		<not applicable>	used e.g. as F1w to denote wheel force on wheel 1 in wheel coordinates
3. Subsystem in vehicles	1. Propulsion	Engine torque	Te	T_e		Nm	
3. Subsystem in vehicles	2. Brake						
3. Subsystem in vehicles	3. Steering	Steering wheel torque	Tsw	T_{sw}	SWT	Nm	
3. Subsystem in vehicles	4. Suspension	Caster angle	CA			rad	
3. Subsystem in vehicles	4. Suspension	Caster offset	c			m	
3. Subsystem in vehicles	4. Suspension	Kingpin inclination angle	KPI			rad	
3. Subsystem in vehicles	4. Suspension	Pneumatic trail	t			m	

1.5.3 Mechanical engineering

Vehicle dynamics originates from Mechanical engineering (in Swedish "Maskinteknik", in German "Machinenbau"). Therefore, it is important to be familiar with the following basic relationships:

- Energy = time integral of Power
- [Torque or Moment] = Force · Lever
- Power = Torque · Rotational speed   *or*   Power = Force · Translational speed
- (Torque) Ratio = Output torque / Input torque
- (Speed) Ratio = Input speed / Output speed
- Efficiency = Output power / Input power   *or, in a wider meaning,*   Efficiency = Useful / Used

1.5.3.1 Free-body diagrams

An example of a free-body diagram is given in Figure 1-4.

Division into sub-systems is often needed, e.g. to implement moment less connection points or other models of the vehicle internal behaviour. The sub-system split typically goes through:

- Connection point between towing unit and towed unit (typical interface quantities: 2 positions (with their derivative, velocities) and 2 forces)
- Driveshaft close to each wheel (typical interface quantities: 1 shaft torque, 3 forces, and 2 angles (steering and shaft rotation), sometimes 1 wheel camber angle)
- Surface between driver's hand and steering wheel (typical interface quantities: 1 angle and 1 torque)

The free-body diagram is important as part of the physical model and it helps setting up the equilibrium equations in the mathematical model. Relevant notes for this are:

- A short-cut that can be taken when drawing the diagram is to assume forces are already in equilibrium, which makes one equilibrium equation unnecessary. An example of this could be to use F_{fz} instead of F_{fz0} in Figure 1-4, which would make the vertical force equilibrium for the front axle ($F_{fz} - F_{fz} = 0$) unnecessary.
- In the free-body diagram, one draws arrows and names corresponding vector quantities, typically forces and velocities. You can either use a standard sign rule and let mathematics decide the sign ('+' or '-') of the variable, or, try to "feel" which direction the force or speed will have and define your arrows and names according to this, to get positive numerical values. It is a matter of taste which is best, but it is recommended that care is taken – it is very easy to make sign mistakes.

You will notice that most mechanical models in Vehicle Dynamics are combinations of (Static or Dynamic) Equilibrium, Compatibility and Constitutive relationships:

- (Static) Equilibrium (using Newtonian mechanics):
    - Sum of forces in one direction = 0
    - Sum of moments around an axis in one direction = 0
- Dynamic equilibrium (or "Equation of motion" or "Newton's 2nd law"):
    - Sum of forces (including "fictive forces" = "d'Alambert forces") in one direction = 0, **or** sum of forces in one direction = *Mass·Acceleration* in the forces' direction.
    - Sum of moments (including "fictive moments") in one direction = 0, **or** sum of moments in one direction = *Moment of inertia around centre of gravity·Rotational acceleration* in the moment's direction.
    - If fictive forces or moments are included on equation left-hand side, it is recommended that they are introduced in the free-body diagram (see dashed force arrow in Figure 1-4). These forces shall be opposite to the positive direction of acceleration and act through the centre of gravity.

- Compatibility: Relation between positions or velocities, e.g. "Speed=Radius*Rotational speed" for a rotating wheel
- Constitutive relations: Relation between forces and positions or between forces and velocities, e.g.
    - "Force = constant1+constant2·deformation" or "$\frac{d}{dt}$Force= constant2·$\frac{d}{dt}$deformation" for a (linear) spring,
    - "Force = constant * deformation speed" for a (linear) damper,
    - "Force = constant * sign(sliding speed)" for a dry friction contact
- (An alternative to Newton mechanics is Lagrange mechanics, which is sometimes an easier way to find the same equations. Lagrange mechanics formulates the equations in kinetic and potential energy in a way which has similarities with using velocities of bodies and (time) derivatives of forces in compliances as state variables, as described in Section 1.5.2.2.)
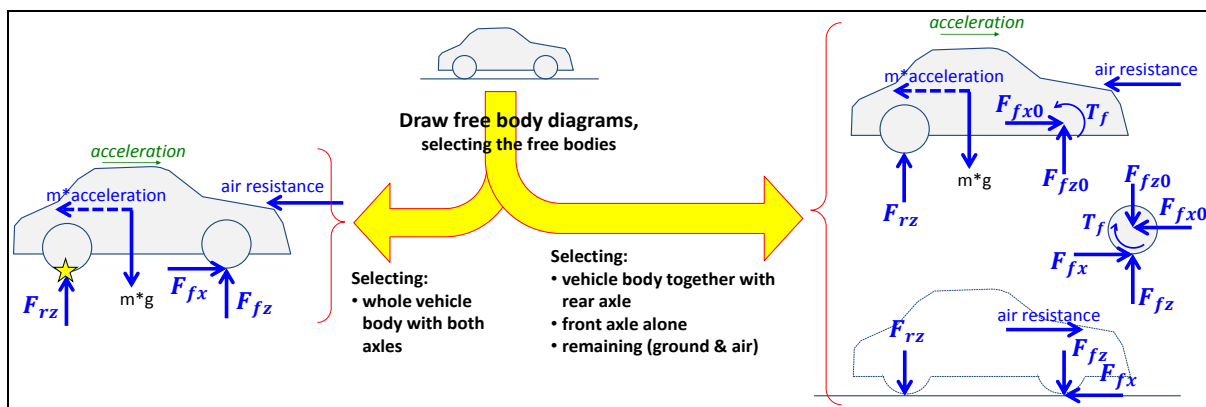
Figure 1-4: Free body diagram. The dashed arrow is a "fictive force". The star is a way to mark around which point(s) moment equilibrium is taken in the later stage "Mathematical model".

1.5.3.2 Operating conditions

The operating conditions of a vehicle lend expressions from general dynamics, as listed below.

- (*Static* conditions, meaning that vehicle is standing still, are seldom relevant to study. Static means that the all velocities are zero, i.e. that all positions are constant.)

- *Steady State* operation means that time history is irrelevant for the quantities studied. Seen as a manoeuvre over time, the studied quantities are constant.

- *Transient* (or Transient State, as opposed to Steady State) manoeuvres means that time history is relevant; i.e. there are delays, represented by "state variables" when simulated.

- *Stationary (oscillating) dynamics* is a special case of transient, where cyclic variations continues over long time with a constant pattern. This pattern is often assumed to be harmonic, meaning that the variable varies in sinus and cosine with constant amplitudes and phases. An example is sinusoidal steering, where also the vehicle response is harmonic if steering amplitude is small enough to assume the vehicle response is governed by a linear dynamic system.

- *Quasi-static* and *Quasi-steady state* are terms with a more diffuse meaning, which refers rather to analysis methods than the actual operation/manoeuvre. It is used when the analysis neglects the dynamics of a variable which normally is a state variable. An example is when constant non-zero deceleration is assumed, but speed is not changed; then the dynamics "der(speed)=acceleration" is neglected, and speed is instead prescribed.

1.5.4 Control engineering

Vehicle dynamics is more and more influenced by electronics, where the algorithms are a main artefact to engineer. For this reason, this section gives a brief introduction to some relevant theory and methods and their *connection to vehicle models as they are described in vehicle dynamics*. From Figure 1-5, we realize that there are many other types of Vehicle Level Algorithms needed than just the Vehicle (Motion) Controller.
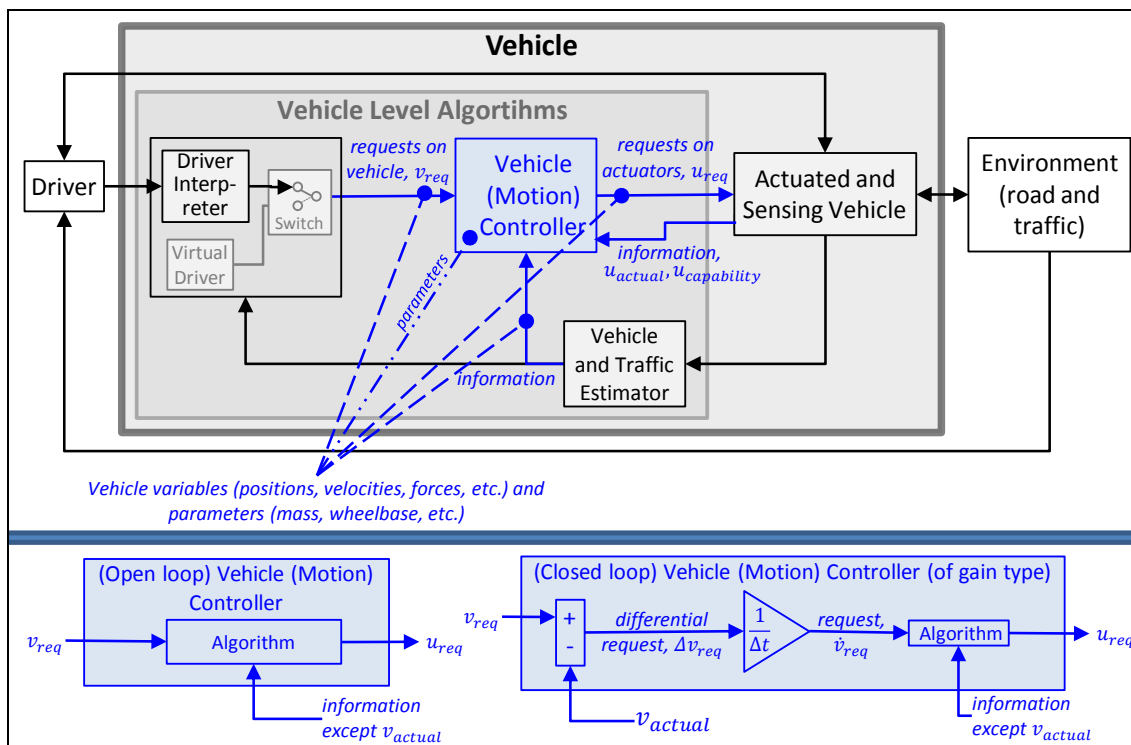
Figure 1-5: Context for Vehicle Level Algorithms and Vehicle (Motion) Controller

Vehicle Controllers can be designed without utilizing knowledge about the controlled system (such as neural networks, tuned only on observations on how the system responds). However, in this section we only consider Model based controllers. For those, the input and output signals, as well as parameters inside, has a clear interpretation in vehicle motion quantities and units. The model base is helpful when tuning the controller parameters. Moreover, the model base helps to find a consistency between derivatives order in the controller and the controlled system, such as if P, I or D gains should be used in a PID-controller.

1.5.4.1 Categorizations of Vehicle Control design

Three categorizations will be presented, which authors thinks is clarifying to be able to discuss control design on a high approximate level.

1.5.4.1.1 Momentaneous or Predictive control

If the controller consider the future (predicted) of its input v_{req} and/or output u_{req}, the controller uses **Predictive control**. If the controller (or more correct, the controller designer) consider both its input v_{req} and its output u_{req} to be at present time instant, the controller uses **Momentaneous control**. This categorization is not strict, but there are cases where it makes sense. Since a controller is normally implemented in a computer with sampled values, the future of the input cannot be known, so future of inputs u_{req} should be seen as prediction e.g. via a time function or desired path ahead. The future of the outputs is easier to understand, since a dynamic model can be used to tell how the system evolves over future time.

A reasons to do predictive control, as opposed to the simpler momentaneous control, is that the control objective requires some strategic planning over future time. One example can be fuel consumption, where the objective is an integral over future time, $Fuel = \int FuelRate \cdot dt$;, where a high $FuelRate$ can be good initially (momentaneously) to minimize the total integral. Another example is braking and steering when entering a curve, where it is generally more strategically optimal to brake before steering.

In Sections 1.5.4.1.2 and 1.5.4.1.3, momentaneous control will be assumed unless else is stated.

1.5.4.1.2 Open or closed loop controllers

As indicated already in Figure 1-5, a **Closed loop controller** uses the actual value (v_{actual}) of the requested quantity v_{req}. Else it is an **Open loop controller**.

Since the driver is in the loop and can correct errors, Open-loop can often work well enough. Especially if the driver is given good feedback, e.g. good steering feel. When automation of driving there is a motivation to go towards more Closed-loop control. However, there can be architectural benefits to close the loop in the Virtual driver instead of the Vehicle Controller, see Figure 1-5, so that same algorithms can used in Vehicle Controller for manual and for automatic driving.

A more including definition of closed loop controller is that the controller uses any signal from the controlled object, not exclusively whether it uses v_{actual}. With that definition, almost all controllers ends up as closed loop controllers. An example is an open-loop controller for a cruise control function: $F_{req} \leftarrow m \cdot a_{req} + F_{res}$;. Here, the requested vehicle quantity is acceleration (a_{req}) but the used information about the vehicle is not a_{actual} but estimated mass (m) and estimated driving resistance force (F_{res}). These estimated quantities are typically updated much slower than the request control loop, but they are still used signals. With the proposed definition it is open loop controller, but with the more including definition it would be a closed loop controller.

The cruise controller example above is an example of **Inverse model controller**, since it is an inverse of the model: $a \leftarrow (F - F_{res})/m$;. The most common implementation of closed loop is when the control error is calculated as an intermediate quantity. In the cruise control example, it would be $a_{error} \leftarrow a_{actual} - a_{req}$; or with opposite sign it is rather a differential request $\Delta a_{req} \leftarrow a_{req} - a_{actual} (= -a_{error})$;. A **Gain controller** could then be: $F_{req} \leftarrow Gain \cdot \Delta a_{req}$;. This can be called a P-control on acceleration or D-control on velocity. The model connection is not obvious since one cannot directly see that $Gain$ corresponds to mass and resistance force is not even present. A similar gain controller could be formulated in another differentiation order, such as velocity instead of acceleration: $F_{req} \leftarrow Gain \cdot \Delta v_{req}$;. This can be called P-control on velocity, I-control on acceleration or D-control on position. The model points out that $Gain$ should be seen as $m/time$ instead, where $time$ is the time to when v_{req} should be reached. Interpretation of gains to physical quantities with units is encouraged, since it facilitates tuning and reuse of the controller. Such interpretation requires a physical model.

It is very typical for automotive engineering, that algorithms are reused, and sometimes incrementally developed, from one platform or vehicle programme to the next. Hence, given a certain controller, it is very relevant to understand/derive its model base, for efficient parameter setting. However, it is important to realize that it is not generally possible to derive the model base from a given controller. So, the controller really has to be developed from a physical model. So, the documentation of which physical model is used is very important output from the control design, beside the controller itself. The documentation should include model equations and declarations of variables and parameters so that next vehicle programme can inherit this as document.

1.5.4.1.3 Degree of over-actuation

Already before designing the controller, it is often clear what vehicle requests v_{req} and actuate-able quantities u_{req} there are. The number (or dimension=dim) of those enables one simple categorization:

- If $dim(u_{req}) = dim(v_{req})$, the vehicle is (formally) Neutral actuated.
- If $dim(u_{req}) > dim(v_{req})$, the vehicle is (formally) Over-actuated.
- If $dim(u_{req}) < dim(v_{req})$, the vehicle is (formally) Under-actuated.

In cases where actuators influence on vehicle motion is saturated in some way, or the vehicle motion is constrained, the above definition is less useful. So, we have to include also a certain operating conditions for the vehicle, to be able to include such effects. Certain operating conditions means that we think there is a certain model which describes the actuated vehicle motion, $f(u_{req}, v_{req}) = 0$;, where f can include time derivave operators ($\frac{d}{dt}$ and $\int \dots \cdot dt$). With a model, we can include saturations and constraints. Instead of dimension, we need to define the property *rank of the model* as the number of dimensions that the vehicle motion can be influenced in by the available actuators. Using the model we can, conceptually, find F such that:

$$\partial v_{req} = \boldsymbol{F} \cdot \partial u_{req};$$
$$where\ \boldsymbol{F}\ is\ a\ \dim(v_{req}) \times \dim(u_{req})\ matrix.$$
$$Rank\ of\ model = rank(\boldsymbol{F}).$$

The rank of a matrix is the number of non-zero diagonal elements in the middle matrix S in the singular value decomposition of F, $svd(F) = U \cdot S \cdot V^T$;. Using the rank, we can define degree of overactuation in a way which better helps us differ between different control design types, see also Figure 1-6:

- If $dim(u_{req}) = rank(F)$, the vehicle is (effectively) **Neutral actuated**.
  Conceptually, u_{req} could be calculated from v_{req}, using the model, which would be an Inverse model control design. I practice, one often makes a closed loop control instead: $u_{req} = GainMatrix \cdot (v_{req} - v_{actual})$;. The model can motivate another time differentiation order of each element in $(v_{req} - v_{actual})$.
- If $dim(u_{req}) > rank(F)$, the vehicle is (effectively) **Over-actuated**.
  Conceptually, there are two ways to convert the problem to a Neutral actuated case: Limit actuation (decrease dimension of u_{req} to $rank(F)$), which always works. The other way is to add control objectives in a way (e.g. increase dimension of v_{req}) so that $rank(F) = \dim(u_{req})$, which require that actuators that influence the added objective are available. A third option is to use an approximate solution found through **optimization**, by introducing a cost function to minimize, e.g. $cost = \|v_{req} - v_{model}(u_{req})\|$; where the function $v_{model}(u_{req})$ is derived from the model.
- If $dim(u_{req}) < rank(F)$, the vehicle is (effectively) **Under-actuated**.
  Conceptually, there is no way to convert the problem to a Neutral actuated case (without adding actuators or disregarding requests), but one can find and approximate solution through **optimization**, as described for Over-actuated above.

A visualisation of these cases and solution is given in Figure 1-6.

If using approximate solutions and the function v_{model} is linear, $v_{model} = B \cdot u_{req}$;, there are many cooking-book methods to minimize $\|W_v \cdot (v_{req} - B \cdot u_{req})\|_2$, where W_v is a diagonal matrix with weigth factors. One such is **Control allocation, CA**, which are based on Least square optimization methods, can be used.

Generally, there is a big conceptual difference between whether an exact or approximate solution is aimed for. Note that approximation applied on the Over-actuated case, leads to optimization problem with non-unique solution, which might give randomly varying and jumping u_{req}. To make solution smoother, one often adds control objectives, such that $u_{req} = 0$;. The addition $u_{req} = 0$; makes the problem Over-actuated with unique solution and the cost function then becomes typically $cost = \|W_u \cdot u_{req}\|_2 + \|W_v \cdot (v_{req} - B \cdot u_{req})\|_2$;. Control allocation can then be applied. Since the added objectives $u_{req} = 0$; are artificial, compared to the original objectives, it makes sense that the weight

factors in W_u are small, or at least reduced along with convergence of the optimization problem. The added objectives $u_{req} = 0$; can then be seen as a way to select among non-unique solutions to an ill-conditioned optimization problem.
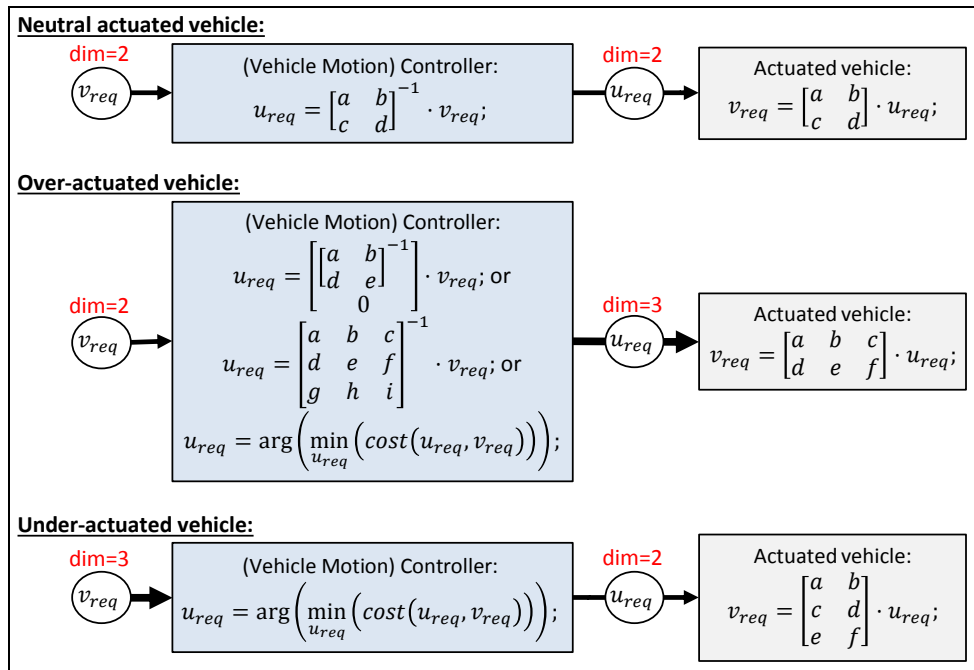
Figure 1-6: Visualisation of possible conceptual controllers for vehicles with different degree of over-actuation. The actuated vehicles are represented by a very conceptual model..

The above in the present section could be seen as valid also for predictive control if we think of u_{req} and v_{req} as having N time more elements, where N is the number of time instants considered in the future. The model can be applied N times, and if it contains state variable, a time integration method is needed to make the sequences of each variable consistent. If model is linear and optimization is to be applied, there are cooking-book methods, such as **Model Predictive Control, MPC**.

1.5.5   Verification methods with real vehicle

1.5.5.1   In traffic

Driving on public roads in real traffic is the most realistic way to verify how a vehicle actually works. It can be used for completely new vehicle models; or new systems, mounted on old models. The drivers can be either ordinary drivers (FOT=Field Operational Test) or test drivers (expeditions). A general existing vehicle population can also be studied by collecting data, e.g. as Accident Statistics Databases.

1.5.5.2   On test track

For vehicles and systems which are not yet allowed on public roads, or tests which are very severe or need a high degree of repeatability, test are carried out at test tracks. There are specialized test tracks for certain conditions, such as hot climate or slippery surfaces.

1.5.5.3   Augmented Reality, AR, manipulates environment

This is a new method. A typical example is: A real driver drives a real vehicle on a real road/test track. Some additional (virtual/simulated) traffic objects are presented to driver, e.g. on a head-up display. The same objects can be fed into the control functions, as if they were detected by the vehicles camera/radar, which enables functions such as automatic braking to be triggered.

1.5.6 Verification methods with virtual vehicle

1.5.6.1 Testing using driver model

Generally, this means that driver, vehicle and environment are modelled and simulated. To perform a serious test there is also need to put effort on test scripts so that the model is run in the intended test manoeuvre and result is pre-processed. When verifying functions partly built with algorithms, the HIL, SIL and MIL below are different ways to represent the algorithm in the vehicle model.

1.5.6.1.1 HIL = Hardware in the loop simulation

The hardware is often one or several ECUs (Electronic Control Units). If several ECUs are tested, the hardware can also contain the communication channel between them, e.g. a CAN bus. The hardware is run with real-time I/O to simulation model of the remaining system (vehicle, driver and environment).

In some cases, there is also mechanical hardware involved, such as if the ECU is the brake system ECU, the actual hydraulic part of the brake system can also be included in the HIL set-up, a so called "wet brake ECU HIL".

1.5.6.1.2 SIL = Software in the loop simulation

The software is often one or several computer programs (intended for download in electronic control units). The software is run with synchronized time-discrete I/O to a simulation model of the remaining system (vehicle, driver and environment).

The software is often used in compiled format (black box format) so that the supplier of the software can retain his intellectual property.

1.5.6.1.3 MIL = Model in the loop simulation

The model, or more correctly, a control algorithm, is a conceptual form of the computer programs (intended for download in electronic control units). The control algorithm is run with I/O to a simulation model of the remaining system (vehicle, driver and environment).

The control algorithms can appear in compiled format so that the supplier of the control algorithms can retain his intellectual property. Then it is hard to tell the difference between MIL and SIL.

1.5.6.2 Testing with real driver

1.5.6.2.1 Simulator = Driver in the loop simulation

This is when a real human, not a driver model, uses real driver devices (pedals, steering wheel) to influence a simulation model of the remaining system (vehicle and environment). The loop is closed by giving the human feedback through display of what would be visible from driver seat, including views outside windscreen. Feedback can be further improved by adding a motion platform to the driver's seat, sound, vibrations in seat, steering wheel torque, etc.

The vehicle model run in the simulator can utilize HIL, SIL and MIL, from Section 1.5.6.1, for some part of the vehicle model.

1.5.7 (Computer) Tools & Methods

1.5.7.1 General mathematics tools

Examples of tool: Matlab, Matrixx, Python

We will take Matlab as example. Matlab is a commercial computer program for general mathematics. It is developed by Mathworks Inc.

Solve linear systems of equations, A*x=b

```
>> x=inv(A)*b;
```

Solve non-linear systems of equations, f(x)=0

```
>> x=fsolve('f',...);
```

Parameter optimization (may be used for trajectory optimization, if trajectory is parameterised)

```
>> (x,fval) = fmincon('f',x0, …)
```

Solve ODE (="systems of Ordinary Differential Equations") as initial value problems, dx/dt=f(t,x), given x(0)

```
>> x=ode23('f',x0,...);
```

Find Eigen vectors (V) and Eigen values (D) to linear systems: D*V=A*V

```
>> [V,D]=eig(A);
```

Matlab is mainly numerical, but also has a symbolic toolbox:

```
>> syms x a; Eq='a/x+x=0'; solve(Eq,x)
ans =   (-a)^(1/2)
        -(-a)^(1/2)
>> diff('a/x+x',x)
ans = 1 - a/x^2
>> int('x^3+log(x)',x)
ans = (x*(4*log(x) + x^3 - 4))/4
```

Some simple Matlab code will be used to describe models in this compendium.

1.5.7.2 Block diagram based modelling and simulation tools

Examples of tools: Simulink, Systembuild

We will take Simulink as example. Graphical definition of non-linear systems of ODE, if known on explicit form $\dot{x} = f(t, x)$;. An example of how the corresponding graphical model may look is given in Figure 1-7.

Simulink is designed for designing/modelling signal processing and control design. It can also be used for modelling the physics of the controlled systems. There are no dedicated vehicle dynamics tools/libraries from Mathworks (but there are in-house developed specific libraries in automotive companies).

From this type of tools it is often possible to automatically generate real time code, which is more and more used instead of typing algorithms. It can be used for rapid prototyping of control functions, or even for generation of executable code for production ECUs.

1.5.7.3 Vehicle dynamics specialized simulation tools

Examples of tools: CarMaker, veDYNA, CarSim.

These tools are specialized for vehicle dynamics. They contain purpose-built and relatively advanced models of vehicles, drivers and scripts for test manoeuvres. They are well prepared for parameter changes, but less prepared for modelling conceptually new designs. However, they often have an interface to Simulink, so that the user can add in their own models.

1.5.7.4 MBS tools

Examples of tools: Adams, Simpack, LMS Virtual Lab

These are general 3D mechanics modelling and simulation tools, so called MBS (Multi-Body Simulation) tools. As one example, Adams contains libraries of general bodies, joints and force elements. But there are toolboxes in Adams for vehicle dynamics, where template models and special

components (such as tyre models and driver models) are available for vehicles dynamics. The models are very advanced and accurate for 3D mechanics, and there are import/export interfaces to Simulink.
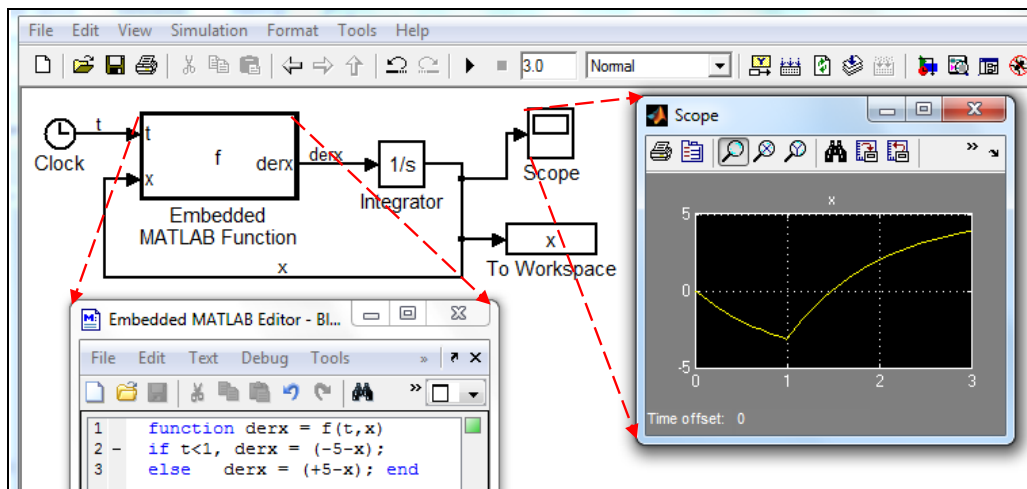

Figure 1-7: Graphical model of dynamic system $\dot{x} = f(t, x)$; using Simulink.

1.5.7.5 Modelica based modelling tools

Examples of tools: Dymola, Maplesim, System-Modeler, AMESim, Optimica Studio, Jmodelica, OpenModelica

Modelica is not a tool but a globally standardized format for dynamic models on DAE form (or Mathematical form, see Mathematical/Declarative modelling in Section 1.5.2). There are a number of tools which supports this format. Specification of Modelica is found at https://www.modelica.org/ and http://www.xogeny.com/ can be helpful when learning Modelica.

The model format itself is non-causal and symbolic. There is one equation part and one declaration part in a model. An example of model is given in Figure 1-8.

The model format is also object oriented, which means that libraries of model components are facilitated. These are often handled with graphical representation, on top of the model code. There are some open-source libraries for various physical domains, such as hydraulic, mechanics, thermodynamics and control. There are also commercial libraries, where we find vehicle dynamics relevant components: Vehicle Dynamics Library and Powertrain Library. Some simple Modelica code will be used to describe models in this compendium.

In one way, Mathematical modelling (Declarative modelling) is more efficient than Explicit form modelling (Imperative modelling), since the engineer does not need to spend time on symbolic/algebraic manipulation of the equations. This is especially true when the natural way of physical modelling generates so called "higher index problems", see Figure 1-9. In this compendium, many models are only driven to Mathematical model, since it is enough if assuming there are modern tools as Modelica tools available. One the other hand, an explicit form model has the value of capturing the causality, i.e. the cause-to-effect chain. The causality can sometimes facilitate the understanding and in that way help the engineer, which is why at least one and rather complete model is shown as explicit form model, see Section 4.5.3.2.

1.5.7.6 FMI supporting simulation tools

Examples of tools: Dymola, Simulink, CarMaker, OpenModelica

FMI (Functional Mock-up Interface) is not a tool but a globally standardized format for dynamic models on explicit form (see Section1.5.2.1). There are a number of tools which supports this format. FMI enables model export/import between tools. It also allows to hide Intellectual Property (IP) by

using "black-box format", i.e. models compiled for certain processors, which is important in relation between OEMs and suppliers.
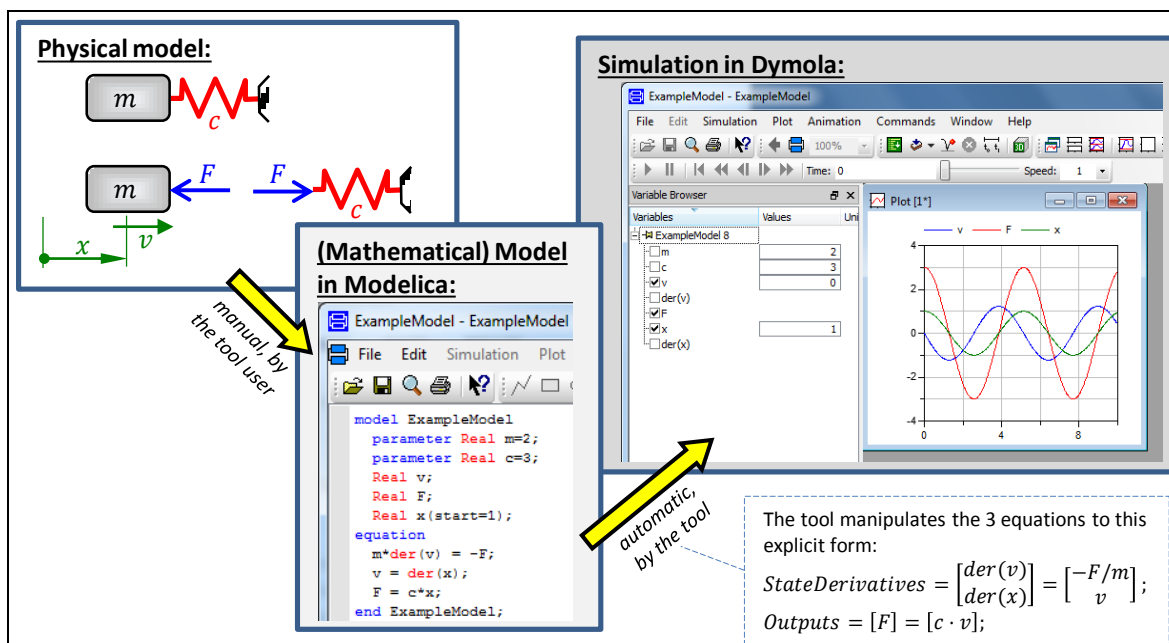
Figure 1-8: Example of model in Modelica format (using the tool Dymola).
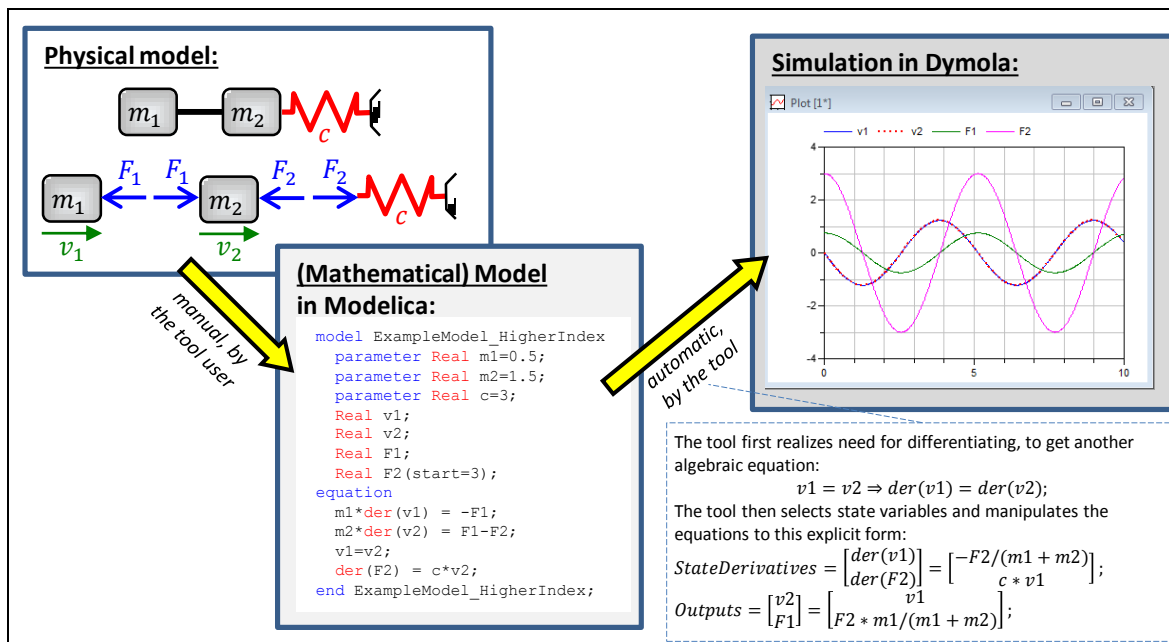
Figure 1-9: Example of "higher index problem" model in Modelica format.

1.5.8 Coordinate Systems

A vehicle's (motion) degrees of freedom are named as in marine and aerospace engineering, such as heave, roll, pitch and yaw, see Figure 1-10. Figure 1-10 also defines the 3 main geometrical planes, such as transversal plane and symmetry plane. For ground vehicles, the motion in ground plane is often treated as the primary motion, which is why longitudinal, lateral and yaw are called in-ground-plane degrees of freedom. The remaining degrees of freedom are referred to as out-of-ground-plane.

The consistent use of parameters that describe the relevant positions, velocities, accelerations, forces, and moments (torques) for the vehicle are critical. Unfortunately there are sometimes disparities

between the nomenclature used in different text books, scientific articles, and technical reports. It is important to apply ISO coordinate system, Reference (ISO8855). It is the predominant coordinate system used nowadays. Historically, a coordinate system with other positive directions, Reference (SAEJ670), has been applied.

The distinction of vehicle fixed and inertial (= earth fixed = world fixed) coordinate systems is important. Figure 1-11 depicts the four most relevant reference frames in vehicle dynamics: the inertial, vehicle, wheel corner and wheel reference frames. All these different coordinate systems allow for the development of equations of motion in a convenient manner.

The orientation of the axes of an inertial coordinate system is typically either along the vehicle direction at the beginning of a manoeuvre or directed along the road or lane. Road or lane can also be curved, which calls for curved longitudinal coordinate.
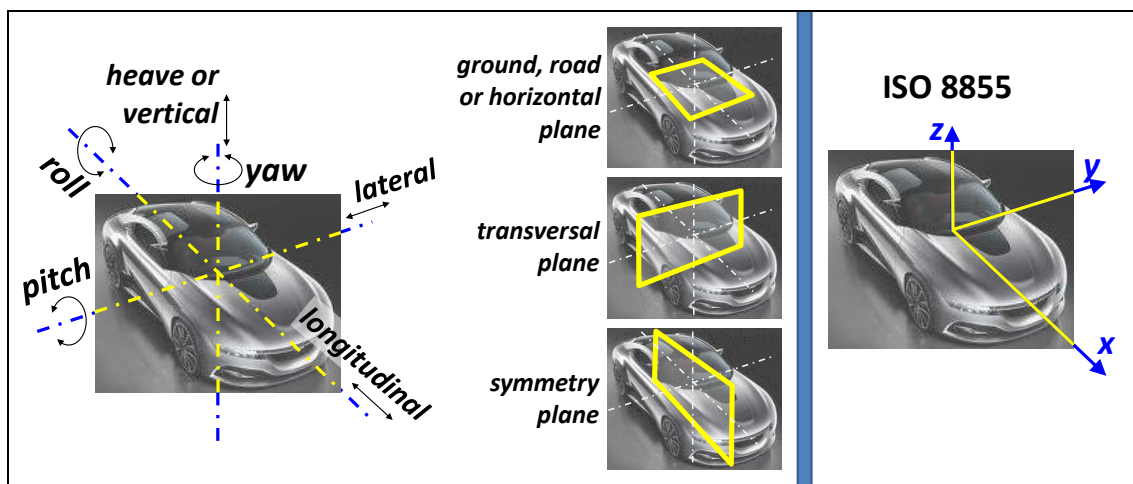
Figure 1-10: Left: Vehicle (motion) degrees of freedom and important planes. Right: ISO coordinate system

Origin for a vehicle fixed coordinate system is often centre of gravity of the vehicle, but other points can be used, such as mid front axle (ground contact or wheel centre height), mid of front bumper, outer edge of body with respect to certain obstacle, etc. Positions often need to be expressed for centre of lane, road edge, other moving vehicle, etc.

In ISO and Figure 1-11, tyre side-slip is defined so that it is positive for positive lateral speed. This means that lateral forces on the wheel will be negative for positive side-slip angles. Some would rather want to have positive force for positive angle. Therefore, one can sometimes see the opposite definition of tyre side-slip angles, as e.g. in (Pacejka, 2005). It is called the "modified ISO" sign convention. This compendium does not use the modified sign convention in equations, but some diagrams are drawn with force-slip-curve in first quadrant. Which is preferable is simply a matter of taste.

Often there is a need to number each unit/axle/wheel. The numbering in Figure 1-12 is proposed. It should be noted that non-numeric notations are sometimes used, especially for two axle vehicles without secondary units. Then front=f, rear=r. Also to differentiate between sides, l=left and r=right.
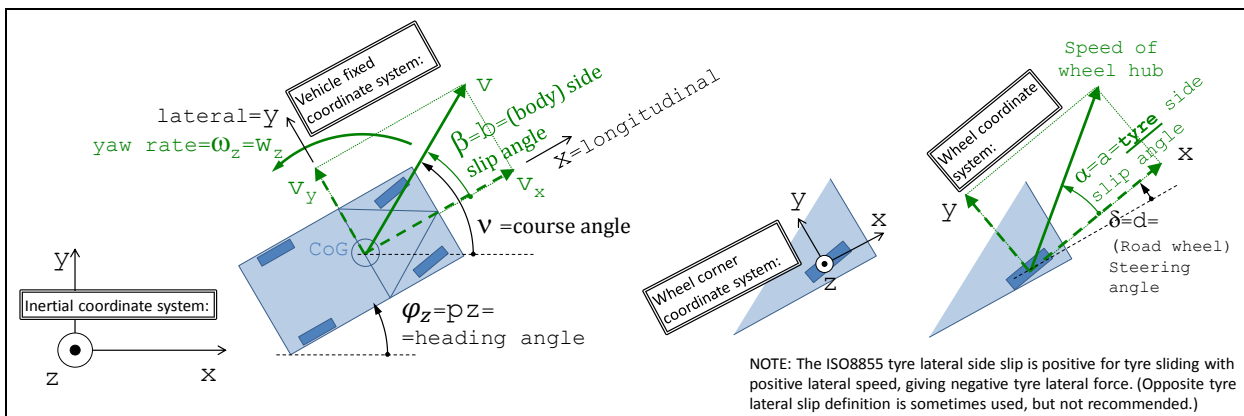
Figure 1-11: Coordinate systems and motion quantities in ground plane
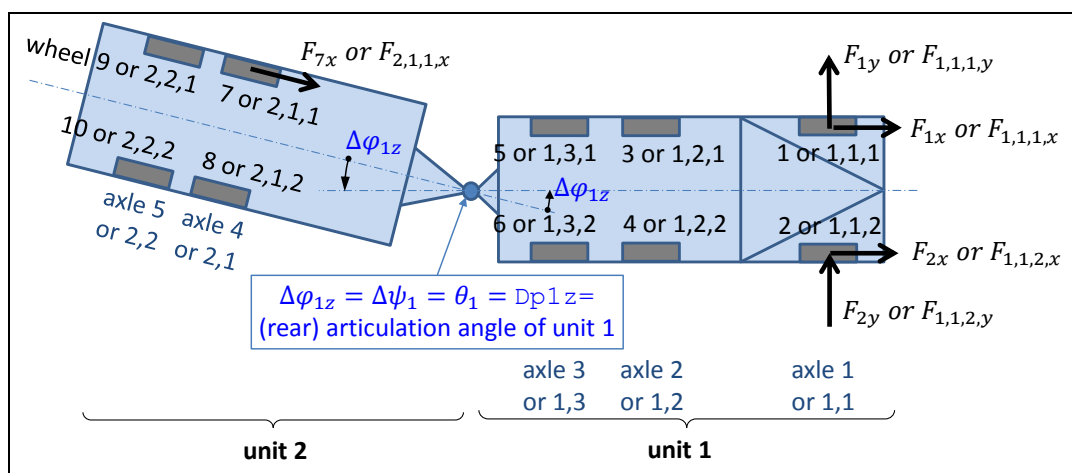
Figure 1-12: Proposed numbering of units, axles, wheels and articulation angle. Example shows a rigid truck with trailer. If multiple units: $\Delta\varphi_{n,z} = \varphi_{n-1,z} - \varphi_{n,z}$;

1.5.9   Terms with special meaning

1.5.9.1   Load levels

The weight of the vehicle varies through usage. For many vehicle dynamic functions it is important to specify the level, which is these definitions are important to know and use.

Kerb weight is the total weight of a vehicle with standard equipment, all necessary operating consumables (e.g., motor oil and coolant), a full tank of fuel, while not loaded with either passengers or cargo. Kerb weight definition differs between different governmental regulatory agencies and similar organizations. For example, many European Union manufacturers include a 75 kilogram driver to follow European Directive 95/48/EC.

Payload is the weight of carrying capacity of vehicle. Depending on the nature of the mission, the payload of a vehicle may include cargo, passengers or other equipment. In a commercial context, payload may refer only to revenue-generating cargo or paying passengers.

Gross Vehicle Weight/Mass (GVW/GVM) is the maximum operating weight/mass of a vehicle as specified by the manufacturer including the vehicle's chassis, body, engine, engine fluids, fuel, accessories, driver, passengers and cargo but excluding that of any trailers.

Other load definitions exist, such as:

- *"**Design Weight**"* (for passenger vehicles, this is typically Kerb weight plus 1 driver and 1 passenger, 75 kg each, in front seats)
- *"**Instrumented Vehicle Weight**"* (includes equipment for testing, e.g. out-riggers)
- *"**Road-allowed GVW/GVM**"* is the maximum GVW/GVM for a certain road, limited by the strength of the road and bridges. It is applicable for heavy trucks.

For vehicle dynamics it is often also relevant to specify where in the vehicle the load is placed because it influences how vertical forces under the wheels/axles distribute as well as moments of inertia.

1.5.9.2 Open loop and Closed loop manoeuvres

Depending on the drivers operation, one can differ between ***Open loop*** and ***Closed loop*** manoeuvres, see Section **2.10.1**.

1.5.9.3 Objective and subjective measures

Two main categories of finding measures are:

- *An **Objective*** measure is a physical measure calculated in a defined and unique way from data which can be logged in a simulation or from sensors in a real test.
- *A **Subjective*** assessment is a rating measure set by a test driver (e.g. on a scale 1-10) in a real-vehicle test or driving simulator test.

One generally strives for objective measures. However, many relevant functions are so difficult to capture objectively, such as Steering feel and Comfort in transient jerks, so subjective assessments are needed and important.

1.5.9.4 Path, Path with orientation and Trajectory

A ***path*** can be $x(y)$ or $y(x)$ for centre of gravity where x and y are coordinates in the road plane. To cope with all paths, it is often necessary to use a curved path coordinate instead, s, i.e. $x(s)$ and $y(s)$. The vehicle also has a varying orientation, $\varphi_z(x)$ or $\varphi_z(s)$, which often is often relevant, but the term "path" does necessarily include this. In those cases, it might be good to use an expression "***path with orientation***" instead.

A ***trajectory*** is a more general term than a path and it brings in the dependence of time, t. One typical understanding is that trajectories can be $[x(t); \; y(t); \; \varphi_z(t)]$. But also other quantities, such as steering angle or vehicle propulsion force can be called trajectory: $\delta(t)$ and $F_x(t)$, respectively. The word "trace" is sometimes used interchangeably with trajectory.

1.5.9.5 Stable and Unstable

Often, in the automotive industry and vehicle dynamics, the words "stable" and "unstable" have a broad meaning, describing whether high lateral slip on any axle is present or not. In more strict physics/mathematical nomenclature, "unstable" would be more narrow, meaning only exponentially increasing solution, which one generally finds only at high rear axle side-slip.

It is useful to know about this confusion. An alternative expression for the wider meaning is "loss of control" or "loss of tracking" or "directional instable", which can include that vehicle goes straight ahead, but road bends.

1.5.9.6 Subject and object vehicle

The ***subject vehicle*** is the vehicle that is studied. Often this is a relevant to have a name for it, since one often study one specific vehicle, but it may interact with other in a traffic situation. Alternative names are ***host vehicle***, ***ego vehicle*** or simply ***studied vehicle***.

If one particular other vehicle is studied, it can be called ***object vehicle*** or ***opponent vehicle***. A special case of object vehicle is ***lead vehicle*** which is ahead of, and travels in same direction as, subject

vehicle. Another special case is ***on-coming vehicle*** which is ahead of, and travels in opposite direction as, subject vehicle.

1.5.9.7   Active Safety and ADAS

The expression *Active Safety* is used a lot in Automotive Engineering. There are at least two different usages:

- Active Safety can refer to the vehicle's ability to avoid accidents, including both functions where the driver is in control (such as ABS and ESC, but also steering response) and functions with automatic interventions based on sensing of the vehicle surroundings (such as AEB and LKA). See http://en.wikipedia.org/wiki/Active_safety. Active Safety can even include static design aspects, such as designing the wind shield and head light for good vision/visibility.
- Alternatively, Active Safety can refer to only the functions with automatic interventions based on sensing of the vehicle surroundings. In those cases it is probably more specific to use Advanced Driver Assistance Systems (ADAS) instead, see http://en.wikipedia.org/wiki/Advanced_Driver_Assistance_Systems. ADAS does not only contain safety functions, but also comfort functions like CC and ACC.

1.5.9.8   Autonomous driving

Functions that off-load the driver the direct tasks during driving can be sorted under Autonomous driving. Fully autonomous driving, e.g. transportation without human driver on-board, is probably a far future vision. On the other hand, it is already a reality that some portion of the driving tasks are autonomous in the latest vehicle on the market, such as Adaptive cruise control, see Section **3.5.2.2**, and Lane Keeping Aid, see Section **4.6.2.1**. If both those are active at the same time, we have already autonomous driving in some sense. Today's version of these systems normally have a way to hand-back responsibility to driver rather immediately in hazardous situations. Future autonomous driving functions will need to always have a safe-stop function. The way to compete between vehicle manufacturers will probably be to avoid hand-backs (maximize up-time) and to allow as long "hand-back times" as possible. So, vehicle dynamics will be important in the development, especially for safety reasons for autonomous driving in higher speeds; hazardous situations where human driver selects to take back the driving.

1.5.10   Architectures

Vehicles are often designed in platforms, i.e. parts of the design solutions are reused in several variants. Typical variants may be different model years or different propulsion system. To be able to reuse solutions, the vehicles have to be built using the same *architecture*.

A **mechanical** architecture may include design decisions about certain type of wheel suspension on front and rear axle. An **electrical and electronic** architecture may include design decisions about electric energy supply system (battery voltage etc.) and electronic hardware for computers (Electronic Control Units, ECUs) and how they are connected in networks, such as Controller Area Network, CAN.

That the mechanical architecture influences vehicle dynamics functions is rather obvious. However, it is noteworthy that also the electronic architecture also is very important for the vehicle dynamics, through all electronic sensors, actuators and control algorithms. One example of this importance is the ABS control of the friction brake actuators. Architectures for functions are therefore motivated, see Section 1.5.10.1.

1.5.10.1   Reference architecture of vehicle functionality

As the number of electronically controlled functions increase, a reference architecture for vehicle functionality, or "Function Architecture", becomes necessary to meet fast introduction of new functionality and to manage different variety of vehicle configurations. A reference architecture is a set of design rules for how functions interact with each other (e.g. signalling between control functions).

An older expression which is related to function architecture is cybernetics. Examples (from Vehicle Dynamics/Vehicle motion function domain) of modern expressions which are related are Integrated Chassis Control (GM), Integrated Vehicle Dynamics Control (Ford), Complete Vehicle Control (Volvo) and Vehicle Dynamics Integrated Management (Toyota). There is no exact and generally well accepted definition of such architecture. However, it becomes more and more essential, driven by increasing content of electronic control in vehicles. One way to visualize a reference architecture is given in Figure 1-13 and Figure 1-14.
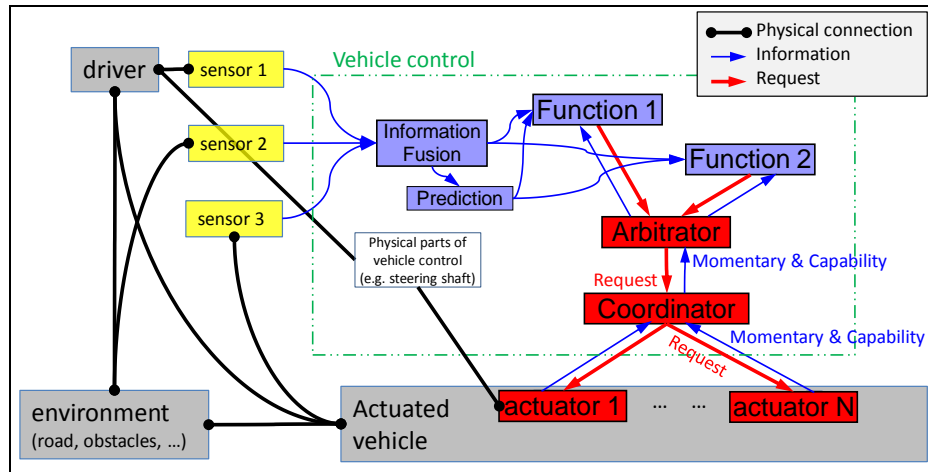

Figure 1-13: Concepts of a reference architecture. Arbitrators, Coordinators (or Allocator) and Actuators are the most important architectural objects for vehicle dynamics (vehicle motion).

In order to be able to formulate design rules in reference architecture of functionality the following are relevant questions:

- Which physical vehicle quantities should be represented on the interface between Sensors and Actuators on one side and Vehicle Level Functionality on the other?

- Partitioning within a reference architecture of vehicle motion functionality could be realised as shown in Figure 1-14. Different Layers/Domains are defined:

  - Motion Support Device Layer: This includes the devices/actuators that can generate vehicle motion. This layer is also consisting sensors which could include the capability and status of each device e.g. max/min wheel torque.

  - Vehicle Motion Layer: This includes the Energy management, powertrain coordination, brake distribution, and vehicle stability such as ESC, ABS. This layer also estimates the vehicle states e.g. v_x, v_y, ω_z. In addition this layer would be able to give vehicle level capability of max/min acceleration and their derivative.

  - Traffic Situation Layer: Interpret the immediate surrounding traffic which the vehicle is in. Automated driving assistance functions such as adaptive cruise control, collision avoidance, and lane steer support are typical functions.

  - Vehicle Environment: Includes surrounding sensors mounted on vehicle but also communication with other vehicles (V2V) and infrastructure (V2I) and map information.

  - Human Machine Interface: This includes the sensors/buttons which the driver use to request services from the vehicle's embedded motion functionality.

- Formalisation of different types of:

  - Blocks, e.g. Controller, Signal Fusion, Arbitrator, and Coordinator.

  - Signals, e.g. Request, Status and Capability.

- Parameters used in Functional blocks. One can differ between Physical parameters (or Model parameters) and Tuning parameters. Some parameters can be common across the whole vehicle, which enables a kind of communication between blocks without normal signals.
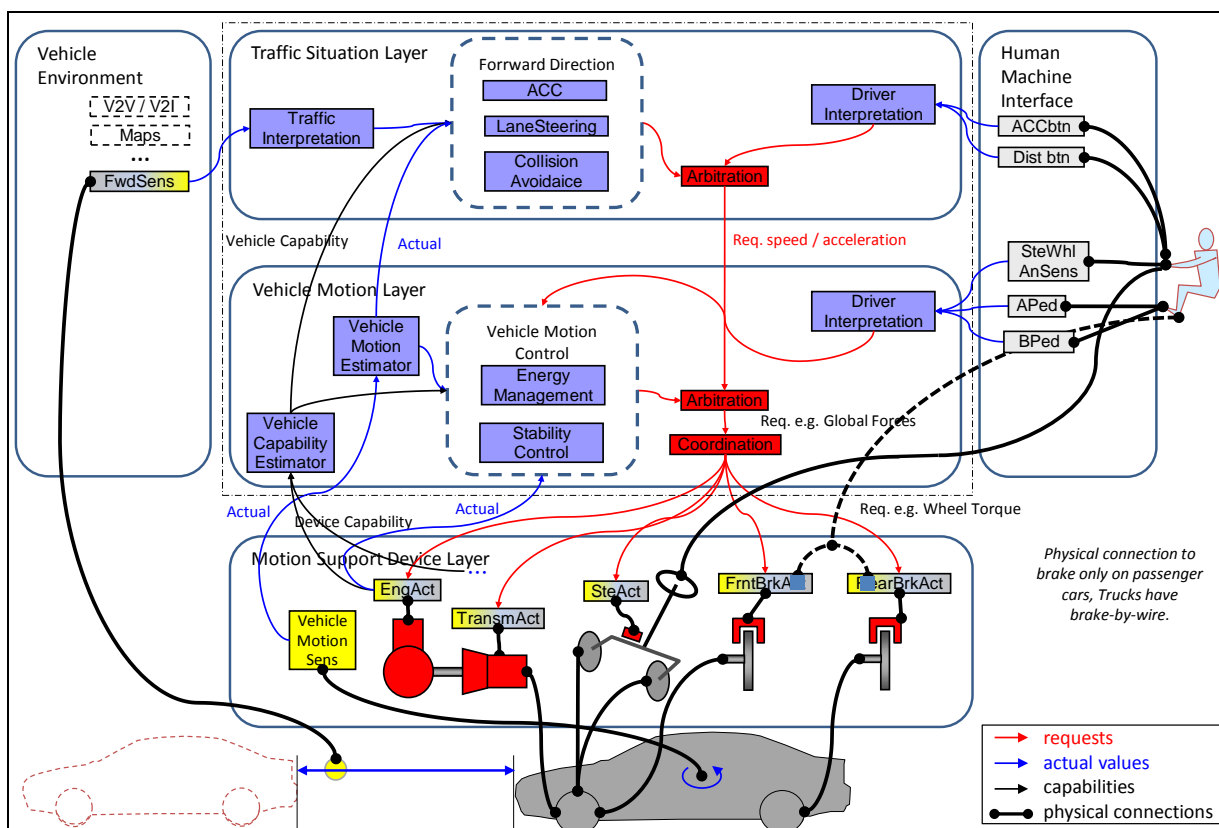
Figure 1-14: One example of reference architecture of vehicle motion functionality. Red arrows: Requests, Blue arrow: Information, Black lines with dot-ends: physical connection.

The functionality is then allocated to ECUs, and signals allocated to network communication. The reference architecture can be used for reasoning where the allocation should be done. Which functionality is sensitive for e.g. time delay and thus should be allocated in the same ECU. Detailed control algorithm design is not stipulated by a reference architecture. Instead the reference architecture assists how detailed control algorithms be managed in the complete problem of controlling the vehicle motion. Whether representation of solutions of Functional Safety (ISO 26262, etc.) is represented in a reference architecture of functionality can vary.

1.5.10.2 Virtual vehicle architecture

Virtual vehicle architecture, VVA, here refers to how to organize complete vehicle models, which can replace some real vehicle pre-series. VVA is a set of rules how a vehicle model should be modularized, such as variable/signal interfaces, parameterization, format- and tool-chains. The vision is that a whole project organisation, within an OEM and it's suppliers, could deliver modules to virtual pre-series and that these modules would fit together. The FMI format, see Section 1.5.7.6, is one example of what could facilitate this.

1.6 Heavy trucks

The following section describes heavy trucks, mainly as compared to passenger vehicles.

1.6.1 General differences

Trucks are normally bought by companies, not private persons. Each truck is bought for a specialized transport task. Life, counted in covered distance, for trucks is typically 10 times passenger cars. The life time cost of fuel is normally 5 times the vehicle cost, compared to passenger car where these costs are about equal. The cost for driver salary is a part of mileage cost, typically same magnitude as fuel cost. If investment cost for vehicle and repairs are distributed over travelled distance, these are typically also of same magnitude. So, the cost for a transport typically comes from one third fuel, one third driver salary and one third vehicle investment and repairs.

1.6.2 Vehicle dynamics differences

A truck has 5..10 times less power installed per vehicle weight. Trucks have their centre of gravity much higher, meaning that roll-over occurs at typically 4 m/s² lateral acceleration, as compared to around 10 m/s² for passenger cars. Trucks have centre of gravity far behind mid-point between axles, where passenger cars have it approximately symmetrical between the axles. Trucks are often driven with more units after, see Figure 1-15. The weight of the load in a truck can be up to 2..4 times the weight of the empty vehicle, while the maximum payload in passenger cars normally are significantly lower than the empty car weight. Trucks often have many steered axles, while passenger cars normally are only steered at front axle.

1.6.3 Definitions

In Figure 1-15, we can find the following units:

- Towing units: Tractor or Rigid (truck)
- Towed units: Full trailer, Semi-trailer, Centre-axle trailer, and (Converter) Dolly
- The couplings between the units can of 2 types:
  - **Fifth-wheel coupling** (e.g. between Tractor and Semi-trailer). Designed to take significant force in all 3 directions. Furthermore, it is designed to be roll-rigid, but free in pitch and yaw. (A **Turn-table** is same as fifth wheel, but might often have rolling bearing instead of greased surface, which leads to less yaw friction.)
  - **Hitch coupling** (e.g. between Rigid and Full trailer). Designed to take significant forces in longitudinal and lateral directions, but only minor in vertical direction. Furthermore, it is rotationally free in all 3 directions.

1.7 Smaller vehicles

This section is about smaller vehicles, meaning bicycles, electric bicycles, motorcycles and 1-2 person car-like vehicles. The last vehicle type refers to vehicles which are rare today, but there are reasons why they could become more common: Increasing focus on energy consumption and congestion in cities can be partly solved with such small car-like vehicles, of which the Twizy in Figure 1-16 is one example. All vehicles in Figure 1-16 can be referred to as Urban Personal Vehicle (UPVs), because they enable personalised transport in urban environments. The transport can be done with low energy consumption per travelled person and distance, compared to today's passenger cars. The transport can be done with high level of flexibility and privacy for the travelling persons, compared to today's public transportation.
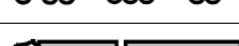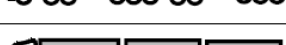
Conventional Combination Vehicles	Tractor-Semitrailer (Tractor-ST)	16.5 m/40 ton	
	Truck-Center Axle Trailer (Tractor-CAT)	18.75 m/40 ton	
	Truck-Full Trailer (Truck-FT)	18.75 m/40 ton	
Existing Longer Combination Vehicles	Tractor-Link Semitrailer-Semitrailer (B-Double)	25.25 m/60 ton	
	Tractor-Semitrailer-Center Axle Trailer (Tractor-ST-CAT)	25.25 m/60 ton	
	Truck-Dolly-Semitrailer (Truck-Dolly-ST)	25.25 m/60 ton	
Prospective Longer Combination Vehicles	Tractor-Semitrailer-Dolly-Semitrailer (A-Double)	31.5 m/80 ton	
	Truck-Duo Center Axle Trailer (Truck-Duo CAT)	27.5 m/66 ton	
	Truck-Dolly-Link Semitrailer-Semitrailer (Truck-B-Double)	34 m/90 ton	

Figure 1-15: An overview over conventional and longer combinations. From (Kharrazi , 2012). The 2 units "Dolly-Semitrailer" can also be replaced by a 1 unit "Full-trailer".
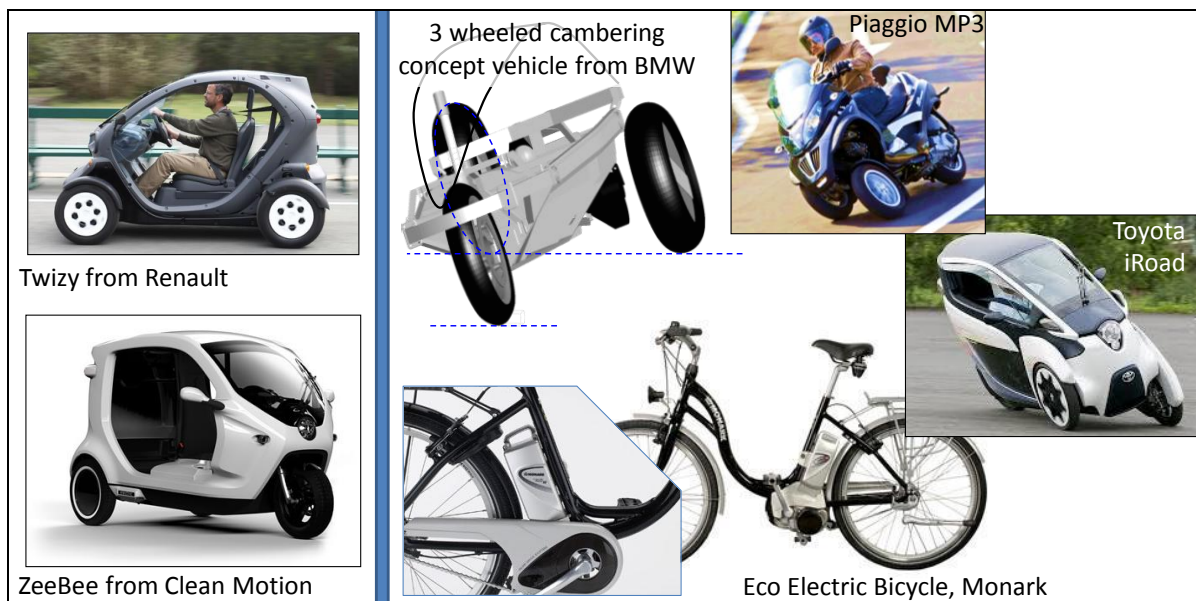
Figure 1-16: Examples of Urban Personal Vehicles. Left: "Roll-stiff". Right: "Cambering". From www.motorstown.com, www.cleanmotion.se, www.monarkexercise.se, www.nycscootering.com.

New solutions as in Figure 1-16 may require some categorization.

- Climate and user type: Sheltered **or** open.
- Transport and user type: Short travels (typically urban, 5-10 km, 50 km/h) **or** long travels (typically inter-urban, 10-30 km, 100 km/h).
- Chassis concept:
  - Narrow (e.g. normal bicycles and motorcycles) **or** wide (at least one axle with 2 wheels, resulting in 3-4 wheels on the vehicle). Note that UPVs in both categories are typically still less wide than passenger cars.

- o Roll moment during cornering carried by suspension roll stiffness or roll moment during cornering avoided by vehicle cambering. The first concept can be called "Roll-stiff vehicle". The second concept can be called "Cambering vehicle" or "Leaning vehicle". 1-tracked are always Cambering vehicles. 2-tracked are normally Roll-stiff, but there are examples of Cambering such (see upper right in Figure 1-16). See Figure 1-17.
- o (This compendium does only consider vehicles which are "Pitch-stiff", i.e. such that can take the pitch moment during acceleration and braking. Examples of vehicles not considered, "Pitching vehicles", are: one-wheeled vehicles as used at circuses and two-wheeled vehicles with one axle, such as Segways.)

Note that also Roll-stiff Vehicles camber while cornering, but **outwards** in curve and only **slightly**, while Cambering Vehicles cambers **inwards** in curve and with a **significant** angle. Cambering Vehicles is more intricate to understand when it comes to how wheel steering is used. In a Roll-stiff Vehicle, the wheel suspension takes the roll-moment (maintains the roll equilibrium), which means that driver can use wheel steering solely for making the vehicle steer (follow an intended path). In a Cambering Vehicles, the driver has to use the wheel steering for both maintaining the roll equilibrium and following the intended path. A model is given in Section 4.5.2.3. Figure 1-17 shows some possible conceptual design of a cambering vehicle. It is not possible to do a partly roll-stiff and partly cambering vehicle, unless one uses suspension springs with negative stiffness, i.e. the suspension would need to consume energy to tilt the vehicle inward in curve.
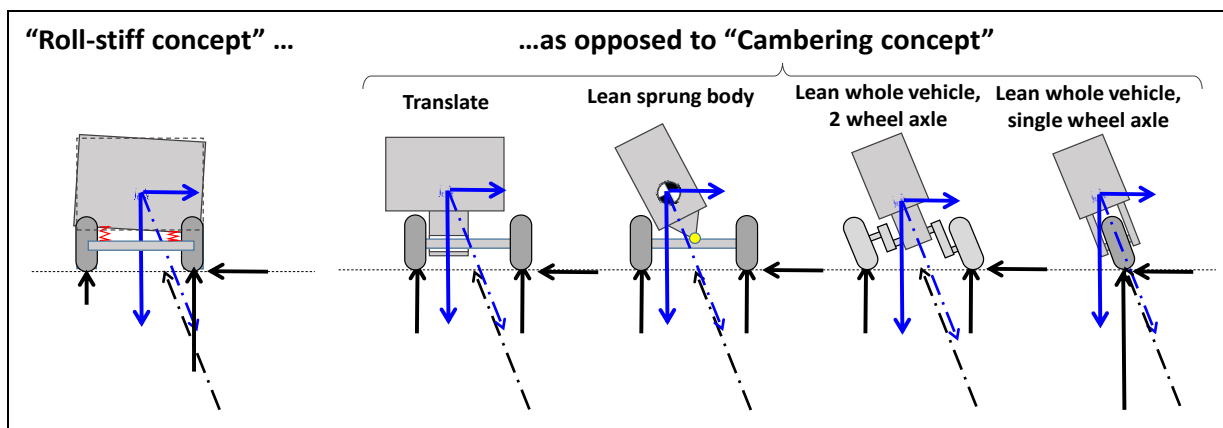
Figure 1-17: How Cambering vehicles avoid to take the roll moment while cornering. The vehicles are viewed from rear and turns to the left. The dash-dotted arrows marks the resulting forces which are equal between the 5 concepts.

Smaller vehicles might have significantly different vehicle dynamics in many ways:

- Influence of driver weight is larger than for other vehicle types. This especially goes for bicycles, where driver weight can be typically 5 times larger than the vehicles own weight. Drivers not only change the total inertia properties, but they can also actively use their weight and move it during driving.
- Ratio between CoG height and wheel base is likely to be larger than passenger cars and trucks. This gives a larger longitudinal load transfer during acceleration and braking. Some concepts might even have the risk of "pitch-over".
- For 2-tracked UPVs, the ratio between CoG height and track width is likely to be larger than passenger cars, rather like trucks, because it is likely that one want to keep swept area low for UPVs.
  - o If Roll-stiff, this gives a larger lateral load transfer and roll angles during cornering. The risk for roll-over is also likely to be larger than passenger cars.
  - o If Cambering, this opens for the risk for slide ("roll-over inwards in curve", so called "low-sider"), which is known from motorcycles.
- For future UPVs it is possible that the part costs need to be kept low, as compared to passenger cars. This, and the fact that new inexperienced OEMs might show up on market, might lead to

low-cost and/or unproven solutions appear for the vehicle design. This might be a challenge for driving experience and (driver and automated) active safety.

- Positive, for safety, is that future UPVs can have significantly lower top speed than passenger cars. However, the acceleration performance up to this top speed might be high, e.g. due to electric propulsion, which might cause new concerns for city traffic with surrounding.

1.8 Typical numerical data

The purpose of the tables in this section is to give approximate numerical values of parameters. Vehicle parameters are often dependent on each other; changing one leads to that it is suitable to change others. The parameters are given with the intention to be consistent with each other, for each vehicle example. The tables balances between being generic and specific, which is difficult. Therefore, please consider the table as very approximate.

Table 1.3: Typical values of parameters, common for typical passenger cars and heavy trucks

Parameter	Notation	Typical Value		Unit
		Passenger car	Heavy truck	
Air density	roh	1		kg/(m^3)
Earth gravity	g	9.80665		m/(s*s)
Road friction, at dry asphalt	mu	1.0		N/N
Road friction, at wet asphalt		0.6		
Road friction, at snow		0.3		
Road friction, at wet ice		0.1		
Tyre slip stiffness, normalized with vertical load	CC	10..15	5..10	(N/rad)/N = (N/1)/N

1.8.1   For passenger vehicle

Table 1.2 gives typical numerical data for a medium sized passenger car.

1.8.2   For heavy vehicle

Compared to passenger cars, trucks differs much more in size and configuration, see Figure 1-15. Also, a certain individual vehicle also differs much more between empty and fully loaded. So, Figure 1-18 and Table 1.5 are really to be seen only as an example. Globally, "Tractor with Semitrailer" is the most common vehicle, which is why it is used as example.

Table 1.4: Typical data for a passenger vehicle

Group/Type	Parameter	Notation	Typical Value	Unit	Note / Typical / Range / Relation to other
1. General	Length, bumper to bumper		5.00	m	
1. General	Longitudinal distance from CoG to front axle	lf	1.3	m	40-50% of wheel base: lf=0.55*L;
1. General	Mass	m	1700	kg	
1. General	Moment of inertia for yaw rotation	Jzz	2900	kg*m*m	Radius of gyration is sligthly less (0.9) than half wheel base: =m*(0.9*L/2)^2
1. General	Unsprung mass	mus	200	kg	Sum of 4 wheels with suspensions
1. General	Track width	W	1.70	m	
1. General	Wheel base	L	2.90	m	
2. Systems	Engine inertia		0.5	kg*m*m	
2. Systems	Transmission ratio, highest gear		5.00	rad/rad= Nm/Nm	Engine to wheel. In magnitude of 5.
2. Systems	Transmission ratio, lowest gear		10.00	rad/rad= Nm/Nm	Engine to wheel. In magnitude of 10.
2. Systems	Brake proportioning, front/rear		70/30	N/N or Nm/Nm	Often tuned so that braking both axles when braking 0.8*g
2. Systems	Rolling resistance		0.01	N/N	
2. Systems	Steering ratio		16	rad/rad	Steering wheel to Road wheel
2. Systems	Wheel radius		0.30	m	
2. Systems	Wheel rotational inertia		0.5	kg*m*m	For one wheel
3. Longitudinal	Projected area in a transversal view	Afront	2.2	m^2	For calculation of air resistance
3. Longitudinal	Aerodynamic coefficients	cd, clf, clr	0.31, 0.10, 0.07	1	For calculation of longitudinal resistance and lift force over front and rear axle
5. Vertical	Suspension heave stiffness (without roll)	cs	100 000	N/m	Vertical stiffness at wheel. Sum of 4 wheels. So that bounce frequency f is between 1 and 2 Hz: sqrt(c/ms)=f*2*pi;
5. Vertical	Suspension roll stiffness, only from anti-roll-bars	carb	14 000	N/m	Vertical stiffness at wheel. Sum of both axles.
5. Vertical	Suspension damping	ds	13 000	N/(m/s)	Wheel rate. Sum of 4 wheels. Some 40..60% of critical damping: d = (0.4..0.6)*2*sqrt(c*m); 2..3 times softer in compression than rebound.
5. Vertical	Tyre vertical stiffness	ct	250 000	N/m	For one wheel

INTRODUCTION
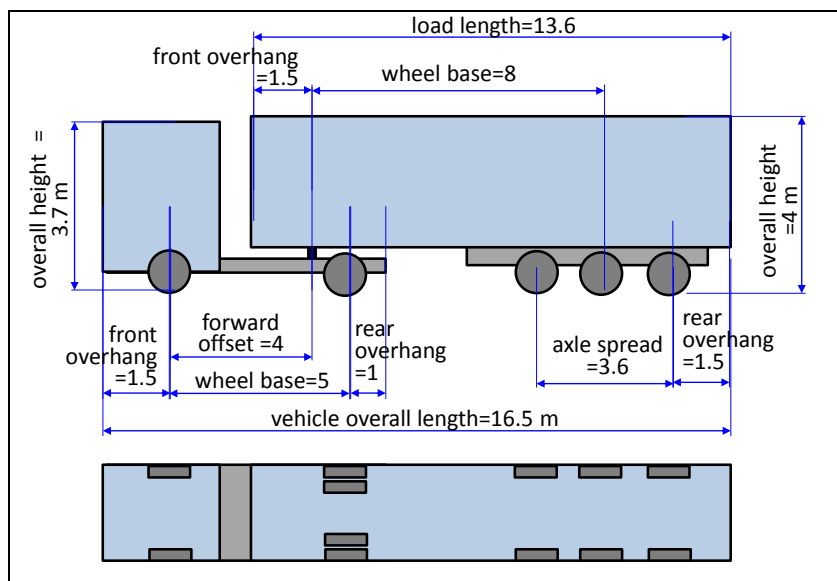
Figure 1-18: Typical data for a heavy vehicle, exemplified with "Tractor with Semi-trailer"

Table 1.5: Typical data for a heavy vehicle, exemplified with "Tractor with Semi-trailer"

Group/Type	Parameter	Typical Value		Unit	Note / Typical / Range / Relation to other
		Empty	With max payload		
Trackwidth	Trackwidth, centre-to-centre for single tyres	2.25		m	Outer tyre edge 2.55
Tractor	CoG heigh	1.00		m	
Semitrailer	CoG heigh	1.00	2.00	m	
Vehicle	CoG heigh	1.00	2.00	m	
Tractor	Mass (total), tractor	7500		kg	
Semitrailer	Mass (total), semi-trailer	10000	32500	kg	
Tractor	Moment of yaw inertia	22500		kg*m*m	Around unit CoG
Semitrailer	Moment of yaw inertia	150000	500000	kg*m*m	Around unit CoG
Tractor	Unsprung mass	1700		kg	Sum of all axles at unit
Semitrailer	Unsprung mass	2400		kg	Sum of all axles at unit
Wheels	Wheel radius	0.50		m	0.4-0.5
Wheels	Wheel rotational inertia	10.0		kg*m*m	For one wheel, single tyre
Tyres	Rolling resistance	0.005		N/N	Or less, 0.003
Propulsion	Engine max power	370		kNm/s=kW	
Propulsion	Engine inertia	5		kg*m*m	
Propulsion	Transmission ratio, highest gear	3		1=rad/rad= Nm/Nm	Engine to wheel
Propulsion	Transmission ratio, lowest gear	30			Engine to wheel
Steering	Steering ratio	20		rad/rad	Steering wheel to Road wheel
Vehicle	Projected area in a transversal view	10.0		m^2	For calculation of air resistance
Vehicle	Aerodynamic coefficient	0.4		1	c_d coefficient in aero dynamic resistance formula

2 VEHICLE INTERACTIONS

2.1 Introduction

The study of vehicle dynamics starts with the interfaces between the vehicle and its environment, see Figure 2-1. The vehicle tyres are the primary structures to transfer loads that produce desired motions (vehicle weight, acceleration, steering, braking) and undesired disturbances (road vibrations, road bumps, etc.). Additionally, the aerodynamic loads on the vehicle will create forces and moments that are often undesirable (wind resistance, side gusts, etc.) but can sometimes be exploited for better contact with the road (down-force). An example of extreme interactions to the vehicle is the impact forces from a crash. An interaction of another kind, but still very influencing, is the driver. One often divide into 3 parts: vehicle, driver and environment, i.e. that environment is all remaining.
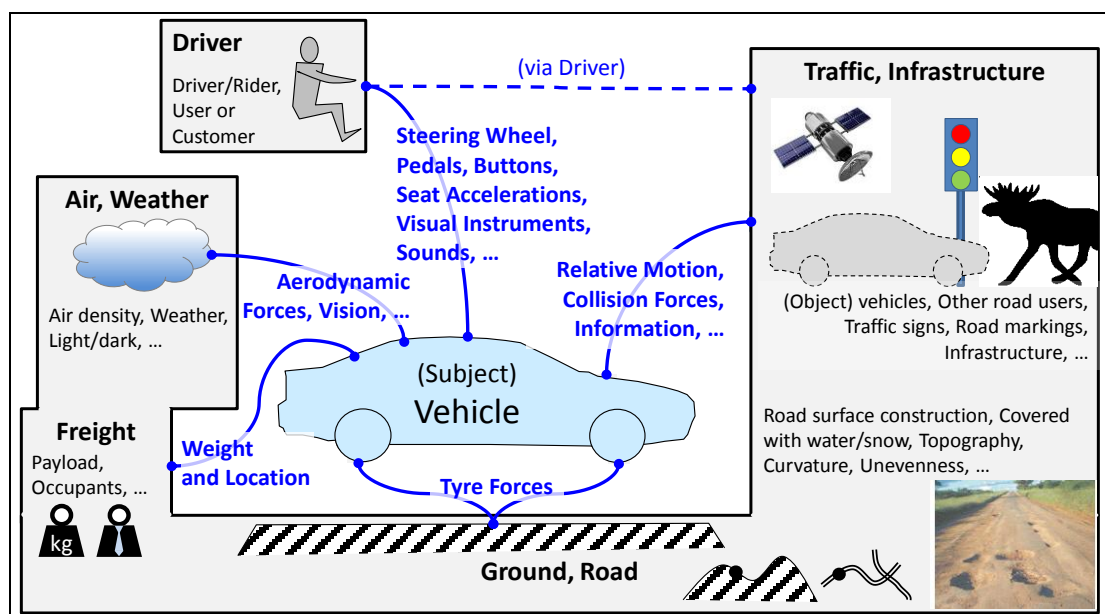
Figure 2-1: Interactions of the vehicle.

Main focus of present chapter is on tyres, including derivation of models. Important aerodynamic models are listed, without ambition on derivation. Driver models are discussed with some selected example models.

2.1.1 References for this chapter

- Tyres: (Pacejka, 2005), (Rill, 2006), and (Michelin, 2003)
- Vehicle Aerodynamics: Reference (Barnard, 2010)
- Driver models: *"Chapter 38 Driver Models in Automobile Dynamics Application"* in Reference (Ploechl, 2013)

2.2 Tyre Terminology

The tyre (or wheel) is best described in its own coordinate system, see Figure 2-2. The three forces and moments are acting on the wheel from the ground. They are needed are recognized in any free body diagrams of the vehicle. The other quantities, such as slip angle α and camber angle ε_w, in Figure 2-2 are examples of variables which have influence on the forces and moments in the coming chapters.
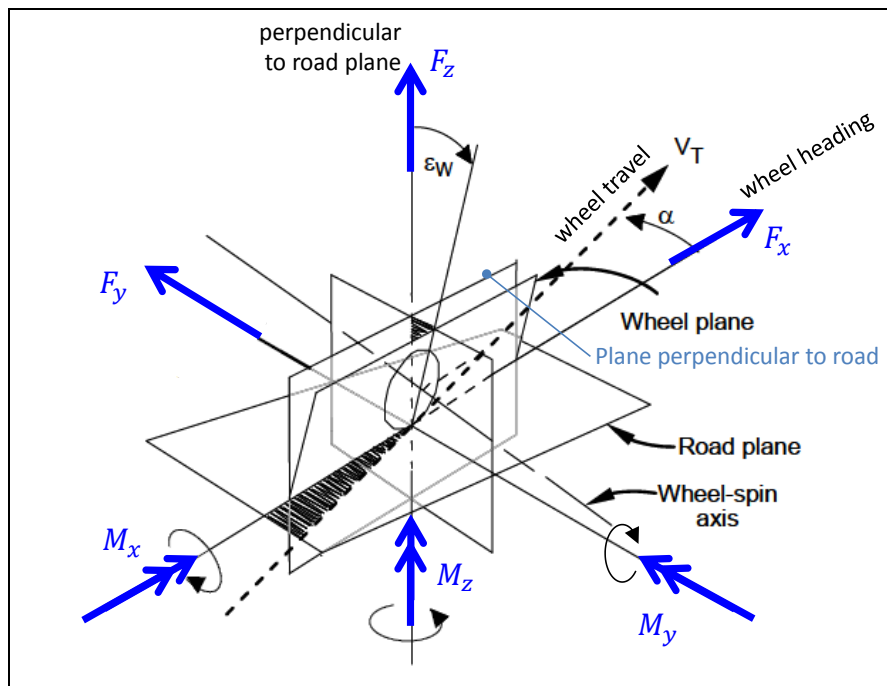
Figure 2-2: Tyre Coordinate System, forces and torques on tyre from ground. According to ISO.

2.2.1 Wheel angles

2.2.1.1 Steering angle

A wheel's steering angle is the angle between the wheel plane and the longitudinal axis of the vehicle. Steering angle can be defined for one wheel or one axle, using averaging of left and right wheel.

2.2.1.2 Camber angle

Camber angle (or sometimes Camber) is the angle between the wheel plane and the vertical, positive when the top of the wheel leans outward. (This definition of sign is only applicable for axles with two wheels. For instance, it is not applicable for motorcycles.) Camber generates lateral forces and gives tyre wear. See also Section 2.5.6.3.

2.2.1.3 Caster angle

The angle in a side-view between the steering axis and the vertical axis is called Caster angle. It is positive if the top of the steering axis is inclined backwards. Caster angle provides an additional aligning torque, see 2.5.6.2 and Section 4.2.3.2, and changes the camber angle when the wheel is steered.

2.2.1.4 Toe Angle

Toe angle (or toe-in) is defined for an axle with two wheels (not for a single wheel), as the difference between right and left wheel's steering angles. Toe angle is positive if front ends of the wheels are pointing inward. Hence, toe can be called toe-in. Negative toe can be called toe-out. Toe angle generates opposing lateral forces on each side.

The toe angles vary with the tyre forces, due to suspension linkage geometry and elasticity in suspension bushings. This means that there is a *static toe angle* (when a vehicle parked in workshop, with a certain load and not tyre forces in ground plane) has one value, while *actual toe angle* (in a particular moment during a manoeuvre) has another value.

Zero toe gives low rolling resistance and low tire wear. Theoretically, toe-out on front axle and toe-in on rear axle makes the vehicle most yaw stable (less over-steered). Tone-in on front axle makes vehicle more yaw agile and improves on-centre steering feel. Normal design choice is toe-in on both axles, and more on front axle.

2.2.1.5   Steering axis inclination

Steering axis inclination (or Kingpin inclination) is defined for a wheel with its suspension linkage (not for an isolated wheel). The angle in a front view between the steering axis (or Kingpin) and the vertical axis is called Kingpin inclination. See Section **4.2.3.2**.

2.3 Tyre Design

The tyres of a vehicle have the following tasks:

o   Carry the vertical load
o   Generate longitudinal (brake, traction) and lateral (steering) forces
o   Isolate vertical disturbances, for comfort, road grip and reduction of suspension fatigue
o   Roll with minimum energy loss, tyre wear, particle emissions and noise emission

Before discussing the mechanics of tyre and road interactions, the physical structure of the wheel assembly should be understood. Consisting of a steel rim and an inflated rubber toroid, pneumatic tyres were invented and patented by Robert William Thomson in 1845 and are essentially the only type of tyre found on motor vehicles today.

The physical construction of the tyre carcass affects the response of the tyre to different road loadings. The carcass is a network of fabric and wire reinforcement that gives the tyre the mechanical strength. The structure of the carcass can be divided into different types of tyres: Bias-ply, Bias-ply Belted, and Radial-ply. Bias-ply tyres were the first types of pneumatic tyres to be used on motor vehicles. Radial ply tyres followed in 1946 and became the standard for passenger car tyres. Figure 2-3 shows the main features of these tyre types.
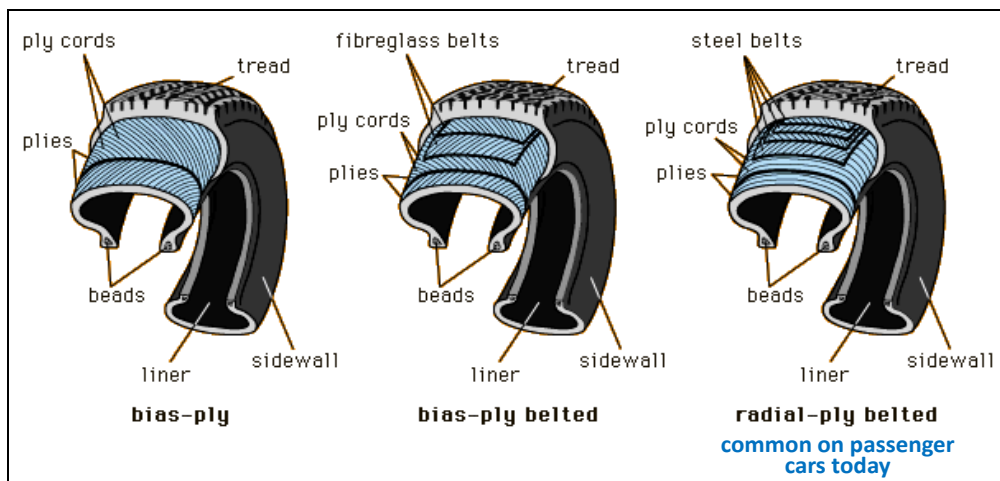
Figure 2-3: Common Tyre Constructions, from (Encyclopædia Britannica Online, 2007)

Note how the bias-ply constructions have textile structures oriented at an angle to the tyre centreline along the x-z plane. This angle is referred to as the crown angle and is further illustrated in Figure 2-4. Note the textile orientation for the bias-ply and radial tyres. Also note the difference in crown angles between the two tyre constructions. This difference plays an important part in the rolling resistance characteristics of the tyre which is Section 2.4.
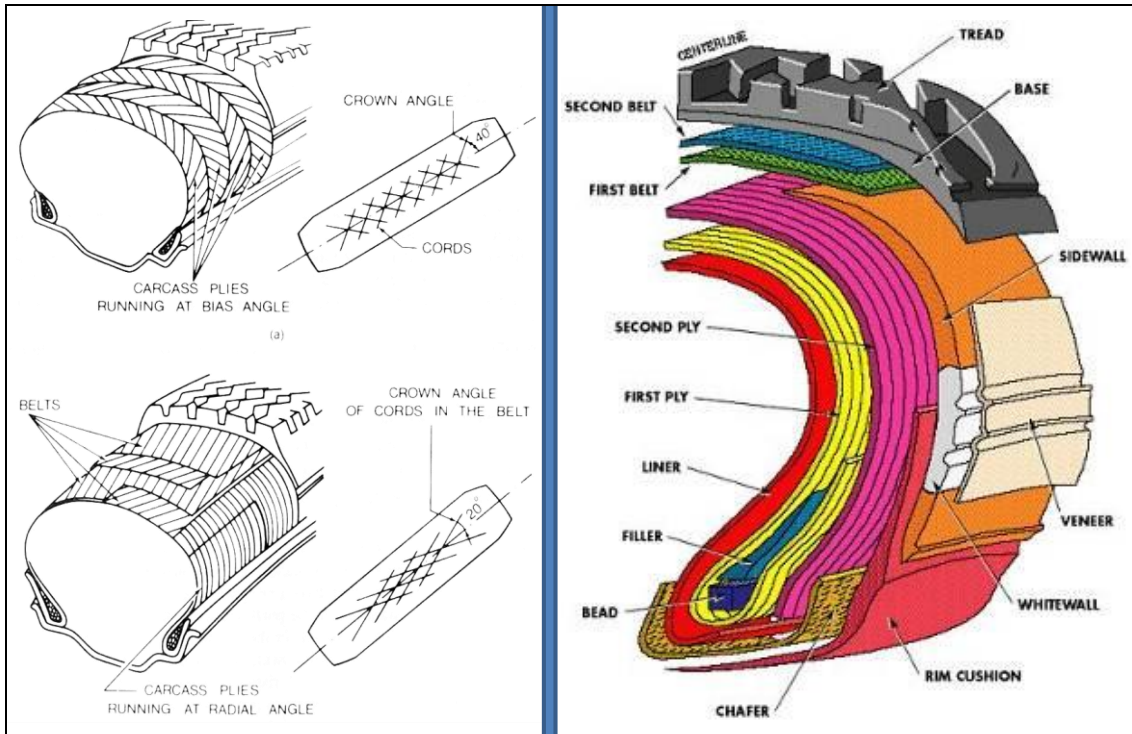
Figure 2-4: <u>Left</u>: Carcass Construction, (Wong, 2001). <u>Left top</u>: Bias-ply construction. <u>Left bottom</u>: Radial construction. <u>Right</u>: Radial Tyre Structure, (Cooper Tire & Rubber Co., 2007)

The tyre components have been constructed to provide the best tyre performance for different loading directions. A trade-off must be made between handling performance and comfort, between acceleration and wear, as well as between rolling resistance and desired friction for generating forces in ground plane. Some of the tyre components have an important role in vehicle performance. For example, the radial tyre components are presented in more detail in Figure 2-4. The rubber components and patterns incorporated in the tread are critical to the friction developed between the tyre and road under all road conditions (wet, dry, snow, etc.). Friction is most relevant in longitudinal and lateral vehicle dynamics. The belts define the circumferential strength of the tyre and thus braking and acceleration performance. The sidewall and plies define the lateral strength of the tyre and thus influence the lateral (cornering) performance of the vehicle. The sidewall as well as the inflation pressure are also significant contributors to the vertical stiffness properties of the tyre and affect how the tyre transmits road irregularities to the remainder of the vehicle. It becomes clear that a tyre that has strong sidewalls will support cornering at the cost of vertical compliance – reducing the comfort in the vehicle.
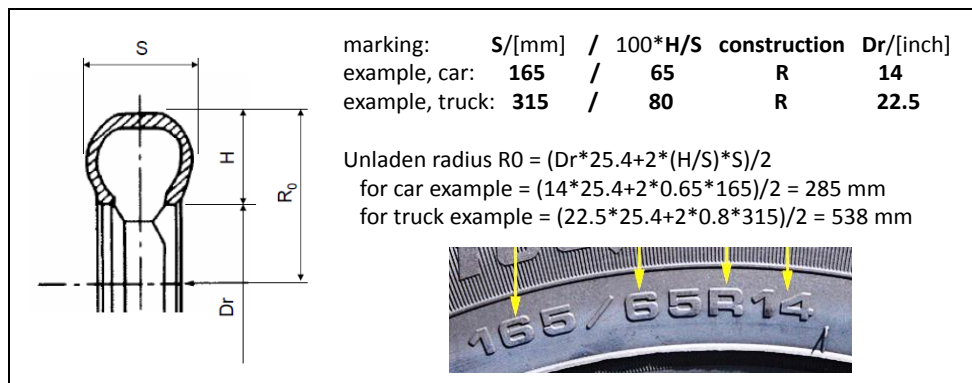
Figure 2-5: Tyre marking (radial tyre)

Figure 2-6 shows how a pneumatic tyre carries the vertical load. In a traditional bicycle or motorbike wheel, the pre-tensioned spokes has a similar role as the air and rubber parts of a pneumatic tyre.
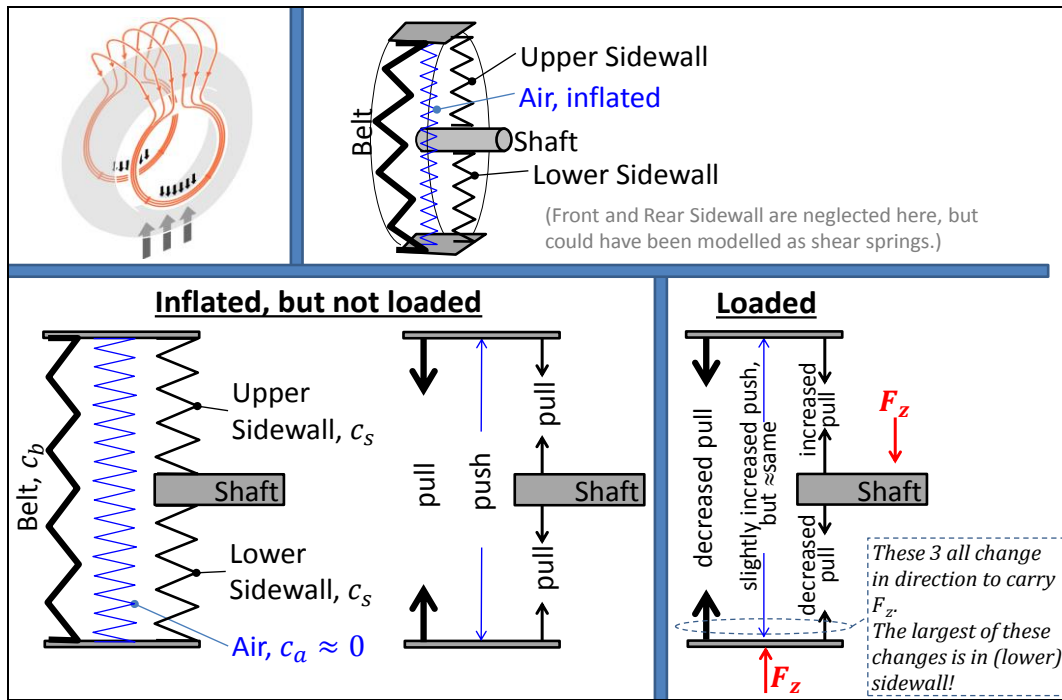
Figure 2-6: A pneumatic tyre is pre-tensioned by inflation pressure. This figure explains how the wheel and tyre takes (vertical) load without (significant) increase of inflation pressure.

2.3.1 Tyre Model Architecture

This section describes how a tyre model can be instantiated once per wheel and integrated in a model together with models of vehicle, driver, and environment. We then need to differ between parameters and variables. The description assumes dynamic models used for simulation. Within each simulation parameters are constant and variables vary. If design optimization, as opposed to simulation, the design parameters becomes variables (are varied) in the optimization.
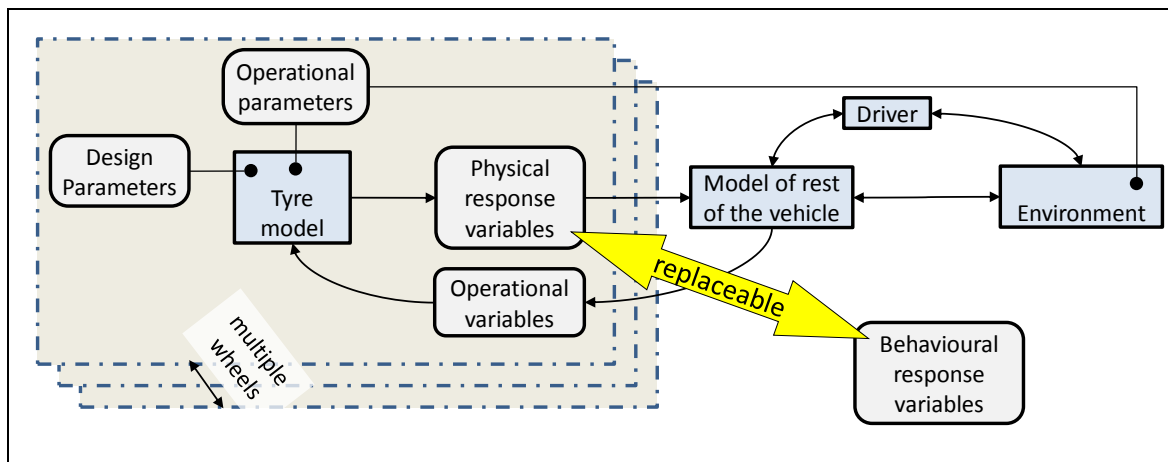
Figure 2-7: How tyre models can come into a model context.

2.3.1.1 Design parameters

We limit ourselves to today's traditional pneumatic tyres. Then the design is captured by:

- Carcass/Material: Rubber quality and plies arrangement.
- Tread/Grooves: Groove pattern, Groove depth, Tread depth, Spikes pattern (if spikes)
- Main dimensions: Outer radius, Width, Aspect ratio
- Installation parameters: Inflation pressure

2.3.1.2   Operational parameters

These are operating conditions which vary slowly, and in this description assumed to be constant during one manoeuvre/driving cycle. These are:

- Road surface (dry/wet, asphalt/gravel/snow/ice, …),
- Road compliance and damping (hard/soft, …),
- Wear state of tyre,
- Age of tyre,
- Temperature

2.3.1.3   Operational variables

These are operating conditions which vary quickly, and in this description assumed to be variable in time during one manoeuvre/driving cycle. These are:

- Longitudinal speed,
- Tyre slip (s_x, s_y, see Equation [2.2]),
- Vertical tyre force, (F_z, see Figure 2-2)
- Camber angle

Tyre forces in road plane (F_x, F_y) can be given instead of tyre slip. Another alternative is to give the corresponding actuation, e.g. wheel shaft torque and wheel steering angle relative to wheel course angle. With those setups, the response variables in Section 2.3.1.4.

Vertical tyre force can be modelled as arbitrarily varying in time or as an offset amplitude for different frequencies where offset is from a mean value. The mean value would then be a parameter instead of a variable. The latter alternative can be more efficient if simulating a longer driving cycle, where following each road wave would be very computational inefficient.

2.3.1.4   Response variables

Response refers to response to both Design changes and Operation changes.

2.3.1.4.1 Physical response variables

The variables from tyre model to model of rest of the vehicle is essential the forces and moments, see Figure 2-2:

- Longitudinal and lateral forces (F_x, F_y)
- Roll moment or Overturning moment (M_x)
- Rolling resistance moment (M_y)
- Spin moment or Aligning moment (M_z)

Other responses are:

- Wear rate [worn rubber mass or tread depth per time unit]
- Loaded radius (R_l)

2.3.1.4.2 Behavioural response variables

The Responses can be modelled as Behavioural variables instead:

- Slip characteristics (C_{sx}, C_{sy}, peak friction coefficient, … or other parameters in physical or empirical tyre slip model, as in Section 2.4.3.2)
- Rolling resistance coefficient and Loaded radius (R_l)
- Vertical stiffness and damping coefficients
- Wear coefficient
- Relaxation length, …

When working with Behavioural instead of Physical, the variables becomes varying model coefficients instead of physical quantities. A model coefficient requires an agreed model to be interpreted, while a physical quantity does not.

2.4 Longitudinal Properties of Tyres

The longitudinal force in ground plane (F_x or $F_{ground,x}$), depends on the design of the tyre, the ground surface and the operational variables, such as velocities (v_x, ω) and vertical force (F_z). This section treats the main phenomena of tyre mechanics that influence the tyre-longitudinal force. The tyre can be under braking, free rolling, pure rolling or traction.

The whole wheel, rim and tyre, can be seen as a transmission from rotational mechanical energy to translational mechanical energy. The shaft is on the rotating side; where we find rotational speed, ω, and the torque, T. The torque T is then the sum of torque on the propulsion shaft and torque on the brake disk or drum. The wheel hub is on the translating side of the transmission; were we find translating speed, v_x, and force, $F_{hub,x}$. See Figure 2-8. Normally, we approximate and denote $F_{ground,x} = F_{hub,x} = F_x$ and $F_{ground,z} = F_{hub,z} = F_z$.
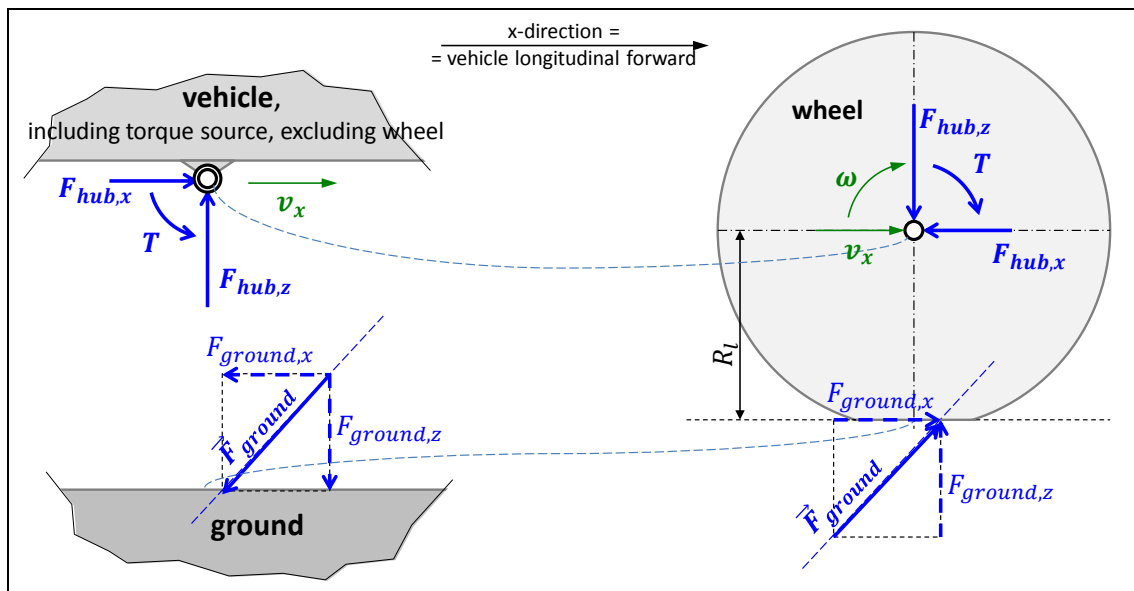
Figure 2-8: A wheel as a transmission from rotational $[\omega; T]$ to translational $[v_x; F_{hub,x}]$.

2.4.1 Tyre Rolling and Radii

In all fundamental engineering mechanics, the radius of an object that rolls without sliding is a compatibility link between the translational velocity and angular velocity as shown in Figure 2-9 a). This relationship does not hold when the tyre is deflected as in Figure 2-9 b). Not even the deflected radius can be assumed to be a proportionality constant between angular and translational velocity, since the tyre contact surface slides, or slips, versus the ground. Then, an even truer picture of a rolling tyre looks like Figure 2-9 c), where the deformation at the leading edge also is drawn. This means that v_x is only $\approx R_l \cdot \omega$ and $\approx R_o \cdot \omega$ for limited slip levels.

There is a difference speed between tyre and the road surface. The ratio between this speed and a reference speed is defined as the "tyre slip". The reference speed can be the translational speed of the tyre or the circumferential speed of the tyre depending on the application. For a driven wheel, the longitudinal (tyre) slip is often defined as:

$$s_x = \frac{R \cdot \omega - v_x}{|R \cdot \omega|};$$

[2.1]
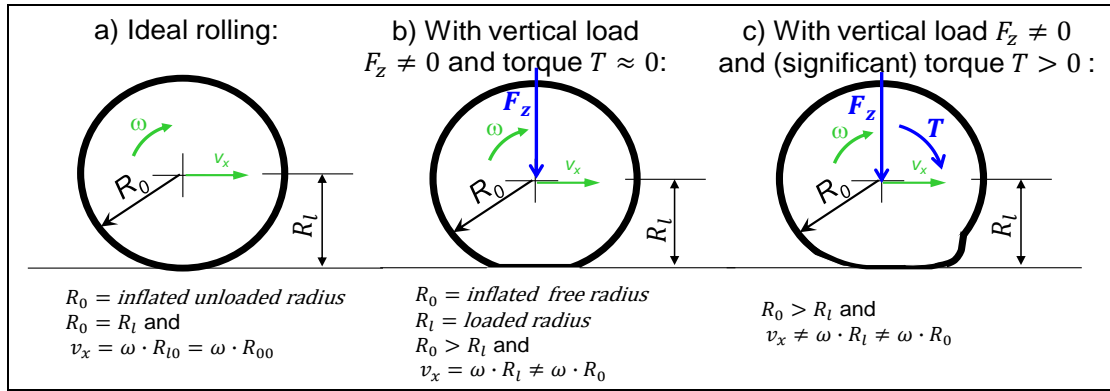
Figure 2-9: Radius and speed relations of a rolling tyre R_0 and R_l do not have exactly the same numerical values across a), b) and c).

For braked wheels it is often defined as:

$$s_x = \frac{R \cdot \omega - v_x}{|v_x|};$$

[2.2]

With the definition in Equation [2.1], the following transformation falls out:

$$\omega = \begin{cases} = \dfrac{1}{1 - s_x} \cdot \dfrac{v_x}{R}; & if \ R \cdot \omega > 0; \\ = \dfrac{1}{1 + s_x} \cdot \dfrac{v_x}{R}; & if \ R \cdot \omega < 0; \end{cases}$$

[2.3]

Whether one should use $R \cdot \omega$ or v_x as reference speed (the denominators in Equations [2.1]..[2.2]), is not obvious and is discussed in Section 2.4.3.

It is also not obvious which R to use in Equations [2.1]..[2.2], e.g. R_0 or R_l. However, this compendium recommends R_0, rather than R_l, because R_0 is a better average value of the radius around the tyre and the tyre's circumference is tangentially stiff so speed has to be same around the circumference.

Sometimes one defines a third radius, the rolling radius $= (v_x/\omega)|_{T=0}$, i.e. a speed ratio with dimension length, between translator and rotating speeds, measured when the wheel is un-driven. This radius can be used for relating vehicle longitudinal speed to wheel rotational speed sensors, e.g. for speedometer or as reference speed for ABS and ESC algorithms. The Rolling radius is normally between R_0 and R_l.

Yet another approach is to use the $R = (v_x/\omega)|_{F_x=0}$, i.e. the ratio when the wheel is pure rolling. Using $R = (v_x/\omega)|_{T=0}$ or $R = (v_x/\omega)|_{F_x=0}$ in the slip definitions shifts $F_x(s_x)$ curve and $T(s_x)$ curve, see more in Section 2.4.3.3.

The variable s_x is the longitudinal slip value, sometimes also denoted as κ. When studying braking, one sometimes uses the opposite sign definition, so that the numerical values of slip becomes positive. It is used to model the longitudinal, traction or braking, tyre force in Section 2.4.3.

2.4.2 Rolling Resistance of Tyres

The rolling resistance force is defined as the loss of longitudinal force on the vehicle body, as compared to the longitudinal force, which would have been transferred with an ideal wheel. The Rolling Resistance Coefficient, f_r, is the rolling resistance force divided by the normal force, F_z. Assuming force equilibria in longitudinal and vertical direction, $F_{hub,z} = F_{ground,z} = F_z$ and $F_{hub,x} =$

$F_{ground,x} = F_x$, see Figure 2-8.

$$f_r = \frac{\frac{T}{R_l} - F_x}{F_z} \qquad [2.4]$$

F_x denotes the longitudinal force on the wheel, T denotes the applied torque and R_l denotes the tyre radius. For a free rolling tyre, where $T = 0$, f_r becomes simply $- F_x/F_z$. One often see definitions of f_r which assumes free rolling tyre; but Eq [2.4] is more generally useful.

Regarding which radius to use, it should rather be R_l than R_0, because R_l represents the lever for the longitudinal tyre force around the wheel hub.

A free body diagram of the forces on the wheel can be used to explain the rolling resistance. Consider Figure 2-10 which represents a free rolling wheel under steady state conditions. The inertia of the wheel is neglected.

The main explanation model of rolling resistance for pneumatic tyres on hard flat surfaces is that the pressure distribution is biased towards the edge towards which the wheel is rolling. Damping and friction, see Figure 2-10, is the main reason for this and it is not dependent on the longitudinal force. Same figure also shows the off-centre effect, which is directly influenced by the longitudinal force. The force offset, e, explains f_r. Additional to what is shown in Figure 2-10 one can motivate even higher e, by including other effects, such as wheel bearing loss, brake disk drag and aerodynamic torque loss.

Longitudinal and vertical force equilibria are already satisfied, due to assumptions above. However, moment equilibrium around wheel hub requires:

$$T - F_x \cdot R_l - F_z \cdot e = 0 \implies F_x = \frac{T}{R_l} - F_z \cdot \frac{e}{R_l}; \qquad [2.5]$$

This result suggests that the force F_x, which pushes the vehicle body forward, is the term T/R_l (arising from the applied propulsion or brake torque T) minus the term $F_z \cdot e/R_l$. The term can be seen as a force F_{roll} and referred to as the rolling resistance force. The dimensionless ratio e/R expression is the rolling resistance coefficient, f_r:

$$f_r = \frac{e}{R_l}; \qquad [2.6]$$

Eq [2.6] is a definition of rolling resistance coefficient based assumed physical mechanisms internally in the tyre with road contact. Rolling resistance coefficient can also be defined based on quantities which are measurable externally, see Eq [2.4]. Sometimes one see $f_r = - F_x/F_z$ as a definition, but that is not suitable since it assumes absence of torque.

It is important to refer to this phenomenon as rolling **resistance** as opposed to rolling **friction**. It is not friction in the basic sense of friction, because $F_x \neq -f_r \cdot F_z$ except for the special case when un-driven wheel ($T = 0$). Figure 2-11 shows an un-driven and pure rolling.

Rolling resistance is a torque loss. Other torque losses, which can be included or not in tyre rolling resistance, are:

- losses associated with friction in gear meshes,
- drag losses from oil in the transmission,
- wheel bearing (and bearing sealings) torque losses, and
- drag losses from aerodynamic around the wheel.

These should, as rolling resistance, be subtracted from propulsion/brake torque when calculating T in Figure 2-11. However, sometimes they are included as part of the tyres rolling resistance coefficient, which is somewhat misleading even if it works if done correctly. The wheel bearing torque loss have

two torque terms: one is proportional to vertical load on the wheel (adds typically 0.0003 to rolling resistance coefficient), and the other is of constant magnitude but counter-directed to rotation speed. The former term can be included in rolling resistance coefficient. The aerodynamic losses due to wheel rotation are special since they vary with wheel rotational speed, meaning that they (for constant vertical load) are relevant to include when studying the variation of rolling resistance coefficient with vehicle speed. A summarizing comment is that one has to be careful with where to include different torque losses, so that they are included once and only once.
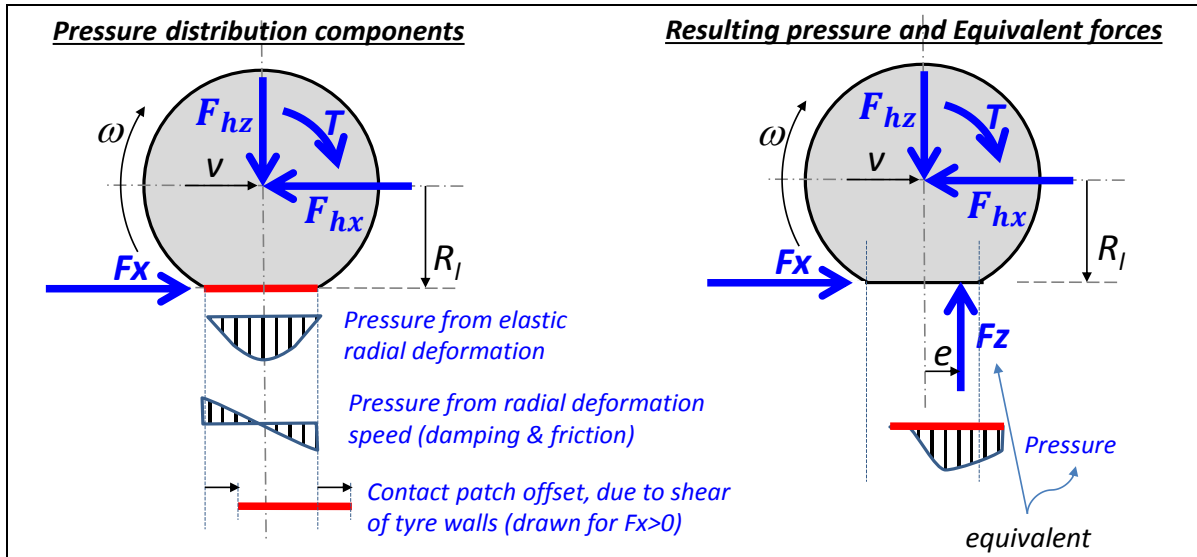
Figure 2-10: Normal force distribution on a tyre. The measure e is the force offset. In steady state, the forces in hub and contact patch are the same: $F_{hx} = F_x$ and $F_{hz} = F_z$.
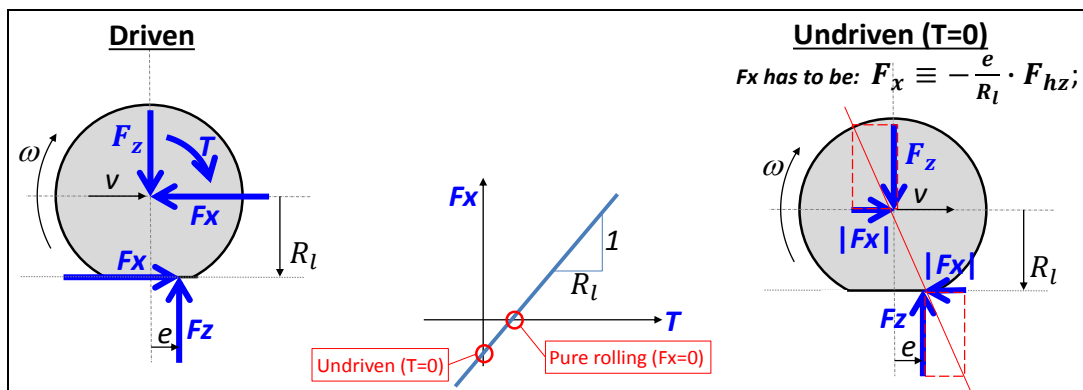
Figure 2-11: Driven wheel with rolling resistance, special cases "Un-driven" and "Pure rolling". Normally, the force in hub and contact patch are the same: $F_{hz} = F_z$.

One should note that torque losses as discussed above are not the only vehicle energy losses related to the tyres. There are also speed losses: speed losses in the tyre slip, both longitudinal and lateral. These cannot be modelled as rolling resistance.

2.4.2.1 Variation of rolling resistance

Several parameters will affect the rolling resistance of tyres. Design parameters:

- Tyre material. Natural rubber often gives lower rolling resistance.
- Radial tyres have more flexible sides, giving lower rolling resistance also bias ply have a greater crown angle causing more internal friction within the tyre during deflection.
- Geometry:
  - Diameter. Large wheels often have lower coefficient of rolling resistance
  - Width

- o Groove depth
- o Tread depth

Usage parameters, long term varying:

- Higher inflation pressure gives lower rolling resistance on hard ground but higher rolling resistance on soft ground (and vice versa), see Figure 2-12 and Figure 2-13.
- Wear. Worn tyres have lower rolling resistance than new ones (less rubber to deform).

Usage parameters, short term varying:

- Tyre loads (traction, braking and lateral forces)
- Speed. Rolling resistance increases with vehicle speed due to rubber hysteresis and air drag.
- High temperatures give low rolling resistance. Tyres need to roll approximately 30 km before the rolling resistance drop to their lowest values.
- Road/ground material. Asphalt, gravel, snow, etc.

2.4.2.1.1 Variation of tyre type

Trucks tyres have a much lower rolling resistance coefficient than passenger vehicle tyres, approximately half or less. Tyres have developed in that way for trucks, because their fuel economy is so critical.

2.4.2.1.2 Variation of speed

As an example, right part of Figure 2-12 shows the influence of tyre construction and speed on rolling resistance. The sudden increase in rolling resistance at high speed is important to note since this can lead to catastrophic failure in tyres. The source of this increase in rolling resistance is a high energy standing wave that forms at the trailing edge of the tyre/road contact.

There are some empirical relationships derived for the tyre's rolling resistance. It is advisable to refer to the tyre manufacturer's technical specifications when exact information is required. This type of information is usually very confidential and not readily available. Some general relationships have been developed, from (Wong, 2001):

Radial-ply passenger car tyres: $\quad f_r = 0.0136 + 0.04 \cdot 10^{-6} \cdot v^2$
Bias-ply passenger car tyres: $\quad f_r = 0.0169 + 0.19 \cdot 10^{-6} \cdot v^2$
Radial-ply truck tyres: $\quad f_r = 0.006 + 0.23 \cdot 10^{-6} \cdot v^2$
Bias-ply truck tyres: $\quad f_r = 0.007 + 0.45 \cdot 10^{-6} \cdot v^2$

As seen in Figure 2-12, a rule of thumb is that rolling resistance coefficient is constant up to around 100 km/h.

2.4.2.1.3 Variation of road surface

The road or ground can mainly vary in two ways: **rigidness** of road and **slipperiness** of road. It is not solely a question of the road, because such rigidness should be judge relative to tyre inflation pressure and such slipperiness should be judged relative to tyre tread pattern, including whether the tyre has spikes or not.

Left part of Figure 2-12 shows how widely the rolling resistance changes due to different road/ground material and inflation pressures. As can be expected, a range of values exist depending on the specific tyre and surface materials investigated. On hard ground, the rolling resistance decreases with increased inflation pressure, which is in-line with the explanation model used above, since higher pressure intuitively reduces the contact surface and hence reduces e. On soft ground the situation is reversed, which requires a slightly different explanation model, see Figure 2-13. On soft ground, the ground is deformed so that the wheel rolls in a "local uphill slope" with inclination angle φ. Intuitively, a higher inflation pressure will lead to more deformation of the ground, leading to a steeper φ.
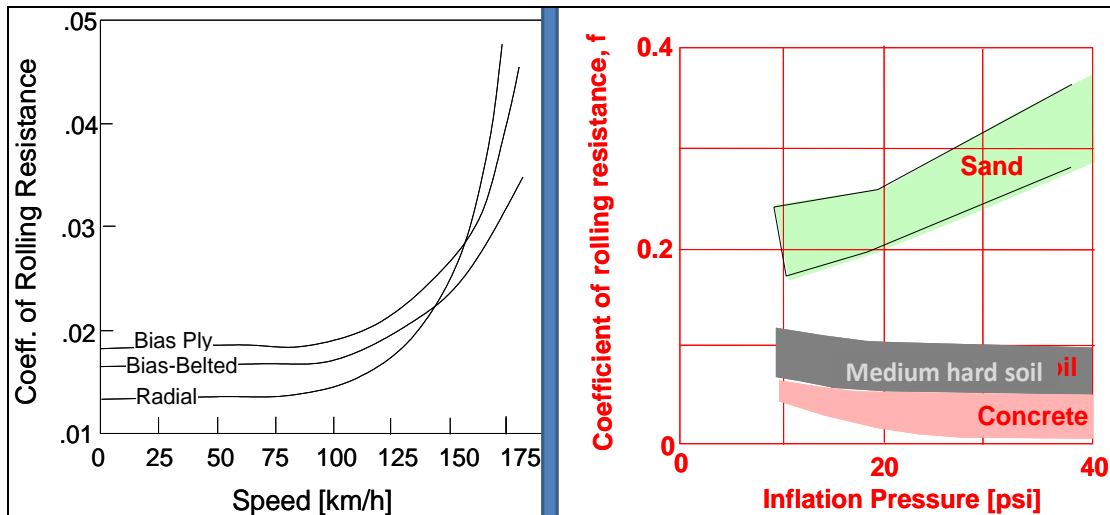
Figure 2-12 : Left: Rolling resistance coefficient variation with speed for different tyre types (Gillespie, 1992). Right: Range of Coefficient of Rolling Resistance for different road/ground material
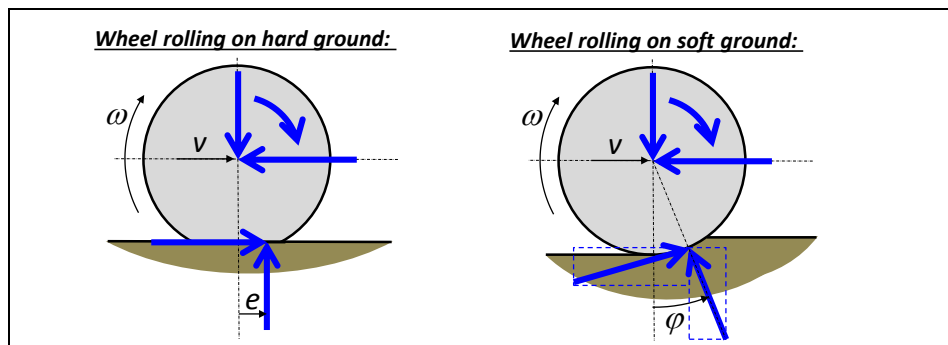
Figure 2-13 : Rolling resistance explanation model for hard and soft ground.

2.4.2.1.4 Variation of longitudinal force, propulsion and braking

There is also a dependency on longitudinal force, see Figure 2-14. RRC increases with positive force and decreases with negative force, due to that the shearing of the sidewall moves the contact forward or rearwards. The wheel radius also decreases with magnitude of force. For negative forces, these two effects have opposite influence, so the change is less for negative force, as seen in Figure 2-14.
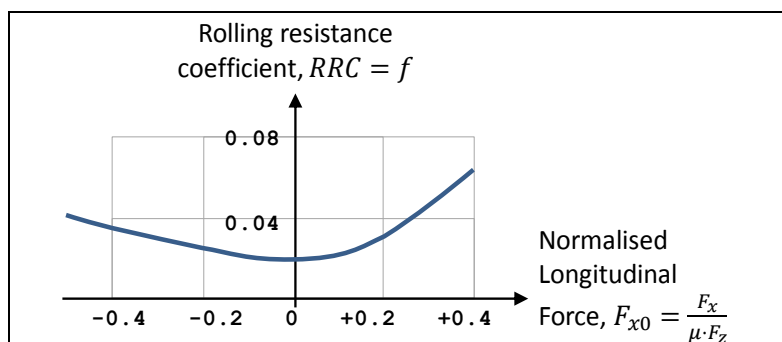
Figure 2-14 : Rolling resistance dependency of longitudinal tyre force. Inspired by (Wong, 2001)

2.4.3   Longitudinal force

The longitudinal force, F_x, between the tyre and ground influences the vehicle propulsion and braking performance. We can see it as a depending on the sliding between the tyre and the ground.

First, compare friction characteristics for a translating block of rubber with a rolling wheel of rubber. Figure 2-2 shows the basic differences between classical dry-friction, or Coulomb friction, of such sliding block and the basic performance of a rolling tyre. Experiments have shown that the relative speed between the tyre and the road produces a frictional force that has an initial linear region that builds to a peak value. After this peak is achieved, no further increase in the tangential (friction) force is possible. There is not always a peak value, which is shown by the dashed curve in the figure. The slope in the right diagram will be explained in Section 2.4.3.1, using the so called "tyre brush model".

Sliding block (or wheel with ω=0)

Rolling wheel of rubber

$(N = F_z)$

$\mu_{stat} \cdot N$ slide
$\mu_{dyn} \cdot N$
stick
$\Delta v = v$
slide

$\mu_{peak} \cdot N$
$\mu_{dyn} \cdot N$
slip=$\Delta v / v_{ref} = (R^* \omega - v_x)/v_{ref}$

- A *stick* mode where Δv=0.
- In *slide* mode, the friction force, F, is only depending on sign(Δv).

- No stick mode (if ω>0).
- The friction force, F, is depending on relative sliding speed, Δv/v_{ref}.
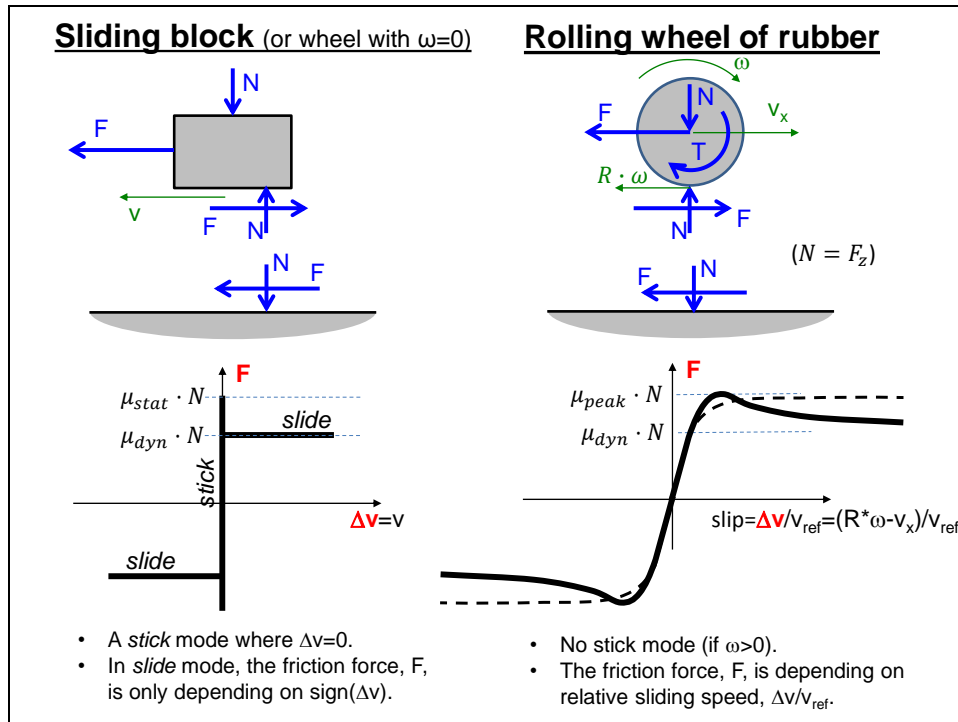
Figure 2-15: Friction characteristics

2.4.3.1   Tyre brush model for longitudinal slip

The brush model is frequently used to explain how tyre develop forces in ground plane, see e.g. References (Pacejka, 2005) and (Svendenius, 2007). The brush model is a physically based model that uses shear stress and dry friction at a local level, i.e. for each contact point in the contact patch. Figure 2-16 shows the starting point for understanding the brush model.

A first simple variant of the brush model, uses the following assumptions:

- o Sliding and shear stress only in **longitudinal** direction (as opposed to combined longitudinal and lateral)
- o Uniform and known **pressure distribution** over a constant an known contact length (as opposed to using a contact mechanics based approach, which can calculate pressure distribution and contact length.)
- o **Contact length** is known (as opposed to function of vertical force).
- o No difference between **static and dynamic** coefficient of friction
- o Only studying the **steady state conditions**, as opposed to including the transition between operating conditions. Steady state as opposed to stationary variations, which would arise for driving on undulated road.
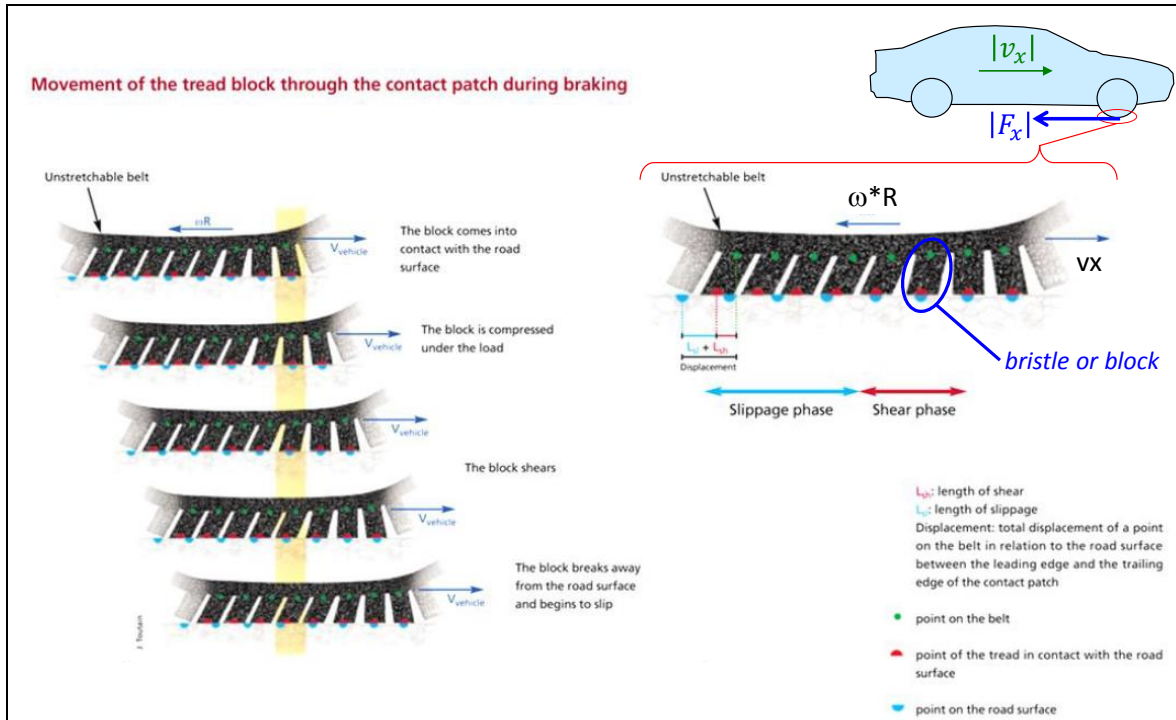
Figure 2-16: Tyre ground contact for braked tyre. Origin to the "Brush model". Picture from Michelin.

2.4.3.1.1 Uniform pressure distribution and known contact length

These assumptions lead to a model as drawn in Figure 2-17. The shear stress is the (tyre-) longitudinal stress in the brushes.

The rubber bristles (rubber elements) are fixed to the wheel and have friction contact to the ground. When going from Figure 2-17 to equations, we move from a view discretized in longitudinal and lateral dimension to a continuous view. So, e.g., forces $[N]$ becomes stress $[N/m^2]$. The shear stress of the element develops as in Hooke's law, see Equation [2.7].

$$\tau = G \cdot \gamma;$$

where $\tau = shear\ stress, G = shear\ modulus$
and $\gamma = shear\ deformation\ angle$;

[2.7]

When a rubber element enters the contact patch, it lands un-deformed, i.e. with $\gamma = 0$. The further into contact, along coordinate ξ, we follow the element, the more sheared will it become. Since the ground end of the element sticks to ground, the increase becomes proportional to the speed difference Δv and the time t it takes to reach the coordinate ξ:

$$\gamma = \frac{\Delta v \cdot t(\xi)}{H} = \frac{(R \cdot \omega - v_x) \cdot t(\xi)}{H};$$

where $t(\xi) = \xi/v_{Transport}$ and $v_{Transport} \approx |R \cdot \omega|$;

[2.8]

The velocity $v_{Transport}$ is the velocity of which the brush bristles are transported through the contact. Combining these equations yields the following, where the slip sx can be identified:

$$\tau = \frac{G}{H} \cdot \underbrace{\frac{R \cdot \omega - v_x}{|R \cdot \omega|}}_{s_x} \cdot \xi = \frac{G}{H} \cdot s_x \cdot \xi = \left\{ C_x = \frac{G \cdot W \cdot L^2}{2 \cdot H} \right\} = \frac{2 \cdot C_x}{W \cdot L^2} \cdot s_x \cdot \xi;$$

[2.9]
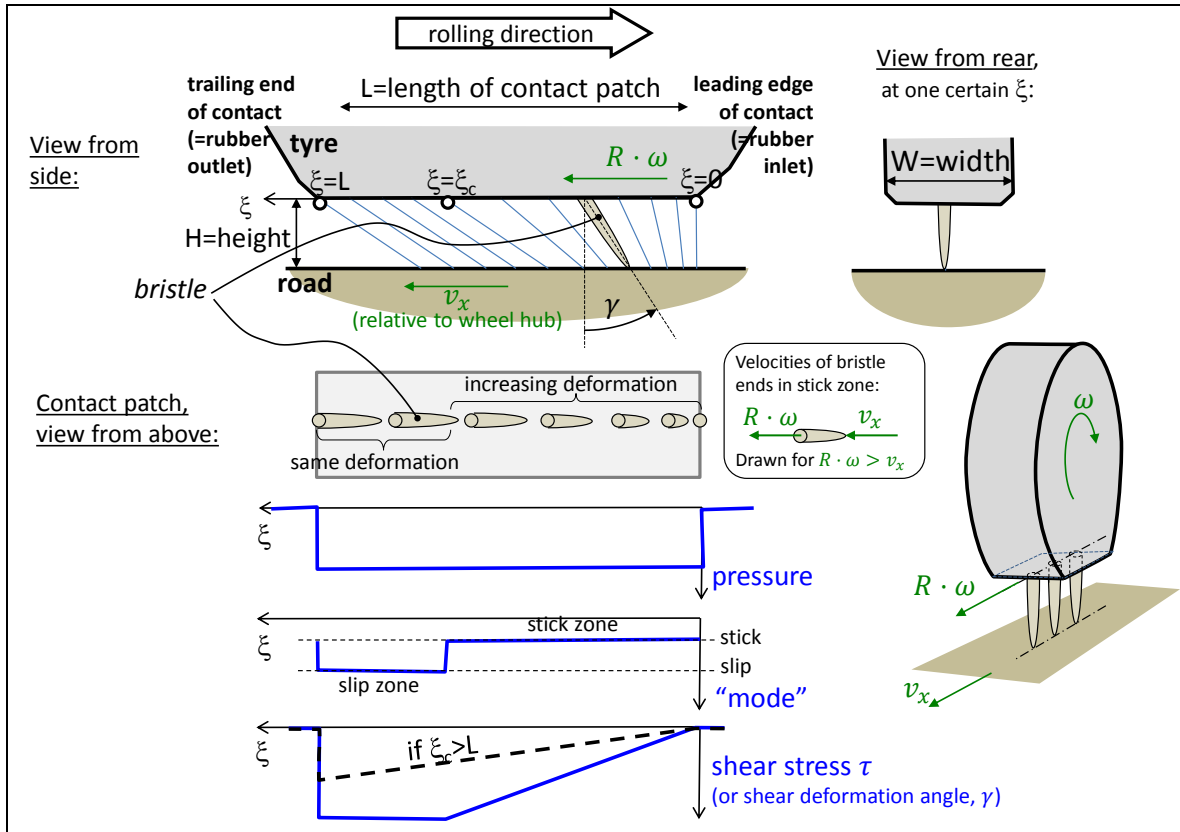
Figure 2-17: The physical model of simple brush model for longitudinal slip. Drawn for propelled tyre. The bristles are to be thought of as the rubber tread outside the belt, so they don't include elasticity in sidewall. Drawn for $R \cdot \omega > v_x$.

With this definition of slip, s_x, we automatically handle ω and v_x both positive and ω and v_x both negative. The case when ω and v_x have different signs will be handled below.

As long as friction limit is not reached ($|\tau| < \mu \cdot p$) within the whole contact, we can find the force as this integral:

$$F_x = W \cdot \int_0^L \tau \cdot d\xi = W \cdot \int_0^L \frac{2 \cdot C_x}{W \cdot L^2} \cdot s_x \cdot \xi \cdot d\xi = C_x \cdot s_x;$$

[2.10]

If friction limit is reached within the contact, i.e. at the break-away point $\xi = \xi_c$, we have to split the integral in two. The point ξ_c is defined by $\tau(\xi_c) = \frac{G}{H} \cdot s_x \cdot \xi_c = \frac{2 \cdot C_x}{W \cdot L^2} \cdot s_x \cdot \xi_c = \mu \cdot p; \Rightarrow \xi_c = \frac{\mu \cdot p \cdot W \cdot L^2}{2 \cdot C_x \cdot s_x} = \frac{\mu \cdot F_z \cdot L}{2 \cdot C_x \cdot s_x};$. For $\xi > \xi_c$, the rubber element will slide with a constant $\tau = \mu \cdot p$.

$$F_x = W \cdot \int_0^L \tau \cdot d\xi = W \cdot \int_0^{\xi_c} \frac{2 \cdot C_x}{W \cdot L^2} \cdot s_x \cdot \xi \cdot d\xi + W \cdot \int_{\xi_c}^L \mu \cdot p \cdot d\xi =$$

$$= \frac{2 \cdot C_x}{L^2} \cdot s_x \cdot \frac{\xi_c^2}{2} + \mu \cdot p \cdot W \cdot (L - \xi_c) = \left\{ p = \frac{F_z}{W \cdot L}; \quad and \quad \xi_c = \frac{\mu \cdot F_z \cdot L}{2 \cdot C_x \cdot s_x}; \right\} =$$

$$= \mu \cdot F_z \cdot \left(1 - \frac{\mu \cdot F_z}{4 \cdot C_x \cdot s_x} \right);$$

[2.11]

The case when ω and v_x have different signs leads to that $\xi_c = 0$;, since the bristles will deform in the opposite direction. So, the whole contact has $\tau = \mu \cdot p$, which leads to:

$$F_x = W \cdot \int_0^L \tau \cdot d\xi = W \cdot \int_0^L \mu \cdot p \cdot d\xi = W \cdot \mu \cdot p \cdot L = \{p \cdot W \cdot L = F_z\} = \mu \cdot F_z;$$ [2.12]

Hence, the total expression for F_x becomes as in [2.13], where a generalisation to cover also when ω and v_x have different signs ($\omega \cdot v_x < 0$) is done. We also add subscript x on G and H, to prepare for a corresponding model for lateral forces, in Section 2.5.

$$F_x = \begin{cases} = \text{sign}(s_x) \cdot \mu \cdot F_z & \text{if } \omega \cdot v_x < 0 \\ = C_x \cdot s_x; & \text{else if } |s_x| \leq \dfrac{\mu \cdot F_z}{2 \cdot C_x} \Leftrightarrow |F_x| \leq \dfrac{\mu \cdot F_z}{2} \\ = \text{sign}(s_x) \cdot \mu \cdot F_z \cdot \left(1 - \dfrac{\mu \cdot F_z}{4 \cdot C_x} \cdot \dfrac{1}{|s_x|}\right); & \text{else} \end{cases}$$

$$\text{where } C_x = \frac{G_x \cdot W \cdot L^2}{2 \cdot H_x}; \quad \text{dimension: } [force] \quad \text{and } s_x = \frac{R \cdot \omega - v_x}{|R \cdot \omega|};$$ [2.13]

The shape of this curve becomes as shown in Figure 2-19, the curves "Reference contact length" and "Constant contact length model". Variation of μ or F_z influence together, via $\mu \cdot F_z$.

The case when $\omega \cdot v_x < 0$ is unusual and can only occur when $|s_x| > 1$. An example is when vehicle moves rearward with $v_x = -1 \, m/s$, would be that the wheel spins forward, e.g. with $R \cdot \omega = 1 \, m/s$. Then $s_x = +2$ and $F_x = \mu \cdot F_z$. Also if increase to $R \cdot \omega = +\infty \, m/s$, we get same $F_x = \mu \cdot F_z$, but with $s_x = +\infty$. One can also note that there is another $R \cdot \omega$, for same v_x, which gives $s_x = +2$. This is $R \cdot \omega = -1/3 \, m/s$ and then $F_x = \mu \cdot F_z \cdot (1 - \mu \cdot F_z/(8 \cdot C_x))$, which is $< \mu \cdot F_z$. So, F_x is uniquely defined for any (ω, v_x), but F_x has double solutions for some s_x, when $|s_x| > 1$.

If we instead hold a certain forward vehicle speed, e.g. $v_x = 1 \, m/s$, and study how F_x varies with ω, we can identify three characteristic levels of ω:

- Full rearward traction: $R \cdot \omega = -\infty \, m/s$. This gives $s_x = -\infty$, with different signs on ω and v_x, and $F_x = -\mu \cdot F_z$;
- Locked wheel: $R \cdot \omega = 0 \, m/s$. This also gives $s_x = -\infty$ and $F_x = -\mu \cdot F_z$;
- Pure rolling wheel: $R \cdot \omega = 1 \, m/s$. This gives $s_x = 0$ and $F_x = 0$;
- Full forward traction: $R \cdot \omega = +\infty \, m/s$. This gives $s_x = +1$ and $F_x = \mu \cdot F_z \cdot (1 - \mu \cdot F_z/(4 \cdot C_x)) \approx \{typically\} \approx (0.95..0.98) \cdot \mu \cdot F_z$, which is $< \mu \cdot F_z$;

The first case is actually a relevant case (e.g. achievable with an electric motor braking, but not with friction brakes) where ω and v_x have different signs. The last case shows that we cannot reach $\mu \cdot F_z$ in the direction the vehicle moves, since there will always be a small part on the inlet side of the contact where the shear stress has not reached $\mu \cdot p$. In practice, we can see it as $\approx \mu \cdot F_z$, but when using the model mathematically, it can be good to note such small phenomena.

2.4.3.1.2 Influence of vertical load and friction in brush model

Eq [2.13] assumes that C_x does not change with F_z. Now, it is empirically found that C_x increases with F_z, almost proportional. The corresponding lateral slip stiffness C_y has a clear degressive tendency. See Figure 2-18.
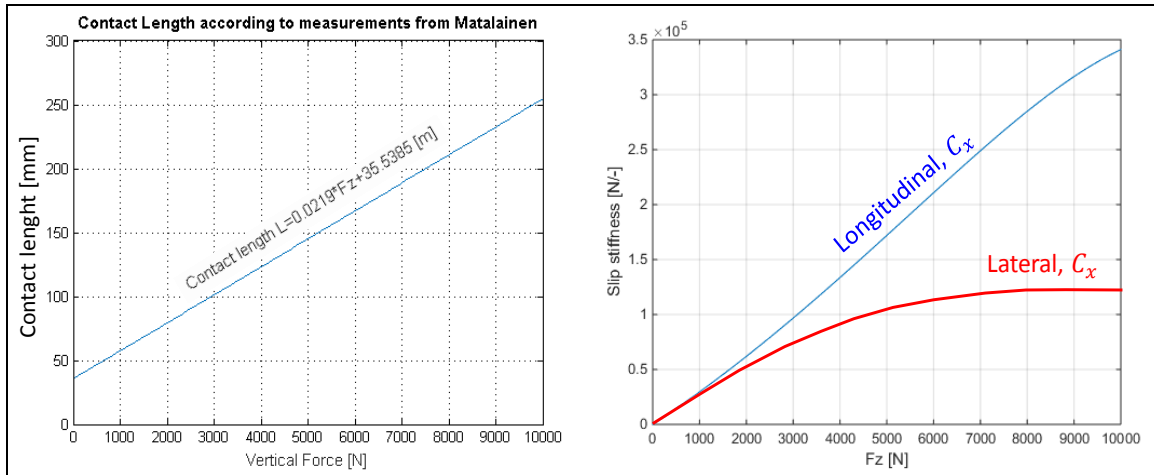
Figure 2-18: Measurements as function of vertical force. Left: Contact length. Right: Slip stiffnesses.

We will now try to explain why variation in F_z gives a variation in slip stiffness. The simplest model for lateral slip stiffness (Section 2.5.1.1) gives same formula as for longitudinal: $C = C_x = C_y = G \cdot W \cdot L^2/(2 \cdot H)$;. The reasoning will therefore be generic for longitudinal both lateral. The parameters G, W and H are reasonably constant for varying F_z, but not L. So, variation of the contact length L with F_z could explain why C varies. One measurement of how contact length vary is seen in Figure 2-18, but there are other which typically show a more degressive character. The contact length L will reasonably vary according to some deformation model. Four deformation models will be compared:

- Constant contact length
- $L \propto \sqrt[3]{F_z}$, which can be motivated by assuming Hertz's contact theory for **point** contact. This is implemented as $L^3 = F_z/k_R$, where k_R is a "material modulus per radius" with dimension $force/(area \cdot length)$. One can understand that length as a weighted average of wheel radius and radius of the tyre toroid.
- $L \propto \sqrt[2]{F_z}$, which can be motivated by assuming Hertz's contact theory for **line** contact. This is implemented as $L^2 = F_z/k$, where k is a material modulus with dimension force/area.
- $L \propto F_z$, which can be motivated by assuming that the tyre is a membrane with constant contact pressure p = inflation pressure p_i (like a balloon).

Note that we use Eq [2.13] which implicitly means that we keep assuming a pressure which is constant over the contact surface (but it varies with F_z). Using also the Hertz's theory elliptic pressure distribution over the contact surface would be more consistent, but we leave pressure distribution uniform until Section 2.4.3.1.3 since it gives the same conceptual influence of F_z. The different deformation models are plotted in Figure 2-19 using a constant value of tyre parameters, but varying F_z and μ.

Studying Figure 2-19, we find:

- Constant contact length model gives $C(F_z) = constant$;.
- Hertz point contact length model gives $\partial C/\partial F_z < 0$; (degressive).
- Hertz line contact length model gives $C(F_z) \propto F_z$; (proportional).
- Membrane contact length model gives $\partial C/\partial F_z > 0$; (progressive).

So, the measurements for $C_x(F_z)$ supports the Hertz line contact length model, while the measurements for $C_y(F_z)$ supports the Hertz point contact length model. The contact length model cannot be different, so the Hertz line contact length model is a credible if the model $C_y = G \cdot W \cdot L^2/(2 \cdot H)$; could be further developed to explain that $C_y(F_z)$ is degressive. In section 2.5.1.2 this is done by involving the compliance in sidewall (as opposed to compliance only in the tread itself).

Studying Figure 2-19, we find that increasing μ only increases the saturation level, while leaving the slope at lower s_x constant, or possibly slightly increased. Variation of F_z involves the contact length model. Hertz's line contact simply scales the curve in force direction, but the other models can motivate a slightly "degressive or progressive" scaling. Overall, it can be concluded that there are arguments for two conceptual ways the tyre characteristics changes, see Figure 2-20.

Figure 2-19: Shape of force/slip relation derived with brush model with uniform pressure distribution and different contact length model. Slope C_x is the longitudinal slip stiffness.
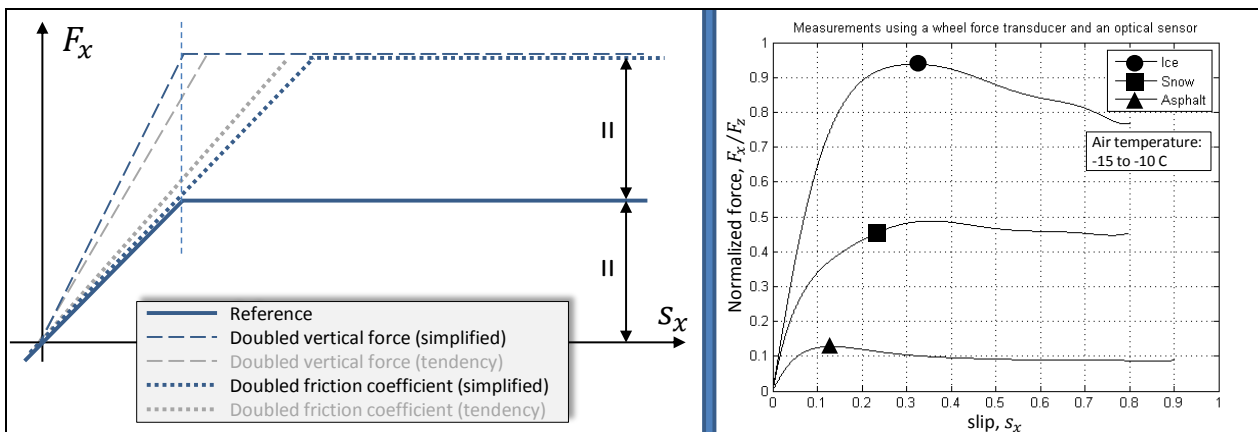
Figure 2-20: How tyre characteristics typically vary due to varying vertical force and road friction. Left: Theory. Right: Measurements with varying friction, i.e. varying surfaces, from PhD course by Ari Tuononen, Aalto university, Finland, Saariselkä, Finland 2014-03-15..22..

In practice, it is relatively straight forward to vary the vertical force. But varying the friction coefficient, for one certain tyre, cannot be done without changing the road surface. The local deformation and friction model in the brush models above, $\tau = G \cdot \gamma$; and $\tau = \mu \cdot p$;, are well motivated on hard and dry road, such as asphalt. When changing the road surface it is reasonable to add snow, water, ice, gravel, etc., which can motivate totally different local models, e.g. $\tau = function(R \cdot \omega - v_x)$, which might even lead to that $F_x = F_x(R \cdot \omega, v_x)$; instead of simply $F_x = F_x(s_x)$;.

2.4.3.1.3 Brush model with parabolic pressure distribution

Hertz's contact theory for line contact motivate an elliptical pressure distribution. A parabolic pressure distribution is an approximation of such elliptical and it gives an alternative brush model, as compared to the one appearing from uniform pressure. The coefficients in the parabolic pressure function have to be chosen such that $\int_0^L p(\xi) \cdot W \cdot d\xi = F_z$ and $p(0) = p(L) = 0$;:

$$p(\xi) = \frac{6 \cdot F_z}{W \cdot L} \cdot \frac{\xi}{L} \cdot \left(1 - \frac{\xi}{L}\right);$$

[2.14]

If we do the corresponding derivation as for the uniform pressure distribution, e.g. assuming a stick and slip zones, the location of where slip starts, ξ_c, becomes:

$$\tau(\xi_c) = (G/H) \cdot s_x \cdot \xi_c = \mu \cdot p(\xi_c) = \mu \cdot \frac{6 \cdot F_z}{W \cdot L} \frac{\xi_c}{L} \cdot \left(1 - \frac{\xi_c}{L}\right); \Rightarrow \xi_c = L - \frac{G \cdot W \cdot L^3 \cdot s_x}{6 \cdot \mu \cdot H \cdot F_z};$$

The slip where ξ_c appears outside $0 < \xi_c < L$ is when ξ_c becomes < 0, which is when the whole contact slips:

$$\xi_c = L - \frac{G \cdot W \cdot L^3 \cdot s_x}{6 \cdot \mu \cdot H \cdot F_z} < 0; \Rightarrow s_x > 3 \cdot \mu \cdot F_z \cdot \frac{2 \cdot H}{G \cdot W \cdot L^2};$$

Total shear force, F_x, becomes:

$$F_x = \begin{cases} = \text{sign}(s_x) \cdot \mu \cdot F_z & \text{if } \omega \cdot v_x < 0 \\ = \text{sign}(s_x) \cdot \left(C_x \cdot |s_x| - \frac{(C_x \cdot |s_x|)^2}{3 \cdot \mu \cdot F_z} + \frac{(C_x \cdot |s_x|)^3}{27 \cdot (\mu \cdot F_z)^2}\right); & \text{else if } |s_x| < \frac{3 \cdot \mu \cdot F_z}{C_x} \Leftrightarrow \\ & \Leftrightarrow |F_x| \leq \mu \cdot F_z \\ = \text{sign}(s_x) \cdot \mu \cdot F_z; & \text{else} \end{cases}$$

$$\text{where } C_x = \frac{G \cdot W \cdot L^2}{2 \cdot H}; \quad \text{dimension: } [force] \quad \text{and } s_x = \frac{R \cdot \omega - v_x}{|R \cdot \omega|};$$

[2.15]

The shape of this curve becomes as shown in Figure 2-21. The uniform pressure distribution model is drawn as reference. Note that the parabolic pressure distribution does not give any linear part, but the derivative at $s_x = 0$ is same, $C_x = G \cdot W \cdot L^2/(2 \cdot H)$.

2.4.3.1.4 Longitudinal tyre (slip) stiffness

In summary for many models (and tests!) the following is a good approximation for small longitudinal slip, and certain normal load and certain friction coefficient:

$$F_x = C_x \cdot s_x$$

[2.16]

For the brush model, or any other model which describes $F_x(s_x, F_z, \mu, \dots)$, one can define the "Longitudinal tyre (slip) stiffness" C_x, which have the unit $N = N/1 = N/((m/s)/(m/s))$. It is the derivative of force with respect to slip. In many cases one means the derivative at sx=0:

$$C_x = \left(\frac{\partial}{\partial s_x} F_x\right)\bigg|_{s_x=0}$$

[2.17]

Note that C_x is not a stiffness in the conventional sense, force/deformation. The tyre also have such a conventional stiffness, defined by force and deformation of a not rotating wheel. Often, it is obvious which stiffness is relevant, but to be unambiguous one can use the wording: "slip stiffness [N/1]" and "deformation stiffness [N/m]".

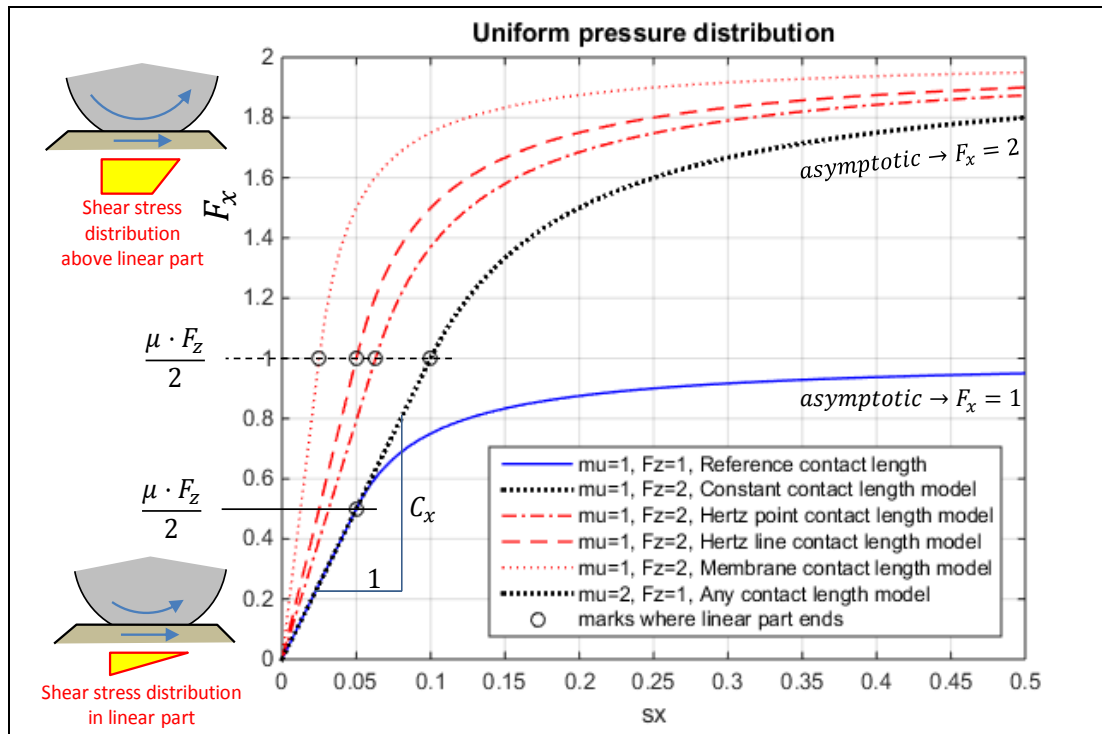*Figure 2-21: Shape of force/slip relation derived with brush model with parabolic pressure distribution and different contact length models.*
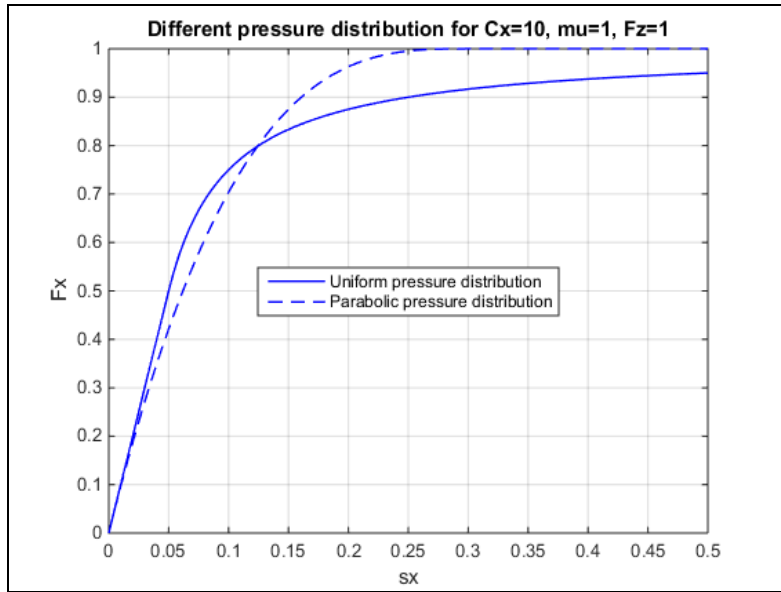
With the brush models with both pressure distributions, Eq [2.13] and Eq [2.15], we get the $C_x = G \cdot W \cdot L^2/(2 \cdot H)$. With $G = 0.5 \ [M \ N/m^2]$; (typical shear modulus in rubber), $W = L = 0.1..0.12 \ [m]$; (typical sizes of contact patch for passenger car) and $H = 0.01 \ [m]$; (approximate tyre tread depth) one gets $25[kN] < C_x = G \cdot W \cdot L^2/(2 \cdot H) <\approx 40[kN]$; which is an interval that contains typically measured stiffnesses for passenger car tyres. This indicates that the brush model models the essential physical phenomena and that the sheared part (the bristles) is rather only the tread than the whole elastic part sidewall and tread together.

The vertical load on the tyre affects the force generation, F_x. An approximation is that F_x is proportional to F_z. Then, one can define the Cornering Coefficient, CC_x:

$$F_x \propto F_z; \ \Rightarrow \ C_x \approx \frac{F_x}{s_x} \propto F_z \ \Rightarrow \ C_x = CC_x \cdot F_z; \ \Rightarrow \ CC_x = \frac{C_x}{F_z}; \qquad \boxed{[2.18]}$$

With the brush models with both uniform pressure distribution we can connect F_z and sizes of contact patch with $F_z = p \cdot W \cdot L$. Assuming approximately same contact pressure as inflation pressure, $p = p_{infl}$, we can express $C_x = G \cdot W \cdot L^2/(2 \cdot H) = G \cdot F_z \cdot L/(2 \cdot p_{infl} \cdot H)$. This gives $CC_x = G \cdot L/(2 \cdot p_{infl} \cdot H)$. With similar values as above, and typical passenger car tyre pressure $p_{infl} = 3 \cdot 10^5 \ [N/m^2]$, we get $CC_x \approx 10$. With typical truck tyre pressure $p_{infl} = 9 \cdot 10^5 \ [N/m^2]$, and slightly larger L and H, we get $CC_x \approx 5$. These are both in the same magnitude and relative relation as one can measure, see Section 1.8.

2.4.3.2 Empirical tyre models

The brush model is a physical model which explains the principles of how the forces are developed. However, if a model is required which is numerically accurate to a certain tyre, one often uses a fitted curve instead of Equation [2.13]. To limit the number of parameters to fit, one often uses a mathematical curve approximation, using trigonometric and exponential formulas. These curve fit models, it can be applied to any type of data with similar characteristics and can thus be used to describe other loading behaviour of the tyre such as lateral stiffness and self-aligning torque.

2.4.3.2.1 Magic Formula Tyre Model

Probably the most well-known curve fit is called "Magic Formula" and it was proposed in (Bakker, 1987). This approach uses trigonometric functions to curve fit the experimental data. The curve fit has the general form:

$$Force = y(x) = D \cdot \sin\left(C \cdot \arctan\left(B \cdot x - E \cdot (B \cdot x - \arctan(B \cdot x))\right)\right);$$

$$Y(x) = y(x) + S_V;$$

$$Slip = x = X + S_H;$$

[2.19]

Where B is a stiffness parameter, C is a shape parameter, D is a peak value parameter, and E is a curvature parameter describing the curve. The variable x is the tyre slip value. The parameters S_V and S_H simply shifts the curve so that it passes through the origin, which might not be the case for measurement data, since there can be errors in tyre radius and correction for rolling resistance. The relationship between these parameter and the tyre slip/friction relation is shown in Figure 2-22.
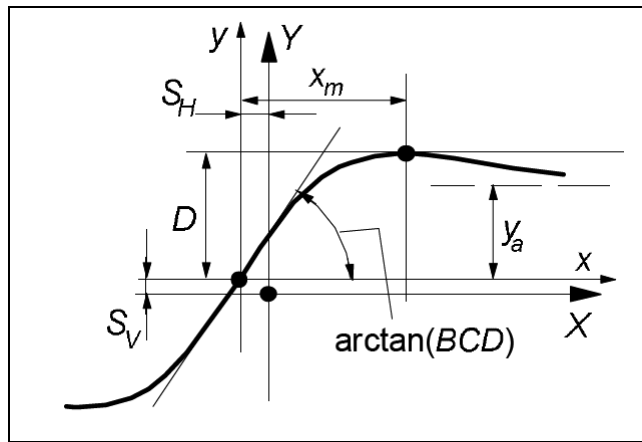
Figure 2-22: Magic Formula Tyre Parameters, (Pacejka, 2005)

2.4.3.2.2 TMsimple and TMeasy Tyre Models

TMsimple and TMeasy are two other curve fit models. TMsimple is shown in Eq [2.20] (without influence of vertical force) and both are shown in Figure 2-23. TMsimple is a simplified variant of TMeasy. For example, in TMsimple, it is not possible to set the maximum force value to a specific slip. Also, torques on the tyre are not described within TMsimple, just the tyre forces. TMeasy is described in Ref (Hirschberg, et al., 2007).

$$F(s) = F_{max} \cdot \sin\left(B \cdot \left(1 - e^{-|s|/A}\right) \cdot \text{sign}(s)\right);$$

$$where\ B = \pi - \arcsin(F_\infty/F_{max});\ and\ A = F_{max} \cdot B/\arctan(C);$$

$$with\ F_{max}, F_\infty\ and\ C\ as\ in\ Eq\ [2.23]$$

[2.20]

2.4.3.2.3 More advanced models

There are numerous of tyre models. Swift and FTire are example on more advanced models with a mixture of physical and curve fit parameters. FTire is almost a finite element model and demands very many parameters.

2.4.3.2.4 Very simple Tyre Models

There are many more models with different degree of curve fitting to experimental data. However, one can often have use for very simple curve fits, such as:

- Linearized: $F_x = C_x \cdot s_x$
- Linearized and saturated: $F_x = sign(s_x) \cdot min(C_x \cdot |s_x|; \mu \cdot F_z)$
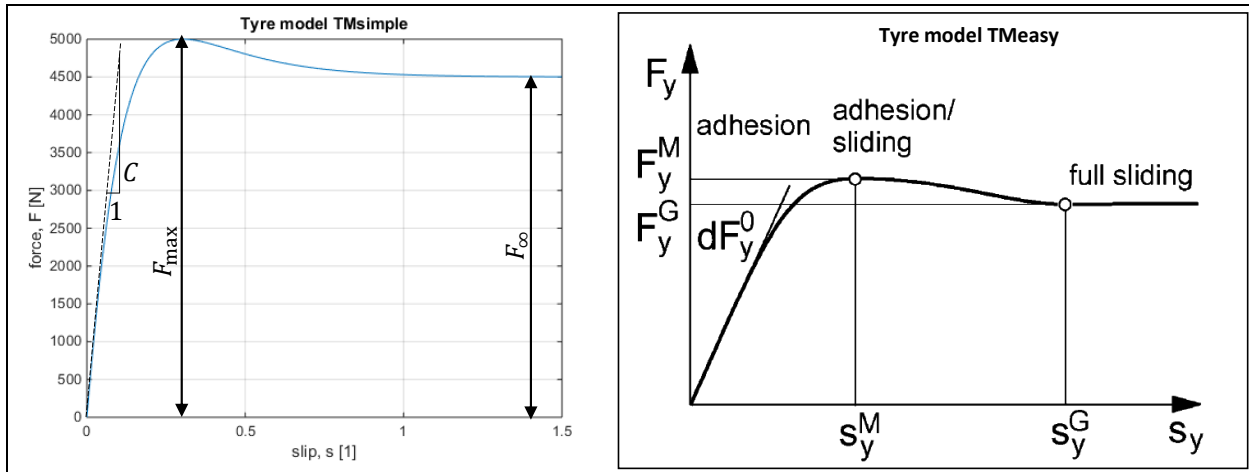
Figure 2-23: Left: TMsimple (Lex, 2015). Right: TM-Easy Tyre Model, (Hirschberg, et al., 2007).

2.4.3.3   Tyre with both rolling resistance and slip

So far, the models in Section 2.4.3 has not included rolling resistance. As we regard rolling resistance as a torque, not a force, it does not affect the $F_x(s_x)$ curve. But the rolling resistance does move the $T(s_x)$ curve vertical. The curve moves upwards if the wheel is rolling forward and downwards if rolling rearwards, see Figure 2-24. The $F_x(s_x)$ curve is normally the suitable view for vehicle level studies, while the $T(s_x)$ curve is sometimes needed for involving a model of the propulsion and brake systems. As mentioned in Section 2.4.1, one can select R in slip definition so that the $F_x = 0$ for $s_x = 0$, as shown in Figure 2-24. This compendium claims this is the most appropriate if one does not know R. As also mentioned in Section 2.4.1, one can alternatively select R in slip definition so that the $T = 0$ for $s_x = 0$. This compendium claims that it is less appropriate and that using $T = F_x(s_x) \cdot R_l + sign(\omega) \cdot \frac{f}{R} \cdot F_z$ is better.
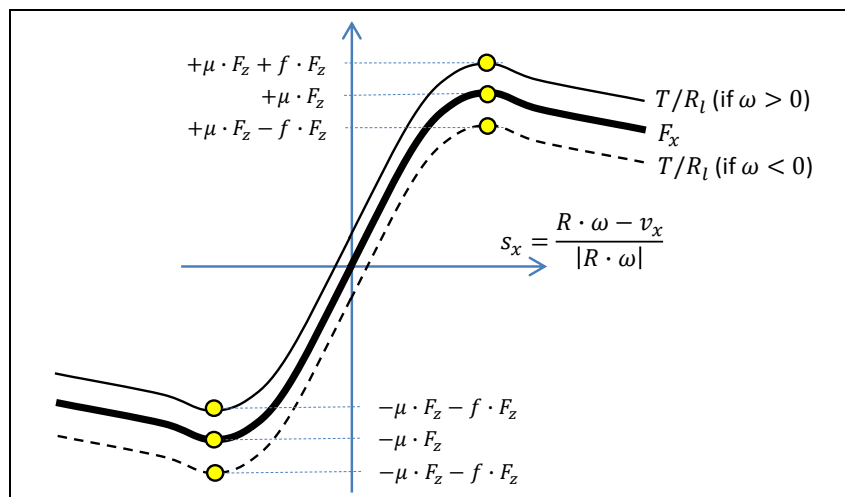
Figure 2-24: Longitudinal tyre force (F_x) and normalized wheel torque (T/R_l) including both rolling resistance and slip. Slip defined so that curve $F_x(s_x)$ passes through diagram origin, which means that $T(s_x)/R_l$ does not.

2.4.3.4   Transients

Both the physical and empirical tyre models discussed above are based on the assumption of steady state condition in the contact patch, meaning steady state deformation pattern and steady state sliding speed distribution. Transients between different steady state conditions take some time and this

process is referred to as relaxation. Often in Vehicle Dynamics, the relaxation is such a quick process that it can be assumed to take place instantaneously, i.e. the $F_x(s_x)$ curve can be used as an algebraic relation. But sometimes it is relevant to model the nature of the transient more carefully. Transients are triggered by variations; variations in slip (v_x and/or ω), vertical force (F_z) and surface conditions (e.g. expressed in varying μ).

Note that also start from stand-still and deceleration to stand-still are examples of strong transients in slip, even if vehicle acceleration/deceleration is small. This is mathematically manifested by that slip goes towards infinity when wheel rotational speed approaches zero. Modelling transients often solve both normal transients in slip, vertical force and surface conditions as well as driving situations involving/close to stand-still.

The physical phenomena to be modelled is elasticity; in tyre sidewalls and/or in contact patch.

2.4.3.4.1 Transients modelled as due to Elasticity of Sidewalls

Figure 2-25 shows a physical model which can model how the force change is delayed during quick changes in slip. The model can also handle vehicle stand-still. This type of model is often called a *rigid ring tyre model*, because the belt is modelled as a rigid ring. The ring is here massless, but can assumed to have mass and rotational inertia. The longitudinal and vertical support are here rigid, but they can be modelled as compliant. If no significant inertia in wheel hub, the driveshaft compliance will be series coupled with the rotational compliance, c_{sw}. The torque T_{rim} is the sum of torque from propulsion system and brake system. Damper elements can be added beside the compliances.
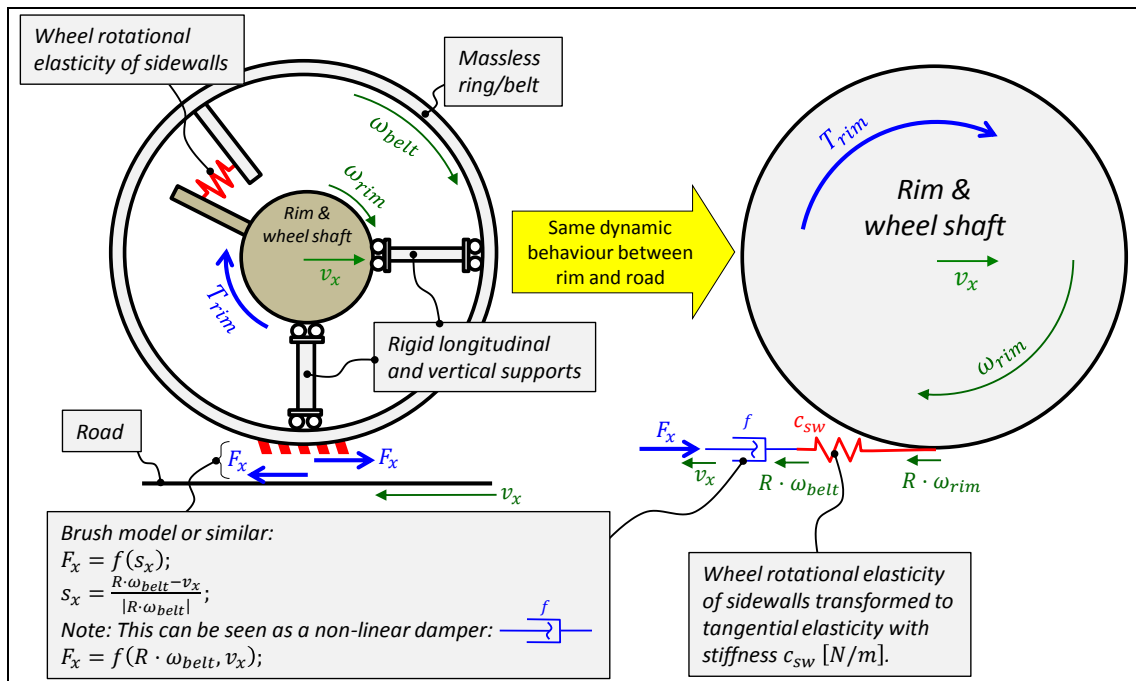
Figure 2-25: Tyre model including the rotational elasticity of tyre sidewalls.

The mathematical model becomes as follows, where f_{SS} denotes a steady state tyre model, e.g. from Section 2.4.3.1 or 2.4.3.2:

$$\dot{F}_x = c_{sw} \cdot (R \cdot \omega_{rim} - R \cdot \omega_{belt});$$

$$F_x = f_{SS}(s_x, F_z, \mu, \dots); \quad where \quad s_x = \frac{R \cdot \omega_{belt} - v_x}{|R \cdot \omega_{belt}|};$$

[2.21]

Damping in parallel with the elasticity is often motivated also:

$$F_x = F_{xs} + F_{xd};$$

$$\dot{F}_{xs} = c_{sw} \cdot (R \cdot \omega_{rim} - R \cdot \omega_{belt});$$

$$F_{xd} = d_{sw} \cdot (R \cdot \omega_{rim} - R \cdot \omega_{belt});$$

$$F_x = f_{SS}(s_x, F_z, \mu, \dots); \quad where \quad s_x = \frac{R \cdot \omega_{belt} - v_x}{|R \cdot \omega_{belt}|};$$

[2.22]

If used in a system where ω_{rim} and v_x are input variables to tyre, the force F_x will become a state variable. It is then not a problem that slip is undefined for $\omega = 0$, because the explicit form of equations will become as follows. Note that we simplify by only considering the case when $\omega_{belt} \cdot v_x > 0$. And the model validity is limited to $F_x, F_z, \mu, \dots$ such that uniquely defines s_x.

$$s_x \leftarrow g_{SS}(F_x, F_z, \mu, \dots);$$

$$\omega_{belt} \leftarrow \frac{v_x}{R \cdot (1 - s_x \cdot \text{sign}(v_x))}; \quad (only\ valid\ for\ \omega_{belt} \cdot v_x > 0)$$

$$\dot{F}_x \leftarrow c_{sw} \cdot (R \cdot \omega_{rim} - R \cdot \omega_{belt});$$

$$where\ g_{SS}\ is\ the\ inverse\ of\ function\ f_{SS}\ such\ that\ s_x = g_{SS}(F_x, F_z, \mu);$$

[2.23]

With $f_{SS} = C_x \cdot s_x$;, and $\omega_{rim} > 0$; and $v_x > 0$;, we can simplify Eq [2.23] to Eq [2.24]:

$$\dot{F}_x = c_{sw} \cdot R \cdot \omega_{rim} - \frac{c_{sw} \cdot v_x}{1 - \frac{F_x}{C_x}}; \quad \Rightarrow \left\{ s_x = \frac{F_x}{C_x}\ is\ small \right\} \Rightarrow$$

$$\Rightarrow \dot{F}_x \approx c_{sw} \cdot R \cdot \omega_{rim} - c_{sw} \cdot v_x;$$

[2.24]

Eq [2.23] means that we read the function f_{SS} from force F_x to slip s_x. When knowing slip, we can calculate the rotational speed ω_{belt}. Then, the state derivative $\dot{F}_x$ can be calculated, so that the state F_x can be updated in each time step.

With any reasonable tyre function f_{SS}, there is a maximum magnitude of force, $|F_x| = \mu \cdot F_z$, above which there is no slip s_x that gives that F_x. In most problems, one never ends up there in the simulations, since when approaching $|F_x| = \mu \cdot F_z$, the velocity ω_{belt} changes quickly in the direction that makes $|F_x|$ stays $< \mu \cdot F_z$. But, due to numerical errors in solutions, or if $\mu \cdot F_z$ decreases stepwise, one might end up there anyway for short time periods. In that case, it often gives physically acceptable solutions on vehicle level, to simply saturate s_x so that $|F_x|$ is saturated at a certain level, e.g. $0.95 \cdot \mu \cdot F_z$. For the brush model with uniform pressure distribution, Eq [2.13], the inverted function g becomes as follows, including such saturation:

$$s_x = g(F_x, F_z, \mu) = \begin{cases} = \dfrac{F_x}{C_x}; & for\ |F_x| \leq \dfrac{\mu \cdot F_z}{2}; \\[2ex] = \dfrac{\mu \cdot F_z}{4 \cdot C_x} \cdot \dfrac{\text{sign}(F_x)}{1 - \dfrac{|F_x|}{\mu \cdot F_z}}; & for\ |F_x| < 0.95 \cdot \mu \cdot F_z; \\[2ex] = \dfrac{\mu \cdot F_z}{4 \cdot C_x} \cdot \dfrac{\text{sign}(F_x)}{1 - 0.95}; & else \end{cases}$$

$$where\ C_x = \frac{G \cdot W \cdot L^2}{2 \cdot H}; \quad dimension: [force]$$

[2.25]

2.4.3.4.2 Transients modelled as due to Relaxation in Contact patch

The elasticity in the side walls, modelled in Section 2.4.3.4.1, explains delay; e.g. when changing ω_{rim} stepwise, the force F_x will not follow f_{SS} directly, but with a delay. Another phenomena that causes delay is that the bristles in the contact patch needs to adopt to a new deformation pattern and sliding speed distribution. Following the brush model, the physically correct way would be to formulate the equations as a partial differential equation (*PDE*), with derivatives with respect to both time and position along the contact patch, ξ. A "quasi-physical" way to model this is to apply a 1st order time delay of force:

$$\dot{F}_x = (1/\tau) \cdot (f_{SS}(s_x, F_z, \mu, \dots) - F_x);$$

where $f_{SS}(s_x, F_z, \mu, \dots)$ is the force according to a steady state model, e.g.Eq [2.13] and the time delay, $\tau = \frac{L_r}{v_{Transport}} = \frac{L_r}{|R \cdot \omega_{rim}|}$ and L_r is the relaxation length, which often is given as a fraction ($\approx 25..50\%$) of tyre circumference.

[2.26]

Alternatively, one can also express the delay as a 1st order time delay of the slip, as follows:

$$F_x = f_{SS}(s_{x,delayed}, F_z, \mu, \dots);$$

$$\dot{s}_{x,delayed} = (1/\tau) \cdot (s_x - s_{x,delayed});$$

where $f_{SS}(s_{x,delayed}, F_z, \mu, \dots)$ is the force according to a steady state model, e.g. Eq [2.13] and τ is as defined in Eq [2.26].

[2.27]

To delay force (Eq [2.26]) is more physical than delaying the slip (Eq [2.27]), since the nature of the delay is motivated by elasticity and delay in an elasticity is modelled with *force* (or *deformation*) as state variable. The delay in slip rather proposes that *relative speed* as state variable, which is not physical in this context. However, the delayed force has the non-physical effect that F_x sometimes can become $> \mu \cdot F_z$ in cases when wheel is off-loaded quickly, i.e. when $\dot{F}_z$ is a large negative value. So, an extension to $F_x = \max(f_{SS}(s_{x,delayed}, F_z, \mu, \dots), \ \mu \cdot F_z)$; can be motivated.

It would make sense from physical point of view, if the relaxation length was approximately same magnitude as the contact length, or possibly the length of the sticking zone. However, commonly given size of relaxation length is 25..50% of tyre circumference, which is normally several times larger than the contact length. This can be because one measures delays due to sidewall elasticity also, but then interpreted as a relaxation length.

With $f_{SS} = C_x \cdot s_x$;, and $\omega_{rim} > 0$; and $v_x > 0$;, we can simplify Eq [2.26] to Eq [2.28]:

$$\dot{F}_x = \frac{C_x}{L_r} \cdot R \cdot \omega_{rim} - \frac{C_x}{L_r} \cdot v_x - \frac{R \cdot \omega_{rim}}{L_r} \cdot F_x; \quad \Rightarrow \left\{ s_x = \frac{F_x}{C_x} \text{ is small} \right\} \Rightarrow$$

$$\Rightarrow \dot{F}_x \approx \frac{C_x}{L_r} \cdot R \cdot \omega_{rim} - \frac{C_x}{L_r} \cdot v_x;$$

[2.28]

2.4.3.4.3 Relation between the two Transients models

The models in Section 2.4.3.4.1 and 2.4.3.4.2 describe two different phenomena which both are present in the real world. Since it is difficult to distinguish between the two delay-creating parameters, c_{sw} and C_x/L_r, one often model only one phenomena. But then, one adjust the numerical value of the used parameter so that the model captures about the same delay as a real-world test. If $c_{sw} = C_x/L_r$;, the two models coincide approximately.

This compendium does not give any recommendation of which of the two models is best.

2.5 Lateral Properties of Tyres

After a vehicle starts moving, controlling the direction of travel becomes a high priority for the operator. For wheeled vehicles, the primary mode to control travel direction is to change the orientation of the tyre, i.e. to apply a steering angle. Tyres generate a lateral force when they are oriented at an angle different to the direction of the vehicle motion. The tyre typically deforms as in Figure 2-26.
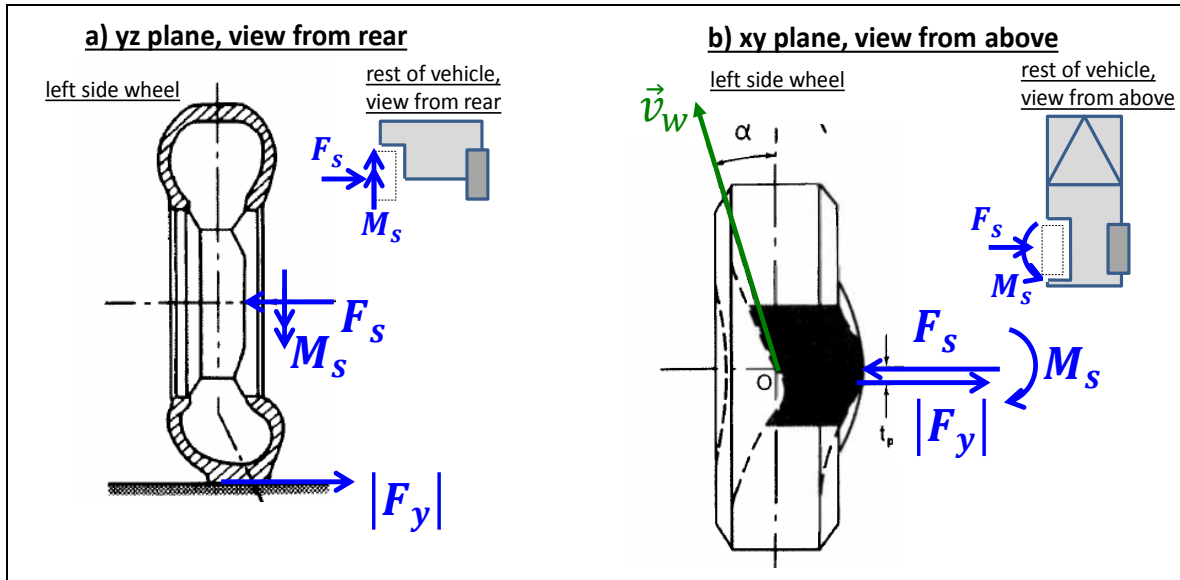
Figure 2-26: Deformation and forces of a Cornering Tyre, (Clark, 1971)

It is essential to distinguish between the steering angle and (lateral or side) slip angle of the tyre. Lower right part of Figure 1-11 shows this difference. The steering angle, δ or d, is the angle between vehicle longitudinal direction and tyre longitudinal direction. The tyre side slip angle, α is the angle between tyre longitudinal direction and the tyre translational velocity (=wheel hub velocity).

The relation between the lateral force of a tyre and the tyre side slip angle is typically as shown in Figure 2-30. The behaviour of the curve is similar to that exhibited for longitudinal forces Figure 2-22 and Figure 2-23. It becomes even more similar if lateral slip angle is replaced by lateral wheel slip, $tan(\alpha)$.

2.5.1 Tyre brush model for lateral slip

With corresponding simplification as in Section 2.4, we now use the brush model to also explain the lateral properties.

2.5.1.1 Model with independent bristles

Figure 2-27 shows the model for pure lateral slip and should be compared to Figure 2-17. The difference is that the model for lateral slip has the deformation of the bristles perpendicular to drawing in the upper left view in the figure.

Each bristle in Figure 2-27 is thought of as a part of the tread in series with a part of the sidewall. Further, the bristles are considered as independent of each other, which is debatable. However, it is enough for a quantitative explanation of the brush model for lateral slip. The derivation of model equations becomes similar as for the longitudinal model:

$$\tau_y = G_y \cdot \gamma_y = G_y \cdot \frac{\Delta v_y \cdot t(\xi)}{H_y} = G_y \cdot \frac{-v_y \cdot t(\xi)}{H_y} = \begin{cases} t(\xi) = \xi/v_{Transport}; \\ v_{Transport} \approx |R \cdot \omega|; \end{cases} =$$

$$= G_y \cdot \frac{-v_y \cdot \xi}{H_y \cdot |R \cdot \omega|} = -\frac{G_y}{H_y} \cdot \underbrace{\frac{v_y}{|R \cdot \omega|}}_{s_y} \cdot \xi = \left\{ C_y = \frac{G_y \cdot W \cdot L^2}{2 \cdot H_y} \right\} = -\frac{2 \cdot C_y}{W \cdot L^2} \cdot s_y \cdot \xi; \qquad \text{[2.29]}$$
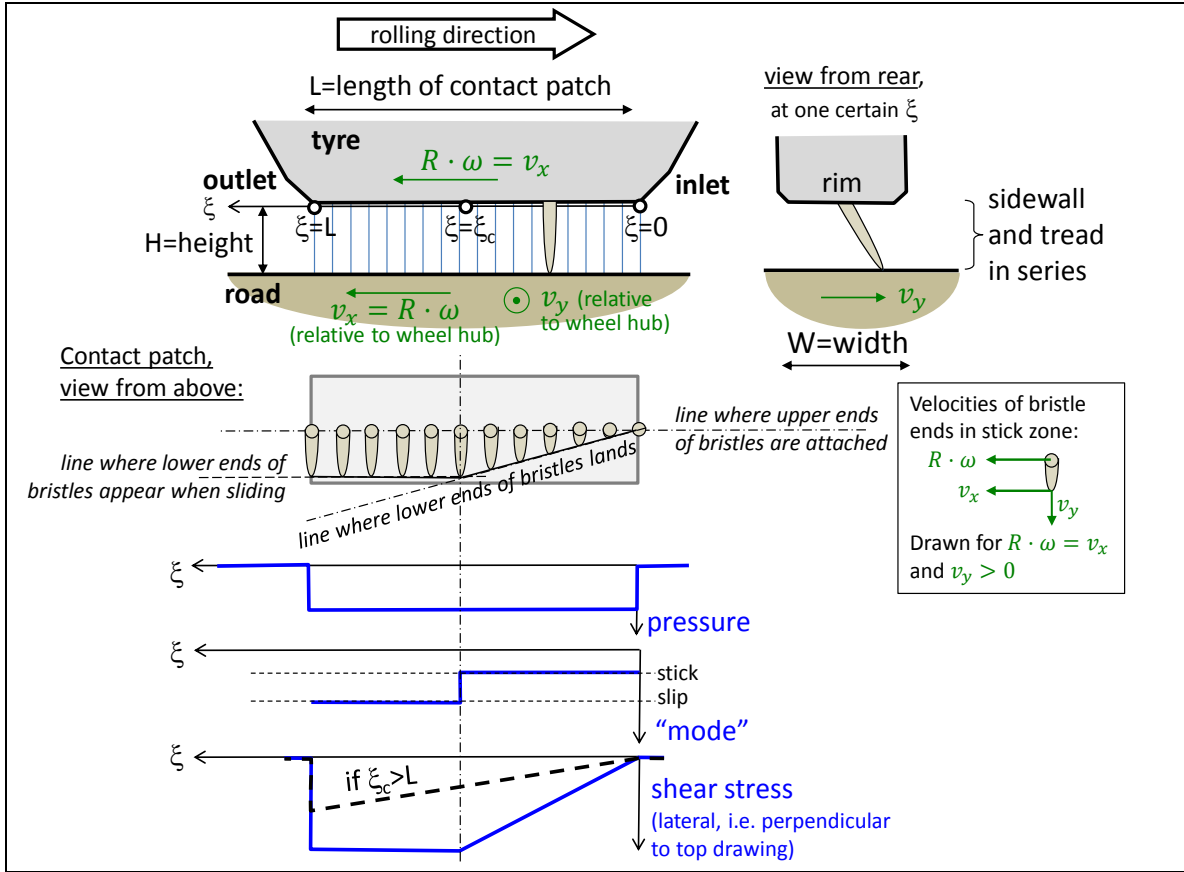
*Figure 2-27: The brush model's physical model for lateral slip. The bristles are to be thought of as the **tread in series with sidewall** lateral elasticity.*

The lateral tyre slip s_y is now defined as:

$$s_y = \frac{-v_y}{|R \cdot \omega|}; \qquad \text{[2.30]}$$

Note that subscript y has been introduced where we need to differ towards the longitudinal brush model. Correspondingly, subscript x should be used in longitudinal model. As for longitudinal model, we have to express the force differently for when friction limit is not reached within the contact and when it is reach at inlet and outlet.

$$F_y = \begin{cases} = -C_y \cdot s_y; & \text{if } |s_y| \leq \frac{\mu \cdot F_z}{2 \cdot C_y} \Leftrightarrow |F_y| \leq \frac{\mu \cdot F_z}{2} \\ = -\text{sign}(s_y) \cdot \mu \cdot F_z \cdot \left(1 - \frac{\mu \cdot F_z}{4 \cdot C_y} \cdot \frac{1}{|s_y|}\right); & \text{else} \end{cases}$$

$$\text{where } C_y = \frac{G_y \cdot W \cdot L^2}{2 \cdot H_y}; \quad \text{dimension: [force]} \quad \text{and } s_y = \frac{v_y}{|R \cdot \omega|};$$

(Only valid for pure lateral slip, i.e. pure longitudinal rolling: $v_x = R \cdot \omega$;)

[2.31]

2.5.1.2   Model with dependent bristles, String model

Opposed to the assumption in Section 2.5.1.1, the lateral deformation of the bristles are dependent on each other, especially since the tread is mounted on the belt and the belt is rather like a string. So, we assume a certain deformation of the sidewall, expressed in ε_{in} and ε_{out} for the belt="string" in Figure 2-28. This gives a slightly different model compared to Section 2.5.1.1. Models with such belt deformation are called "tyre string models". The shape of the string is dependent on the sidewall elasticity, e.g. tyre profile height, but also of the side force itself. So, the model is intrinsically implicit; the string shape influences the side force and the side force influences the string shape.
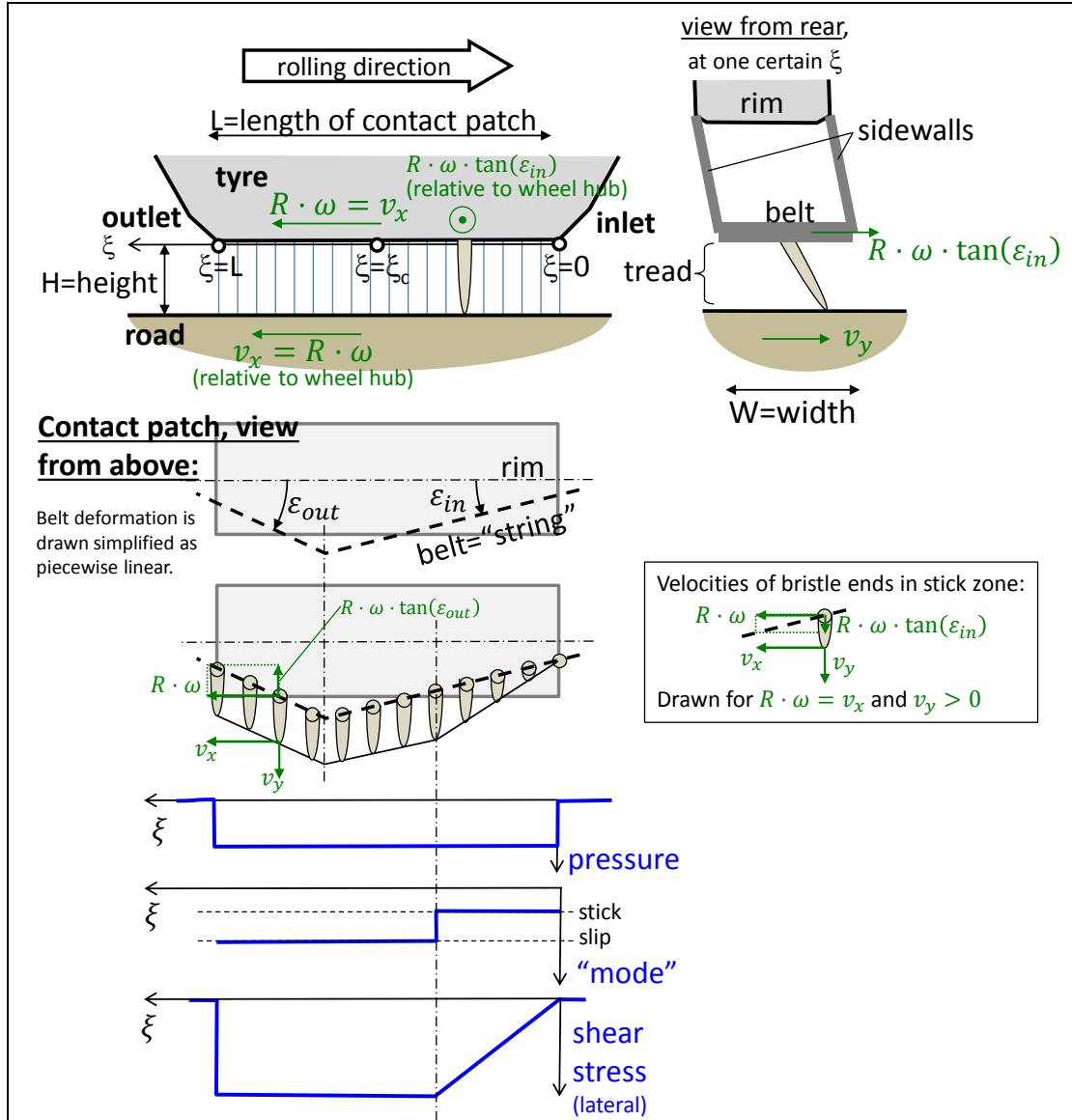
Figure 2-28: Tyre sidewall deformation and tread deformation with belt="string" in between. The drawn bristles are here assumed to represent only tread parts, while the sidewall is treated as an elastic structure between rim and belt="string".

The derivation of model equations becomes similar as for the longitudinal model. Here is an intermediate result, an expression for the shear stress τ_y:

$$\tau_y = G_{y,tr} \cdot \gamma_y = G_{y,tr} \cdot \frac{\Delta v_y \cdot t(\xi)}{H_{y,tr}} = G_{y,tr} \cdot \frac{\left(R \cdot \omega \cdot \tan(\varepsilon_{in}) - v_y\right) \cdot t(\xi)}{H_{y,tr}} =$$

$$\begin{aligned}
&= \begin{cases} t(\xi) = \xi/v_{Transport}; \\ v_{Transport} \approx |R \cdot \omega|; \end{cases} = G_{y,tr} \cdot \frac{(R \cdot \omega \cdot \tan(\varepsilon_{in}) - v_y) \cdot \xi}{H_{y,tr} \cdot |R \cdot \omega|} = \\
&= \frac{G_{y,tr}}{H_{y,tr}} \cdot \left(\tan(\varepsilon_{in}) \cdot \text{sign}(\omega) - \underbrace{\frac{v_y}{|R \cdot \omega|}}_{s_y} \right) \cdot \xi = \left\{ C_{y,tr} = \frac{G_{y,tr} \cdot W \cdot L^2}{2 \cdot H_{y,tr}} \right\} = \\
&= -\frac{2 \cdot C_{y,tr}}{W \cdot L^2} \cdot \underbrace{\left(s_y - \tan(\varepsilon_{in}) \cdot \text{sign}(\omega) \right)}_{s_{y\varepsilon}} \cdot \xi;
\end{aligned}$$

Comparing to Section 2.5.1.1, we can note that subscript tr is added to underline that $C_{y,tr}$ and $G_{y,tr}/H_{y,tr}$ now means only the tread, not including the sidewall. Sidewall elasticity is instead handled with ε_{in}. The variable $s_{y\varepsilon}$ is to be seen as an auxiliary mathematical variable introduced only to make the expressions more manageable; it will be eliminated later.

We have to express the force differently for when friction limit is not reached within the contact and when it is reach at inlet and outlet.

$$F_y = \begin{cases} = -C_{y,tr} \cdot s_{y,\varepsilon}; & \quad if \; |F_y| \leq \dfrac{\mu \cdot F_z}{2} \\[2ex] = -\text{sign}(s_{y,\varepsilon}) \cdot \mu \cdot F_z \cdot \left(1 - \dfrac{\mu \cdot F_z}{4 \cdot C_{y,tr}} \cdot \dfrac{1}{|s_{y,\varepsilon}|} \right); & \quad else \end{cases}$$

$$where \; C_{y,tr} = \frac{G_{y,tr} \cdot W \cdot L^2}{2 \cdot H_{y,tr}}; \; dimension: [force]$$

$$and \; s_y = \frac{v_y}{|R \cdot \omega|} \quad and \; s_{y,\varepsilon} = s_y - \tan(\varepsilon_{in}) \cdot \text{sign}(\omega);$$

Now, we have to remember that this model is still **implicit** because ε_{in} depends on $\tau(\xi)$. Introducing simplest possible (linear) constitutive equation for this dependency as in Eq [2.32]:

$$\int \tau \cdot d\xi = F_y = -C_{sw,\varepsilon,in} \cdot \tan(\varepsilon_{in}); \qquad \boxed{[2.32]}$$

Eq [2.32] makes it possible to derive the following **explicit** model:

$$F_y = \begin{cases} = -\dfrac{C_{sw,\varepsilon,in} \cdot C_{y,tr}}{C_{sw,\varepsilon,in} + C_{y,tr}} \cdot s_y; & if \; |F_y| \leq \dfrac{\mu \cdot F_z}{2} \\[4ex] = -\text{sign}(s_y) \cdot \mu \cdot F_z \cdot \dfrac{1 + \dfrac{C_{sw,\varepsilon,in} \cdot |s_y|}{\mu \cdot F_z} - \sqrt{\left(1 - \dfrac{C_{sw,\varepsilon,in} \cdot s_y}{\mu \cdot F_z} \right)^2 + \dfrac{C_{sw,\varepsilon,in}}{C_{y,tr}}}}{2}; & else \end{cases}$$
$$[2.33]$$
$$where \; s_y = \frac{v_y}{|R \cdot \omega|}; \quad and \; C_{y,tr} = \frac{G_{y,tr} \cdot W \cdot L^2}{2 \cdot H_{y,tr}}; \; dimension: [force]$$
(Only valid for pure lateral slip, i.e. pure longitudinal rolling: $v_x = R \cdot \omega$;)

It should be noted that the constitutive relation in Eq [2.32] only states how the string is angled. It is still physically consistent to separately add, outside the tyre model, a constitutive equations for the lateral translational deformation of the sidewall; something as $F_y = c_{sw,transaltion} \cdot \delta_{tyre,y}$;, where $\delta_{tyre,y}$ would be the lateral deformation between wheel rim and contact patch. Such sidewall elasticity would appear in series with the lateral tyre slip force model, in a similar way as the torsional sidewall elasticity in Section Transients modelled as due to Elasticity of Sidewalls2.4.3.4.1 appeared in series with the longitudinal tyre slip force model.

2.5.1.3   Comparison of the models

Eq [2.33] (dependant bristles) is to be compared to Eq [2.31] (independent bristles). Using $C_{ysw} = C_{sw,\varepsilon,in} \cdot C_{y,tr}/(C_{sw,\varepsilon,in} + C_{y,tr})$; the models are identical up to $\mu \cdot F_z/2$ and have the same asymptot for $s \to \infty$. See Figure 2-29.
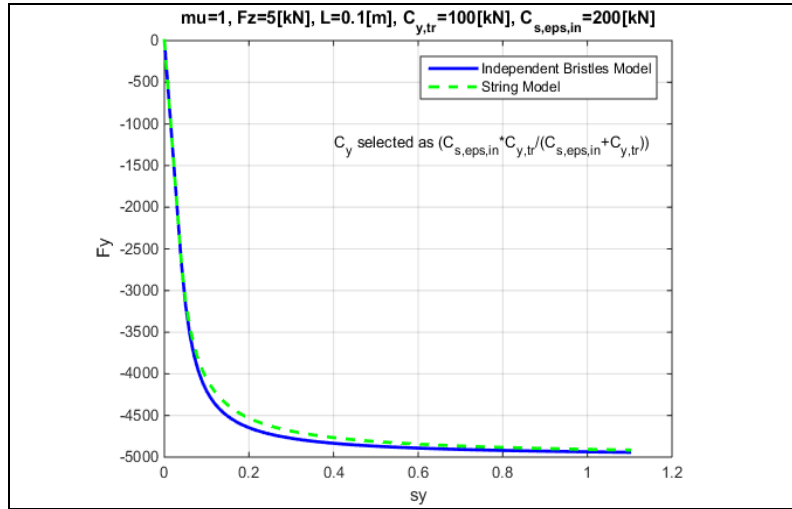

Figure 2-29: Comparison of model with independent bristles and dependent bristles (String model).

The influence of vertical load F_z, discussed already in Section 2.4.3.1.2, is better explained with dependent bristles. Assumes that only the tread stiffness $C_{y,tr}$ (and not $C_{sw,\varepsilon,in}$) varies with contact length, and that this variation is proportional, $C_{y,tr}(F_z) \propto F_z$;, as we found in Section 2.4.3.1.2. This indicates a degressive characteristics of $C_y(F_z)$, which is also observed in measurements.

Notes, for both models:

- The tyre lateral slip is the sliding speed in lateral direction, divided by the same "transport speed" as for longitudinal slip, i.e. the longitudinal transport speed.
- There is a minus sign appearing, because of sign conventions.
- The **tyre** lateral slip definition in Eq [2.31] and Eq [2.33] is to be compared to lateral **wheel** slip $tan(\alpha) = v_y/v_x$, mentioned in context of Figure 2-26:
  - "Lateral **wheel** slip"= $s_{y,wheel} = v_{y,wheel}/v_{x,wheel} = \arctan(\alpha)$, which is defined by how wheel hub moves over ground and independent of wheel rotational speed.
  - "Lateral **tyre** slip" = $s_{y,tyre} = v_y/|R \cdot \omega|$, valid as slip in the constitutive relation $F_y = F_y(s_{y,tyre})$.
  - If no longitudinal tyre slip, i.e. if $R \cdot \omega = v_x$, we have $s_{y,wheel} = s_{y,tyre}$. Then $s_{y,wheel}$ can be used in the constitutive relation.
- For a linearization, the most correct way is that lateral force is $F_y \propto s_y$, not $F_y \propto \alpha$. Often one find $F_y \propto \alpha$ as starting point in the literature, but this compendium uses $F_y \propto s_y$.
  (The advantage with using $F_y \propto \alpha$ is that the vehicle dynamics equations becomes linear in v_y and ω_z, e.g. see derivation of Equation [4.55]. However, the compendium suggests that the tyre model itself should be seen as linear $F_y \propto s_y$ and. It then becomes a deliberate and conscious approximation that $s_y \approx \alpha$. If no longitudinal tyre slip, the approximation is exact.)

The model with dependent bristles is probably more correct. Anyway, we will use the other most in this compendium, since it is much easier to combine with the longitudinal model (Eq [2.13]) to model combined (longitudinal and lateral) slip.

2.5.2 Lateral tyre (slip) stiffness

In summary for many models (and tests!) the following is a good approximation for small lateral slip (and negligible longitudinal slip and constant normal load):

$$F_y = -C_y \cdot s_y; \quad \text{or} \quad F_y = -C_\alpha \cdot \alpha; \qquad [2.34]$$

For the brush model, or any other model which describes $F_y(s_y, F_z, \mu, \dots)$ or $F_y(\alpha, F_z, \mu, \dots)$, one can define the "Lateral tyre slip stiffness" or "Tyre Cornering Stiffness", C_y or C_α, which have the unit N/1 or N/rad. It is the derivative of force with respect to slip or slip angle. Reference (ISO8855) defines the cornering stiffness as C_α for slip angle $\alpha = 0$;:

$$C_\alpha = -\left(\frac{\partial}{\partial \alpha} F_y\right)\Big|_{\alpha=0} \quad = \quad C_y = -\left(\frac{\partial}{\partial s_y} F_y\right)\Big|_{s_y=0} \qquad [2.35]$$

When using only small slip, it does not matter if the cornering stiffness is defined as the slope in an F_y versus α diagram or F_y versus $s_y = tan(\alpha)$ diagram. Therefore, the notation for cornering stiffness varies between C_α and C_y. Cornering stiffness has the unit N which can be interpreted as $N = N/1 = N/((m/s)/(m/s))$ or $N = N/rad$.

The longitudinal tyre slip stiffness, C_x, is normally larger than the lateral tyre slip stiffness, C_y, which can be explained with that the tyre is less stiff in lateral direction. Since it is the same rubber one could argue that both G and H should be the same, but both due to longitudinal grooves in the tread and due to lateral deformable sidewall it is motivated to introduce different subscripts: $(G/H)_x > (G/H)_y$. One could elaborate with different friction coefficients μ_x and μ_y, but in this compendium it is claimed that friction is well modelled as isotrop. More about this in Section 2.6

2.5.3 Empirical tyre models

The cornering tyre forces initially exhibit a linear relation with the slip angle. A non-linear region is then exhibited up to a maximum value. In

Figure 2-30, the maximum slip angle is only 16 degrees (or sy=tan(16 deg)=0.29) and one can expect that the tyre forces will drop as the slip angle approaches 90 degrees. The general form of the lateral force versus slip angle curve is also suitable for the Magic Formula, TM-Easy, or similar curve fitting approach when sufficient test data is available.

2.5.4 Influence of vertical load

As discussed for longitudinal slip and the rolling resistance behaviour of tyres, the vertical load on the tyre affects the force generation. The general behaviour of the tyre's cornering performance as the vertical load changes is presented in

Figure 2-31. These figures show that the cornering stiffness is influenced by vertical load. One term is used to describe the dependence of cornering stiffness on vertical load: cornering coefficient, and is defined as:

$$CC_\alpha = \frac{C_\alpha}{F_z} \quad = \quad CC_y = \frac{C_y}{F_z}; \qquad [2.36]$$

The influence of vertical tyre force on the generated lateral forces is an important aspect of vehicle performance in cornering and will be further discussed in **4**.
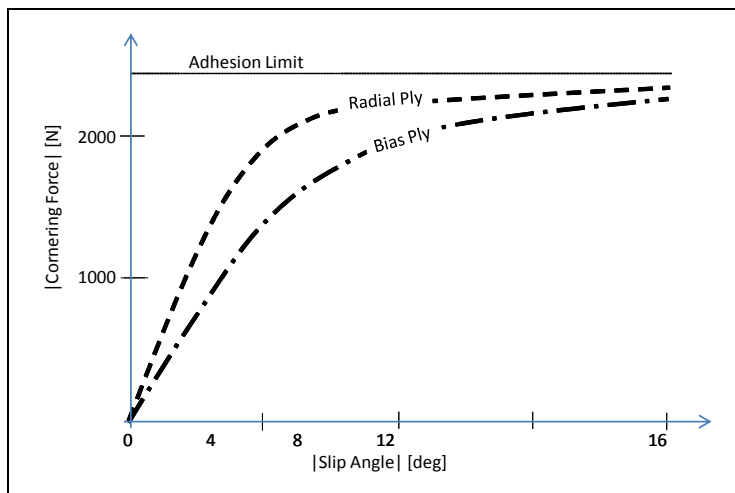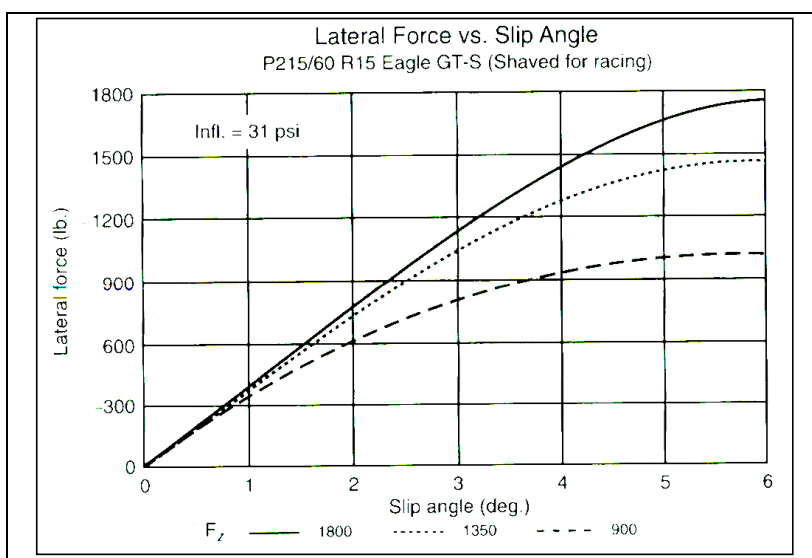
Figure 2-30: Cornering Forces of Tyres

Figure 2-31: Left: Influence of Vertical Load on Lateral Force, (Gillespie, 1992). Right: Cornering stiffness versus vertical load
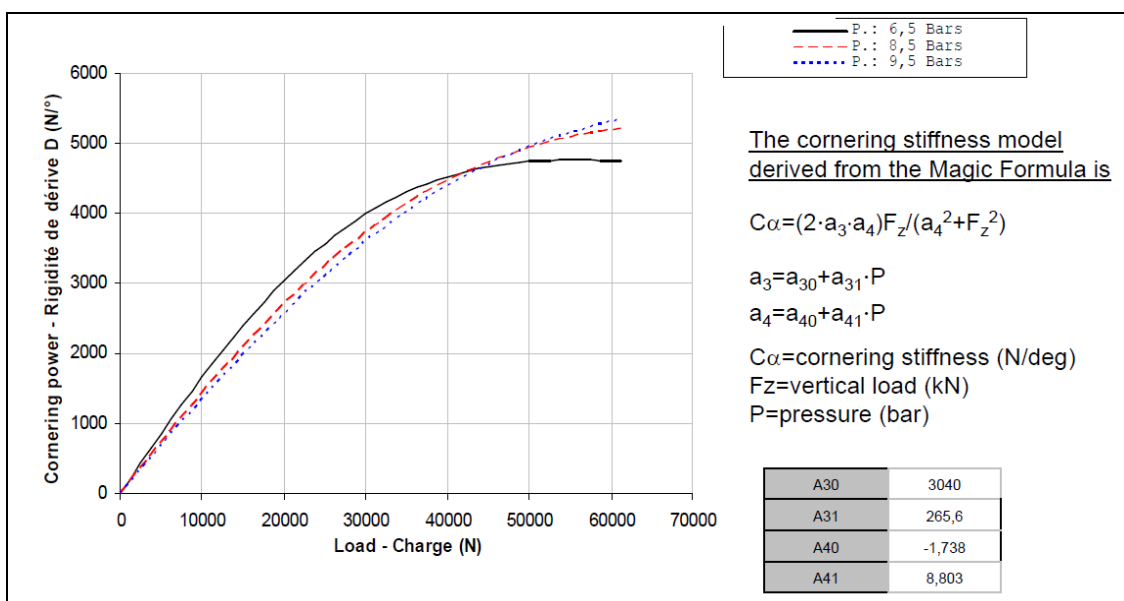
Figure 2-32: Example of cornering stiffness versus vertical load for a truck tyre 295/80R22.5.
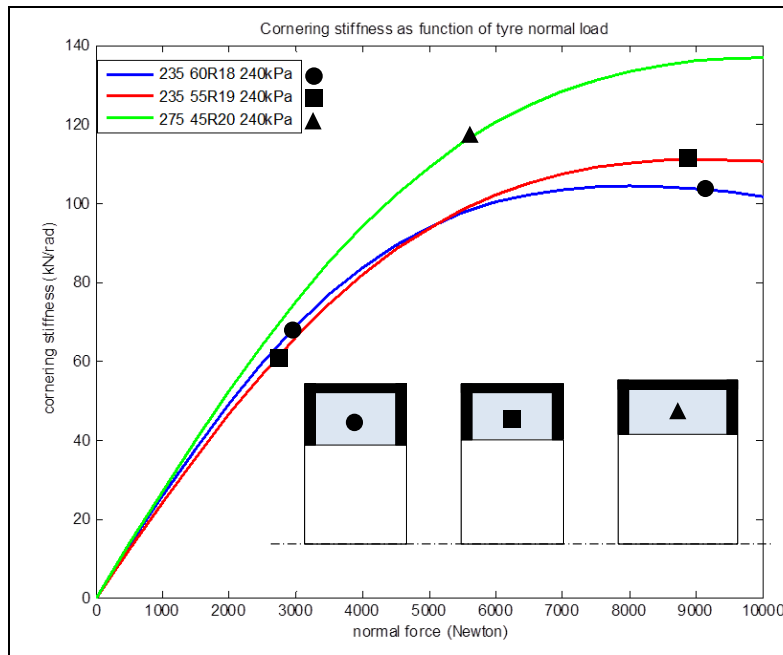
Figure 2-33: Cornering stiffness versus vertical load for some passenger car tyres. From flat track tests.

2.5.5   Relaxation in contact patch

As for longitudinal, there is a delay in how fast the steady state conditions can be reached in contact patch, which is sometimes important to consider. A similar model, as for relaxation in longitudinal direction Section 2.4.3.4.2, is to add a first order delay of the force:

$$\dot{F}_y = A \cdot \left(f\left(s_y, F_z, \mu, \dots\right) - F_y \right);$$

where $f\left(s_y, F_z, \mu, \dots\right)$ is the force according to a steady state model and $A = \frac{v_{Transport}}{L_r} = \frac{|R \cdot \omega|}{L_r}$ or $A = \frac{|v_x|}{L_r}$ and L_r is the relaxation length, which is a fraction ($\approx 25..50\%$) of tyre circumference.

[2.37]

2.5.6   Other effects due to lateral slip

The deformations of the tyre during cornering are quite complex when compared to the case of pure longitudinal motion, see Figure 2-26. Hence, there are more effects than simply a lateral force. Some of these will be discussed in the following.

2.5.6.1   Overturning moment

The contact patch is deflected laterally from the centre of the carcass. This creates an overturning moment M_x due to the offset position of the normal force. The lateral force F_y also contributes to the overturning moment.

2.5.6.2   Tyre aligning moment

*(This section has large connection with Section **4.2.3.2 Steering system forces**.)*

In the lowest diagram in Figure 2-27, one can see that shear stress is concentrated to the outlet side of the contact patch for small slip angles. So the equivalent lateral force acts behind the centre of wheel rotation for small slip angles. As seen in Figure 2-26 b) it acts at a position t_p behind the wheel's y axis. This distance is referred to as the pneumatic trail, see Figure 4-5, and the resulting moment of the lateral force acting on the ground and the reaction of wheel on the suspension creates a moment, M_z,

which is an aligning torque. More commonly the moment M_z is referred to the as the aligning moment since it (with a positive caster offset) tends to align the tyre to zero tyre slip angle. The reason why pneumatic trail can become slightly negative is because pressure centre is in front of wheel centre, see Figure 2-10.
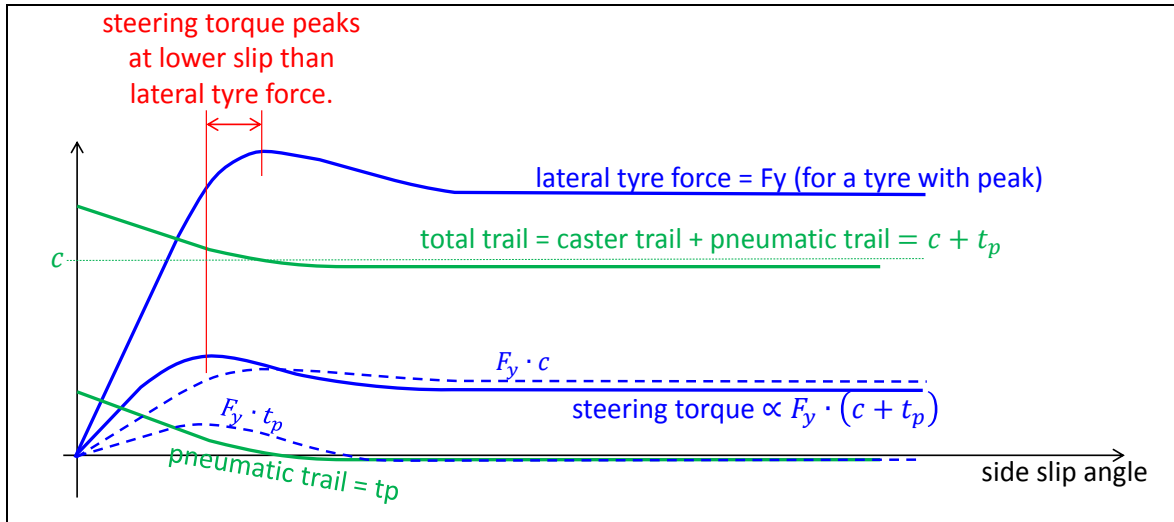
Figure 2-34: General Response of Steering torque to Side slip angle. Tyre aligning moment = $F_y \cdot t_p$ is one part of the steering moment.

Figure 2-34 shows the combined response of lateral force and slip angle. It is interesting to note that the steering torque reaches a peak before the maximum lateral force capacity of the tyre is reached. It can be used by drivers to find, via steering wheel torque, a suitable steering angle which gives a large lateral force but still does not pass the peak in lateral force.

2.5.6.2.1 Aligning Torque Model

A model for (yawing) aligning moment around a vertical axle through centre of contact point, M_z, will now be derived. Any model for lateral shear stress can be used, but we will here only use the uniform pressure distribution and independent bristles, Eq [2.29]. A corresponding expression as Eq [2.31] is derived, but for M_z instead of F_y.

$$M_z = -W \cdot \int_0^L \tau \cdot \left(\xi - \frac{L}{2}\right) \cdot d\xi = \cdots$$

$$= \begin{cases} = -C_y \cdot \dfrac{L}{6} \cdot s_y; & for \ F_y < \dfrac{\mu \cdot F_z}{2} \Leftrightarrow s_y < \dfrac{\mu \cdot F_z}{2 \cdot C_y} \\ = -\dfrac{\mu^2 \cdot F_z^2 \cdot L}{8 \cdot C_y \cdot s_y} \cdot \left(1 - \dfrac{\mu \cdot F_z}{3 \cdot C_y \cdot s_y}\right); & else \end{cases}$$

$$where \ C_y = \frac{G_y \cdot W \cdot L^2}{2 \cdot H_y};$$

[2.38]

The curve of Eq [2.38] is plotted in Figure 2-35.

The lateral force and the aligning torque can be used to calculate the steering forces. If also the steering assistance is known, the steering wheel torque can be calculated. It can be noted that the model does not include the moment from steering rotation itself, i.e. the torque counteracting $\dot{\delta}$.

Figure 2-35: Aligning moment (M_z) around contact patch center for uniform pressure distribution.

2.5.6.3   Camber force

Camber force (also called Camber thrust) is the lateral force caused by the cambering of a wheel. One explanation model is shown in Figure 2-36. It is that Camber force is generated when a point on the outer surface of a leaning (cambered) and rotating tyre, that would normally follow a path that is elliptical when projected onto the ground, is forced to follow a straight path due to friction with the ground. This deviati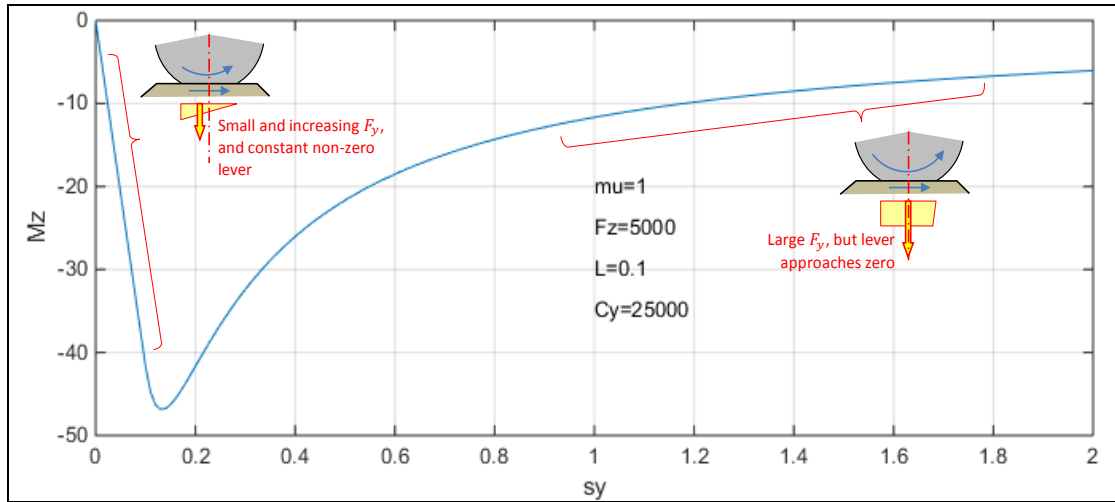on towards the direction of the lean causes a deformation in the tyre tread and carcass that is transmitted to the vehicle as a force in the direction of the lean. Another explanation model is that the tyre "climbs" sideways as the inlet edge is directed, because there is more stick and less slip in the inlet edge as compared to the outlet edge; see brush model.

Camber thrust is approximately linearly proportional to camber angle for small angles: Camber thrust= $F_{yc} = C_\gamma \cdot \gamma$. The camber stiffness, C_γ, is typically 5-10 % of the cornering stiffness and opposite sign. The camber force is superimposable for small lateral slip and small camber angle. The approximate Eq [2.34], can then be developed to:

$$F_y = F_{y,SideSlip} + F_{y,Camber} = C_y \cdot s_y + C_\gamma \cdot \gamma; \quad \text{or} \quad F_y = C_\alpha \cdot \alpha + C_\gamma \cdot \gamma \qquad \text{[2.39]}$$

There is also a rotation perpendicular to the ground due to the camber. The total rotation vector of the wheel is directed along the wheel rotation axis. The component of this vector that is perpendicular to ground creates friction moment which steers the wheel towards the side it tilts; on a cambering vehicle like a bicycle, the wheel is steered "into the fall", which counteracts falling.

2.6 Combined Longitudinal and Lateral Slip

The operation of motor vehicles often involves a combination of turning, braking, and steering actions. Hence, the performance of the tyre under combined (tyre) slip is important.

If the tyre has isotropic adhesion properties in the lateral and longitudinal direction, one can assume that the maximum force magnitude F_{xy} is determined by the maximum resultant friction force, $\mu \cdot F_z$.

$$F_{xy}{}^2 = F_x{}^2 + F_y{}^2 \le (\mu \cdot F_z)^2 \Rightarrow \left(\frac{F_x}{F_z}\right)^2 + \left(\frac{F_y}{F_z}\right)^2 \le \mu^2 \qquad \text{[2.40]}$$

Equation [2.40] can be plotted as a circle, called the "Friction Circle". Since the lateral and longitudinal properties are not really isotropic (due to carcass deflection, tread patterns, camber, etc) the shape may be better described as a "Friction Ellipse" or simply "Friction limit".
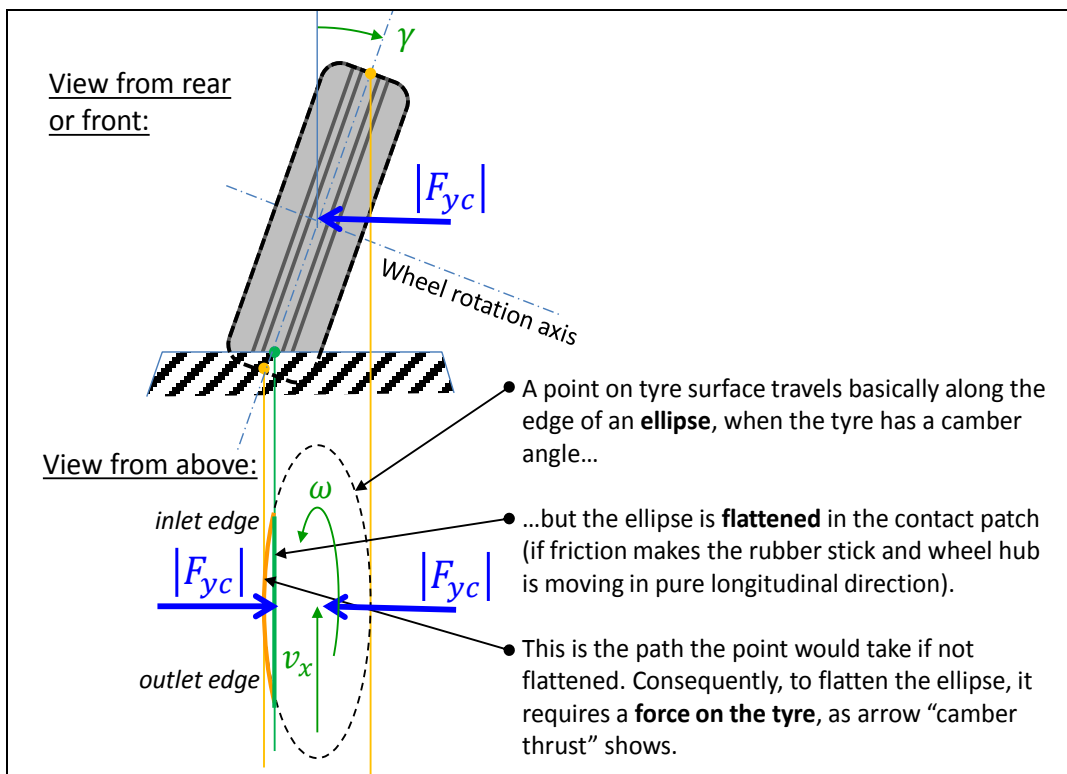
Figure 2-36: Camber thrust

When not cornering, the tyre forces are described by a position between -1 (braking) and +1 (acceleration) along the Y-axis. Note that the scales of both axes are normalized to the maximum value for friction.

The "actuation" of the wheel means the propulsion, braking and steering (and sometimes suspension control) of the wheel. An ideal actuation allows all conditions within the boundaries of the friction circle to be achieved anytime during a vehicle manoeuvre. An example of limitation in actuation is a wheel on a non-steered rear axle. They cannot access any of the lateral parts of the circle; unless the vehicle slides laterally.
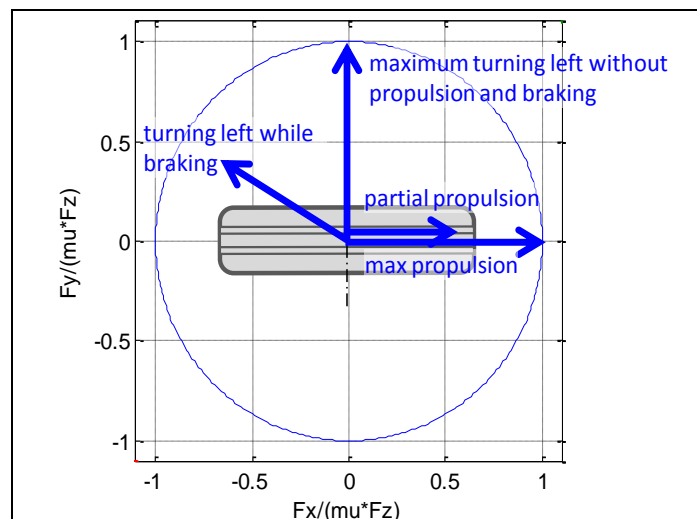
Figure 2-37: Friction Circle with some examples of utilization. View from above, forces on tyre.

At the boundary of the friction circle, tyres become more sensitive to changes in slip. It is therefore extra important to model the direction of the force in relation to shear deformation and relative slip motion in the tyre contact patch. Here, isotropic shear and friction properties are assumed:

$$\frac{lateral\ sliding\ speed}{longitudinal\ sliding\ speed} = \frac{v_y}{R \cdot \omega - v_x} = -\frac{F_y}{F_x}; \qquad [2.41]$$

Significant testing and modelling work have been undertaken to quantify the relationship between tyre slip (s_x and s_y, or s_x and α) and tyre forces (F_x and F_y). As an example, Figure 2-38 presents one method to present the maximum lateral force for different longitudinal slips. Note that each line represents a constant slip angle and that the maximum lateral force occurs for a slip angle between 10 and 18 degrees. Also the maximum value for longitudinal slip does not occur at zero, but for a slight braking condition (around 0.05), which can be motivated using slip definition in Eq [2.1], but not from Eq [2.2].
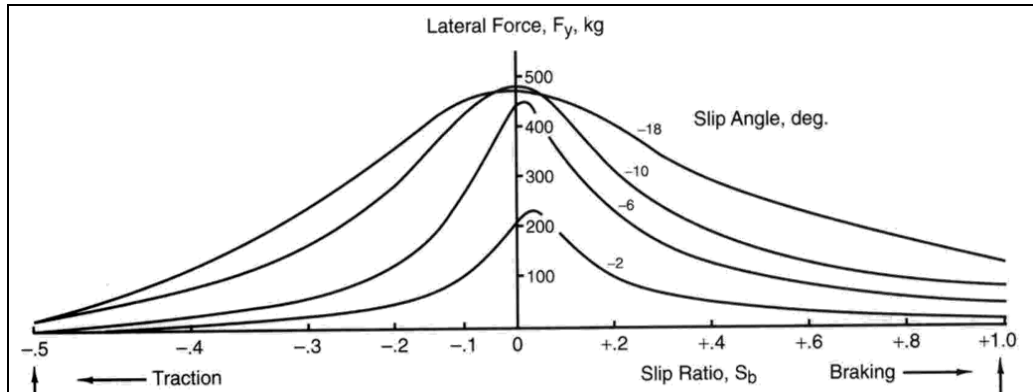
Figure 2-38: Combined Longitudinal and Lateral Slip
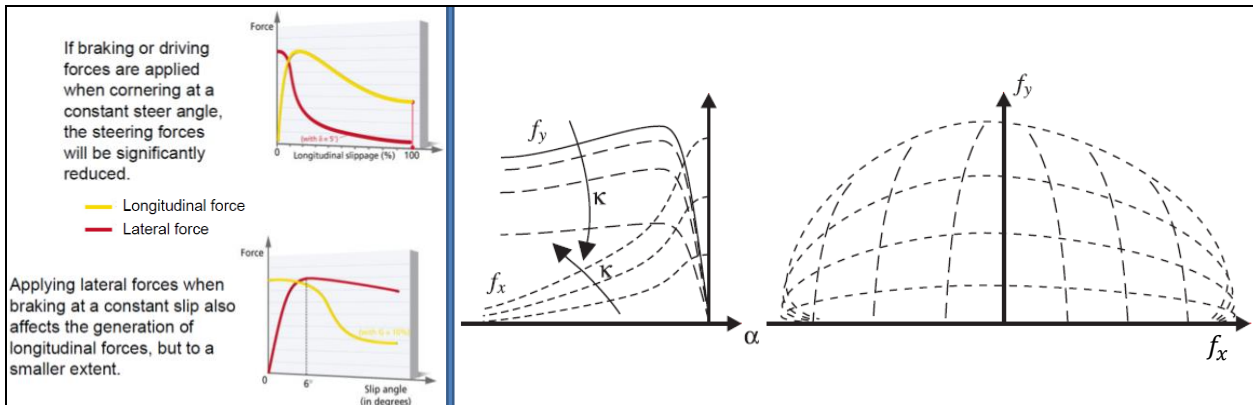
Figure 2-39: Left: Effects of combined longitudinal and lateral utilization of friction. Right: Tyre force diagrams with iso-curves for longitudinal and lateral slip. From (Andreasson, 2007). κ is longitudinal slip and f_i is F_i/F_z.

2.6.1   Isotropic combined slip using any $F = f(s)$;

A simple but physically consistent combined slip model can be expressed using "effective slip, s", as shown in Equation [2.42].

$$\left\{ \begin{aligned} & \begin{bmatrix} F_x \\ F_y \end{bmatrix} = \begin{bmatrix} +s_x \\ -s_y \end{bmatrix} \cdot \frac{F_{xy}}{s_{xy}} = \begin{bmatrix} R_w \cdot \omega - v_x \\ -v_y \end{bmatrix} \cdot \frac{F_{xy}}{\sqrt{(R_w \cdot \omega - v_x)^2 + (v_y)^2}}; \\ & s_{xy}^2 = s^2 = s_x^2 + s_y^2; \\ & \quad s_x = \frac{R_w \cdot \omega - v_x}{v_{Transport}}; \quad and \quad s_y = \frac{v_y}{v_{Transport}}; \quad and \quad v_{Transport} = |R_w \cdot \omega|; \\ & F_{xy} = \mu \cdot F_z \cdot f(s_{xy}); \\ & \quad e.g.\ f(s_{xy}) = \{Eq\ [2.13]\ or\ [2.15]]\}; \\ & \quad or\ f(s_{xy}) = \min\left(\frac{C_0}{\mu} \cdot s_{xy}; 1\right); \quad C_0 \approx \{typically\} \approx 5..15\ [\text{non-dimensional}]; \end{aligned} \right. \qquad [2.42]$$

The model becomes singular if $\sqrt{(R_w \cdot \omega - v_x)^2 + (v_y)^2} \to 0;$. This can be avoided for some such conditions using that $f(s) \approx linear$ for small s_{xy}. Inserting $f(s) = \min\left(\frac{C_0}{\mu} \cdot s_{xy}; 1\right);$ in Eq [2.42] gives:

$$\begin{bmatrix} F_x \\ F_y \end{bmatrix} = \left\{ \begin{aligned} & = \begin{bmatrix} R_w \cdot \omega - v_x \\ -v_y \end{bmatrix} \cdot \frac{F_z \cdot C_0}{|R_w \cdot \omega|} = \begin{bmatrix} +s_x \\ -s_y \end{bmatrix} \cdot F_z \cdot C_0; \\ & \qquad \dots if\ \sqrt{(R_w \cdot \omega - v_x)^2 + (v_y)^2} < \mu \cdot C_0 \cdot |R_w \cdot \omega| \\ & = \begin{bmatrix} R_w \cdot \omega - v_x \\ -v_y \end{bmatrix} \cdot \frac{\mu \cdot F_z}{\sqrt{(R_w \cdot \omega - v_x)^2 + (v_y)^2}}; \qquad \dots else \end{aligned} \right. \qquad [2.43]$$

2.6.2   Isotropic brush model for combined slip

The brush model can be applied also for combined slip. If doing that, with uniform pressure distribution and same $(G/H)_x = (G/H)_y \Leftrightarrow C_x = C_y = C_{xy}$ (isotropic stiffness), the expression for F_{xy} in Eq [2.42] will be as follows.

$$F_{xy} = \left\{ \begin{aligned} & = C_{xy} \cdot s; \qquad \dots if\ s \le \frac{\mu \cdot F_z}{2 \cdot C_{xy}} \Leftrightarrow |F_{xy}| \le \frac{\mu \cdot F_z}{2} \\ & = \mu \cdot F_z \cdot \left(1 - \frac{\mu \cdot F_z}{4 \cdot C_{xy}} \cdot \frac{1}{s}\right); \qquad \dots else \end{aligned} \right. \qquad where\ C_{xy} = \frac{G \cdot W \cdot L^2}{2 \cdot H}$$

Or, equivalent:

$$F_{xy} = \left\{ \begin{aligned} & = C_0 \cdot \mu \cdot F_z \cdot s; \quad \dots if\ s \le \frac{1}{2 \cdot C_0} \Leftrightarrow |F_{xy}| \le \frac{\mu \cdot F_z}{2} \\ & = \mu \cdot F_z \cdot \left(1 - \frac{1}{4 \cdot C_0} \cdot \frac{1}{s}\right); \qquad \dots else \end{aligned} \right. \qquad where\ C_0 = \frac{C_{xy}}{\mu \cdot F_z};$$

[2.44]

2.6.3   Anisotropic brush model for combined slip

The longitudinal model (Eq [2.13]) and the lateral model with independent bristles (Section 2.5.1.1) will now be used with the anisotropy $C_x \ne C_y;$, motivated by that sidewall contributes more to lateral bristle elasticity than to longitudinal bristle elasticity. With significantly different tread grooves in longitudinal and lateral direction, one could motivate also difference in friction coefficient μ, but here

we assume same μ in both directions. The derivation of model equations becomes similar as for the pure longitudinal and lateral models. For the stick zone:

$$\tau_x = \frac{2 \cdot C_x}{W \cdot L^2} \cdot s_x \cdot \xi; \quad and \quad \tau_y = \frac{2 \cdot C_y}{W \cdot L^2} \cdot s_y \cdot \xi;$$

If no slip in contact:

$$F_x = W \cdot \int_0^L \tau_x \cdot d\xi = W \cdot \int_0^L \frac{2 \cdot C_x}{W \cdot L^2} \cdot s_x \cdot \xi \cdot d\xi = \frac{2 \cdot C_x}{L^2} \cdot s_x \cdot \int_0^L \xi \cdot d\xi = \frac{2 \cdot C_x}{L^2} \cdot s_x \cdot \frac{L^2}{2} = C_x \cdot s_x;$$

$$F_y = W \cdot \int_0^L \tau_y \cdot d\xi = W \cdot \int_0^L \frac{2 \cdot C_y}{W \cdot L^2} \cdot s_y \cdot \xi \cdot d\xi = \frac{2 \cdot C_y}{L^2} \cdot s_y \cdot \int_0^L \xi \cdot d\xi = \frac{2 \cdot C_y}{L^2} \cdot s_y \cdot \frac{L^2}{2} = C_y \cdot s_y;$$
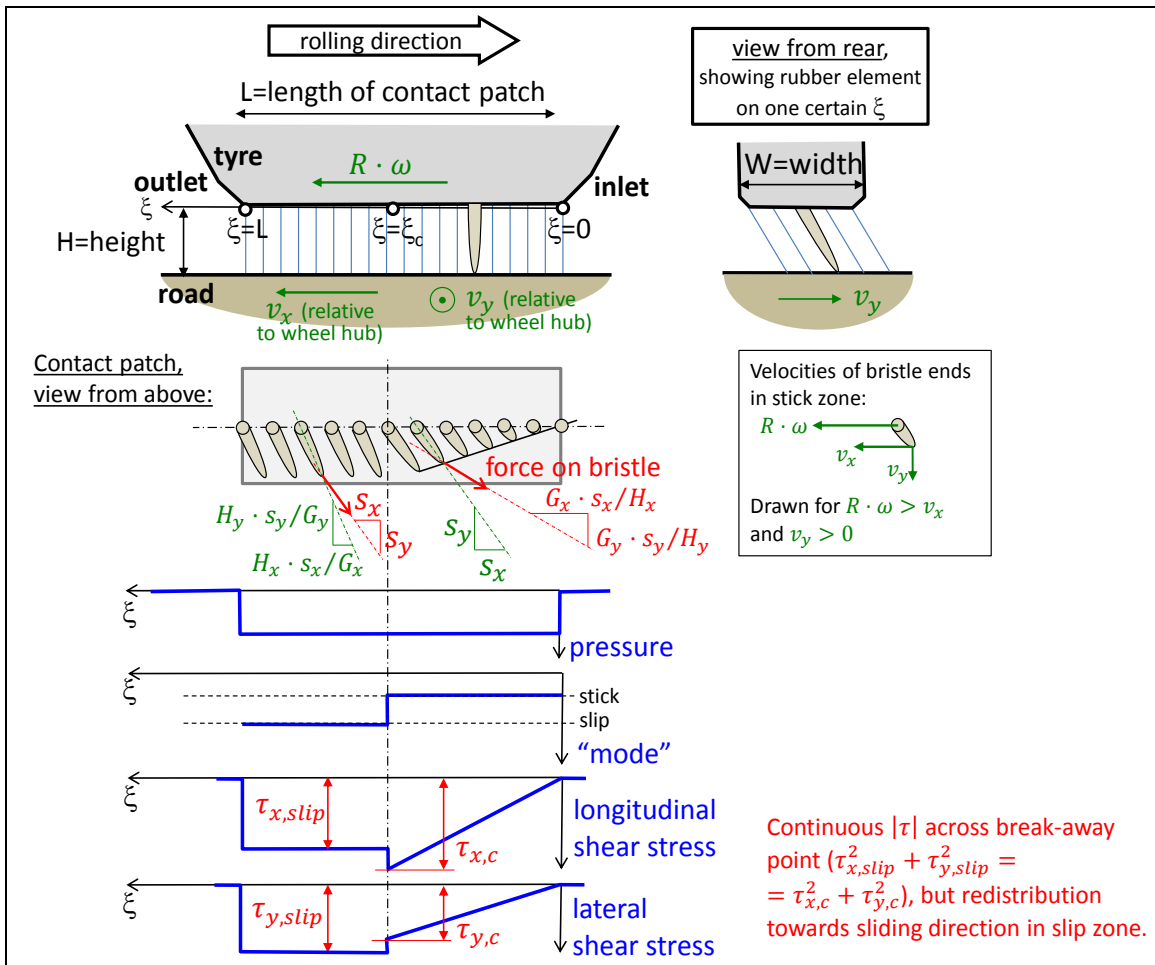
Figure 2-40: Physical model for deriving brush model for combined slip.

Now, if there is a break-away point (ξ_c) where slip starts, we can find it from $\tau(\xi_c) = \mu \cdot p; \Rightarrow \tau_x^2 + \tau_y^2 = \mu^2 \cdot p^2;$. Introducing an auxiliary parameter, $k = C_x/C_y$;, and an auxiliary variable, $s_k = \sqrt{(k \cdot s_x)^2 + s_y^2}$;, gives the following break-away point:

$$\tau(\xi_c) = \mu \cdot p; \Rightarrow \tau_x^2 + \tau_y^2 = \mu^2 \cdot p^2; \Rightarrow \cdots \Rightarrow \xi_c = \frac{\mu \cdot F_z \cdot L}{2 \cdot C_y \cdot s_k};$$

The forces, when $0 < \xi_c < L$ and $\omega \cdot v_x > 0$ becomes:

$$F_x = W \cdot \int_0^L \tau_x \cdot d\xi = W \cdot \int_0^{\xi_c} \frac{2 \cdot C_x}{W \cdot L^2} \cdot s_x \cdot \xi \cdot d\xi + W \cdot \int_{\xi_c}^L \tau_{x,slip} \cdot d\xi =$$

$$= W \cdot \int_0^{\xi_c} \frac{2 \cdot C_x}{W \cdot L^2} \cdot s_x \cdot \xi \cdot d\xi + W \cdot \int_{\xi_c}^L \mu \cdot p \cdot \frac{s_x}{\sqrt{s_x{}^2 + s_y{}^2}} \cdot d\xi = \cdots =$$

$$= \mu \cdot F_z \cdot \frac{s_x}{s} \left(1 - \frac{\mu \cdot F_z}{2 \cdot C_y \cdot s_k} \cdot \left(1 - \frac{1}{2} \cdot \frac{k \cdot s}{s_k}\right)\right); \text{ and}$$

$$-F_y = W \cdot \int_0^L \tau_y \cdot d\xi = \cdots = W \cdot \int_0^{\xi_c} \frac{2 \cdot C_y}{W \cdot L^2} \cdot s_y \cdot \xi \cdot d\xi + W \cdot \int_{\xi_c}^L \mu \cdot \frac{F_z}{W \cdot L} \cdot \frac{s_y}{s} \cdot d\xi = \cdots =$$

$$= \mu \cdot F_z \cdot \frac{s_y}{s} \cdot \left(1 - \frac{\mu \cdot F_z}{2 \cdot C_y \cdot s_k} \cdot \left(1 - \frac{1}{2} \cdot \frac{s}{s_k}\right)\right);$$

Arranging for all combinations of (v_x, v_y, ω), we find:

$$
\begin{bmatrix} F_x \\ F_y \end{bmatrix} =
\begin{cases}
= \begin{bmatrix} +\mu \cdot F_z \cdot \dfrac{k \cdot s_x}{s_k} \\[2mm] -\mu \cdot F_z \cdot \dfrac{s_y}{s_k} \end{bmatrix}; & \text{if } \omega \cdot v_x < 0 \\[6mm]
= \begin{bmatrix} +C_x \cdot s_x \\ -C_y \cdot s_y \end{bmatrix}; & \text{else if } s_k \leq \dfrac{\mu \cdot F_z}{2 \cdot C_y} \Leftrightarrow F_{xy} = \sqrt{F_x^2 + F_y^2} \leq \dfrac{\mu \cdot F_z}{2} \\[6mm]
= \begin{bmatrix} +\mu \cdot F_z \cdot \dfrac{s_x}{s} \left(1 - \dfrac{\mu \cdot F_z}{2 \cdot C_y \cdot s_k} \cdot \left(1 - \dfrac{1}{2} \cdot \dfrac{k \cdot s}{s_k}\right)\right) \\[3mm] -\mu \cdot F_z \cdot \dfrac{s_y}{s} \cdot \left(1 - \dfrac{\mu \cdot F_z}{2 \cdot C_y \cdot s_k} \cdot \left(1 - \dfrac{1}{2} \dfrac{s}{s_k}\right)\right) \end{bmatrix}; & \text{else}
\end{cases}
$$

$$\text{where } s_x = \frac{R \cdot \omega - v_x}{|R \cdot \omega|}; \quad s_y = \frac{-v_y}{|R \cdot \omega|}; \quad s = \sqrt{s_x{}^2 + s_y{}^2};$$

$$\text{and } k = \frac{C_x}{C_y}; \quad s_k = \sqrt{(k \cdot s_x)^2 + s_y{}^2};$$

[2.45]

Figure 2-41 shows results from the model. It can be observed that F_x is independent of s_y and F_y is independent of s_x for $F_{xy} \leq \mu \cdot F_z/s$. This is a reasonable consequence of that no sliding occurs so that forces are purely defined by the elasticity, not the friction. At $s_y \approx 0.01..0.04$, we see that F_y increases with utilization of $|F_x|$ at some areas. This is a redistribution of force from longitudinal to lateral, due to that the tyre stiffer in longitudinal than lateral.
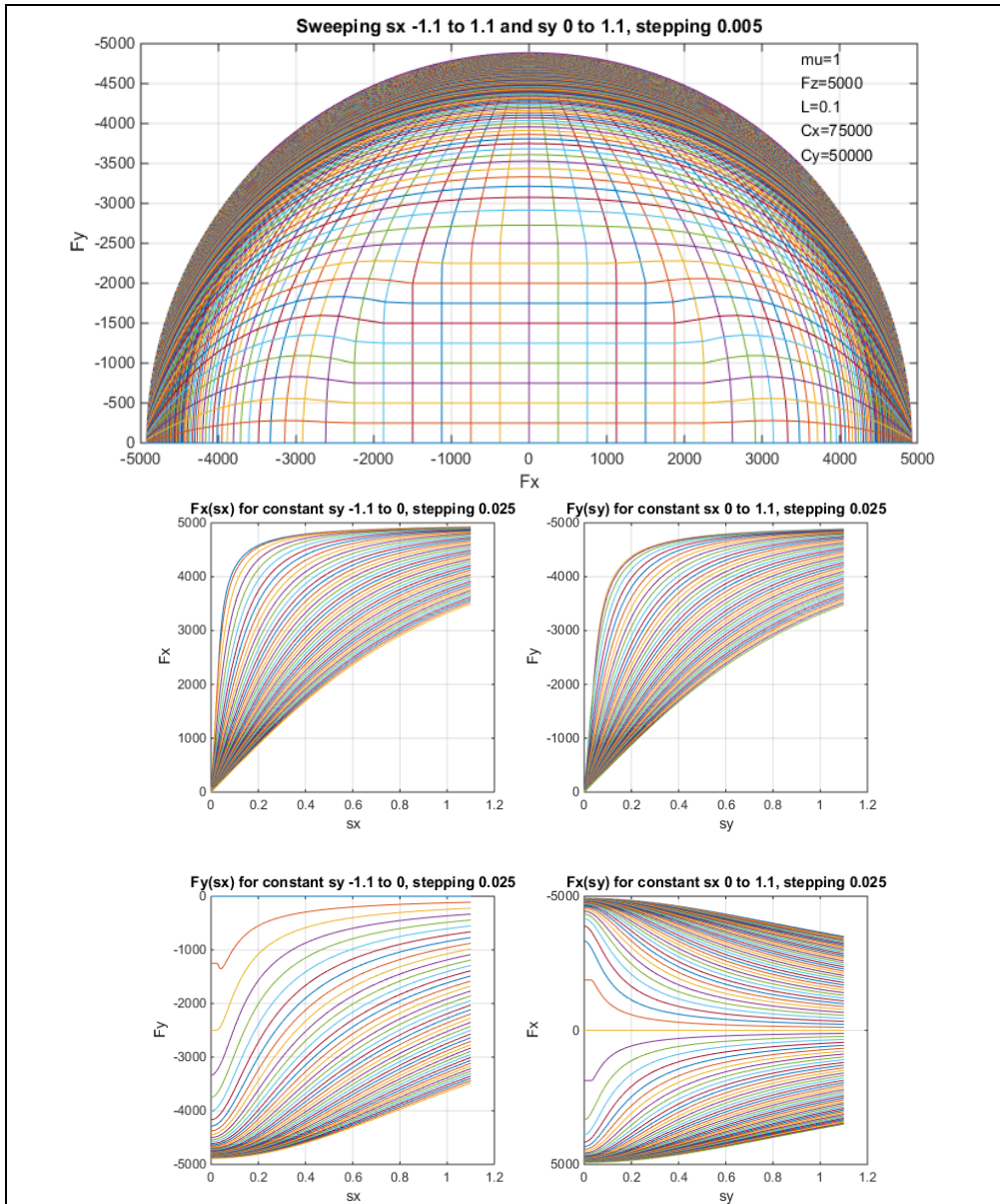
Figure 2-41:Tyre force diagrams with iso-curves for longitudinal and lateral slip. Results from Eq [2.45].

2.6.4 An approximate combined slip model

A combined model for cases when one knows F_x without involving s_x is shown in Equation [2.46]. It can be if we know the wheel torque, e.g. by prescribed propulsion or braking. The equation is not completely physically motivated, but works relatively well. One can consider it as "a mathematical scaling, inspired by the friction circle".

$$F_y \approx \sqrt{1 - \left(\frac{F_x}{\mu \cdot F_z}\right)^2} \cdot F_{y0}; \quad where\ F_{y0} = F_y\big|_{s_x=0}$$

[2.46]

Less usual, but not impossible, is that one would like to prescribe a certain lateral force. Then, the corresponding version of the model becomes:

$$F_x \approx \sqrt{1 - \left(\frac{F_y}{\mu \cdot F_z}\right)^2} \cdot F_{x0}; \quad where \; F_{x0} = F_x|_{s_y=0} \qquad \text{[2.47]}$$

2.6.5   Transients and Relaxation

The models above for combined slip assume steady state conditions. For separate longitudinal and lateral slip, there is a delay in how fast the steady state conditions can be reached, which is sometimes important to consider. A similar model, as for relaxation in longitudinal direction Section 2.4.3.4.2, is to add a first order delay of the force:

$$[\dot{F}_x; \; \dot{F}_y] = [A_x \cdot (f_x(s_x, s_y, F_z, \mu, \dots) - F_x); \; A_y \cdot (f_y(s_x, s_y, F_z, \mu, \dots) - F_y)];$$

where $[f_x; \; f_y]$ are the forces according to steady state models and $[A_x; \; A_y]$ are relaxation lengths, as defined in Eq [2.26] and Eq [2.37].

[2.48]

Most reasoning in Section 2.4.3.4 is applicable also for combined slip relaxation.

2.7 Vertical Properties of Tyres

The most important vertical property of a tyre is probably the stiffness. It mainly influences the vertical dynamics, see **5**. For normal operation, the vertical force of the tyre can be assumed to vary linearly with vertical deflection. If comparing a tyre with different pressures, the stiffness increases approximately linear with pressure. See Figure 2-42.

Figure 2-42: Vertical properties of a truck tyre.

Figure 2-43: Different tyre models which will filter road irregularities differently. Picture from Peter Zegelaar, Ford Aachen.

2.8 Tyre wear

There are many other aspects of tyres, for instance the wear. Wear models are often based around the Archard's (or Reye's) wear hypothesis: worn material is proportional to work done by friction, i.e. friction force times sliding distance. Wear rate (worn mat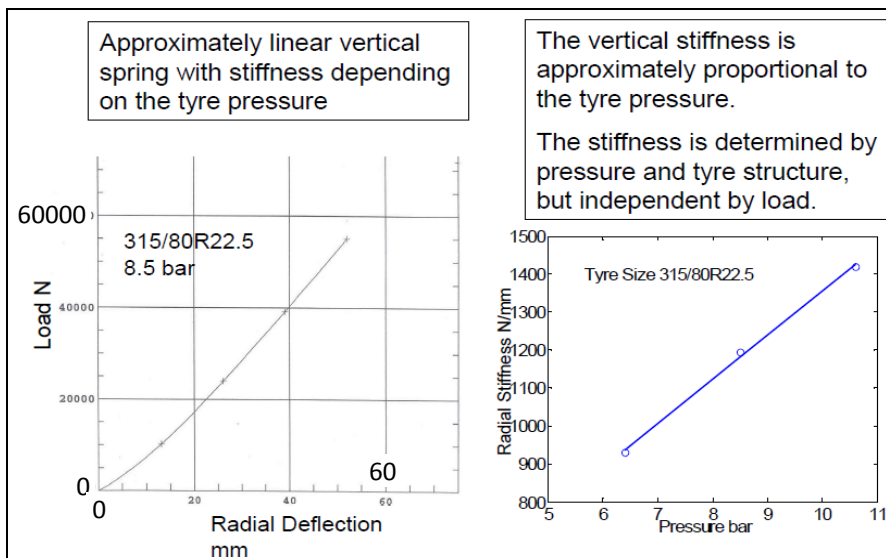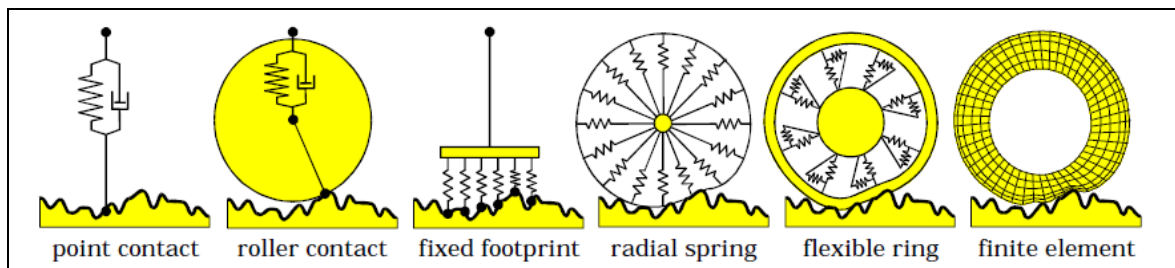erial per time) is therefore friction force times sliding speed. Different approaches to apply this to tyres and expanding to temperature dependency etc. is found for instance in Reference (Grosch, et al., 1961). A generalization of $WearRate$ [in mass/s or mm tread depth/s], for one certain tyre at constant temperature, becomes as follows:

$$WearRate \propto FrictionForce \cdot SlidingSpeed \Rightarrow$$

$$\Rightarrow WearRate = k \cdot F \cdot \Delta v \approx k \cdot (C \cdot s) \cdot \left(s \cdot v_{Transport}\right) \approx k \cdot C \cdot s^2 \cdot v_x;$$

where $F = \sqrt{F_x{}^2 + F_y{}^2}$; $s = \sqrt{s_x{}^2 + s_y{}^2}$; $v_{Transport}$ defined as in Eq [2.8] and

k is a constant for a certain tyre with a certain temperature, rolling on a certain road surface.

[2.50]

2.9 Vehicle Aerodynamics

The flow of air around the vehicle body produces different external forces and moments on the vehicle. Considerable research and engineering has been carried out, and the fluid mechanics will not be covered in this course. However practical first order models for aerodynamics forces have been established and are presented here.

2.9.1 Longitudinal wind velocity

The most relevant force of interest in this course is the resistance force to forward motion, aerodynamic drag $F_{x,air}$, which is proportional to the square of the longitudinal component of the wind speed relative to the vehicle, $v_{x,rel}$. For aerodynamic loads resisting forward motion of the vehicle, the Equation [2.51] can be used. The parameters c_d, ρ and A_{front} represent the drag coefficient, the air density and a reference area, respectively. The reference area is the area of the vehicle projected on a vehicle transversal plane.

$$F_{x,air} = -\frac{1}{2} \cdot c_d \cdot \rho \cdot A_{front} \cdot v_{x,rel}{}^2;$$

[2.51]

Typical values of drag coefficients (cd) for cars can be found from sources such as: (Robert Bosch GmbH, 2004), (Barnard, 2010) and (Hucho, 1998). These coefficients are derived from coast down tests, wind tunnel tests or CFD (Computational Fluid Dynamics) calculations. For light vehicles (cars, SUVs, pick-up trucks) the air resistance can often be neglected for city traffic up to 30-50 km/h, but not at highway speeds.

Since a car structure moving through the air is not unlike an aircraft wing, there are also aerodynamic lift forces. Considering the forward motion only, a lift force and pitch moment will develop. This affects the normal loads on front and rear axle, and consequently the tyre to road grip. Hence, it affects the lateral stability.

$$F_{z,air} = \frac{1}{2} \cdot c_l \cdot \rho \cdot A_{front} \cdot v_{x,rel}{}^2;$$

$$M_{y,air} = \frac{1}{2} \cdot c_{pm} \cdot \rho \cdot A_{front} \cdot L_c \cdot v_{x,rel}{}^2;$$

[2.52]

The coefficient c_l represents the lift characteristics of the vehicle. The lift force is here assumed to act through the centre of gravity. The c_{pm} (pitch moment coefficient) and L_c (characteristic length, usually wheelbase) must be reported together.

With identical effect on the (rigid) vehicle body one can replace the lift force in centre of gravity, $F_{z,air}$, and the pitch moment, $M_{y,air}$, with lift forces at two different longitudinal positions, typically over each axle:

$$F_{air,fz} = \frac{1}{2} \cdot c_{lf} \cdot \rho \cdot A_{front} \cdot v_{x,rel}{}^2;$$
$$F_{air,rz} = \frac{1}{2} \cdot c_{lr} \cdot \rho \cdot A_{front} \cdot v_{x,rel}{}^2;$$

[2.53]

The coefficients c_{lf} and c_{lf} are lift coefficient over front and rear axle, respectively. Relations between Equation [2.52] and Equation [2.53] are: $c_l = c_{lf} + c_{lr}$; and $c_{pm} = (c_{lr} - c_{lf}) \cdot L_c$;.

2.9.2   Lateral wind velocity

When the wind comes from the side, there can be direct influences on the vehicle lateral dynamics. Especially sensitive are large but light vehicles (such as buses or vehicles with unloaded trailers). The problem can be emphasized by sudden winds (e.g. on bridges or exiting a forested area). Besides direct effects on the vehicle lateral motion, side-winds can also disturb the driver through disturbances in the steering wheel feel.

Similar expressions to the longitudinal loads are derived for lateral forces and from side-winds.

$$F_{y,air} = \frac{1}{2} \cdot c_s \cdot \rho \cdot A \cdot v_{y,rel}{}^2;$$
$$M_{z,air} = \frac{1}{2} \cdot c_{ym} \cdot \rho \cdot A \cdot L_c \cdot v_{y,rel}{}^2;$$

[2.54]

The speed $v_{y,rel}$ is the lateral component of the vehicle velocity relative to the wind. Note that A and Lc may now have other interpretations and values than in Equations [2.51]-[2.53].

2.10   Driver interactions with vehicle dynamics

To study how different vehicle designs work in a vehicle operation some driver model is needed. In its easiest form, a driver model can be steering angle $\delta_{stw} \equiv 0$;. Another extreme interpretation of what can be called a driver model is an implicit/inverse statement, like "driver will push accelerator pedal so that speed $v_x \equiv 20\ [m/s]$ during the manouvre", which leads to that accelerator pedal position becomes an output, as opposed to input, to the vehicle model. Beyond those very simple driver models, there is often need for a driver model which react on vehicle states **in relation to an environment or traffic**. In this section, driver models are primarily thought of as models of the driver of the subject vehicle, but when modelling surrounding traffic carefully, each object vehicle can also use a driver model.

The driver interacts with the vehicle mainly through steering wheel, accelerator pedal and brake pedal. In addition to these, there are clutch pedal, gear stick/gear selector, and various buttons, etc., see Figure 2-44, but we focus here on the first 3 mentioned.

```
Acceleration Pedal Position, Brake Pedal Force,
              Steering Wheel Angle
     (and Clutch Pedal Force, Gear Stick/Selector Position,
   Parking Brake Request, Direction indicators, HMI buttons, …)
```

```
              Acceleration Pedal Force,
      Brake Pedal Position, Steering Wheel Torque
           (and HMI Lamps, Sounds, Haptics, …)
```
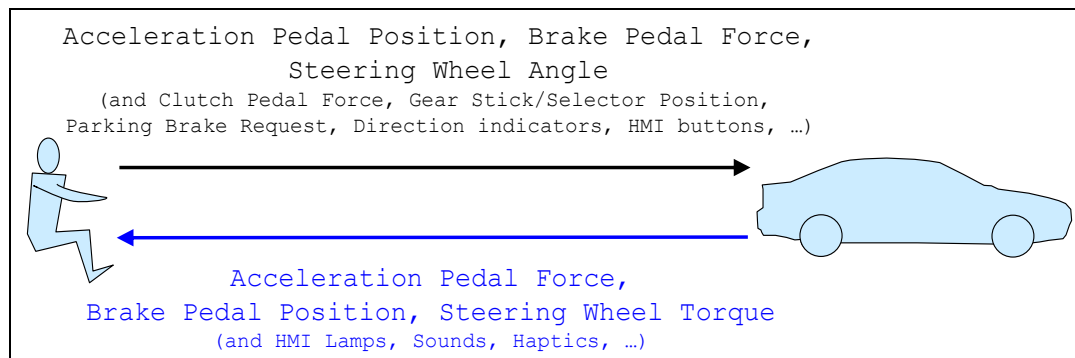
Figure 2-44: Commonly assumed causality (direction of cause and effect).

Driver's control of vehicle dynamics, or vehicle motion including position, can be discussed in longitudinal (mainly pedals) and lateral (mainly steering wheel).

Driver reacts on several stimuli, such as motion (mainly through seat), sounds, and optical. Among motion, it is primarily the accelerations (and their time derivative, jerk) that is sensed by the driver, but also rotational velocity in yaw can be sensed by human. Among the optical there is looming (optical expansion of an object in the driver's field of view) is often used as a cause for how driver uses the pedals. The optical flow (the pattern of apparent motion of objects, surfaces, and edges in the driver's field of view) is often used as a cause for highest comfortable speed and yaw rate.

Driver models are here discussed as models of the "human driver" for use in vehicle verification simulations. However, driver models can also be understood as models of "virtual driver", and then they are actually implemented as algorithms in the vehicle product, e.g. as prediction algorithms or autonomous driving controllers. In the first context, it is often important to vary the driver model (at least its parameters, maybe even its equations) for robustness, as mentioned in Figure 1-2. In the latter context, the driver model of the subject vehicle is rather varied for optimization/satisficing, see Figure 1-2 again.

2.10.1 Open-loop and Closed-loop Manoeuvres

Two common expressions used in vehicle dynamics are "Open-loop" and "Closed-loop". These concepts are used to describe how the vehicle control systems are manipulated in a "driving" event.

An **open-loop** manoeuvre refers to the case where the driver controls (steering wheel, brake pedal and accelerator pedal) are operated in a specific sequence, i.e. as functions of time. A typical case is a sine wave excitation of the steering wheel. The time history of the steering wheel angle is defined as a function that is independent of the road environment or driver input. This type of manoeuvre is a practical design exercise to study the steering response of the system, but has little relation to a real-world driving case. Theoretical simulation and real testing with a steering robot are examples of how such studies can be made.

A **closed-loop** manoeuvre refers to the case when (human) driver feedback via driver controls is included. This represents real-world driving better. In real vehicle or driving simulator testing, a real driver is used. This enables collection of the drivers' subjective experience. In cases of theoretical simulation, a "driver-model" is needed. A driver-model can have varying levels of complexity but in all cases simulates the response of a human driver to different effects, such as lateral acceleration, steering wheel torque, various objects appearing outside the vehicle, etc.

A test with real vehicle, carried out with a steering-robot (and/or pedal robot) can also be called closed-loop if the robot is controlled with a control algorithm which acts differently depending on the vehicle states, i.e. if the algorithm is a driver model.

The concepts of open- and closed-loop control are demonstrated in Figure 2-45. The important difference to note is that in open-loop control there is no feedback to the driver. The figure also shows a "Virtual driver" which represents today's automatic functions based on environment sensing, such as

adaptive cruise control (section 3.5.2.2) and lane keeping aid (section 4.6.2.1). Closed loop control incorporates the different types of feedback to the driver. Drivers automatically adapt to the different feedback. Understanding driver response to different feedback, and expressing it in mathematical descriptions, is an active area of research, particularly for driver support functions.
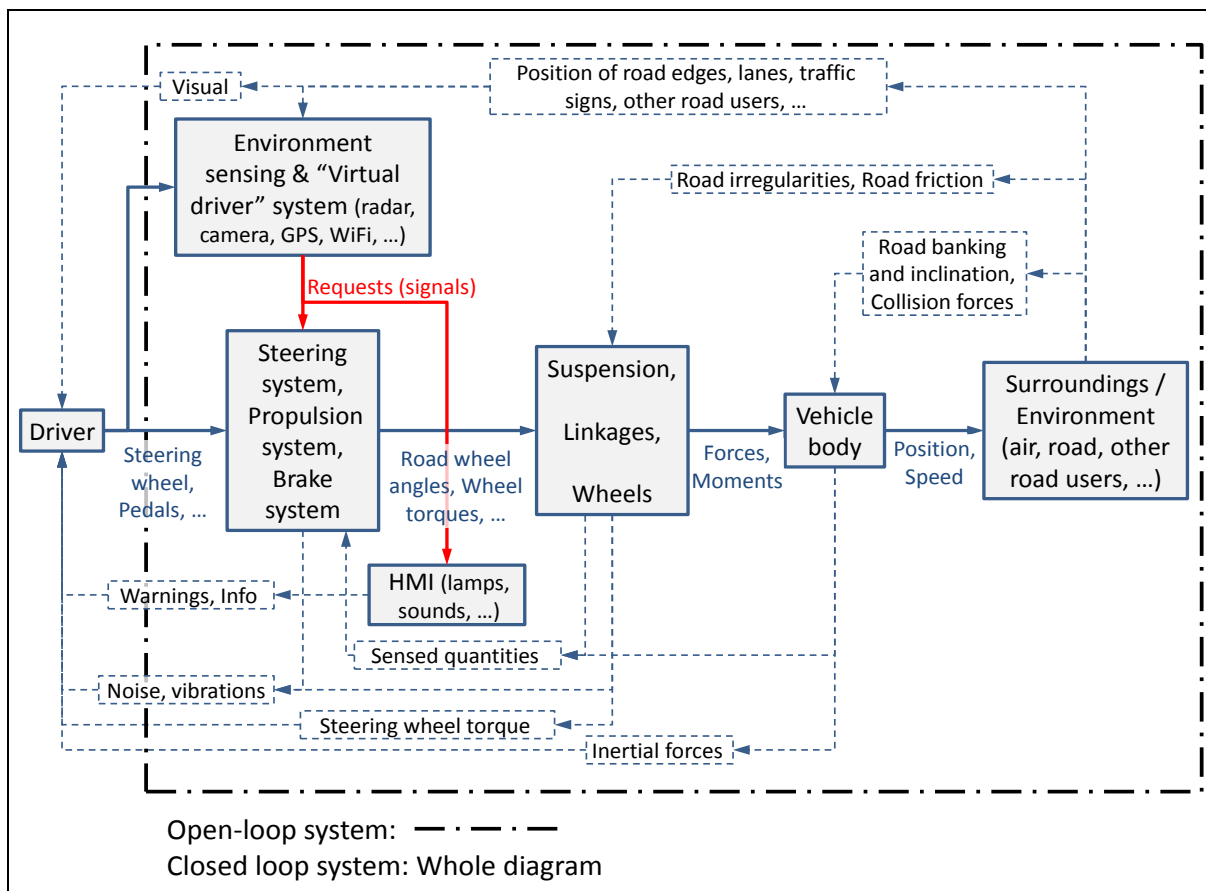
Figure 2-45: Open and closed loop representations of vehicle dynamic systems

2.10.2 Driver Longitudinal or Pedals

Each pedal has both pedal position and pedal force as communication channels to the driver.

In broad terms, the accelerator pedal position is interpreted by a control system as a certain requested engine torque, which means a certain wheel shaft torque on the propelled axle/axles. In some advanced solutions, one could think of using accelerator pedal force as a feedback channel from vehicle to driver.

In broad terms, the brake pedal force gives a certain friction brake torque application on each axle. In some advanced solutions, one could think of changing brake pedal position versus force characteristics as a feedback channel from vehicle to driver. But already with traditional (hydraulic) brake systems for passenger cars, the brake pedal gives a feedback to driver in that ABS interventions is felt.

For electric and hybrid vehicles the brake pedal can typically influence the propulsion system as well, in that at low levels of pedal braking, the electric propulsion motors give negative wheel shaft torque. This is for regenerating energy. Regenerative braking can even be engaged at low levels of accelerator pedal position.

The propulsion and brake systems are more described in 3. LONGITUDINAL DYNAMIC.

How driver operates the pedals can also be called a longitudinal driver model. But different manoeuvres calls for different driver models. Examples of manoeuvres/situations are:

- Full acceleration or deceleration, including driver delays
- Keep constant speed
- Keep distance to lead vehicle
- When a cut-in happens in front of object vehicle: Expand to comfortable/safe gap
- Approach slower subject vehicle from behind: Reduce to comfortable/safe gap
- Longitudinal speed control during overtaking
- Longitudinal speed control to stand-still

An example of longitudinal model for approaching a slower vehicle from behind is defined through simple kinematic relations and some assumptions, see Figure 2-46 which indicates how to calculate the required (constant) acceleration to reach a certain safe gap. The safe gap can be defined by "gap needed to exactly avoid collision if braking as object vehicle but with a certain reaction time". In traffic schools one is often taught that safe time gap STG is $STG = 3\ [s]$, as a rule of thumb. In Eq [2.56], it is shown how such a model is derived, subscripts: *s=subject, o=object, 0=present, p=predicted*. The requested acceleration a_{req} just have to be converted to pedal force or position.

Prediction, of object and subject:

$$s_{op} = s_{o0} + v_o \cdot t_p;\ \text{(object vehicle assumed to not accelerate)}$$

$$v_{sp} = v_{s0} + a_{req} \cdot t_p;$$

$$s_{sp} = s_{s0} + v_{s0} \cdot t_p + a_{req} \cdot t_p^2/2;$$

Requirement on prediction at t_p:

$$s_{op} - s_{sp} = (s_o - s_s)_{safe} = v_o \cdot SafeTimeGap = v_o \cdot STG;$$

$$v_{sp} = v_o;$$

Solve for a_{req} and t_p gives the driver model on explicit form:

$$a_{req} = \frac{-(v_o - v_{s0})^2}{2 \cdot (s_{o0} - s_{s0} - STG \cdot v_o)};$$

$$t_p = \frac{2 \cdot (s_{s0} - s_{o0} + STG \cdot v_o)}{v_o - v_{s0}};$$

Use only if $t_p > 0$, else "prediction" happens in passed time.

[2.55]

Examples of applying the driver model in Eq [2.56] is shown in Figure 2-46, where also a general PVA-time-diagrams (PVA=position, velocity, acceleration) is shown. PVA-time-diagrams are often useful when studying vehicle operations with other moving objects, see Figure 2-46. Different scenarios can be tested, and driver models can be derived using simple formulas, such as constant speed and constant acceleration.

2.10.3 Driver Lateral or Steering Wheel

The driver interacts with steering wheel through two channels, steering wheel angle and steering wheel torque.

A frequently used model is that the driver decides a steering wheel angle and expects a certain steering wheel torque, T_{sw}, feedback. Only in extreme situations, the causality is modelled the other way, e.g. studying what happens if driver takes hands-off, i.e. steering wheel torque =0. However, it should be noted that, from neuromuscular point-of-view, it is not motivated to model a driver as controlling the torque or forces, but only the position.
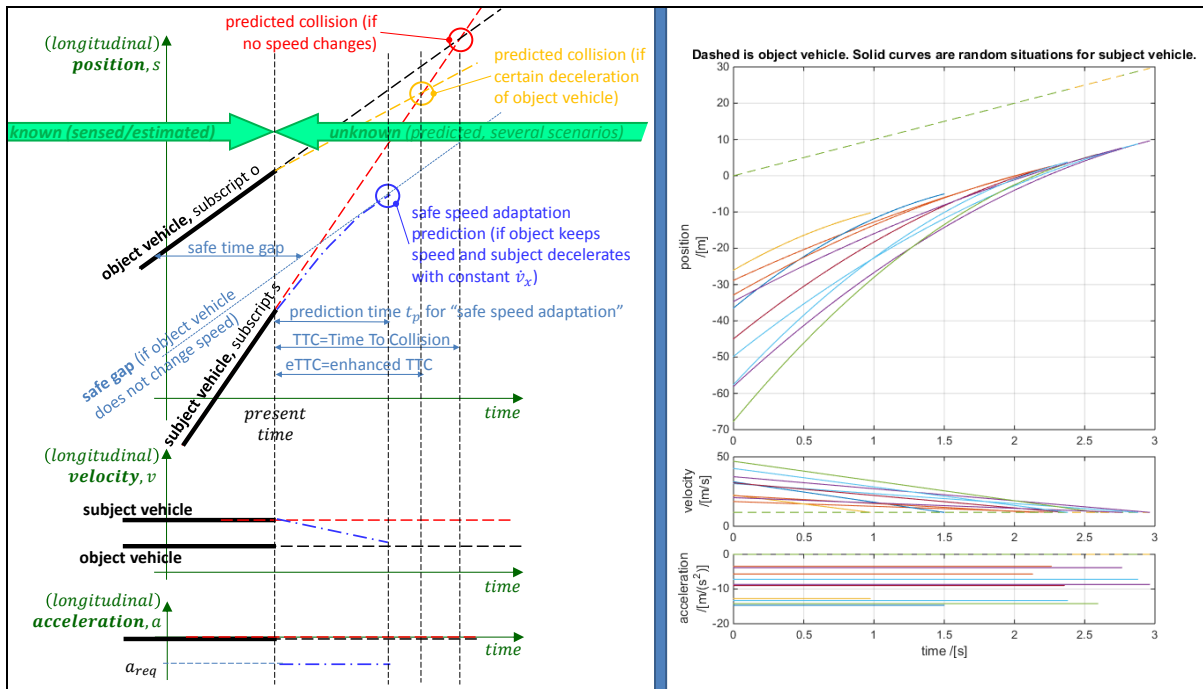
Figure 2-46: Left: PVA-time-diagrams (PVA=position, velocity, acceleration) for studying longitudinal interaction with an object vehicle ahead. Right: PVA diagram for the driver model in Eq [2.56] using $SafeTimeGap = 2$ [s] and some randomly selected s_{s0} and v_{v0}.

In a broad view, the angles of the road wheels are functions of steering wheel angle, independent of forces and torques in the steering system. Further, the steering wheel torque is a function of the lateral force on the front axle, possibly scaled down with assistance from the power steering or steering servo. Some more detailed aspects on the two latter sentences are discussed below. See more about steering system in Section 4.2.3.

How driver operates the steering wheel can also be called a lateral driver model. But different manoeuvres calls for different driver models. Examples of manoeuvres/situations are:

- Going into curve from straight and vice versa
- Turning in intersection
- Avoidance manoeuvre
- Stabilizing vehicle when sudden lose yaw stability, e.g. in curve
- Compensating road unevenness which cause lateral disturbance
- Lateral speed control during overtaking

An example of driver model is the Salvucci and Gray model in Figure 2-47 and Eq [2.56]. The steering wheel angle is denoted δ_{stw}. The 3 k coefficients are parameters that have to be tuned to certain driver, vehicle and operation. Additionally, the distance to nearpoint needs to be tuned. Also, exactly how to position the far and near point is also open for tuning, such as if there should be extra margins on top of $W/2$ and whether W is vehicle, road or lane width. Further on, all these assumptions can change during a simulation, e.g. as driving on a windy country road and suddenly a meeting vehicle shows up might make the far point jump. So, even if the model might look simple, it is not obvious how to tune and use it. Hence, there are variants of it which has only one aim-point.
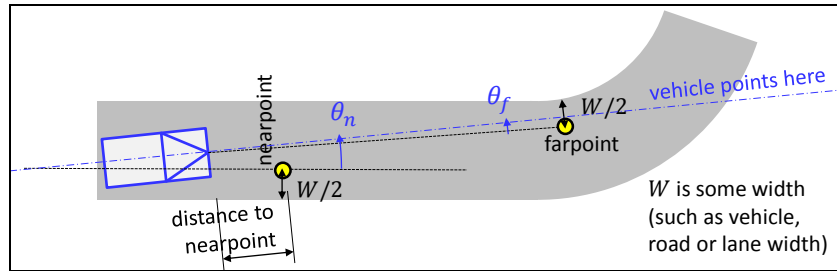
Figure 2-47: Salvucci and Gray model for how driver steers.

$$\dot{\delta}_{stw} = k_f \cdot \dot{\theta}_f + k_n \cdot \dot{\theta}_n + k_I \cdot \theta_n; \Leftrightarrow$$

$$\Leftrightarrow \delta_{stw} = \delta_{stw}(t_0) + k_f \cdot \theta_f + k_n \cdot \theta_n + k_I \cdot \int_{t_0}^{t} \theta_n \cdot dt;$$

[2.56]

The advantage of this kind of models is that most assumptions can be based on vehicle and environment states. A drawback is that the dynamic vehicle behaviour is built into the k coefficients, meaning that if vehicle dynamics is changed, e.g. adding a trailer or reducing road friction, the k factors reasonable have to be re-tuned. If identifying the k coefficients to a dynamic vehicle model, and let them vary with vehicle model parameters one can reduce the need for such re-tuning, but it leads too far to show this in this compendium.

Above driver model can be categorized as having a look ahead. Simpler driver model can be based on only where the vehicle is at present time, such as present lateral position in lane. More advanced driver models uses a dynamic model for prediction. The vehicle dynamics model is especially needed in predicting models.

3 LONGITUDINAL DYNAMICS

3.1 Introduction

The primary purpose of a vehicle is transportation, which requires longitudinal dynamics. The chapter is organised with one group of functions in each section as follows:

- 3.2 Steady State Function
- 3.3 Functions over longer events
- 3.4 Functions in shorter events
- 3.5 Control functions

Most of the functions in "3.5 Control functions", but not all, could be parts of "3.4 Functions in shorter events". However, they are collected in one own section, since they are special in that they partly rely on software algorithms.

There are a lot of propulsion related functions, originating from the attribute Driving dynamics. Examples of such, not covered in this compendium are:

- Off-road accessibility: Ability to pass obstacles of different kind, such as uneven ground, extreme up- and down-hills, mud depth, snow depth, etc.
- Shift quality: Quick and smooth automatic/automated gear shifts
- Shunt & shuffle: Absence from oscillation for quick pedal apply, especially accelerator pedal.

3.1.1 References for this chapter

- *"Chapter 23. Driveline" in Reference* (Ploechl, 2013)*.*
- *"Chapter 24. Brake System Dynamics" in Reference* (Ploechl, 2013)*.*
- *"Chapter 27 Basics of Longitudinal and Lateral Vehicle Dynamics" in Reference* (Ploechl, 2013)
- *"Chapter 6: Adaptive Cruise Control" in Reference* (Rajamani, 2012)

3.2 Steady State Functions

Functions as top speed and grade-ability are relevant without defining a certain time period. For such functions it is suitable to observe the vehicle in steady state, i.e. independent of time. Those functions are therefore called steady state functions, in this compendium.

The main subsystems that influences here are the propulsion system, see Section 3.2.1, and the (Friction) Brake system, see Section 3.4.3.

3.2.1 Propulsion System

A generalised propulsion system is shown in Figure 3-11, along with a specific example of a conventional one. There are 1+2=3 control degrees of freedom marked for the generalized one (e.g. engine power, transmission ratio and storage power) while there is only 1+1=2 for the conventional.

Note that the approach in Figure 3-1 is one-dimensional: we consider neither the differential between left and right wheel on the driven axle nor distribution between axles. Instead, we sum up the torques at all wheels and assume same rotational speed.
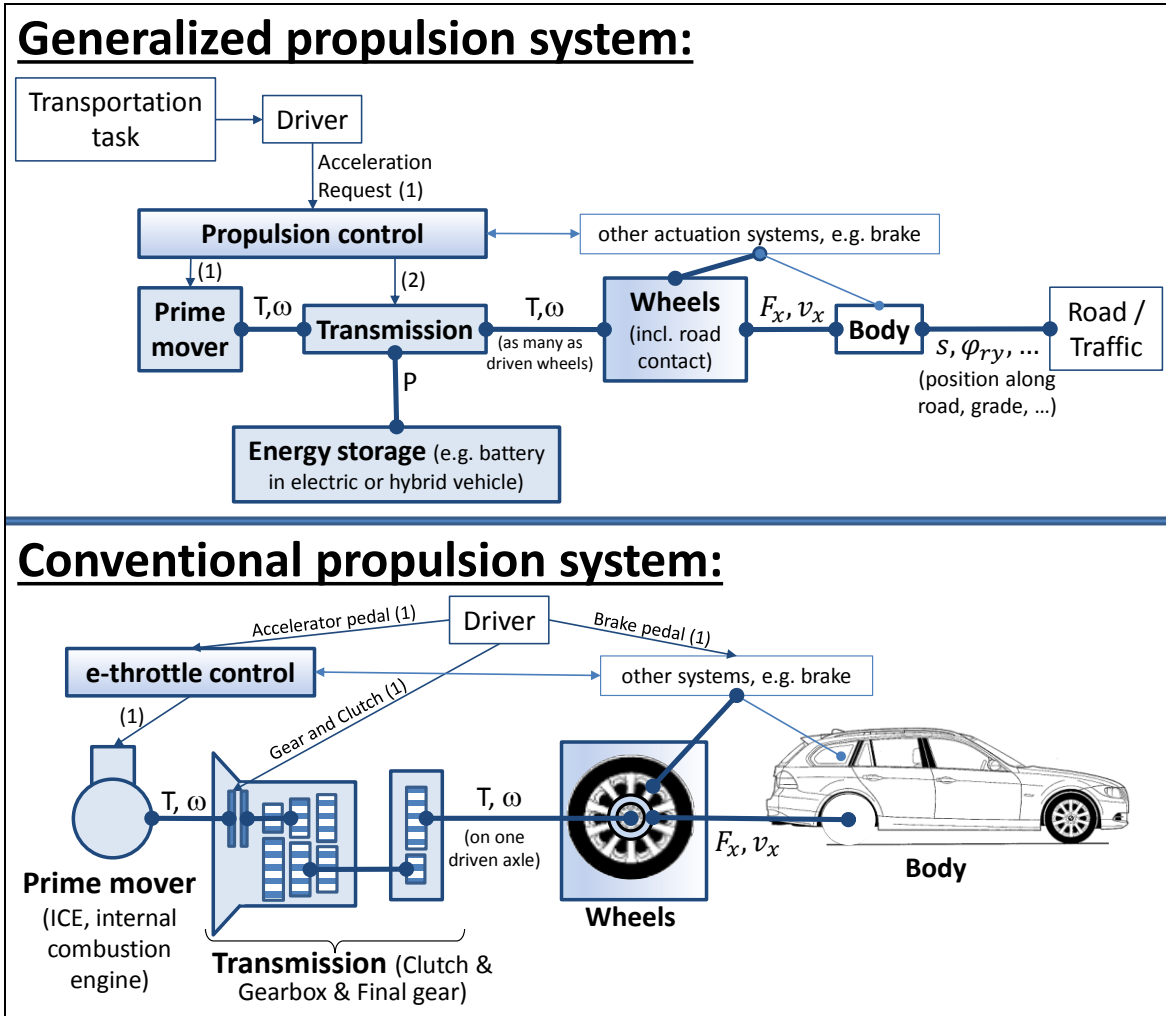
Figure 3-1: Propulsion system

It is often suitable to model propulsion systems "connecting in nodes", see Section 1.5.2.5.1. Notation and sign conventions then becomes as in Figure 3-2.
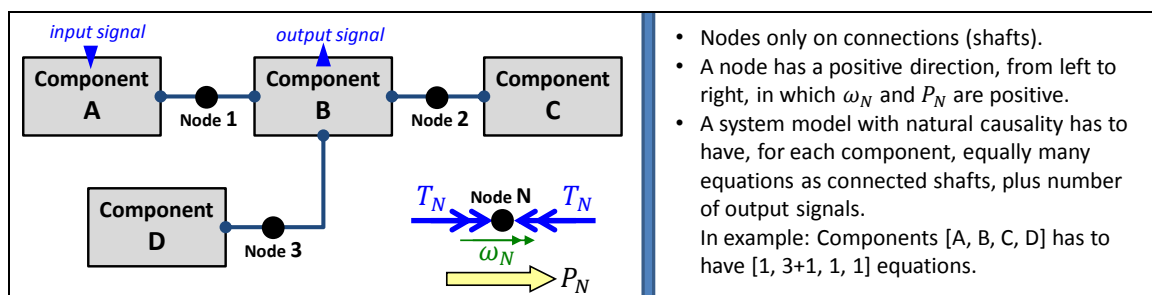
Figure 3-2: Propose notation and sign conventions for Propulsion system models.

3.2.1.1 Prime movers

The conversion of stored energy to power occurs in the prime mover, see Figure 3-1. Details of the conversion processes and transmission of power to the tyres are not covered in this compendium. Some basic background is still necessary to describe the longitudinal performance of the vehicle. The main information that is required is a description of the torque applied to the wheels over time and/or as a function of speed. Sketches of how the maximum torque varies with speed for different prime movers (internal combustion engine (ICE), electric motor or similar) are shown in Figure 3-3. The torque speed characteristics vary dramatically between electric and internal combustion engines. Also, gasoline and diesel engines characteristics vary.

The curve for electric motors in Figure 3-3 shows that the main speciality, compared to ICEs, is that their operation range is nearly symmetrical for negative speeds and torques. However, the curve should be taken as very approximate, since electric motors can work at higher torque for short periods of time. The strong time duration dependency makes electric motors very different to ICEs from a vehicle dynamics point of view. Other properties that makes them special are quick and accurate response, well known actual torque and that it is much more realistic to divide them into several smaller motors, which can operate on different wheels/axles.
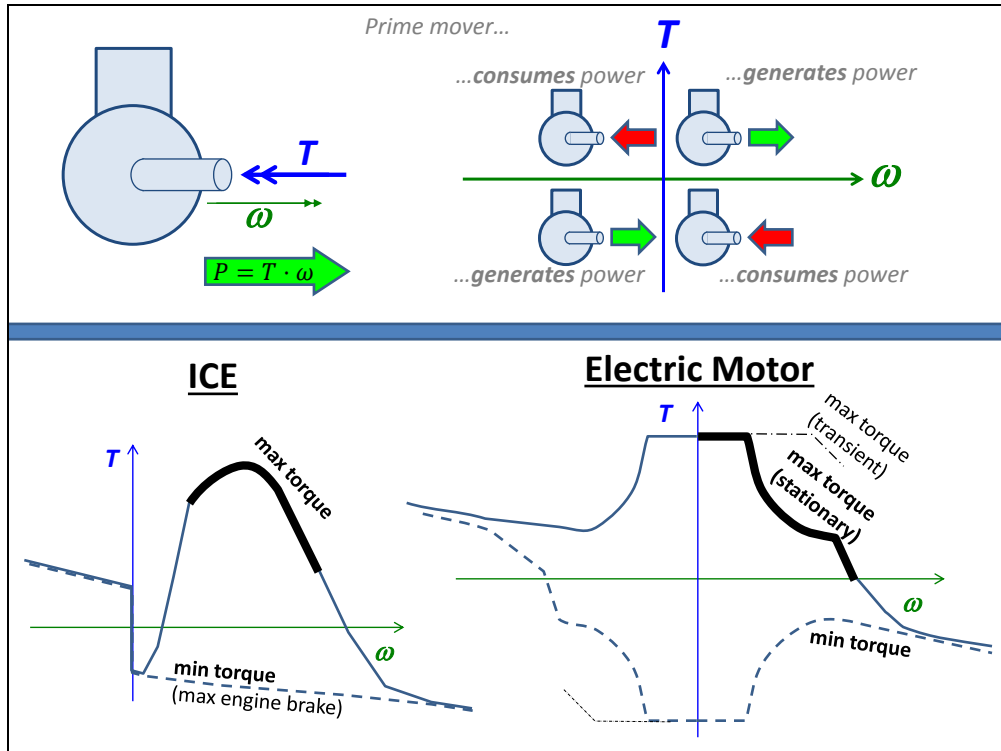
Figure 3-3: Torque Characteristics of Prime Movers

3.2.1.2 Transmissions

In some contexts "transmission" means the 1-dimensional transmission of rotational mechanical power from an input shaft to one output shaft. Such is called "Main transmission", Section 3.2.1.2.1. In other contexts, "transmission" means the system that distributes the energy to/from an energy buffer and to/from multiple axles and/or wheels. Such is called "Distribution transmission", Section 3.2.1.2.2.

3.2.1.2.1 Main transmissions

Main transmission can be either stepped transmissions or continuously variable transmissions. Among stepped transmissions, there are manual an automatic. Among automatic, there are those with power transmission interruption during shifting and other with powershifting, see Section 3.2.1.3 . Clutches and torque converters can also be part of models of main transmissions, see Sections 3.2.1.4 and 3.2.1.5. A stepped transmission, can be modelled e.g. as:

$$T_{out} = r \cdot T_{in} \cdot \eta_{CoggMeshes} - \Delta T_0 \cdot \text{sign}(\omega_{out}) ;$$

$$\omega_{out} = \frac{\omega_{in}}{r};$$

$$\text{where } r = r_1, r_2, \cdots r_N; \quad r \neq 0;$$

[3.1]

ΔT_0 is the "parasitic" or "load independent" losses, arising from oil, sealings and bearings. Eq [3.1] is not valid for neutral gear, because then there is no speed equation, but instead two torque equations: $T_{out} = -\Delta T_{0,out} \cdot \text{sign}(\omega_{out})$; and $T_{in} = \Delta T_{0,in} \cdot \text{sign}(\omega_{in})$;.

For any 1-dimensional transmission of rotational mechanical power between two rotating shafts, the total efficiency, $\eta_{total} = P_{out}/P_{in} = T_{out} \cdot \omega_{out}/(T_{in} \cdot \omega_{in})$;, is depending on operating condition. If

assuming a nominal ratio, r, the total efficiency can be decomposed in $\eta_{total} = \eta_T \cdot \eta_\omega$;, where $\eta_T = T_{out}/(r \cdot T_{in})$; and $\eta_\omega = \omega_{out}/(\omega_{in}/r)$;.

3.2.1.2.2 Distribution transmissions

The distribution to energy buffer and multiple axles and/or wheels can basically be done in two ways:

- Distribute in certain fractions of (rotational) speed. A (rotationally) rigid shaft between left and right wheel is one example of this. We find this in special vehicles, such as go-carts, and in more common vehicles when a differential lock is engaged. There are 3 shafts in such an axle: input to the axle and two outputs (to left and right wheel). The equations will be:

$$
\begin{aligned}
\omega_{in} &= \omega_{left}; \\
\omega_{in} &= \omega_{right}; \\
T_{in} &= T_{left} + T_{right};
\end{aligned}
\qquad [3.2]
$$

- Distribute in certain fraction of torque. This requires some type of planetary gear arrangement. A conventional (open) differential gear is one example of this, where the equations will be:

$$
\begin{aligned}
\omega_{in} &= \frac{\omega_{left} + \omega_{right}}{2}; \\
T_{left} &= T_{right}; \\
T_{in} &= T_{left} + T_{right};
\end{aligned}
\qquad [3.3]
$$

Generally speaking, the open differential is rather straight-forward to use in most vehicle dynamics manoeuvres: The speeds are given by vehicle motion (e.g. curve-outer wheel runs faster than curve-inner wheel, defined by vehicle yaw rate and track width). The torques are defined by the differential, as half of the propulsion torque at each side.

Also, a locked differential, it is generally more complex to model and understand in a vehicle manoeuvre. Here, the wheels are forced to have same rotational speed and, in a curve, that involves the tyre longitudinal slip characteristics. The solution involves more equations with shared variables.

So, open/locked differential is the basic concept choice. But there are additions to those: One can build in friction clutches which are either operated automatically with mechanical wedges or similar or operated by control functions. One can also build in electric motors which moves torque from one wheel to the other. However, the compendium does not intend to go further into these designs.

Part of the distribution transmissions are also shafts. If oscillations is to be studied, these has to be modelled with energy storing components:

- Rotating inertias or Flywheels ($J \cdot \dot\omega = T_{in} - T_{out}$;) and

- Elasticities, compliances or springs: ($\dot T = c \cdot (\omega_{in} - \omega_{out})$).

3.2.1.3   Powershifting transmissions

The most common powershifting transmission is using planetary gears and torque converter, see Figure 3-13. During 20100-2010, developments in mechatronics has enabled to leave out the torque converter and the planetary gears resulting in what often meant with powershifting transmissions, see concept in Figure 3-4. In practice, one can often manage with 2 clutches, and instead select different paths through gear wheels with synchronisers. An advanced design of powershifting transmission for a hybrid propulsion system is seen in Figure 3-5. A dummy sequence of shifting is simulated in Figure 3-6.
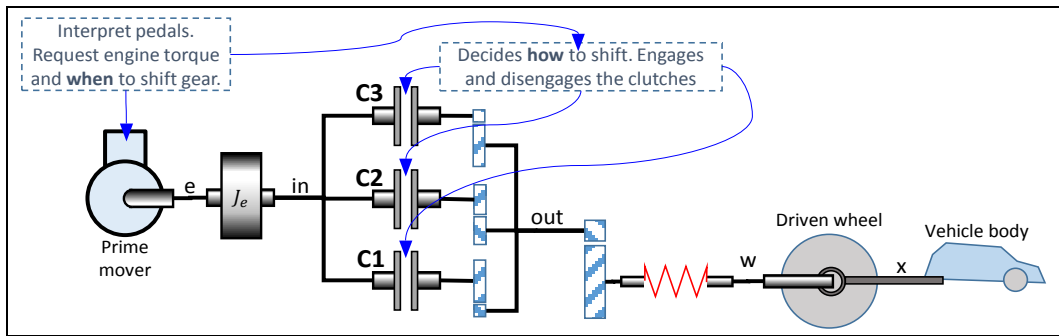
Figure 3-4: Conceptual design of powershifting transmission with 3 gears.
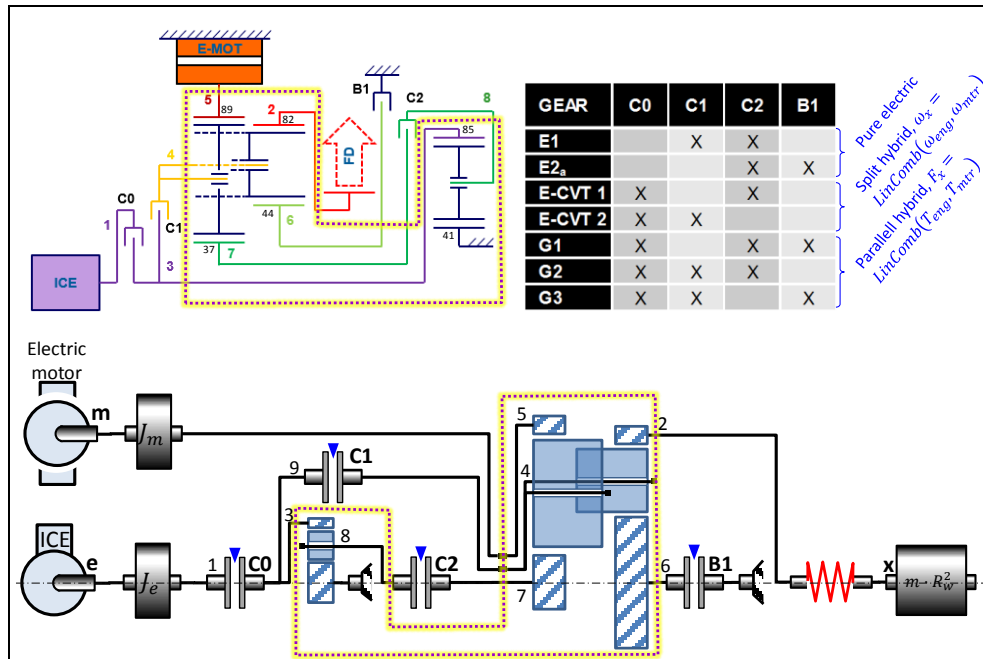

Figure 3-5: Hybrid propulsion system with powershifting, designed using planetary gears. Upper left: Design. Upper right: Gear/Clutch schedule. Lower half: Dynamic model.
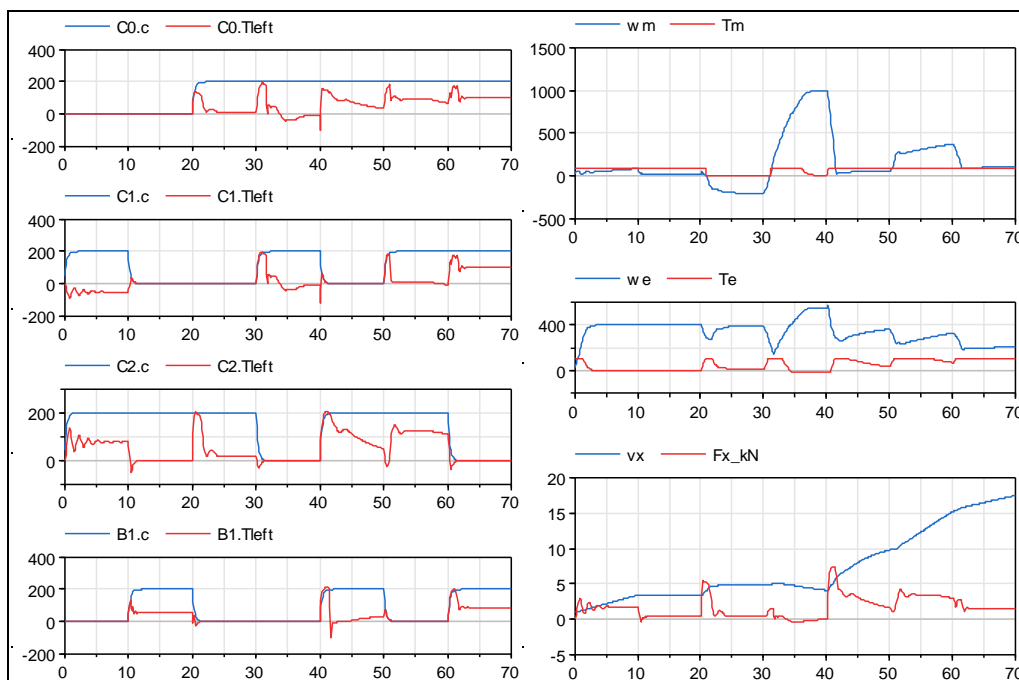

Figure 3-6: Simulation of the transmission in Figure 3-5 (with approximate clutch model from Eq [3.5]). Example sequence of shifts: Simply shift each 10th second, in order as in table in Figure 3-5.

3.2.1.4   Clutches and Brakes

In this content, clutches includes brakes as a special cases, characterised by that one of the clutch halves is not rotating. Clutches with dry friction characteristics are often difficult to model in dynamic systems since they introduce "discrete dynamics" by sticking and slipping. The general mathematical model of a controlled clutch is given in Eq[3.4]. Here, the interface variables are $T_{left}, T_{right}, \omega_{left}, \omega_{right}$ and c. The capability, c /[Nm], is an input signal. It tells the magnitude of torque in the case that clutch is slipping. In the model below, a discrete state variable, $slip = -1, 0 \; or + 1$, is introduced to model the discrete dynamics.

$$T_{left} = T_{right};$$
$$0 = \begin{cases} = T_{left} + c; & if \; slip = -1 \\ = \omega_{left} - \omega_{right}; & if \; slip = 0 \\ = T_{left} - c; & if \; slip = +1 \end{cases}$$
$$when \left(slip \equiv -1 \; AND \; when \; \omega_{left} > \omega_{right} \right): change \; slip \; to \; 0;$$
$$when \left(slip \equiv 0 \; AND \; when \; T_{left} < -c \right): change \; slip \; to - 1;$$
$$when \left(slip \equiv 0 \; AND \; when \; T_{left} > +c \right): change \; slip \; to + 1;$$
$$when \left(slip \equiv +1 \; AND \; when \; \omega_{left} < \omega_{right} \right): change \; slip \; to \; 0;$$

[3.4]

The clutch model is to be connected between surrounding components, which have shaft ends as connectors, see examples in Figure 3-8. The implementation can be almost as Eq [3.4]. But slightly different implementations is generally needed for different surroundings; energy dissipating/generating components (dampers/power sources), kinetic energy storing components (flywheels) or potential energy storing components (elasticities). The challenge is to handle that the set of state variables can change between the different discrete states. Modelling format and tools have to allow discrete state events and resetting of states when events occurs. For automatic transmissions, where there are several clutches involved, the implementation of the ideal model in Eq [3.4] can be very demanding.
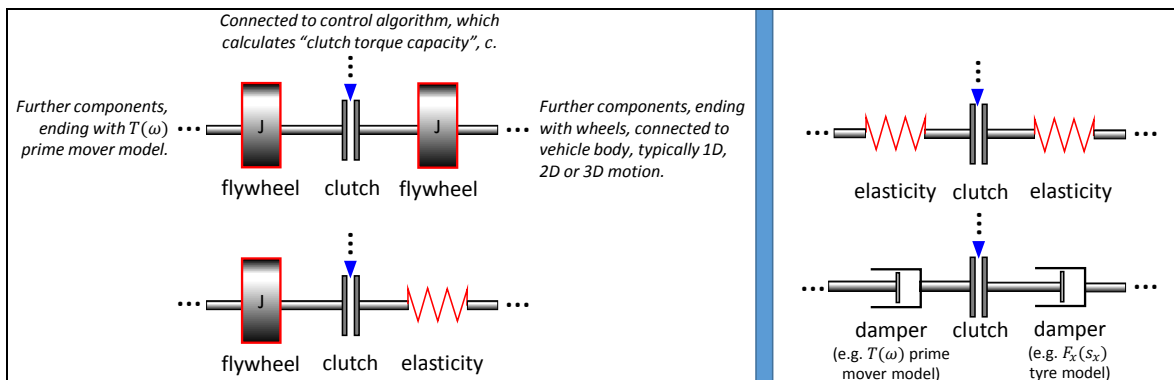
Figure 3-8: Examples of differently modelled surroundings of a clutch.


```
//Clutch:
if abs(slip) == 1 then der(T) = sign(slip)*der(cclu);
                  else w1 = wx; end if;

if pre(slip) == +1 and w1 < wx then      slip = 0;
elseif pre(slip) == -1 and w1 > wx then  slip = 0;
elseif pre(slip) == 0 and T > +cclu then slip = +1;
elseif pre(slip) == 0 and T < -cclu then slip = -1;
else                                     slip = pre(slip);
end if;

when slip == -1 or slip == +1 then
  reinit(T, slip*cclu);
end when;

//Spring:
der(T) = cspr*(wx-w2);
```

```
//Clutch and Spring:
der(T) = if T > cclu and w1 > w2 then +der(cclu)
elseif T < -cclu and w1 < w2 then -der(cclu) else cspr *(w1-w2);
```
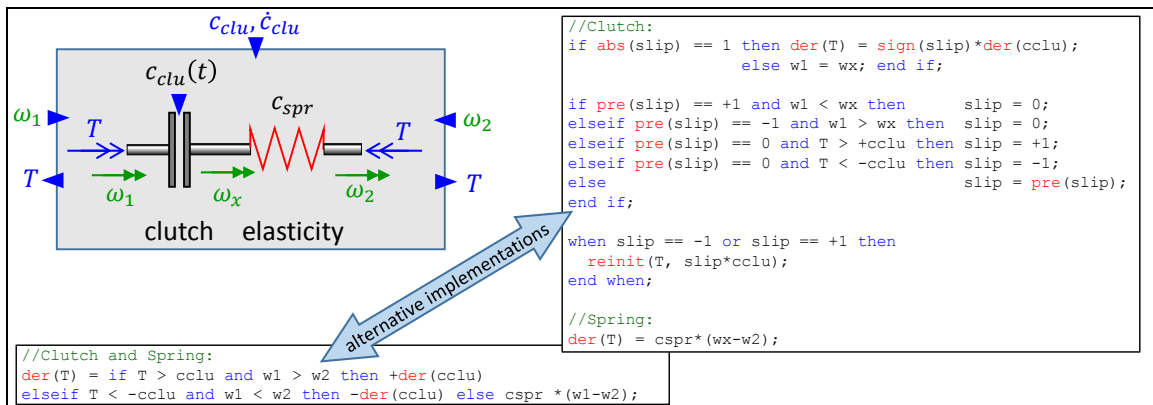
Figure 3-9: Model of clutch and spring in series, modelled so that speed is input from both sides.

3.2.1.4.1 Implementation as approximate clutch characteristics

A way around these problems is to use an approximate clutch model as in Eq [3.7]. The advantage is that it can handle any surrounding without leading to changing set of state variables. The drawback is that it has a trade-off between modelling the intended physics (Eq [3.7]) and the computational efficiency in simulation; the more $d \to \infty$, the closer to the intended model we come, but the simulation time will increase towards infinity. The approximation can be seen as putting a stiff dampers in direct series with an ideal clutch. There are also other approximations, which could be seen as putting a stiff spring with stiffness c in series with an ideal clutch. This will work if clutch is surrounded by inertias:

$$T_{left} = T_{right}; \quad and \quad \omega_{rel} = \omega_{left} - \omega_{right};$$

$$\frac{T_{left}}{c} \cdot sign(\omega_{rel}) =$$

$$= \begin{cases} = \min\left(\dfrac{1-\varepsilon}{\varepsilon} \cdot \dfrac{|\omega_{rel}|}{\omega_{nom}} \quad ; \quad 1 + \dfrac{\varepsilon}{1-\varepsilon} \cdot \left(\dfrac{|\omega_{rel}|}{\omega_{nom}} - 1\right)\right); & if \dfrac{|\omega_{rel}|}{\omega_{nom}} < 1 \\[4mm] = \max\left(\dfrac{1}{1 + \dfrac{\varepsilon}{1-\varepsilon} \cdot \left(\dfrac{\omega_{nom}}{|\omega_{rel}|} - 1\right)} \quad ; \quad \dfrac{\varepsilon}{1-\varepsilon} \cdot \dfrac{|\omega_{rel}|}{\omega_{nom}}\right); & else \end{cases}$$

[3.5]
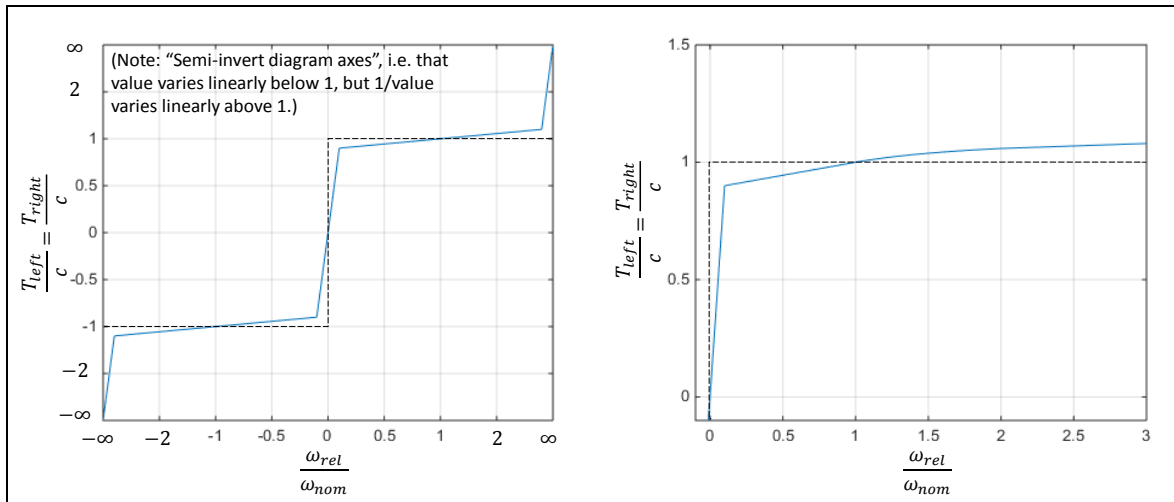
Figure 3-10: Example of approximation of clutch model. Strategies: ω_{nom}= typical slip speed of clutch, $\varepsilon \ll 1$. Dashed curve shows before approximation.

Figure 3-11 shows an example that the ideal and approximate models can give similar results with respect to torques and speeds. About computational efficiency, the ideal needs around 5 ms time step with Euler forward integration, while the approximate needs 100 times smaller time step. If better agreement than in Figure 3-11 is needed, ε needs to be reduced, which slows down the approximation even more. Note also that, for energy dissipation, the approximate model of course calculates a higher energy dissipation, since it assumes the clutch has to slip to transfer torque.

There are clutch models also in the standard Modelica (see Section 1.5.7.5) library, see Figure 3-12. Note that the library is built such that the "small inertia" is needed, which forces down computational efficiency during clutch slip.

Brakes, one-way clutches and backlashes often causes similar difficulties and can be modelled similarly as clutches.
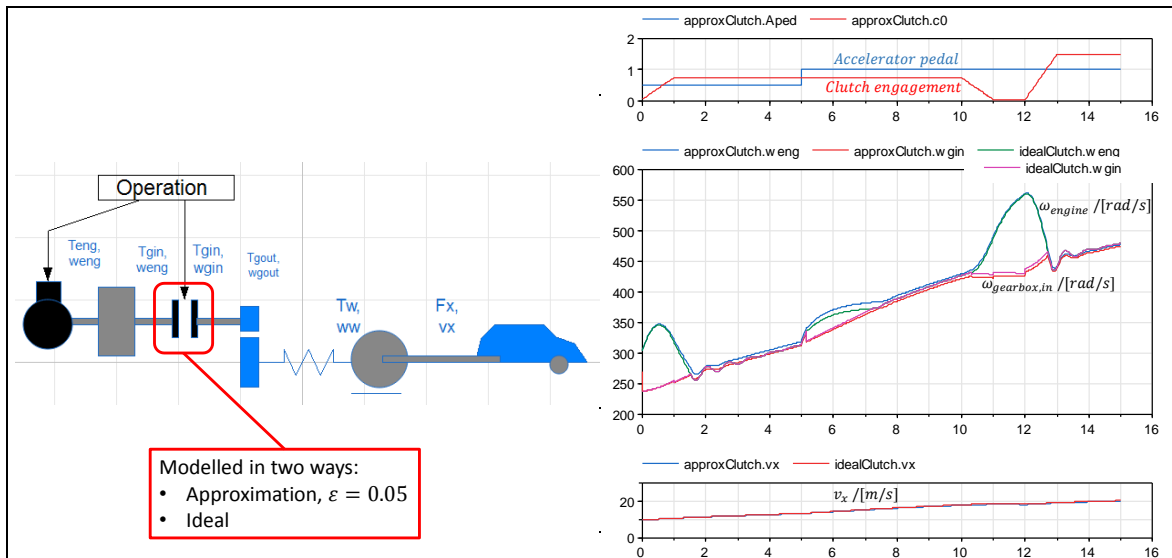
Figure 3-11: Example with clutch, modelled in two ways.

(Inputs to "eninge" and "clutch" governed by equations)
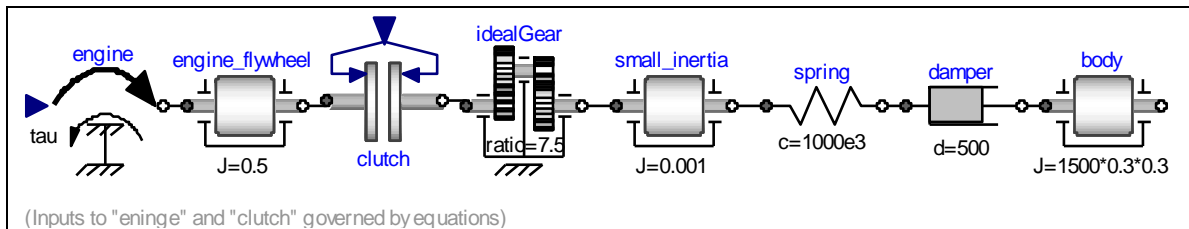
Figure 3-12: Similar example, but built with standard Modelica library "Modelica.Mechanics.Rotational".

3.2.1.5 Hydrodynamic torque converters

Hydrodynamic torque converters serve almost same purpose as a clutch, but it is much less complex to model as a member of a dynamic system. Such converters have a pump in input side and turbine on output side. They can operate with substantial slip, and when slip, there is a torque amplification, which leads to that a vehicle with converter have typically good acceleration performance and driveability also without the corresponding lowest gear needed on same vehicle without converter.

The following model gives the steady state characteristics of a hydrodynamic torque converter. Steady state characteristics are often enough, but combined with that hydrodynamic torque converters often are possible to look-up with a clutches which is mounted parallel to impellers.

$$\frac{T_{out}}{T_{in}} = \mu(v); \quad \frac{T_{in}}{\omega_{in}^2} = \lambda(v); \quad where\ \mu\ and\ \lambda\ are\ functions\ and\ v = \frac{\omega_{out}}{\omega_{in}};$$

But if locked-up: $\frac{T_{out}}{T_{in}} = 1; \quad and \quad \frac{\omega_{out}}{\omega_{in}} = 1;$

[3.6]

The moment capacity, λ, is often given on a dimensionless form
$\lambda = T_{in}/(\omega_{in}^2 \cdot OilDensity \cdot OuterRadius^5)$.
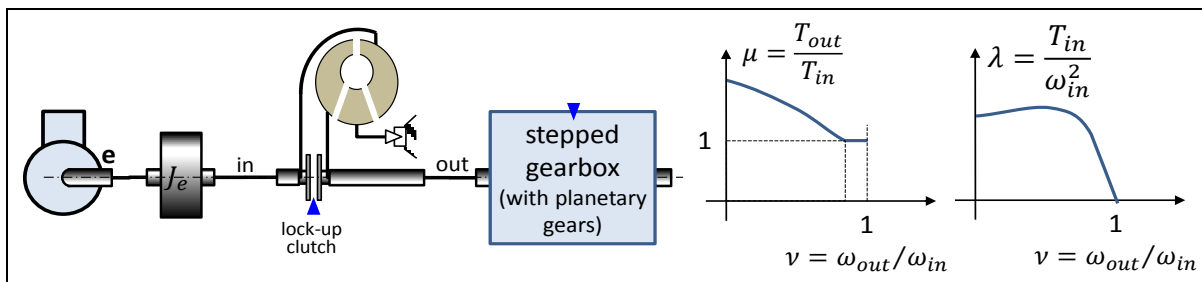
Figure 3-13: Left: Traditional automatic transmission. Right: Conceptual curves of the torque converter.

3.2.1.6 Energy storages

Fuel tank and battery are two examples of energy storages. An "energy buffer" often refers to an energy storage that can not only be emptied (during propulsion), but also refilled by regenerating energy from the vehicle during deceleration. A fuel tank is an energy storage, but not an energy buffer. Also, a battery which can only be charged from the grid, and not from regenerating deceleration energy, is not an energy buffer.

Energy buffers in vehicles are today often electro-chemical batteries. However, other designs are possible, such as flywheels and hydrostatic accumulators. A simple model of a buffer is as follows:

$$\dot{E} = \begin{cases} = (P_{in} - P_{out}) \cdot \eta_{charge}; & for\ P_{in} > P_{out}; \\ = (P_{in} - P_{out})/\eta_{use}; & else; \end{cases}$$

$$where\ P_{in} = T_{in} \cdot \omega_{in};\ and\ P_{out} = T_{out} \cdot \omega_{out};$$

[3.7]

Including how the buffer is connected, one more equation can be found: Typically $\omega_{in} = \omega_{out}$; or $T_{in} = T_{out}$;.

The model uses stored energy, E. For batteries one often uses state of charge, SoC, instead. Conceptually, $SoC = E/E_{max}$;, where E_{max} is a nominal maximum charge level.

A first approximation of the efficiencies, can be $\eta_{charge} = \eta_{use} = constant < 1$, but typically the efficiency is dependent of many things, such as $P_{in} - P_{out}$. The model above does not consider any leakage when buffer is "resting": $P_{in} = P_{out}$.

3.2.2 Traction diagram

The force generated in the prime mover is transmitted through a mechanical transmission to the wheel which then generates the propulsive forces in the contact patch between tyre and road. In an electric in-wheel motor, the transmission can be as simple as a single-step gear. In a conventional vehicle it is a stepped transmission with several gear ratios (i.e. a gearbox). Then, the drivetrain can be drawn as in Figure 3-14. The torque and rotational speed of the engine is transformed into force and velocity curves via the mechanical drivetrain and driven wheel. The result is a Traction diagram. The transformation follows the following formula, if losses are neglected:

$$F = ratio \cdot \frac{T}{WheelRadius}; \quad and \quad v = WheelRadius \cdot \frac{\omega}{ratio};$$

[3.8]

A traction diagram for a truck is given in Figure 3-15, which also shows that there will be one curve for each gear.

Losses in transmission can be included by using equations including loss models for transmission, such as:

$$F = \eta_T \cdot ratio \cdot \frac{T}{radius}; \ where\ \eta_T \leq 1;$$

$$v = \eta_\omega \cdot radius \cdot \frac{\omega}{ratio}; \ where\ \eta_\omega \leq 1;$$

$$where \quad \eta_T \cdot \eta_\omega = \eta_{total} = \frac{P_{vehicle}}{P_{engine}} = \frac{F \cdot v}{T \cdot \omega} \leq 1$$

[3.9]

This will basically move the curves in the first quadrant downwards and to the left.

Tyre rolling friction is a loss mechanism, which on its own yields $\eta_\omega = 1$ and $\eta_T < 1$. Tyre longitudinal slip is a loss mechanism, which on its own yields $\eta_\omega < 1$ and $\eta_T = 1$. See Section 2.4.
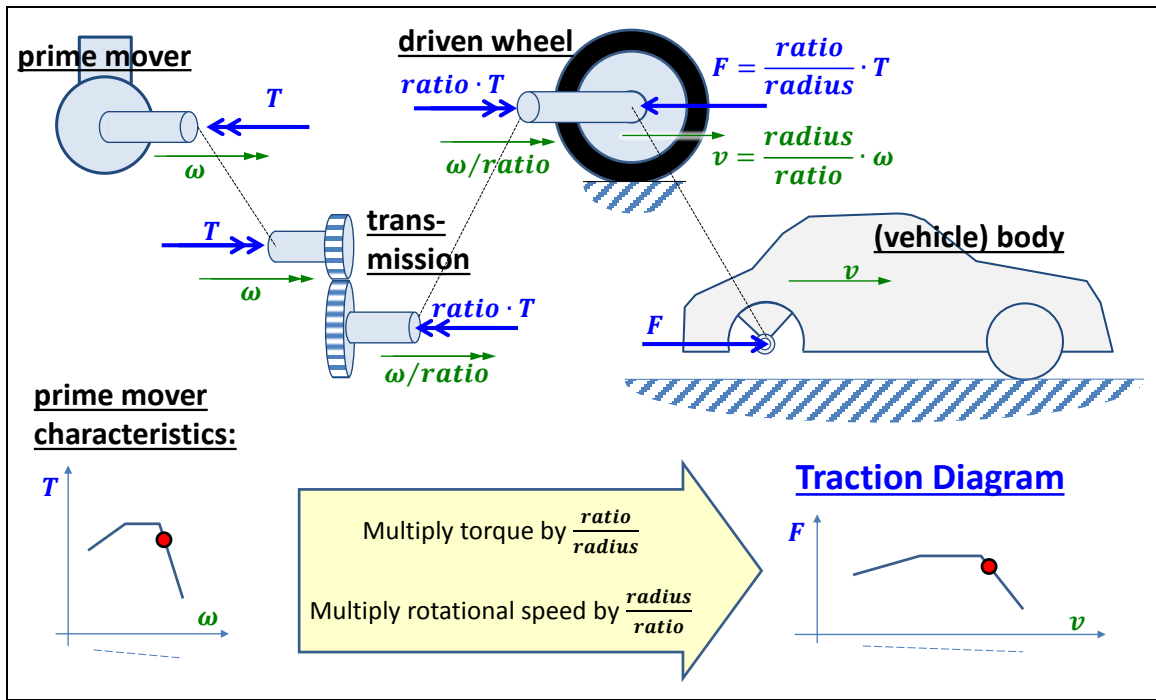
Figure 3-14: Construction of Traction Diagram, i.e. diagram for transmission of torque to longitudinal force on vehicle.
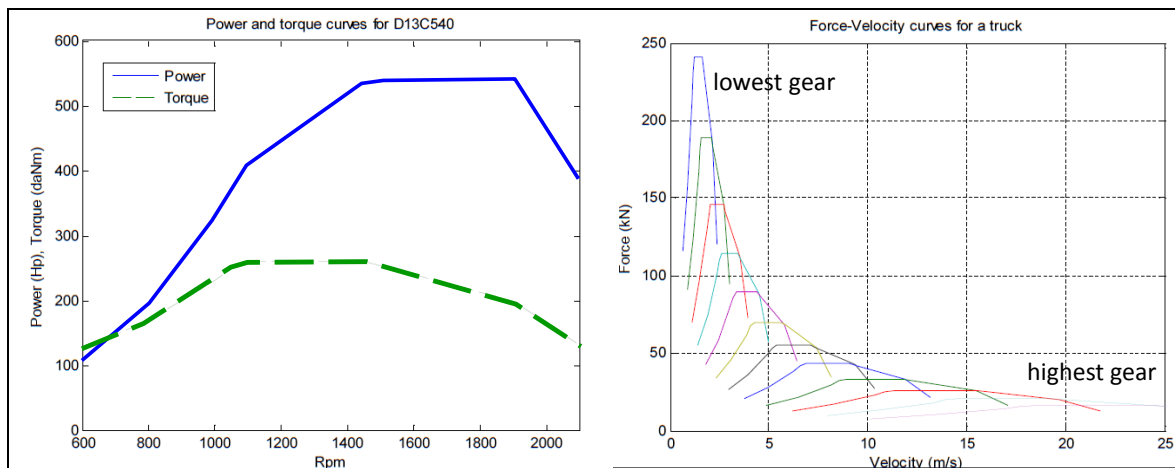
Figure 3-15: Example of engine map and corresponding traction diagram map from a truck. (D13C540 is an I6 diesel engine of 12.8-litre and 540 hp for heavy trucks.)

A traction diagram is a kind of one degree of freedom graphical model. The diagram can be extended with, e.g., the longitudinal force from the brake system.

3.2.3 Driving Resistance

From studying Figure 3-15 one could extrapolate that a very low transmission ratio, i.e., a very high gear, we would enable almost infinite speed. We know that this is not possible. Something obviously limits the top speed: the limit comes from "driving resistance". As presented in Chapter **2**, there are tyre rolling-resistance forces and aerodynamic driving-resistance forces. Also, there can be an additional resistance force to be considered when going uphill: the grade or gravitational load on the vehicle. This resistance can also be negative, i.e. act as propulsion down-hill. The formula for driving resistance becomes as follows, using Equation **[2.51]**. Notation *f* means rolling resistance coefficient.

$$F_{resistance} = m \cdot g \cdot \sin(\varphi) + f \cdot m \cdot g \cdot \cos(\varphi) + \frac{1}{2} \cdot c_d \cdot \rho \cdot A \cdot \left(v_x - v_{wind,x}\right)^2 \qquad \boxed{[3.10]}$$

Superimposing the external loads on the Traction Diagram allows us to identify when the "demands" can be met by the "supply". As seen in Figure 3-16, the combination of external resistance loads and the internally generated drive forces can be presented on the same figure. The resulting intersection of supply (prime mover) and demand (driving resistance) identifies the top speed of the vehicle. These results hold only for steady state (no acceleration) conditions.
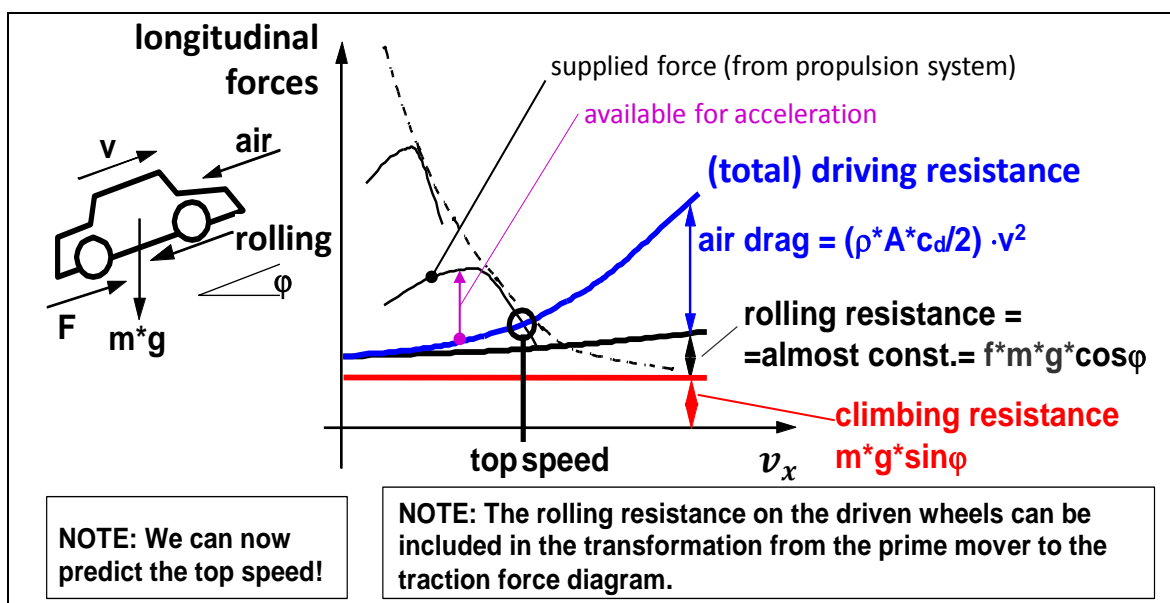
Figure 3-16: Top speed can be found from Traction diagram with Driving Resistance curves. Head wind speed, $v_{wind,x}$, is assumed to be zero. Note that "rolling" actually is a moment loss on the wheels, why it is more correct to let it influence the "supplied force curve" for driven axles and the driving resistance curve for the non-driven axles, see Figure 3-20.

As seen in Figure 3-16, the acceleration can be identified as a vertical measure in the traction diagram, divided by the mass. However, one should be careful when using the traction diagram for more than steady state driving. We will come back to acceleration performance later, after introducing the two effects "Load transfer" and "Rotating inertia effect".

3.2.3.1   Losses due to lateral tyre slip

(Section 3.2.3.1 might require some studying of Chapter 4 for full understanding.)

There are more driving-resistance effects than covered in Equation [3.10]. One example is that none-Ackermann steering geometry (toe or parallel steering on an axle, or two non-steered axles).

Another effect, which appears also for Ackermann steering geometry, is that power is lost due to lateral axle slip. Now, we use the same simple model as in Figure 4-25, but additionally use $a_y = v_x/\omega_z$; and define power losses P_{loss} as sliding velocity counterdirected to force:

$$P_{loss} = -F_{fy} \cdot v_{fy} - F_{ry} \cdot v_{ry} = -F_{fy} \cdot s_{fy} \cdot v_x - F_{ry} \cdot s_{ry} \cdot v_x;.$$

We also define a Cornering Reistance Coefficient, f_{CRC}:

$$f_{CRC} = \frac{P_{loss}/v_x}{m \cdot g} = \frac{m \cdot a_y^2}{g} \cdot \left(\left(\frac{l_f}{L}\right)^2 \cdot \frac{1}{C_r} + \left(\frac{l_r}{L}\right)^2 \cdot \frac{1}{C_f} \right);$$

f_{CRC} is such that the extra propulsion force needed is $= f_{CRC} \cdot m \cdot g$

[3.11]

During a transport operation, the cornering in each time instant is typically described by two variables, e.g. (v_x, R_p), but only the combined scalar measure $a_y = v_x^2/R_p$ influences f_{CRC}. Hence we can plot the following graph:

Figure 3-17: Left: Cornering Resistance Coefficient. Right: Required steering angle.
Vehicle data: $m = 1500\ kg$; $L = 3$; $l_f = 1.25$; $C_f = 60\ [kN/s]$; $C_r = 80\ [kN/1]$.

Notes:

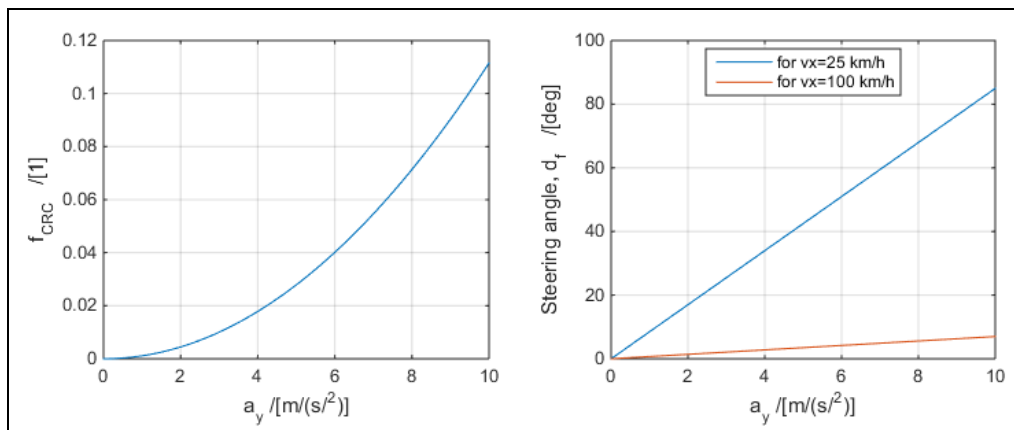- The model used above is not advanced enough to differ between which axle is driven. For such purpose one would need e.g. the model in Figure 4-21.
- Normal driving is often below 2 or 3 m/s^2, so the coefficient typically stays below 0.01. However, the influence on energy consumption, during such "maximum normal" negotiation of corners, is still of the same magnitude as rolling resistance coefficient.
- For ideally tracking axles, see Section 4.2.5, $C_f \to \infty$ and $C_r \to \infty$, which gives that $f_{CRC} \to 0$ and consequently no power loss and no required propulsion force. So, high cornering stiffness is fuel efficient when cornering.

3.2.4　Top speed *

*Function definition: **Top speed** is the maximum longitudinal forward speed the vehicle can reach and maintain on level and rigid ground without head-wind.*

The top speed can be read out from a traction diagram with driving resistance, see Figure 3-16. Top speed is the speed where the sum of all driving resistance terms is equal to the available propulsion forces.

3.2.5　Starting with slipping clutch

As seen in previous traction diagrams, there is no available positive propulsion force at zero speed. This means that the diagram can still not explain how we can start a vehicle from stand-still.

The concepts in Figure 3-14 were used to create the force-velocity diagram in

Figure 3-18. It shows the smooth curve of a Continuous Variable ratio Transmission (CVT) in comparison to the stepped transmission. The CVT is the ideal situation for the engine since it can always let the engine work at a maximum power or minimum fuel consumption (minimum for the momentarily required power). If the CVT has unlimited high ratio, it can actually have a non-zero propulsion force at zero vehicle speed. Without losses, this force would be infinite, but in reality it is limited, but still positive, so the vehicle can start from stand-still.

A stepped transmission, as well as a CVT with limited ratio range, instead needs a clutch to enable starting from vehicle stand-still. This is shown in Figure 3-18. The highest force level on each curve can be reached at all lower vehicle speeds, because the clutch can slip. It requires the clutch to be engaged carefully to the torque level just below the maximum the engine can produce. In traditional automatic transmissions the slipping clutch is replaced with a hydrodynamic torque converter, to enable start from stand-still.
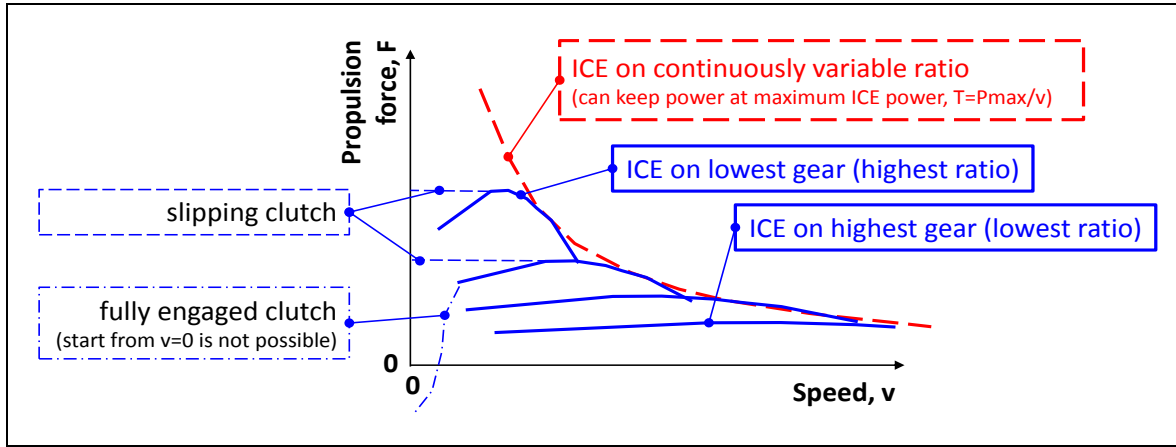
Figure 3-18: Force/Speed Curves for a Multiple Gear Transmission and for CVT.

3.2.6   Steady state load distribution

The vehicle performance discussed previously does not rely on knowing the distribution of (vertical) load between the axles. To be able to introduce limitations due to road friction, this distribution must be known. Hence we set up the free-body diagram in Figure 3-19.
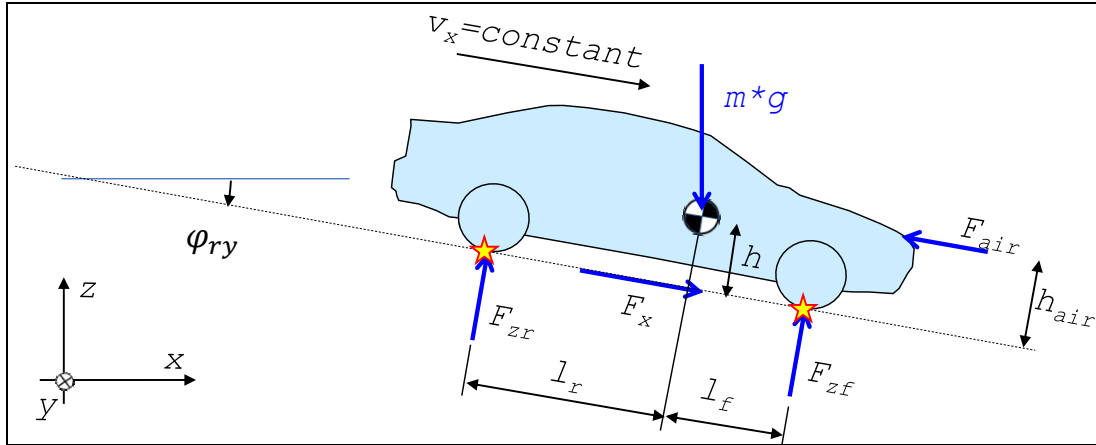
Figure 3-19: Free Body Diagram for steady state vehicle. With ISO coordinate system, the road gradient is positive when downhill. (Rolling resistance force on non-driven axles is included in F_x.)

From the free-body diagram we can set up the equilibrium equations as follows and derive the formula for load on front and rear axle:

Moment equilibrium, around rear contact with ground:
$$m \cdot g \cdot \left(l_r \cdot \cos(\varphi_{ry}) + h \cdot \sin(\varphi_{ry})\right) - F_{air} \cdot h_{air} - F_{zf} \cdot (l_f + l_r) = 0; \Rightarrow$$

$$\Rightarrow F_{zf} = m \cdot g \cdot \frac{l_r \cdot \cos(\varphi_{ry}) + h \cdot \sin(\varphi_{ry})}{l_f + l_r} - F_{air} \cdot \frac{h_{air}}{l_f + l_r}$$

Moment equilibrium, around front contact with ground:
$$F_{zr} \cdot (l_f + l_r) - m \cdot g \cdot \left(l_f \cdot \cos(\varphi_{ry}) - h \cdot \sin(\varphi_{ry})\right) - F_{air} \cdot h_{air} = 0; \Rightarrow$$

$$\Rightarrow F_{zr} = m \cdot g \cdot \frac{l_f \cdot \cos(\varphi_{ry}) - h \cdot \sin(\varphi_{ry})}{l_f + l_r} + F_{air} \cdot \frac{h_{air}}{l_f + l_r}$$

[3.12]

For most vehicles and reasonable gradients one can neglect $h \cdot \sin(\varphi_{ry})$ since it is $\ll |l_f \cdot \cos(\varphi_{ry})| \approx |l_r \cdot \cos(\varphi_{ry})|$.

3.2.7   Friction limit

With a high-powered propulsion system, there is a limitation to how much the vehicle can be propelled, due to the road friction limit. It is the normal load and coefficient of friction, which limits this. For a vehicle which is driven only on one axle, it is only the normal load on the driven axle, $F_{z,driven}$, that is the limiting factor:

$$F_x = \min\left(F_{x,PropSyst} \; ; \; \mu \cdot F_{z,driven}\right) \qquad \text{[3.13]}$$

One realises, from Figure 2-11, that the rolling resistance on the driven axle works as a torque loss and that the road friction limitation will be limiting $T_{eng} \cdot ratio - e \cdot F_{z,driven}$ rather than limiting $T_{eng} \cdot ratio$. Expressed using the rolling resistance coefficient, f_{roll}, gives:

$$F_x = \min\left(F_{x,PropSyst} \; ; \; \mu \cdot F_{z,driven}\right) = \min\left(\frac{T_{eng} \cdot ratio}{radius} - f_{roll} \cdot F_{z,driven} \; ; \; \mu \cdot F_{z,driven}\right) \qquad \text{[3.14]}$$

This is shown in the traction diagram in Figure 3-20, where it should also be noted that the rolling resistance curve only consists of the rolling resistance on the non-driven axles. See also Figure 2-11.
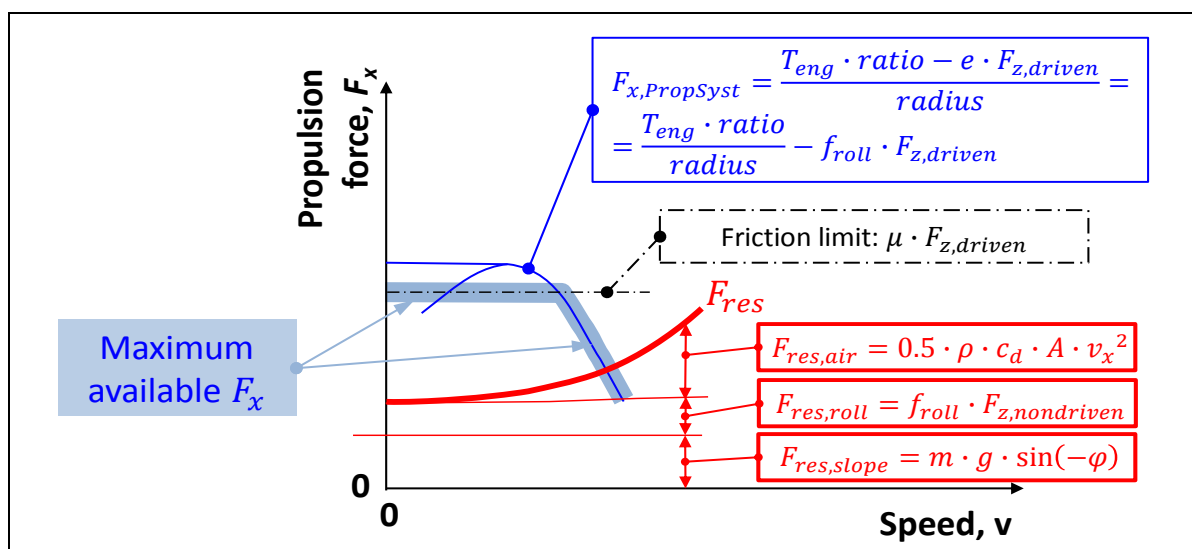
Figure 3-20: Traction diagram with Road Friction limitation and Driving Resistance curves.

3.2.8   Uphill performance

3.2.8.1   Start-ability *

*Function definition: **Start-ability** is the maximum grade that a vehicle is capable to start in and maintain the forward motion at a certain road friction level and a certain load. (Reference (Kati, 2013))*

Figure 3-21 shows how we find the start-ability in the traction diagram. There are two phenomena that can limit start-ability: propulsion system or road friction. Also, in each case, we can theoretically reach somewhat higher start-ability by allowing clutch or tyre to slip. However, in practice the start-ability has to require "forward motion without significant slip in clutch or tyre", because there will be a lot of wear and heat in the slipping clutch or tyre. Hence, the lower curves in Figure 3-21 are used. The reduction is however very small, since the resistance curves does not change very much during this small speed interval (the resistance curves in the figure have exaggerated slope; the air resistance can typically be neglected for start-ability).

However, the energy loss (heat, wear) in clutch and tyre should be limited also **during the starting sequence**. This can limit the start-ability more severely than the slope of the resistance curves, but it cannot be shown in the traction diagram, since it is limited by energy losses in clutch or tyre, which is a

time integral of $T \cdot \omega_{clutch}$ and $T_{wheel} \cdot \omega_{wheel}$. There can also be quite other limitations of start-ability, such as deliberately limited engine torque at low gears, to save drive shafts.
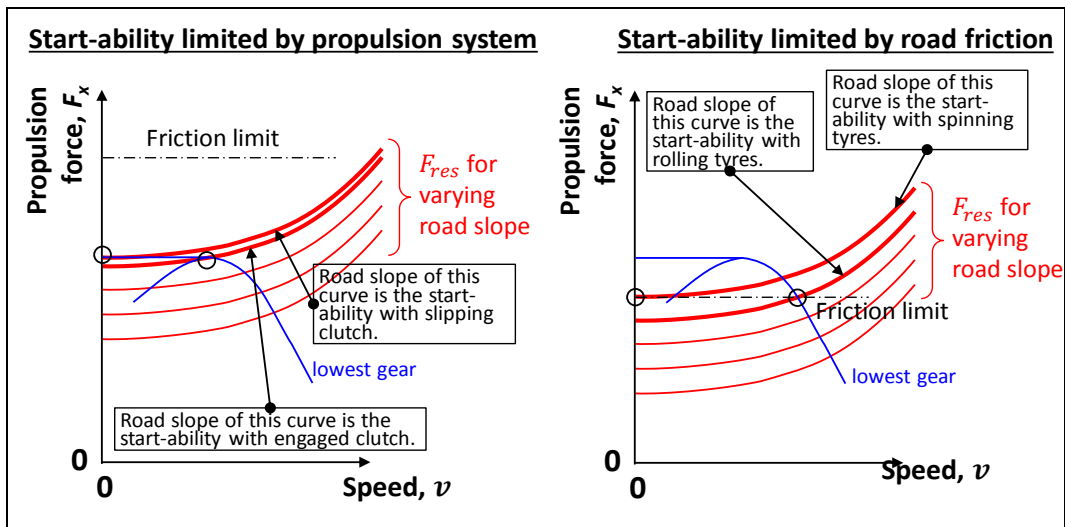
Figure 3-21: How Start-ability is read-out from Traction diagram.

3.2.8.2   Grade-ability *

*Function definition: **Grade-ability** is the maximum grade that a vehicle is capable to maintain the forward motion on an uphill road at a certain constant speed, at a certain road friction level and with a certain load. (from Reference (Kati, 2013))*

Figure 3-22 shows how we find the start-ability in the traction diagram. For vehicles with high installed propulsion power per weight, the road friction can be limiting, but this is not visualised in Figure 3-22. Since the speeds are higher than for start-ability, the air resistance cannot be neglected.
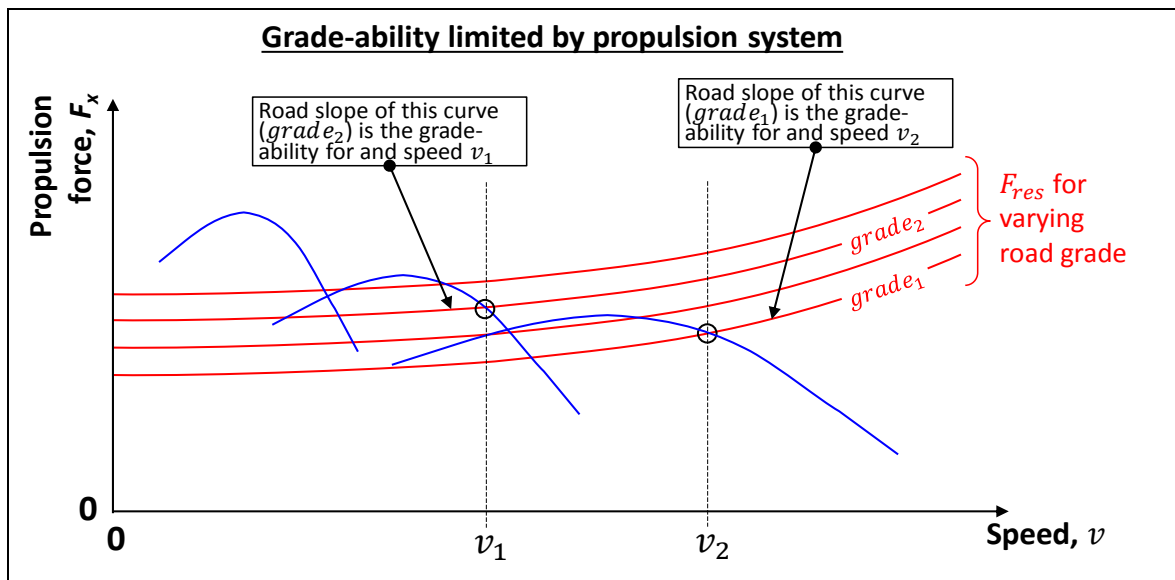
Figure 3-22: How Grade-ability is read-out from Traction diagram.

3.2.8.3   Down-grade holding capability

*Function definition: **Down-grade holding capability** is defined as the maximum down-grade in which the vehicle with certain weight is able to maintain a certain speed without using friction brakes.*

The function is typically of interest for heavy trucks and certain typical certain weight and certain speed is payload corresponding to maximum allowed weight and 80 km/h downhill.

The function is defined assuming there are clear friction brakes and other brakes, where the other brakes are typically engine brake and retarders. For newer vehicle concepts having electric

propulsion, also regenerative braking via reversed electric propulsion motors can be discussed to be allowed. However, because sometimes the energy storage will be full so that regenerative braking cannot be applied. Also, a small energy storage will have a limited downhill length, which might call for also prescribing a certain downhill distance.

3.2.8.4 Towing capacity *

Function definition: **Towing capacity** *is the maximum vehicle-external longitudinal force the vehicle can have on its body and start and maintain a certain forward speed at a certain road friction and a certain up-hill gradient.*

The driving situation for defining towing capacity is similar to the one for defining grade-ability. Towing capacity describes how much load the vehicle can tow, P_x in Figure 3-23, on a certain up-hill gradient. Since towing a load is more relevant as part of a longer transport mission, it is normally also for a particular constant speed, typically in range 80 to 100 km/h. Since the speed is that large, the air resistance may not be neglected. It is also important consider air resistance of the trailer and that axle loads can change, which changes both friction limitation and rolling resistance. A free-body diagram is shown in Figure 3-23. It is noticeable, that there can also be an additional air resistance of the trailer which will influence in a test of Towing capacity.

For pure off-road vehicles and agriculture tractors, the term "towing" can mean the maximum pulling force at very low forward speeds at level ground. This is related but different to the above described towing capacity for road vehicles.
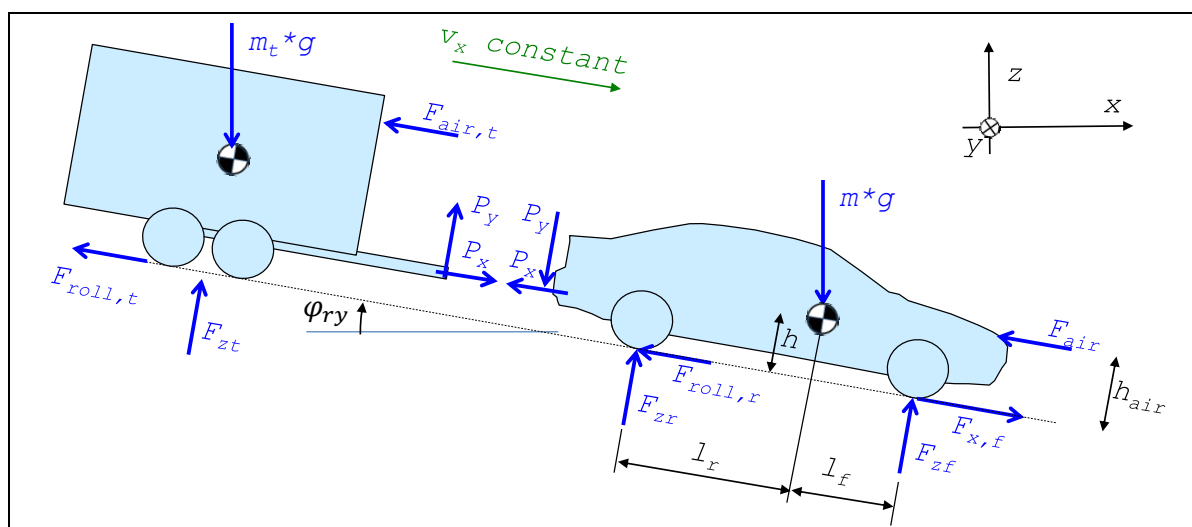
Figure 3-23: Towing Loads. The towing vehicle is front axle driven.

3.3 Functions over longer events

Functions as fuel or energy consumption and emissions are relevant only over certain but longer periods of driving, typically some seconds (typically ≥10 s) to hours of driving. There are different ways of defining such driving events.

3.3.1 Vehicle operation over longer events

The heading of this section, "vehicle operation", refers to how "all except the vehicle", e.g. road, traffic, driver and payload. The overall idea is to model the vehicle operation as *independent of the vehicle*, so that different vehicles, or various designs or configurations of a certain vehicle, can be compared in a fair way.

3.3.1.1 Driving cycles

One way to model vehicle operation is a so called driving cycle; where the relevant variables are pre-scribed as function of time. At least on defines speed as a function of time. Examples of commonly used driving cycles are given in Figure 3-24 and Figure 3-25. In addition, it can also be relevant to give road

inclination as function of time. Engine temperature and selected gear as functions of time may also be defined. For hybrid vehicles, the possibility to regenerate energy via electric machines is limited in curves, so curvature radius can also be prescribed as function of time. For heavy vehicles, the weight of transported goods can be another important measure to prescribe.
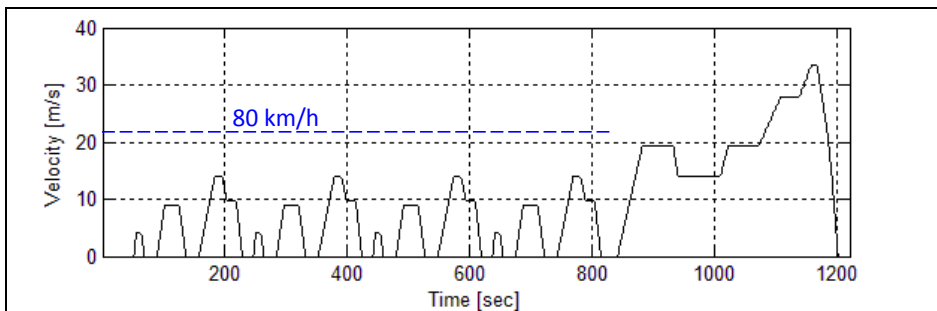
Figure 3-24: New European Driving Cycle (NEDC). From (Boerboom, 2012)
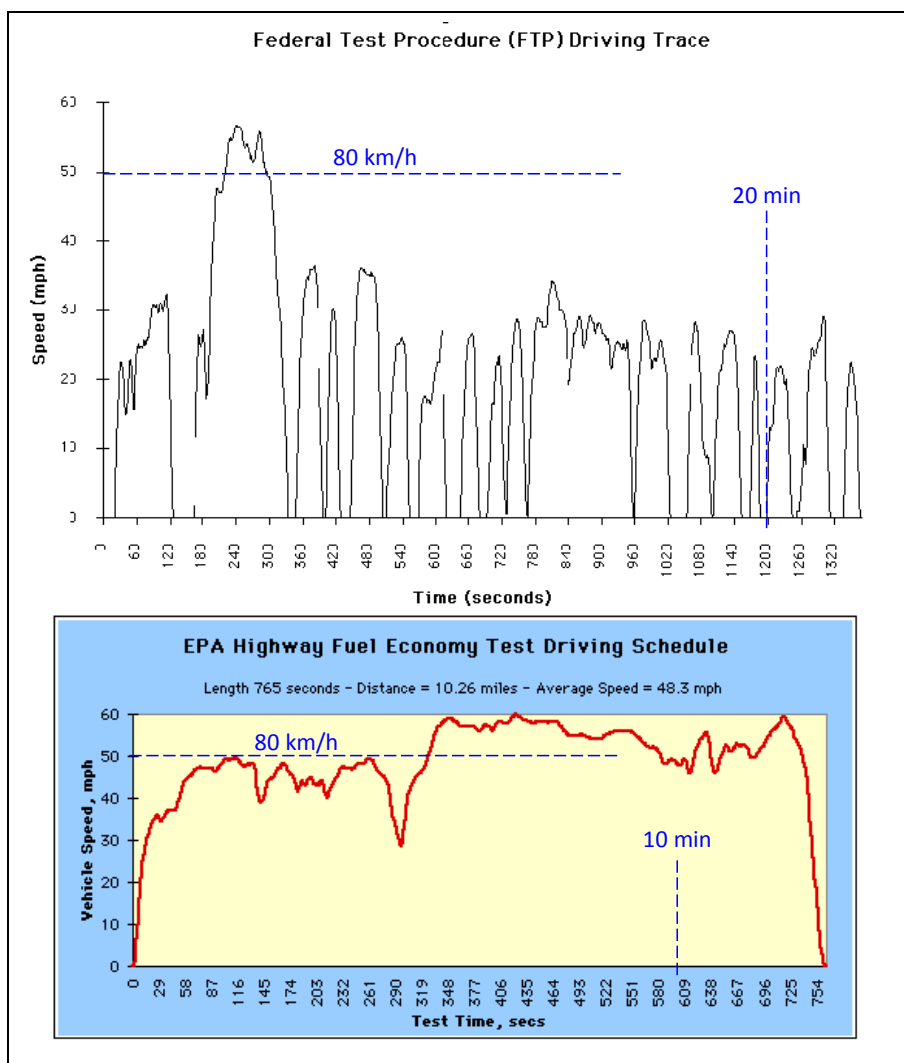
Figure 3-25: Top: FTP cycle from http://www.epa.gov/oms/regs/ld-hwy/ftp-rev/ftp-tech.pdf. Bottom: HFTP cycle from http://www.epa.gov/nvfel/methods/hwfetdds.gif.

FTP and HFTP are examples of cycles derived from logging actual driving, mainly used in North America. NEDC is an example of a "synthetically compiled" cycle, mainly used in Europe. Worldwide harmonized Light duty driving Test Cycle (WLTC) is a work with intention to be used world-wide, see Figure 3-26. WLTC exists in different variants for differently powered vehicle [power/weight].
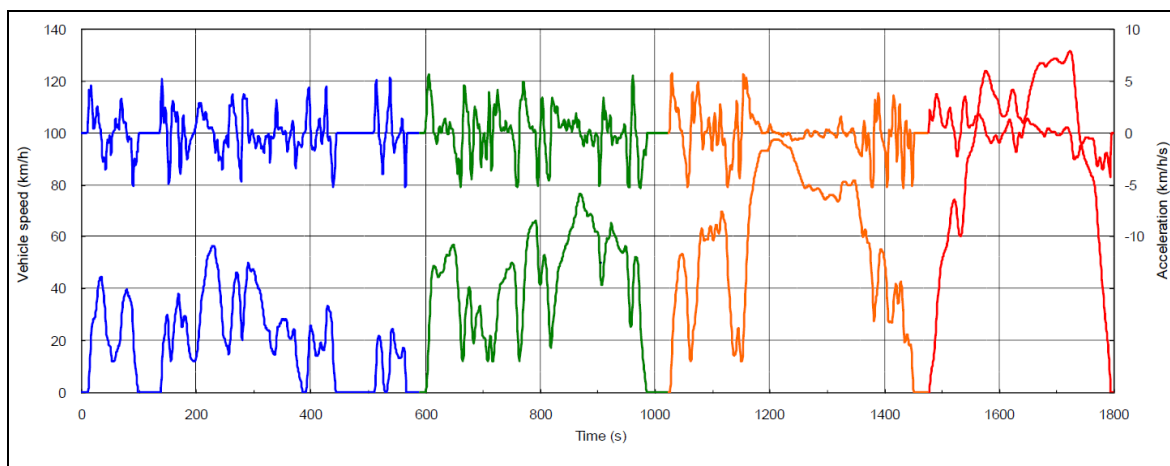
Figure 3-26: WLTC cycle from http://www.unece.org.

3.3.1.2   Driving pattern

A driving cycle can be condensed into a Driving pattern, i.e. a 2-dimensional function of speed and acceleration, as shown in Figure 3-27. Note that the chronological order is no longer represented in such representation; it is not a dynamic model. Figure 3-27 shows simply a scatter plot of time-sampled combinations of speed and acceleration. Using the same diagram axis, such information can also be shown as durations (in seconds or fractions of total time or frequency). A Driving pattern can only be combined with a steady state model of the vehicle, such as "fuel consumption=function(speed, acceleration)", as opposed to a dynamic model of the vehicle. The Driving pattern itself includes the driver, so no driver model is needed.

Driving patterns can use more than 2 dimensions, such as [speed, acceleration, road gradient]. In principle, they can also use less than 2 dimensions, maybe only [speed]. The (steady state) vehicle model has to reflect the corresponding dimensions.
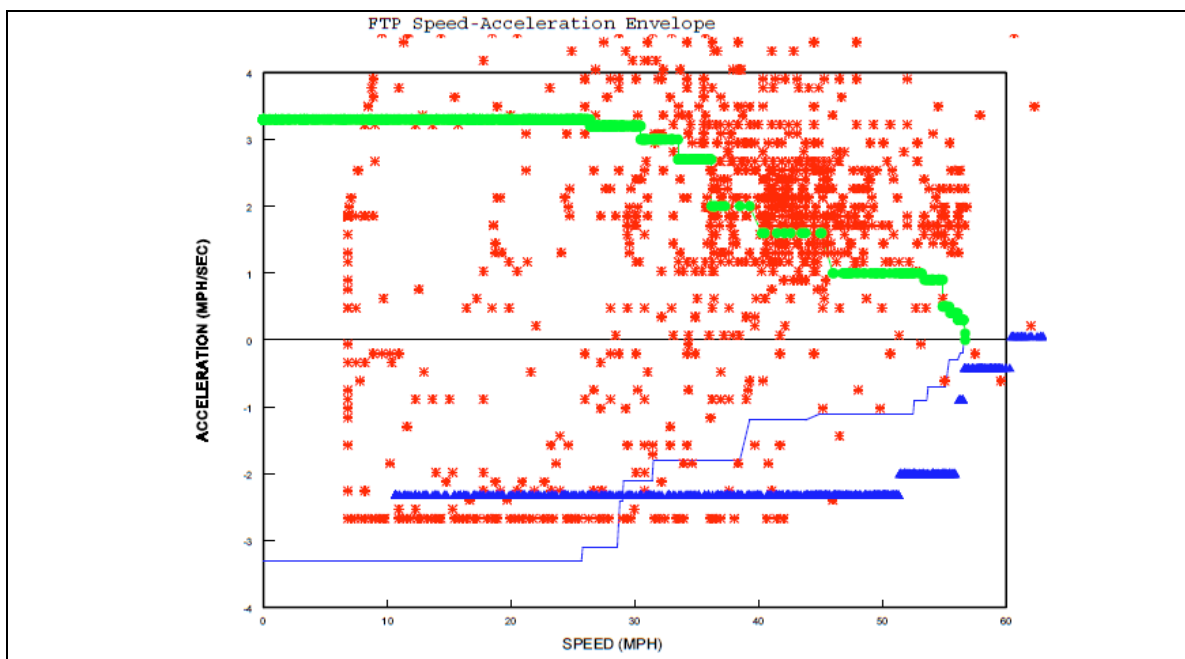
Figure 3-27: FTP cycle converted to a Driving pattern, i.e. a distribution of operating duration in speed and acceleration domain. From http://www.epa.gov/oms/regs/ld-hwy/ftp-rev/ftp-tech.pdf.

3.3.1.3   Transport task/Operating cycle

Desired speed, road inclination, weight of transported goods etc. are defined in position rather than time. For stops along the route, the stop duration or departure time has to be separately defined. This

is a more advanced and realistic description of the vehicle usage. It can be extended to include operation at stand-still, e.g. idle and loading/unloading cargo.

Simulation of such vehicle usage require some kind of driver model. A consequence is that different driver models will give different results, e.g., different fuel consumption due to different driver preferred acceleration. Hence, the driver model itself can be seen as a part of the vehicle usage definition.

3.3.2 Rotating inertia effects

In Figure 3-16 it was shown that the acceleration cannot be found directly as a force difference (distance between curves) divided by vehicle mass. This is because the Traction Diagram does not contain any dynamics, and dynamics are more complicated than simply accelerating the vehicle mass. The phenomenon that occurs is referred to here as "rotating inertia effect". The rotating part of the propulsion system, e.g. engine and wheels, must be synchronically accelerated with the vehicle mass. This "steals" some of the power from the propulsion system. This affects the required propulsion force when following accelerations in a driving cycle.

Consider a wheel rolling which is ideally rolling (no slip), with a free-body diagram and notations as in Figure 3-28. Setting up 2 equilibrium equations and 1 compatibility equation gives:

$$\begin{aligned} m \cdot \dot{v} &= F; \\ J \cdot \dot{\omega} &= T - F \cdot R; \\ v &= R \cdot \omega \Rightarrow \dot{v} = R \cdot \dot{\omega}; \end{aligned}$$

[3.15]
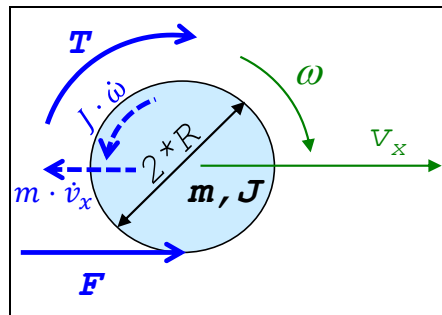
Figure 3-28: Rolling wheel

Assume that we know torque T and want to compare this with the situation without rotational inertia:

$$m \cdot \dot{v} = \frac{T}{R}; \quad and \quad F = \frac{T}{R};$$

[3.16]

Then we use the compatibility equation to eliminate ω in Equation [3.15], which then becomes:

$$k \cdot m \cdot \dot{v} = \frac{T}{R}; \quad and \quad F = \frac{1}{k} \cdot \frac{T}{R};$$
$$where \quad k = \frac{m + J/R^2}{m} = \frac{m + J_{transf}}{m};$$

[3.17]

Thus, we can see the effect of the rotating inertia as making the mass a factor k larger and making the reaction force correspondingly lower. We call the factor k the "rotational inertia coefficient".

In a vehicle propulsion system, there are rotational inertias mainly at two places:

- Rotating inertias before transmission, i.e. elements rotating with the same speed as the engine: J_e
- Rotating inertias after transmission, i.e. elements rotating with same speed as the wheel: J_w

The effective mass, $k \cdot m$, will be dependent on the gear ratio as well:

$$k \cdot m = m + \frac{J_w}{R^2} + \frac{J_e \cdot ratio^2}{R^2};$$

[3.18]

Typically for a passenger car, k=1.4 in the first gear and k=1.1 in the highest gear. So, in the first gear, approximately one third of the engine torque is required to rotationally accelerate the driveline, and only two thirds is available for accelerating the vehicle!

When the clutch is slipping, there is no constraint between engine speed and vehicle. The term with J_e disappears from Equation [3.18]. If the wheel spins, both rotational terms disappear.

We can now learn how to determine acceleration from the Traction Diagram, see Figure 3-29.
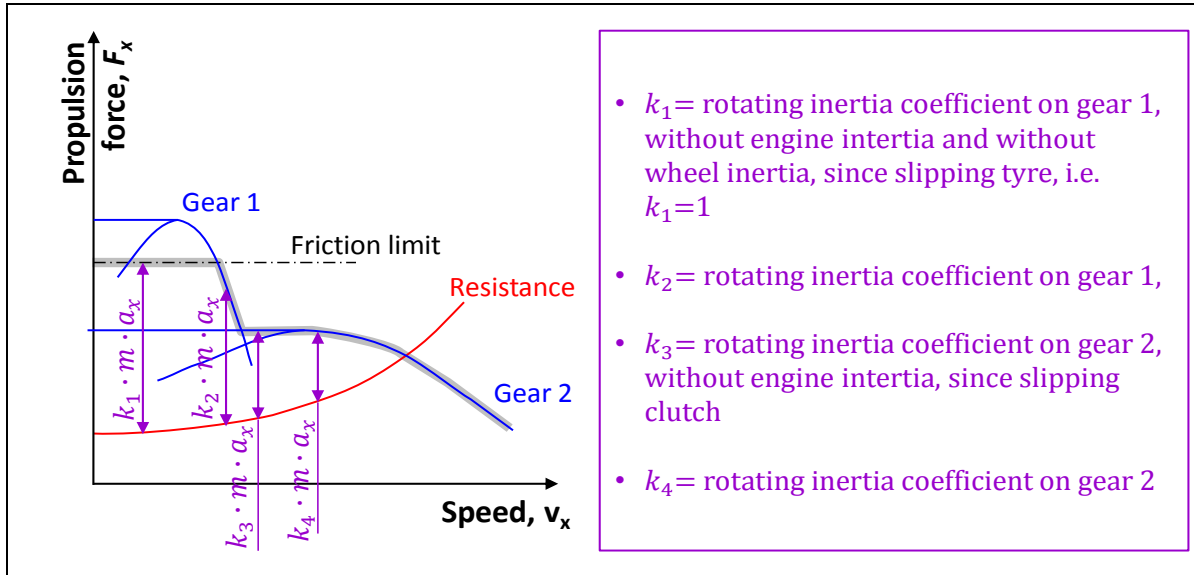
Figure 3-29: Acceleration in Traction Diagram. Rotating inertia effects are shown assuming that the engine is run on its maximum curve and the gear (or slipping clutch) for highest acceleration is selected.

3.3.3 Four quadrant traction diagram

When the driving cycle shows a deceleration which is larger than can be achieved with resistance force, we need to brake with a combination of engine braking and friction brakes. If only friction braking is used, it can be with engaged or disengaged clutch. That influences the rotating inertia coefficient by using or not using the J_e term in Equation [3.18], respectively. The traction diagram can be extended to also cover engine braking and friction braking. However, the friction brake system is seldom limiting factor for how negative the longitudinal force can be. But the road friction is, see Figure 3-30.

3.3.4 Fuel or energy consumption *

Function definition: **Fuel (or Energy) Consumption** *is the amount of fuel [kg or litre] (or energy [J]) consumed by the vehicle per performed transportation amount. Transportation amount can e.g. be measured in km, person*km, ton*km or m³*km. The vehicle operation has to be defined, e.g. with a certain driving cycle (speed as function of time or position), including road gradient, cargo load, road surface conditions, etc.*

The consumption arises in the prime mover. The consumption is dependent on the operating point in the speed vs torque diagram, or map, for the prime mover. Each point have a consumption rate [g/s] or [Nm/s=W], but it is often given as a specific consumption or an efficiency. Specific consumption is the consumption rate divided with output power=speed*torque; for a fuel consuming prime mover this leads to the unit [(g/s)/(Nm/s)] or [g/J] or [g/(Ws)] or [g/(kWh)]. Efficiency is, conceptually, the inverse of specific consumption; "out/in" instead of "in/out". The units for efficiency becomes [W/W=1]. An example of a map for an ICE is given in Figure 3-31. Maps with similar function can be found for other types of prime movers, such as the efficiency map for an electric motor, see Figure 3-32.
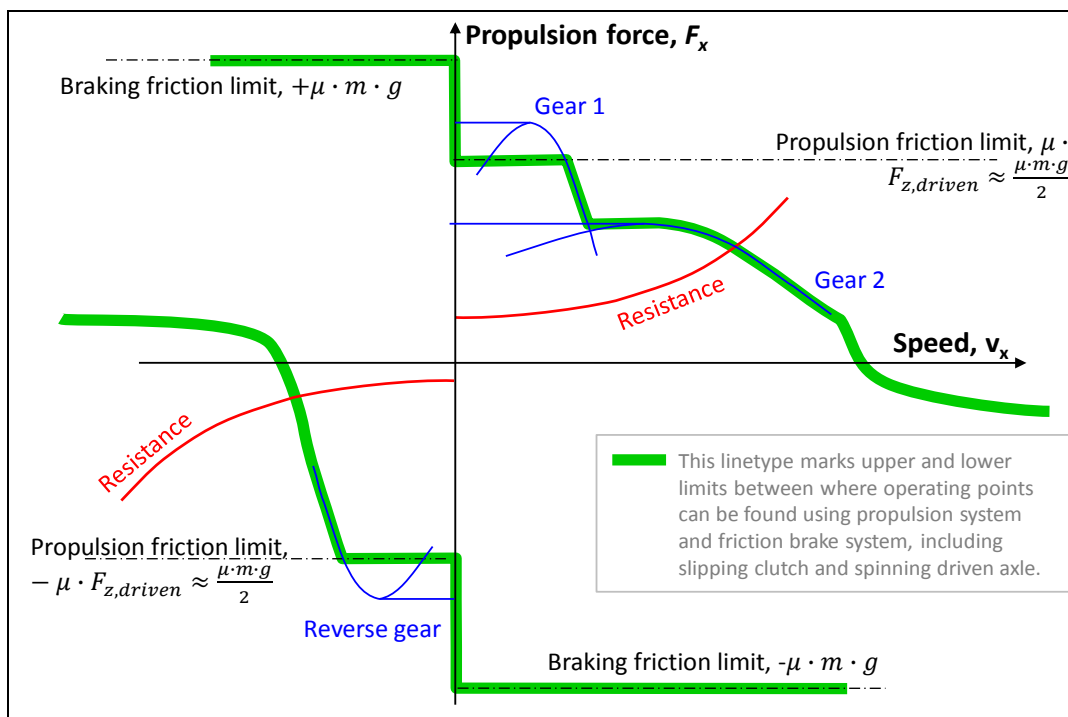
Figure 3-30: Traction Diagram in 4 quadrants. One of two axles is assumed to be driven, which limits propulsion to approximately half of braking friction limit. Up-hill slope is assumed, which is seen as asymmetric resistance.

Figure 3-31 and Figure 3-32 also show that the efficiencies can be transformed to the traction diagram. The maps for different gears partly overlap each other, which show that an operating point of the vehicle can be reached using different gears. The most fuel or energy efficient way to select gear is to select the gear which gives the lowest specific fuel consumption, or highest efficiency. Such a gear selection principle is one way of avoiding specifying the gear selection as a function over time in the driving cycle. For vehicles with automatic transmission, that principle can be programmed into the control algorithms for the transmission.
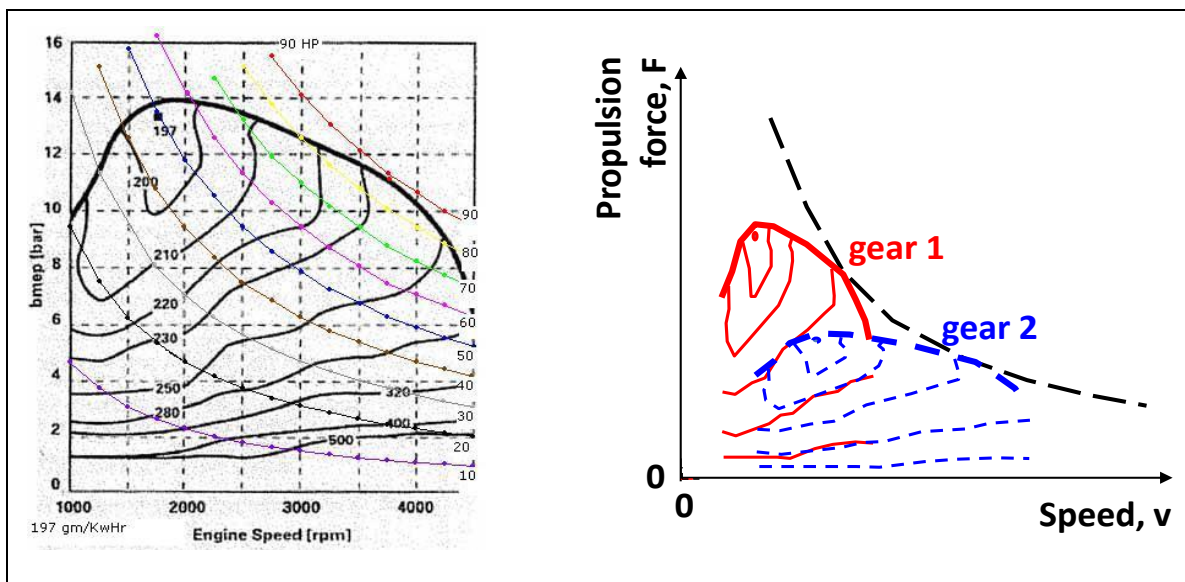
Figure 3-31: Left: Fuel consumption map. Curves show where specific fuel consumption $[g/(kW \cdot h)]$ is constant. For a specific fuel, this is proportional to $1/efficiency$. Right: Specific fuel consumption curves can also be transformed in Traction Diagram, for a given gear.

How to predict the consumption for a vehicle during a certain driving cycle is rather straight-forward using what has been presented earlier in this chapter. Since a driving cycle is a prediction of how the vehicle is moving, it actually stipulates the acceleration of a mass, which calls for an "inverse dynamic analysis". In such one assumes that the driving cycle is met exactly, which means that both required wheel speed and required wheel torque can be calculated for each time instant. Then, via a propulsion

and brake system model, the corresponding fuel consumption in the engine can also be found for each time instant. A summary of such an inverse dynamic algorithm for prediction of fuel or energy consumption is given in Equation [3.19].
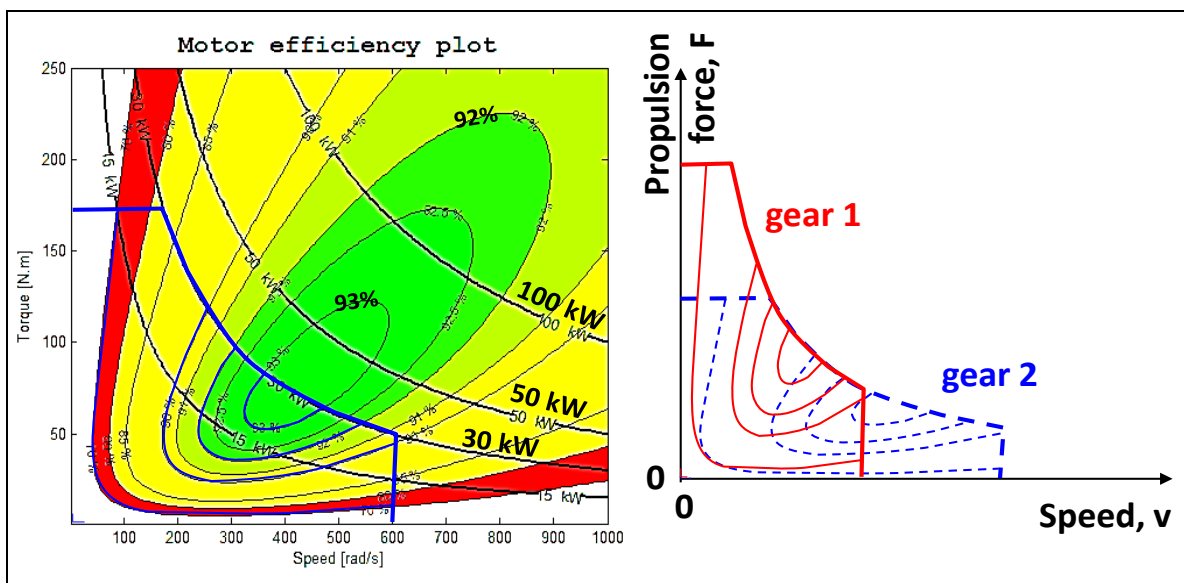
Figure 3-32: <u>Left</u>: Efficiency map for a typical brushless DC motor, from (Boerboom, 2012). Elliptic curves show where efficiency is constant. <u>Right</u>: The efficiency curves can also be transformed in Traction Diagram, for a given gear.

```
For each time step in the driving cycle:

  • Calculate operating point for vehicle (speed and acceleration) from
    driving cycle. Acceleration is found as slope of v(t) curve. Other
    quantities, such as road slope, also needs to be identified;
  • Select gear (and clutch state, tyre spin, friction brake state, etc)
    to obtain this operating point. Select also friction brake, especially
    for operating points which can be reached using only friction brake.
    If the vehicle has an energy buffer, regenerative braking is also an
    option;
  • Calculate required actuation from propulsion system on the driven
    wheel, i.e. rotational speed and shaft torque;
  • Calculate backwards through propulsion system, from wheel to prime
    motor. It gives the operating point for prime mover (rotational speed
    and torque);
  • Read prime mover consumption [in kg/s or W=J/s, not specific
    consumption, not efficiency] from prime mover consumption map;
  • Sum up consumption [in kg or J] with earlier time steps, e.g. using
    the Euler forward integration method: AccumulatedConsumption =
    AccumulatedConsumption + Consumption*TimeStepLength;

end;
```

[3.19]

The final accumulated consumption [in kg or J] is often divided by the total covered distance in the driving cycle, which gives a value in kg/km or J/km. If the fuel is liquid, it is also convenient to divide by fuel density, to give a value in litre/(100*km). It can also be seen as a value in m^2, which is the area of the "fuel pipe" which the vehicle "consumes" on the way.

We should note that the calculation scheme in Equation [3.19] does not always guarantee a solution. An obvious example is if the driving cycle prescribes such high accelerations at such high speeds that the propulsion system is not enough, i.e. we end up outside maximum torque curve in engine diagram. This is often the case with "inverse dynamic analysis", i.e. when acceleration of inertial bodies is prescribed and the required force is calculated. An alternative is to do a dynamic analysis, which means that a driver model calculates the pedals in order to follow the driving cycle speed as closely as possible, but not exactly. Inverse dynamic analysis is often more computational efficient, but limits what can phenomena that can be modelled in the propulsion and brake system. Inverse dynamics and

dynamic simulations are sometimes referred to as backward and forward analysis, respectively; see Reference (Wipke, o.a., 1999).

For hybrid vehicles with energy buffers the same driving cycle can be performed but with quite different level of energy in the buffer after completing the driving cycle. Also, the level when starting the driving cycle can be different. This can make it unfair to compare energy efficiency only by looking at fuel consumption in kg/km or litre/km.

Driving cycles are used for legislation and rating for passenger cars. For commercial vehicles, the legislation is done for the engine alone, and not for the whole vehicle. Rating for commercial vehicles is under development, see http://ec.europa.eu/clima/events/docs/0096/vecto_en.pdf.

3.3.5   Emissions *

Function definition: As Energy consumption, but amount of certain substance instead of amount of energy.

There are emission maps where different emission substances (NOx, HC, etc.) per time or per produced energy can be read out for a given speed and torque. This is conceptually the same as reading out specific fuel consumption or efficiency from maps like in Figure 3-31 and Figure 3-32. A resulting value can be found in mass of the emitted substance per driven distance.

Noise is also sometimes referred to as emissions. It is not relevant to integrate noise over the time for the driving cycle, but maximum or mean values can have relevance. Noise emissions are very peripheral to vehicle dynamics.

3.3.6   Tyre wear *

*Function definition: **Tyre wear** is the worn out tyre tread depth on a vehicle per performed transportation amount. Transportation amount can be measured as for Energy consumption. Tyre wear as a vehicle function has to consider all tyres on the vehicle, e.g. as maximum over the wheels (assuming that all tyres are changed when one is worn out) or average (assuming that single tyres are exchanged when worn out).*

There are models for tyre wear (e.g. outputting "worn tread depth per time"), see Equation **[2.50]**. For a certain driving cycle we can integrate the $WearRate$ [in mass/s or mm tread depth/s], over time similar to energy consumption rate, which becomes worn material [in mass or mm tread depth]. The wear rate per wheel is a function of the total slip, so it can include both longitudinal slip (propulsion and brake) and lateral slip (from cornering and toe angles).

Generally, the worn material will be different for different axles, or wheels, so a tyre change strategy might be necessary to assume to transform the worn material on several axles into one cost. The cost will depend on whether one renews all tyres on the vehicle at once or if one change per axle. The tyre wear is a cost which typically sums up with energy cost and cost of transport time (e.g. driver salary, for commercial vehicles).

3.3.7   Range *

*Function definition: **Range** [km] is the inverted value of Energy consumption [kg/km, litre/km or J/km], and multiplied with fuel tank size [kg or litre] or energy storage size [J].*

The range is how far the vehicle can be driven without refilling the energy storage, i.e. filling up fuel tank or charging the batteries from the grid. This is in principle dependent on how the vehicle is used, so the driving cycle influences the range. In principle, the same prediction method as for energy consumption and substance emissions can be used. In the case of predicting range, you have to integrate speed to distance, so that you in will know the travelled distance.

3.3.8 Acceleration reserve *

Function definition: **Acceleration reserve** *is the additional acceleration the vehicle will achieve within a certain time (typically 0.1..1 s) without manual gear-shifting by pressing accelerator pedal fully, when driving in a certain speed on level ground without head-wind. For vehicles with automatic transmissions or CVTs the certain time set can allow automatic gear-shift (or ratio-change) or not. The reserve can also be measured in propulsion force.*

In general terms, the lowest consumption is found in high gears. However, the vehicle will then tend to have a very small reserve in acceleration. It will, in practice, make the vehicle less comfortable and less safe to drive in real traffic, because one will have to change to a lower gear to achieve a certain higher acceleration. The gear shift gives a time delay.

Figure 3-33 shows one way of defining a momentary acceleration reserve. The reserve becomes generally larger the lower gear one selects.

A characteristic of electric propulsion systems is that an electric motor can be run at higher torque for a short time than stationary, see

Figure 3-3. On the other hand, the stationary acceleration reserve is less gear dependent, since an electric motor can work at certain power levels in large portions of its operating range.

One can calculate the acceleration reserve at each time instant over a driving cycle. However, integration of acceleration reserve, as we did with fuel, emissions and wear, makes less sense. Instead, a mean value of acceleration reserve tells something about the vehicle's driveability. Minimum or maximum values can also be useful measures.

Acceleration reserve was above described as limited by gear shift strategy. Other factors can be limiting, such as energy buffer state of charge for parallel hybrid vehicles or how much overload an electric machine can take short term, see right part of Figure 3-33.
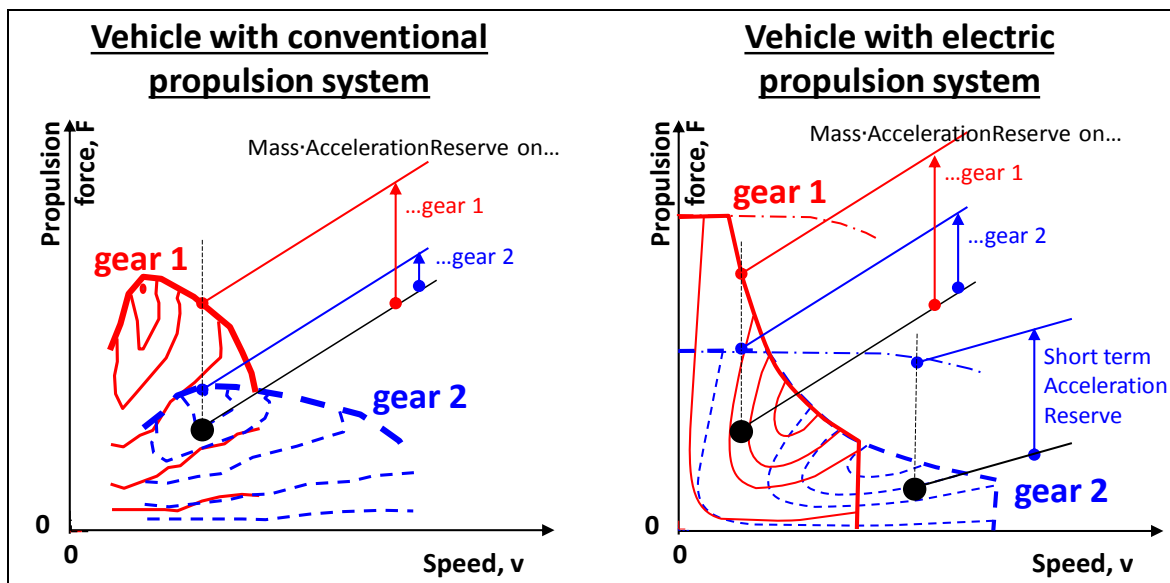
Figure 3-33: Acceleration reserves for different gears. Large dots mark assumed operating points, each with its acceleration reserve shown.

3.3.9 Load Transfer, without delays from suspension

It is useful to understand longitudinal load transfer because unloading one axle often limits the traction and braking. This is because the propulsion and brake systems are normally designed such that axle torques cannot always be ideally distributed.

We start with the free-body diagram in Figure 3-34, which includes acceleration, a_x.
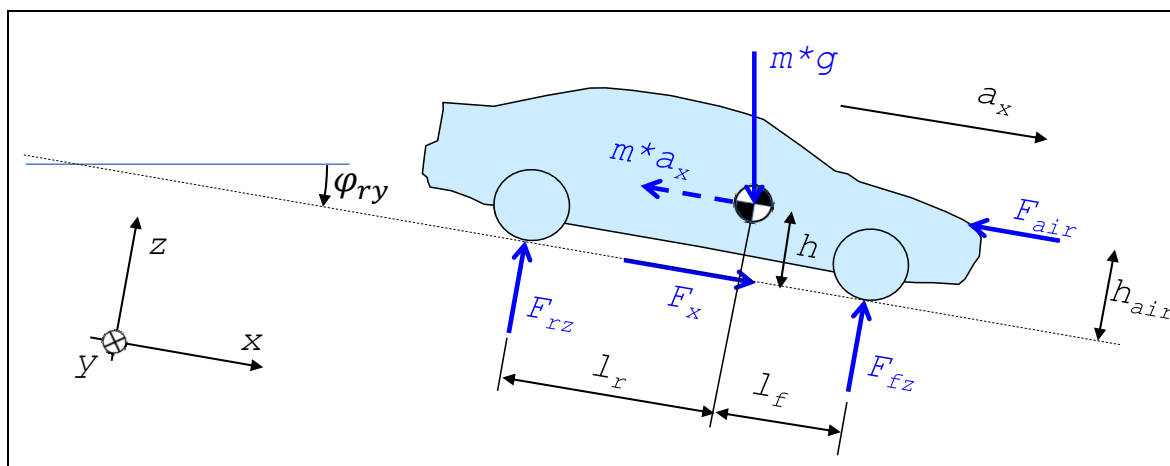
Figure 3-34: Free Body Diagram for accelerating vehicle. (Rolling resistance included in F_x.)

Note that the free-body diagram and the following derivation is very similar to the derivation of Equation [3.12], but we now include the fictive force $m \cdot a_x$.

Moment equilibrium, around rear contact with ground:
$$-F_{fz} \cdot \left(l_f + l_r\right) + m \cdot g \cdot \left(l_r \cdot \cos(\varphi_{ry}) + \text{h} \cdot \sin(\varphi_{ry})\right) - F_{air} \cdot h_{air} - m \cdot a_x \cdot h = 0; \Rightarrow$$

$$\Rightarrow F_{fz} = m \cdot \left(g \cdot \frac{l_r \cdot \cos(\varphi_{ry}) + \text{h} \cdot \sin(\varphi_{ry})}{l_f + l_r} - a_x \cdot \frac{h}{l_f + l_r}\right) - F_{air} \cdot \frac{h_{air}}{l_f + l_r}$$

Moment equilibrium, around front contact with ground:
$$+F_{rz} \cdot \left(l_f + l_r\right) - m \cdot g \cdot \left(l_f \cdot \cos(\varphi_{ry}) - \text{h} \cdot \sin(\varphi_{ry})\right) - F_{air} \cdot h_{air} - m \cdot a_x \cdot h = 0; \Rightarrow$$

$$\Rightarrow F_{rz} = m \cdot \left(g \cdot \frac{l_f \cdot \cos(\varphi_{ry}) - \text{h} \cdot \sin(\varphi_{ry})}{l_f + l_r} + a_x \cdot \frac{h}{l_f + l_r}\right) + F_{air} \cdot \frac{h_{air}}{l_f + l_r}$$

[3.20]

These equations confirm what we know from experience, the front axle is off-loaded under acceleration with the load shifting to the rear axle. The opposite occurs under braking.

The load shift has an effect on the tyre's grip. If one considers the combined slip conditions of the tyre (presented in Chapter 2), a locked braking wheel limits the amount of lateral tyre forces. The same is true for a spinning wheel. This is an important problem for braking as the rear wheels become off-loaded. This can cause locking of the rear wheels if the brake pressures are not adjusted appropriately.

Consider the different conditions for a vehicle where either the front axle or rear axle is locked.

Figure 3-35 shows the vehicle's response to a small disturbance and argues for that:

- A vehicle with **locked front** wheels will have a **stable** straight-ahead motion. However, steering ability is lost.
- A vehicle with **locked rear** wheels will be **unstable**. It turns around and ends up in stable sliding, i.e. with the rear first.

Usually, it is preferred that the front wheels lock first. But it is of course also important that both axles are used as much as possible during braking, to improve braking efficiency. Hence, there are trade-offs when designing the brake torque distribution, see Section 3.4.6.
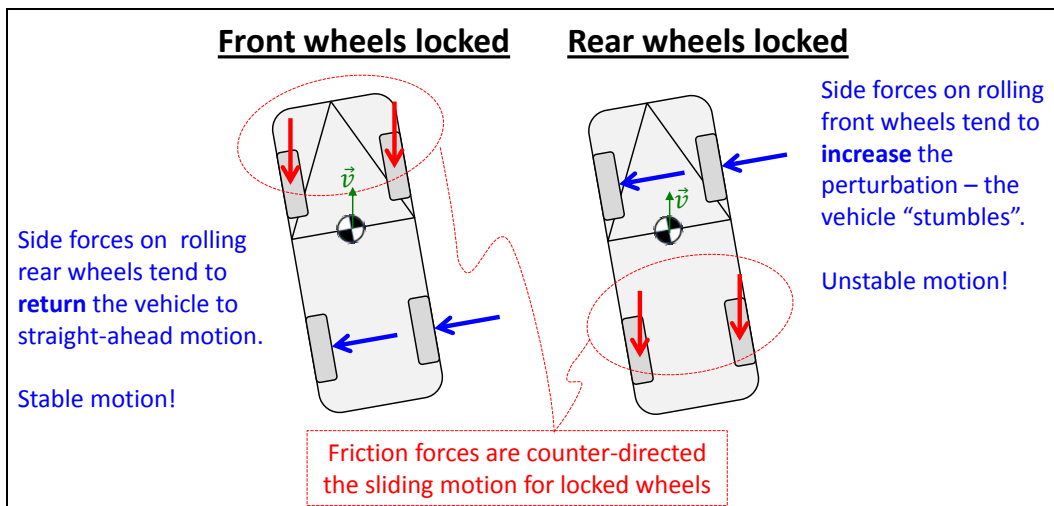
Figure 3-35: Locked Axle Braking. Same reasoning works for propulsion, if "locked" is replaced by "large longitudinal tyre slip".

3.3.10 Acceleration – simple analysis

3.3.10.1 Acceleration performance *

Function definition: **Acceleration performance** *is the time needed to, with fully applied accelerator pedal, increase speed from a certain speed to another certain higher speed, at certain road friction on level ground without head-wind and certain load.*

Acceleration events will be considered in Section 3.4, as being shorter events, where more dynamic aspects become important. If we are interested in a prediction of acceleration performance over longer time, typically 0-100 km/h, over 5..10 s, we can use a simpler model.

3.3.10.2 Solution using integration over time

A front-wheel-drive passenger car with a stepped gearbox should accelerate from 0 to 100 km/h. A Matlab code is given in Equation [3.21], which simulates the acceleration uphill from stand-still, using simple numerical integration. The code calculates the possible acceleration in each of the gears, and one mode with slipping clutch. In each time step it selects that which gives the highest acceleration. The numerical data and results are not given in the code, but some diagrams are shown in Figure 3-36. The code is not fully documented, only using equations so far presented in this compendium.

```
dt=0.1; t_vec=[0:dt:10]; vx_vec(1)=0;
for i=1:length(t_vec)
    vx=vx_vec(i);
    Fres=m*g*sin(p)+froll*m*g*cos(p)+0.5*roh*A*cd*vx*vx;

    %if gear 1 (clutch engaged)
    ratio=ratios(1);
    we=vx*ratio/radius;
    Te=interp1(Engine_w,Engine_T,we);
    Fx=Te*ratio/radius;
    ax=(Fx-Fres)/(m+(Jw+Je*(ratio^2))/(radius^2));
    Fzf=m*(g*lr/(lf+lr)-ax*h/(lf+lr));
    if Fx>mu*Fzf
        Fx=mu*Fzf;
        ax=(Fx-Fres)/m;
    end
    ax1=ax;

    %if gear 2 (clutch engaged)
    ratio=ratios(2);
    … then similar as for gear 1
    ax2=ax;

    %if gear 3 (clutch engaged)
    ratio=ratios(3);
    … then similar as for gears 1 and 2
    ax3=ax;
```

[3.21]

```
%if clutch slipping on gear 2
ratio=ratios(2);
wc=vx*ratio/radius; %speed of output side of clutch
Te=max(Engine_T);
we=Engine_w(find(Engine_T>=Te)); %engine runs on speed where max torque
Fx=Te*ratio/radius;
ax=(Fx-Fres)/(m+Jw/(radius^2));
Fzf=m*(g*lr/(lf+lr)-ax*h/(lf+lr));
if Fx>mu*Fzf
    Fx=mu*Fzf;
    ax=(Fx-Fres)/m;
end
if wc>we %if vehicle side (wc) runs too fast, we cannot slip on clutch
    ax=-inf;
end
ax0=ax;

[ax,gear_vec(i)]=max([ax0,ax1,ax2,ax3]);
vx_vec(i+1)=vx+ax*dt;
end
```

Phenomena that are missing in this model example are:

- Gear shifts are assumed to take place instantly, without any duration
- The option to use slipping clutch on 1st and 3rd gear is not included in model
- The tyre slip is only considered as a limitation at a strict force level, but the partial slip is not considered. The code line "we=vx*ratio/radius;" is hence not fully correct. Including the slip, the engine would run at somewhat higher speeds, leading to that it would lose its torque earlier, leading to worse acceleration performance. The calculation scheme in Equation [3.21] would be much less explicit.
- Load transfer is assumed to take place instantly quick; Suspension effects as described in Section 3.3 are not included.
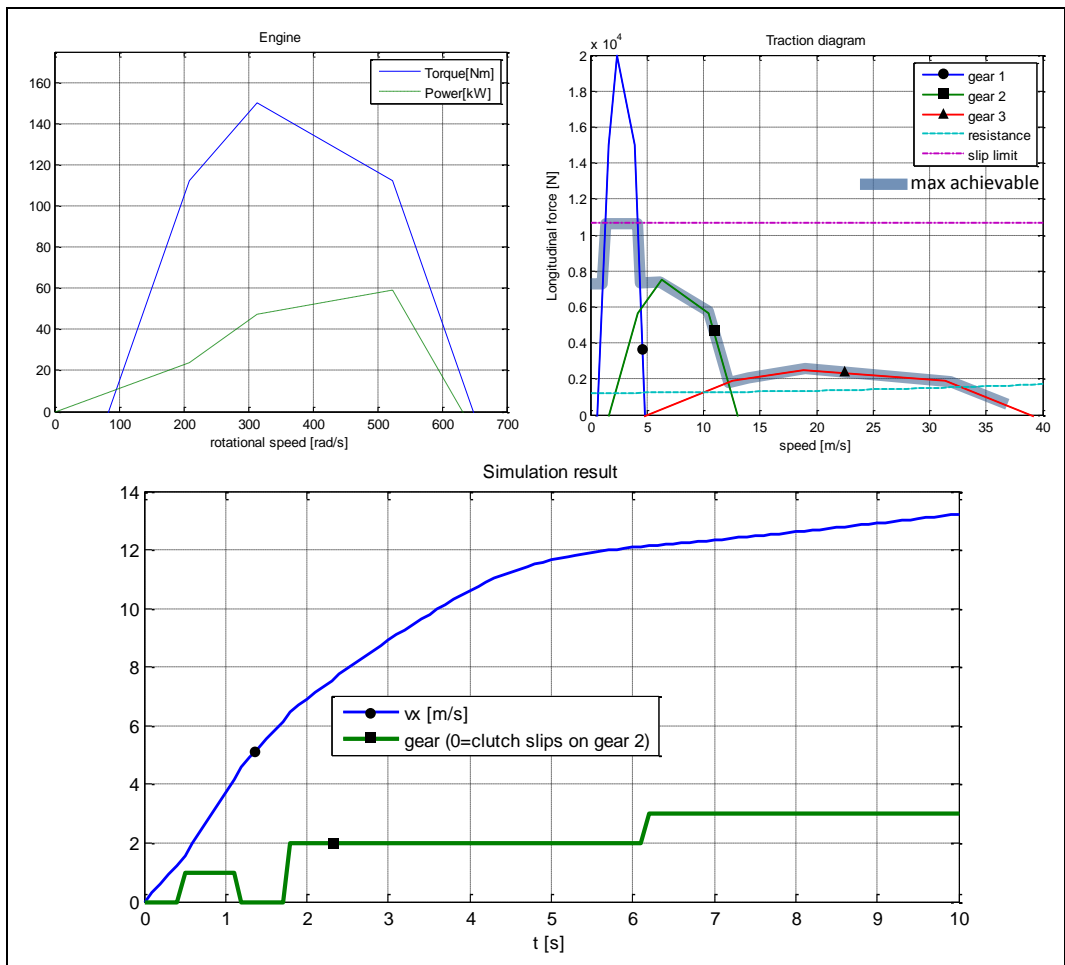

Figure 3-36: Example of simulation of acceleration, using the code in Equation [3.21].

3.3.10.3 Solution using integration over speed

An alternative way to calculate how speed varies with time is to separate the differential equation as follows:

$$m \cdot a = m \cdot \frac{dv}{dt} = F(v) - F_{res}(v); \Rightarrow \frac{m \cdot dv}{F(v) - F_{res}(v)} = dt \Rightarrow$$

$$\Rightarrow \int_0^v \frac{m \cdot dv}{F(v) - F_{res}(v)} = \int_0^t dt \Rightarrow \quad t = \int_0^v \frac{m \cdot dv}{F(v) - F_{res}(v)};$$

[3.22]

Now, the time is calculated by means of integration over speed, as opposed to integration over time. If simple mathematic functions are used to describe $F(v)$ and $F_{res}(v)$ the solution can potentially be mathematically explicit, but the previous integration over time is more general and works for more advanced models.

3.4 Functions in shorter events

This section targets models and methods to define and predict functions in a certain and shorter time frame, typically 0.5 to 5 seconds. It can be both acceleration and deceleration. (Friction) Brake system and phenomena as load transfer then becomes important, why these are presented early. But first, some typical driving manoeuvres are presented.

3.4.1 Typical test manoeuvres

When applying the longitudinal actuator systems (propulsion system and brake system) there are a couple of different situations which are typical to consider:

- Straight line maximum braking from, typically 100 km/h to stand-still for passenger cars.
- Braking in curve with significant lateral acceleration, see References (ISO, 2006) and (ISO, 2011).
- Straight line acceleration, typically 0 to 100 km/h and 80-100 km/h.
- Accelerating in curve with significant lateral acceleration.

For these four main situations, one can also vary other, typically:

- At high road friction and at low friction, often called "hi-mu" and "lo-mu"
- At different road friction left and right, often called "split-mu"
- At sudden changes in road friction, called "step-mu"
- At high speed, typically 200 km/h, for checking stability
- At different up-hill/down-hill gradients
- At different road banking (slope left to right)

A propelled or braked wheel or axle develops a longitudinal force, F_x, counter-acting the rotation of the wheel. F_x is limited by the road friction: $|F_x|_{max} = \mu \cdot F_z$;. (NOTE: $|F_x|_{max}$ is **not** $\mu \cdot F_z - f_r \cdot F_z$, see Figure 2-11.)

Braking coefficient $= -F_x/F_z$, is a property defined for an axle (or a single wheel) = brake force/normal load. It can be seen as the utilized friction coefficient. A suitable notation can be μ_{util}. The coefficient should not be mixed up with friction coeeficient, μ; the relation between them is $\mu_{util} \leq \mu$.

3.4.2 Deceleration performance

There are some different functions that measures braking performance or deceleration performance.

3.4.2.1 Braking efficiency *

Function definition: **Braking Efficiency** *is the ratio of vehicle deceleration and the best brake-utilized axle (or wheel), while a certain application level of the brake pedal at a certain speed straight ahead, at certain road friction on level ground without head-wind and certain load at a certain position in the vehicle.*

In equation form, the Braking Efficiency becomes $= \frac{-a_x/g}{\max_{\forall axles} \mu_{util}}$;. If Braking Efficiency=1=100%, the distribution of braking is optimal.

3.4.2.2 Braking Distance *

Function definition: **Braking Distance** *is the distance travelled during braking with fully applied brake pedal from a certain speed straight ahead to another certain lower speed, at certain road friction on level ground without head-wind and certain load at a certain position in the vehicle.*

For passenger cars one typically brakes fully from 100 km/h and then the braking distance is typically around 40 m (average deceleration 9.65 m/s²). For a truck it is typically longer, 51..55 m (7.5..7 m/s²).

3.4.2.3 Stopping Distance *

Function definition: **Stopping Distance** *is the distance travelled from that an obstacle becomes visible to driver have taken the vehicle to stand-still. Certain conditions, as for Braking Distance, have to be specified, but also a certain traffic scenario and a certain driver to be well defined.*

Stopping Distance is the braking distance + the "thinking/reaction distance", which depends on the speed and the reaction time. The reaction time of a driver is typically 0.5..2 seconds.

3.4.3 (Friction) Brake system

Generally speaking, there are several systems that can brake a vehicle:

- Service brake system (brake pedal and ABS/ESC controller, which together applies brake pads to brake discs/drums)
- Parking brake (lever/button that applied brake pads to brake discs/drums, normally on rear axle on cars but all axles on heavy vehicles)
- Engine braking (ICE operates at "engine brake" as marked in Figure 3-3)
- Electric machines (machines can be used symmetrical, i.e. both for positive and negative torques, see Figure 3-3)
- Retarders, or auxiliary brakes, for heavy vehicles. They normally use hydraulic or Eddy current to dissipate engine, as opposed to dry-friction. So, they cannot brake at low speeds or stand-still.
- Large steering angles will decelerate the vehicle, see Section 3.2.3.1.

This section is about Friction brakes, meaning Service brakes and Parking brake. In vehicle dynamics perspective these have the following special characteristics:

- Friction brakes are almost unlimited in force for a limited time since they can lock the wheels for most driving situations and road friction (ICE and electric motors are often limited by their maximum power, since it is often smaller than available road friction.) If, however, the friction brakes are used for a long time the brake lining will start to fade, e.g. lose friction coefficient due to high temperature (oxidation and melting of pad/lining material).
- Friction brakes can only give torque in opposite direction to wheel rotation. (Electric motors can brake so much that wheel spins rearwards.)
- Friction brakes can hold the vehicle at exact standstill. (If using electric machines for holding stand-still in a slope, a closed loop control would be necessary, resulting in that vehicle "floats" a little.)

The basic design of a passenger car brake system is a hydraulic system is show in Figure 3-37. Here, the brake pedal pushes a piston, which causes a hydraulic pressure (pressure = pedal force/piston

area). The hydraulic pressure is then connected to brake callipers at each wheel, so that a piston at each wheel pushes a brake pad towards a brake disc ($disc\ force = pressure \cdot piston\ area$). The brake torque on each wheel is then simply: $torque = number\ of\ friction\ surfaces \cdot disc\ coefficient\ of\ friction \cdot disc\ force \cdot disc\ radius$. (Normally, there are 2 friction surfaces, since double-acting brake calipers.) By selecting different piston area and disc radii at front and rear, there is a basic hydro mechanical brake distribution ratio between front and rear axle. There are normally two circuits for redundancy.

Brake systems for heavy trucks are generally based on pneumatics, as opposed to hydraulics, see Figure 3-39.
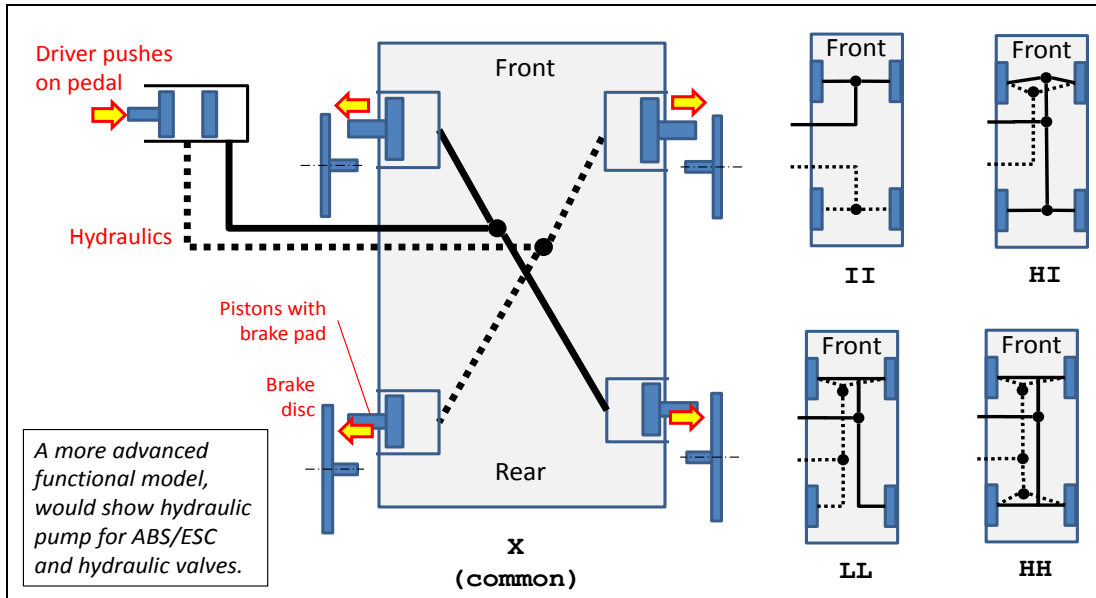
Figure 3-37: Layouts of a hydraulically applied brake system, which is conventional on passenger cars.
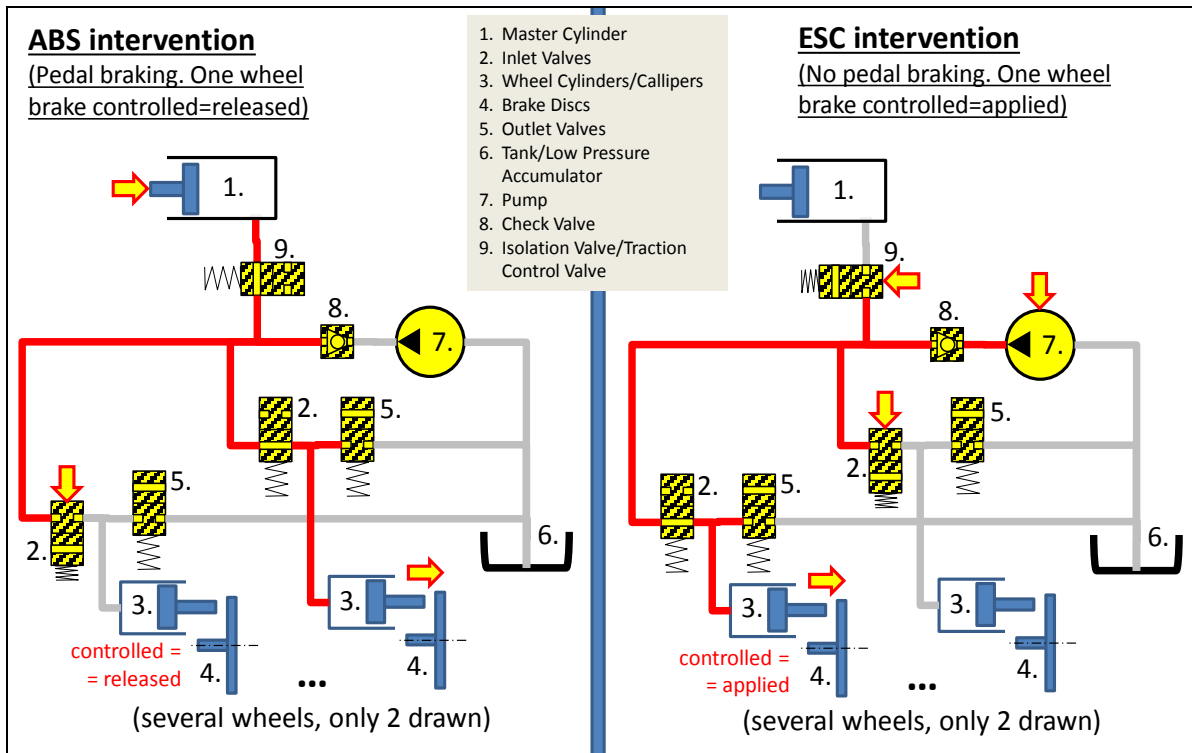
Figure 3-38: Concept of hydraulically applied brake system for ABS and ESC functions.
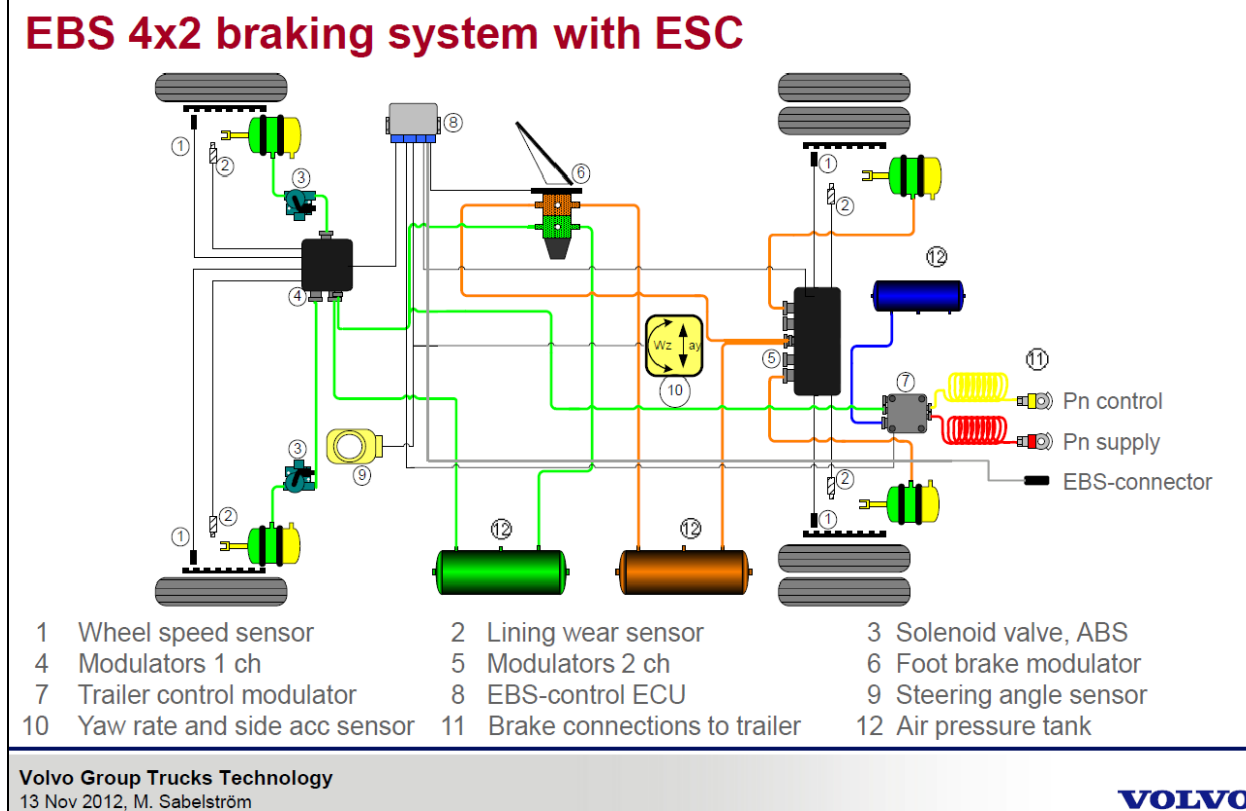
Figure 3-39: Pneumatically applied brake system for heavy vehicles. Electronics Brake System, EBS, from Volvo GTT, Mats Sabelström.

3.4.4   Pedal Response *

Function definition: **Accelerator pedal response** *is how vehicle acceleration varies with accelerator pedal position, for a certain vehicle speed and possibly certain gear, on level ground without pressing the brake pedal.*

Function definition: **Brake pedal response** *is how vehicle deceleration varies with brake pedal force, for a certain vehicle speed, on level ground without pressing the accelerator pedal.*

These functions, together with the functions in Section 3.4.5, enable the driver to operate the vehicle longitudinally with precision and in an intuitive and consequent way. The requirements based on above function definitions, are typically that the translation of pedal position (or force) to vehicle acceleration (or deceleration) should be consistent, progressive and oscillation-free.

For accelerator pedal steps, there should be enough acceleration, but also absence of "shunt and shuffle" (driveline oscillations). When accelerator pedal is suddenly lifted off, there shall be certain deceleration levels, depending on vehicle speed and gear selected.

3.4.5   Pedal Feel *

Function definition: **Accelerator pedal feel** *is the pedal's force response to pedal position.*

Function definition: **Brake pedal feel** *is the pedal's position response to pedal force.*

These functions, together with the functions in Section 3.4.4, enable the driver to operate the vehicle longitudinally with precision and in an intuitive and consequent way.

3.4.6   Brake proportioning

The basic function of a brake system is that brake pressure (hydraulic on passenger cars and pneumatic on trucks) is activated so that it applies brake pads towards brake discs or drums. In a first

approximation, the pressure is distributed with a certain fraction on each axle. For passenger cars this is typically 60..70% of axle torque front. In heavy trucks, the proportioning varies a lot, e.g. 90% for a solo tractor and 30% for heavy off-road construction rigid truck. The intention is to utilize road friction in proportion to the normal load, but not brake too much rear to avoid yaw instability, see Figure 3-35.

If neglecting air resistance and slope in Equation [3.20], the vertical axle loads can be calculated as function of deceleration ($= -a_x$). An ideal brake distribution would be if each axle always utilize same fraction of friction: $F_{fx}/F_{fz} = F_{rx}/F_{rz}$. This requirement gives the optimal F_{fx} and F_{rx} as:

$$\frac{F_{fx}}{\mu \cdot F_{fz}} = \frac{F_{rx}}{\mu \cdot F_{rz}} \Rightarrow \frac{F_{fx}}{F_{rx}} = \frac{F_{fz}}{F_{rz}} \Rightarrow \frac{F_{fx}}{F_{rx}} = \frac{m \cdot \left(g \cdot \dfrac{l_r}{l_f + l_r} - a_x \cdot \dfrac{h}{l_f + l_r}\right)}{m \cdot \left(g \cdot \dfrac{l_f}{l_f + l_r} + a_x \cdot \dfrac{h}{l_f + l_r}\right)} = \frac{g \cdot l_r - a_x \cdot h}{g \cdot l_f + a_x \cdot h};$$

$$F_{fx} + F_{rx} = m \cdot a_x;$$

$$\Rightarrow F_{fx} = m \cdot a_x \cdot \frac{g \cdot l_r - a_x \cdot h}{g \cdot (l_f + l_r)}; \quad and \quad F_{rx} = m \cdot a_x \cdot \frac{g \cdot l_f + a_x \cdot h}{g \cdot (l_f + l_r)};$$

[3.23]

Equation [3.23] is plotted for some variation in centre of gravity height and longitudinal position in Figure 3-40.

The proportioning is done by selecting pressure areas for brake calipers, so the base proportioning will be a straight line, marked as "Hydrostatic brake proportioning". For passenger cars, one typically designs this so that front axle locks first for friction below 0.8 for lightest vehicle load and worst variant. For heavier braking than $0.8 \cdot g$, or higher (or front-biased) centre of gravity, rear axle will lock first, if only designing with hydrostatic proportioning..
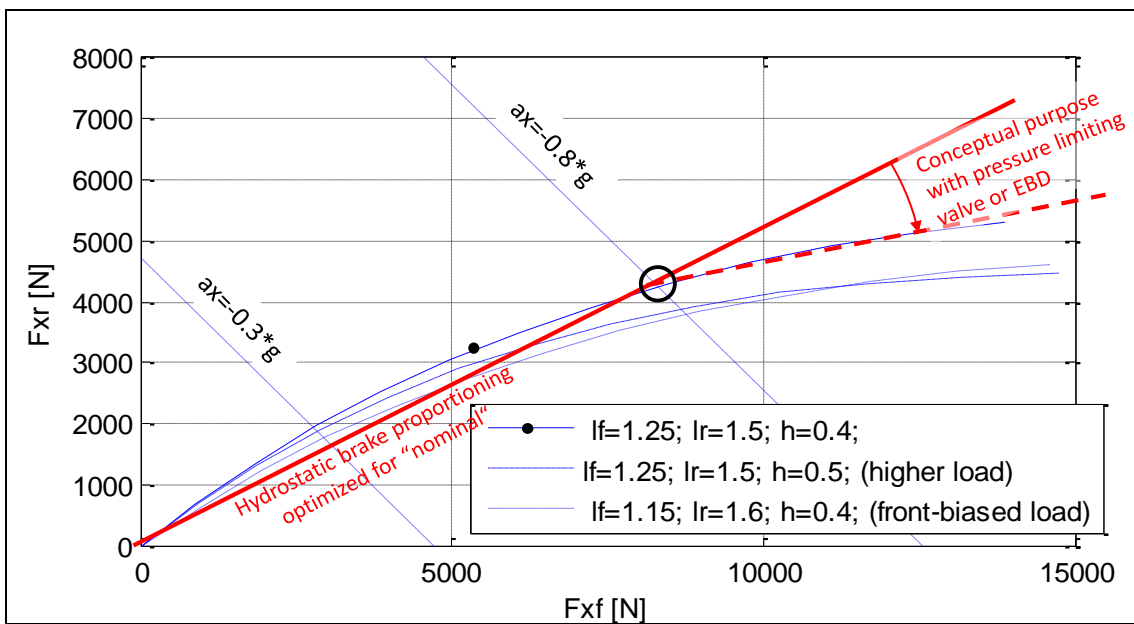
Figure 3-40: Brake Proportioning diagram. The curved curves mark optimal distribution for some variation in position of centre of gravity.

To avoid rear axle lock up, one restricts the brake pressure to the rear axle. This is done by pressure limiting valve, brake pads with pressure dependent friction coefficient or Electronic Brake Distribution (EBD). In principle, it bends down the straight line as shown in Figure 3-40. With pressure dependent values one gets a piece-wise linear curve, while pressure dependent friction coefficient gives a continuously curved curve. EBD is an active control using same mechatronic actuation as ABS. EBD is the design used in today's passenger cars, since it comes with ABS, which is now a legal requirement on most markets.

On heavy vehicles with EBS (Electronic Brake System) and vertical axle load sensing, the brake pressure for each axle can be tailored. For modest braking (corresponding to deceleration $\leq 2 \; m/s^2$) all axles are braked with same brake torque, to equal the brake pad wear which is importance for vehicle maintenance. When braking more, the brake pressure is distributed more in proportion to each axle's vertical load.
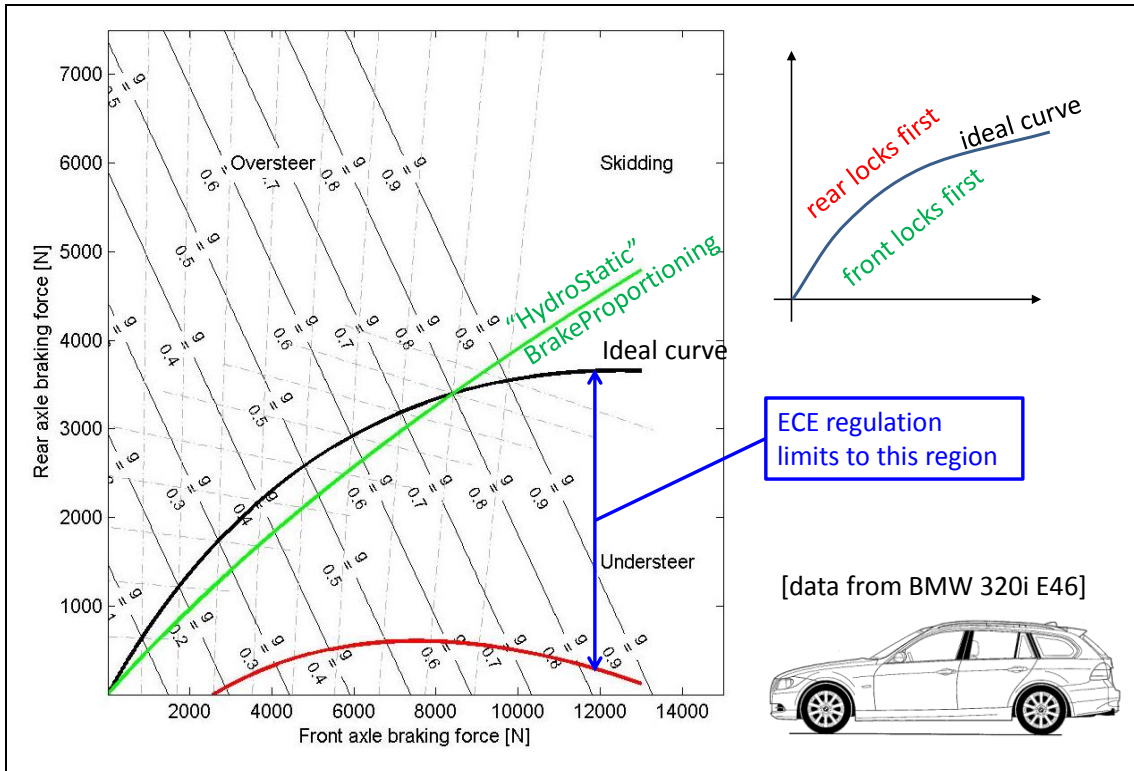
Figure 3-41: Brake Proportioning. From (Boerboom, 2012). If looking carefully, the "HydroStatic" curve is weakly degressive, which is thanks to brake pads with pressure dependent friction coefficient.

3.4.7   Varying road pitch

The model in Figure 3-34 assumes constant grade, i.e. a constant road pitch angle, φ_{ry} in Figure 3-42. An example where φ_{ry} varies is when passing a *crest* or a *hollow*, or *meeting uphill* or *meeting downhill*.
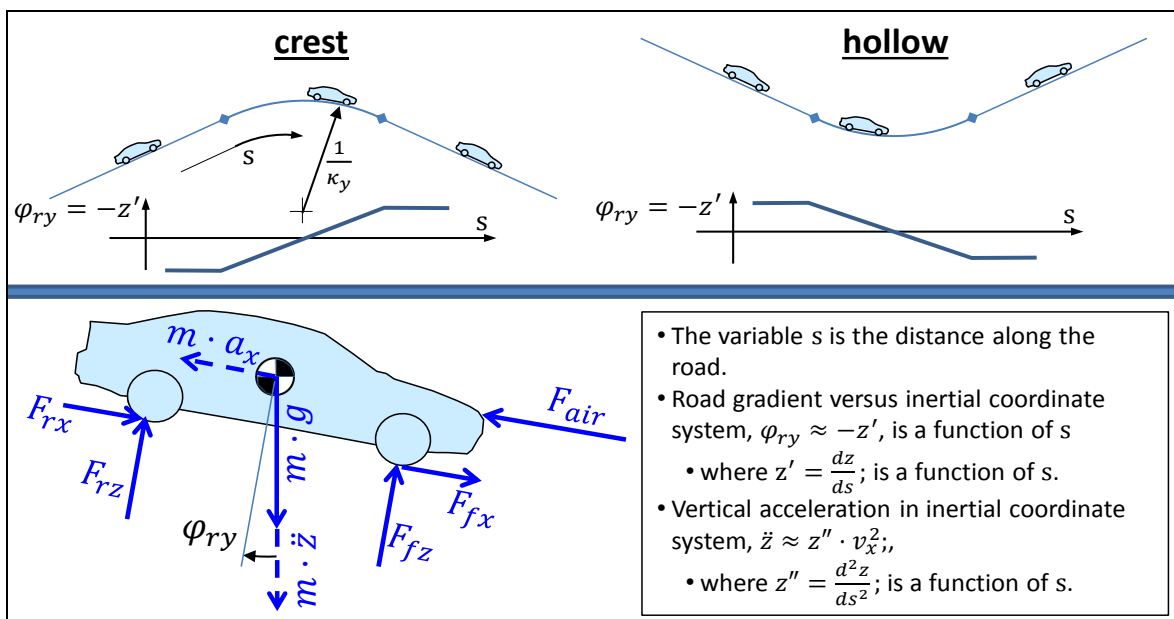
Figure 3-42: Free Body Diagram for driving over arbitrary vertical road profile.

Moment equilibrium, around rear and front wheel contact with ground gives:

$$F_{zf} = m \cdot \left((g + z'' \cdot v_x^2) \cdot \frac{l_r \cdot \cos(\varphi) + h \cdot \sin(\varphi)}{L} - a_x \cdot \frac{h}{L} \right) - F_{air} \cdot \frac{h_{air}}{L};$$

$$F_{zr} = m \cdot \left((g + z'' \cdot v_x^2) \cdot \frac{l_f \cdot \cos(\varphi) - h \cdot \sin(\varphi)}{L} + a_x \cdot \frac{h}{L} \right) + F_{air} \cdot \frac{h_{air}}{L};$$

[3.24]

Assuming that we have the road as $z(s)$, then $\varphi = -\arctan\left(\frac{dz}{ds}\right) \approx -\frac{dz}{ds}$; and $z'' = \frac{d^2 z}{ds^2}$;.

Note that this model is assuming that vertical variations of road are larger than wheel base and track width and same on left and right side of the road/vehicle. Else the variation would be called road unevenness, which will be more treated in Chapter **5**.

If models with body vertical and pitch motion and suspension springs, such as in Sections 3.4.7 and 3.4.9 it is often suitable to express the vertical fictive force, $m \cdot \ddot{z}$, with $v_x \cdot \omega_y$ instead of $m \cdot z'' \cdot v_x^2$. The fictive force downwards will then be $-m \cdot v_x^2 \cdot \kappa_y = -m \cdot v_x \cdot \omega_y$ instead. This can be understood from basic geometry, $z'' \approx -\kappa_y$, where κ_y is the road pitch curvature $[1/length]$, see Figure 3-42.

3.4.8 Quasi-steady state body heave and pitch due to longitudinal wheel forces

Additional to that the axle vertical loads change due to acceleration ax, there are also change in displacement (heave and pitch). In the following section, a model assuming "quasi-steady state" will be derived, see Figure 3-44. We hereby mean that the accelerations and speeds are constant, except for in longitudinal direction. The model is approximately valid for heave and pitch during such a constant braking and acceleration. The model differs between the "unsprung mass" (wheels and the part of the suspension that does not heave) and the "sprung mass" or "body" (parts that heaves and pitches as one rigid body).

It is especially noted that the model in Figure 3-44 models the suspension in a very trivial way; purely vertical. It can be seen as a very trivial (suspension) linkage. The model will be further developed in Section 3.4.9, to model linkage in the suspension better, which allows validity for transients braking and acceleration. It will also generally improve the validity also for quasi-steady state acceleration or braking.

There is no damping included in model, because their forces would be zero, since there is no displacement velocity, due to the "quasi-steady-state" assumption. As constitutive equations for the compliances (springs) we assume that displacements are measured from a static conditions and that the compliances are linear. The road is assumed to be smooth, i.e. $z_{fr} = z_{rr} = 0$.

$$F_{zf} = F_{zf0} + c_f \cdot (z_{fr} - z_f) \quad and \quad F_{zr} = F_{zr0} + c_r \cdot (z_{rr} - z_r)$$
$$where \ F_{zf0} + F_{zr0} = m \cdot g \quad and \quad F_{zf0} \cdot l_f - F_{zr0} \cdot l_r = 0$$

[3.25]

Suspension design is briefly discussed at these places in this compendium: Section 3.4.7, Section 4.3.9.4 and Section **5.2**. The stiffnesses c_f and c_r are the effective stiffnesses at each axle. The physical spring may have another stiffness, but its effect is captured in the effective stiffness. An example of different physical and effective stiffness is given in Figure 3-43. Note that the factor $(a/b)^2$ is not the only difference between effective and physical stiffness, but the effective can also include compliance from other parts than just the spring, such as bushings and tyre. A common alternative name for the effective stiffness is axle rate, or wheel (spring) rate if measured per wheel. There will also be a need for a corresponding effective damping coefficient, see Section 3.4.9.2, or wheel (damping) rate.
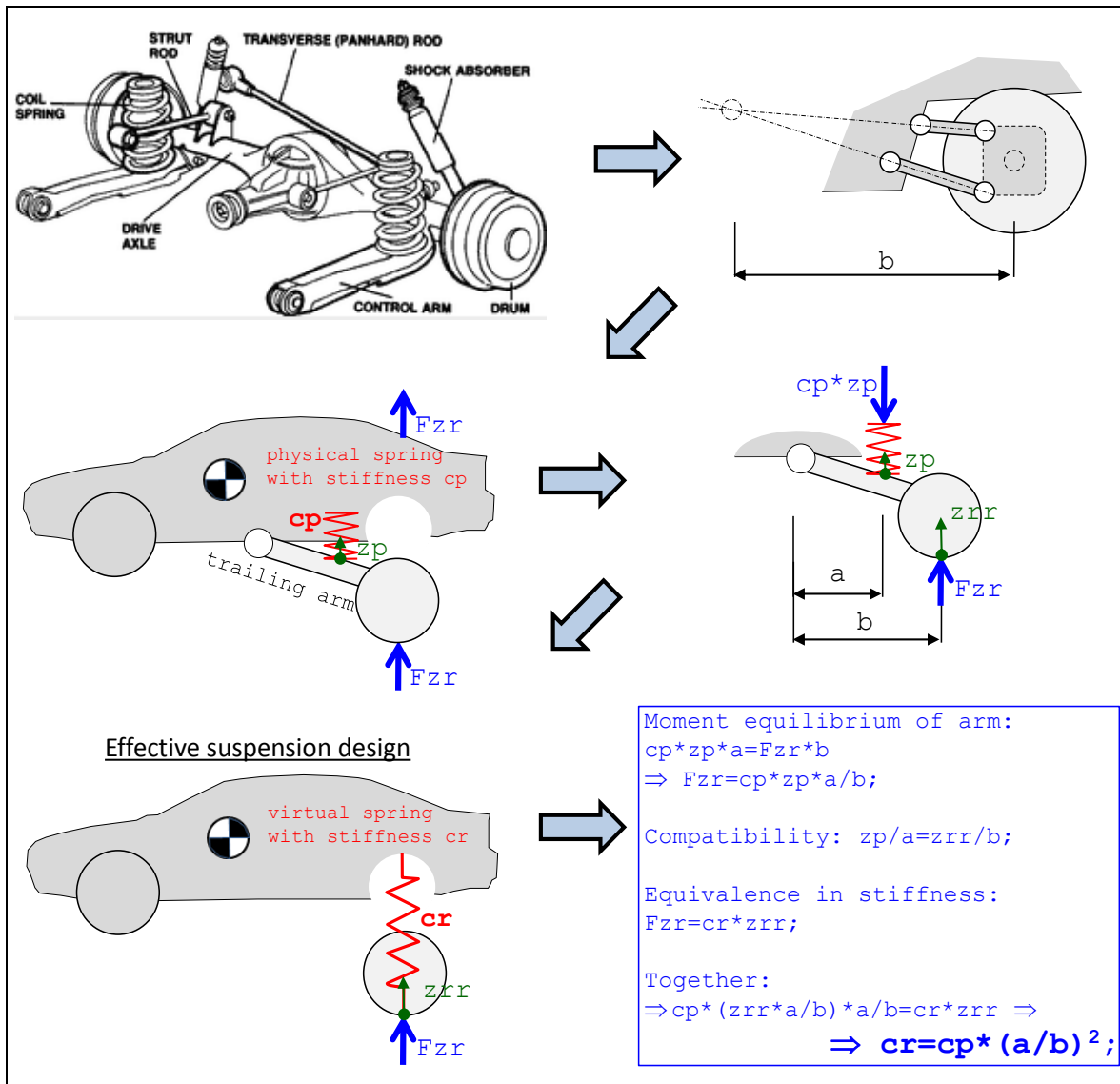
Figure 3-43: From physical suspension design to effective stiffness. Upper left: From http://www.procarcare.com/icarumba/resourcecenter/encyclopedia/icar_resourcecenter_encyclopedia_suspster3.asp.
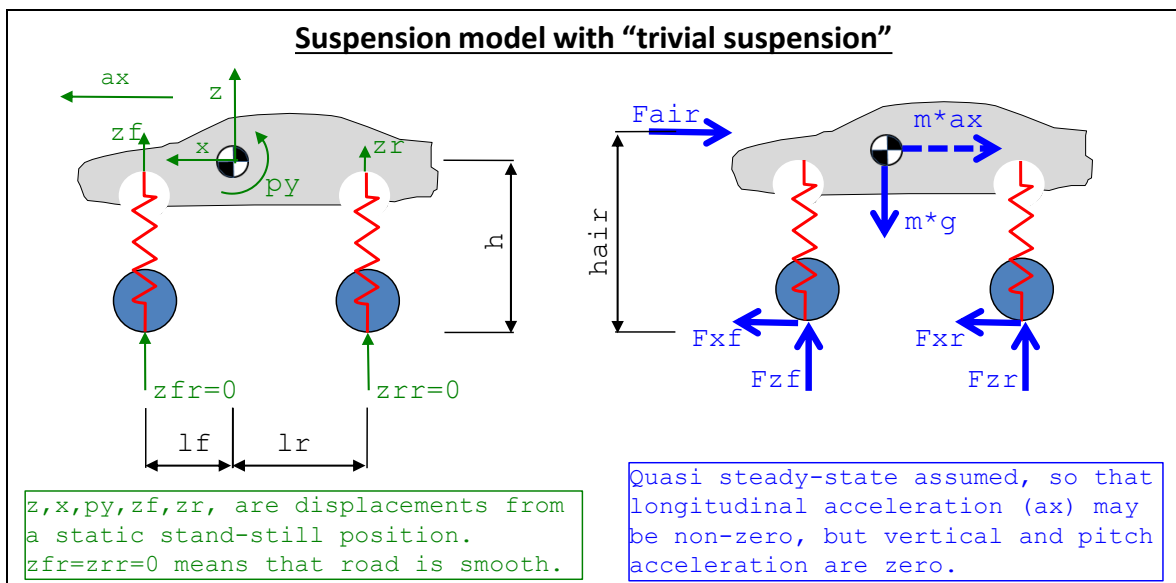
Figure 3-44: Model for quasi-steady state heave and pitch due to longitudinal accelerations.

We see already in free-body diagram that F_{xf} and F_{xr} always act together, so we rename $F_{xf} + F_{xr} = F_{xw}$, where w refers to wheel. This and equilibrium give:

$$-F_{air} - m \cdot a_x + F_{xw} = 0;$$
$$m \cdot g - F_{zf} - F_{zr} = 0;$$
$$F_{zr} \cdot l_r - F_{zf} \cdot l_f - F_{xw} \cdot h - F_{air} \cdot (h_{air} - h) = 0;$$

[3.26]

Compatibility, to introduce body displacements, z and p_y, gives:

$$z_f = z - l_f \cdot p_y; \quad and \quad z_r = z + l_r \cdot p_y;$$

[3.27]

Combining constitutive relations, equilibrium, compatibility and renaming $F_{xf} + F_{xr} = F_{xw}$, where w refers to wheel), gives, as Matlab script:

```
clear, syms zf zr Fzf Fzr Fzf0 Fzr0 ax z py
sol=solve( ...
    'Fzf=Fzf0-cf*zf', ...
    'Fzr=Fzr0-cr*zr', ...
    'Fzf0+Fzr0=m*g', ...
    'Fzf0*lf-Fzr0*lr=0', ...
    '-Fair-m*ax+Fxw=0', ...
    'm*g-Fzf-Fzr=0', ...
    'Fzr*lr-Fzf*lf-Fxw*h-Fair*(hair-h)=0', ...
    'zf=z-lf*py', ...
    'zr=z+lr*py', ...
    zf, zr, Fzf, Fzr, Fzf0, Fzr0, ax, z, py);
```

[3.28]

The solution from Matlab script in Equation [3.28] becomes:

$$a_x = \frac{F_{xw} - F_{air}}{m};$$
$$z = -\frac{c_f \cdot l_f - c_r \cdot l_r}{c_f \cdot c_r \cdot (l_f + l_r)^2} \cdot \left(F_{xw} \cdot h + F_{air} \cdot (h_{air} - h)\right)$$
$$p_y = -\frac{c_f + c_r}{c_f \cdot c_r \cdot (l_f + l_r)^2} \cdot \left(F_{xw} \cdot h + F_{air} \cdot (h_{air} - h)\right)$$

[3.29]

In agreement with intuition and experience the body dives (positive pitch) when braking (negative F_{xw}). Further, the body centre of gravity is lowered (negative z) when braking and weaker suspension front than rear ($c_f \cdot l_f < c_r \cdot l_r$), which is normally the chosen design for cars.

The air resistance force is brought into the equation. It can be noted that for a certain deceleration, there will be different heave and pitch depending on how much of the decelerating force that comes from air resistance and from longitudinal wheel forces. But, as already noted, heave and pitch does not depend on how wheel longitudinal force is distributed between the axles.

3.4.9 Load Transfer including suspension linkage effects

In previous model of load transfer, see Section 3.3.9, we assumed nothing about the transients of transfer (vertical wheel) loads between front and rear axle. So, if we study longer events when the wheel force is applied and then kept constant for a longer time (1-5 s), it is often a good enough model. But if the wheel forces vary more, we need to capture the transients better. Then it is important to consider that the linkage can transfer some of the wheel longitudinal forces. When studying the transients, it is also relevant to consider the damping.

Another reason for doing a better model than in Section 3.3.9 can be that one is interested in the displacements, heave and pitch, which are not covered in the model in Section 3.3.9.

There are basically two modelling ways to include the suspension in the load transfer: through a pitch centre or through a pivot point for each axle, see Figure 3-45.
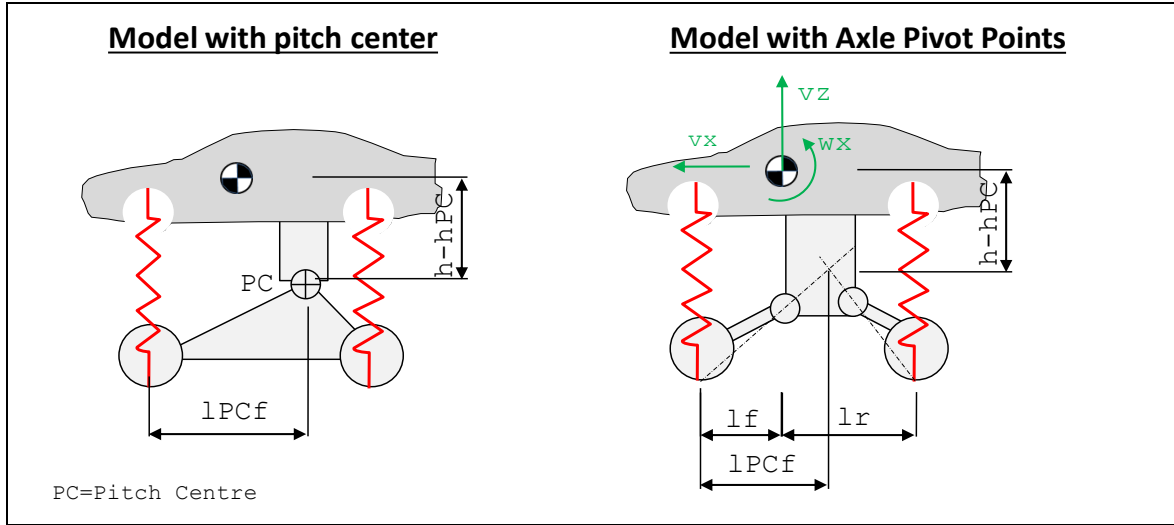
Figure 3-45: Models for including suspension effects in longitudinal load transfer

3.4.9.1   Load Transfer model with Pitch Centre

This model will not be deeply presented in this compendium. It has drawbacks in that it has only one suspended degree of freedom. Also, it does not take the distribution of longitudinal wheel forces between the axles into account. These short comings is not very important for studying dive and squat, but they are essential when studying rapid individual wheel torque changes in time frames of 0.1 s, such as studying ABS or traction control. So, since the model with axle pivot points is more generally useful and not much more computational demanding (and probably more easy intuitively), that model is prioritized in this compendium.

3.4.9.2   Load Transfer model with Axle Pivot Points

Behold the free-body diagram in Figure 3-46. The road is assumed to be flat, $z_{fr} = z_{rr} \equiv 0$. The force play in the rear axle is shown in more detail. P_{xr} and P_{zr} are reaction forces in the pivot point. F_{sr} is the force in the elasticity, i.e. where potential spring energy is stored. The torque T_{sr} is the shaft torque, i.e. from the propulsion system. Both torque from propulsion and brake system contribute to F_{xr}. But torque from friction brake $T_{reac,r}$ is not visible in free-body diagram, unless decomposed in suspension and wheel, as in the right-most part of Figure 3-46. This is because the friction braking appears as internal torque (or, depending on the brake design, probably forces) between brake pad and brake calliper. Any part of the longitudinal wheel force that is applied via reaction torque to unsprung parts will not add to shaft torque, such as an electric motor mounted on unsprung parts. The term $\omega_y \cdot v_x$ in a_z is often negelctable, except for during high speed, i.e. large v_x. The term can be explained as the other centripetal accelerations (giving centrifugal (fictive) forces) in Section 4.4.2.2.

We assume that displacements are measured from the forces F_{sf0} and F_{sr0}, respectively, and that the compliances are linear. The total constitutive equations become:

$$F_{sf} = F_{sf0} + c_f \cdot \left(z_{ff} - z_f \right) \quad and \quad F_{sr} = F_{sr0} + c_r \cdot \left(z_{rr} - z_r \right) \qquad \text{[3.30]}$$

Now, there are two ways of representing the dynamics in spring-mass systems: Either as second order differential equations in position or first order differential equations in velocity and force. We select the latter, because it is easier to select suitable initial values. Then we need the differentiated versions of the compliances constitutive equations:

$$\dot{F}_{sf} = 0 + c_f \cdot \left(\dot{z}_{ff} - \dot{z}_f \right) = -c_f \cdot v_{zf} \quad and \quad \dot{F}_{sr} = 0 + c_r \cdot \left(\dot{z}_{rr} - \dot{z}_r \right) = -c_r \cdot v_{zr} \qquad \text{[3.31]}$$
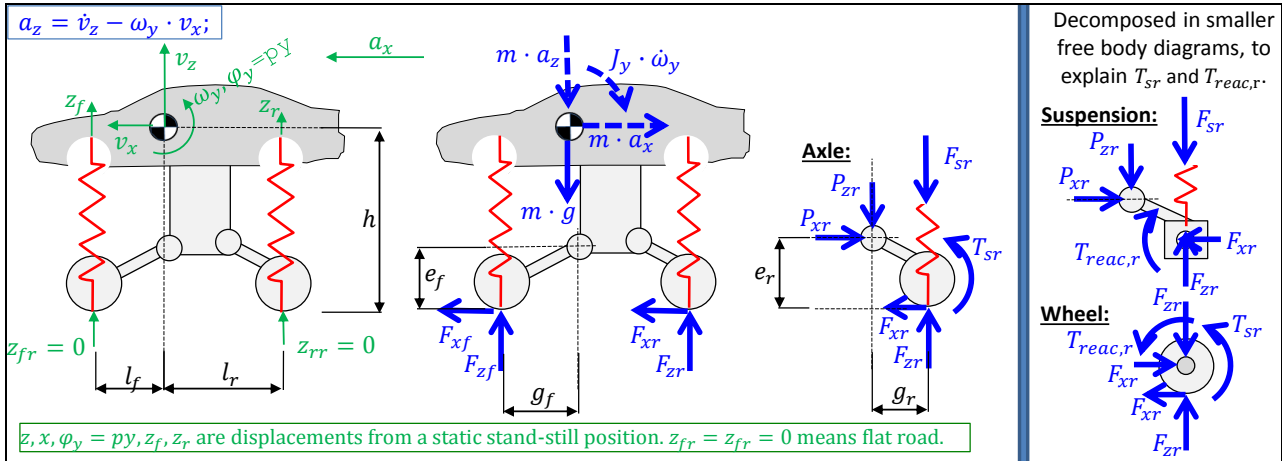
Figure 3-46: Free-body diagram for model with Axle Pivot Points

Damping is included in the model, but it is not drawn in Figure 3-46, for graphical simplicity. The damper forces are denoted F_{df} and F_{dr}. They will appear in the equilibrium equations quite similar to F_{sf} and F_{sr}. Note that the damping coefficients, d_f and d_r, are the effective ones, i.e. the ones defined at the wheel contact point with ground, as opposed to the physical ones defined for the actual physical damper. C.f. effective stiffness in Section 3.4.7.

$$F_{df} = d_f \cdot \left(\dot{z}_{fr} - \dot{z}_f \right) = -d_f \cdot v_{zf} \quad and \quad F_{dr} = d_r \cdot \left(\dot{z}_{rr} - \dot{z}_r \right) = -d_r \cdot v_{zr} \qquad [3.32]$$

Now, 3 equilibria for whole vehicle and one moment equilibria around pivot point for each axle gives:

$$
\begin{aligned}
&-m \cdot \dot{v}_x + F_{xf} + F_{xr} = 0; \\
&-m \cdot \left(\dot{v}_z + \omega_y \cdot v_x \right) - m \cdot g + F_{zf} + F_{zr} = 0; \\
&-J \cdot \dot{\omega}_y + F_{zr} \cdot l_r - F_{zf} \cdot l_f - \left(F_{xf} + F_{xr} \right) \cdot h = 0; \\
&\left(F_{zr} - F_{sr} - F_{dr} \right) \cdot g_r - F_{xr} \cdot e_r + T_{sr} = 0; \\
&\left(F_{sf} + F_{df} - F_{zf} \right) \cdot g_f - F_{xf} \cdot e_f + T_{sf} = 0;
\end{aligned}
\qquad [3.33]
$$

It can be noted that a "trivial suspension" (wheel kinematics simply vertically supported), the same equations is valid if we let $g_r \to \infty$ and $g_f \to \infty$. It is then no difference if the vehicle is actuated with a F_{xi} via shaft torque T_{si} or via reaction to unsprung parts, $T_{reac,i}$.

Compatibility, to connect to body displacements, z and p_y, gives:

$$
\begin{aligned}
&z_f = z - l_f \cdot p_y; \quad and \quad z_r = z + l_r \cdot p_y; \\
&v_{zf} = v_z - l_f \cdot \omega_y; \quad and \quad v_{zr} = v_z + l_r \cdot \omega_y; \\
&\dot{z} = v_z; \quad and \quad \dot{p}_y = \omega_y;
\end{aligned}
\qquad [3.34]
$$

By combining constitutive relations, equilibrium and compatibility we can find explicit function so that:

$$
\begin{aligned}
&StateDerivatives = function(States, Inputs); \\
&States = \begin{bmatrix} v_x & v_z & \omega_y & F_{sf} & F_{sr} & z & p_y \end{bmatrix}; \\
&StateDerivatives = \begin{bmatrix} \dot{v}_x & \dot{v}_z & \dot{\omega}_y & \dot{F}_{sf} & \dot{F}_{sr} & \dot{z} & \dot{p}_y \end{bmatrix}; \\
&Inputs = \begin{bmatrix} F_{xf} & F_{xr} & T_{sf} & T_{sr} \end{bmatrix};
\end{aligned}
\qquad [3.35]
$$

Equation [3.35] can be solved with well-established methods for numerical ode solution, if *Inputs* are known as functions of time and initial values of *States* are known. Such simulation of Equation [3.35] is shown in Section 3.4.13.

3.4.9.3 Quasi-steady state heave and pitch due to longitudinal wheel forces

If we study long term quasi-steady state (all derivatives, except $\dot{v}_x$, zero and $\omega_y \cdot v_x$ zero) for the model described in Section 3.4.9.2 we find a model comparable with the model in Section 3.4.7 but also including non-zero displacements, heave z and pitch φ_y. So, Equations [3.30] to [3.34] are combined. We also neglect air resistance force for clarity of equations. Equation [3.30] becomes, in Matlab format:

```
clear, syms zf zr Fzf Fzr Fsf0 Fsr0 ax Fsf Fsr z py
sol=solve( ...
    'Fsf=Fsf0-cf*zf',    'Fsr=Fsr0-cr*zr', ...
    'Fsf0+Fsr0=m*g',     'Fsf0*lf-Fsr0*lr=0', ...
    '-m*ax+Fxf+Fxr=0', ...
    '-m*(0+0)-m*g+Fzf+Fzr=0', ...
    '-J*0+Fzr*lr-Fzf*lf-(Fxf+Fxr )*h=0', ...
    '(Fzr-Fsr-0 )*gr-Fxr*er+Tsr=0', '(Fsf+0-Fzf )*gf-Fxf*ef+Tsf=0', ...
    'zf=z-lf*py',        'zr=z+lr*py', ...
    zf, zr, Fzf, Fzr, Fsf0, Fsr0, ax, Fsf, Fsr, z, py);

%results:

% ax = (Fxf + Fxr)/m

% z  = -(Tsr*cf*gf*lf^2 - Tsf*cr*gr*lr^2 + Tsr*cf*gf*lf*lr - Tsf*cr*gr*lf*lr
- Fxr*cf*er*gf*lf^2 + Fxf*cr*ef*gr*lr^2 + Fxf*cf*gf*gr*h*lf +
Fxr*cf*gf*gr*h*lf - Fxf*cr*gf*gr*h*lr - Fxr*cr*gf*gr*h*lr -
Fxr*cf*er*gf*lf*lr + Fxf*cr*ef*gr*lf*lr)/(cf*cr*gf*gr*(lf + lr)^2)

% py = -(Tsr*cf*gf*lf + Tsr*cf*gf*lr + Tsf*cr*gr*lf + Tsf*cr*gr*lr +
Fxf*cf*gf*gr*h + Fxr*cf*gf*gr*h + Fxf*cr*gf*gr*h + Fxr*cr*gf*gr*h -
Fxr*cf*er*gf*lf - Fxf*cr*ef*gr*lf - Fxr*cf*er*gf*lr -
Fxf*cr*ef*gr*lr)/(cf*cr*gf*gr*(lf + lr)^2)
```

[3.36]

The solution should be compared with corresponding solution in Equation [3.29]. One can see that ax is in complete alignment between the two models. Then, a general reflection is that the displacement, z and py, in Equation [3.36] follows a complex formula, but that they are dependent on how the $F_{xw} = F_{xf} + F_{xr}$ is applied: both dependent on distribution between axles and dependent on how much of the axle forces (F_{xf} and F_{xr}) that are actuated with shaft torques (T_{sf} and T_{sr}, respectively). In Figure 3-50, dashed lines show the quasi-steady state solutions from Equation [3.29].

3.4.9.4 Examples of real suspension designs

In Figure 3-46, some kind of "trailing arm" is drawn both for front and rear axle. For rear axle, that is a realistic design even if other designs are equally common. However, for front axle a so called McPherson suspension is much more common, see Figure 3-47.
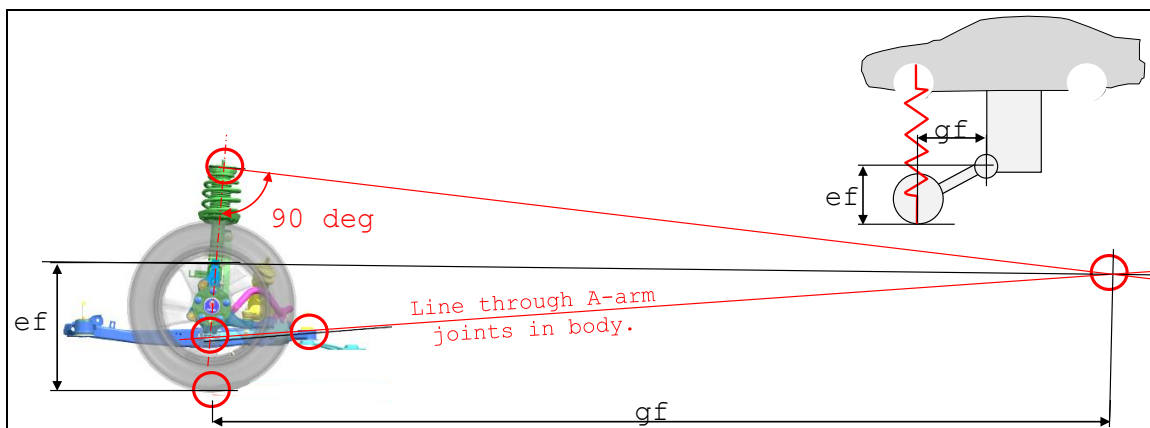
Figure 3-47: Example of typical front axle suspension, and how pivot point is found. The example shows a McPherson suspension. From Gunnar Olsson, LeanNova.
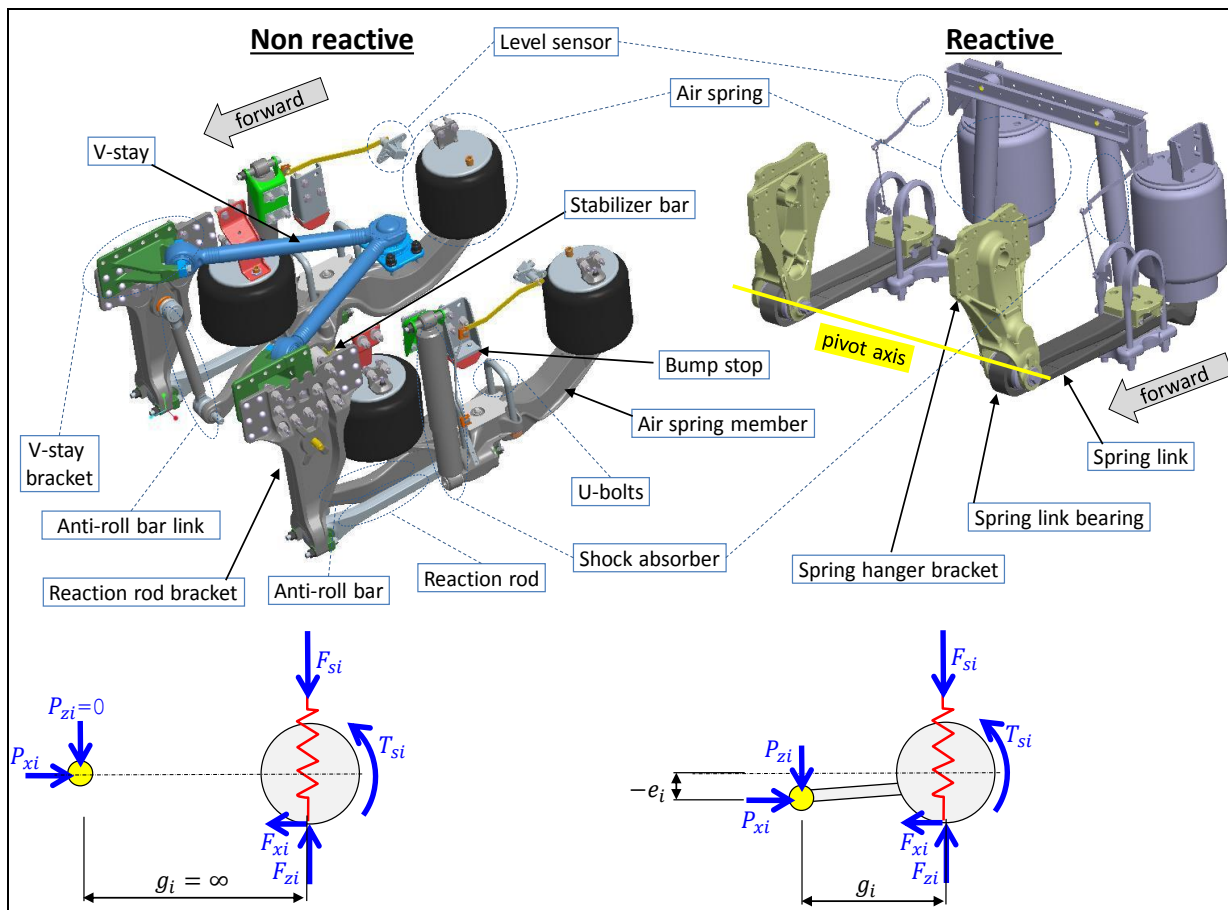
Figure 3-48: Axle suspensions/installations for heavy vehicles.

3.4.9.5 Additional phenomena

It is relevant to point out the following, which are not modelled in this compendium:

- **Stiffness** and **damping** may be dependent of **wheel (vertical) displacement** and **wheel steering angle**. One way of inserting this in the model is to make the coefficients varying with spring force, which is a measure of how much compressed the suspension is. Here, non-linearity within spring working range, as well as bump stops, can be modelled. Also, **position of pivot points (or pitch and roll centres)** can be dependent of wheel displacement steering angle.
- Dampers are often **deformation direction dependent**, i.e. different damping coefficients are suitable to use for compression and rebound. Typical is 2..4 times softer (smaller d [N/(m/s)]) in compression than in rebound.

3.4.10 Dive at braking *

*Function definition: **Dive at braking** is pitch angle change that the vehicle body experience when brake pedal is applied to a certain deceleration level, from driving straight ahead. Either the peak or steady state pitch angle can be addressed.*

Now, study the suspension at front axle in Figure 3-46. When the axle is braked, F_{xf} will be negative and push the axle rearwards, i.e. in under the body. The front of the vehicle will then be lifted as in pole jumping. This means that this design counter-acts the (transient) dive of the front. (Only the transient dive will be reduced, while the dive after a longer time of kept braking is dependent only on the stiffnesses according to Equation [3.29].) The design concept for front axle suspension to place the pivot point behind axle and above ground is therefore called "anti-dive".

If the braking is applied without shaft torque T_{sf}, a good measure of the Anti-dive mechanism is e_f/g_f. This is the normal way for braking, since both the action and reaction torque acts on the axle. For in-

board brakes, or braking via propulsion shaft, the reaction torque is not taken within the axle, but the reaction torque is taken by the vehicle body. The action torque T_{sf} then appears in the equilibrium equation for the axle, as shown in Equation [3.33]. If we neglect the wheel rotational dynamics for a while, we can insert $T_{sf} = F_{xf} \cdot R_w$ in the equation with T_{sf} in Equation [3.33]:

$$
\begin{aligned}
&\left(F_{sf} + F_{df} - F_{zf}\right) \cdot g_f - F_{xf} \cdot e_f + T_{sf} = 0; with\ T_{sf} = F_{xf} \cdot R_w;\ \Rightarrow \\
&\Rightarrow \left(F_{sf} + F_{df} - F_{zf}\right) \cdot g_f - F_{xf} \cdot e_f + F_{xf} \cdot R_w = 0; \Rightarrow \\
&\Rightarrow \left(F_{sf} + F_{df} - F_{zf}\right) \cdot g_f - F_{xf} \cdot \left(e_f - R_w\right) = 0;
\end{aligned}
$$

[3.37]

We can then see that a good measure of the Anti-dive mechanism is $\left(e_f - R_w\right)/g_f$ instead.

3.4.11   Squat at propulsion *

Function definition: **Squat at propulsion** *is pitch angle change that the vehicle body experience when accelerator pedal is applied to a certain acceleration level, from driving straight ahead. Either the peak or steady state pitch angle can be addressed.*

Now, study the suspension at rear axle in Figure 3-46. When the axle is propelled, F_{xr} will push the axle in under the body. This means that this design reduces the rear from squatting (transiently). The design concept for rear axle suspension to place the pivot point ahead of axle and above ground is therefore called "anti-squat".

3.4.12   Anti-dive and Anti-squat designs

With Anti-dive front and Anti-squat rear, we avoid front lowering at braking and rear lowering at acceleration, respectively. But how will the designs influence the parallel tendencies: that rear tend to lift at braking and front then to lift at propulsion? Well, they will luckily counteract also these: Braking at rear axle will stretch the rear axle rearwards and upwards relative to the body. When propelling the front axle, the propulsion force will stretch the front axle forwards and upwards relative to the body. (If one brakes at one axle and propels at the other, the reasoning is not valid. This mode may seem irrelevant, but could be desired for a hybrid vehicle with ICE on front axle and electric motor on rear axle, if one would like to charge batteries "via the road". This is an example of that novel designs may rise new issues.)

In summary: Anti-dive and anti-squat refer to the front diving when braking and the rear squatting when acceleration. Anti-dive and anti-squat can be measured in fractions: Anti-dive for $=e_f/g_f$ or $= \left(e_f - R_w\right)/g_f$ and Anti-squat$=e_r/g_r$ or $= (e_r - R_w)/g_r$. Normal values are typically 0.05..0.15.

Figure 3-49: Anti-Dive Geometry, (Gillespie, 1992)

3.4.13   Deceleration performance *

Function definition: See Section 3.4.2.2.

Deceleration performance can now be predicted, including the suspension mechanisms. It is a very important function, and every decimetre counts when measuring braking distance in standard tests like braking from 100 to 0 km/h. The active control of the brake torques (ABS function) is then very important, and this is so fast dynamics that the suspension mechanisms of Anti-lift and Anti-dive influences. The position of the load in the vehicle will influence, since it influences the load transfer.

We will now set up a mathematical model, see Equation [3.38], which shows how the normal forces change during a braking event. It is based on the physical model in Figure 3-46. Note that we can **not neglect** the term $\omega_y \cdot v_x$ as we did in Section 3.4.9.3, since the manoeuvre cannot be seen as quasi-steady state. Driving resistance contributes normally with a large part of the deceleration, but we will neglect this for simplicity, just to show how the suspension mechanism works. The equations in the

model are presented in the dynamic modelling standardized format "Modelica", and are hence more or less identical to Equation [3.31] to [3.34].

```
Fxf = if 1 < time and time < 3 then -0.4*m*g else 0;
Fxr = if 3 < time and time < 7 then -0.4*m*g else 0;
Tsf/Rw = 0;
Tsr/Rw = if 5 < time and time < 7 then -0.4*m*g else 0;

// Motion equations:
der(z) = vz;
der(py) = wy;

// Constitutive equations for the springs:
der(Fsf) = -cf*vzf;
der(Fsr) = -cr*vzr;

// Constitutive equations for the dampers:
Fdf = -df*vzf;
Fdr = -dr*vzr;

//(Dynamic) Equilibrium equations:
-m*der(vx) + Fxf + Fxr = 0;
-m*(der(vz)-wy*vx) - m*g + Fzf + Fzr = 0;
-Jy*der(wy) + Fzr*lr - Fzf*lf - (Fxf + Fxr)*h = 0;
(Fzr - Fsr - Fdr)*gr - Fxr*er + Tsr = 0;
(Fsf + Fdf - Fzf)*gf - Fxf*ef + Tsf = 0;

//Compatibility:
zf = z - lf*py;
zr = z + lr*py;
vzf = vz - lf*wy;
vzr = vz + lr*wy;
```

[3.38]

The simulation results are shown in Figure 3-50. It shows a constant deceleration, but it is changed how the decelerating force is generated. At time=3 s, there is a shift from braking solely on front axle to solely on rear axle. The braking is, so far, only done with friction brakes, i.e. generating torque by taking reaction torque in the axle itself. At time=5 s, there is a shift from braking with friction brakes to braking with shaft torque. It should be noted that if we shift axle or shift way to take reaction torque, gives transients even if the deceleration remains constant.

One can also see, at time=1 s, that the normal load under the braked axle first changes in a step. This is the effect of the Anti-dive geometry. Similar happens when braking at rear axle, due to the Anti-squat geometry. Since brake performance is much about controlling the pressure rapidly, the transients are relevant and the plots should make it credible that it is a control challenge to reach a high braking efficiency.

3.4.14   Acceleration performance *

Function definition: See Section 3.3.10.1.

The model presented in Equation [3.38] can also be used to predict acceleration performance in a more accurate way compared to Section 3.3.10. Especially, the more accurate model is needed when propelling or braking on the limit of tyre to road adhesion, since the normal load of each tyre then is essential. It is a challenge to control the propulsion and brake wheel torques to utilize the varying normal loads under each axle.
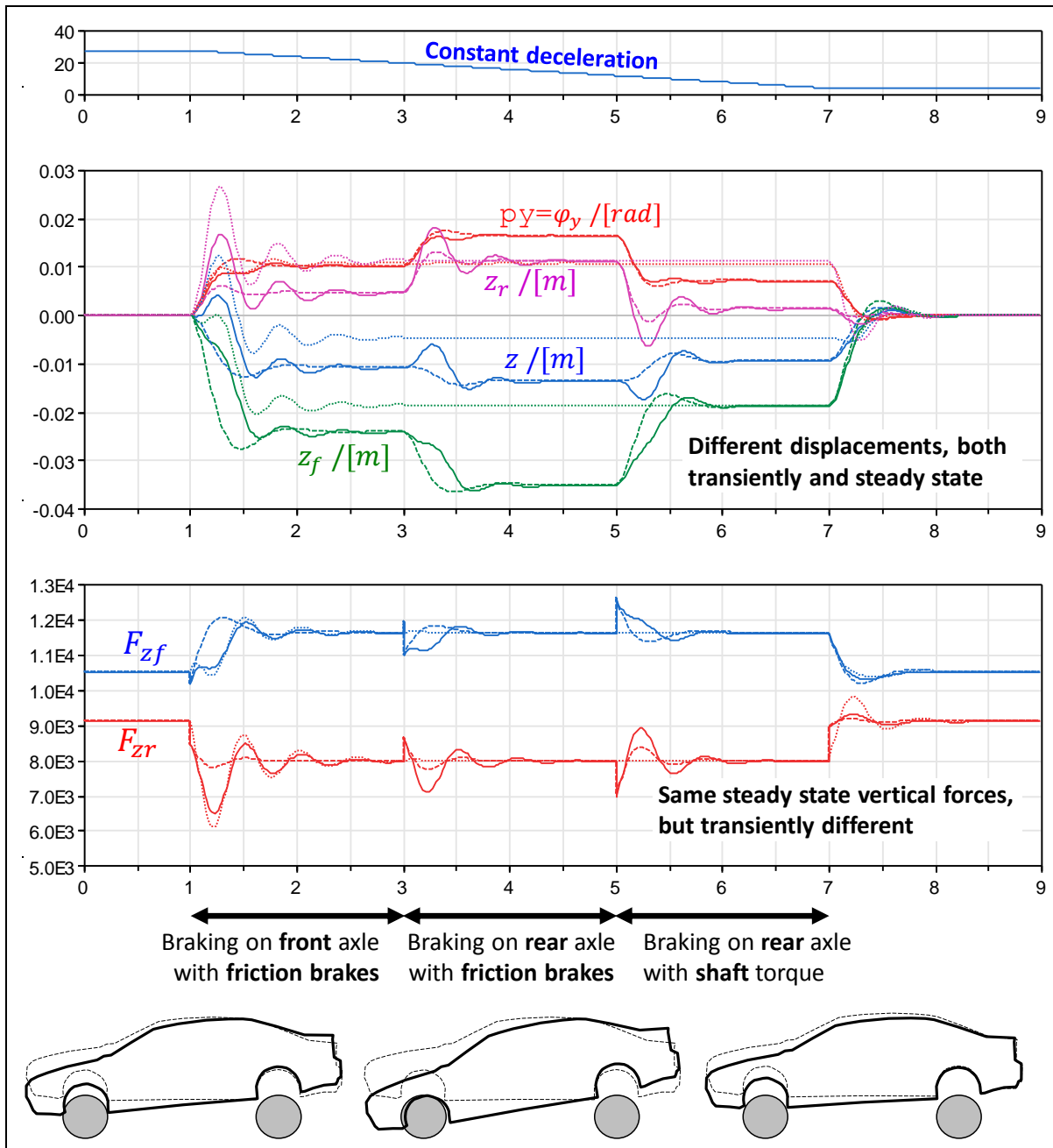
Figure 3-50: Deceleration sequence with constant vehicle deceleration, but changing between different ways of actuation. (With the centripetal term $\omega_y \cdot v_x$ (solid) and without (dashed). Dotted shows without anti-dive/-squat geometry, i.e. $g_f = g_r = \infty$.)

3.5 Control functions

Some control functions will be presented briefly. There are more, but the following are among the most well-established ones. First, some general aspects on control are given.

3.5.1 Longitudinal Control

Some of the most important sensors available in production vehicles and used mainly for longitudinal control are listed below. (Sensors for instrumented vehicles for testing can be many more.)

- **Wheel Speed Sensors**, WSS. For vehicle control design, one can often assume that "sensor-close" software also can supply information about longitudinal vehicle speed.

- **Vehicle body inertial sensors.** There is generally a yaw rate gyro and a lateral accelerometer available, but sometimes also a longitudinal accelerometer. The longitudinal accelerometer is useful for longitudinal control and longitudinal velocity estimation.
- **Pedal sensors**. Accelerator pedal normally has a position sensor and brake pedal force can be sensed via brake system main pressure sensor. Heavy vehicles often have both a brake pedal position and brake pressure sensors.
- High specification modern vehicles have **environment sensors** (camera, radar, GPS with electronic map, etc.) that can give information (relative distance and speed, etc.) about objects ahead of subject vehicle. It can be both fixed objects (road edges, curves, hills, …) and moving objects (other road users, animals, …).
- Information about what actuation that is **actually applied at each time instant** is available, but it should be underlined that the confidence in that information often is questionable. Information about axle propulsion torque is generally present, but normally relies on imprecise models of the whole combustion process and torque transmission, based on injected amount of fuel and gear stick position. (Electric motors can typically give better confidence in estimation, especially if motor is close to the wheel without too much transmission in between.) Wheel individual friction brake torque is available, but normally rely on imprecise models of the brake systems hydraulic/pneumatic valves and disc friction coefficient, based on brake main cylinder pressure.
- Information about what **actuation levels that are possible** upon request (availability or capability) is generally not so common. It is difficult to agree of general definitions of such information, because different functions have so different needs, e.g. variations in accepted time delay for actuation.
- Sometime **wheel/axle forces** can be sensed. One case is when pneumatic suspension. More extreme variants are under development, such as sensors in the wheel bearings which can sense forces (3 forces and roll and yaw moment) (SKF) and sensors in drive shafts (ABB).

3.5.2 Longitudinal Control Functions

3.5.2.1 Pedal driving *

Function definition: See Section 3.4.4.

These functions, Pedal Response *, are often not seen as comparable with other control functions, but they become more and more relevant to define as such, since both accelerator and brake pedals tend to be electronically controlled, and hence they become increasingly tuneable. Also, more and more functions, such as those below in section 3.5.2, will have to be arbitrated with the pedals.

In modern passenger vehicles, Accelerator pedal is normally electronically controlled but the Brake pedal is basically mechanical. In modern heavy commercial vehicles, both functions are electronically controlled.

The functions in Section "3.4.5 Pedal Feel *" are normally not actively controlled, but in there are concept studies with active pedals, where also the pedal feel can be actively changed to give feedback to driver.

3.5.2.2 Cruise Control and Adaptive Cruise Control (CC, ACC) *

*Function definition: **Cruise Control, CC,** controls the vehicle's longitudinal speed. Driver can activate the function and decide desired speed.*

*Function definition: **Adaptive Cruise Control, ACC,** is an addition to CC. ACC controls the vehicle's time gap to a lead vehicle. Driver can activate the function and decide desired gap. When there is no lead vehicle, CC controls the vehicle's speed.*

The purpose of CC is to keep the vehicle at a driver selected longitudinal speed, while driver not pushes the accelerator pedal. The actuator used is the propulsion system. In heavy vehicles also the braking system (both retarders and service brakes) is used to maintain or regulate the vehicle speed.

ACC is an addition to CC. The purpose of ACC is to keep a safe distance to the lead vehicle (vehicle ahead of subject vehicle). ACC uses also friction brake system as actuator, but normally limited to a deceleration of $2..4\ m/s^2$.

The safe distance which ACC aims for, is often expressed as a time gap, driver adjustable in the range $2..3\ s$. A model behind this is that the time gap is the driver reaction time and the subject vehicle can decelerate as much as the object vehicle. More advanced models can allow smaller time gap in certain situations. This is desired because it reduces the risk that other vehicles cut in between subject and leading object vehicle. Such models can take into account, e.g., acceleration of the object vehicle, pedal operation of subject vehicle, road gradient, road curvature, road friction and deceleration capabilities of subject and object vehicles.

CC is normally only working down to $30..40\ km/h$. ACC can have same limitation, but with automatic transmission, good forward looking environment sensors, brake actuators and speed sensing, ACC can be allowed all the way down to stand-still.

3.5.2.3   Anti-lock Braking System, ABS *

*Function definition: **Anti-lock Braking System, ABS**, prohibits driver to lock the wheels while braking. The wheel brake torques requested are limited by ABS in a way that each individual wheel's longitudinal slip stays above a certain (negative) value. An extended definition of ABS also includes vehicle deceleration requested by other functions than pedal braking, such as AEB. ABS only uses friction brake as actuator.*

The purpose of ABS is to avoid losing vehicle brake force due to that the tyre force curve drops at high slips AND to leave some friction for steering and cornering, see Sections **2.4**, **0** and **2.6**. ABS is a wheel slip closed loop control, active when driver brakes via brake pedal. It keeps the slip above a certain value, typically -15..-20 %. ABS uses the friction brakes as actuator.

Each wheel is controlled individually, but all wheels speed sensors contribute to calculation of vehicle longitudinal speed (which is needed to calculate actual slip value). In the ABS function, it may be included how slip are distributed between the wheels, such as normally the front axle is controlled to a slip closer to locking than the rear axle. Also, a sub function called "select-low" which means that the wheel closest to locking decides the pressure also for the other wheel at the same axle. Select-low is typically used at rear axles.
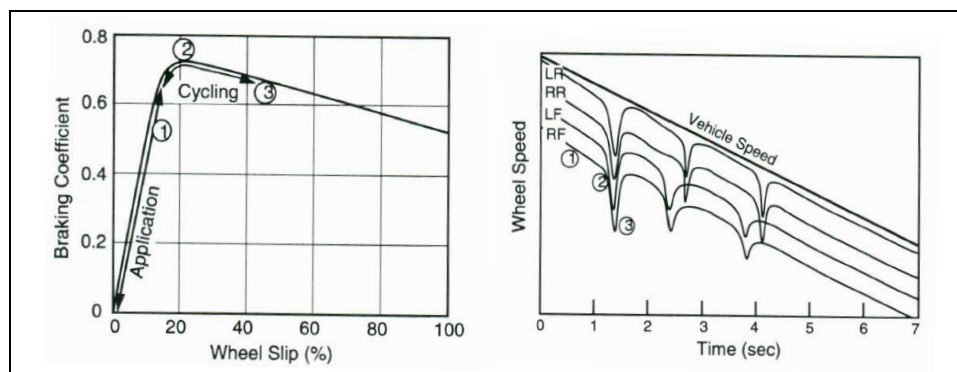
Figure 3-51: ABS control. Principle and control sequence

3.5.2.4   Electronic Brake Distribution, EBD *

*Function definition: **Electronic Brake Distribution** prohibits driver to over-brake the rear axle while braking. An extended definition of EBD also includes vehicle deceleration requested by other functions than pedal braking, such as AEB. EBD only uses friction brake as actuator.*

With a fix proportioning between front and rear axle braking, there is a risk to over-brake rear axle when friction is very high, since rear axle is unloaded so much then. Before electronic control was available, it was solved by hydraulic valves, which limited the brake pressure to rear axle when pedal force became too high. In today's cars, where electronic brake control is present thanks to legislation of ABS, the software base function EBD fulfils this need. In heavy vehicles, pneumatic valves are used

that limits the brake pressure in relation to the rear axle load (deflection of mechanical spring suspension or air pressure in air suspension).
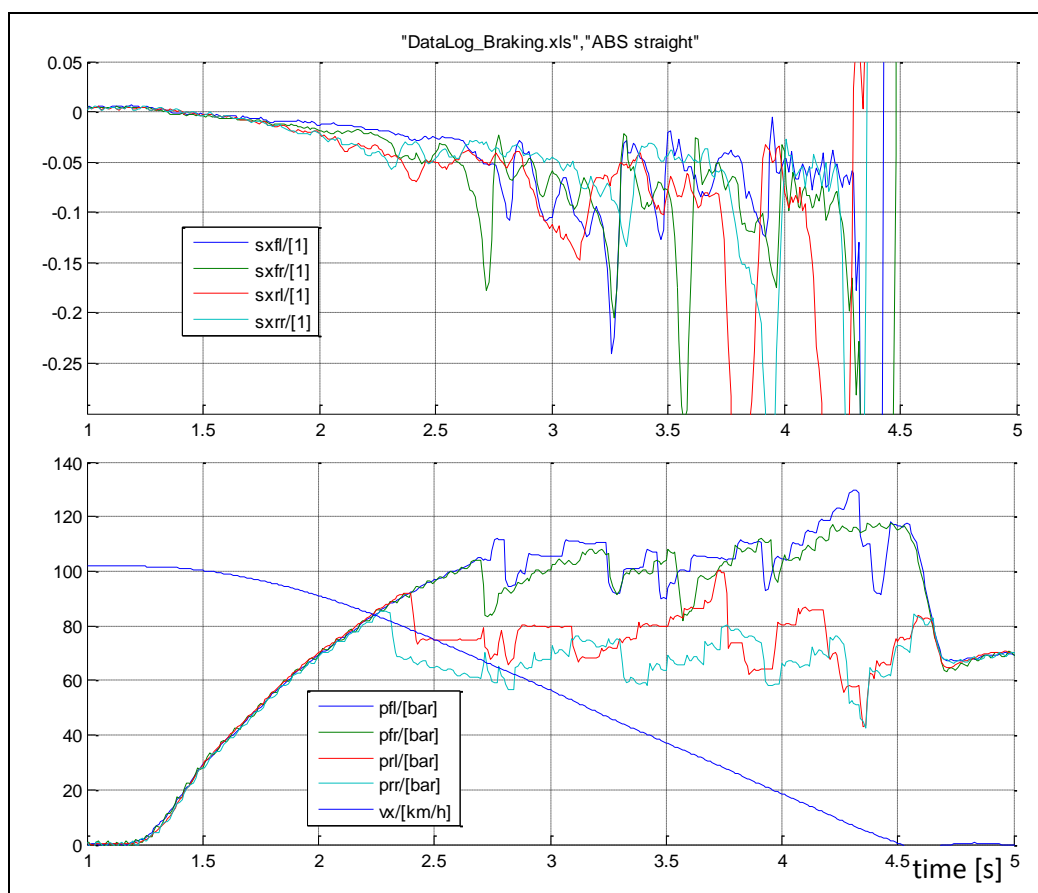
Figure 3-52: ABS control, Data log from passenger car test.

There are other side functions enabled by having ABS on-board. Such are "select low", which means that the brake pressure to both wheels on an axel is limited by the one with lowest pressure allowed from ABS. So, if one wheel comes into ABS control, the other gets the same pressure. This is most relevant on rear axle (to reduce risk of losing side grip) but one tries to eliminate the need of it totally, because it reduces the brake efficiency when braking in curve or on different road friction left/right.

It is often difficult to define strict border between functions that is a part of ABS and which is part of EBD, which is why sometimes one say ABS/EBD as a combined function.

3.5.2.5 Traction Control, TC *

*Function definition: **Traction Control** prohibits driver to spin the driven axle(s) in positive direction while accelerating. An extended definition of TC also includes vehicle acceleration requested by other functions than pedal braking, such as CC. TC uses both friction brakes and propulsion system as actuators.*

The purpose of Traction Control is to maximise traction AND to leave some friction for lateral forces for steering and cornering. Traction control is similar to ABS, but for keeping slip below a certain value, typically +(15..20)%.

Traction control can use different ways to control slip, using different actuators. One way is to reduce engine torque, which reduces slip on both wheels on an axle if driven via differential. Another way is to apply friction brakes, which can be done on each wheel individually. Vehicles with propulsion on several axles can also redistribute propulsion from one axle to other axles, when the first tends to slip. Vehicles with transversal differential clutch or differential lock can redistribute between left and right wheel on one axle.

3.5.2.6 Engine Drag Torque Control, EDC *

Function definition: **Engine Drag Torque Control** *prohibits over-braking of the driven axle(s) while engine-braking. EDC uses both friction brakes and propulsion system as actuators.*

The purpose of Engine Drag Torque Control is as the purpose of ABS, but the targeted driving situation is when engine braking at low road friction, when engine drag torque otherwise can force the wheels to slip too much negative. Similarly to ABS, it keeps the slip above a certain negative value. However, it does it by increasing the engine torque from negative (drag torque) to zero (or above zero for a short period of time).

3.5.2.7 Automatic Emergency Brake, AEB *

Function definition: **Automatic Emergency Brake** *decelerates vehicle without driver having to use brake pedal when probability for forward collision is predicted as high.*

The purpose of AEB is to eliminate or mitigate collisions where subject vehicle collides with a lead vehicle. AEB uses friction brake system as actuator, up to full brake which would be typically 10 m/s2. An AEB system is often limited by that it cannot be designed to trigger too early, because driver would be disturbed or it could actually cause accidents. Therefore, in many situations, AEB will rather mitigate than avoid collisions. (The A in the abbreviation AEB can be for either of "Automatic", "Autonomous" or "Advanced".)

Conceptually, an AEB algorithm can be assumed to know physical quantities as marked in Figure 3-53. The quantity time-to-collision, TTC, can then be defined as $TTC = x_o/(v_x - v_{ox})$, which means the time within a collision will appear if no velocities changes. Also, one can define enhanced time-to-collision measure, eTTC, which takes into account the present accelerations of the lead vehicle. TTC and eTTC can also be drawn in PVA-time-diagram, see Figure 2-46. TTC shall not be mixed up with another time measure, "time gap" (TG), which is the time when subject vehicle will reach the present position of the lead vehicle, $TG = x_o/v_x$;.

AEB function shall, continuously, decide whether or not to trigger AEB braking. AEB shall intervene by braking when driver can be assumed to collide without intervention. If no other information, this can be predicted as when driver can NOT avoid by normal driving. Avoidance manoeuvres that have to be considered are (normal) deceleration and (normal) lateral avoidance to the left and to the right. What to assume as normal driving is a question of tuning; here the following limits are used $|\dot{v}_x| < a_{xn} = e.g.\ 4\ m/s^2$ and $|\dot{v}_y| < a_{yn} = e.g.\ 6\ m/s^2$. A physical model based algorithm can start from the following simple models. (The notation "$(\cdot)$" means "over a time interval".)

- Normal **deceleration** ($\dot{v}_x = -a_{xn} = -4\ m/s^2$) leads to **collision if**:
$$\min_{t > 0}(x_o(\cdot)) < 0 \Rightarrow \min_{t > 0}\left(x_o + v_{ox} \cdot t - \left(v_x \cdot t + a_{xn} \cdot \frac{t^2}{2}\right)\right) < 0 \Rightarrow$$
$$\Rightarrow \left. \left(x_o + v_{ox} \cdot t - \left(v_x \cdot t + a_{xn} \cdot \frac{t^2}{2}\right)\right)\right|_{t=\frac{v_{ox}-v_x}{a_{xn}}} < 0 \Rightarrow$$
$$\Rightarrow x_o - \frac{1}{2 \cdot (-a_{xn})} \cdot (v_x - v_{ox})^2 < 0 \Rightarrow \frac{x_o}{v_x - v_{ox}} = TTC < \frac{v_x - v_{ox}}{2 \cdot (-a_{xn})} = \frac{v_x - v_{ox}}{8};$$

- Normal **avoidance to the left** ($\dot{v}_y = a_{yn} = 6\ m/s^2$) leads to **collision if**:
$$\left. \left(y_{ol}(\cdot) + \frac{w}{2}\right)\right|_{x_o=0} < 0 \Rightarrow \left. \left(y_{ol} - a_{yn} \cdot \frac{t^2}{2} + \frac{w}{2}\right)\right|_{t=\frac{x_o}{v_x - v_{ox}}} < 0 \Rightarrow$$
$$\Rightarrow \frac{x_o}{v_x - v_{ox}} = TTC < \sqrt{2 \cdot \frac{y_{ol} + w/2}{a_{yn}}} = \{e.g.\} = \sqrt{\frac{0.6 + 1.8/2}{3}} \approx 0.4\ s;$$

- Normal **avoidance to the right** ($\dot{v}_y = -a_{yn} = -6\ m/s^2$) leads to **collision if**:
$$\cdots \Rightarrow \frac{x_o}{v_x - v_{ox}} = TTC < \sqrt{2 \cdot \frac{-y_{or} - w/2}{a_{yn}}} = \sqrt{\frac{-y_{or} + w/2}{3}};$$

- Assuming that the AEB intervention decelerates the vehicle with $-\dot{v}_x = a_{xAEB} = -8\ m/s^2$, a forward collision can be avoided if AEB intervenes AND if:
$$\cdots \Rightarrow \frac{x_o}{v_x - v_{ox}} = TTC > \frac{v_x - v_{ox}}{2 \cdot (-a_{xAEB})} = \frac{v_x - v_{ox}}{16};$$

Figure 3-53 shows a diagram where different condition areas are marked. The sectioned area shows where AEB will be triggered, using above rules. The smaller of the sectioned areas shows where it also will be possible to trigger AEB so timely that a collision is actually avoided; with the assumed numbers, this is for speeds up to 6.4 m/s≈23 km/h.

The reasoning above is very simplified. Additional information can improve effectiveness of AEB, such as knowing if a lateral avoidance on one side of object vehicle is blocked, the acceleration of the object vehicle, pedal operation of subject vehicle, road gradient, road curvature and road friction is. The vehicle dynamics model used is simply a point mass with predicted constant velocity and certain assumed acceleration capability, which of course can be extended a lot; both with taking actual accelerations into account and more advanced vehicle dynamics models. The decision to intervene is dependent of many pieces of information and simple models; vehicle dynamics and driver behaviour (in both subject and object vehicles) as well as road characteristics. AEB function has to be designed together with other similar functions, such as ACC and Forward Collision Warning (FCW).

AEB is on market and legal requirement for both passenger vehicles and heavy vehicles.

Related functions are, e.g. extra force assistance in brake pedal when driver steps quickly onto brake. Another related function is automatic braking triggered by a first impact and intended to mitigate or avoid secondary accident events, starts to appear at market, see Reference (Yang, 2013). In semantic meaning this could be seen as AEB, but they are normally not referred to as AEB; AEB normally refers to functions that use environment sensors (forward directed radar, camera, etc.).

When designing and evaluating AEB, it is important to also know about the function Forward Collision Warning, FCW. FCW is a function that warns the driver via visual and/or audio signals when a forward collision is predicted. FCW is typically triggered earlier than AEB.
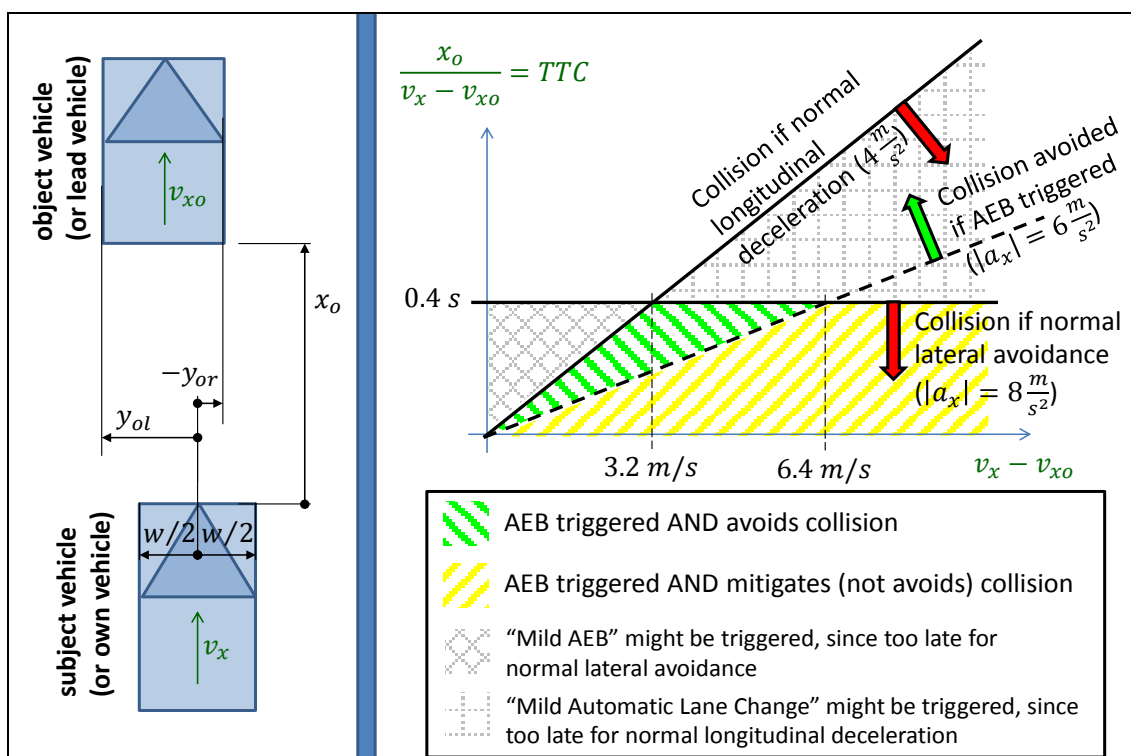
Figure 3-53: Left: Quantities known for an AEB algorithm in the subject vehicle, assuming forward directed camera or radar. Right: Model based decision of triggering AEB and effectiveness of AEB if triggered.

3.5.3 Longitudinal Motion Functionality shown in a reference architecture

All control functions controls have to cooperate and they have to be transferable between platforms and vehicle variants. It is very complex to take all functions into consideration, but with a scope limited to the longitudinal Motion functionality

Figure 3-54 can be drawn as a solution within the reference architecture.

By using a reference architecture it can be illustrated that Adaptive Cruise control and cruise control can be seen as part of Traffic Situation Layer (ACC=CC if no vehicle ahead). The Traffic Situation Layer has the purpose and scope to understand the ego vehicle's surrounding traffic by looking at e.g. Forward Sensors. The forward looking sensor is in this case part of Vehicle Environment sensors.

Vehicle Motion and Coordination Layer would include the arbitration of Driver's Acceleration and Brake pedal input and Traffic functionality, see Figure 3-54. In addition, Vehicle Motion and Coordination Layer would perform the powertrain coordination and brake distribution. The coordinated requests are then sent to Motion Support Device Layer.

The Human Machine Interface would include the services available for the driver to activate or request, E.g. ACC activation to Traffic Situation or Deceleration by pressing the brake pedal.
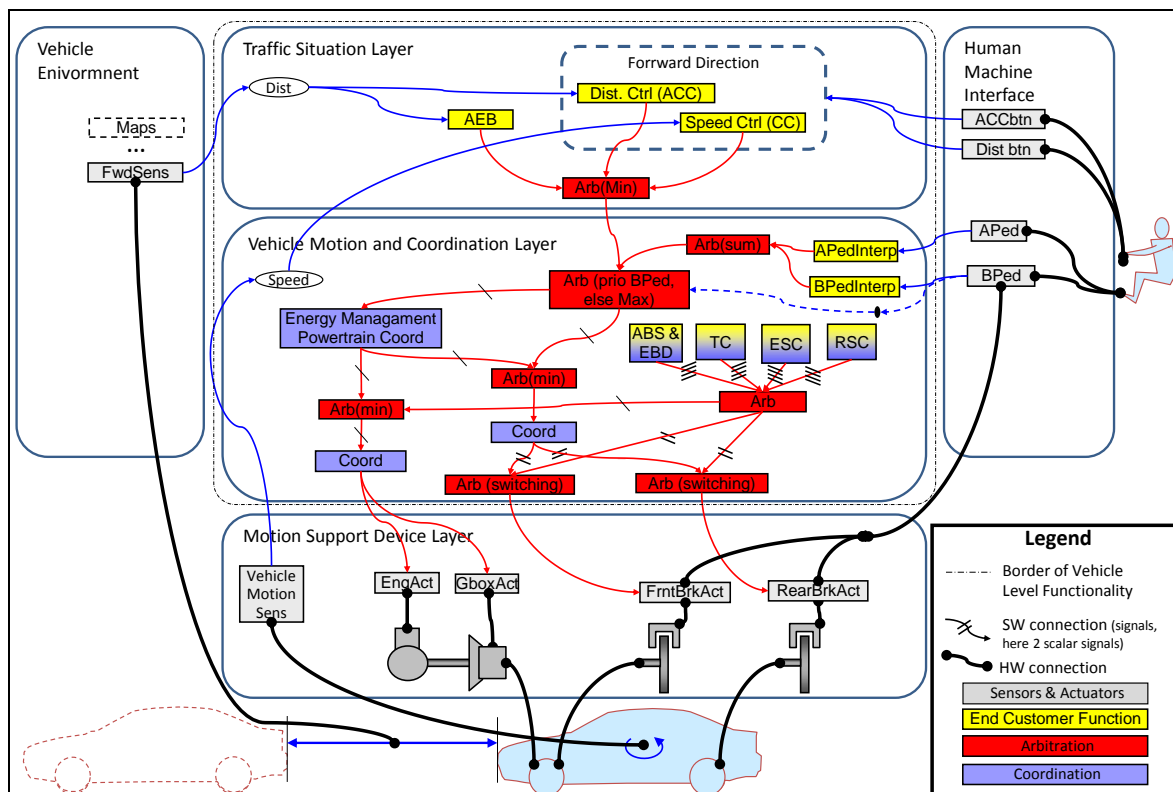
Figure 3-54: Functional architecture for conventional front axle driven passenger car. Mainly longitudinal functions (plus ESC, RSC) are shown, e.g. no steering. Cf Figure 1-14.

If a reference architecture is used, it can assist function developers from OEM's Electrical, Powertrain, and Chassis departments and suppliers to have a common view of how vehicle's embedded motion functionality is intended to be partitioned and to understand how different functions relate and interact with each other and what responsibilities they have.

4 LATERAL DYNAMICS

4.1 Introduction

The lateral motion of a vehicle is needed to follow the roads' curves and select route in intersections as well as to laterally avoid obstacles that appear. The vehicle needs to be steerable. With some simplification, one can say that lateral dynamics is about how steerable the vehicle is for different given longitudinal speeds. Vehicle steering is studied mainly through the vehicle degrees of freedom: yaw rotation and lateral translation.

A vehicle can be steered in different ways:

- Applying steering angles on, at least one, road wheel. Normally both of front wheels are steered.
- Applying longitudinal forces on road wheels. Either unsymmetrical between left and right side of vehicle, e.g. one sided braking, or deliberately use up much friction longitudinally on one axle in a curve, so that that axle loses lateral force.
- Articulated steering, where the axles are fixed mounted on the vehicle but the vehicle itself can bend.

The chapter is organised with one group of functions in each section as follows:

- 4.2 Low speed manoeuvrability
- 4.3 Steady state cornering at high speed
- 4.4 Stationary oscillating steering
- 4.5 Transient handling
- 4.6 Lateral Control Functions

Most of the functions in "4.6 Lateral Control Functions", but not all, could be parts of "4.5 Transient handling". However, they are collected in one own section, since they are special in that they partly rely on software algorithms.

The lateral dynamics of vehicles is often experienced as the most challenging for the new automotive engineer. Longitudinal dynamics is essentially motion in one plane and rectilinear. Vertical dynamics may be 3 dimensional, but normally the displacements are small and in this compendium the vertical dynamics is mainly studied in one plane as rectilinear. However, lateral dynamics involves motion in the vehicle coordinate system which introduces curvilinear motion since the coordinate system is rotating as the vehicle yaws.

The turning manoeuvres of vehicles encompass two concepts. Handling is the driver's perception of the vehicle's response to the steering input. Cornering is usually used to describe the physical response (open-loop) of the vehicle independent of how it influences the driver.

4.1.1 References for this chapter

- *"Chapter 25 Steering System" in Reference* (Ploechl, 2013)*.
- *"Chapter 27 Basics of Longitudinal and Lateral Vehicle Dynamics" in Reference* (Ploechl, 2013)*.
- *"Chapter 8: Electronic Stability Control" in Reference* (Rajamani, 2012)

4.2 Low speed manoeuvrability

This section is about operating vehicles in low speeds, including stand-still and reverse. Specific for low speed is that inertial effects can be neglected, i.e. one can assume that left hand side in motion equation ($Mass \cdot LateralAcceleration = sum\ of\ Forces$) is zero.

In low speed, one often needs to find the path with orientation and understand the steering system and how tyres can be modelled to track ideally. This, and the resulting one-track model for low speeds, is described in Sections 4.2.1, ...,4.2.6.

4.2.1   Path with orientation

The path and path with orientation was introduced in Section 1.5. The path, in global coordinate system, is related to vehicle speeds, in vehicle fix coordinates, as given in Figure 4-1 and Equation [4.1].

Knowing $(v_x(t), v_y(t), \omega_z(t))$, we can determine "path with orientation" $(x(t), y(t), \varphi_z(t))$, by time integration of the right hand side of the equation. Hence, the positions are typically "state variables" in lateral dynamics models.
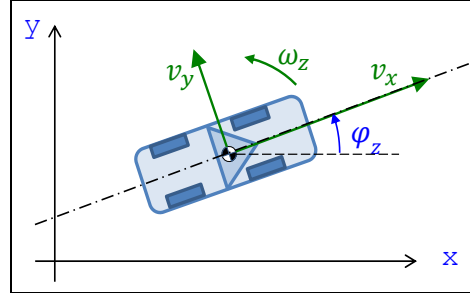
Figure 4-1: Model for connecting "path with orientation" to speeds in vehicle coordinate system.

$$\begin{bmatrix} \dot{x} \\ \dot{y} \end{bmatrix} = \begin{bmatrix} \cos(\varphi_z) & -\sin(\varphi_z) \\ \sin(\varphi_z) & \cos(\varphi_z) \end{bmatrix} \cdot \begin{bmatrix} v_x \\ v_y \end{bmatrix};$$

$$\dot{\varphi}_z = \omega_z;$$

[4.1]

It should be noted that in some problems, typically manoeuvring at low speed, the real time scale is of less interest. Then, the problem can be treated as time independent, e.g. by introducing a coordinate, s, along the path, as in Equation [4.2].

$$x' = \frac{v_x}{\dot{s}} \cdot \cos(\varphi_z) - \frac{v_y}{\dot{s}} \cdot \sin(\varphi_z);$$

$$y' = \frac{v_y}{\dot{s}} \cdot \cos(\varphi_z) + \frac{v_x}{\dot{s}} \cdot \sin(\varphi_z);$$

$$\varphi_z' = \frac{\omega_z}{\dot{s}};$$

where prime notes differentation with respect to s

[4.2]

Here, $\dot{s}$ can be thought of like an arbitrary time scale, with which all speeds are scaled. One can typically chose $\dot{s} = 1 \ [m/s]$. However, in this compendium we will keep notation t and the dot notation for derivative.

4.2.2   Vehicle and wheel orientations

For steered wheels, there are often reason to translate forces and velocities between vehicle coordinate system and wheel coordinate system, see Figure 4-2 and Equation [4.3].

Figure 4-2: Transformation between forces and velocities in vehicle coordinate system and wheel coordinate system.

Transformation from wheel coordinates to vehicle coordinates:

$$\begin{bmatrix} v_{xv} \\ v_{yv} \end{bmatrix} = \begin{bmatrix} \cos(\delta) & -\sin(\delta) \\ \sin(\delta) & \cos(\delta) \end{bmatrix} \cdot \begin{bmatrix} v_{xw} \\ v_{yw} \end{b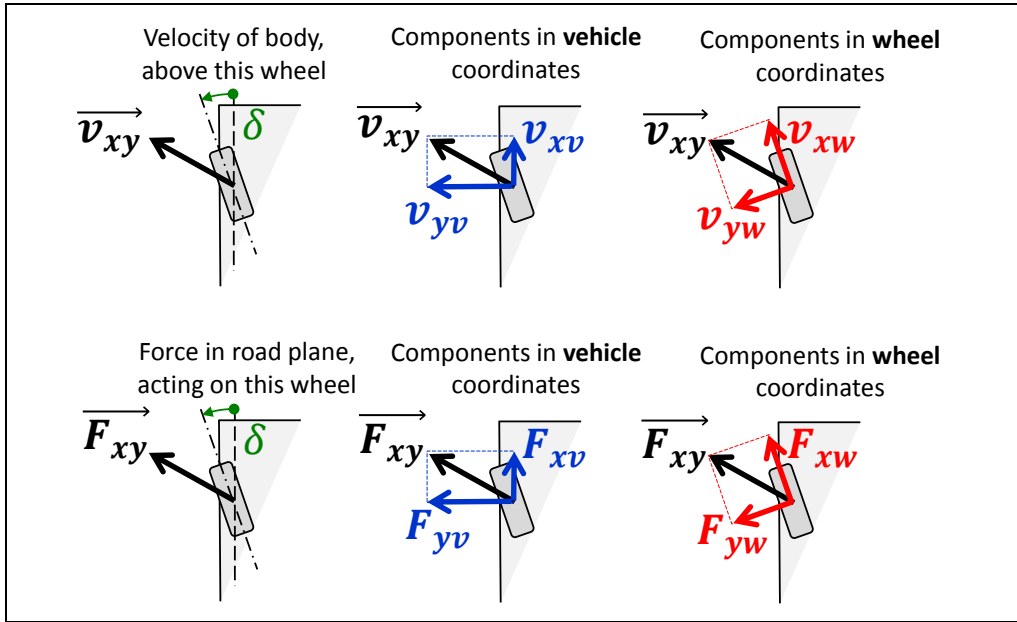matrix}; \quad and \quad \begin{bmatrix} F_{xv} \\ F_{yv} \end{bmatrix} = \begin{bmatrix} \cos(\delta) & -\sin(\delta) \\ \sin(\delta) & \cos(\delta) \end{bmatrix} \cdot \begin{bmatrix} F_{xw} \\ F_{yw} \end{bmatrix};$$

Transformation from vehicle coordinates to wheel coordinates:

$$\begin{bmatrix} v_{xw} \\ v_{yw} \end{bmatrix} = \begin{bmatrix} \cos(\delta) & \sin(\delta) \\ -\sin(\delta) & \cos(\delta) \end{bmatrix} \cdot \begin{bmatrix} v_{xv} \\ v_{yv} \end{bmatrix}; \quad and \quad \begin{bmatrix} F_{xw} \\ F_{yw} \end{bmatrix} = \begin{bmatrix} \cos(\delta) & \sin(\delta) \\ -\sin(\delta) & \cos(\delta) \end{bmatrix} \cdot \begin{bmatrix} F_{xv} \\ F_{yv} \end{bmatrix};$$

[4.3]

4.2.3 Steering System

The steering system is here referred to the link between steering wheel and the road wheel's steering, on the steered axle. It is normally the front axle that is steered. Driver's interaction is two-folded, both steering wheel angle and torque, which is introduced in Section 2.10. In present section, we will focus on how wheel steering angles are distributed between the wheels.

4.2.3.1 Chassis steering geometry

The most basic intuitive relation between the wheels steering angles is probably that all wheels rotation axes always intersect in one point. This is called Ackermann geometry and is shown in Figure 4-3. The condition for having Ackermann geometry is, for the front axle steered vehicle that:

$$\left. \begin{aligned} \frac{1}{\tan(\delta_i)} &= \frac{R_r - w/2}{L}; \\ \frac{1}{\tan(\delta_o)} &= \frac{R_r + w/2}{L}; \end{aligned} \right\} \Rightarrow \frac{1}{\tan(\delta_o)} = \frac{1}{\tan(\delta_i)} + \frac{w}{L};$$

[4.4]

The alternative to Ackermann steering geometry is parallel steering geometry, which is simply that $\delta_i = \delta_o$. Note that Ackermann geometry is defined for a vehicle, while parallel steering is defined for an axle. This means that, for a vehicle with 2 axles, each axle can be parallel steered, which means that the vehicle is non-Ackermann steered. However, the vehicle can still be seen as Ackermann steered with respect to mean steering angles at each axle.
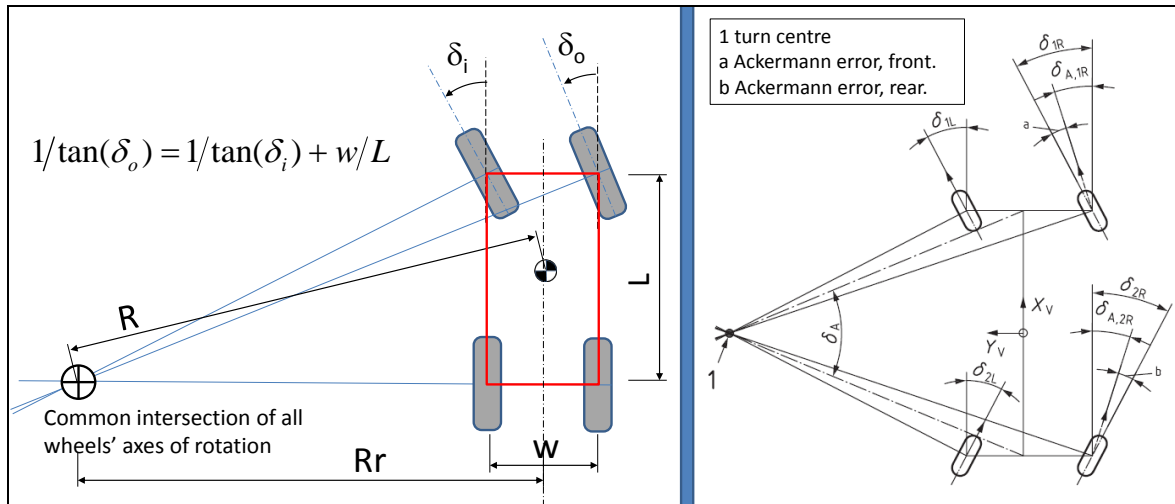
Figure 4-3: Ackermann steering geometry. <u>Left</u>: One axle steered. <u>Right</u>: Both axles steered and including "Ackermann errors". From (ISO8855).

For low-speed, Ackermann gives best manoeuvrability and lowest tyre wear. For high-speed, Parallel is better in both aspects. This is because vehicles generally corner with a drift outwards in curves, which means that the instantaneous centre is further away than Ackermann geometry assumes, i.e. more towards optimal for parallel. Hence the chosen geometry is normally somewhere between Ackermann and parallell.

Practical arrangement to design the steering geometry is shown in Figure 4-7. The design of linkage will also make the transmission from steering wheel angle to road wheel steering angle non-linear. This can lead to different degrees of Ackerman steering for small and large steering wheel angles.

In traditional steering systems, the steering wheel angle has a monotonically increasing function of the steering angle of the two front axle road wheels. This relation is approximately linear with a typical ratio of 15..17 for passenger cars. For trucks the steering ratio is typically 18..22. Differences between left and right wheels are discussed in 4. In some advanced solutions, steering on other axles is also influenced (multiple-axle steering, often rear axle steering). There are also advanced solutions for adding an additional steering angle to the basic steering ratio gives, so called AFS=Active Front Steering.

4.2.3.2   Steering system forces

*(This section has large connection with Section **2.5.6.2 Tyre aligning moment**.)*

The steering wheel torque, T_{sw}, should basically be a function of the tyre/road forces, mainly the wheel-lateral forces. This gives the driver a haptic feedback of what state the vehicle is in. The torque/force transmission involves a servo actuator, which helps the driver to turn the steering system, typically that assists the steering wheel torque with a factor varying between 1 and 10, but less for small T_{sw} (highway driving) than large T_{sw} (parking), see Figure 4-4. Here, the variation in assistance is assumed to be hydraulic and follows a so called boost curve. At $T_{sw} = 0$, the assistance is $\approx 0.45/0.55 \approx 1$ and for $T_{sw} = 4$ Nm, it is $\approx 0.9/0.1 \approx 10$.

For vehicle dynamics, one important effect of a steered axle, is that the lateral force on the axle tries to align the steering in the direction that the body (over the steered axle) moves, i.e. towards a zero tyre side slip. This is designed in via the sign of the caster trail, see Figure 4-5. Also, asymmetry in longitudinal tyre forces (wheel shaft torques and/or brake torques) affects the steering wheel torque. This is analysed in the following.

On a steered axle, there is a *Steering axis* (or *Kingpin axis*) around which the wheel is rotated when it is steered. The steering axis intersects with the ground plane at a point which normally has an offset from the contact patch centre, both longitudinally and laterally. The offsets are called *Castor offset at ground* and *Steering axis offset at ground*, respectively, see Figure 4-5. (Steering axis offset at ground is

sometimes called *Scrub radius*, but that is also used for the resulting distance of both offsets, so it is an ambiguous name.) This figure also defines *Normal steering axis offset at wheel centre* . We will use the 3 latter measures to explain why steering is affected by differences in shaft torque left/right, differences in brake torque left/right, and lateral wheel forces. The steering axis distance from wheel centre in side view, is called *Castor offset at wheel centre* .
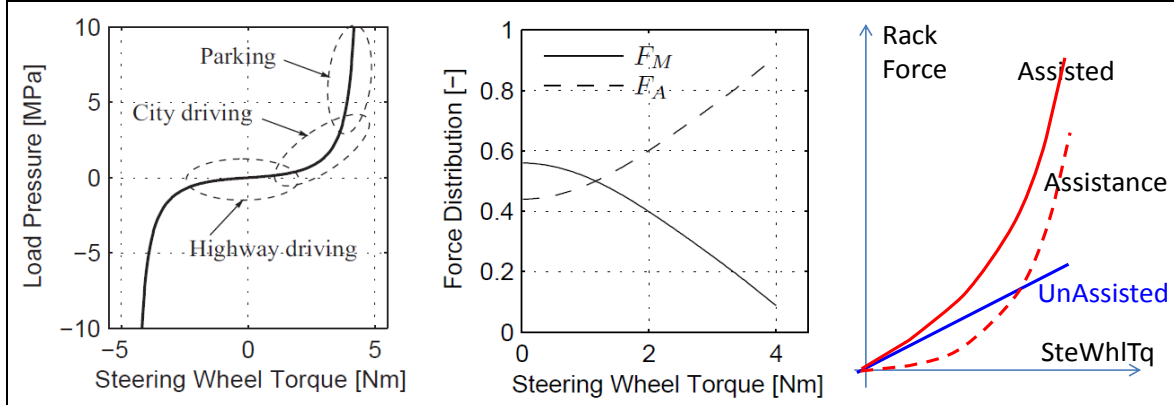

Figure 4-4: Left: Boost Curve with different working areas depending on the driving envelope. Middle: Torque distribution between manual torque, FM, and assisting torque, FA, depending on applied steering wheel torque. From Reference (Rösth, 2007). Right: Unassisted and assisted steering wheel torque.

Often, the actual forces between tyre and ground are not in the exact centre of the nominal contact patch, which also creates "effective" version of caster offset and scrub radius. For instance, the *Pneumatic trail* adds to the Castor offset at ground due to the lateral force distribution being longitudinally offset from nominal contact point; so that the lever becomes not only c, but $c + t$. The moment, T_{steer}, on steering system (around Steering axis, turning towards increasing steering angle) is affected by tyre forces on a steered axle as in Equation [4.5].

Castor offset at ground is, on passenger vehicles, 15-20 mm (at motorcycles approximately 100 mm). On rear wheel driven passenger vehicles it can typically be 5 mm, due to higher Castor Angle which gives a beneficial higher Camber angle gain at cornering. On a front wheel driven passenger vehicle a non-zero caster offset is not chosen due to drive axle lateral displacement. Caster offset gives a self-aligning steering moment, which generally improves the steering feel.

(Notations in Equation [4.5] are defined in Figure 4-5.)

$$
\begin{aligned}
T_{steer} &= \frac{-(T_{b1} + T_{s1})}{R} \cdot s \cdot \cos(KPI) + \frac{-T_{s1}}{R} \cdot R \cdot \sin(KPI) + \\
&+ \frac{(T_{b2} + T_{s2})}{R} \cdot s \cdot \cos(KPI) + \frac{T_{s2}}{R} \cdot R \cdot \sin(KPI) + \\
&+ (-1) \cdot \left(F_{y1} \cdot (c + t_1) + F_{y2} \cdot (c + t_2) \right) \cdot \cos(CA) = \\
&= \frac{T_{b2} - T_{b1}}{R} \cdot s \cdot \cos(KPI) + \frac{T_{s2} - T_{s1}}{R} \cdot k - \left(F_{y1} \cdot (c + t_1) + F_{y2} \cdot (c + t_2) \right) \cdot \cos(CA) ;
\end{aligned}
$$

[4.5]

The equation shows that difference in both brake torque and shaft torque affects steering. So does the sum of lateral forces. For reducing torque steer and disturbances from one-sided longitudinal forces due to road irregularities, kingpin offset, scrub radius different road friction should be as small as possible, but it is limited by geometrical conflicts between brake disc, bearing, damper, etc.

Positive scrub radius contributes to self-centring, thanks to lifting the car body, see below. Negative scrub radius compensates for split-μ braking, or failure in one of the brake circuits. Hence, the scrub is a balance between these two objectives. Scrub radius is often slightly negative on modern passenger cars. Scrub radius is often positive on trucks, maybe 10 cm, due to packaging.

The geometry in Figure 4-6 shows one part of the lifting effect. This is that if steering angle is changed from zero, it lifts the vehicle slightly which requires a steering torque. One can see this as a kind of "return spring effect".

Figure 4-6 shows how KPI and scrub radius causes the vehicle body to lift a distance $s''' = s \cdot \cos(KPI) \cdot (1 - \cos(|\varphi_{steer}|)) \cdot \sin(KPI)$. This will require a work $T_{steer} \cdot \varphi_{steer} = F_{iz} \cdot s'''$. This leads to an T_{steer} (additional to Eq [4.5]) as follows:

$$(additional)\ T_{steer} = \sum_{i=left\ and\ right} \frac{F_{iz} \cdot s'''}{\varphi_{steer}} =$$

$$= \frac{s \cdot \cos(KPI) \cdot (1 - \cos(|\varphi_{steer}|)) \cdot \sin(KPI)}{\varphi_{steer}} \cdot F_{axle,z};$$

[4.6]

It should be noted that Eq [4.6] is not complete with respect to all "returning effects". There are also effects from Castor angle and Caster trail as well as that the tyre has a width and radius. However, in total, these give rise to a returning steering torque which is depending on the steering angle.

It can also be noted that steering effort for low speed or stand-still is largely influenced by whether brakes are applied or not, due to the magnitude (not sign) of scrub radius.
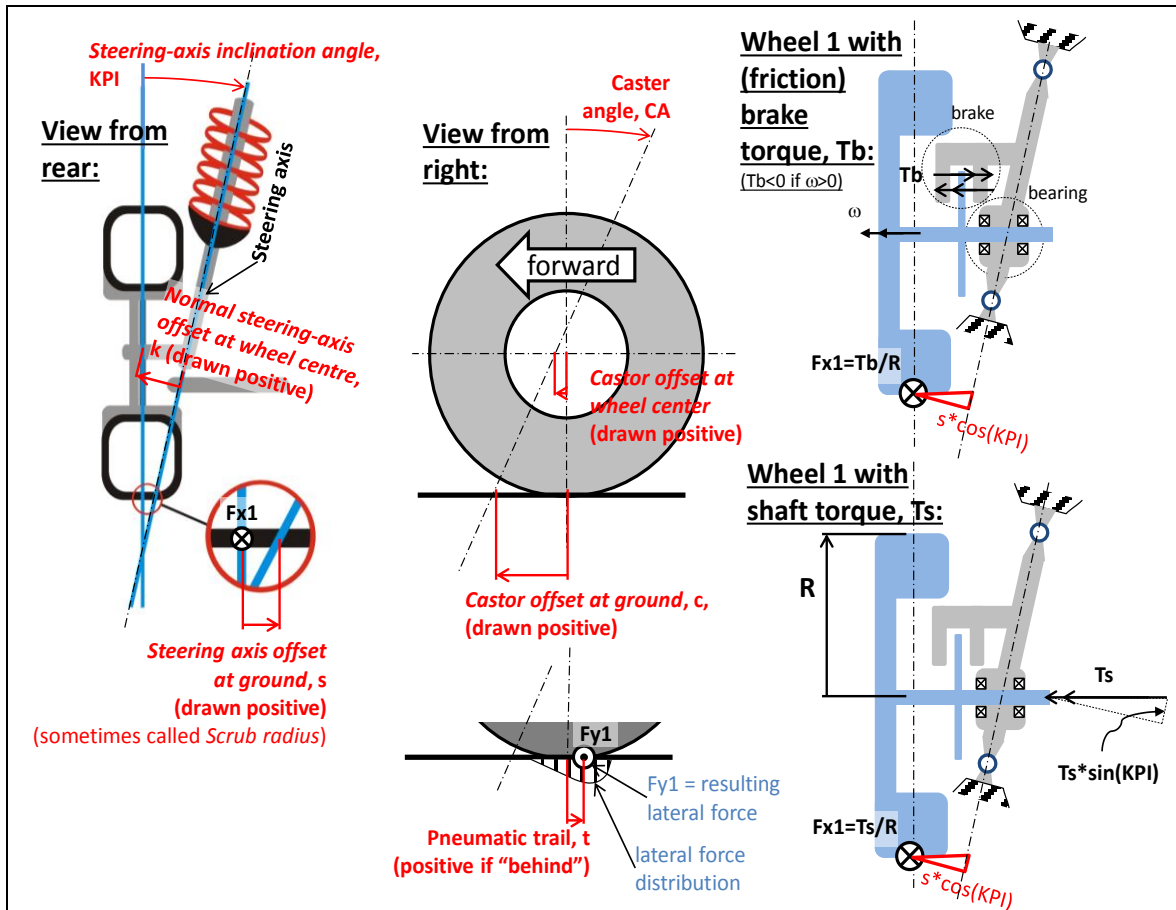
Figure 4-5: Steering geometry and offsets.
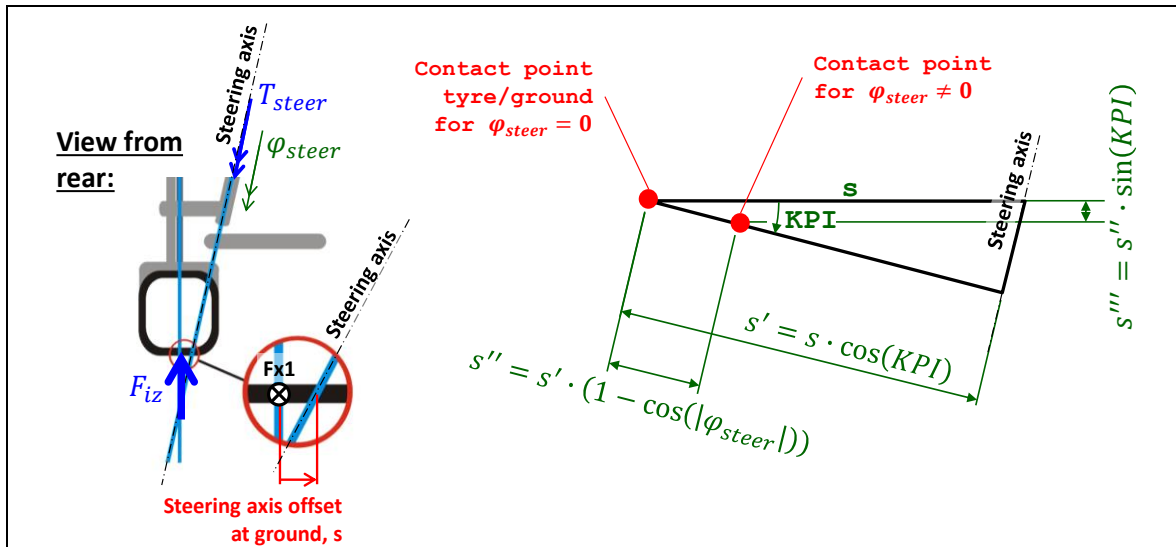
Figure 4-6: Lift effect due to steering angle and positive Steering axis offset at ground.

4.2.4   One-track models

When studying the vehicle cornering response, it is useful to combine the effects of all tyres on the axle into one virtual tyre. This assumption, referred to as the one-track model (or single-track model or bicycle model), facilitates understanding but can also capture most important phenomena. A one-track model of a two-axle vehicle is shown in Figure 4-8. One-track model for truck with trailer is exemplified in Figure 4-9.

$$\delta_{left} = func(position_{rack}) = = func(r_{rack} \cdot \delta_{sw});$$

$$\delta_{right} = -func(-position_{rack}) = = -func(-r_{rack} \cdot \delta_{sw});$$
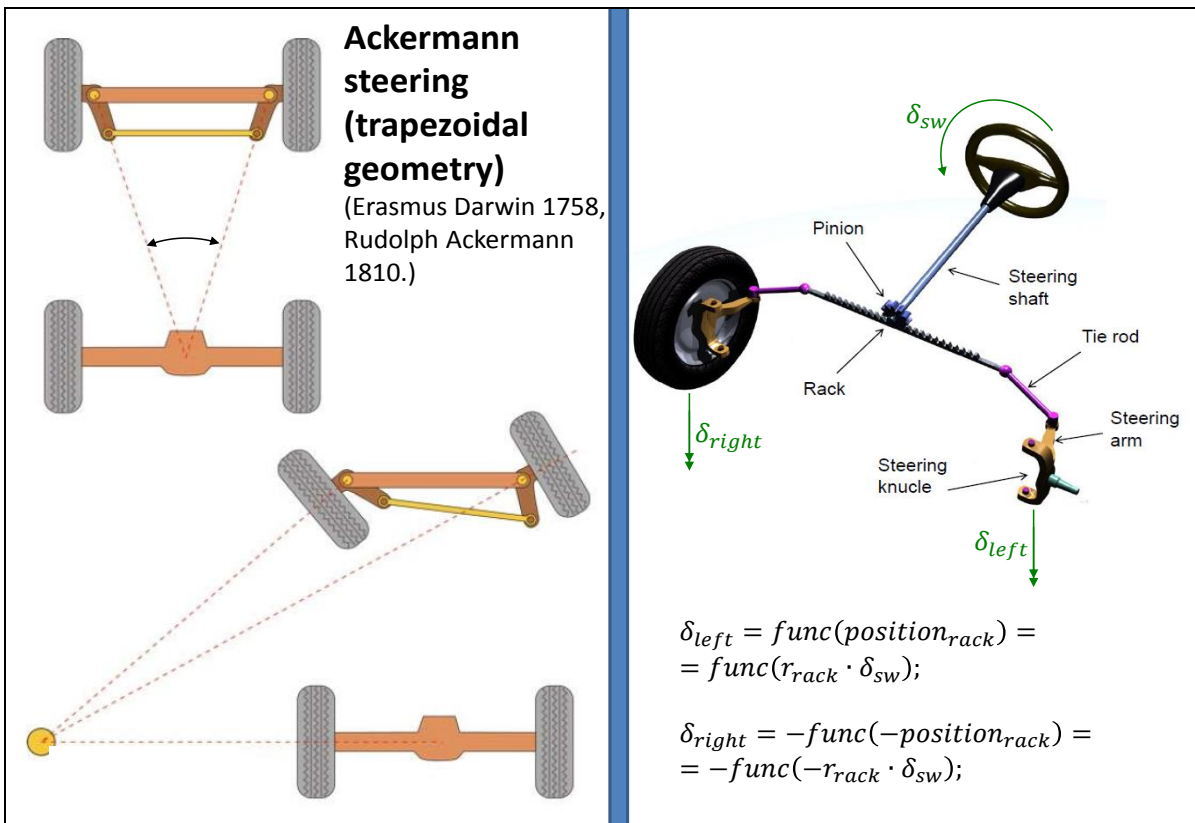
Figure 4-7: Example of Trapezoidal Steering. Left: Conceptual use of steering arms. Right: More exact design, common today. From Gunnar Olsson, LeanNova.
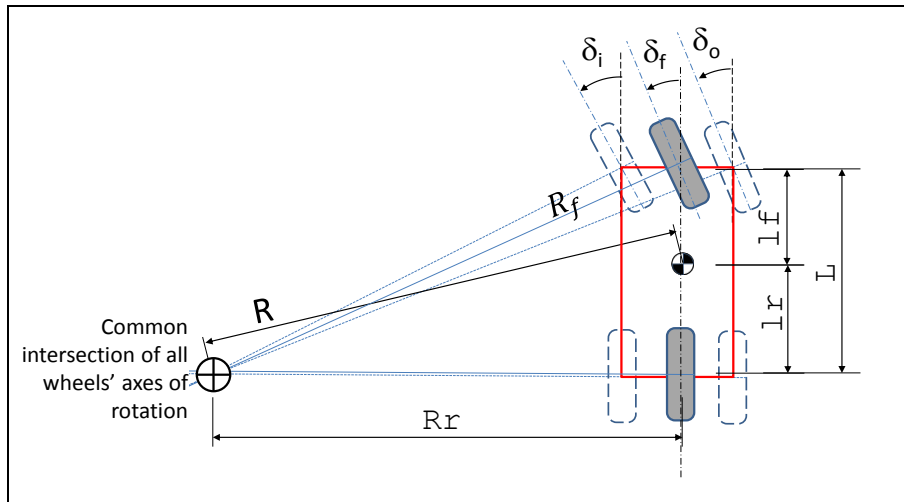
Figure 4-8: Collapsing to one-track model.
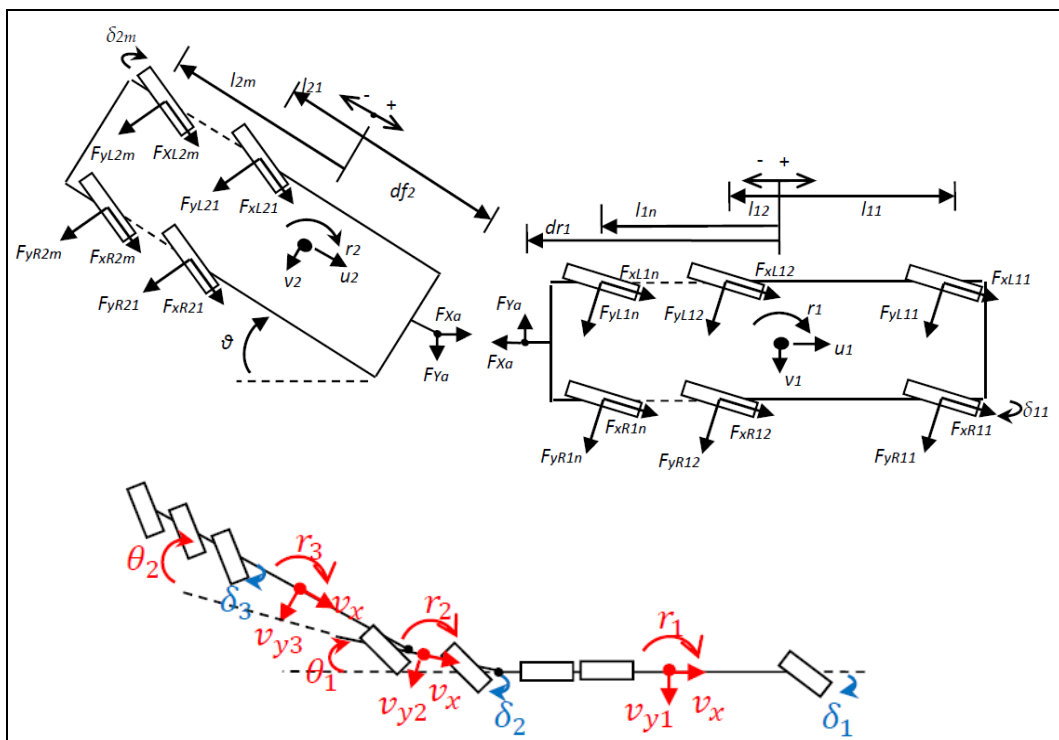
Figure 4-9: Upper: Two-track model of 3-axle truck with 2-axle trailer. Lower: One-track model of a 3-axle truck with a 2+5 axle trailer. Note: SAE coordinate system used. (Kharrazi , 2012).

Phenomena which one-track models not capture are, e.g.:

- Large deviations from Ackerman geometry within an axle.
- Varying axle cornering stiffness due to lateral load shift and axle propulsion/braking, see Section 4.3.
- Additional yaw moment due to non-symmetrical wheel torque interventions, such as ESC interventions.

These effects can, however, be approximately captured with a one-track vehicle model, extended with sub-models for the axles. The axle sub-models, can propagate the varying cornering stiffnesses and yaw moments to the superior one-track vehicle model.

4.2.5 Ideally tracking wheels and axles

In Section 2.5, lateral slip models for tyres were introduced. It is the constitutive equation $F_y = -C_y \cdot s_y$. If the tyre force, F_y, is small compared to cornering stiffness, C_y, one would expect side slip, s_y, to be very small. If this assumption is taken to its extreme, one get something we can call "ideal tracking" for a tyre or for an axle, which is that side slip is zero and side force can be any (finite) value. For low speed this is often a good enough model of the tyre. The validity of this assumption is limited by when lateral force becomes large with respect to available lateral force, $\mu \cdot F_z$. Hence, the speed border between low speed and high speed is lowered on low road friction.

Models using ideally tracking wheels are sometimes referred to as "kinematic models". However, a strictly kinematic model does not contain the forces at all, why validity cannot be checked.

The assumption about ideally tracking wheel or axle is a constitutive assumption, although that the equation (tyre lateral speed=tyre side slip=0) does not couple force and speed, but only stipulates speed. If forces should be calculated, it has to be done using the equilibrium.

4.2.6 One-track model for low speeds, with Ackermann geometry

Low speed manoeuvres are characterised by that the inertial forces are neglected, i.e. $m \cdot a = 0$. If the geometry is according to Ackermann, it is reasonable to assume ideal tracking axles. This means that the intersection point of the wheels rotational axes coincides with the instantaneous centre of vehicle rotation in ground plane. We can there through connect steering angles and path radius. For the model in Figure 4-8 this connection becomes:

$$\left.\begin{array}{l} \tan(\delta_f) = \dfrac{L}{R_r}; \\ R^2 = R_r{}^2 + l_r{}^2; \end{array}\right\} \Rightarrow \delta_f = \arctan\left(\dfrac{L}{\sqrt{R^2 - l_r{}^2}}\right) \cdot \text{sign}(R) \approx \dfrac{L}{\sqrt{R^2 - l_r{}^2}} \cdot \text{sign}(R) \approx \dfrac{L}{R}; \qquad [4.7]$$

where $R > 0$ means that instantaneous centre of rotation is left of the vehicle

The model in Eq [4.7] predicts a motion without involving forces, or actually assuming forces are zero. To get a more complete model, where more variables can be extracted, we can set up the model in Figure 4-10.
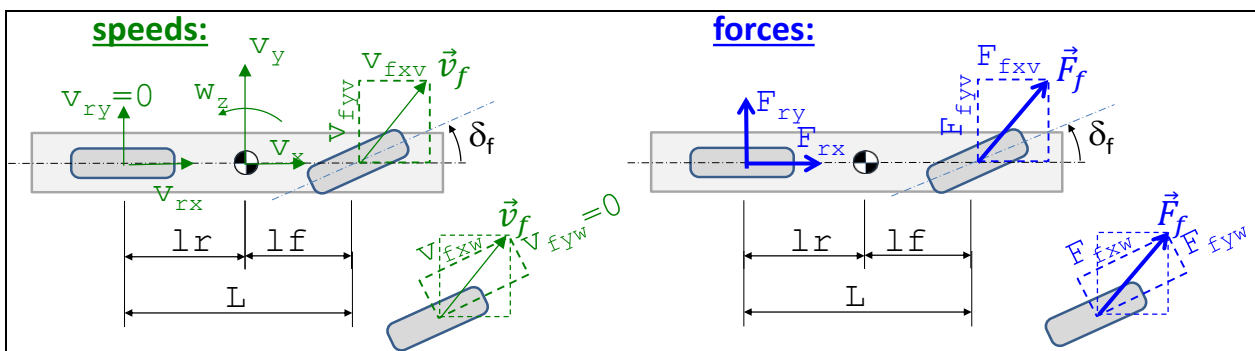

Figure 4-10: One-track model with ideally tracking axles. Lower view of front wheel shows conversion between wheel and vehicle coordinate systems.

The "physical model" in Figure 4-10 gives the following "mathematical model":

Equilibrium (longitudinal, lateral and yaw-rotational):

$$0 = F_{fxv} + F_{rx};$$
$$0 = F_{fyv} + F_{ry};$$
$$0 = F_{fyv} \cdot l_f - F_{ry} \cdot l_r;$$

Transformation between vehicle and wheel coordinate systems:

$$F_{fxv} = F_{fxw} \cdot \cos(\delta_f) - F_{fyw} \cdot \sin(\delta_f);$$
$$F_{fyv} = F_{fxw} \cdot \sin(\delta_f) + F_{fyw} \cdot \cos(\delta_f);$$
$$v_{fxv} = v_{fxw} \cdot \cos(\delta_f) - v_{fyw} \cdot \sin(\delta_f);$$
$$v_{fyv} = v_{fxw} \cdot \sin(\delta_f) + v_{fyw} \cdot \cos(\delta_f);$$

Compatibility:

$$v_{fxv} = v_x; \quad and \quad v_{fyv} = v_y + l_f \cdot \omega_z;$$
$$v_{rx} = v_x; \quad and \quad v_{ry} = v_y - lr \cdot \omega_z;$$

[4.8]

Ideal tracking (Constitutive relation, but without connection to forces):

$$v_{fyw} = 0; \quad and \quad v_{ry} = 0;$$

Path with orientation:

$$\dot{x} = v_x \cdot \cos(\varphi_z) - v_y \cdot \sin(\varphi_z);$$
$$\dot{y} = v_y \cdot \cos(\varphi_z) + v_x \cdot \sin(\varphi_z);$$
$$\dot{\varphi}_z = \omega_z;$$

Prescription of actuation:

$$\delta_f = \begin{cases} = (35 \cdot \pi/180) \cdot \sin(0.5 \cdot 2 \cdot \pi \cdot t); & if\ t < 4.5; \\ = 35 \cdot \pi/180; & else \end{cases}$$

Rear axle undriven, which gives drag from roll resistance:

$$F_{rx} = -100;$$

The "Compatibility" in Eq [4.8] neglects the influence of steering axis offsets at ground, see Section 4.2.3.2. The terms neglected are of the type $LateralOffset \cdot \dot{\delta}$; in the equation for v_{fxv} and $LongitudinalOffset \cdot \dot{\delta}$ in the equation for v_{fyv}. This is generally well motivated for normal road vehicles, except for quick steering when vehicle is stand-still.

Equation [4.8] is written in Modelica format in Equation [4.9]. Comments are marked with //. The subscript v and w refers to vehicle coordinate system and wheel coordinate system, respectively. The actual assumption about ideal tracking lies in that $v_{fyw} = v_{ry} = 0$. Global coordinates from Figure 4-1 is also used.

```
//Equilibrium:
  0 = Ffxv + Frx;
  0 = Ffyv + Fry;
  0 = Ffyv*lf - Fry*lr;

//Ideal tracking (Constitutive relation, but without connection to forces):
  vfyw = 0;      vry = 0;

//Compatibility:
  vfxv = vx;     vfyv = vy + lf*wz;
  vrx = vx;      vry = vy - lr*wz;

//Transformation between vehicle and wheel coordinate systems:
  Ffxv = Ffxw*cos(df) - Ffyw*sin(df);
  Ffyv = Ffxw*sin(df) + Ffyw*cos(df);
```

[4.9]

```
    vfxv = vfxw*cos(df) - vfyw*sin(df);
    vfyv = vfxw*sin(df) + vfyw*cos(df);

//Path with orientation:
    der(x) = vx*cos(pz) - vy*sin(pz);
    der(y) = vy*cos(pz) + vx*sin(pz);
    der(pz) = wz;

// Prescription of actuation:
    df = if time < 4.5 then (35*pi/180)*sin(0.5*2*pi*time) else 35*pi/180;
//Rear axle undriven, which gives drag from roll resistance:
    Frx = -100;
```

The longitudinal speed is a parameter, $v_x = 10 \ km/h$. A simulation result from the model is shown in Figure 4-11. It shows the assumed steering angle function of time, which is an input. It also shows the resulting path, $y(x)$. The variables x, y, p_z are the "state variables" of this simulation.
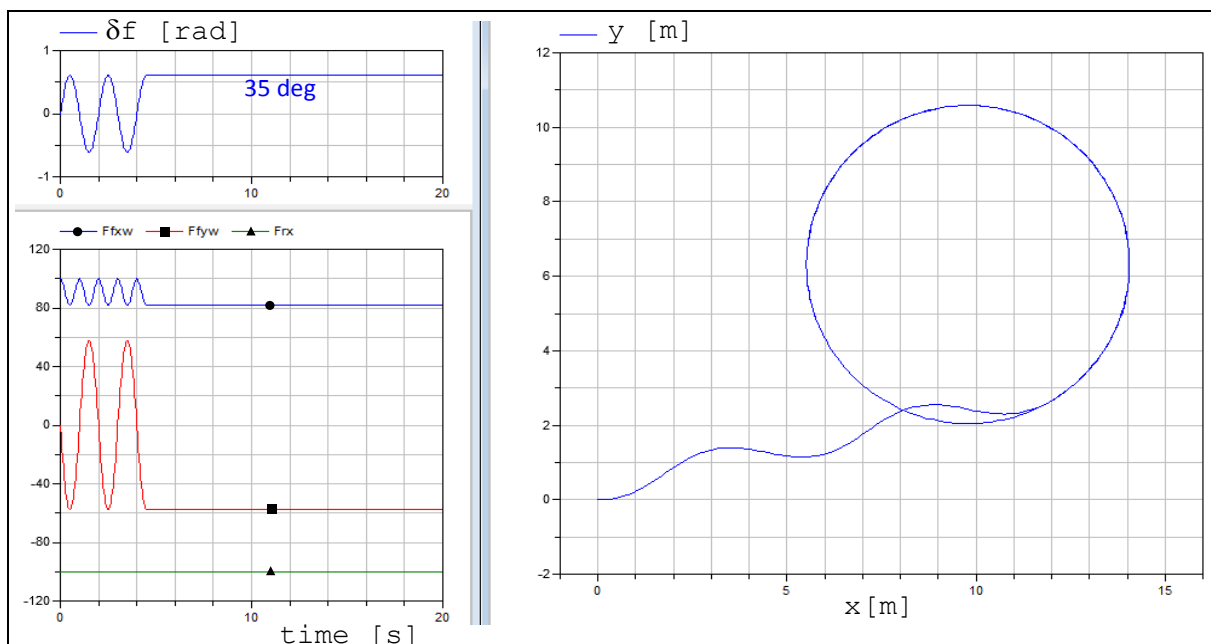
Figure 4-11: Simulation results of one-track model with ideal tracking.

The variables x, y, p_z are the only "state variables" of this simulation. If not including the path model (Equation [4.1]), the model would actually not be a differential equation problem at all, just an algebraic system of equations. That system of equations could be solved isolated for any value of steering angle without knowledge of time history. These aspects are the same for the steady state model in section 4.3.2.

A driving resistance of 100 N is assumed on the rear axle ($F_{rx} = -100;$). This is to exemplify that forces does not need to be zero, even if forces normally are not so interesting for low speed manoeuvres. Anyway, one should note that the speeds and forces are not coupled, since there are no inertial forces modelled. The modelling of forces is really a preparation for the case where we don't have Ackerman geometry. For a two-axle one-track model we always have Ackermann geometry, because there is always an intersection point between the front and rear wheels rotational axes.

4.2.7   Turning circle *

Function definition: **Turning diameter** *is the diameter of the smallest possible circular path obtained steady state at low speed, measured to a certain point at the vehicle. The certain point can be either outer-most point on wheel (Kerb Turning diameter) or outer-most point on body (Wall Turning diameter).*

155

The turning circle (or turning diameter) is the diameter of the smallest circular turn that the vehicle is capable of making at low speed. The value should be as low as possible to enable best manoeuvrability in e.g. U-turns.

The end of the simulation in Figure 4-11 is made with constant steering angle. If we assume that it is the maximum steering angle, the circle actually shows the turning circle (diameter) for centre of gravity. If we add the path for the outermost wheels, we get the kerb or kerb-to-kerb turning circle diameter, see Figure 4-12. If we add the path for the outermost point at the vehicle body we get the wall or wall-to-wall turning circle diameter, also shown in Figure 4-12. The outermost point at the vehicle body is normally the front outer corners of the vehicle body, i.e. the outer front bumper end.
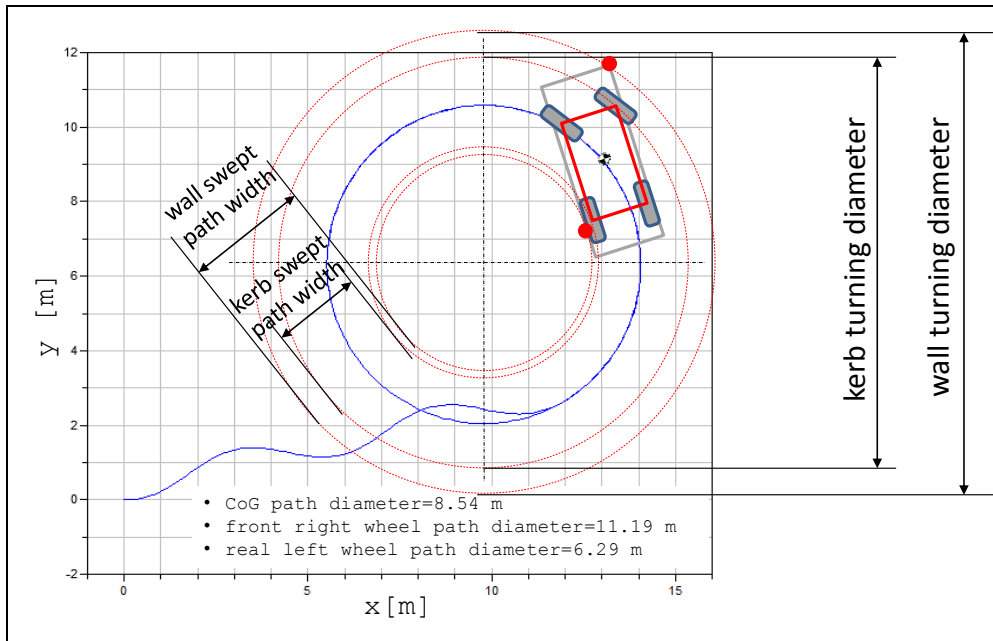
Figure 4-12: Adding paths for wheels and body points, on top of result in Figure 4-11.

If we have a vehicle with Ackermann geometry, it is tempting to model without involving forces, using Eq [4.7]. But the influence of forces from rolling resistance is often significant, see Figure 4-10. When introducing rolling resistance on the un-driven axle, the force equilibrium is obtained by counter-directed forces on the two axles. Due to the steering angle, a lateral force on the front wheel is required, which gives a lateral tyre slip, $\alpha_f \neq 0$. This changes the motion compared to Figure 4-8.
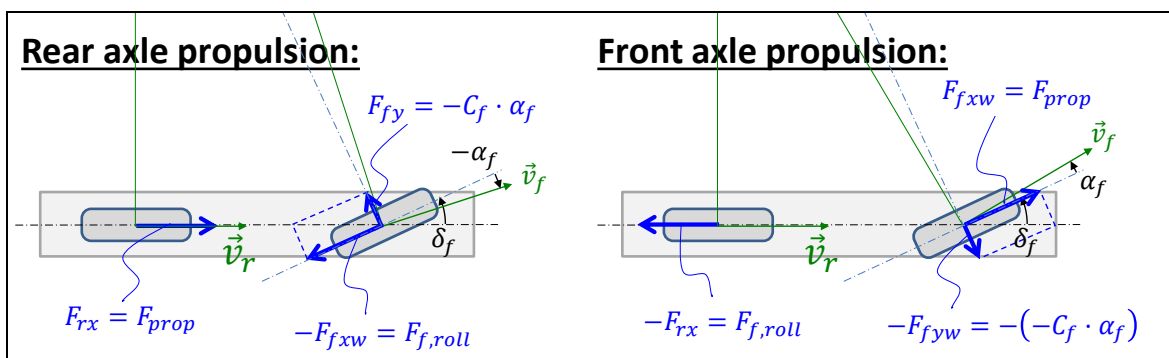
Figure 4-13: Smaller turning circle diameter for front axle propulsion, as compared to rear axle propulsion due to rolling resistance on the un-driven axle.

For heavy combination vehicles these effects can be significant, adding also rolling resistance from many towed units and non-Ackermann effects of several non-steered axles on some units. Then, the function to turn can be quantified by required road friction on steered and driven axle, as opposed to radius at maximum steering angle.

A turning circle can also be defined for high speed, but it is then more conventional to define and set requirement on curvature gain. Curvature gain is not the curvature at maximum steering angle, but the curvature per steering angle, see Section 4.2.12.

4.2.8   Swept path width and Swept Area *

*Function definition: **Swept path width** is the distance between the outermost and innermost trajectories of wheels (or body edges). The trajectories are then from a certain turning or lane change manoeuvre at a certain speed.*

*Function definition: **Swept path area** is the area between the outermost and innermost trajectories in the definition of Swept path width.*

For manoeuvrability, there is a function which is complementary to turning radius diameter. It is "Swept path width" (SPW), see Figure 4-12. It can occur as a kerb and wall version as well as turning circle radius can. It is the distance between the outermost and innermost wheel/point on the vehicle. The SPW should be as small as possible for improving manoeuvrability.

Another way of measuring approximately the same is "Swept Area", which is the area between the outer and inner circle in Figure 4-12. Again, one can differ between kerb and wall version of this measure.

"Swept path width" and "Swept Area" is often used for low vehicle speeds. For higher speeds it is more common to talk about off-tracking, see next section.

4.2.9   Off-tracking *

*Function definition: **Off-tracking** is the distance between the outermost and innermost trajectories of centre points of the axles. The trajectories are then from a certain turning or lane change manoeuvre at a certain speed.*

Another measure of manoeuvrability is "Off-tracking", see Figure 4-14. It is like swept area width, but for the centre point of the axles. It is also used for higher speeds, and then the rear axle can track on a larger circle than front axle.

Off-tracking is most relevant for vehicles with several units, such as truck with trailer. Off-tracking for driving several rounds in a circle is well defined since it is a steady state, but seldom the most relevant. Often, it is a more relevant to set requirements on off-tracking when driving from straight, via curve with certain radius, to a new straight in a certain angle from the first straight, e.g. 90 degrees. A way to predict off-tracking for this is to simulate with time integration, even if no traditional dynamics (mass inertia times acceleration) is modelled. The states in such simulation are the path coordinates with orientation (x, y, φ_z).
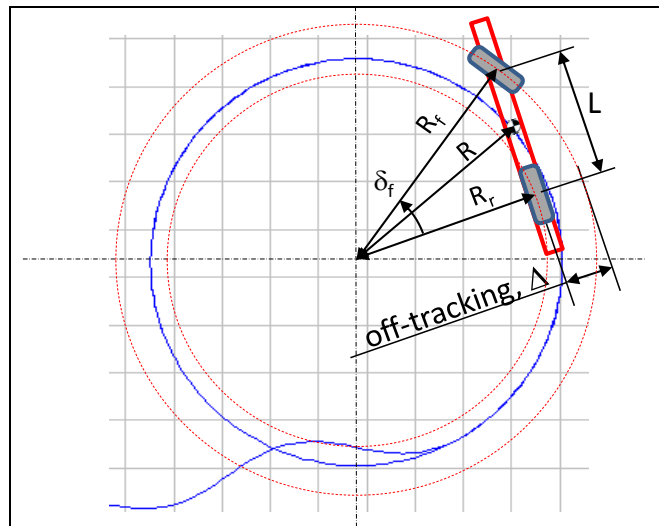

Figure 4-14: Adding one-track model, on top of result in Figure 4-11.

From geometry in Figure 4-14 on can find an expression for off-tracking at low speed:

$$\Delta = R_f - R_r = \frac{R_r}{\cos(\delta_f)} - R_r = R_r \cdot \left(\frac{1}{\cos(\delta_f)} - 1\right) =$$

$$= \sqrt{R^2 - {l_r}^2} \cdot \left(\frac{1}{\cos(\delta_f)} - 1\right) \approx R \cdot \left(\frac{1}{\cos(\delta_f)} - 1\right) \approx R \cdot (1 - \cos(\delta_f))$$

[4.10]

4.2.10 Steering effort *

Function definition: **Steering effort at low speed** *is the steering wheel torque needed to turn the steering wheel a certain angle at a certain angular speed at vehicle stand-still on high road friction.*

Function definition: **Steering effort at high speed** *is the steering wheel torque (or subjectively assessed effort) needed to perform a certain avoidance manoeuvre at high road friction.*

At low or zero vehicle speed, it is often difficult to make steering wheel torque low enough. This has mainly two reasons:

See the Caster offset in Figure 4-5. It gives the wheel a side slip when steering and hence a tyre lateral force is developed. Tyre lateral forces times the caster offset is one part that steering efforts has to overcome.

Additionally, there is a spin moment in the contact patch, M_{ZT} in Figure 2-2. (M_{ZT} does not influence very much, except for at very low vehicle speed, which is why quantitative models for M_{ZT} are not presented in this compendium.) The spin moment also has to be overcome by steering efforts.

A critical test for steering effort at low speed is to steer a parked vehicle with a certain high steering wheel rotational speed, typically some hundred deg/s. The steering wheel torque is then required to stay under a certain design target value, normally a couple of Nm. The torque needed will be dependent on lateral force, spin moment and steering geometry (which is not steering speed dependent) and dependent on the capability of the power steering system (which is dependent on steering, due to delays in the steering assistance actuator). A failure in this test is called "catch-up", referring to that driver catches up with the power steering system. It can be felt as a soft stop and measured as a step in steering wheel torque.

At higher vehicle speeds, the steering effort is normally less of a problem since unless really high steering wheel rate. Hence, steering wheel torque in avoidance manoeuvres in e.g. 70 km/h can be a relevant requirement. In these situations, the subjective assessment of steering effort can also be the measure. Then, steering effort is probably assessed based on both steering wheel rate and steering wheel torque.

4.2.11 One-track model for low speeds, with non-Ackerman geometry

The model in Figure 4-10 can rather easily be extended to more axles, more units and two-track model, if Ackermann geometry. However, if not Ackermann geometry, one has to do a structural change in the model, because ideal tracking is no longer consistent with geometry. One example is a two-track model of a two-axle vehicle which has parallel steering on one axle. Another example is a one-track model of a truck with three axles, whereof the two last are non-steered, see Figure 4-15.

We will go through model changes needed in the latter example. In order to compare the models as closely as possible, we simply split the rear axle into two rear axles, in the example in Section 4.2.6. The physical model becomes as in Figure 4-15. The measures appear in

Figure 4-17, and you see that it is not a truck, but a very unconventional passenger size car with two rear axles.
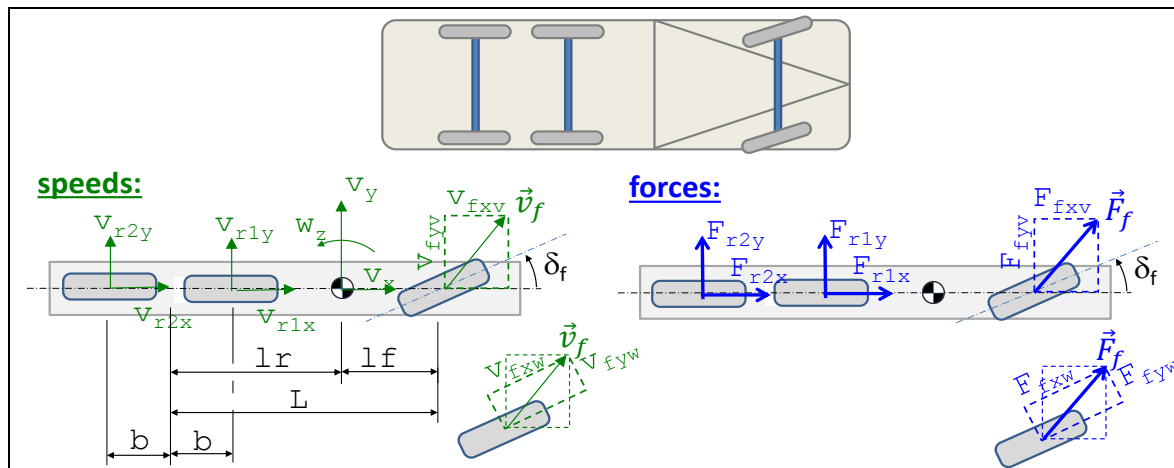
*Figure 4-15: Top: Rigid Truck with 3 axles, whereof only the first is steered.
Bottom: One-track model. Not Ackermann geometry, due to un-steered rear axles.*

The changes we have to do in the model appear as underlined in Equation [4.11]. There has to be double variables for v_{rx}, v_{ry}, F_{rx}, F_{ry}, denoted 1 and 2 respectively. Also, we cannot use $v_{fyw} = v_{ry} = 0$ anymore, but instead we have to introduce a lateral tyre force model, as described in Section 2.5.

```
//Equilibrium:
  0 = Ffxv + Fr1x + Fr2x;
  0 = Ffyv + Fr1y + Fr2y;
  0 = Ffyv*lf - Fr1y*(lr - b) - Fr2y*(lr + b);

//Constitutive relation, i.e.
Lateral tyre force model (instead of Ideal tracking):
  Ffyw = -Cf*sfy;
  Fr1y = -Cr1*sr1y;
  Fr2y = -Cr2*sr2y;
  sfy = vfyw/vfxw;
  sr1y = vr1y/vr1x;
  sr2y = vr2y/vr2x;

//Compatibility:
  vfxv = vx;
  vfyv = vy + lf*wz;
  vr1x = vx;
  vr2x = vx;
  vr1y = vy - (lr - b)*wz;
  vr2y = vy - (lr + b)*wz;

//Transformation between vehicle and wheel coordinate systems:
  Ffxv = Ffxw*cos(df) - Ffyw*sin(df);
  Ffyv = Ffxw*sin(df) + Ffyw*cos(df);
  vfxv = vfxw*cos(df) - vfyw*sin(df);
  vfyv = vfxw*sin(df) + vfyw*cos(df);

//Path with orientation:
  der(x) = vx*cos(pz) - vy*sin(pz);
  der(y) = vy*cos(pz) + vx*sin(pz);
  der(pz) = wz;

// Prescription of steering angle:
  df = if time < 4.5 then (35*pi/180)*sin(0.5*2*pi*time) else 35*pi/180;
//Rear axles undriven, which gives drag from roll resistance:
  Fr1x = -100/2;
  Fr2x = -100/2;
```

[4.11]

The new result is shown in Figure 4-16, which should be compared to Figure 4-11. The radius of the final path radius increases a little. If we read out more carefully, we can draw the different locations of the instantaneous centre for both cases. This is shown, in scale, in

Figure 4-17.
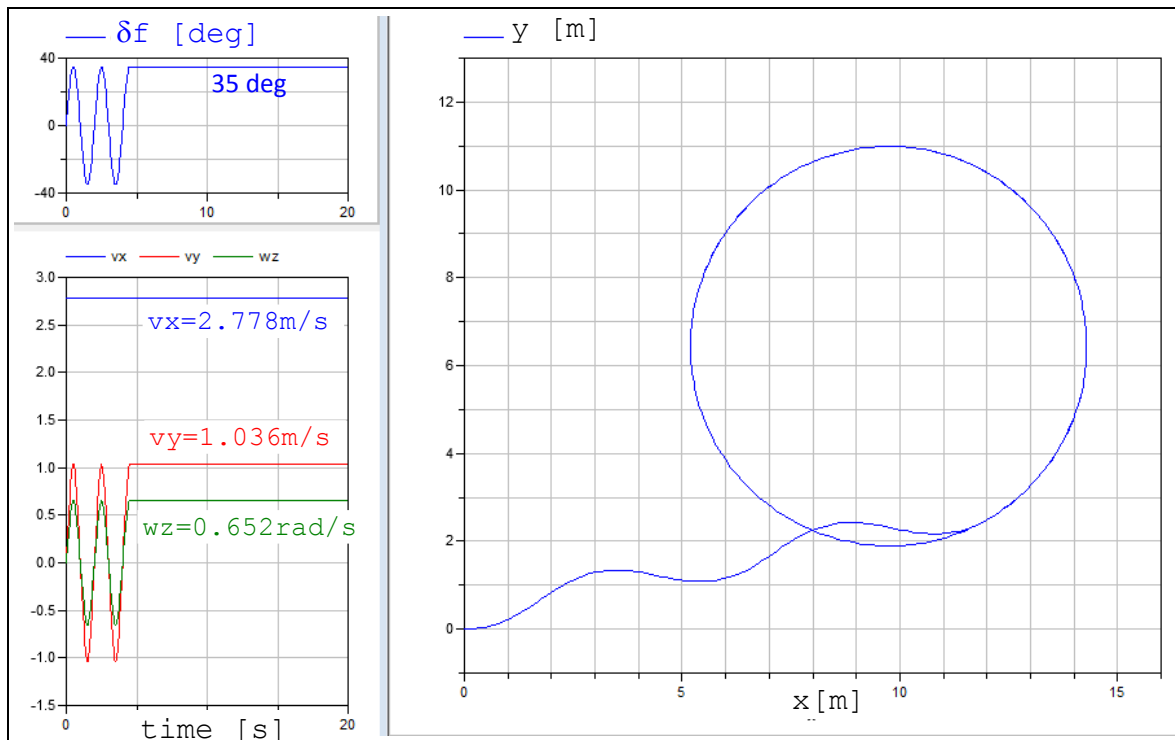
Figure 4-16: Simulation results of one-track model with ideal tracking. Non-Ackermann geometry due to two non-steered rear axles.

We could tune the steering angle required to reach exactly the same path radius as for the 2-axle reference vehicle. Then, we would have to steer a little more than the 35 degrees used, and we could find a new instantaneous centre, and we could identify a so called Equivalent wheelbase. This leads us to a definition: The equivalent wheel base of a multi-axle vehicle is the wheel base of a conventional two-axle vehicle which would exhibit the same turning behaviour as exhibited by the multi-axle vehicle, given same steering angle and similar axle cornering stiffnesses.
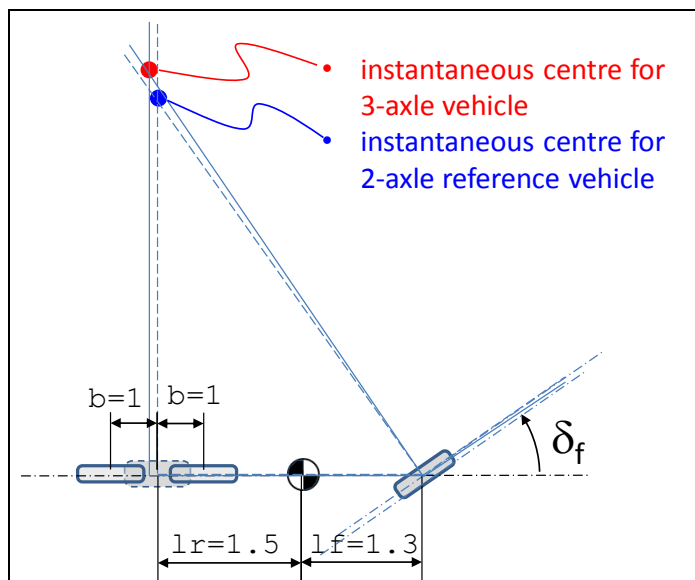
Figure 4-17: Instantaneous centre with a 3-axle vehicle, with the corresponding 2-axle vehicle as reference.

Section 4.2.11 shows that the lateral tyre force model, which is a constitutional relation, can sometimes be needed also at low speeds. However, it is always needed in next section about high speed cornering, Section 4.2.12.

4.2.12 One-track model for low speeds, with trailer

When the vehicles has an articulation point, also the low speed case (disregarding inertias) has transients in the sense that the articulation angles changes transiently. Consider the case of instantaneous step steer. For a vehicle without articulation point, a steady state is reached directly, since inertia is not considered. But for an articulated vehicle it takes some travelled distance (not time, since it can be studied independent of speed and time) before a steady state articulation angle is achieved.

So, for articulated vehicles, a scalar requirement on turning radius is not so relevant as for two axle vehicles. But, the function "4.2.8 Swept path width and Swept Area *" and "4.2.9 Off-tracking *" is, if road geometry is reflected, e.g. through outer radius and total angle of turning.

4.3 Steady state cornering at high speed

Steady state cornering refers to that all time derivatives of vehicle speeds (v_x, v_y, ω_z) are zero. The physical understanding is then that the vehicle drives on a circle with constant yaw rate, see Figure 4-18. Alternatively, this can be described as driving with constant tangential speed (v), on a constant path radius (R) with and with a constant side slip angle (β).

Steady state cornering can be defined by either 3 or 2 quantities, depending on assumptions:

- For a **general vehicle** it is fully defined only by all **3 quantities**, e.g. $[v_x, v_y, \omega_z]$ or $[v, \beta, R]$.

- For a **certain vehicle** it is often considered as fully defined by **2 inputs from driver**: accelerator pedal position and steering wheel angle. Then, one should keep in mind that one have neglected possible inputs from driver, such as brake pedal and parking brake, all wheel drive distribution, etc.

Figure 4-18: Steady state cornering.

4.3.1 Steady state driving manoeuvres

When testing steady state function, one usually runs on a so called "skid-pad" which appears on most test tracks, see Figure 4-8. It is a flat circular surface with typically 100 m diameter and some concentric circles marked. A general note is that tests in real vehicles are often needed to be performed in simulation also, and normally earlier in the product development process.

Typical steady state tests are:

- Constant path radius. Driven for different longitudinal speeds.
- Constant longitudinal speed. Driven for different path radii.
- Constant steering wheel angle. Then increase accelerator pedal (or apply brake pedal) gently. (If too quick, the test would fall under transient handling instead.)

Standards which are relevant to these test manoeuvres are, e.g. References (ISO 4138) and (ISO 14792).
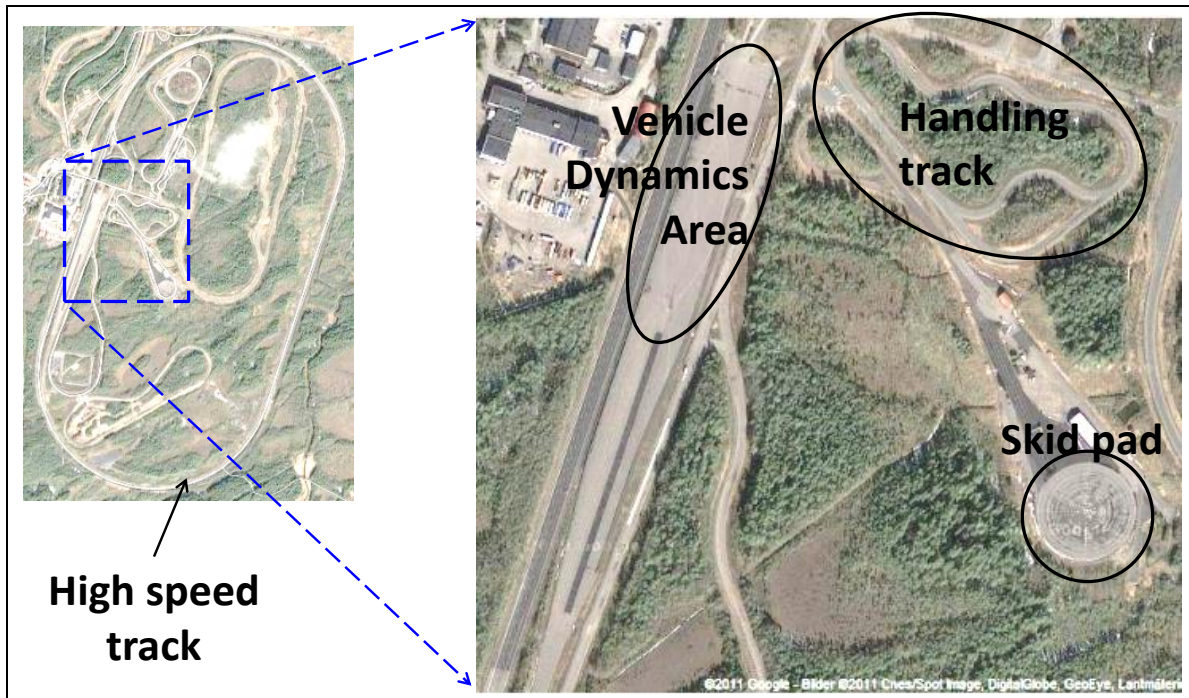
Figure 4-19: An example of test track and some parts with special relevance to Vehicle Dynamics. The example is Hällered Proving Ground, Volvo Car Corporation.
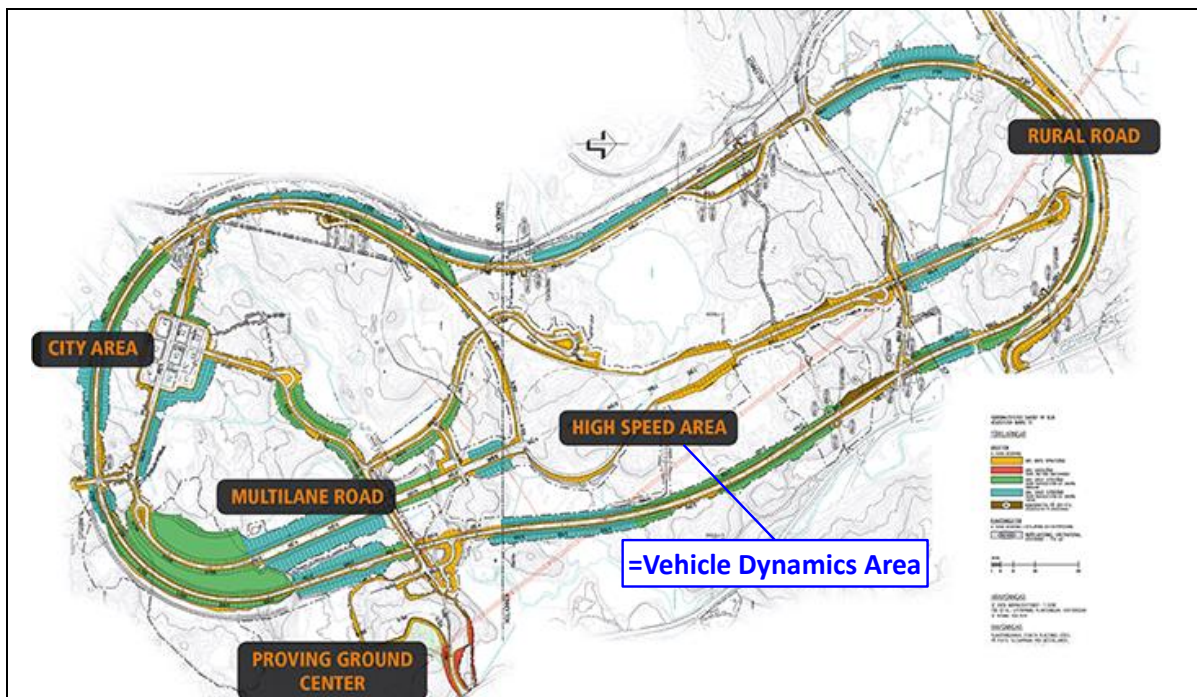
Figure 4-20: An example of test track. The example is AstaZero (Active Safety Test Arena), SP Technical Research Institute of Sweden and Chalmers University of Technology.

4.3.2 Steady state one-track model

In steady state we have neither inertial effects from changing the total vehicle speed ($v = \sqrt{v_x{}^2 + v_y{}^2}$ is constant) nor from changing the yaw rate (w_z is constant). However, the inertial "centrifugal" effect of the vehicle must be modelled. The related acceleration is the centripetal acceleration, $a_c = R \cdot \omega_z{}^2 = v^2/R = \omega_z \cdot v$.

A vehicle model for this is sketched in Figure 4-21. The model is a development of the model for low-speed in Figure 4-10 and Equation [4.9], with the following changes:

- Longitudinal and lateral accelerations are changed from zero to components of centripetal acceleration, ac, as follows (see Figure 4-21):
  - $a_x = -a_c \cdot \sin(\beta) = -\omega_z \cdot v \cdot \sin(\beta) = -\omega_z \cdot v_y$;
  - $a_y = +a_c \cdot \cos(\beta) = +\omega_z \cdot v \cdot \cos(\beta) = +\omega_z \cdot v_x$;
- The constitutive assumptions for the axles are changed from ideal tracking to a (linear) relation between lateral force and lateral slip. The relations should capture the slip characteristics for the tyres, see Section 2.5, but they can also capture steering system compliance (see Section 4.3.5.3), roll steering (see Section 4.3.5.5) and side force steering (see Section 4.3.5.4). The total mathematical relations can anyway be written as:
  - $F_{fyw} = -C_f \cdot s_{fy}$; where $s_{fy} = v_{fyw}/v_{fxw}$;
  - $F_{ry} = -C_r \cdot s_{ry}$; where $s_{ry} = v_{ry}/v_{rx}$;
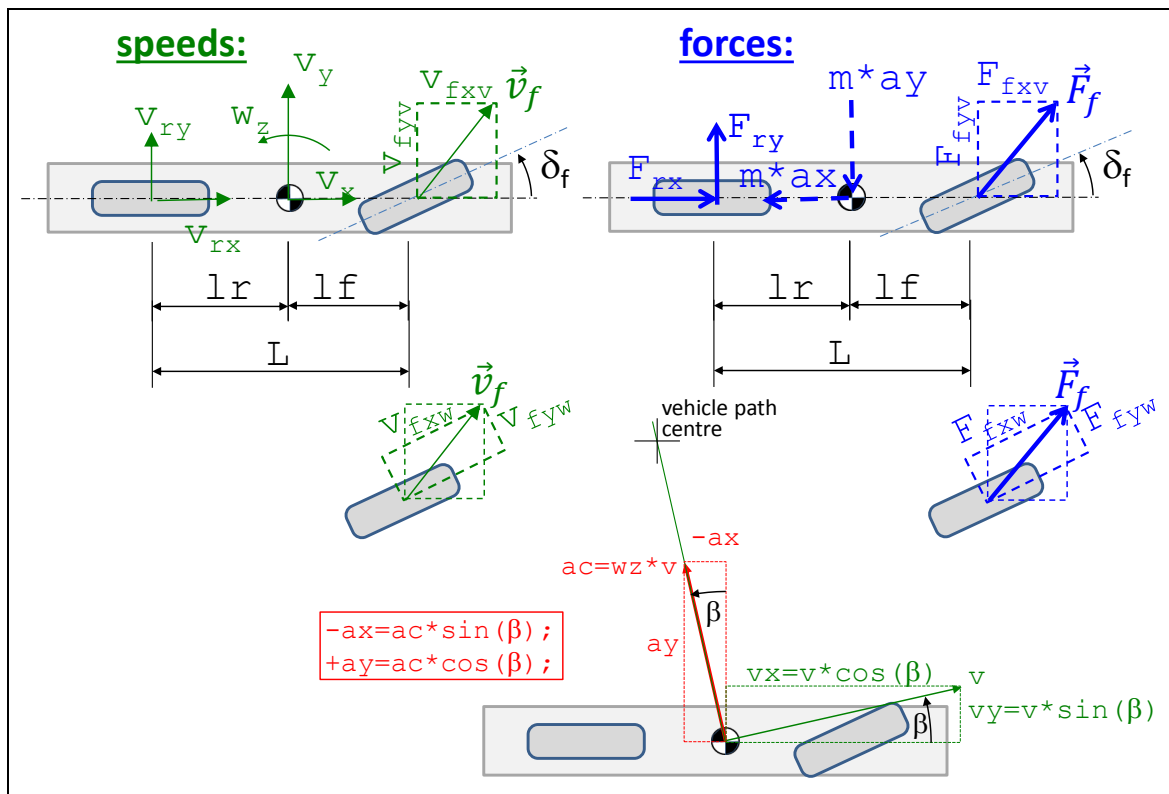
Figure 4-21: One-track model. Dashed forces and moment are fictive forces.

The model in Figure 4-21 is documented in mathematical form in Equation [4.12] (in Modelica format). The subscript v and w refers to vehicle coordinate system and wheel coordinate system, respectively.

```
//Equilibrium:
m*ax = Ffxv + Frx;    //Air and grade resistance neglected
m*ay = Ffyv + Fry;
J*0 = Ffyv*lf - Fry*lr;    // der(wz)=0
-ax = wz*vy;
+ay = wz*vx;

//Constitutive relation, i.e. Lateral tyre force model:
Ffyw = -Cf*sfy;
Fry = -Cr*sry;
sfy = vfyw/vfxw;
sry = vry/vrx;

//Compatibility:
```

[4.12]

```
vfxv = vx;
vfyv = vy + lf*wz;
vrx = vx;
vry = vy - lr*wz;

//Transformation between vehicle and wheel coordinate systems:
Ffxv = Ffxw*cos(df) - Ffyw*sin(df);
Ffyv = Ffxw*sin(df) + Ffyw*cos(df);
vfxv = vfxw*cos(df) - vfyw*sin(df);
vfyv = vfxw*sin(df) + vfyw*cos(df);

//Path with orientation:
der(x) = vx*cos(pz) - vy*sin(pz);
der(y) = vy*cos(pz) + vx*sin(pz);
der(pz) = wz;

// Prescription of steering angle:
df = if time < 2.5 then (5*pi/180)*sin(0.5*2*pi*time) else 5*pi/180;
// Rear axle undriven, which gives drag from roll resistance:
Frx = -100; // =10000; //
//Ffxw=0;
```

The longitudinal speed is a parameter, $v_x = 100\ km/h$. A simulation result from the model is shown in Figure 4-22. It shows the assumed steering angle function of time, which is an input. It also shows the resulting path, y(x). A driving resistance of 100 N is assumed on the rear axle (Frx=100;). This is to exemplify that longitudinal forces does not need to be zero, even if longitudinal forces normally are not so interesting for steady state high speed manoeuvres.

The variables x, y and $pz = \varphi_z$ are the only "state variables" of this simulation. If not including the path model (Equation [4.1]), the model would actually not be a differential equation problem at all, just an algebraic system of equations. That system of equations could be solved isolated for any value of steering angle without knowledge of time history. These aspects are the same for the low speed model in section 4.2.6.

Now, the validity of a model always have to be questioned. There are many modelling assumptions which could be checked, but in the following we only check the assumption $a_y = \omega_z \cdot v_x$; instead of the more correct $a_y = \dot{v}_y + \omega_z \cdot v_x$;, which we will learn in Section "4.4.2 Transient one-track model". Comparison of the terms gives $\left|\dot{v}_y\right|_{max} \approx |\omega_z \cdot v_x|_{max} \approx 10\ m/s^2$, so $|\omega_z \cdot v_x|$ is large and this jeopardizes the validity. Large $|\omega_z \cdot v_x|$ happens during $0 < t <\approx 2\ s$, so the model is not very valid there. But, at $t >\approx 2\ s$, the model is valid, at least in this aspect, since there $|\omega_z \cdot v_x| \ll \left|\dot{v}_y\right|$. So, the model is not very valid during the initial sinusoidal steering. This shows that a steady state *models* should not be thrusted outside steady state *conditions*.

Equation [4.12] is a complete model suitable for simulation, but it does not facilitate understanding very well. We will reformulate it assuming small δ_f (i.e. $\cos(\delta_f) = 1$, $\sin(\delta_f) = 0$, and $\delta_f^2 = 0$). Eliminate slip, all forces that are not wheel longitudinal, and all velocities that are not CoG velocities:

$$
\begin{aligned}
&-m \cdot \omega_z \cdot v_y \cdot \left(v_x + (v_y + l_f \cdot \omega_z) \cdot \delta_f\right) = \\
&= F_{fxw} \cdot \left(v_x + (v_y + l_f \cdot \omega_z) \cdot \delta_f\right) + C_f \cdot (v_y + l_f \cdot \omega_z) \cdot \delta_f + F_{rx} \cdot \left(v_x + (v_y + l_f \cdot \omega_z) \cdot \delta_f\right); \\
&m \cdot \omega_z \cdot v_x \cdot \left(v_x + (v_y + l_f \cdot \omega_z) \cdot \delta_f\right) = \\
&= -C_f \cdot \left(-v_x \cdot \delta_f + (v_y + l_f \cdot \omega_z)\right) + F_{fxw} \cdot \delta_f \cdot v_x - C_r \cdot \frac{v_y - l_r \cdot \omega_z}{v_x} \cdot \left(v_x + (v_y + l_f \cdot \omega_z) \cdot \delta_f\right); \\
&C_f \cdot \left(-v_x \cdot \delta_f + (v_y + l_f \cdot \omega_z)\right) \cdot l_f - F_{fxw} \cdot \delta_f \cdot l_f \cdot v_x = C_r \cdot \frac{v_y - l_r \cdot \omega_z}{v_x} \cdot l_r \cdot \left(v_x + (v_y + l_f \cdot \omega_z) \cdot \delta_f\right);
\end{aligned}
\qquad [4.13]
$$

Equation [4.13] is a complete model, which we can see as a dynamic system without state variables.

- Actuation: Steering and wheel torque on each axle: $\delta_f, F_{fxw}, F_{rx}$.
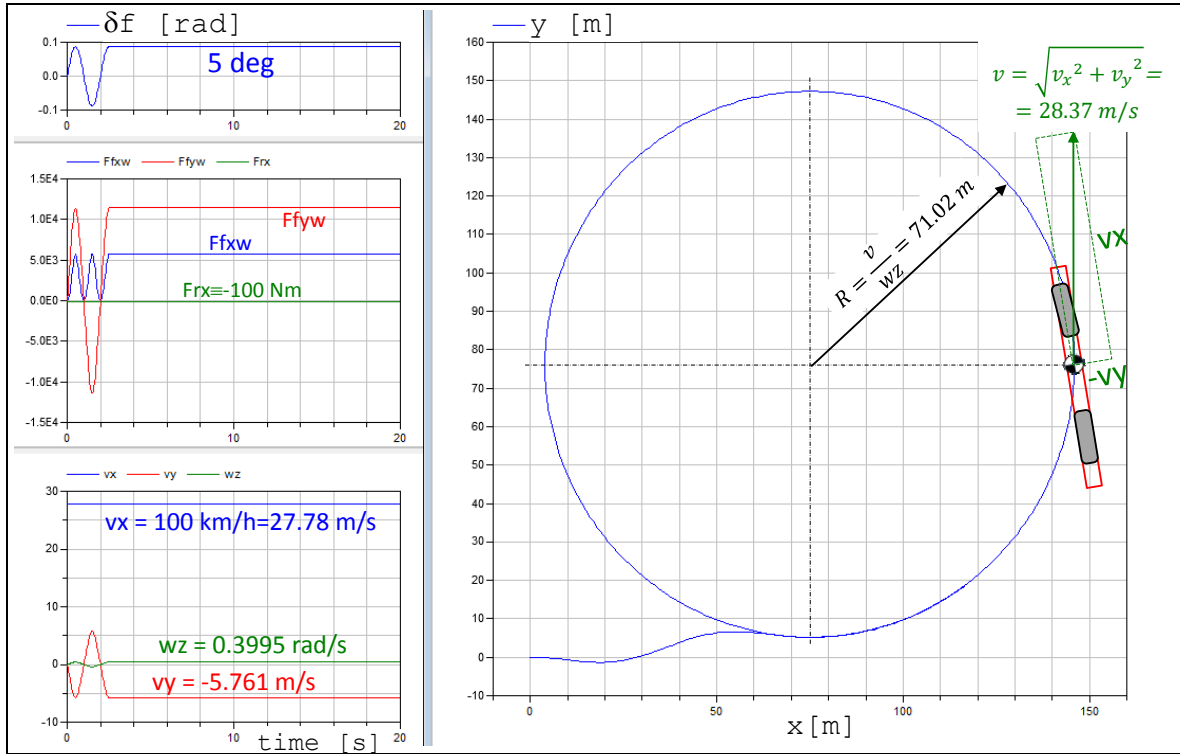- Motion quantities: v_x, v_y, ω_z

Figure 4-22: Simulation results of steady state one-track model. The vehicle sketched in the path plot is not in scale, but correctly oriented.

For example, we can chose δ_f, F_{fxw}, v_x and use the 3 equations to calculate F_{rx}, v_y, ω_z. In steady state manoeuvres, one can often disregard the longitudinal equilibrium, which means to skip 1st equation and the unknown F_{rx}:

$$\omega_z = \frac{C_f \cdot C_r \cdot L + (C_r \cdot l_f + C_r \cdot l_r) \cdot F_{fxw}}{C_f \cdot C_r \cdot L^2 + (C_r \cdot l_r - C_f \cdot l_f) \cdot m \cdot v_x^2} \cdot v_x \cdot \delta_f;$$

$$v_y = \frac{C_f \cdot (C_r \cdot L \cdot l_r - l_f \cdot m \cdot v_x^2) + (C_r \cdot L \cdot l_r - l_f \cdot m \cdot v_x^2) \cdot F_{fxw}}{C_f \cdot C_r \cdot L^2 + (C_r \cdot l_r - C_f \cdot l_f) \cdot m \cdot v_x^2} \cdot v_x \cdot \delta_f;$$

[4.14]

4.3.2.1 Relation δ_f, v_x and R

Solving the first equation in Equation [4.14] yields:

$$\delta_f = \frac{C_f \cdot C_r \cdot L^2 + (C_r \cdot l_r - C_f \cdot l_f) \cdot m \cdot v_x^2}{C_f \cdot C_r \cdot L + (C_r \cdot l_f + C_r \cdot l_r) \cdot F_{fxw}} \cdot \frac{\omega_z}{v_x} \approx$$

$$\approx \{assume: F_{fxw} \approx 0\} \approx \left(L + \frac{C_r \cdot l_r - C_f \cdot l_f}{C_f \cdot C_r \cdot L} \cdot m \cdot v_x^2\right) \cdot \frac{\omega_z}{v_x} =$$

$$= \left\{define: K_u = \frac{C_r \cdot l_r - C_f \cdot l_f}{C_f \cdot C_r \cdot L} = \frac{l_r}{C_f \cdot L} - \frac{l_f}{C_r \cdot L}\right\} = L \cdot \frac{\omega_z}{v_x} + K_u \cdot m \cdot a_y \approx$$

$$= \{use\ steady\ state: a_y = \omega_z \cdot v_x\} = L \cdot \frac{\omega_z}{v_x} + K_u \cdot m \cdot \omega_z \cdot v_x \approx$$

$$\approx \left\{assume\ small\ v_y \Rightarrow \frac{\omega_z}{v_x} \approx \frac{1}{R}\right\} \approx \frac{L}{R} + K_u \cdot \frac{m \cdot v_x^2}{R};$$

[4.15]

The coefficient K_u is the *understeer gradient* and it will be explained in next section.

4.3.2.2   Relation δ_f, v_x and β

Solving the second equation in Equation [4.14] yields:

$$\delta_f = \frac{C_f \cdot C_r \cdot L^2 + (C_r \cdot l_r - C_f \cdot l_f) \cdot m \cdot v_x^2}{C_f \cdot (C_r \cdot L \cdot l_r - l_f \cdot m \cdot v_x^2) + (C_r \cdot L \cdot l_r - l_f \cdot m \cdot v_x^2) \cdot F_{fxw}} \cdot \frac{v_y}{v_x} \approx$$

$$\approx \{use: F_{fxw} = 0\} \approx \frac{C_f \cdot C_r \cdot L^2 - (C_f \cdot l_f - C_r \cdot l_r) \cdot m \cdot v_x^2}{C_f \cdot C_r \cdot l_r \cdot L - C_f \cdot l_f \cdot m \cdot v_x^2} \cdot \frac{v_y}{v_x} \approx$$

$$\Rightarrow \begin{cases} \delta_f \xrightarrow[v_x \to 0]{} \dfrac{L}{l_r} \cdot \dfrac{v_y}{v_x}; \\ \delta_f \xrightarrow[v_x \to \infty]{} \dfrac{C_f \cdot l_f - C_r \cdot l_r}{C_f \cdot l_f} \cdot \dfrac{v_y}{v_x} = -K_u \cdot C_r \cdot \dfrac{L}{l_f} \cdot \dfrac{v_y}{v_x}; \end{cases}$$

[4.16]

We can see that there is a speed dependent relation between steering angle and side slip, $\frac{v_y}{v_x}$. The side slip can also be expressed as a side slip angle, $\beta = \arctan\left(\frac{v_y}{v_x}\right)$. Since normally $K_u > 0$, the side slip changes sign, when increasing speed from zero to sufficient high enough. This should feel intuitively correct, if agreeing on the conceptually different side slip angles at low and high speed, as shown in Figure 4-23. We will come back to this equation in context of Figure 4-34.
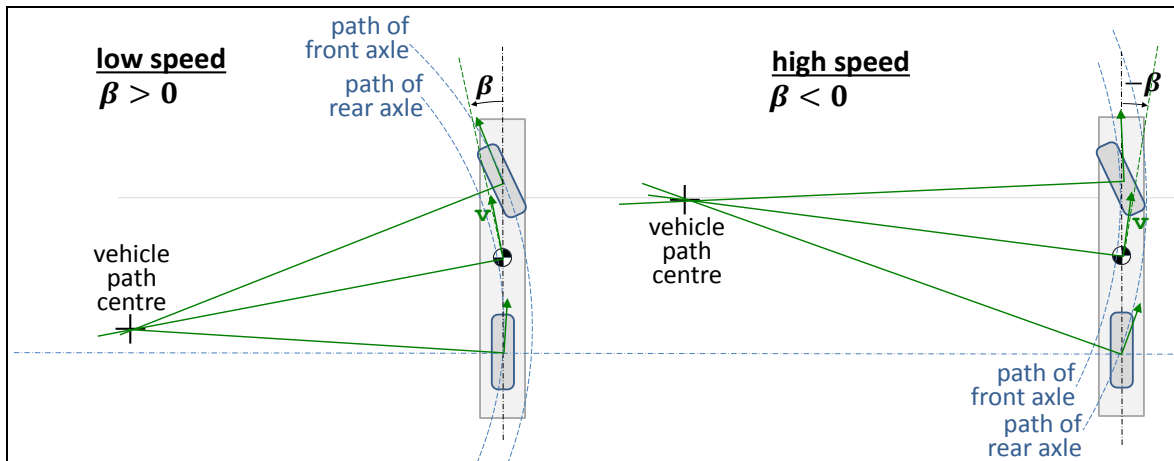
Figure 4-23: Body Slip Angle for Low and High Speed Steady State Curves

4.3.2.3   Relation v_x, R and β

If we approximate $F_{fxw} = 0$ and use both equations in Equation [4.14] to eliminate δ_f we get:

$$\frac{C_r \cdot L \cdot l_r - l_f \cdot m \cdot v_x^2}{C_r \cdot L} = l_r - \frac{l_f \cdot m \cdot v_x^2}{L \cdot C_r} = \frac{v_y}{\omega_z} = \frac{v_x}{\omega_z} \cdot \frac{v_y}{v_x} \approx R \cdot \tan(\beta); \Rightarrow$$

$$\Rightarrow \frac{v_y}{v_x} = \tan(\beta) = \left(l_r - \frac{l_f \cdot m \cdot v_x^2}{L \cdot C_r}\right) \cdot \frac{1}{R};$$

[4.17]

4.3.2.4   Simpler derivation of same model

A simpler way to reach almost same expression as first expression in Eq [4.14] is given in Figure 4-25. Here, the simplifications are introduced earlier, already in physical model, which means e.g. that the influence of F_{fxw} is not identified.

Physical model:
- Path radius >> the vehicle. Then, all forces (and centripetal acceleration) are approximately co-directed.
- Small tyre and vehicle side slip. Then, angle=sin(angle)=tan(angle).
  (Angles are not drawn small, which is the reason why the forces not appear co-linear in figure.)

Mathematical model:

Equilibrium:

$$m \cdot \frac{v_x{}^2}{R} \approx F_{fy} + F_{ry}; \quad 0 \approx F_{fy} \cdot l_f - F_{ry} \cdot l_r;$$

Constitution:

$$F_{fy} = -C_f \cdot s_{fy}; \quad F_{ry} = -C_r \cdot s_{ry};$$

Compatibility:

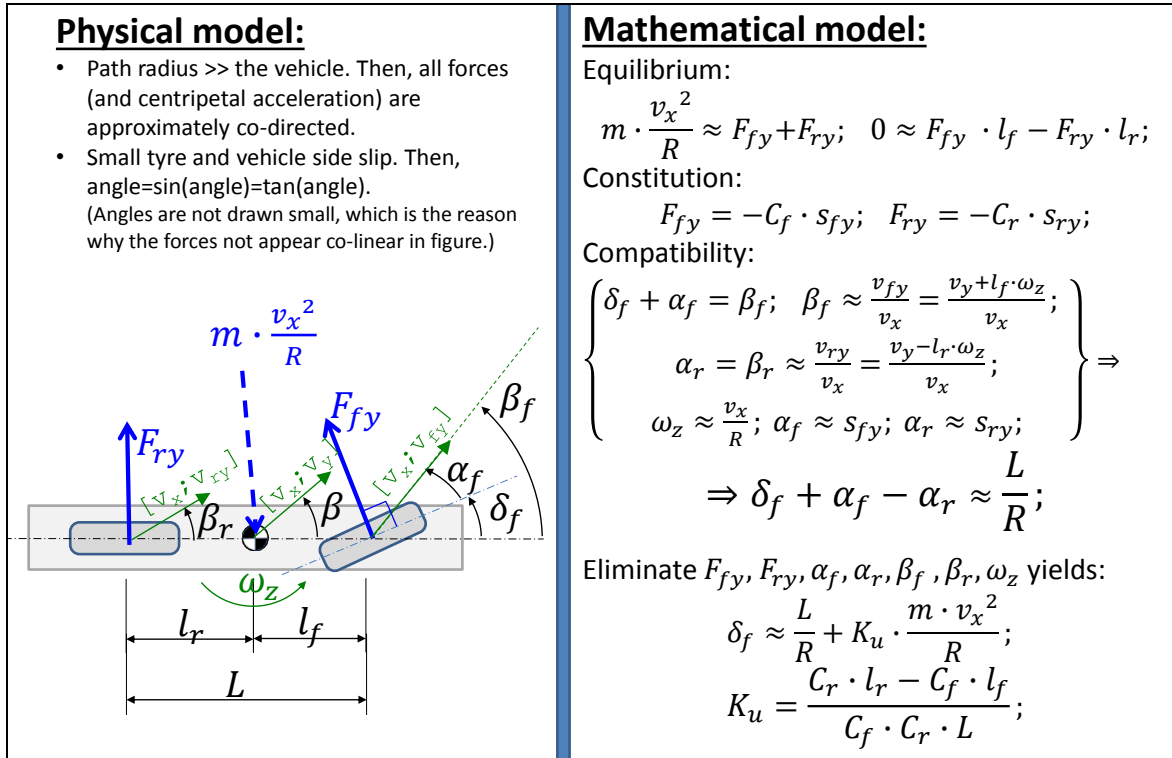$$\begin{cases} \delta_f + \alpha_f = \beta_f; \quad \beta_f \approx \frac{v_{fy}}{v_x} = \frac{v_y + l_f \cdot \omega_z}{v_x}; \\ \alpha_r = \beta_r \approx \frac{v_{ry}}{v_x} = \frac{v_y - l_r \cdot \omega_z}{v_x}; \\ \omega_z \approx \frac{v_x}{R}; \; \alpha_f \approx s_{fy}; \; \alpha_r \approx s_{ry}; \end{cases} \Rightarrow$$

$$\Rightarrow \delta_f + \alpha_f - \alpha_r \approx \frac{L}{R};$$

Eliminate $F_{fy}, F_{ry}, \alpha_f, \alpha_r, \beta_f, \beta_r, \omega_z$ yields:

$$\delta_f \approx \frac{L}{R} + K_u \cdot \frac{m \cdot v_x{}^2}{R};$$

$$K_u = \frac{C_r \cdot l_r - C_f \cdot l_f}{C_f \cdot C_r \cdot L};$$

Figure 4-25: Simpler derivation final step in Equation [4.15].

The validity of the steady state model described in this section, section 4.3.2, is of course limited by if the manoeuvre is transient which would mean that steady state is not reached. But it is also limited by if the assumption of linear tyre characteristics, $F_y = -C \cdot s_y$;, is violated. Therefore, one should check if some axle (or wheel) is calculated to use more than some certain fraction of available friction, $F = \sqrt{F_x^2 + F_y^2} > fraction \cdot \mu \cdot F_z$;. In many cases, one can argue for this limiting fraction to be in the order of 0.5.

4.3.3 Under-, Neutral- and Over-steering *

4.3.3.1 Understeering as built-in measure

Function definition: **Understeering (gradient)** *is the additional steering angle needed per increase of lateral force (or lateral acceleration) when driving in high speed steady state cornering on level ground and high road friction. Additional refers to low speed. The gradient is defined at certain high speed steady state cornering conditions, including straight-line driving. Steering angle can be either road wheel angle or steering wheel angle.*

K_u in Equation [4.15] is called "understeer gradient" and has hence the unit rad/N or 1/N. Sometimes one can see slightly other definitions of what to include in definition of understeer gradient, which have different units, see K_{u2} and K_{u3} in Equation [4.18]. (When defined as K_{u3}, one can sometimes see the unit "rad/g" used, which present compendium recommended to not use.)

$$\delta_f = \frac{L}{R} + \frac{C_r \cdot l_r - C_f \cdot l_f}{C_f \cdot C_r \cdot L} \cdot \frac{m \cdot g \cdot v_x{}^2}{g \cdot R} =$$

$$= \left\{ use: K_{u2} = m \cdot g \cdot \frac{C_r \cdot l_r - C_f \cdot l_f}{C_f \cdot C_r \cdot L} [1 \; or \; rad] \right\} = \frac{L}{R} + K_{u2} \cdot \frac{v_x{}^2}{g \cdot R};$$

$$\delta_f = \frac{L}{R} + \frac{C_r \cdot l_r - C_f \cdot l_f}{C_f \cdot C_r \cdot L} \cdot \frac{m \cdot v_x{}^2}{R} =$$

$$= \left\{ use: K_{u3} = m \cdot \frac{C_r \cdot l_r - C_f \cdot l_f}{C_f \cdot C_r \cdot L} \left[\frac{1}{m/s^2} \; or \; \frac{rad}{m/s^2} \right] \right\} = \frac{L}{R} + K_{u3} \cdot \frac{v_x{}^2}{R};$$

[4.18]

The first term in the final expression in Equation [4.15], L/R, can be seen as a reference steering angle. This is referred to as either "low speed steering angle" or "Ackermann steering angle". The understanding of this steering angle can be expanded to cover more general vehicles: It is the angle required for low speed turning. For a general vehicle, e.g. with other steering geometry than Ackermann, the angle cannot be calculated as simple as L/R, but with some specific derived formula, or it can be measured on a real vehicle. It is common to use the subscript A. It can be defined for front axle road wheel steering angle, δ_{fA}. It can also be defined for steering wheel angle, δ_{swA}.

The understeering gradient, K_u, is normally positive, which means that most vehicles require more steering angle for a given curve, the higher the speed is. Depending on the sign of K_u a vehicle is said to be oversteered (if $K_u < 0$), understeered (if $K_u > 0$) and neutral steered (if $K_u = 0$). In practice, all vehicles are designed as understeered, because over steered vehicle would become instable very easily.

The understeering gradient K_u can be understood as how much additionally to the Ackermann steering angle one have to steer, in relation to centrifugal force, F_c:

$$\delta_f = \delta_{fA} + K_u \cdot \frac{m \cdot v_x{}^2}{R} = \delta_{fA} + K_u \cdot F_c; \quad \Rightarrow \quad K_u = \frac{\delta_f - \delta_{fA}}{F_c} = \frac{\Delta\delta_f}{F_c};$$

Or, using the steering ratio, $\delta_f = \delta_{sw}/r_{ste}$:

$$\delta_{sw} = \delta_{swA} + K_u \cdot \frac{r_{ste} \cdot m \cdot v_x{}^2}{R} = \delta_{fA} + K_u \cdot r_{ste} \cdot F_c; \quad \Rightarrow \quad K_u = \frac{\delta_{sw} - \delta_{swA}}{r_{ste} \cdot F_c} = \frac{\Delta\delta_{sw}}{r_{ste} \cdot F_c};$$

[4.19]

4.3.3.2 Understeering as varying with steady state lateral acceleration

So far, the understeering gradient is presented as a fix built-in vehicle parameter. There is nothing that says that a real vehicle behaves linear, so in order to get a well-defined value of K_u, the $\Delta\delta_f$ and the F_c should be small when using Eq [4.20]. However, if we accept that K_u can change with F_c, K_u can be defined as a differential quantity:

K_u can also be understood as how much the additional steering angle, $\Delta\delta_f$, has to increase per increased centrifugal force, F_c, or per lateral acceleration, a_y:

$$K_u = \frac{\partial(\Delta\delta_f)}{\partial F_c} = \frac{\partial}{\partial F_c}(\delta_f - \delta_A) = \frac{\partial\Delta\delta_f}{\partial F_c}; \quad or \quad K_{u3} = \frac{\partial(\Delta\delta_f)}{\partial a_y} = \frac{\partial}{\partial a_y}(\delta_f - \delta_A) = \frac{\partial\delta_f}{\partial a_y};$$

[4.20]

Equation [4.20] shows the understeering gradient as a (mathematical) function, rather than a scalar parameter. But it is still fix and built-in in the vehicle. If assessing understeering for a lateral forces up to near road friction limit, Equation [4.20] is more relevant than Equation [4.15], because it reflects that understeering gradient changes.

4.3.3.3 Understeering as a varying quantity during a transient manoeuvre

A third understanding of the word understeering is quite different and less strictly defined. It is to see the understeering as a variable during a transient manoeuvre. For instance, a vehicle can be said to understeer if tyre side slip is larger on front axle than on rear axle, $|\propto_f| > |\propto_r|$, and over-steer if opposite, $|\propto_r| > |\propto_f|$. This way of defining understeering and oversteering is not built in, but varies over time through a (transient) manoeuvre. E.g., when braking in a curve a vehicle loses grip on rear axle due to temporary load transfer from rear to front. Then the rear axles can slide outwards significantly and the vehicle can be referred to as over-steering at this time instant, although the built-in understeering gradient is >0. This "instantaneous" under-/over-steering can be approximately found from log data with this simple approximation:

$$\delta_{neutral} = \frac{L}{R} \approx \{v_x \approx R \cdot \omega_z\} \approx \frac{L \cdot \omega_z}{v_x} \approx \{a_y \approx v_x \cdot \omega_z\} \approx \frac{L \cdot a_y}{v_x^2};$$

[4.21]

If the actual vehicle has $|\delta| > |\delta_{neutral}|$ the vehicle oversteers ($|\alpha_r| > |\alpha_f|$), and vice versa. This is often very practical since it only requires simply logged data, δ, v_x and a_y. Note that when δ and a_x have different signs, neither understeer or oversteers is suitable as classification, but it can sometimes be called "counter-steer".
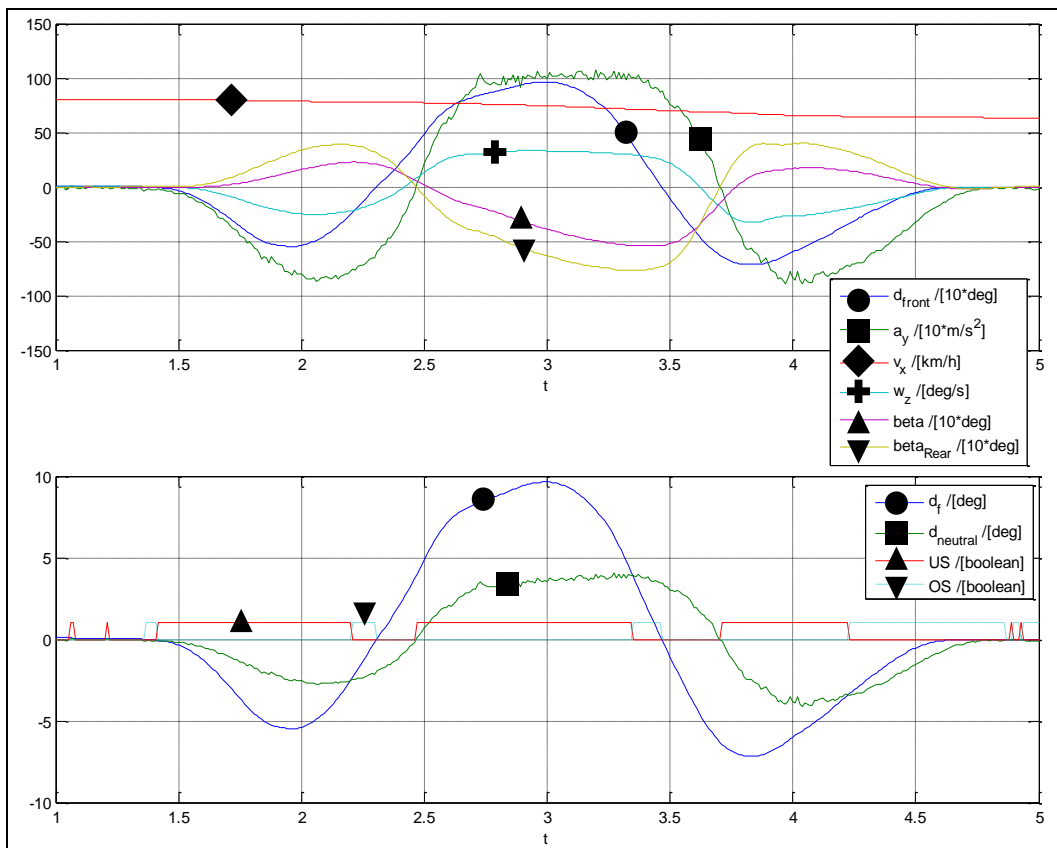

Figure 4-26: Upper: Log data from passenger car with ESC system in a double lane change. Lower: $\delta_{neutral}$ can be used to approximately assess "instantaneous" under-/over-steering (US/OS).

A second look at Equation [4.15] tells us that we have to assume absence of propulsion and braking on front axle, $F_{fxw} = 0$, to get the relatively simple final expression. When propulsion on front axle ($F_{fxw} > 0$), the required steering angle, δ_f, will be smaller; the front propulsion pulls in the front end of the vehicle. When braking on front axle ($F_{fxw} < 0$), the required steering angle, δ_f, will be larger; the front braking hinders the front end to turn in. To keep v_x constant, which is required within

definition of steady state, one have to propel the vehicle because there will always be some driving resistance to overcome. Driving fast on a small radius is a situation where the driving resistance from tyre lateral forces becomes significant, which is a part of driving resistance which was only briefly mentioned in Section 3.2.

Above reasoning was made for steady-state both longitudinally and laterally. If longitudinal acceleration, we can still assume lateral steady-state and study under-steering gradient. This is discussed in Section 4.3.5.1.

4.3.3.4　Neutral steering point

An alternative measure to understeering coefficient is the longitudinal position of the *neutral steering point*. The point is defined for lateral force disturbance during steady state **straight-ahead** driving, as opposed to steady state cornering without lateral force disturbance. The point is where a vehicle-external lateral force, such as wind or impact, can be applied on the vehicle without causing a yaw velocity ($\omega_z = 0$), i.e. only causing lateral velocity ($v_y \neq 0$). From this definition we can derive a formula for calculating the position of the neutral steering point, see Figure 4-27.

Physical model:
- Steady state ($\dot{v}_x = \dot{v}_y = \dot{\omega}_z = 0$)
- Straight ahead driving ($\omega_z = 0$)
- No steering
- Small tyre and vehicle side slip. Then, angle=sin(angle)=tan(angle).

Mathematical model:

Equilibrium:
$$0 = F_{fy} + F_{ry} + F_e;$$
$$0 = F_{fy} \cdot l_f - F_{ry} \cdot l_r + F_e \cdot l_s;$$

Constitution:
$$F_{fy} = -C_f \cdot s_{fy};$$
$$F_{ry} = -C_r \cdot s_{ry};$$

Compatibility:
$$s_{fy} = s_{ry} = \frac{v_y}{v_x};$$

Eliminate $F_{fy}, F_{ry}, s_{fy}, s_{ry}, F_e$ yields:
$$l_s = \frac{C_f \cdot l_f - C_r \cdot l_r}{C_f + C_r};$$

Express with understeering gradient,
$K_u = \frac{C_r \cdot l_r - C_f \cdot l_f}{C_f \cdot C_r \cdot L}$:
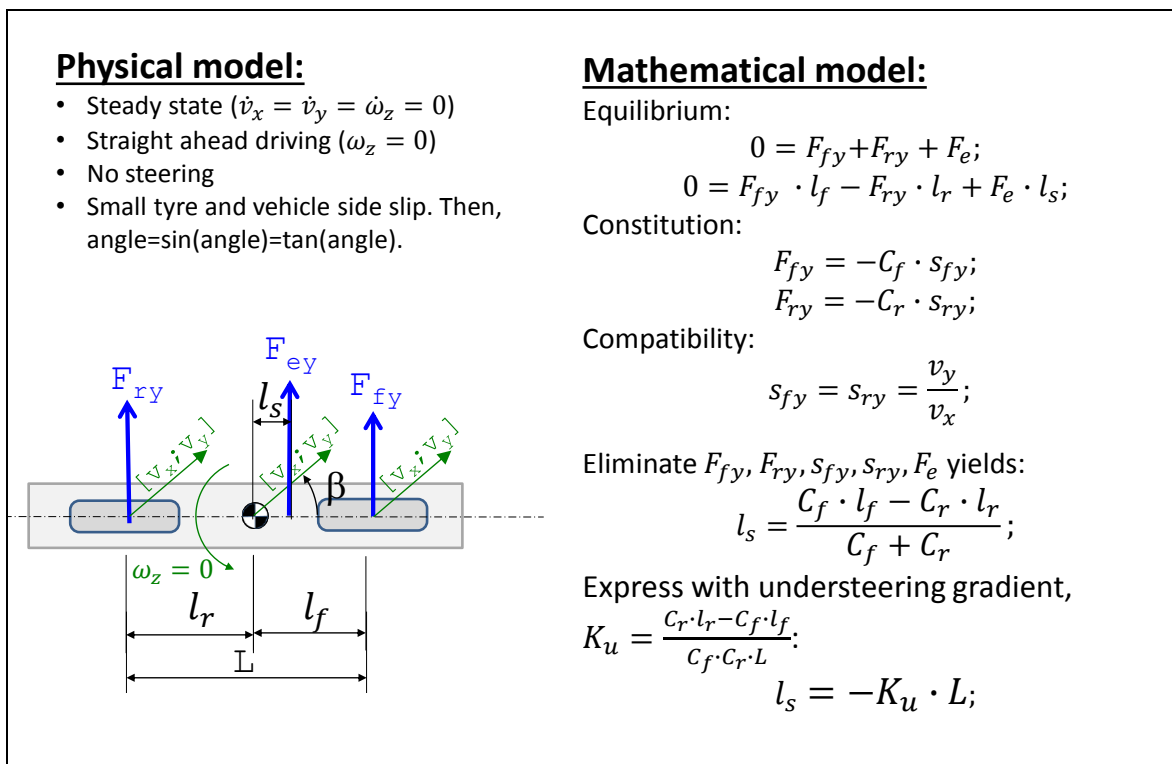$$l_s = -K_u \cdot L;$$

Figure 4-27: Model for definition and calculation of neutral steering point.

The result is condensed in Eq [4.22].

$$l_s = \frac{C_f \cdot l_f - C_r \cdot l_r}{C_f + C_r} = -K_u \cdot L; \quad where \; K_u = \frac{C_r \cdot l_r - C_f \cdot l_f}{C_f \cdot C_r \cdot L};$$
[4.22]

We can see that the understeer gradient from steady state cornering model appears also in the formula for neutral steering point position, l_s. This is why l_s (or rather l_s/L) and K_u can be said to be alternative measures for the same vehicle function/character, the yaw balance. It also proposes an alternative understanding of the understeering gradient; if $K_u = 0.1$, the neutral steering point is located $0.1 \cdot L$ rear of CoG.

4.3.4   Normalized required steering angle

A fundamental property of the vehicle is what steering angle that is required to negotiate a certain curvature (=1/path radius = $1/R_p$). This value can vary with longitudinal speed and it can be normalized with wheel base, L. From Equation [4.15], we can conclude:

$$\text{\textit{\textbf{Normalized required steering angle}}} = \frac{\delta_f \cdot R}{L} = 1 + K_u \cdot \frac{m \cdot v_x^2}{L}; \qquad [4.23]$$

The normalized required steering angle is plotted for different understeering gradients Figure 4-28. It is the same as the inverted and normalized curvature gain, see 4.3.6.2.
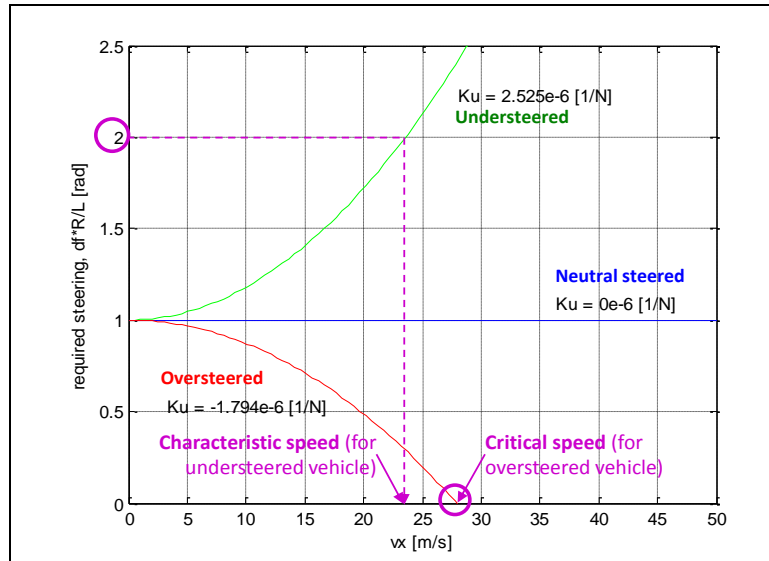

Figure 4-28: Normalized steering angle ($\delta_f \cdot R/L$) for Steady State Cornering

4.3.4.1   Critical and Characteristic speed *

Function definition: **Critical speed** *is the speed above which the vehicle becomes instable in the sense that the yaw rate grows significantly for a small disturbance in, e.g., steering angle.*

Function definition: **Characteristic speed** *is the speed at which the vehicle requires twice as high steering angle for a certain path radius as required at low speed (Figure 4-28). (Alternative definitions: The speed at which the yaw rate gain reaches maximum (Figure 4-31). The speed at which the lateral acceleration gain per longitudinal speed reaches its highest value. (Figure 4-33).)*

We can identify that zero steering angle is required for the over-steered vehicle at 28 m/s. This is the so called Critical Speed, which is the speed where the vehicle becomes unstable. It should be noted here, that there are stable conditions also above critical speed, but one has to steer in the opposite direction then. Normal vehicles are built understeered, which is why a Critical speed is more of a theoretical definition. However, if studying (quasi-steady state) situations where the rear axle is heavily braked, the cornering stiffness rear is reduced, and a critical speed can be relevant.

For understeered vehicles, we can instead read out another measure, the Characteristic Speed. The understanding of Characteristic Speed is, so far just that required steering increases to over twice what is needed for low speed at the same path radius. A better feeling for Characteristic Speed is easier suggested in a later section, see Section 4.3.6.3.

From Equation [4.15], we can find a formula for critical and characteristic speeds:

$$\delta_f = \frac{L}{R} + K_u \cdot \frac{m \cdot v_{x,crit}^2}{R} = 0 \;\Rightarrow\; v_{x,crit} = \sqrt{\frac{L}{-K_u \cdot m}} = \sqrt{\frac{C_f \cdot C_r \cdot L^2}{(C_f \cdot l_f - C_r \cdot l_r) \cdot m}} \;;$$

$$\delta_f = \frac{L}{R} + K_u \cdot \frac{m \cdot v_{x,char}^2}{R} = 2 \cdot \frac{L}{R} \;\Rightarrow\; v_{x,char} = \sqrt{\frac{L}{K_u \cdot m}} = \sqrt{\frac{C_f \cdot C_r \cdot L^2}{(C_r \cdot l_r - C_f \cdot l_f) \cdot m}} \;;$$

[4.24]

4.3.5 How to design for understeer gradient

The values of cornering stiffness for each axle are design parameters to influence understeer gradient. However, cornering stiffness is an abstract design parameter, in the sense that one cannot put it on a drawing. Instead, cornering stiffness is a combined effect from various, more concrete, design parameters. Such more concrete design parameters are briefly presented in the following.

4.3.5.1 Tyre design, inflation pressure and number of tyres

(This section discusses also influence of longitudinal acceleration, which is no tyre design parameter. However, it is logical in the sense that longitudinal acceleration influence yaw balance via how the tyres cornering stiffness varies with tyre normal load, which is directly influenced by the longitudinal acceleration.)

The cornering stiffness of each tyre is an obvious parameter which influences the axle stiffness. The cornering stiffness of an axle is influence by the sum of cornering stiffness for all tyres. There are normally two tyres per axle, but there are also vehicles with one tyre (e.g. bicycles) or 4 (typically 2 double mounted on each side in heavy trucks).

Tyre design influences, which is geometrical dimensions and material selection. Inflation pressure is in this context very close to a design parameter.

In a first approximation, tyre cornering stiffness is approximately proportional to vertical load: $C_i = k_i \cdot F_{iz}$. For a vehicle with equally many and same tyres front and rear, this means that it will be neutral steered. This is because, in steady state cornering, vertical loads distributes in same relation as lateral loads. Using definition of understeer gradient:

$$\frac{K_{u2}}{m \cdot g} = \frac{l_r}{C_f \cdot L} - \frac{l_f}{C_r \cdot L} = \frac{l_r}{k_f \cdot F_{fz} \cdot L} - \frac{l_f}{k_r \cdot F_{rz} \cdot L} = \left\{ \begin{array}{c} longitudinal \\ load\ transfer \\ m \cdot a_x \cdot h/L \end{array} \right\} \Rightarrow$$

$$\Rightarrow K_{u2} = \frac{m \cdot g \cdot l_r}{k_f \cdot \left(m \cdot g \cdot \frac{l_r}{L} - m \cdot a_x \cdot \frac{h}{L} \right) \cdot L} - \frac{m \cdot g \cdot l_f}{k_r \cdot \left(m \cdot g \cdot \frac{l_f}{L} + m \cdot a_x \cdot \frac{h}{L} \right) \cdot L} =$$

$$= \frac{l_r/L}{k_f \cdot \left(\frac{l_r}{L} - \frac{a_x}{g} \cdot \frac{h}{L} \right)} - \frac{l_f/L}{k_r \cdot \left(\frac{l_f}{L} + \frac{a_x}{g} \cdot \frac{h}{L} \right)} = \left\{ \begin{array}{c} if\ a_x = 0 \\ and \\ k_f = k_r \end{array} \right\} = 0;$$

[4.25]

Longitudinal load transfer (influence of a_x in the equations) show that braking increases over-steering tendency. It is actually so, that the critical speed $v_{x,crit} = \sqrt{L/(-K_u \cdot m)}$ (see Equation [4.24]) can come down to quite reachable levels when braking hard; i.e. hard braking at high speed may cause instability. This is especially so for front biased CoG location. See Figure 4-29, inspired by Reference (Drenth, 1993).
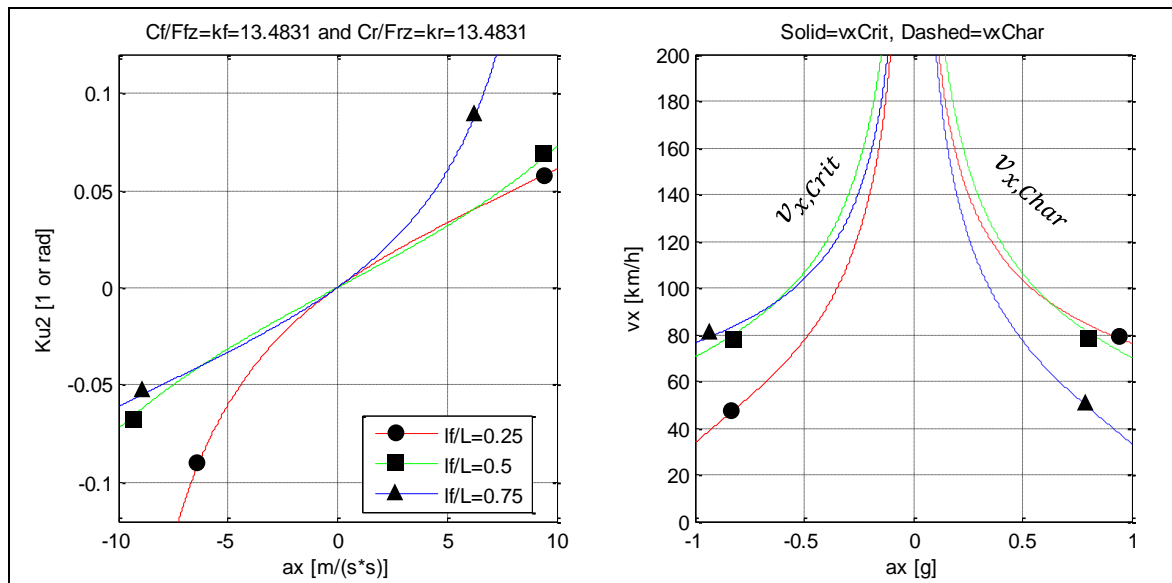
Figure 4-29: Left: Under-steering gradient as function of longitudinal acceleration, ax, and static load distribution, lf/L. Right: Critical and characteristic velocity as function of acceleration and load distribution.

However, the cornering stiffness varies degressively, e.g. $C_i = k_{ip} \cdot F_{iz} - k_{id} \cdot F_{iz}^2$. This is further studied in Reference (Drenth, 1993).

If taking the degressiveness of tyre cornering stiffness into account, the weight distribution plays a role also without longitudinal load transfer; front biased weight distribution gives under-steered vehicles and vice versa. Also, the number of wheel per axle influence stronger; single wheel front (or double-mounted rear) gives under-steered vehicles and vice versa.

It should be noted that if the longitudinal acceleration is due to wheel torques, as opposed to road grade or aerodynamic forces, the tyre combined slip effects influences the curves in Figure 4-29. Basically as the axle that takes most longitudinal force gets reduced cornering stiffness.

4.3.5.2 Roll stiffness distribution between axles

During cornering, the vertical load is shifted towards the outer wheels. Depending on the roll stiffness of each axle, the axles take differently much of this lateral load transfer. This also influences the yaw balance. The more roll stiff an axle is, the more of the lateral load shift it takes. Tyre cornering stiffness varies degressively with vertical load. Together, this means that increasing the roll stiffness on the front axle, leads to less front cornering stiffness, see Figure 2-31, and consequently more understeered vehicle. Increasing roll stiffness on rear axle makes the vehicle more oversteered. The total roll stiffness of the vehicle does not influence the understeering gradient. Normally one makes the front axle more roll stiff than the rear axle. This means that vehicle becomes more and more understeered for increased lateral acceleration, e.g. more steering angle is needed to maintain a certain path radius if speed increases. One can change the roll stiffness of an axle by changing roll centre height, wheel stiffness rate and anti-roll bar stiffness.
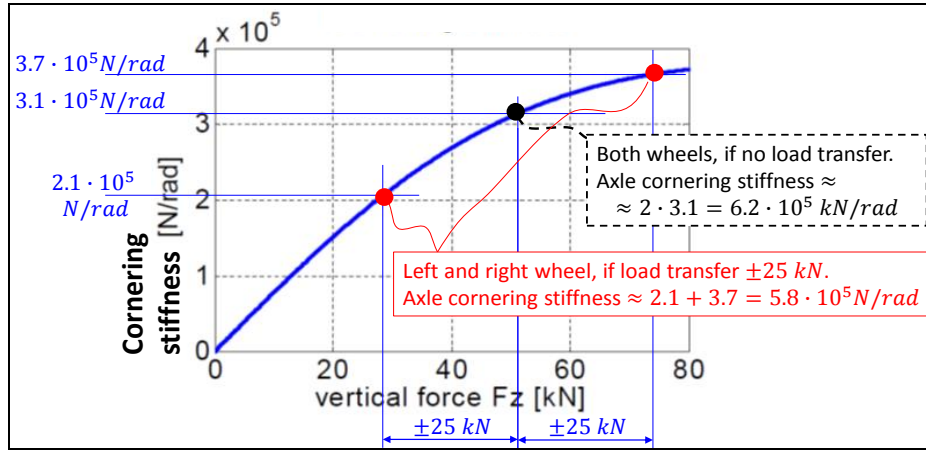
Figure 4-30: The wheels cornering stiffness $(\partial/\partial\alpha\,(F_y))|_{s_y=0})$ changes degressively with vertical load. The axle cornering stiffness therefore decreases with increased load transfer.

4.3.5.3   Steering system compliance

A compliant steering system will reduce the effective cornering stiffness on the steered axle. With normal front axle steering, a compliant steering means a more understeered vehicle.

4.3.5.4   Side force steer gradient

Side force steer gradient, c_{iSFS}, is defined for an axle and it is how much the wheels on an axle steers [deg] per lateral force [N]. Also a non-steered axle steers due to side force steering, which depends on the compliance of the suspension bushings.

It can be modelled as an extra compliance, with the constitutional equations: $F_{fy} = -c_{fSFS} \cdot \Delta\delta_f$; and $F_{ry} = -c_{rSFS} \cdot \Delta\delta_r$;, where the Δ marks additional steering angle due to the lateral force. These extra compliances comes into play as series connected with the tyre cornering compliances. If we update Equation [4.15] with side force steering it becomes:

$$\delta_f = \frac{L}{R} + K_u \cdot \frac{m \cdot v_x{}^2}{R};$$

$$where\ K_u = \frac{l_r}{C_{f,tot} \cdot L} - \frac{l_f}{C_{r,tot} \cdot L} = \frac{C_{r,tot} \cdot l_r - C_{f,tot} \cdot l_f}{C_{f,tot} \cdot C_{r,tot} \cdot L};$$

$$where\ C_{f,tot} = \frac{1}{\frac{1}{C_f} + \frac{1}{c_{fSFS}}} \quad and \quad C_{r,tot} = \frac{1}{\frac{1}{C_r} + \frac{1}{c_{rSFS}}};$$

[4.26]

4.3.5.5   Roll steer gradient

Roll steer gradient, c_{iRS}, is defined for an axle and it is how much the wheels on an axle steers [deg] per vehicle roll angle [deg]. Also a non-steered axle steers due to roll-steering, which depends on the suspension linkage geometry. The added steering angle can hence be expressed: $\Delta\delta_i = -c_{iRS} \cdot \varphi_x$;

If one assumes steady state cornering, the vehicle roll angle depends on the vehicle's roll gradient, c_{roll} as: $\varphi_x = c_{roll} \cdot a_y$;.For steady state, it is also possible to express $F_{iy} = m \cdot a_y \cdot (L - l_f)/L$;. In total: $\Delta\delta_i = -c_{iRS} \cdot c_{roll} \cdot F_{iy} \cdot L/\big(m \cdot (L - l_f)\big) = -c_{iRS,F} \cdot F_{iy}$;. The parameter $c_{iRS,F}$ comes into the equations in exactly the same way as side force steering gradient, c_{iSFS}, so:

$$\delta_f = \frac{L}{R} + K_u \cdot \frac{m \cdot v_x^2}{R};$$

$$where \ K_u = \frac{l_r}{C_{f,tot} \cdot L} - \frac{l_f}{C_{r,tot} \cdot L} = \frac{C_{r,tot} \cdot l_r - C_{f,tot} \cdot l_f}{C_{f,tot} \cdot C_{r,tot} \cdot L};$$

$$where \ C_{f,tot} = \frac{1}{\frac{1}{C_f} + \frac{1}{c_{fRS,F}}} \quad and \quad C_{r,tot} = \frac{1}{\frac{1}{C_r} + \frac{1}{c_{rRS,F}}};$$

[4.27]

Side force steering and roll-steering are very similar. Side force steering does not require a roll angle change, so side-force steering has basically no delay (or at least same magnitude of delay as the tyre cornering forces). However, roll-steering requires that sprung body changes roll angle which takes significantly longer time, typically roll eigen-frequency for a passenger vehicle is around 1.5 Hz. Roll-steering also come into play for one-sided road unevenness, i.e. also without cornering.

Side force steering and roll-steering compliances often represent a significant part of the front axle cornering compliance, e.g. 20-50% on a passenger car.

4.3.5.6 Camber steer

Negative camber (wheel top leaning inwards) increases the cornering stiffness. One explanation to this is that curve outer wheel gets more vertical load than the curve inner wheel. Hence, the inwards directed camber force from outer wheel dominates over outwards directed camber force from the inner wheel. Negative camber is often used at rear axle at passenger cars. Drawback with non-zero camber is tyre wear.

4.3.5.7 Toe angle

Toe has some, but limited effect on an axles cornering stiffness. Non-zero toe increases tyre wear. Toe-angle: When rolling ahead, tyre side forces pre-tension bushes.

If toe (=toe-in) is positive there are tyre-lateral forces on each tyre already when driving straight ahead, even if left and right cancel out each other: $F_{ay} = \left(C_{left} - C_{right}\right) \cdot \frac{toe}{2} = 0;$. Then, if the axle takes a side force, the vertical load of the wheels are shifted between left and right wheel, which also changes the tyre cornering stiffnesses. The outer wheel will get more cornering stiffness. Due to positive toe, it will also have the largest steering angle. So, the axle will generate larger lateral force than with zero toe. For steady-state cornering vehicle models, this effect comes in as an increased axle cornering stiffness, i.e. a linear effect.

4.3.5.8 Wheel Torque effects

Wheel torque give tyre longitudinal force, directed as the wheel is pointing. If the wheel is steered, the wheel longitudinal forces can influence the yaw balance, see also Ffxw in Equation [4.15].

Unsymmetrical wheel torques (left/right) will give a **direct yaw moment** in the yaw equilibrium in Equation [4.12]. The actuated yaw moment around CoG is then of the magnitude of wheel longitudinal wheel force times half the track width. ESC and Torque vectoring interventions have such effects.

High longitudinal utilization of friction on an axle leads to that lateral grip is reduced on that axle. The changed yaw moment, compared to what one would have without using friction longitudinally, can be called an **indirect yaw moment**. The actuated change in yaw moment around CoG is then of the magnitude of change in wheel lateral wheel force times half the wheel base. It influences the yaw balance. That is the reason why a front axle driven vehicle may be more understeered than a rear axle driven one. On the other hand, the wheel-longitudinal propulsion force on the front axle does also help the turn-in, which acts towards less understeering.

4.3.5.9   Transient vehicle motion effects on yaw balance

The effects presented here are not so relevant for steady state understeering coefficient. However, they affect the yaw balance in a more general sense, why it is relevant to list them in this section.

- Longitudinal load transfer changes normal forces. E.g. strong deceleration by wheel forces helps against under-steering, since front axle gets more normal load. This effect has some delay. Also, it vanishes after the transient.
  (This effect can be compared with the effect described in Section 4.3.5.2, which is caused by tyre cornering stiffness varying degressively with vertical load, while the longitudinal load transfer effect can be explained solely with the proportional variation.)
- Change of longitudinal speed helps later in manoeuvre. E.g. deceleration early in a manoeuvre makes the vehicle easier to manoeuvre later in the manoeuvre. It is the effect of the term $\omega_z \cdot v_x$ that is reduced.

4.3.5.10   Some other design aspects

High cornering stiffness is generally desired for controllability.

Longer wheel base (with unchanged yaw inertia and unchanged steering ratio) improves the transient manoeuvrability, because the lateral forces have larger levers to generate yaw moment with.

4.3.6   Steady state cornering gains *

*Function definition: **Steady state cornering gains** are the amplification from steering angle to certain vehicle response measures for steady state cornering at a certain longitudinal speed.*

From Equation [4.15], we can derive some interesting ratios. We put steering angle in the denominator, so that we get a gain, in the sense that the ratio describes how much of something we get "per steering angle". If we assume $F_{fxw} = 0$, we get Equation [4.28].

Yaw rate gain $=$

$$\frac{\omega_z}{\delta_f} = \left\{ use: \frac{\omega_z}{v_x} \approx \frac{1}{R} \right\} \approx \frac{v_x/R}{\frac{L}{R} + K_u \cdot \frac{m \cdot v_x^2}{R}} = \frac{v_x}{L + K_u \cdot m \cdot v_x^2};$$

Curvature gain $=$

$$= \frac{\kappa}{\delta_f} = \frac{1/R}{\delta_f} = \frac{1/R}{\frac{L}{R} + K_u \cdot \frac{m \cdot v_x^2}{R}} = \frac{1}{L + K_u \cdot m \cdot v_x^2};$$

Lateral acceleration gain $=$

$$= \frac{a_y}{\delta_f} = \left\{ \begin{array}{l} use: \\ a_y = \omega_z \cdot v_x; \\ and\ \frac{\omega_z}{v_x} \approx \frac{1}{R}; \end{array} \right\} \approx \frac{\frac{v_x^2}{R}}{\frac{L}{R} + K_u \cdot \frac{m \cdot v_x^2}{R}} = \frac{v_x^2}{L + K_u \cdot m \cdot v_x^2};$$

[4.28]

Yaw rate gain is also derived for $F_{fxw} \neq 0$, and then we get Equation [4.29].

With F_{fxw} taken into account: **Yaw rate gain** $=$

$$= \frac{\omega_z}{\delta_f} = \frac{C_f \cdot C_r \cdot L + (C_r \cdot l_f + C_r \cdot l_r) \cdot F_{fxw}}{C_f \cdot C_r \cdot L^2 - (C_f \cdot l_f - C_r \cdot l_r) \cdot m \cdot v_x^2} \cdot v_x$$
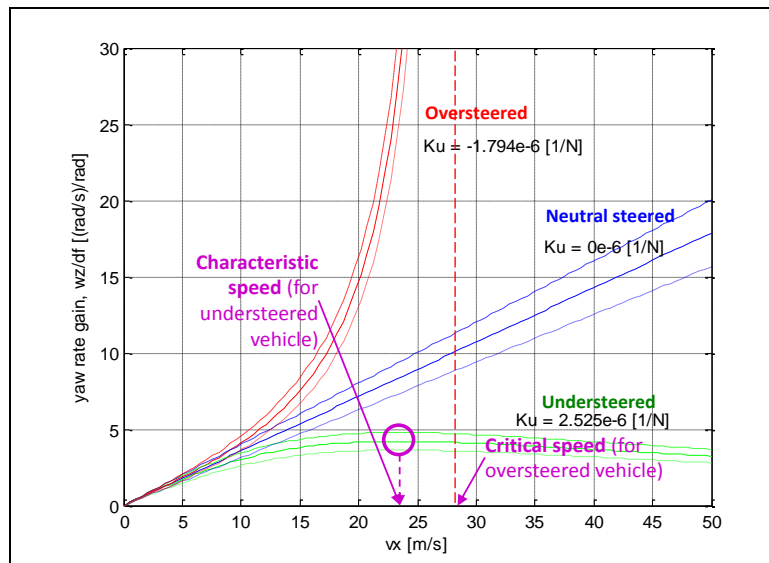
[4.29]

4.3.6.1 Yaw Rate gain

Figure 4-31: Yaw rate gain (ω_z/δ_f) for Steady State Cornering. Each "cluster of 3 curves": Mid curve $F_{fxw} = 0$. Upper $F_{fxw} = +0.25 \cdot F_{fz}$. Lower $F_{fxw} = -0.25 \cdot F_{fz}$.

The yaw rate gain gives us a way to understand Characteristic Speed. Normally one would expect the yaw rate to increase if one increases the speed along a circular path. However, the vehicle will also increase its path radius when speed is increased. At the Characteristic Speed, the increase in radius cancel out the effect of increased speed, so that yaw rate in total decrease with increased speed. One can find the characteristic speed as the speed where one senses or measures the highest value of yaw rate increase for a given steering angle step.

The curves for $F_{fxw} = +0.25 \cdot F_{fz}$ and $F_{fxw} = -0.25 \cdot F_{fz}$ in

Figure 4-31 are generated using the first stages in Eq [4.15], before assuming $F_{fxw} \approx 0$.
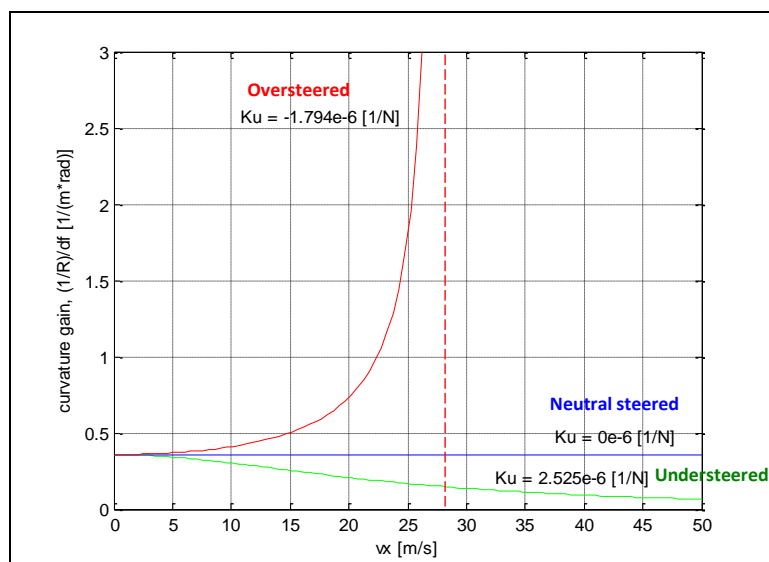
4.3.6.2 Curvature gain

Figure 4-32: Curvature gain ($\frac{1/R}{\delta_f}$) for Steady State Cornering

If driving on a constant path radius, and slowly increase speed from zero, an understeered vehicle will require more and more steering angle ("steer-in"), to stay at the same path radius. For an over-steered vehicle one has to steer less ("open up steering") when increasing the speed.

4.3.6.3 Lateral Acceleration gain

Figure 4-34 shows the lateral acceleration gain as function of vehicle speed. The characteristics speed is once again identified in this diagram, and now as the speed when lateral acceleration gain per longitudinal speed ($(a_y/\delta_f)/v_x$) reaches its highest value. This is an alternative definition of characteristic speed, cf Section 4.3.4.1.
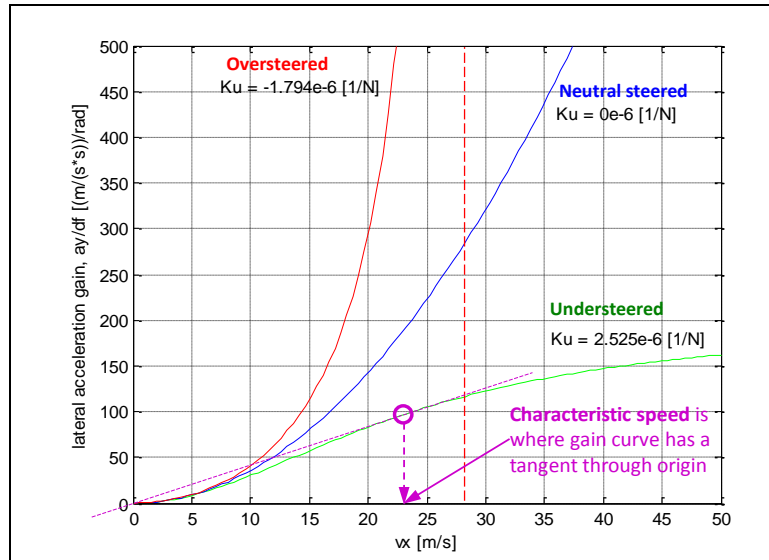

Figure 4-33: Lateral acceleration gain ($\frac{a_y}{\delta_f}$) for Steady State Cornering

From the previous figures the responsiveness of the vehicle can be identified for different understeer gradients. In all cases the vehicle which is understeered is the least responsive of the conditions. Both the yaw rate and lateral acceleration cannot achieve the levels of the neutral steered or over-steered vehicle. The over-steered vehicle is seen to exhibit instability when the critical speed is reached since small changes in the input result in excessive output conditions. In addition, the over-steered vehicle will have a counter-intuitive response for the driver. To maintain a constant radius curve, an increase in speed requires that the driver turns the steering wheel opposite to the direction of desired path. The result of these characteristics leads car manufacturers to produce understeered vehicles that are close to neutral steering to achieve the best stability and driver feedback.

4.3.6.4 Side slip gain as function of speed

All gains above can be found from solving wz from Equation [4.15]. If instead solving the other unknown, vy, we can draw "side slip gain" instead. Equation [4.30] shows the formula for this.

$$\frac{v_y}{v_x \cdot \delta_f} = \frac{C_f \cdot C_r \cdot l_r \cdot L - C_f \cdot l_f \cdot m \cdot v_x{}^2}{C_f \cdot C_r \cdot L^2 - (C_f \cdot l_f - C_r \cdot l_r) \cdot m \cdot v_x{}^2} \qquad [4.30]$$

It is not solely the understeering gradient that sets the curve shape, but we can still plot for the some realistic numerical data, which are under-, neutral and over-steered, see Figure 4-34.

All cases in Figure 4-34 goes from positive side slip to negative when speed increases. This is the same as we expected already in Figure 4-23.
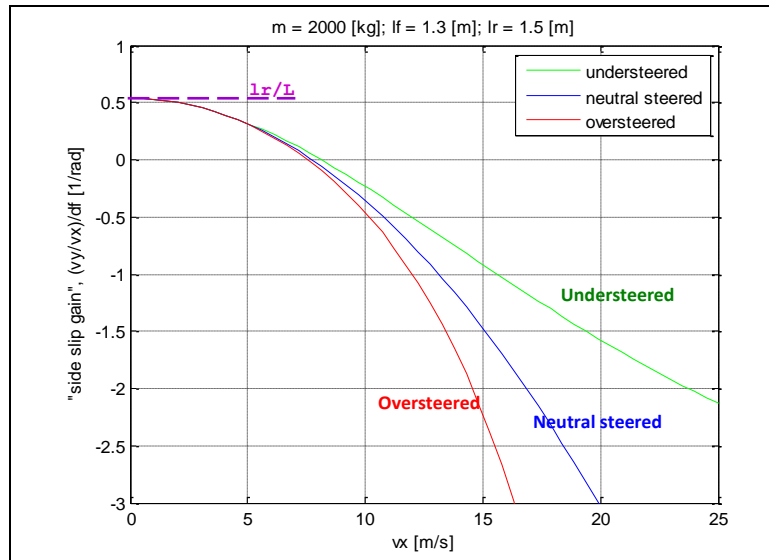
Figure 4-34: "Side slip gain" ($\frac{v_y}{v_x \cdot \delta_f}$) for Steady State Cornering.

4.3.7 Manoeuvrability and Stability

The overall conclusion of previous section is that all gains become higher the more over-steered (or less understeered) the vehicle is. Higher gains are generally experienced as a sportier vehicle and it also improves safety because it improves the manoeuvrability. A higher manoeuvrability makes it easier for the driver to do avoidance manoeuvres. This would motivate a design for low understeering gradient.

However, there is also the effect that a vehicle with too small understeer gradient becomes very sensitive to the steering wheel angle input. In extreme, the driver would not be able to control the vehicle. This limits how small the understeering gradient one can design for.

The overall design rule today is to make the understeering as small as possible, but the neutral steer is a limit which cannot be passed.

It is not impossible for a driver to keep an unstable vehicle (Ku<0 and vx>Critical Speed) on an intended path, but it requires an active compensation with steering wheel. If adding support systems, such as yaw damping by steering support or differentiated propulsion torques, it can be even easier. If one could rely on a very high up time for such support systems, one could move today's trade-off between manoeuvrability and stability. This conceptual design step has been taken for some airplanes, which actually are designed so that they would be instable without active control.

4.3.8 Handling diagram

This section gives a brief introduction to handling diagram, which is a useful tool for discussing yaw stability during different steady state cornering situations, as initiated with Equation [4.20].

There are many frequently used graphical tools or diagrams to represent vehicle characteristics. One is the "handling diagram", which is constructed as follows. Same simplifying assumptions are done as in Figure 4-25, with the exception that we don't assume linear tyre models.

Equilibrium:
$$\left\{ m \cdot \frac{v_x^2}{R} = m \cdot a_y = F_{fy} + F_{ry}; \quad 0 = F_{fy} \cdot l_f - F_{ry} \cdot l_r; \right\} \Rightarrow F_{fy} = \frac{l_r}{L} \cdot m \cdot a_y; \; F_{ry} = \frac{l_f}{L} \cdot m \cdot a_y$$

Constitution:
$$F_{fy} = F_{fy}(\alpha_f) \Rightarrow \alpha_f = F_{fy}^{-1}(F_{fy}); \quad F_{ry} = F_{ry}(\alpha_r) \Rightarrow \alpha_r = F_{ry}^{-1}(F_{ry});$$

Solving for $\alpha_f - \alpha_r$ yields:

$$\alpha_r - \alpha_f = F_{ry}{}^{-1}(F_{ry}) - F_{fy}{}^{-1}(F_{fy}) = F_{ry}{}^{-1}\left(\frac{l_f}{L} \cdot m \cdot a_y\right) - F_{fy}{}^{-1}\left(\frac{l_r}{L} \cdot m \cdot a_y\right);$$

So, we can plot $\alpha_r - \alpha_f$ as function of a_y. This relation is interesting because compatibility ($\delta_f + \alpha_f - \alpha_r = L/R$;) yields $\alpha_r - \alpha_f = \delta_f - L/R = \delta_f - \delta_A$. And $\delta_f - \delta_A$ is connected to one of the understandings of K_u in Equation [4.20], ($K_u = \frac{\partial}{\partial a_y}(\delta_f - \delta_A)$;). If we plot $\alpha_r - \alpha_f = \delta_f - \delta_A$ on abscissa axis and a_y on ordinate axis, we get the most common way of drawing the handling diagram, see Figure 4-35. The axle's constitutive relations can be used as graphical support to construct the diagram, but then the constitutive relations should be plotted as: $a_{yi}(\alpha_i) = \frac{L}{L - l_i} \cdot \frac{1}{m} \cdot F_{iy}(\alpha_i)$;. The quantity a_{yi} can be seen as the lateral force on the axle, but scaled so that both axles' values correspond to the same vehicle lateral acceleration.

Figure 4-35 shows the construction of a handling diagram from axle slip characteristics. Figure 4-36 show examples of handling diagrams constructed via tests with simulation tools. Handling diagrams can be designed from real vehicle tests as well. The slope in the handling diagram corresponds to understeering gradient K_{u3} in Equation [4.18].
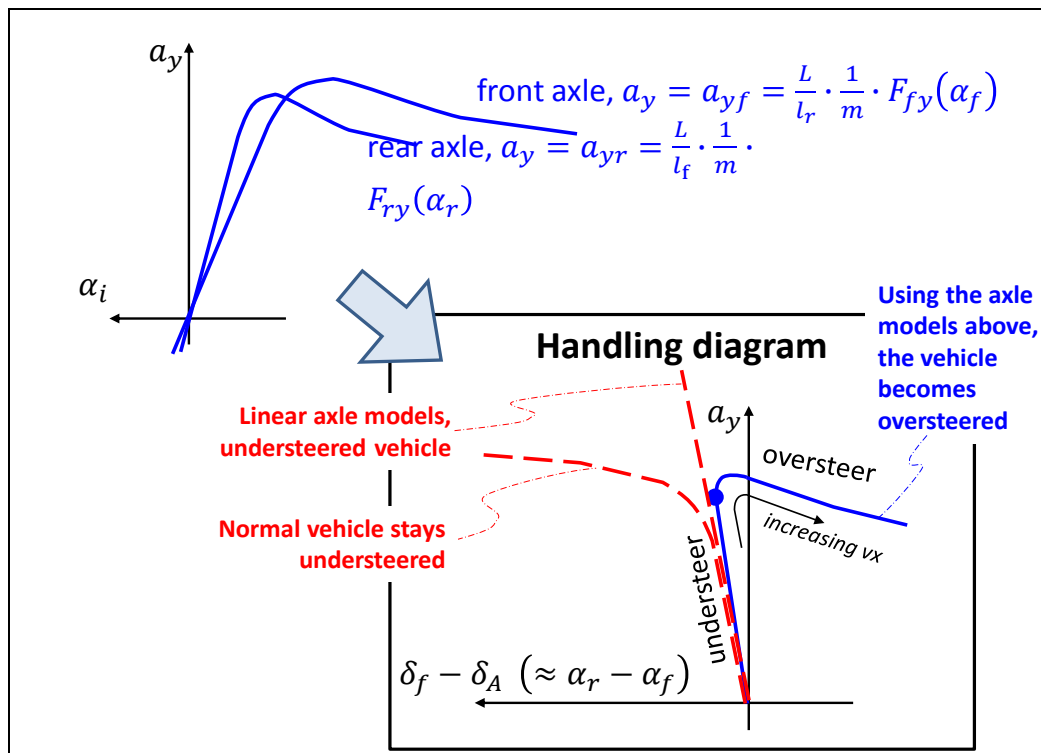

Figure 4-35: Construction of the "Handling diagram". The axle's slip characteristics (solid) are chosen so that vehicle transits from understeer to over-steer with increased longitudinal speed, vx. The dashed shows two other examples.
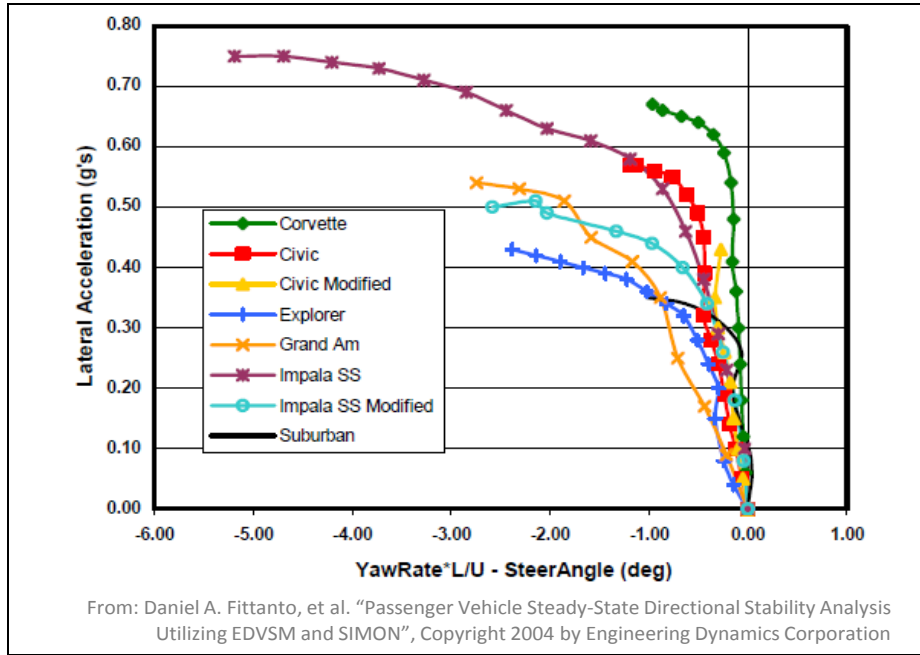
Figure 4-36: Example of handling diagram.

Using a one-track model of a two axle vehicle, there is one unique such curve as drawn in Figure 4-35. However, from a more advanced model, a vehicle with non-Ackermann steering or a real test or an articulated vehicle, there are different curves. This is so because a certain lateral acceleration can be reached in different ways. For instance, the sweep along the lateral acceleration axis can be made by driving at a constant radius with increasing speed (R-handling diagram) or driving with constant speed on a decreasing radius (V-handling diagram). An R-handling diagram can be drawn for each combination of vehicle and radius, so that in one diagram one can often see several curves which are for different radii. These diagrams are often seen for heavy trucks with several non-steered axles. With data according to Section 4.2.11 and $C_r = 2 \cdot C_{r1} = 2 \cdot C_{r2}$; one can derive different handling curves for different v_x:

$$\delta = \frac{L}{R} + K_u \cdot \frac{v_x^2}{R} + \frac{b^2}{L} \cdot \left(1 + \frac{C_r}{C_f}\right) \cdot \frac{1}{R}; \quad K_{u3} = m \cdot \frac{C_r \cdot l_r - C_f \cdot l_f}{C_f \cdot C_r \cdot L};$$

$$\delta = \frac{L}{R} + \left(K_u + \underbrace{\frac{b^2}{L} \cdot \left(1 + \frac{C_r}{C_f}\right) \cdot \frac{1}{v_x^2}}_{influence\ of\ 2\ rear\ axles}\right) \cdot a_y;$$

[4.31]

Alternatively, one can identify an "equivalent wheelbase":

$$\delta = \frac{L}{R} + K_u \cdot \frac{v_x^2}{R} + \frac{b^2}{L} \cdot \left(1 + \frac{C_r}{C_f}\right) \cdot \frac{1}{R} = \underbrace{\left(L + \frac{b^2}{L} \cdot \left(1 + \frac{C_r}{C_f}\right)\right)}_{equivalent\ wheelbase} \cdot \frac{1}{R} + K_u \cdot \frac{v_x^2}{R};$$

[4.32]

4.3.9 Steady state cornering at high speed, with Lateral Load Transfer

In the chapter about longitudinal dynamics we studied (vertical tyre) load transfer between front and rear axle. The corresponding issue for lateral dynamics is load transfer between left and right side of

the vehicle. Within the steady state lateral dynamics, we will cover some of the simpler effects, but save the more complex suspension linkage dependent effects to Sections 4.5.

The relevance to study the load transfer during steady state cornering is to limit the roll during cornering (for comfort) and yaw balance (understeering gradient, see Section 4.3.5.2). Additionally, the load transfer influence the transient handling; see Section 4.4 and Section 4.5.

4.3.9.1   Load transfer between vehicle sides

The total load transfer can be found without involving suspension effects.

Moment equilibrium, around left contact with ground: $\Rightarrow$

$$\Rightarrow m \cdot g \cdot \frac{w}{2} + m \cdot a_y \cdot h - F_{zr} \cdot w = 0 \Rightarrow F_{zr} = m \cdot \left(\frac{g}{2} + a_y \cdot \frac{h}{w}\right);$$

[4.33]

Moment equilibrium, around right contact with ground: $\Rightarrow F_{zl} = m \cdot \left(\frac{g}{2} - a_y \cdot \frac{h}{w}\right);$

These equations confirm what we know from experience, the left side if off-loaded if turning left. Generally, curve inner side is off-loaded.
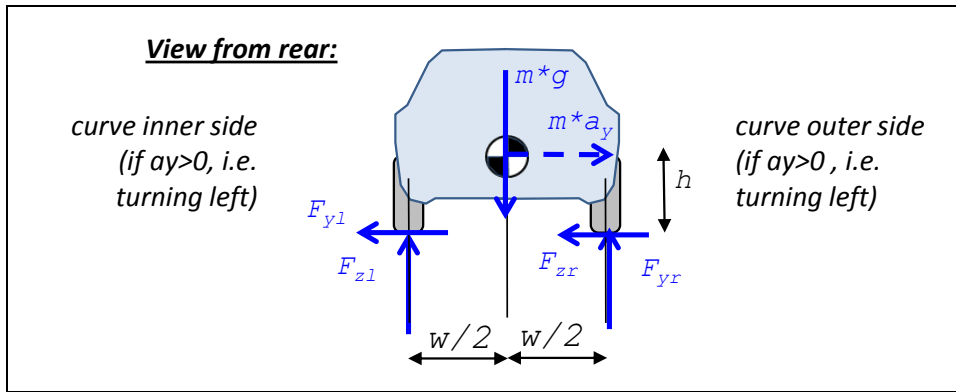

Figure 4-37: Free Body Diagram for cornering vehicle.
The force m*ay is a fictive force. Subscript l and r here means left and right.

4.3.9.2   Body heave and roll due to lateral wheel forces

Now, we shall find out how much the vehicle rolls and heaves during steady state cornering. First, we decide to formulate the model in "effective stiffnesses", in the same manner as for longitudinal load transfer in previous chapter.

There is no damping included in model, because their forces would be zero, since there is no displacement velocity, due to the "quasi-steady-state" assumption. As constitutive equations for the compliances (springs) we assume that displacements are measured from a static conditions and that the compliances are linear. The road is assumed to be smooth, i.e. $z_{lr} = z_{rr} = 0$.

$$F_{zl} = F_{zl0} + c_{side} \cdot (z_{lr} - z_l) + c_{arb} \cdot \left((z_{lr} - z_l) - (z_{rr} - z_r)\right) =$$
$$= \{z_{lr} = z_{rr} = 0\} = F_{zl0} - (c_{side} + c_{arb}) \cdot z_l + c_{arb} \cdot z_r;$$

$$F_{zr} = \cdots = F_{zr0} - (c_{side} + c_{arb}) \cdot z_r + c_{arb} \cdot z_l;$$

$$where \ F_{zl0} + F_{zr0} = m \cdot g; \quad and \quad F_{zl0} \cdot w/2 - F_{zr0} \cdot w/2 = 0;$$

[4.34]

The stiffnesses c_{side} and c_{arb} are effective stiffnesses as measurable under the wheels. The physical springs are mounted inside in some kind of linkage and have different stiffness values, but their effect is captured in the effective stiffnesses. Some examples of different physical spring and linkage design are given in Section 4.3.9.4.
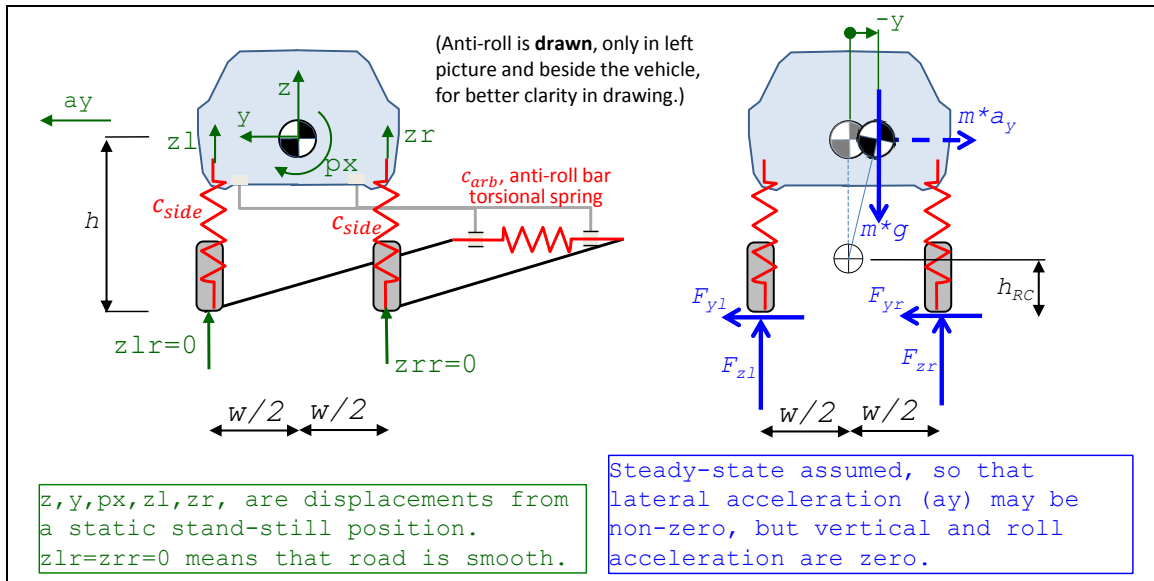
Figure 4-38: Model for steady state heave and roll due to lateral acceleration. Suspension model is no linkage (or "trivial linkage") and without difference front and rear.

We see already in free-body diagram that F_{yl} and F_{yr} always act together, so we rename $F_{yl} + F_{yr} = F_y$. This and equilibrium gives:

$$\begin{aligned} &F_y - m \cdot a_y = 0; \\ &m \cdot g - F_{zl} - F_{zr} = 0; \\ &F_{zl} \cdot (w/2) - F_{zr} \cdot (w/2) + F_y \cdot h + m \cdot g \cdot (-y) = 0; \end{aligned}$$

[4.35]

The term $m \cdot g \cdot (-y)$ is taken into account, but not corresponding for $m \cdot a_y$, since symmetry of the vehicle motivates that the roll takes place around a point on the vertical symmetry axis. Therefore y is significant but corresponding displacement in vertical direction is not. If we assume a height for the point where the roll takes place, h_{RC} ,we can expressed $-y = (h - h_{RC}) \cdot p_x$. We don't know the value of it, until below where we study the suspension design, but it can be mentioned already here that most vehicles have an $h_{RC} \ll h$. This causes a significant "pendulum effect", especially for heavy trucks.

Compatibility, to introduce body displacements, z and px, gives:

$$z_l = z + (w/2) \cdot p_x; \quad and \quad z_r = z - (w/2) \cdot p_x;$$

[4.36]

Combining constitutive relations, equilibrium and compatibility, gives, as Matlab script:

```
clear, syms zl zr Fzl Fzr Fzl0 Fzr0 Fy z px
sol=solve( ...
    'Fzl=Fzl0-(cside+carb)*zl+carb*zr', ...
    'Fzr=Fzr0-(cside+carb)*zr+carb*zl', ...
    'Fzl0+Fzr0=m*g', ...
    'Fzl0*w/2-Fzr0*w/2=0', ...
    'Fy-m*ay=0', ...
    'm*g-Fzl-Fzr=0', ...
    'Fzl*(w/2)-Fzr*(w/2)+Fy*h+m*g*(h-hRC)*px=0', ...
    'zl=z+(w/2)*px', ...
    'zr=z-(w/2)*px', ...
    ' Fzl1=-1/((Fzl/m-g/2)*w/(ay*h))', ...
    zl, zr, Fzl, Fzr, Fzl0, Fzr0, Fy, z, px);
```

[4.37]

The results from the Matlab script in Equation [4.37]:

$$F_y = m \cdot a_y;$$

$$z = 0;$$

$$p_x = \frac{2 \cdot m \cdot a_y \cdot h}{(c_{side} + 2 \cdot c_{arb}) \cdot w^2 - 2 \cdot m \cdot g \cdot (h - h_{RC})};$$

$$F_{zl} = m \cdot \left(\frac{g}{2} - \frac{a_y \cdot h}{w} \cdot \left(\frac{1}{1 - \frac{2 \cdot m \cdot g}{c_{side} + 2 \cdot c_{arb}} \cdot \frac{h - h_{RC}}{w^2}} \right) \right);$$

$$F_{zr} = m \cdot \left(\frac{g}{2} + \frac{a_y \cdot h}{w} \cdot \left(\frac{1}{1 - \frac{2 \cdot m \cdot g}{c_{side} + 2 \cdot c_{arb}} \cdot \frac{h - h_{RC}}{w^2}} \right) \right);$$

[4.38]

In agreement with intuition and experience the body rolls with positive roll when steering to the left (positive F_{yw}). Further, the body centre of gravity is unchanged in heave (vertical motion, z). The formula uses h_{RC} which we cannot estimate without modelling the suspension. Since front and rear axle normally are different, we could expect that h_{RC} is expressed in some similar quantities for each of front and rear axle, which also is the case, see Equation [4.45].

4.3.9.2.1 Steady-state roll-gradient *

Function definition: **Steady state roll-gradient** *is the body roll angle per lateral acceleration for the vehicle during steady state cornering with a certain lateral acceleration and certain path radius on level ground.*

4.3.9.3   Lateral load transfer

For longitudinal load transfer, during purely longitudinal dynamic manoeuvres, the symmetry of the vehicle makes it reasonable to split vertical load on each axle equally between the left and right wheel of the axle. For lateral dynamics it is not very realistic to assume symmetry between front and rear axle. Hence, the suspension has to be considered separately for front and rear axle. The properties that are important to model for each axle is not only left and right elasticity (as we modelled the whole vehicle in Figure 4-38). It is also how the lateral tyre forces are transmitted from road contact patches to the vehicle body. We end up with conceptually the same two possible linkage modelling concepts as we found for longitudinal load transfer, see Figure 3-45. Either we can introduce roll centre heights for each axle (c.f. pitch centre in Section 3.4) or we can introduce the pivot point for each wheel (c.f. axle pivot points in Section 3.4). A difference for lateral load transfer, compared to longitudinal load transfer, is that it is significant also at steady state (due to centrifugal force).

The two modelling ways to include the suspension in the load transfer are shown in Figure 4-39. Generally speaking, they can be combined, so that one is used on front axle and the other on rear axle. However, in this compendium we will not combine, but select one of the concepts to describe.

4.3.9.3.1 Load Transfer model with Wheel Pivot Points

This model will not be deeply presented in this compendium. However, it should be mentioned as having quite a few advantages:

- The model has both heave and roll degree of freedom. (Roll centre model is restricted to roll around roll centre.)
- The model does take the distribution of longitudinal wheel forces between left and right side into account. (Roll centre model only uses the sum of lateral forces per axle.)

Generally spoken, this model is more accurate and not much more computational demanding and probably more easy to intuitively understand. (For non-individual, rigid axles or beam axles, the roll centre model is accurate enough and probably more intuitive.)

Cases when this model is recommended as opposed to the model with roll centres are:

- Steady state and transient manoeuvres where the heave displacement is important.
- When large differences between lateral load on left and right wheels are present, such as:
- Large load transfer, i.e. high CoG and large lateral accelerations. One example is when studying wheel lift and roll-over tendencies.
  - Large differences between longitudinal slip, while axle skids sideways. Then one wheel might have zero lateral force, due to that friction is used up longitudinally, while the other can have a large lateral force.
  - If individual steering within an axle would be studied. One could think of an extreme case if actuating a sudden toe-in or toe-out, which would causes large but counter-directed lateral forces on left and right wheel.
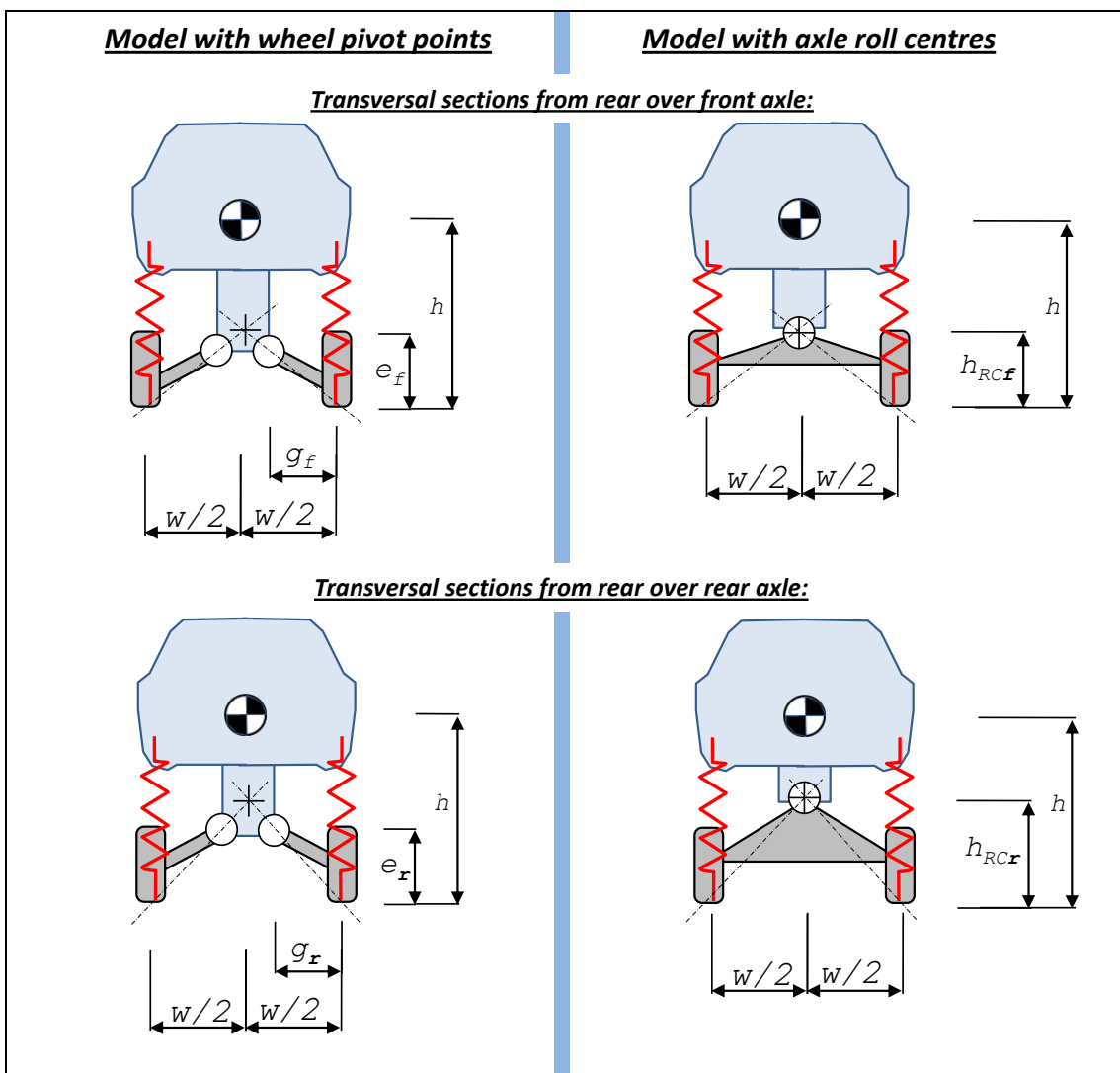

Figure 4-39: Two alternative models for including suspension linkage effects (kinematics) in lateral load transfer. Anti-roll bars not drawn.

4.3.9.3.2 Load Transfer model with Axle Roll Centres

The model with axle roll centres has some drawback as listen before. To mention some advantages, it is somewhat less computational demanding. However, the main reason why using the roll centre

based model in this compendium is that the compendium then cover two different concepts with longitudinal and lateral load transfer.

Behold the free-body diagrams in Figure 4-40. The road is assumed to be flat, $z_{flr} = z_{frr} = z_{rlr} = z_{rrr} = 0$. In free-body diagram for the front axle, Pfz and Pfy are the reaction force in the rear roll-centre. Corresponding reaction forces are found for rear axle. Note that roll centres are free of roll moment, which is the key assumption about roll centres! $F_{sfl}, F_{sfr}, F_{srl}$ and F_{srr} are the forces in the compliances, i.e. where potential spring energy is stored. One can understand the roll-centres as also unable to take vertical force, as opposed to constraining vertical motion (as drawn). Which of vertically force-free or vertically motion-free depends on how one understand the concept or roll-centre, and it does not influence the equations.

Note carefully that the "pendulum effect" is NOT included here, in section 4.3.9.3, as it was in section 4.3.9.2. The motivation is to get simpler equations for educational reasons.
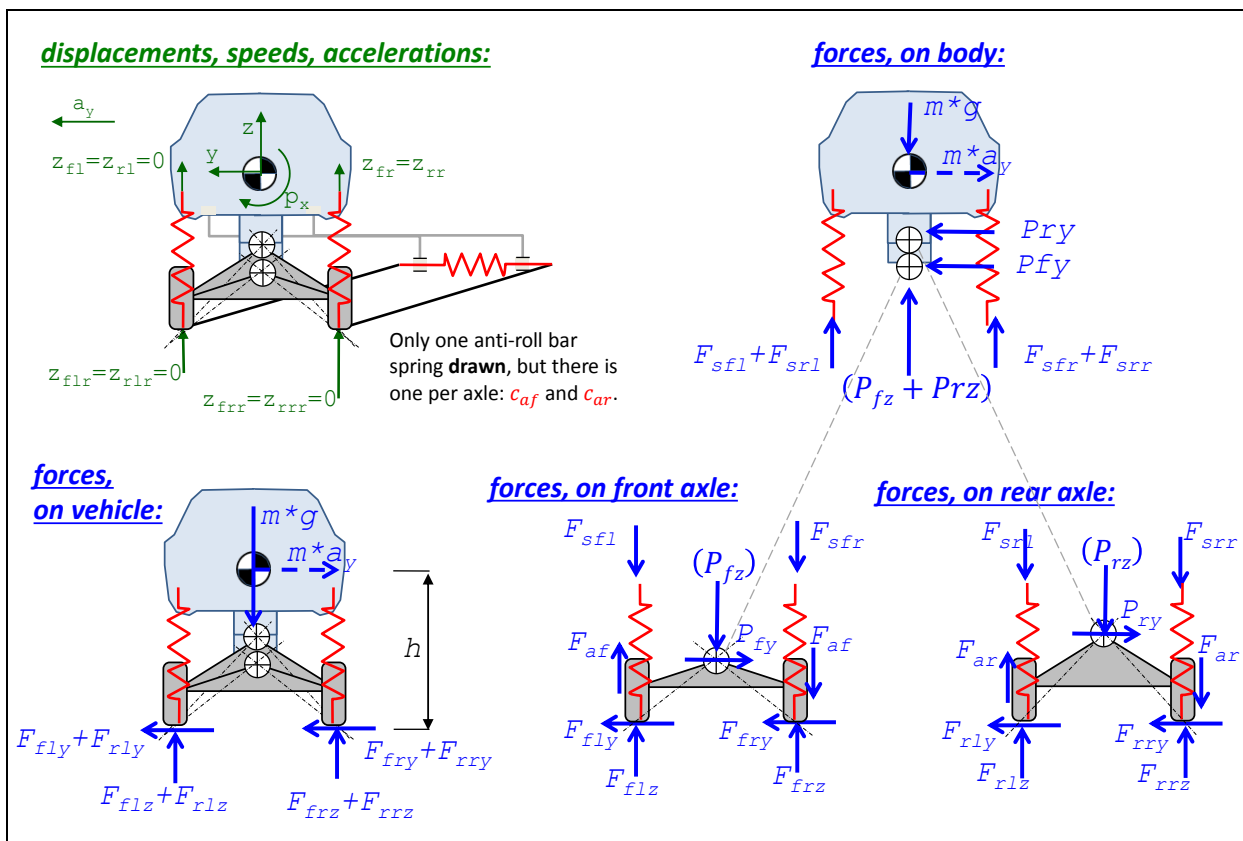

Figure 4-40: Model for steady state heave and roll due to lateral acceleration, using roll centres, which can be different front and rear.

There is no damping included in model, because their forces would be zero, since there is no displacement velocity, due to the steady-state assumption. As constitutive equations for the compliances (springs) we assume that displacements are measured from a static conditions and that the compliances are linear. Note that there are two elasticity types modelled: springs per wheel (c_{fw} per front wheel and c_{rw} per rear wheel) and anti-roll bars per axle (c_{af} front and c_{ar} rear). The road is assumed to be smooth, i.e. $z_{flr} = z_{frr} = z_{rlr} = z_{rrr} = 0$.

$$F_{sfl} = F_{sfl0} + c_{fw} \cdot \left(\cancel{z_{flr}} - z_{fl}\right);$$
$$F_{sfr} = F_{sfr0} + c_{fw} \cdot \left(\cancel{z_{frr}} - z_{fr}\right);$$
$$F_{srl} = F_{srl0} + c_{rw} \cdot \left(\cancel{z_{rlr}} - z_{rl}\right);$$
$$F_{srr} = F_{srr0} + c_{rw} \cdot \left(\cancel{z_{rrr}} - z_{rr}\right);$$
$$F_{af} = 0 + c_{af} \cdot \left(\left(\cancel{z_{flr}} - z_{fl}\right) - \left(\cancel{z_{frr}} - z_{fr}\right)\right);$$
$$F_{ar} = 0 + c_{ar} \cdot \left(\left(\cancel{z_{rlr}} - z_{rl}\right) - \left(\cancel{z_{rrr}} - z_{rr}\right)\right);$$
$$\text{where } F_{sfl0} = F_{sfr0} = \frac{m \cdot g \cdot l_r}{2 \cdot L}; \quad \text{and} \quad F_{srl0} = F_{srr0} = \frac{m \cdot g \cdot l_f}{2 \cdot L};$$

[4.39]

The stiffnesses $c_{fw}, c_{rw},\ c_{af}$ and c_{ar} are the effective stiffnesses per wheel. We see already in free-body diagram that F_{fly} and F_{fry} always act together, so we rename $F_{fly} + F_{fry} = F_{fy}$ and $F_{rly} + F_{rry} = F_{ry}$.

Equilibrium for whole vehicle (vertical, lateral, yaw, pitch, roll):

$$F_{flz} + F_{frz} + F_{rlz} + F_{rrz} = m \cdot g;$$
$$m \cdot a_y = F_{fy} + F_{ry};$$
$$0 = F_{fy} \cdot l_f - F_{ry} \cdot l_r;$$
$$-\left(F_{flz} + F_{frz}\right) \cdot l_f + \left(F_{rlz} + F_{rrz}\right) \cdot l_r = 0;$$
$$\left(F_{flz} + F_{rlz}\right) \cdot \frac{w}{2} - \left(F_{frz} + F_{rrz}\right) \cdot \frac{w}{2} + \left(F_{fy} + F_{ry}\right) \cdot h = 0;$$

[4.40]

Equilibrium for each axle (roll, around roll centre):

$$\left(F_{flz} - F_{sfl} + F_{af}\right) \cdot \frac{w}{2} - \left(F_{frz} - F_{sfr} - F_{af}\right) \cdot \frac{w}{2} + F_{fy} \cdot h_{RCf} = 0;$$
$$\left(F_{rlz} - F_{srl} + F_{ar}\right) \cdot \frac{w}{2} - \left(F_{rrz} - F_{srr} - F_{ar}\right) \cdot \frac{w}{2} + F_{ry} \cdot h_{RCr} = 0;$$

[4.41]

Compatibility, to introduce body displacements, z, px and py, gives:

$$z_{fl} = z + \frac{w}{2} \cdot p_x - l_f \cdot p_y; \quad \text{and} \quad z_{fr} = z - \frac{w}{2} \cdot p_x - l_f \cdot p_y;$$
$$z_{rl} = z + \frac{w}{2} \cdot p_x + l_r \cdot p_y; \quad \text{and } z_{rr} = z - \frac{w}{2} \cdot p_x + l_r \cdot p_y;$$
$$z_{fl} + z_{fr} = 0; \quad \text{and} \quad z_{rl} + z_{rr} = 0;$$

[4.42]

The measure Δh is redundant and can be connected to the other geometry measures as follows. The geometrical interpretation is given in Figure 4-41.

$$\Delta h = h - \frac{l_r \cdot h_{RCf} + l_f \cdot h_{RCr}}{L};$$

[4.43]

Combining Equations [4.39] to [4.43] gives, as Matlab script and solution:

```
clear, syms zfl zfr zrl zrr Fflz Ffrz Frlz Frrz Fsfl Fsfr Fsrl
Fsrr Faf Far Fsfl0 Fsfr0 Fsrl0 Fsrr0 Ffy Fry z px py h
sol=solve( ...
    'Fsfl=Fsfl0-cfw*zfl', ...
    'Fsfr=Fsfr0-cfw*zfr', ...
    'Fsrl=Fsrl0-crw*zrl', ...
    'Fsrr=Fsrr0-crw*zrr', ...
    'Faf=0-caf*(-zfl+zfr)', ...
    'Far=0-car*(-zrl+zrr)', ...
      'Fsfl0=(1/2)*m*g*lr/L', ...
      'Fsfr0=(1/2)*m*g*lr/L', ...
      'Fsrl0=(1/2)*m*g*lf/L', ...
      'Fsrr0=(1/2)*m*g*lf/L', ...
    'Fflz+Ffrz+Frlz+Frrz=m*g', ...
    'm*ay=Ffy+Fry', ...
    '0=Ffy*lf-Fry*lr', ...
    '-(Fflz+Ffrz)*lf+(Frlz+Frrz)*lr=0', ...
    '(Fflz+Frlz)*w/2-(Ffrz+Frrz)*w/2+(Ffy+Fry)*h=0', ...
      '(Fflz-Fsfl+Faf)*w/2-(Ffrz-Fsfr-Faf)*w/2+Ffy*hRCf=0', ...
      '(Frlz-Fsrl+Far)*w/2-(Frrz-Fsrr-Far)*w/2+Fry*hRCr=0', ...
    'zfl=z+(w/2)*px-lf*py', ...
    'zfr=z-(w/2)*px-lf*py', ...
    'zrl=z+(w/2)*px+lr*py', ...
    'zrr=z-(w/2)*px+lr*py', ...
      'zfl+zfr=0', ...
      'zrl+zrr=0', ...
    'dh=h-(lr*hRCf+lf*hRCr)/(lf+lr)', ...
    zfl,   zfr,  zrl,   zrr, ...
    Fsfl,  Fsfr,  Fsrl,  Fsrr, Faf, Far, ...
    Fsfl0, Fsfr0, Fsrl0, Fsrr0, ...
    Fflz,  Ffrz,  Frlz,  Frrz, ...
    Ffy, Fry, z, px, py, h);
```

[4.44]

The result from the Matlab script in Equation [4.44], but in a prettier writing format:

$$F_{fy} = m \cdot a_y \cdot \frac{l_r}{L}; \quad and \quad F_{ry} = m \cdot a_y \cdot \frac{l_f}{L};;$$

$$z = 0; \quad and \quad p_x = \frac{m \cdot a_y \cdot \Delta h}{c_{vehicle,roll}} = \frac{(F_{fy} + F_{ry}) \cdot \Delta h}{c_{vehicle,roll}}; \quad and \quad p_y = 0;$$

$$F_{flz} = m \cdot \left(\frac{g \cdot l_r}{2 \cdot L} - a_y \cdot \left(\frac{h_{RCf} \cdot l_r}{L \cdot w} + \frac{\Delta h}{w} \cdot \frac{c_{f,roll}}{c_{vehicle,roll}} \right) \right);$$

$$F_{frz} = m \cdot \left(\frac{g \cdot l_r}{2 \cdot L} + a_y \cdot \left(\frac{h_{RCf} \cdot l_r}{L \cdot w} + \frac{\Delta h}{w} \cdot \frac{c_{f,roll}}{c_{vehicle,roll}} \right) \right);$$

$$F_{rlz} = m \cdot \left(\frac{g \cdot l_f}{2 \cdot L} - a_y \cdot \left(\frac{h_{RCr} \cdot l_f}{L \cdot w} + \frac{\Delta h}{w} \cdot \frac{c_{r,roll}}{c_{vehicle,roll}} \right) \right);$$

$$F_{rrz} = m \cdot \left(\frac{g \cdot l_f}{2 \cdot L} + a_y \cdot \left(\frac{h_{RCr} \cdot l_f}{L \cdot w} + \frac{\Delta h}{w} \cdot \frac{c_{r,roll}}{c_{vehicle,roll}} \right) \right);$$

[4.45]

where, roll stiffnesses in [moment/angle], are:

$$c_{f,roll} = 2 \cdot (c_{fw} + 2 \cdot c_{af}) \cdot \left(\frac{w}{2}\right)^2 \quad \left[\frac{Nm}{rad}\right];$$

$$c_{r,roll} = 2 \cdot (c_{rw} + 2 \cdot c_{ar}) \cdot \left(\frac{w}{2}\right)^2 \quad \left[\frac{Nm}{rad}\right];$$

$$c_{vehicle,roll} = c_{f,roll} + c_{r,roll} \quad \left[\frac{Nm}{rad}\right];$$

The axle roll stiffnesses, $c_{f,roll}$ and $c_{r,roll}$ are identified beside vehicle roll stiffness $c_{vehicle,roll}$. We should compare Equation [4.45] with Equation [4.38]. Equation [4.38] considers the "pendulum

effect", but not the differentiation between front and rear suspension. Equation [4.45] does the opposite.

Assume $h = h_{RC}$ and look at the sum of vertical force on one side, F_{zl} in Equation [4.38]. Compare F_{zl} in Equation [4.38] and $F_{flz} + F_{rlz}$ in Equation [4.45]; the equations agree if:

$$F_{flz} + F_{rlz} = F_{zl} \Rightarrow m \cdot \left(\frac{g}{2} - a_y \cdot \left(\frac{h_{RCf} \cdot l_r + h_{RCr} \cdot l_f}{L \cdot w} + \frac{\Delta h}{w}\right)\right) = m \cdot \left(\frac{g}{2} - a_y \cdot \frac{h}{w}\right) = F_{zl} \Rightarrow$$

$$\Rightarrow \frac{h_{RCf} \cdot l_r + h_{RCr} \cdot l_f}{L \cdot w} + \frac{\Delta h}{w} = \frac{h}{w} \Rightarrow h_{RCf} \cdot l_r + h_{RCr} \cdot l_f = (h - \Delta h) \cdot L;$$

This is exactly in agreement with the definition of the redundant geometric parameter Δh, see Equation [4.43]. This means that a consistent geometric model of the whole model is as drawn in Figure 4-41. Here the artefact roll axis is also defined.
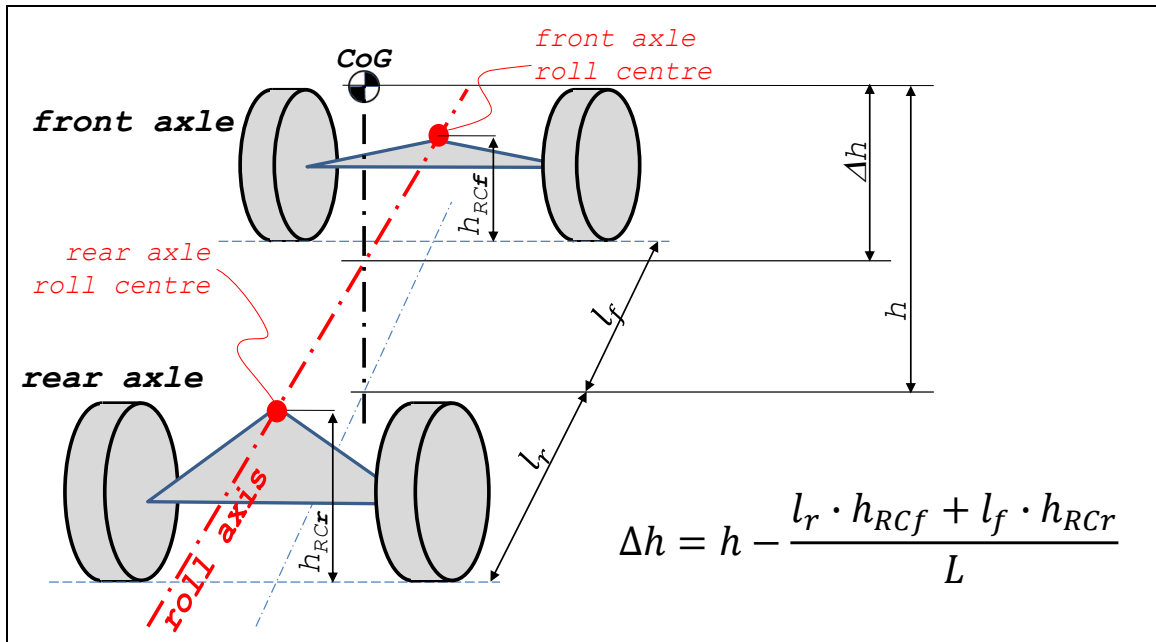
Figure 4-41: Roll axis for a two axle vehicle. (Note that the picture may indicate that the roll centres and roll axis are above wheel centre, but this is normally not the case.)

The terms of type $h_{RCi} \cdot l_j/(L \cdot w)$ in Equation [4.45] can be seen as the part of the lateral tyre forces that goes via the stiff linkage. The terms of type $(\Delta h/w) \cdot \left(c_{iw}/(c_{iw} + c_{jw})\right)$ in Equation [4.45] can be seen as the part of the lateral tyre forces that goes via the compliance. The latter part is distributed in proportion to roll stiffness of the studied axle, as a fraction of the vehicle roll stiffness. This should be in agreement with intuition and experience from other preloaded mechanical systems (load distributes as stiffness).

Body rolls with positive roll when steering to the left, as long as CoG is above roll axle. Further, the body centre of gravity is unchanged in heave (vertical z) because the model does not allow any vertical displacements, which is a drawback already mentioned.

4.3.9.4 Axle suspension system

Suspension design is briefly discussed at these places in this compendium: Section 3.4.7, Section 4.3.9.4 and Section **5.2**.

There are axles with dependent wheel suspensions, which basically look as the roll centre axle model in Figure 4-39 , i.e. that left right wheel are rigidly connected to each other. Then, there are axles with dependent wheel suspensions, which look more like the model with wheel pivot points in Figure 4-39. For these, there are no (rigid) connections between left and right wheel.

Many axles have a so called anti-roll bar, which is a elastic connection between left and right side. It is connected such that if the wheel on one side is lifted, it lifts also the wheel on the other side. Note that, if an anti-roll bar is added to an independent wheel suspension it is still called independent, because the connection is not rigid.

Figure 4-42 and Figure 4-43 show design of two axles with independent wheel suspensions. Figure 4-44 shows an axle with dependent wheel suspension. In all these figures it is shown how to find wheel pivot points and roll centre. In the McPherson suspension in Figure 4-43, one should mention that the strut is designed to take bending moments. For the rigid axle in Figure 4-44, one should mention that the leaf spring itself takes the lateral forces. Symmetry between left and right wheel suspension is a reasonable assumption and it places the roll centre symmetrically between the wheels, which is assumed in the previous models and equations regarding roll centre. (Symmetry is not reasonable to assume for pitch centre.)
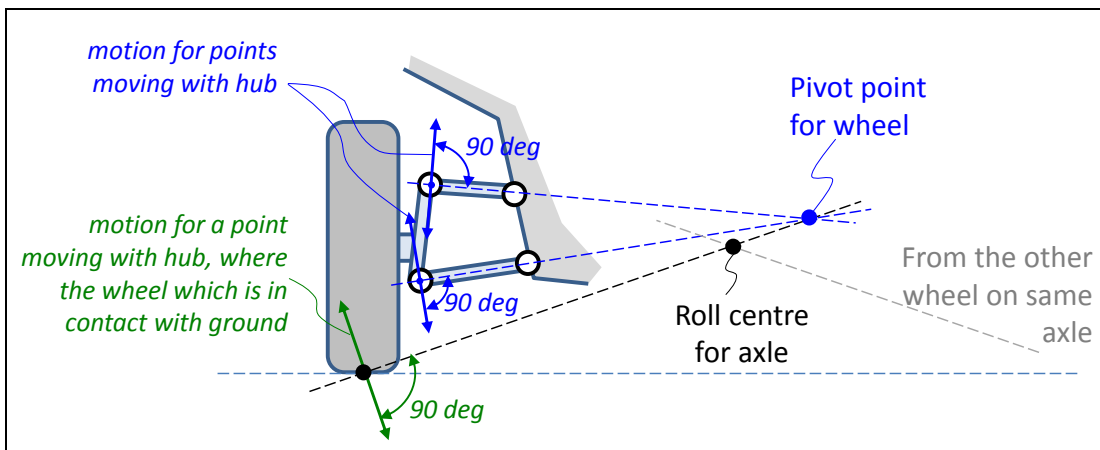
Figure 4-42: Example of how to appoint the pivot point for one wheel and roll centre for axle with double wishbone suspension.
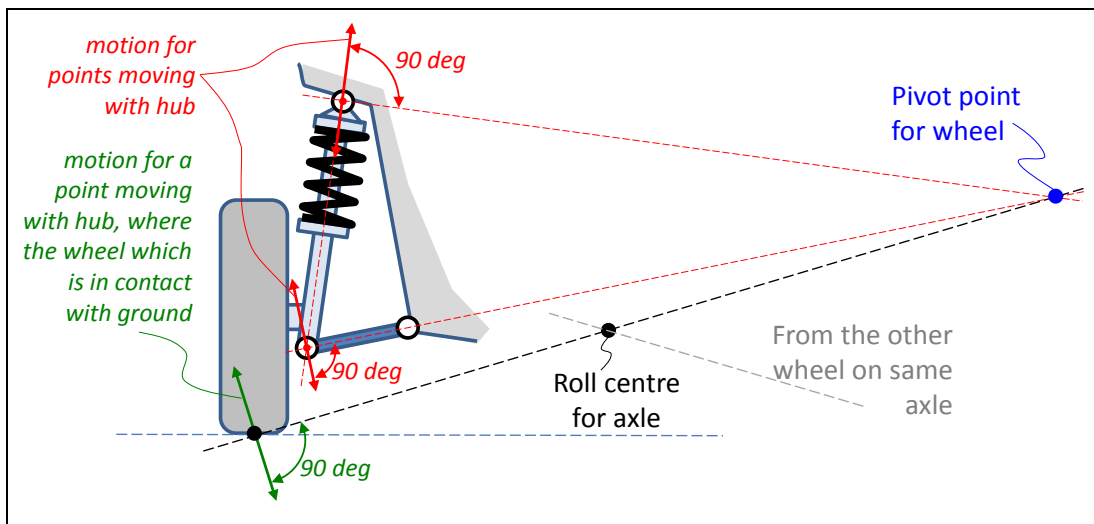

Figure 4-43: Example of how to appoint the pivot point for one wheel and roll centre for axle with double McPherson suspension.

Generally, a "rigid axle" gives roll centre height on approximately the same magnitude as wheel radius, see Figure 4-44. With individual wheel suspension one have much larger flexibility, and typical chosen designs are 30..90 mm front and 90..120 mm rear.
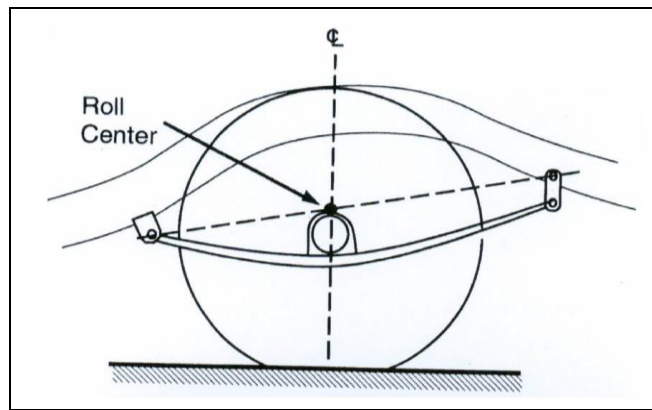
190

Figure 4-44: Example of how to appoint the pivot point for one wheel and roll centre for axle with rigid axle suspended in leaf springs. From (Gillespie, 1992).

The design of roll centre height is a trade-off. On one side, high roll centre is good because it reduces roll in steady state cornering. On the other side, low roll centre height is good because it gives small track width variations due to vehicle heave variations. Track width variations are undesired, e.g. because it makes the left and right tyre lateral force fight against each other, leaving less available friction for longitudinal and lateral grip. Roll centre is normally higher rear than front. One reason for that is that the main inertia axis leans forward, and parallelism between roll axis and main inertia axis is desired.

4.3.10   Steering feel *

Function definition: **Steering feel** *is the steering wheel torque response to steering wheel angle. The function is used in a very wide sense; on a high level, it is a measure of steering wheel torque, or its variation, for certain driving situations. Often, it can only be subjectively assessed.*

At steady state driving at high speed, there are basically three aspects of steering feel:

- Lateral steering feel feedback at cornering. The steering wheel torque is normally desired to increase monotonously with lateral forces on the front axle. This is basically the way the mechanics work due to caster trail. Some specifications on steering assistance system is however needed to keep the steering wheel torque low enough for comfort.
- Steering torque drop when cornering at low-friction. It is built into the mechanics of the caster trail and the pneumatic trail that steering wheel torque drops slightly when one approaches the friction limit on front axle. This is normally a desired behaviour because it gives driver feedback that the vehicles is approach the limits.
- On-centre feel in straight line driving. When the vehicle is driven in straight line, the steering wheel is normally desired to return to centre position after small perturbations. This is a comfort function, which OEMs works a lot with and it is often rather subjectively assessed.

4.3.11   Tracking-ability on straight path*

Function definition: **Tracking-ability on straight path** *is the swept width between outer-most axle centres when driving at a road with certain cross-fall and certain road friction at a certain speed.*

The axles on any vehicle driving at a road with cross-fall will not track exactly in each others trajectories. This is especially pronounced if long vehicles with many articulation points. The driving situation is straight steady state low or high speed.
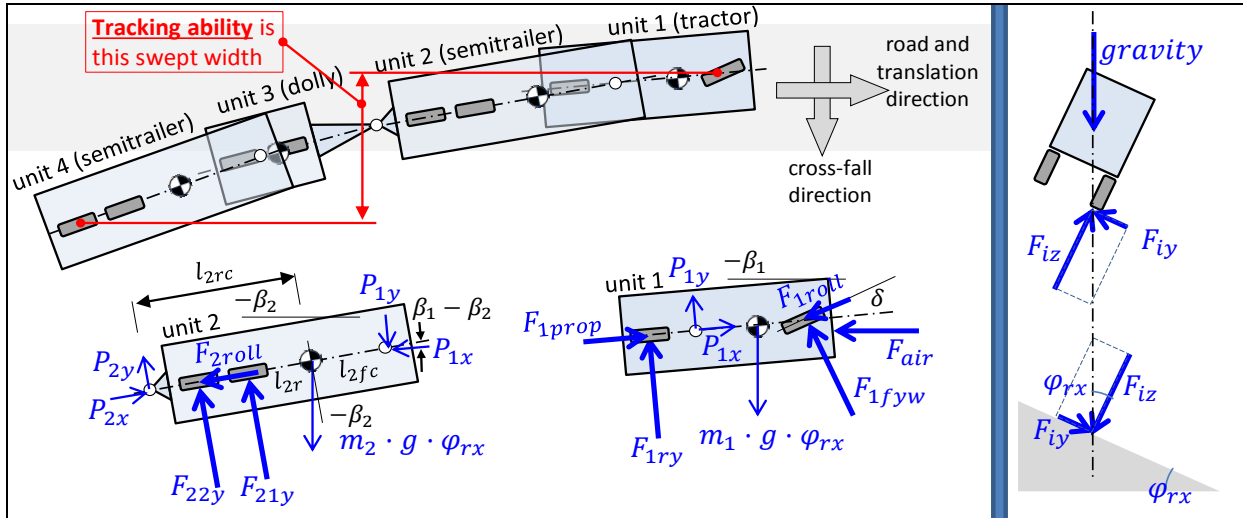
Figure 4-45: Tracking ability on straight path for an "A-double" (Tractor-SemiTrailer-Dolly-SemiTrailer).

An example is seen in Figure 4-45. If we neglect longitudinal forces and combined tyre slip effects, and assume same cornering coefficient, CC, on all axles we can derive these equations:

- $F_{1fyw} = -CC \cdot F_{1fz} \cdot (\beta_1 - \delta)$;
- $F_{1ry} = -CC \cdot F_{1rz} \cdot \beta_1$;
- $F_{iy} = -CC \cdot F_{iz} \cdot \beta_i$; $\quad for\ i = 2..4$

Since the levers for moment equilibria in road x-y-plane and in road x-z-plane are equal, the distribution of the axles' vertical forces and lateral forces becomes identical. So, relation between lateral force and vertical force becomes $\frac{F_{iy}}{F_{iz}} = \tan(\varphi_{rx}) \approx \varphi_{rx}$ for all axles:

- $\varphi_{rx} = -CC \cdot (\beta_1 - \delta)$;
- $\varphi_{rx} = -CC \cdot \beta_i$; $\quad for\ i = 1..4$

Solving for steering angle and side slip angles:

- $\beta_i = -\frac{\varphi_{rx}}{CC} = \beta$; $\quad for\ i = 1..4$;
- $\delta = \beta_1 + \frac{\varphi_{rx}}{CC} = 2 \cdot \frac{\varphi_{rx}}{CC}$;

The swept width becomes: $SweptWidth = \left(l_{1f} + l_{1rc}\right) \cdot \frac{\varphi_{rx}}{CC} + \left(l_{2fc} + l_{2rc}\right) \cdot 2 \cdot \frac{\varphi_{rx}}{CC} + \left(l_{3fc} + l_{3rc}\right) \cdot 3 \cdot \frac{\varphi_{rx}}{CC} + \left(l_{4fc} + l_{4rc}\right) \cdot 4 \cdot \frac{\varphi_{rx}}{CC}$; This can be expressed as:

$$SweptWidth = \frac{\varphi_{rx}}{CC} \cdot \left(\left(l_{1f} + l_{1rc}\right) + \sum_{i=2}^{4} \left(\left(l_{ifc} + l_{irc}\right) \cdot i \right) \right); \qquad [4.46]$$

There is no influence of longitudinal speed. There is influence of cornering coefficient CC but not cornering coefficient C_y.

Model validity assumes that the influence of longitudinal force is small. These will affect via articulation angles and via combined tyre slip effects. So, the model will be less valid if low road friction and if strong up- or downhill.

4.3.12 Roll-over in steady state cornering

When going in curves, the vehicle will have roll angles of typically some degrees. At that level, the roll is a comfort issue. However, there are manoeuvres which can cause the vehicle to roll-over, i.e. roll ≥

90 *deg* so that vehicle body crashes into ground. Roll-over can be seen as a special event, but if sorting into the chapters of this compendium it probably fits best in present chapter, about lateral dynamics.

One can categorize roll-overs in e.g. 3 different types:

- **Tripped roll-over**. This is when the car skids sideways and hits an edge, which causes the roll-over. It can be an uprising edge, e.g. pavement or refuge. It can be the opposite, a ditch or loose gravel outside road. In both these cases, it is strong lateral forces on the wheels on one side of the vehicle that causes the roll-over.
  Tripped roll-over can also be when the vehicle is exposed to large one-sided vertical wheel forces, e.g. by running over a one-sided bump.
  A third variant of tripped roll-over is when the vehicle is hit by another vehicle so hard that it rolls over.
- **Un-tripped roll-over** or on-road roll-overs. These happen on the road and triggered by high tyre lateral forces. This is why they require high road friction. For sedan passenger cars these event are almost impossible, since road friction seldom is higher than approximately 1. For SUVs, un-tripped roll-overs can however occur but require dry asphalt roads, where friction is around 1. For trucks, un-tripped roll-over, can happen already at very moderate friction, like 0.4, due to their high CoG in relation to track width. Within un-tripped roll-overs, one can differ between:
  - **Steady state roll-over**. If lateral acceleration is slowly increased, e.g. as running with into a hairpin curve or a highway exit, the vehicle can slowly lift off the inner wheels and roll-over. This is the only case of roll-over for which a model is given in this compendium.
  - **Transient roll-over**. This is when complex manoeuvres, like double lane changes or sinusoidal steering, are made at high lateral accelerations. This can trigger roll eigen-modes, which can be amplified due to unlucky timing between the turns. Models from Section 4.5 can be used as a start, but it is required that load transfer is modelled carefully and includes wheel lifts, suspension end-stops and bump stops.

4.3.12.1 Roll-over threshold definitions

An overall requirement on a vehicle is that the vehicle should not roll-over for certain manoeuvres. Heavy trucks will be possible to roll-over on high-mu conditions. The requirement for those are based on some manoeuvres which not utilize the full road friction. For passenger cars, it is often the intended design that they should be impossible to roll-over, even at high mu. Any requirement need a definition of what exactly roll-over is, i.e. a Roll over threshold definition. Candidates for Roll over threshold definition are:

- **One wheel** lift from ground
- All wheels on **one side** lift from ground
- Vehicle **CoG** passes its **highest point**

Note that:

- It is the 3rd threshold which really is the limit, but other can still be useful in requirement setting. To use the 3rd for requirement setting makes the verification much more complex, of course in real vehicles but also in simulation.
- The 1st is not a very serious situation for a conventional vehicle with 4 wheels. However, for a 3-wheeled vehicle, such as small "Tuctucs" or a 3-wheel moped, it is still a relevant threshold.
- The 2nd threshold is probably the most useful threshold for two-tracked vehicles, because it defines a condition from which real roll-over is an obvious risk, and still it is relatively easy to test and simulate. For 3-wheeled vehicle, 2nd and 3rd threshold generally coincide. The 2nd threshold will be used in this compendium.

Figure 4-46 shows how the inner wheels lift off subsequently during a slowly increasing lateral force (or lateral acceleration) build-up. Before any wheel is lifted, the load transfer is proportional to roll-

centre heights and roll stiffnesses, as shown in Equation [4.45]. But every time a wheel lifts, the distribution changes, so that a "knee" on the curves appears, see Figure 4-46. So, the relation of type as Equation [4.45] is no longer valid. For instance, it is not physically motivated to keep the roll-centre model for an axle which has lifted one side. So, the prediction of critical lateral acceleration for roll-over is not trivial, especially for heavy vehicles which has many axles, and often also a fifth wheel which can transfer roll-moment to a certain extent. There are approximate standards for how to calculate steady state roll-over thresholds for such vehicle, e.g. UN ECE 111 (http://www.unece.org/fileadmin/DAM/trans/main/wp29/wp29regs/r111e.pdf).
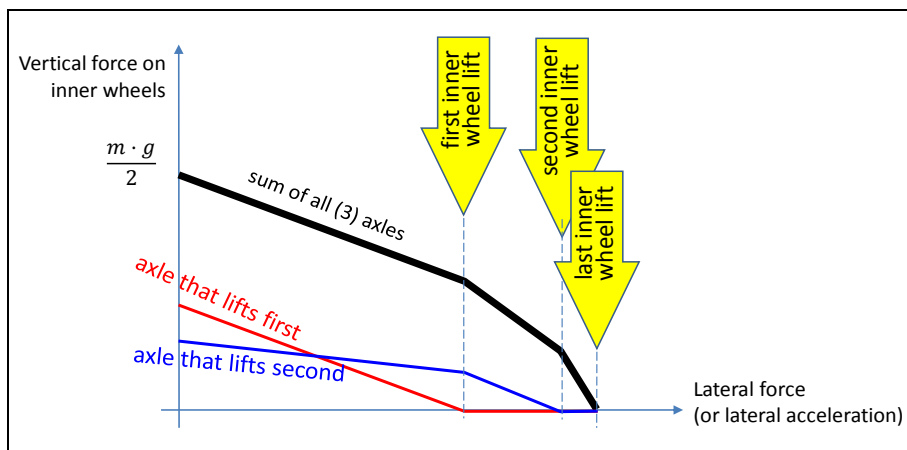
Figure 4-46: Example of 3-axle vehicle steady state roll-over wheel lift diagram.

4.3.12.2 Static Stability Factor, SSF

One very simple measure of the vehicles tendency to roll-over is the Static Stability Factor, SSF. It is proposed by NHTSA, http://www.nhtsa.gov/cars/rules/rulings/roll_resistance/, and it is simply defined as:

$$\text{SSF} = \frac{Half\ TrackWidth}{HeigthOfCoG} = \frac{w/2}{h};$$

[4.47]

A requirement which requires *SSF>number* cannot be directly interpreted in terms of certain manoeuvre and certain roll-over threshold. It is not a *performance based requirement*, but a *design based requirement*. However, one of many possible performance based *interpretations* is that the vehicle shall not roll-over for steady-state cornering on level ground with a certain friction coefficient, using one-sided wheel lift as threshold. Since the requirement is not truly performance based, each interpretation will also stipulate a certain verification method; here it would be theoretical verification using a rigid suspension model. Such model and threshold is shown in Figure 4-47.

The derivation of the SSF based requirement looks as follows:

$$Model: \begin{cases} F_{iz} \cdot w + m \cdot a_y \cdot h = m \cdot g \cdot \dfrac{w}{2}; \\ F_{iz} + F_{oz} = m \cdot g; \\ m \cdot a_y = F_y = \mu \cdot (F_{iz} + F_{oz}); \end{cases} \Rightarrow F_{iz} = m \cdot g \cdot \left(\dfrac{1}{2} - \dfrac{h \cdot \mu}{w}\right); \atop Requirement: F_{iz} \geq 0; \Bigg\} \Rightarrow$$

[4.48]

$$\Rightarrow Requirement: \frac{1}{2} > \frac{h \cdot \mu}{w} \Rightarrow \frac{w}{2 \cdot h} = SSF > \mu;$$

Maximum road friction, μ, is typically 1, which is why SSF>μ=1 would be a reasonable. However, typical values of SSF for passenger vehicles are between 0.95 and 1.5. For heavy trucks, it can be much lower, maybe 0.3..0.5, much depending on how the load is placed. There are objections to use SSF as a

measure, because SSF ignores suspension compliance, handling characteristics, electronic stability control, vehicle shape and structure.
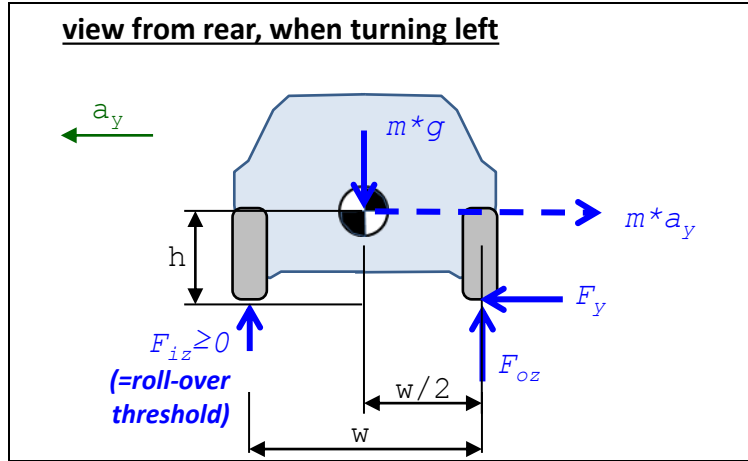

Figure 4-47: Model for verification of requirement based on Static Stability Factor, SSF.

4.3.12.3 Steady-state cornering roll-over *

A function defined for requirement setting can be:

Function definition: **Steady state cornering roll-over acceleration** *is the maximum lateral acceleration the vehicle can take in steady state cornering without lifting all inner wheels. On level ground with enough road friction and certain weight and position of payload.*

For a long combination-vehicle with several articulation points, one often need to drive a long distance after a steering angle change before steady state values on articulation angles are reached. Hence, it can be more relevant to formulate a corresponding roll-over function in terms of curvature to follow, total yaw angle for turn and longitudinal speed. A common way is also the, somewhat artificial, tilt-table test, which means that one measure steady-state roll-over with a (real or virtual) tilt-table where the maximum road pitch angle before wheel lift on one side is the measure to set requirement on.

Consider a roll-stiff vehicle in steady state cornering. Assume lateral acceleration is subsequently increased. If the vehicle is a two-axle vehicle, Eq [4.45] is valid until first axle lifts its inner wheel, since for larger lateral accelerations, the constitutive equation Eq [4.39] is invalid for the inner wheel, since the lifted inner wheel has zero force from ground. We can identify the terms of one of the inner wheel (if $a_y > 0$) equations in Eq Eq [4.45] as follows:

$$F_{flz} = m \cdot \left(\frac{g \cdot l_r}{2 \cdot L} - a_y \cdot \left(\frac{h_{RCf} \cdot l_r}{L \cdot w} + \frac{\Delta h}{w} \cdot \frac{c_{f,roll}}{c_{roll,vehicle}} \right) \right) =$$

$$= \frac{1}{2} \cdot \underbrace{\frac{m \cdot g \cdot l_r}{2 \cdot L}}_{VerticalForceOnAxle} - \underbrace{m \cdot a_y \cdot \frac{l_r}{L}}_{LateralForceOnAxle} \cdot \frac{h_{RCf}}{w} - \underbrace{m \cdot a_y}_{LateralForceOnVehicle} \cdot \frac{\Delta h}{w} \cdot \underbrace{\frac{c_{f,roll}}{c_{roll,vehicle}}}_{RollStiffnessFractionOnAxle} =$$

$$= \frac{F_{iz}}{2} - F_{iy}(a_y) \cdot \frac{h_{RCi}}{w} - F_y(a_y) \cdot \frac{\Delta h}{w} \cdot \frac{c_{i,roll}}{c_{roll,vehicle}};$$

If the vehicle has more axles, Eq [4.45] is generalized to Eq [4.49], which also is valid until first inner wheel lifts from ground.

For axle *i* of a roll-stiff vehicle:

$$F_{ilz} = \frac{F_{iz}}{2} - F_{iy}(a_y) \cdot \frac{h_{RCi}}{w} - F_y(a_y) \cdot \frac{\Delta h_i}{w} \cdot \frac{c_{i,roll}}{c_{roll,vehicle}};$$

[4.49]

For a vehicle with >2 axles, the parameter Δh_i can not be calculated from Eq [4.43], but can still be understood as the vertical distance between roll axis and the axles roll centre. It should be noted that the pendulum effect is **not** included in Eq [4.49], and this is often a significant approximation if applied on high CoG vehicles, like heavy trucks.

4.3.12.3.1   Model assuming all inner wheels lifts at the same lateral acceleration

An approximation of Steady state cornering roll-over acceleration $a_{y,crit}$ (lateral acceleration when all inner wheels lifted) can be found for vehicles where Eq [4.49] gives $F_{ilz} = 0$ for all axles at same a_y. Then, summing the Eq [4.49] for all axles leads to the Eq [4.50] which is the same $a_{y,crit}$ as the simple SSF model in Figure 4-47 and Section 4.3.12.2 gives.

$$a_{y,crit} = \frac{w \cdot g}{2 \cdot h};$$ [4.50]

In the following, we will elaborate with 4 additional effects, which marked in Figure 4-48.

- The tyre will take the vertical load on its **outer edge** in a roll-over situation. This suggests a change of performance and requirement to: $\frac{a_y}{g} < \frac{w+w_{tyre}}{2 \cdot h} > \mu$. This effect is accentuated when low tyre profile and/or high inflation pressure. This effect **decreases** the risk for roll-over.
- Due to suspension and tyre **lateral deformation**, the body will translate laterally outwards, relative to the tyre. This could motivate $\frac{a_y}{g} < \frac{w-Def_y}{2 \cdot h} > \mu$. This effect **increases** the risk for roll-over.
- Due to suspension linkage and compliances, the **body will roll**. Since the CoG height above roll axis, Δh, normally is positive, this could motivate $\frac{a_y}{g} < \frac{w-\Delta h \cdot \varphi_x}{2 \cdot h} > \mu$. This effect **increases** the risk for roll-over. At heavy vehicle this "pendulum effect" is large.
- Due to suspension linkage and compliances, the body will also heave. This requires a suspension model with pivot points per wheel, as opposed to roll-centre per axle, to be taken into account. The heave is normally positive. This could motivate $\frac{a_y}{g} < \frac{w}{2 \cdot (h+z)} > \mu$. The effect is sometimes called "jacking" and it **increases** the risk for roll-over.
- Road leaning left/right (road banking), or driving with one side on a different level (e.g. out-side road or on pavement) also influence the roll-over performance.
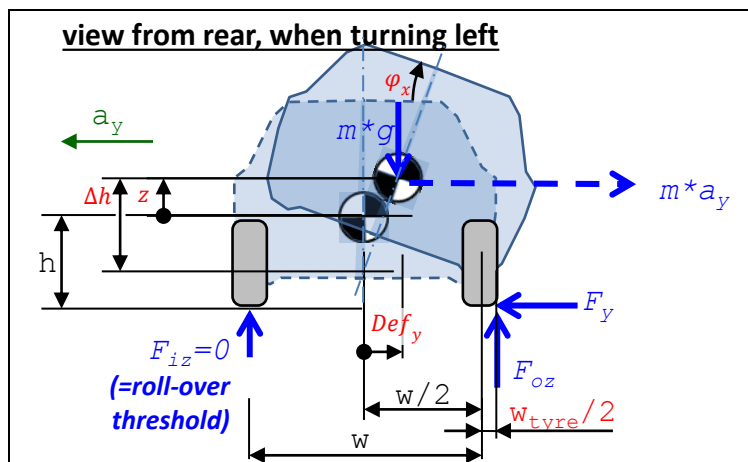

Figure 4-48: Steady-state roll-over model, with fore/aft symmetry. The measures $w_{tyre}, Def_y, \Delta h \cdot \varphi_x$ and z mark effects additional to what is covered with a simple SSF approach.

4.3.12.3.2   Model with subsequent inner wheel lift

A model which does not assume wheel lift at same lateral acceleration will be sketched. For each axle that has lifted, the equations have to be changed. Instead of simply the constitutive equation $(F_{ilz} - F_{irz}) \cdot w/2 = c_{i,roll} \cdot \varphi_x$; one need to assure $F_{ilz} = 0$;. The axle will then position itself so that it

keeps $F_{ilz} + F_{irz} = F_{iz,static}$;. That means both roll and vertical translation of the axle centre, why also the vertical suspension compliance needs to be modelled. A new position variable has to be declared, e.g. the lift distance of the inner wheel, $lift_{ilz}$. This variable is contrained to $lift_{ilz} = 0$; before lift, but after lift the constraint is $F_{ilz} = 0$;. So, the model is suitably implemented as a state event model with the event "*when F_{ilz} becomes < 0*". If a_y is swept from zero and upwards, the result will be something like shown in Figure 4-46.

4.3.12.3.3   Using a transient model for steady-state roll-over

Another work-around to avoid complex algebra is to run a fully transient model, including suspension, and run it until a steady state cornering conditions occur. If then, the lateral acceleration is slowly increased, one can identify when or if the roll-over threshold is reached. Lateral acceleration increase can be through either increase of longitudinal speed or steering angle. It should be noted that the model should reasonably be able to manage at least lift of one wheel from the ground. This way of verifying steady state cornering roll-over requirements has the advantage that, if using tyre models with friction saturation, the limitation discussed in Section 4.3.12.3.2 does not have to be checked separately.

4.3.12.4   Roll-over and understeering/propulsion

With the above formulas for roll-over there will always be a certain lateral acceleration that leads to roll-over, because neither limitation due to road friction nor propulsion power modelled yet. Since vehicles generally are understeered, they are limited to develop lateral acceleration, see Figure 4-33. For propulsion-weak vehicles, there is also the limitation of lateral acceleration due to limited longitudinal speed, which in turn is due to driving resistance from the steered wheels (=wheel lateral force * sin(steering angle)) and loosing propulsion power due to longitudinal wheel slip. However, one should take into account that the propulsion limitation is less in down-hill driving, which increases the roll-over risk again. Also, if the vehicles goes relatively quickly into steady state cornering, the longitudinal speed will not have time to decelerate to its real (longitudinal) steady state value.

For heavy trucks, the critical lateral acceleration is typically 0.3..0.4 g, which is quite possible to reach during normal road conditions, because road friction is there around 1. For passenger cars, the critical lateral acceleration is typically in the region of 1, so it is not obvious that it is possible to reach the roll-over-critical lateral acceleration. This is also the case for heavy trucks on low road friction.

4.4 Stationary oscillating steering

In between steady state and transient manoeuvres, one can identify stationary oscillations as an intermediate step.

Generally, a mechanical system can be excited with a stationary oscillating disturbance. The response of the system is, after possible transients are damped out, a stationary oscillation. If staying within the linear region for the system and the excitation is harmonic (sinus and cosine), the ratio between the response amplitude and the excitation amplitude is only dependent of the frequency. The ratio is called transfer function.

For lateral vehicle dynamics, the excitation is typically steering wheel angle and the response is amplitudes of yaw rate, curvature or lateral acceleration. The corresponding transfer functions are a frequency version of the gains defined in Equation [4.28].

Also, there will be a delay between excitation and response. This is another important measure, beside the amplitude ratio.

4.4.1   Stationary oscillating steering tests

When testing Stationary oscillating steering functions, one usually drives on a longer part of the test track. It might be a high speed track, see Figure 4-8, because one generally need to find the response at

high speeds, rather than driving close to lateral limits. So the track rather needs to be long than wide. If the available Vehicle Dynamics Area, see Figure 4-8, is long enough this can be a safer option. A Vehicle Dynamics Area is a flat surface with typically 100..300 m diameter. It normally has entrance roads for accelerating up to a certain speed.

Typical tests in this part of lateral vehicle dynamics are:

- Sweeping frequency and/or amplitude
- Random frequency and amplitude

There are ISO standards for both these tests. The response will be very dependent of the vehicle longitudinal speed, why the same tests are typically done at different such speeds.

4.4.2 Transient one-track model

The model needed for stationary oscillation is only a linearization of the model needed for fully transient handling, in Section 4.5. However, a rather complete model will be derived already in present section, to capture the physical assumptions in a proper way. (If the reader is satisfied with the linearized model, it can be found directly in Equation [4.56], and a less general derivation of this equation in Figure 4-52.)

The vehicle model is sketched in Figure 4-50. The model is a development of the model for steady state cornering in Figure 4-21, with the following changes:

- Longitudinal and lateral accelerations don't only have the components of centripetal acceleration ($\omega_z \cdot v_y$ and $\omega_z \cdot v_x$), but also the derivatives $\dot{v}_x$ and $\dot{v}_y$:

$$
\begin{aligned}
a_x &= der(v_x) - \omega_z \cdot v_y = \dot{v}_x - \omega_z \cdot v_y; \\
a_y &= der(v_y) + \omega_z \cdot v_x = \dot{v}_y + \omega_z \cdot v_x;
\end{aligned}
$$

[4.52]

- The yaw acceleration, der(wz), is no longer zero.
- The speed vx is no longer defined as a parameter, but a variable. Then, one more prescription is needed to be a consistent model. For this purpose, an equation that sets front axle propulsion torque to 1000 Nm is added.

The difference between acceleration $\vec{a} = [a_x; a_y]$ and [der(vx); der(vy)]=$[\dot{v}_x; \dot{v}_y]$ can be confusing. A way to understand those could be to think of $\vec{a}$ as the (geometric vector) acceleration in the inertial coordinate system and $[\dot{v}_x; \dot{v}_y]$ as a (mathematical) vector, with derivatives of the scalar mathematical variables v_x and v_y, which are the velocities in the vehicle fix (and moving) coordinate system. A graphical derivation of Equation [4.52] is found below, in Figure 4-53.

The model in Figure 4-50 is documented as mathematical model in Equation [4.53]. The equation is given in Modelica format. The subscript v and w refers to vehicle coordinate system and wheel coordinate system, respectively. The model is a development of the model for low-speed in Equation [4.12], with the changes marked with underlined text:
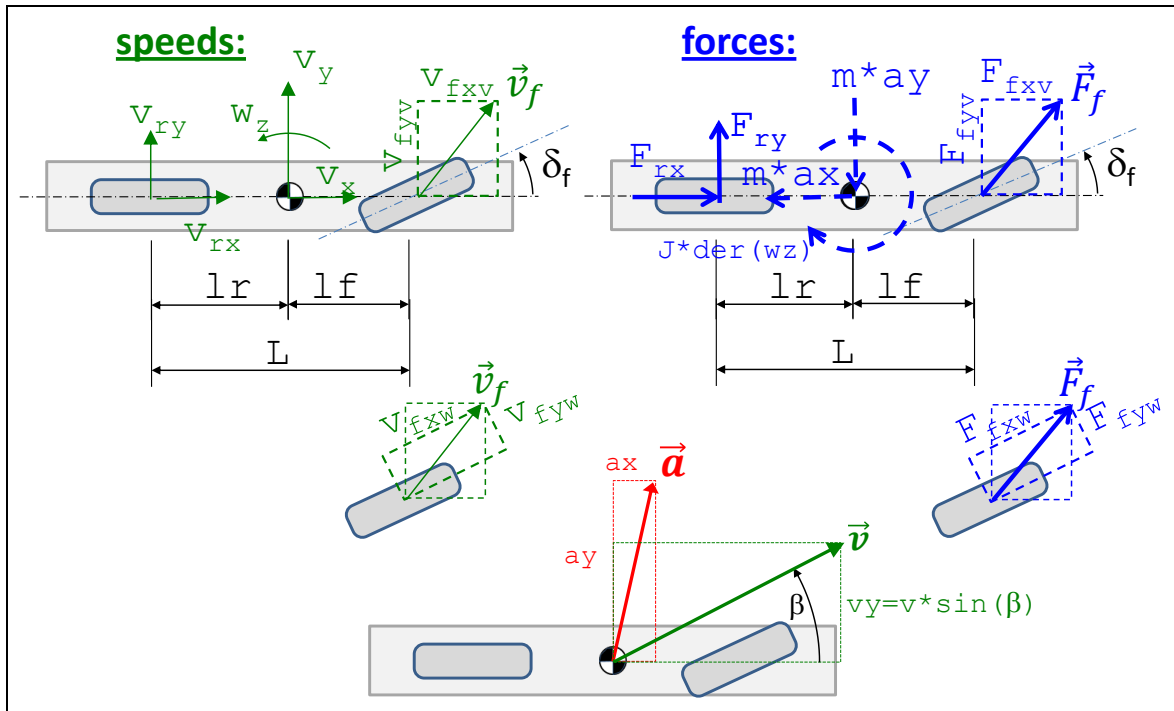
Figure 4-50: One-track model for transient dynamics. Dashed forces and moment are fictive forces. Compare to Figure 4-21.

```
//(Dynamic) Equilibrium:
m*ax = Ffxv + Frx;
m*ay = Ffyv + Fry;
J*der(wz) = Ffyv*lf - Fry*lr;
ax=der(vx)-wz*vy;
ay=der(vy)+wz*vx;

//Constitutive relation (Lateral tyre force model):
Ffyw=-Cf*sfy;
Fry=-Cr*sry;
sfy=vfyw/vfxw;
sry=vry/vrx;

//Compatibility:
vfxv = vx;
vfyv = vy + lf*wz;
vrx = vx;
vry = vy - lr*wz;

//Transformation between vehicle and wheel coordinate systems:
Ffxv = Ffxw*cos(df) - Ffyw*sin(df);
Ffyv = Ffxw*sin(df) + Ffyw*cos(df);
vfxv = vfxw*cos(df) - vfyw*sin(df);
vfyv = vfxw*sin(df) + vfyw*cos(df);

//Path with orientation:
der(x) = vx*cos(pz) - vy*sin(pz);
der(y) = vy*cos(pz) + vx*sin(pz);
der(pz) = wz;

// Prescription of steering angle:
df = if time < 2.5 then (5*pi/180)*sin(0.5*2*pi*time) else 5*pi/180;
//Shaft torques:
Ffxw = +1000; // Front axle driven.
Frx  = -100; // Rolling resistance on rear axle.
```

[4.53]

The initial longitudinal speed is a parameter, vx=100 km/h. A simulation result from the model is shown in Figure 4-51. The manoeuvre selected is same steering wheel function of time as in Figure 4-22, for better comparison of the different characteristics of the models.
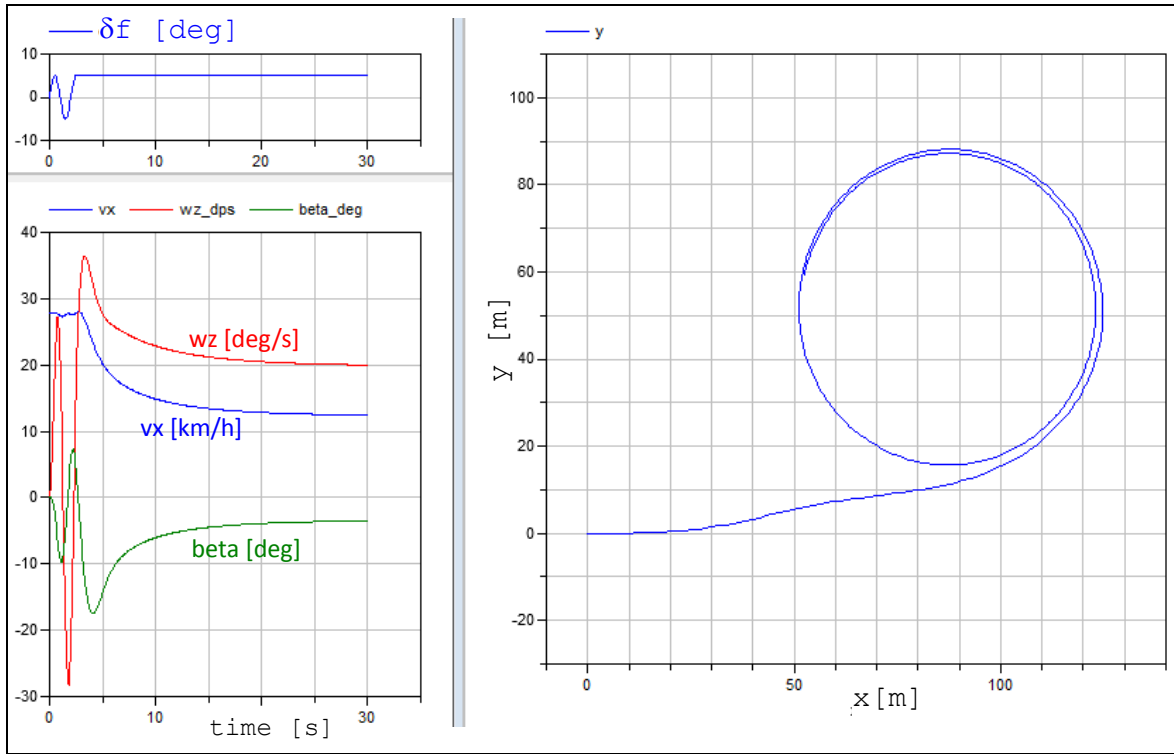
Figure 4-51: Simulation results of one-track model for transient dynamics.

Both position variables $[x, y, \varphi_y=pz]$ and speed variables $[v_x, v_y, \omega_z=wz]$ are "state variables" of this simulation. For each continuation from one time instant, the future solution requires knowledge of the previous states. This means that in the beginning, initial values were needed on the state variable. The only non-zero initial value was for v_x, which was given to $100\ km/h$.

Equation [4.53] is a complete model suitable for simulation. Eliminating some variable and rewrite in prettier format gives:

Equilibrium:

$$m \cdot (\dot{v}_x - \omega_z \cdot v_y) = F_{fxw} \cdot \cos(\delta_f) - F_{fyw} \cdot \sin(\delta_f) + F_{rx};$$
$$m \cdot (\dot{v}_y + \omega_z \cdot v_x) = F_{fxw} \cdot \sin(\delta_f) + F_{fyw} \cdot \cos(\delta_f) + F_{ry};$$
$$J \cdot \dot{\omega}_z = \left(F_{fxw} \cdot \sin(\delta_f) + F_{fyw} \cdot \cos(\delta_f)\right) \cdot l_f - F_{ry} \cdot l_r;$$

Constitution:

$$F_{fyw} = -C_f \cdot s_{fy}; \quad and \quad F_{ry} = -C_r \cdot s_{ry};$$

Compatibility:

$$s_{fy} = \frac{v_{fyw}}{v_{fxw}}; \quad and \quad s_{ry} = \frac{v_y - l_r \cdot \omega_z}{v_x};$$

Transformation from vehicle to wheel coordinate system on front axle:

$$v_{fxw} = \left(v_y + l_f \cdot \omega_z\right) \cdot \sin(\delta_f) + v_x \cdot \cos(\delta_f);$$
$$v_{fyw} = \left(v_y + l_f \cdot \omega_z\right) \cdot \cos(\delta_f) - v_x \cdot \sin(\delta_f);$$

[4.54]

Typically, this model is used for simulation, where δ_f, F_{fxw} and F_{rx} are input variables. Suitable state variables are then v_x, v_y and ω_z. It is a model suitable for arbitrary transient manoeuvres and we will

come back to this in Section 4.5. It is non-linear with respect to angles, but linear with respect to tyre slip model. It is also non-linear with respect to that the states appear as multiplied with each other, e.g. $\omega_z \cdot v_x$.

For the stationary oscillation events, this compendium will be limited to manoeuvres where far from saturating tyre grip and at constant v_x ($\Rightarrow \dot{v}_x = 0$). We assume:

- Low usage of lateral tyre force, i.e. small tyre slip angle (α_f): $s_{fy} = tan(\alpha_f) \approx \alpha_f$;
- Low level of cornering, i.e.
  - small steering angle: $sin(\delta_f) \approx \delta_f$; $cos(\delta_f) \approx 1$;
  - small front body slip angle (β_f): $\alpha_f = \beta_f - \delta_f$;
    where $\beta_f = arctan\left(\frac{v_{fyv}}{v_{fxv}}\right) \approx \frac{v_{fyv}}{v_{fxv}} = \frac{v_y + l_f \cdot \omega_z}{v_x}$;

We then rewrite the two last equations in Equation [4.54]:

$$\begin{cases} m \cdot (\dot{v}_y + \omega_z \cdot v_x) = F_{fxw} \cdot \delta_f - C_f \cdot \left(\frac{v_y + l_f \cdot \omega_z}{v_x} - \delta_f\right) - C_r \cdot \frac{v_y - l_r \cdot \omega_z}{v_x}; \\ J \cdot \dot{\omega}_z = \left(F_{fxw} \cdot \delta_f - C_f \cdot \left(\frac{v_y + l_f \cdot \omega_z}{v_x} - \delta_f\right)\right) \cdot l_f + C_r \cdot \frac{v_y - l_r \cdot \omega_z}{v_x} \cdot l_r; \end{cases} \Rightarrow$$

$$\Rightarrow \begin{cases} -m \cdot \omega_z \cdot v_y = F_{fxw} + F_{rx} + C_f \cdot \left(\frac{v_y + l_f \cdot \omega_z}{v_x} - \delta_f\right) \cdot \delta_f; \\ m \cdot \dot{v}_y + \frac{C_f + C_r}{v_x} \cdot v_y + \left(\frac{C_f \cdot l_f - C_r \cdot l_r}{v_x} + m \cdot v_x\right) \cdot \omega_z = (C_f + F_{fxw}) \cdot \delta_f; \\ J \cdot \dot{\omega}_z + \frac{C_f \cdot l_f - C_r \cdot l_r}{v_x} \cdot v_y + \frac{C_f \cdot l_f^2 + C_r \cdot l_r^2}{v_x} \cdot \omega_z = (C_f + F_{fxw}) \cdot l_f \cdot \delta_f; \end{cases}$$

[4.55]

This equation is written on matrix form (for the two state variables, v_y and ω_z) and one algebraic equation for the longitudinal equilibrium. Then:

$$\begin{bmatrix} m & 0 \\ 0 & J \end{bmatrix} \cdot \begin{bmatrix} \dot{v}_y \\ \dot{\omega}_z \end{bmatrix} + \begin{bmatrix} \dfrac{C_f + C_r}{v_x} & \dfrac{C_f \cdot l_f - C_r \cdot l_r}{v_x} + m \cdot v_x \\ \dfrac{C_f \cdot l_f - C_r \cdot l_r}{v_x} & \dfrac{C_f \cdot l_f^2 + C_r \cdot l_r^2}{v_x} \end{bmatrix} \cdot \begin{bmatrix} v_y \\ \omega_z \end{bmatrix} =$$

$$= \begin{bmatrix} C_f + F_{fxw} \\ (C_f + F_{fxw}) \cdot l_f \end{bmatrix} \cdot \delta_f;$$

[4.56]

Neglecting the longitudinal equilibrium and assuming that propulsion forces can be neglected for lateral and yaw equilibrium:

$$\begin{bmatrix} m & 0 \\ 0 & J \end{bmatrix} \cdot \begin{bmatrix} \dot{v}_y \\ \dot{\omega}_z \end{bmatrix} + \begin{bmatrix} \dfrac{C_f + C_r}{v_x} & \dfrac{C_f \cdot l_f - C_r \cdot l_r}{v_x} + m \cdot v_x \\ \dfrac{C_f \cdot l_f - C_r \cdot l_r}{v_x} & \dfrac{C_f \cdot l_f^2 + C_r \cdot l_r^2}{v_x} \end{bmatrix} \cdot \begin{bmatrix} v_y \\ \omega_z \end{bmatrix} = \begin{bmatrix} 1 \\ l_f \end{bmatrix} \cdot C_f \cdot \delta_f;$$

[4.57]

It should be noted that the assumption about small front body slip angle (β_f) makes the linearization questionable at high curvature, i.e. at small path radii.

The longitudinal equilibrium (first equation in Equation [4.54]) is often not mentioned, because the longitudinal dynamics is prescribed as a constant speed, v_x. However, this equation can be used to

calculate required propulsion on the axles to maintain the constant longitudinal speed. Note that it is complemented with air and grade resistance force.

$$F_{fxw} \cdot \cos(\delta_f) + F_{rx} =$$

$$= F_{air} + F_{grade} - m \cdot \omega_z \cdot v_y - C_f \cdot \frac{(v_y + l_f \cdot \omega_z) \cdot \cos(\delta_f) - v_x \cdot \sin(\delta_f)}{(v_y + l_f \cdot \omega_z) \cdot \sin(\delta_f) + v_x \cdot \cos(\delta_f)} \cdot \sin(\delta_f);$$

If $\delta_f, \alpha_f, \beta_f$ are small and $\beta_f \cdot \delta_f \approx 0$; $\delta_f \cdot \delta_f \approx 0$:

$$F_{fxw} + F_{rx} = F_{air} + F_{grade} - m \cdot \omega_z \cdot v_y;$$

If **front** axle driven: $F_{fxw} = \frac{T_f}{R_w} - f \cdot F_{fz};$ and $F_{rx} = f \cdot F_{rz};$

If **rear** axle driven: $F_{rx} = \frac{T_r}{R_w} - f \cdot F_{rz};$ and $F_{fxw} = f \cdot F_{fz};$

[4.58]

4.4.2.1 Simpler derivation of same model

A simpler derivation of Equation [4.57] is given in Figure 4-52. Here, the simplifications are introduced earlier, already in physical model, which means e.g. that the influence of F_{fxw} is not found.

Physical model:
- Path radius >> the vehicle. Then, all forces (and centripetal acceleration) are approximately co-directed.
- Small tyre and vehicle side slip. Then, angle=sin(angle)=tan(angle).
  (Angles are not drawn small, which is the reason why the forces not appear co-linear in figure.)

$$a_x = (\dot{v}_x - \omega_z \cdot v_y);$$
$$a_y = (\dot{v}_y + \omega_z \cdot v_x);$$

Mathematical model:

Equilibrium:
$$m \cdot (\dot{v}_x - \omega_z \cdot v_y) \approx F_{fx} + F_{rx}; where\ \dot{v}_x = 0;$$
$$m \cdot (\dot{v}_y + \omega_z \cdot v_x) \approx F_{fy} + F_{ry};$$
$$J \cdot \dot{\omega}_z \approx F_{fy} \cdot l_f - F_{ry} \cdot l_r;$$

Constitution: $F_{fy} = -C_f \cdot s_{yf};$ $F_{ry} = -C_r \cdot s_{yr};$

Compatibility:
$$\begin{cases} \delta_f + \alpha_f = \beta_f; \ \ \beta_f \approx \frac{v_{fy}}{v_x} = \frac{v_y + l_f \cdot \omega_z}{v_x}; \\ \alpha_r = \beta_r \approx \frac{v_{ry}}{v_x} = \frac{v_y - l_r \cdot \omega_z}{v_x}; \\ \alpha_f \approx s_{yf}; \ \ \alpha_r \approx s_{yr}; \end{cases}$$

Eliminate $F_{fy}, F_{ry}, \alpha_f, \alpha_r, \beta_f, \beta_r$ yields:
$$m \cdot \dot{v}_y + \frac{C_f + C_r}{v_x} \cdot v_y + \left(\frac{C_f \cdot l_f - C_r \cdot l_r}{v_x} + m \cdot v_x\right) \cdot \omega_z \approx$$
$$\approx C_f \cdot \delta_f;$$
$$J \cdot \dot{\omega}_z + \frac{C_f \cdot l_f - C_r l_r}{v_x} \cdot v_y + \frac{C_f \cdot l_f^2 + C_r \cdot l_r^2}{v_x} \cdot \omega_z \approx$$
$$\approx C_f \cdot l_f \cdot \delta_f;$$
$$F_{fx} + F_{rx} \approx -m \cdot \omega_z \cdot v_y;$$

Figure 4-52: Simpler derivation final step in Equation [4.57].

4.4.2.2 Relation between accelerations in inertial system and velocity derivatives in vehicle fix system

See Equation [4.52]. The relation between accelerations in inertial system, $\vec{a} = [a_x; a_y]$, and velocity derivatives in vehicle fix system, [der(vx); der(vy)]=$[\dot{v}_x; \dot{v}_y]$, is $[a_x; a_y] = [\dot{v}_x; \dot{v}_y] + [+v_x; -v_y] \cdot \omega_z$. The terms proportional to ω_z can be understood as a centrifugal force.

Another explanation is given in left part of Figure 4-53 and the following reasoning. We can express the velocity in direction of the x axis at time t, at the two time instants:

- Velocity at time $= t$: $\boldsymbol{v_x}$
- Velocity at time $= t + \Delta t$: $(v_x + \Delta v_x) \cdot \cos(\Delta \psi) - (v_y + \Delta v_y) \cdot \sin(\Delta \psi) = (v_x \cdot \cos(\Delta \psi) + \Delta v_x \cdot \cos(\Delta \psi)) - (v_y \cdot \sin(\Delta \psi) + \Delta v_y \cdot \sin(\Delta \psi)) \approx \{\Delta \psi \ small\} \approx (v_x + \Delta v_x) - (v_y \cdot \Delta \psi + \Delta v_y \cdot \Delta \psi) \approx \{\Delta v_y \cdot \Delta \psi \ small\} \approx \boldsymbol{(v_x + \Delta v_x) - v_y \cdot \Delta \psi}$

Using these two expressions, we can express a_x as the change of that speed per time unit:

- Acceleration=Velocity change per time $= \boldsymbol{a_x} = \frac{\{(v_x + \Delta v_x) - v_y \cdot \Delta \psi\} - v_x}{\Delta t} = \frac{\Delta v_x - v_y \cdot \Delta \psi}{\Delta t} = \frac{\Delta v_x}{\Delta t} - v_y \frac{\Delta \psi}{\Delta t} \approx \dot{v}_x - v_y \cdot \dot{\psi} = \boldsymbol{\dot{v}_x - v_y \cdot \omega_z}$

Corresponding for the lateral direction gives, in total, the Equation [4.52]. In Equation [4.52], the term $\omega_z \cdot v_x$ is generally more important than the term $\omega_z \cdot v_y$. This is because v_x is generally much larger than v_y.
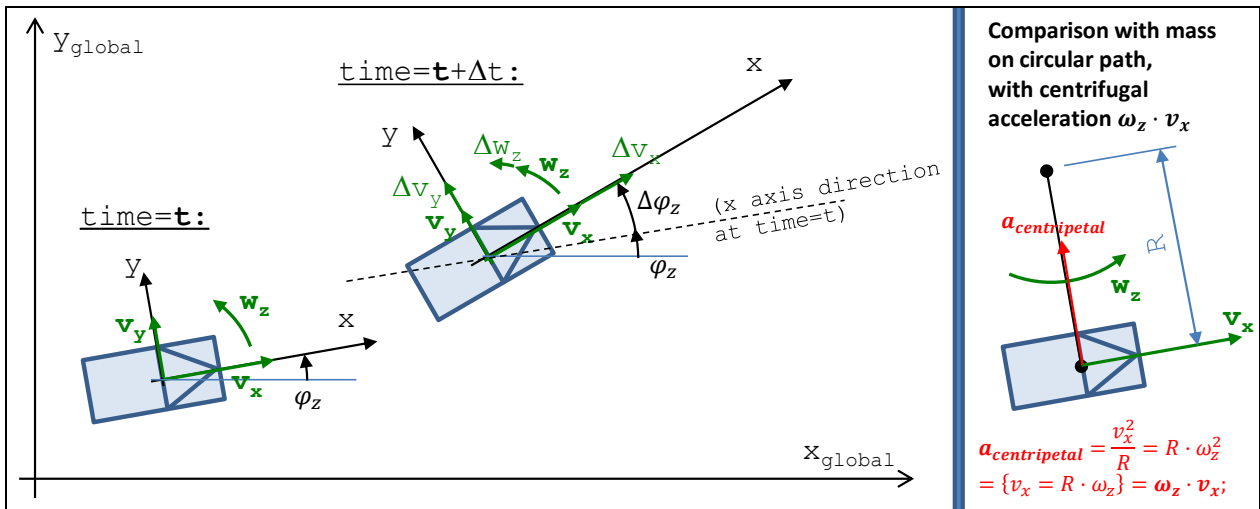
Figure 4-53: How to understand the acceleration term $\omega_z \cdot v_x$ for vehicle motion in ground plane. Left: Two consecutive time instants. Right: Comparison with circular motion, to identify the centripetal acceleration.

A generalisation gives that these centripetal acceleration terms appears as $v_i \cdot \omega_j$ where $i \neq j$, i.e. for rotation perpendicular to translational velocity, see right part of Figure 4-53:

$$\begin{bmatrix} a_x \\ a_y \\ a_z \end{bmatrix} = \begin{bmatrix} \dot{v}_x \\ \dot{v}_y \\ \dot{v}_z \end{bmatrix} + \begin{bmatrix} 0 & +v_z & -v_y \\ -v_z & 0 & +v_x \\ +v_y & -v_x & 0 \end{bmatrix} \cdot \begin{bmatrix} \omega_x \\ \omega_y \\ \omega_z \end{bmatrix} = \begin{bmatrix} \dot{v}_x \\ \dot{v}_y \\ \dot{v}_z \end{bmatrix} + \begin{bmatrix} 0 & -\omega_z & +\omega_y \\ +\omega_z & 0 & -\omega_x \\ -\omega_y & +\omega_x & 0 \end{bmatrix} \cdot \begin{bmatrix} v_x \\ v_y \\ v_z \end{bmatrix} =$$

$$= \begin{bmatrix} \dot{v}_x + v_z \cdot \omega_y - v_y \cdot \omega_z \\ \dot{v}_y - v_z \cdot \omega_x + v_x \cdot \omega_z \\ \dot{v}_z + v_y \cdot \omega_x - v_x \cdot \omega_y \end{bmatrix} \approx \left\{ \begin{array}{c} in \ most \ relevant \\ vehicle \ operations: \\ v_x \gg v_y \ and \ v_x \gg v_z \end{array} \right\} \approx \begin{bmatrix} \dot{v}_x \\ \dot{v}_y \\ \dot{v}_z \end{bmatrix} + \begin{bmatrix} 0 \\ +\omega_z \\ -\omega_y \end{bmatrix} \cdot v_x ;$$

[4.59]

In most vehicle operations, the most important centripetal acceleration terms are: $\omega_z \cdot v_x$ and $\omega_y \cdot v_x$. The first comes into play in Equation [4.52], and the latter in Figure 3-46, Eq [3.33], and Section 3.4.13.

4.4.2.3   Validity of solution

When only studying the response as yaw rate and curvature response, it is easy to forget that one very easily comes into manoeuvres where road friction is limited, i.e. where the linear tyre model is not valid. Hence it is good to look at lateral acceleration response, because we can roughly say that for $|a_y|$ in the same magnitude as $\mu \cdot m \cdot g$, it is doubtful if the model is valid. If the wheel torques are significant, the validity limit is even lower. For high CoG vehicles, another invalidating circumstance is wheel lift, which can be approximately checked by checking that $|a_y| \ll SSF = \frac{g \cdot w}{2 \cdot h}$.

If one really wants to include nonlinear tyre models in stationary oscillation response, one can simulate using time integration (same method as usually used for transient handling) over several excitation cycles, until the response shows a clear stationary oscillation. This consumes more computational efforts and the solutions become approximate and numerical.

4.4.3   Steering frequency response gains *

Function definition: **Steering frequency response gains** *are the amplifications from steering angle amplitude to certain vehicle response measure's amplitudes for stationary oscillating harmonic steering at a certain longitudinal speed.*

Equation [4.57] (or resulting equation in Figure 4-52) can be seen as a state-space-model:

$$\text{State space form:} \begin{cases} \begin{bmatrix} \dot{v}_y \\ \dot{\omega}_z \end{bmatrix} = \boldsymbol{A} \cdot \begin{bmatrix} v_y \\ \omega_z \end{bmatrix} + \boldsymbol{B} \cdot \delta_f; \\ \begin{bmatrix} \omega_z \\ a_y \end{bmatrix} = \boldsymbol{C} \cdot \begin{bmatrix} v_y \\ \omega_z \end{bmatrix} + \boldsymbol{D} \cdot \delta_f; \end{cases}$$

$$\text{where } \boldsymbol{A} = -\begin{bmatrix} m & 0 \\ 0 & J \end{bmatrix}^{-1} \cdot \begin{bmatrix} \dfrac{C_f + C_r}{v_x} & \dfrac{C_f \cdot l_f - C_r \cdot l_r}{v_x} + m \cdot v_x \\ \dfrac{C_f \cdot l_f - C_r \cdot l_r}{v_x} & \dfrac{C_f \cdot l_f^2 + C_r \cdot l_r^2}{v_x} \end{bmatrix};$$

$$\text{and } \boldsymbol{B} = \begin{bmatrix} m & 0 \\ 0 & J \end{bmatrix}^{-1} \cdot \begin{bmatrix} 1 \\ l_f \end{bmatrix} \cdot C_f;$$

$$\text{and } \boldsymbol{C} = \begin{bmatrix} 0 & 0 \\ 1 & 0 \end{bmatrix} \cdot \boldsymbol{A} + \begin{bmatrix} 0 & 1 \\ 0 & v_x \end{bmatrix}; \text{ and } \boldsymbol{D} = \boldsymbol{B};$$

[4.60]

When studying "stationary oscillating steering":

$$\begin{bmatrix} \dot{v}_y \\ \dot{\omega}_z \end{bmatrix} = A \cdot \begin{bmatrix} v_y \\ \omega_z \end{bmatrix} + B \cdot \delta(t) = A \cdot \begin{bmatrix} v_y \\ \omega_z \end{bmatrix} + B \cdot \hat{\delta} \cdot \cos(\omega \cdot t)$$

(Note similar notation for vehicle yaw rate, ω_z, and steering angular frequency, ω.) Knowing $\hat{\delta}$ and ω, it is possible to calculate the responses $\hat{v}_y$, $\hat{\omega}_z$, φ_y and φ_z:

$$\begin{bmatrix} v_y \\ \omega_z \end{bmatrix} = \begin{bmatrix} \hat{v}_y \\ \hat{\omega}_z \end{bmatrix} \cdot \cos\left(\omega \cdot t - \begin{bmatrix} \varphi_{v_y} \\ \varphi_{\omega_z} \end{bmatrix}\right);$$

$$\begin{bmatrix} \omega_z \\ a_y \end{bmatrix} = \begin{bmatrix} \hat{\omega}_z \\ \hat{a}_y \end{bmatrix} \cdot \cos\left(\omega \cdot t - \begin{bmatrix} \varphi_{\omega_z} \\ \varphi_{a_y} \end{bmatrix}\right);$$

Different methods are available for calculation of the responses:

- **Fourier** transform
- **Complex mathematics**, using $e^{j \cdot \omega \cdot t}$
- **Real trigonometry**, using $\cos(\omega \cdot t + phase)$, $\sin(\omega \cdot t + phase)$ or $\cos(\omega \cdot t) + \sin(\omega \cdot t)$.

For each of these, depending on the problem, it can be ether scalar or matrix algebra. Matrix based Fourier transform is generally the most efficient, especially if Matlab is available and numerical solutions can be accepted.

4.4.3.1   Single frequency response

4.4.3.1.1 Solution with Fourier transform

Equation [4.60] can be transformed to the frequency domain (where the Fourier transform of a function, $\xi(t)$, is denoted $\mathcal{F}(\xi(t)) = \int_0^\infty e^{-j \cdot \omega \cdot t} \cdot \xi(t) \cdot dt$):

$$\begin{cases} \mathrm{j} \cdot \omega \cdot \mathcal{F}\left(\begin{bmatrix} v_y \\ \omega_z \end{bmatrix}\right) = \boldsymbol{A} \cdot \mathcal{F}\left(\begin{bmatrix} v_y \\ \omega_z \end{bmatrix}\right) + \boldsymbol{B} \cdot \mathcal{F}(\delta_f); \\ \mathcal{F}\left(\begin{bmatrix} \omega_z \\ a_y \end{bmatrix}\right) = \boldsymbol{C} \cdot \mathcal{F}\left(\begin{bmatrix} v_y \\ \omega_z \end{bmatrix}\right) + \boldsymbol{D} \cdot \mathcal{F}(\delta_f); \end{cases}$$

Solving for states and outputs:

$$\begin{cases} \begin{bmatrix} v_y \\ \omega_z \end{bmatrix} = \mathcal{F}^{-1}\left(\mathcal{F}\left(\begin{bmatrix} v_y \\ \omega_z \end{bmatrix}\right)\right) = \mathcal{F}^{-1}\left((\mathrm{j} \cdot \omega \cdot \mathrm{I} - \boldsymbol{A})^{-1} \cdot \boldsymbol{B} \cdot \mathcal{F}(\delta_f)\right); \\ \begin{bmatrix} \omega_z \\ a_y \end{bmatrix} = \mathcal{F}^{-1}\left(\mathcal{F}\left(\begin{bmatrix} \omega_z \\ a_y \end{bmatrix}\right)\right) = \mathcal{F}^{-1}\left(\boldsymbol{C} \cdot \mathcal{F}\left(\begin{bmatrix} v_y \\ \omega_z \end{bmatrix}\right) + \boldsymbol{D} \cdot \mathcal{F}(\delta_f)\right); \end{cases}$$

Expressed as transfer functions:

$$\begin{cases} H_{\delta_f \to \begin{bmatrix} v_y \\ \omega_z \end{bmatrix}} = \dfrac{\mathcal{F}\left(\begin{bmatrix} v_y \\ \omega_z \end{bmatrix}\right)}{\mathcal{F}(\delta_f)} = \dfrac{(\mathrm{j} \cdot \omega \cdot \mathrm{I} - \boldsymbol{A})^{-1} \cdot \boldsymbol{B} \cdot \mathcal{F}(\delta_f)}{\mathcal{F}(\delta_f)} = (\mathrm{j} \cdot \omega \cdot \mathrm{I} - \boldsymbol{A})^{-1} \cdot \boldsymbol{B}; \\ H_{\delta_f \to \begin{bmatrix} \omega_z \\ a_y \end{bmatrix}} = \dfrac{\mathcal{F}\left(\begin{bmatrix} \omega_z \\ a_y \end{bmatrix}\right)}{\mathcal{F}(\delta_f)} = \boldsymbol{C} \cdot H_{\delta_f \to \begin{bmatrix} v_y \\ \omega_z \end{bmatrix}} + \boldsymbol{D} = \boldsymbol{C} \cdot (\mathrm{j} \cdot \omega \cdot \mathrm{I} - \boldsymbol{A})^{-1} \cdot \boldsymbol{B} + \boldsymbol{D}; \end{cases}$$

[4.61]

We have derived the transfer functions. The subscript tells that the transfer function is for the vehicle operation with excitation=input= δ_f and response=output= $\begin{bmatrix} v_y \\ \omega_z \end{bmatrix}$ and output= $\begin{bmatrix} \omega_z \\ a_y \end{bmatrix}$. The transfer functions has dimension 2x1 and it is complex. They operate as follows:

Amplitudes: $\begin{cases} \begin{bmatrix} \hat{v}_y \\ \hat{\omega}_z \end{bmatrix} = \left| H_{\delta_f \to \begin{bmatrix} v_y \\ \omega_z \end{bmatrix}} \right| \cdot \hat{\delta}_f; \\ \begin{bmatrix} \hat{\omega}_z \\ \hat{a}_y \end{bmatrix} = \left| H_{\delta_f \to \begin{bmatrix} \omega_z \\ a_y \end{bmatrix}} \right| \cdot \hat{\delta}_f; \end{cases}$

Phase delays: $\begin{cases} \begin{bmatrix} \varphi_{v_y} \\ \varphi_{\omega_z} \end{bmatrix} = \begin{bmatrix} \arg(v_y) \\ \arg(\omega_z) \end{bmatrix} - \begin{bmatrix} 1 \\ 1 \end{bmatrix} \cdot \arg(\delta_f) = \left\{ \begin{matrix} \arg(\delta_f) \\ = 0 \end{matrix} \right\} = \arg\left(H_{\delta_f \to \begin{bmatrix} v_y \\ \omega_z \end{bmatrix}} \right); \\ \begin{bmatrix} \varphi_{\omega_z} \\ \varphi_{a_y} \end{bmatrix} = \begin{bmatrix} \arg(\omega_z) \\ \arg(a_y) \end{bmatrix} - \begin{bmatrix} 1 \\ 1 \end{bmatrix} \cdot \arg(\delta_f) = \left\{ \begin{matrix} \arg(\delta_f) \\ = 0 \end{matrix} \right\} = \arg\left(H_{\delta_f \to \begin{bmatrix} \omega_z \\ a_y \end{bmatrix}} \right); \end{cases}$

[4.62]

4.4.3.1.2 Solution with complex mathematics

This section avoids requiring skills in Fourier transform. This makes the derivation quite long to reach the final results Equation [4.67] and Equation [4.66]. With Fourier Transform, the expression for the Transfer Function, H, can be reached with less algebra. Knowing H, it can be used in Equation [4.66].

The fundamental situation for steering frequency response is that the excitation is: $\delta_f = \hat{\delta}_f \cdot \cos(2 \cdot \pi \cdot f \cdot t) = \{e^{j \cdot a} = \cos(a) + j \cdot \sin(a)\} = \mathrm{Re}(\hat{\delta}_f \cdot e^{j \cdot 2 \cdot \pi \cdot f \cdot t})$, where f is the (time) frequency in Hz and j is the imaginary unit. We rewrite $2 \cdot \pi \cdot f$ as ω (angular frequency), which has to be carefully distinguished from ω_z (yaw rate). Insert this in Equation [4.56] and neglecting the longitudinal force F_{fxw}. The full (complex) equation is used:

$$\mathrm{Re}\left[\begin{bmatrix} m & 0 \\ 0 & J \end{bmatrix} \cdot \begin{bmatrix} \dot{v}_{yc} \\ \dot{\omega}_{zc} \end{bmatrix} + \begin{bmatrix} \dfrac{C_f + C_r}{v_x} & \dfrac{C_f \cdot l_f - C_r \cdot l_r}{v_x} + m \cdot v_x \\ \dfrac{C_f \cdot l_f - C_r \cdot l_r}{v_x} & \dfrac{C_f \cdot l_f{}^2 + C_r \cdot l_r{}^2}{v_x} \end{bmatrix} \cdot \begin{bmatrix} v_{yc} \\ \omega_{zc} \end{bmatrix} = \begin{bmatrix} C_f \\ C_f \cdot l_f \end{bmatrix} \cdot \hat{\delta}_f \cdot e^{j \cdot \omega \cdot t} \right];$$

[4.63]

We intend to solve the complex equation, and then find the solutions as real parts: $v_y = \text{Re}[v_{yc}]$; and $\omega_z = \text{Re}[\omega_{zc}]$;. (Subscript c means complex.)

If only interested in the stationary solution, which is valid after possible initial value dependent transients are damped out, we can assume a general form for the solution.

$$\begin{bmatrix} v_{yc} \\ \omega_{zc} \end{bmatrix} = \begin{bmatrix} \hat{v}_{yc} \\ \hat{\omega}_{zc} \end{bmatrix} \cdot e^{j\cdot\omega\cdot t} \quad \Rightarrow \quad \begin{bmatrix} \dot{v}_{yc} \\ \dot{\omega}_{zc} \end{bmatrix} = j\cdot\omega\cdot\begin{bmatrix} \hat{v}_{yc} \\ \hat{\omega}_{zc} \end{bmatrix} \cdot e^{j\cdot\omega\cdot t}; \qquad [4.64]$$

Inserting the assumption in the differential equation gives:

$$\begin{bmatrix} m & 0 \\ 0 & J \end{bmatrix}\cdot j\cdot\omega\cdot\begin{bmatrix} \hat{v}_{yc} \\ \hat{\omega}_{zc} \end{bmatrix}\cdot e^{j\cdot\omega\cdot t} +$$

$$+ \begin{bmatrix} \dfrac{C_f + C_r}{v_x} & \dfrac{C_f\cdot l_f - C_r\cdot l_r}{v_x} + m\cdot v_x \\ \dfrac{C_f\cdot l_f - C_r\cdot l_r}{v_x} & \dfrac{C_f\cdot l_f{}^2 + C_r\cdot l_r{}^2}{v_x} \end{bmatrix}\cdot\begin{bmatrix} \hat{v}_{yc} \\ \hat{\omega}_{zc} \end{bmatrix}\cdot e^{j\cdot\omega\cdot t} = \begin{bmatrix} 1 \\ l_f \end{bmatrix}\cdot C_f\cdot\hat{\delta}_f\cdot e^{j\cdot\omega\cdot t} \Rightarrow$$

$$\Rightarrow \begin{bmatrix} \hat{v}_{yc} \\ \hat{\omega}_{zc} \end{bmatrix} =$$

$$= \left(\begin{bmatrix} m & 0 \\ 0 & J \end{bmatrix}\cdot j\cdot\omega + \begin{bmatrix} \dfrac{C_f + C_r}{v_x} & \dfrac{C_f\cdot l_f - C_r\cdot l_r}{v_x} + m\cdot v_x \\ \dfrac{C_f\cdot l_f - C_r\cdot l_r}{v_x} & \dfrac{C_f\cdot l_f{}^2 + C_r\cdot l_r{}^2}{v_x} \end{bmatrix} \right)^{-1}\cdot\begin{bmatrix} 1 \\ l_f \end{bmatrix}\cdot C_f\cdot\hat{\delta}_f =$$

$$= H_{\delta_f\rightarrow\begin{bmatrix} v_y \\ \omega_z \end{bmatrix}}\cdot\hat{\delta}_f; \qquad\qquad [4.65]$$

Then, we can assume we know $\hat{v}_{yc}$ and $\hat{\omega}_{zc}$ from Equation [4.65], and consequently we know v_{yc} and ω_{zc} from Equation [4.64]. We have derived the transfer function, $H_{\delta_f\rightarrow\begin{bmatrix} v_y \\ \omega_z \end{bmatrix}}$. The subscript tells that the transfer function is for the vehicle operation with excitation=input= δ_f and response=output= $\begin{bmatrix} v_y \\ \omega_z \end{bmatrix}$ case. This transfer function has dimension 2x1 and it is complex. It operates as follows:

$$\text{Amplitudes: } \begin{bmatrix} \hat{v}_y \\ \hat{\omega}_z \end{bmatrix} = \begin{bmatrix} |v_y| \\ |\omega_z| \end{bmatrix} = \left| H_{\delta_f\rightarrow\begin{bmatrix} v_y \\ \omega_z \end{bmatrix}} \right|\cdot|\delta_f|;$$

$$\text{Phase delays: } \begin{bmatrix} \arg(v_y) \\ \arg(\omega_z) \end{bmatrix} - \begin{bmatrix} 1 \\ 1 \end{bmatrix}\cdot\arg(\delta_f) = \{\arg(\delta_f) = 0\} = \arg\left(H_{\delta_f\rightarrow\begin{bmatrix} v_y \\ \omega_z \end{bmatrix}} \right) \qquad [4.66]$$

However, we can derive expressions for v_{yc} and ω_{zc} on a real (non-complex) form, $amplitude \cdot \cos(angular\ frequency \cdot t - phase\ delay)$, without involving transfer function. That is done in the following:

$$v_y = \text{Re}(v_{yc}) = \text{Re}(\hat{v}_{yc}\cdot e^{j\cdot\omega\cdot t}) = \cdots = |\hat{v}_{yc}|\cdot\cos(\omega\cdot t + \arg(\hat{v}_{yc}));$$

The same rewriting can be done with ω_z, so that in total:

$$\begin{bmatrix} v_y \\ \omega_z \end{bmatrix} = \begin{bmatrix} \hat{v}_y\cdot\cos(\omega\cdot t - \varphi_{vy}) \\ \hat{\omega}_z\cdot\cos(\omega\cdot t - \varphi_{\omega z}) \end{bmatrix} = \begin{bmatrix} |\hat{v}_{yc}|\cdot\cos(\omega\cdot t - (-\arg(\hat{v}_{yc}))) \\ |\hat{\omega}_{zc}|\cdot\cos(\omega\cdot t - (-\arg(\hat{\omega}_{zc}))) \end{bmatrix} \qquad [4.67]$$

Equation [4.65] and Equation [4.67] now gives us the possibility to find vehicle response amplitude and phase delay. The ratios between amplitude of responses and amplitude of excitation, $\hat{v}_y/\hat{\delta}_f$ and $\hat{\omega}_z/\hat{\delta}_f$, are called gains. The difference in argument is the phase delay.

4.4.3.2   Lateral Velocity and Yaw Rate response

The frequency response for the two states, Lateral Velocity and Yaw Rate, can be plotted for given vehicle data, see Equation [4.65], Equation [4.67] and Figure 4-54. The curves show response for same vehicle, but different speed.

See Figure 4-54. The yaw rate gain curve has a knee at 0.5..1 Hz. The decrease after that is a measure of yaw damping. The curve for high speed actually has a weak peak just before the knee. This is not desired, because the vehicle might feel a bit nervous. Yaw damping can also be how fast yaw rate decays after a step response, see Section 4.5.

From Equation [4.24] we can calculate that characteristic speed for the vehicle is 120 km/h. With another understeering coefficient, we could have calculated a critical speed. Studying Figure 4-54 to Figure 4-57, one can find these special speeds in another appearance:

- For an understeered vehicle, speeds above the characteristic speed gives a negative yaw rate delay for low steering frequencies will be negative.
- For over-steered vehicles, speeds above the critical speed gives a yaw rate delay larger than 180 deg and yaw rate amplitudes which are very large for low steering frequencies.
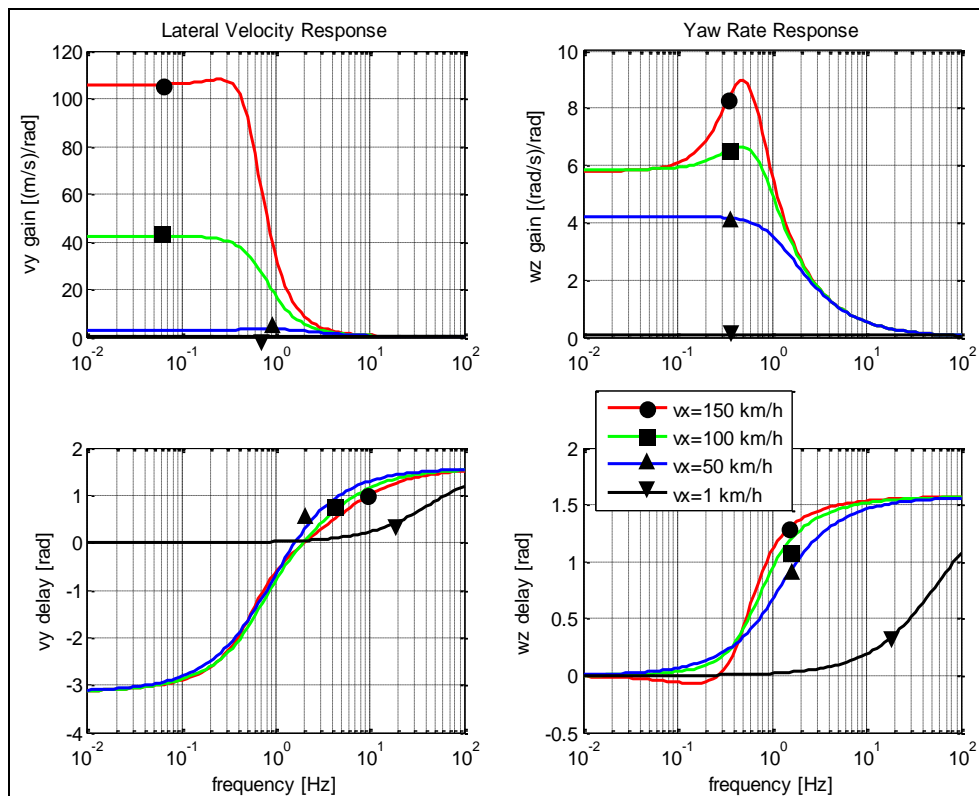
Figure 4-54: Vehicle response to harmonically oscillating steering angle. Vehicle data: $m = 2000\ kg$; $J = 3000\ kg \cdot m^2$; $l_f = 1.3\ m$; $l_r = 1.5\ m$; $C_f = 81400\ N/rad$; $C_r = 78000\ N/rad$; $(K_u = 1.26\ rad/MN)$.

From Equation [4.24] we can calculate that characteristic speed for the vehicle is 120 km/h.

In Figure 4-55 the curves are for same speed and constant understeering gradient, but they show the response for different sums of cornering stiffness (Cf+Cr). Increasing the stiffness increases the yaw rate gain (agility) at high frequencies.
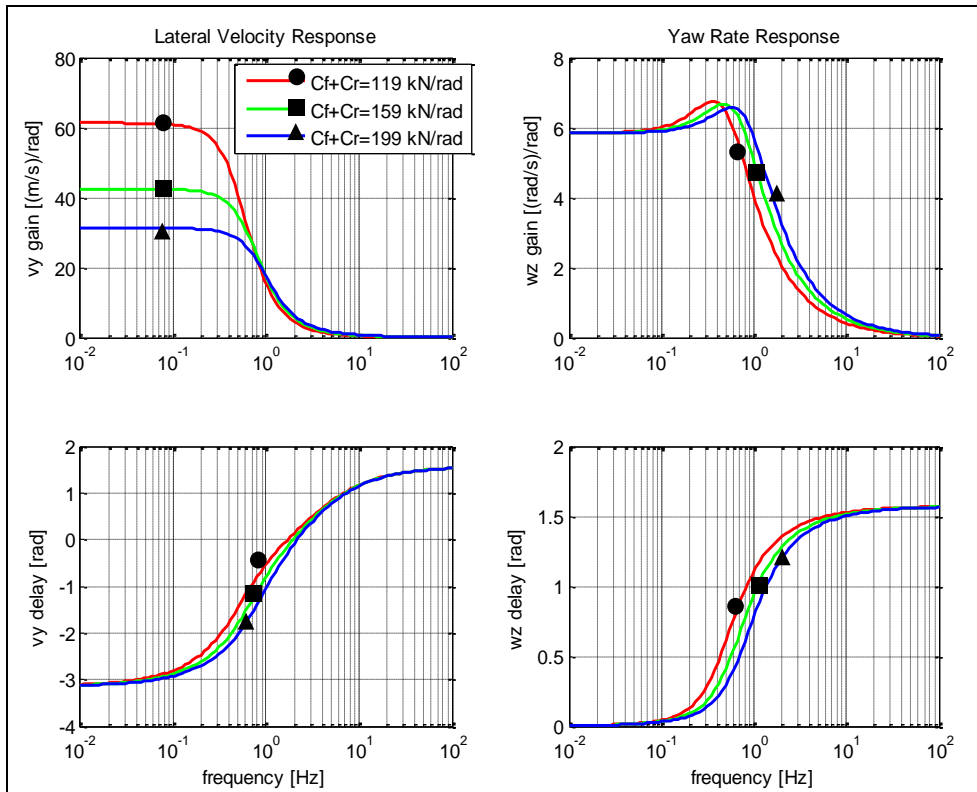
Figure 4-55: Vehicle response to harmonically oscillating steering angle. Same vehicle data as in Figure 4-54, except varying Cf and Cr but keeping understeering gradient Ku constant. Vehicle speed = 100 km/h.

In Figure 4-56 the curves are for same speed and constant sum of cornering stiffness (Cf+Cr), but they show the response for different values of understeering gradient (Ku). Increasing understeer gradient decreases the yaw rate gain (agility) at low frequencies.
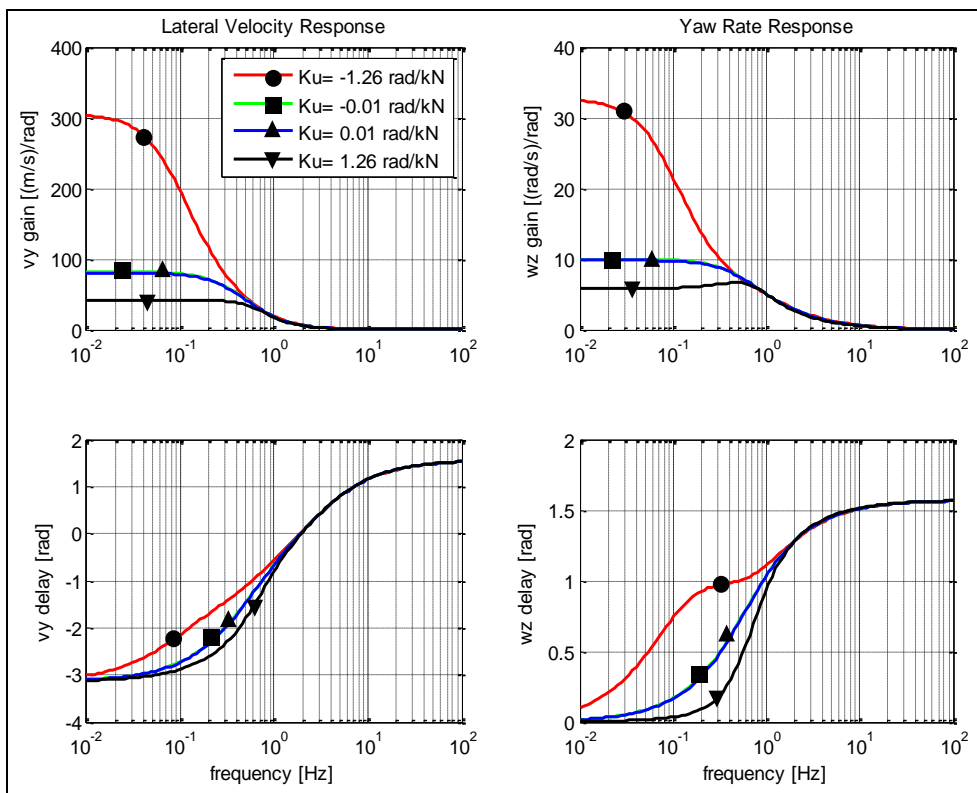
Figure 4-56: Vehicle response to harmonically oscillating steering angle. Same vehicle data as in Figure 4-54, except varying understeering gradient Ku but keeping Cf+Cr constant. Vehicle speed = 100 km/h.

4.4.3.3 Lateral Acceleration response

The lateral acceleration response is another useful response to study and set requirements on. Actually, yaw rate and lateral acceleration are the most frequently used response variables, since they are easily measured, e.g. from ESC sensors in most vehicles.

The transfer function is found (here using Fourier transform and previous results):

$$\text{Amplitude: } \hat{a}_y = |a_{yc}| = \left\{ use: a_y = \frac{\dot{v}_y + \omega_z \cdot v_x}{m} \right\} = \left| \frac{j \cdot \omega \cdot v_{yc} + \omega_{zc} \cdot v_x}{m} \right| =$$

$$= \left| \frac{1}{m} \cdot \begin{bmatrix} j \cdot \omega & v_x \end{bmatrix} \cdot H_{\delta_f \to \begin{bmatrix} v_y \\ \omega_z \end{bmatrix}} \cdot \delta_f \right| = \left| \begin{bmatrix} j \cdot \omega & v_x \end{bmatrix} \cdot H_{\delta_f \to \begin{bmatrix} v_y \\ \omega_z \end{bmatrix}} \cdot \frac{\delta_f}{m} \right|;$$

$$\text{Phase delay: } \arg(a_y) - \arg(\delta_f) = \{ use: \arg(\delta_f) = 0 \} = \arg\left(\begin{bmatrix} j \cdot \omega & v_x \end{bmatrix} \cdot H_{\delta_f \to \begin{bmatrix} v_y \\ \omega_z \end{bmatrix}} \right);$$

[4.68]

Lateral acceleration response is plotted for different vehicle speeds in Figure 4-57.
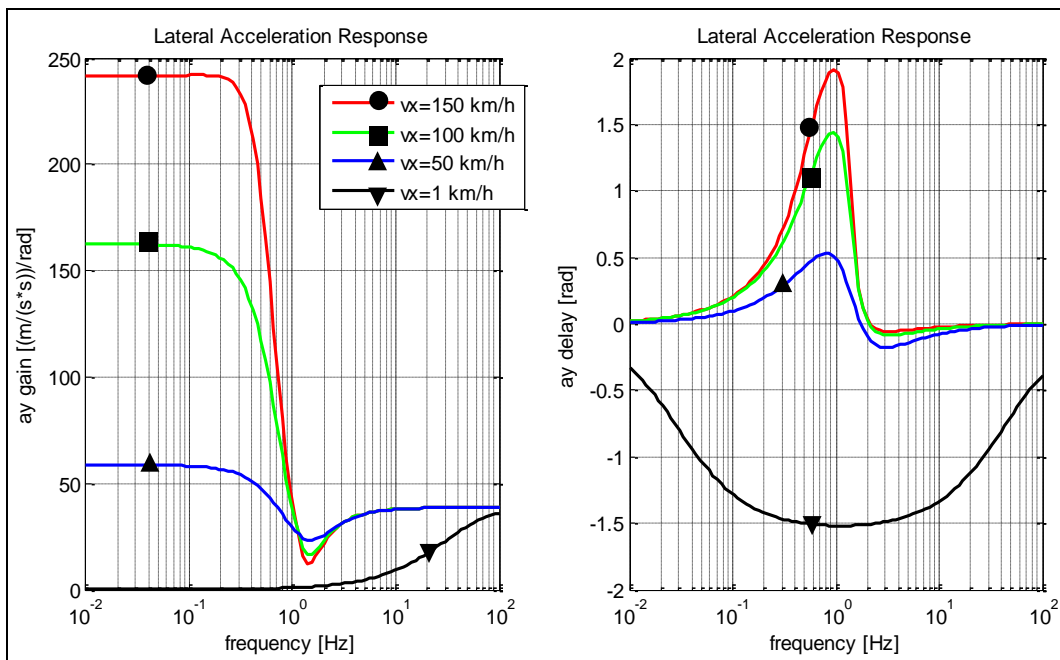
Figure 4-57: Vehicle lateral acceleration response to harmonically oscillating steering angle. Vehicle data: $m = 2000\ kg$; $J = 3000\ kg \cdot m^2$; $l_f = 1.3\ m$; $l_r = 1.5\ m$; $C_f = 81400\ N/rad$; $C_r = 78000\ N/rad$; $(K_u = 1.26\ rad/MN)$.

4.4.3.4 Other responses to oscillating steering

In principle, it is possible to study a lot of other responses, such as Path Curvature response, Side slip response and Lateral Path Width response etc. These are not very standardized in requirement setting, but can be used as such or generally used for comparing different designs during the development work. For combination-vehicles it is common to plot Rearward amplification (RWA) as function of frequency. RWA can be either $RWA_{ay} = \max\limits_{i=2,3,4,\dots} \left(\frac{\hat{a}_i}{\hat{a}_1} \right)$; where i denotes vehicle units or axles, or

$RWA_{ay} = \max\limits_{i=2,3,4,\dots} \left(\frac{\hat{\omega}_{zi}}{\hat{\omega}_{z1}} \right)$; where i denotes vehicle units.

4.4.3.5 Random frequency response

Solutions to harmonic excitation of linear dynamic systems are superimposable. This is also why the response from a mixed frequency excitation can be spliced into separate frequencies, e.g. using Fourier

transformation. Hence, a common way to measure the frequency response diagrams is to log data from a random steering excitation. The frequency response diagram can then be extracted from this test.

4.5 Transient handling

Transient handling in general vehicle dynamics is when the vehicle is manoeuvred in an arbitrary, but not constant or cyclic, way. Generally, this can be turning and braking/accelerating at the same time through a manoeuvre. In this chapter, we only cover transient handling within lateral dynamics. This should be understood as that we assume a reasonably constant longitudinal vehicle speed and modest longitudinal forces on the wheels. The latter assumptions make it possible to base most of the content in this chapter on the model derived in Section 4.4.

4.5.1   Transient driving manoeuvres *

From the manoeuvres defined in this section, there are a large number of relevant function possible to define. Here, only a few is mentioned:

> *Function definition:* **Double Lane Change Capability** *is the highest entry speed that a certain driver (or driver model) can manage without hitting any cones. A certain cone pattern (e.g. as Figure 4-58 or Figure 4-59) and a certain road friction has to be defined. A certain operation principle of pedals needs to be specified, e.g. release both pedals at entry or full brake pedal apply.*

> *Function definition:* **Over-speed into Curve Capability** *is the highest entry speed that a certain driver (or driver model) can manage without hitting any cones. A certain cone pattern e.g. as Figure 4-60) and a certain road friction has to be defined. A certain operation principle of pedals needs to be specified, e.g. release both pedals at entry or full brake pedal apply.*

> *Function definition:* **Steer-In and Release Accelerator Pedal stability** *is a measure (e.g. side slip rear axle peak) after a certain simultaneous steer-in and release of accelerator pedal, starting from a steady state cornering at a certain path radius and speed. A certain road friction has to be defined.*

When testing Transient driving manoeuvres, the typical part of the test track is the Vehicle Dynamics Area or a Handling Track, see Figure 4-8. A Handling Track is a normal width road, intentionally curved and with safety areas beside the curves for safety in case of run-off road during tests.

Typical transient tests are:
* Step steer, where one can measure transient versions of
    o Yaw rate response
    o Lateral acceleration response
    o Curvature response
    o Yaw damping
* Lateral avoidance manoeuvres:
    o Single lane change in cone track
    o Double lane change in cone track, see Figure 4-26, Figure 4-58, and Figure 4-59
    o Figure 4-26
    o Lane change while full braking
    o Sine with dwell
    o Steering effort in evasive manoeuvres
* Tests from steady state cornering
    o Brake or accelerate in curve
    o Lift accelerator pedal and steer-in while cornering
    o Over-speeding into curve, see Figure 4-60
* Handling type tests
    o Slalom between cones
    o Handling track, general driving experience

- Roll-over tests
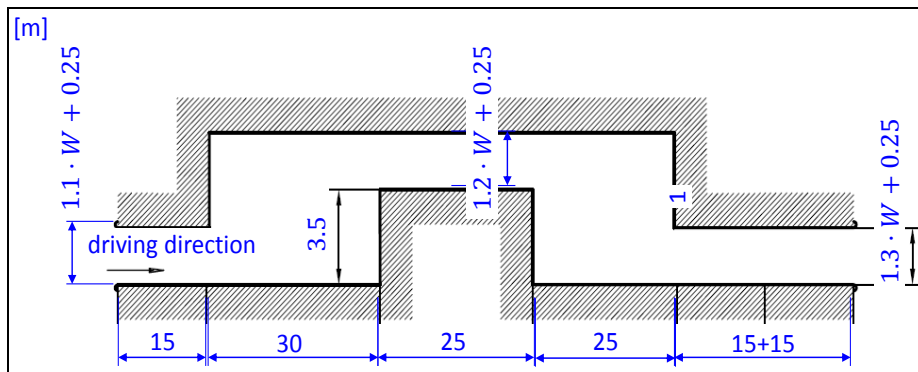
Figure 4-58: Passenger cars - Test track for a severe lane-change manoeuvre - Part 1: Double lane-change. Reference (ISO 3888).
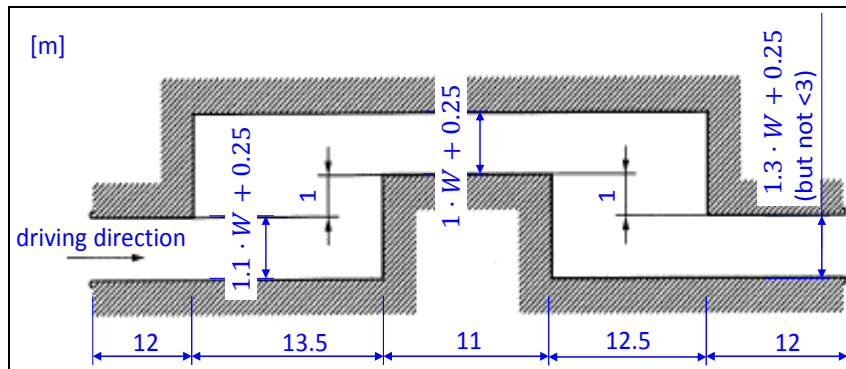
Figure 4-59: Passenger cars - Test track for a severe lane-change manoeuvre - Part 2: Obstacle avoidance. Reference (ISO 3888).
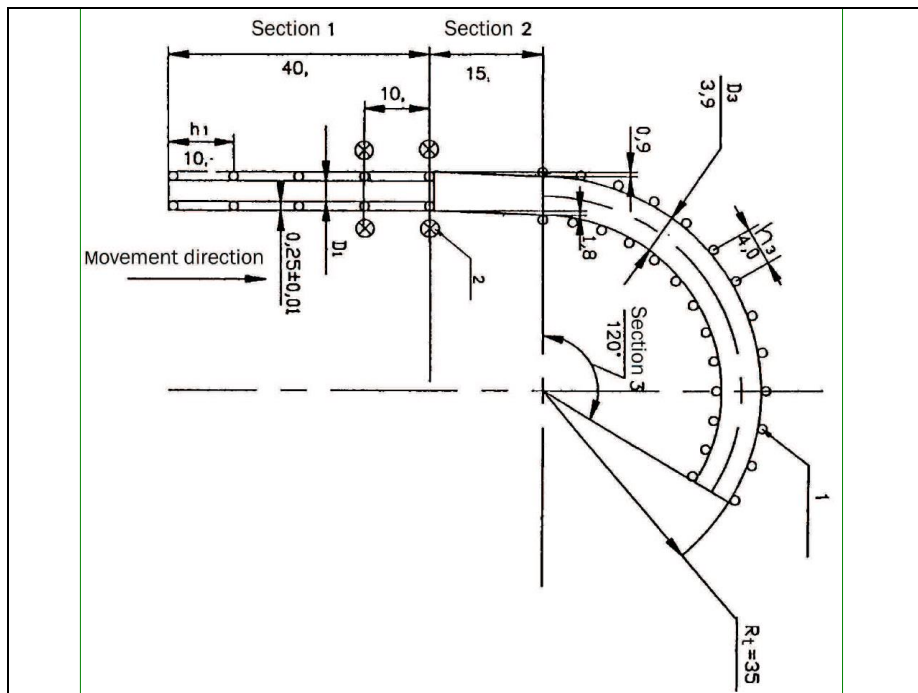
Figure 4-60: Cone track for one standardized test of Over-speeding into curve

Standards which are relevant to these test manoeuvres are, e.g. References (ISO 3888), (ISO 7401), (ISO 7975, 2006), (ISO 11026), (ISO 14791), (ISO 14793), (ISO 14794, 2011) and (NHTSA).

A general note is that tests in real vehicles are often needed to be performed in simulation also, and normally earlier in the product development process.

4.5.2 Transient one-track model, without lateral load transfer

4.5.2.1 Two-axle vehicle without roll influence

Transient handling within lateral vehicle dynamics should be understood as that we assume a reasonably constant longitudinal vehicle speed and modest longitudinal forces on the wheels. The latter assumptions makes it possible to base most of the content in this chapter on the model derived in Figure 4-50 and Equations [4.53] and [4.54]. However, in the context of transient dynamics it is more relevant to use the model for more violent manoeuvres, and also active control such as ESC interventions. Hence, we extend the model in two ways:

- The constitutive relation is saturated, to reflect that each axle may reach friction limit, friction coefficient times normal load on the axle. See max functions in Equation [4.69].
- To be able to do mentioned limitation, the load transfer is modelled, but only in the simplest possible way using stiff suspension models. Basically it is the same model as given in Equation [3.20].
- A yaw moment representing (left/right) unsymmetrical braking/propulsion. See the term $M_{act,z}$ in yaw equilibrium in Equation [4.69].

It should be noted that the model still lacks some: Transients in load transfer and the reduced cornering stiffness and reduced max friction due to load transfer and utilizing friction for wheel longitudinal forces.

Equilibrium in road plane (longitudinal, lateral, yaw):

$$m \cdot (\dot{v}_x - \omega_z \cdot v_y) = F_{fxw} \cdot \cos(\delta_f) - F_{fyw} \cdot \sin(\delta_f) + F_{rx};$$
$$m \cdot (\dot{v}_y + \omega_z \cdot v_x) = F_{fxw} \cdot \sin(\delta_f) + F_{fyw} \cdot \cos(\delta_f) + F_{ry};$$
$$J \cdot \dot{\omega}_z = (F_{fxw} \cdot \sin(\delta_f) + F_{fyw} \cdot \cos(\delta_f)) \cdot l_f - F_{ry} \cdot l_r + M_{act,z};$$

Equilibrium out of road plane (vertical, pitch):

$$F_{fz} + F_{rz} - m \cdot g = 0;$$
$$-F_{fz} \cdot l_f + F_{rz} \cdot l_r - (F_{fxw} \cdot \cos(\delta_f) - F_{fyw} \cdot \sin(\delta_f) + F_{rx}) \cdot h = 0;$$

Constitution:

$$F_{fyw} = -\text{sign}(s_{fy}) \cdot \min(C_f \cdot |s_{fy}|; \ \mu \cdot F_{fz});$$
$$F_{ry} = -\text{sign}(s_{ry}) \cdot \min(C_r \cdot |s_{ry}|; \ \mu \cdot F_{rz});$$

Compatibility:

$$s_{fy} = \frac{v_{fyw}}{v_{fxw}}; \quad and \quad s_{ry} = \frac{v_y - l_r \cdot \omega_z}{v_x};$$

Transformation from vehicle to wheel coordinate system on front axle:

$$v_{fxw} = (v_y + l_f \cdot \omega_z) \cdot \sin(\delta_f) + v_x \cdot \cos(\delta_f);$$
$$v_{fyw} = (v_y + l_f \cdot \omega_z) \cdot \cos(\delta_f) - v_x \cdot \sin(\delta_f);$$

[4.69]

The model in Modelica format is given in Equation [4.70]. Changes compared to Equations [4.53] are marked as underlined code.

```
//Equilibrium, in road plane:
  m*(der(vx)-wz*vy) = Ffxv + Frx;
  m*(der(vy)+wz*vx) = Ffyv + Fry;
  J*der(wz) = Ffyv*lf - Fry*lr + Mactz;
//Equilibrium, out of road plane:
  Ffz + Frz - m*g = 0;
  -Ffz*lf + Frz*lr -(Ffxv + Frx)*h = 0;

//Compatibility:
  vfxv = vx;
  vfyv = vy + lf*wz;
  vrx = vx;
  vry = vy - lr*wz;

//Lateral tyre force model:
  Ffyw = -sign(sfy)*min(Cf*abs(sfy), mu*Ffz);
  Fry  = -sign(sry)*min(Cr*abs(sry), mu*Frz);
  sfy = vfyw/vfxw;
  sry = vry/vrx;

//Transformation between vehicle and wheel coordinate systems:
  Ffxv = Ffxw*cos(df) - Ffyw*sin(df);
  Ffyv = Ffxw*sin(df) + Ffyw*cos(df);
  vfxv = vfxw*cos(df) - vfyw*sin(df);
  vfyv = vfxw*sin(df) + vfyw*cos(df);

//Shaft torques
  Ffxw = +1000; // Front axle driven.
  Frx  = -100; // Rolling resistance on rear axle.
  Mactz=0;
```

[4.70]

A simulation of this model, with same steering input as used in Figure 4-51. $M_{act,z}$ is zero. Cornering stiffnesses are chosen so that the vehicle is understeered in steady state. Road friction coefficient is 1. We can see that the vehicle now gets instable and spins out with rear to the right. This is mainly because longitudinal load transfer unloads the rear axle, since the kept steering angle decelerates the vehicle. In this manoeuvre, it would have been reasonable to model also that the rear cornering stiffness decreases with the decreased rear normal load, and opposite on front. Such addition to the model would make the vehicle spin out even more. On the other hand, the longitudinal load shift is modelled to take place immediately. With a suspension model, this load shift would require some more time, which would calm down the spin-out. In conclusion, the manoeuvre is violent enough to trigger a spin-out, so a further elaboration with how to control $M_{act,z}$ could be of interest. However, it is beyond the scope of this compendium.

The vehicle reaches zero speed already after 7 seconds, because the wide side slip decelerates the vehicle a lot. The simulation is stopped at time=7 seconds, because the model cannot handle zero speed. That vehicle models become singular at zero speed is very usual, since the slip definition becomes singular due to zero speed in the denominator. The large difference compared to Figure 4-51 is due to the new constitutive equation used, which shows the importance of checking validity region for any model one uses.

```
//Compatibility:
```
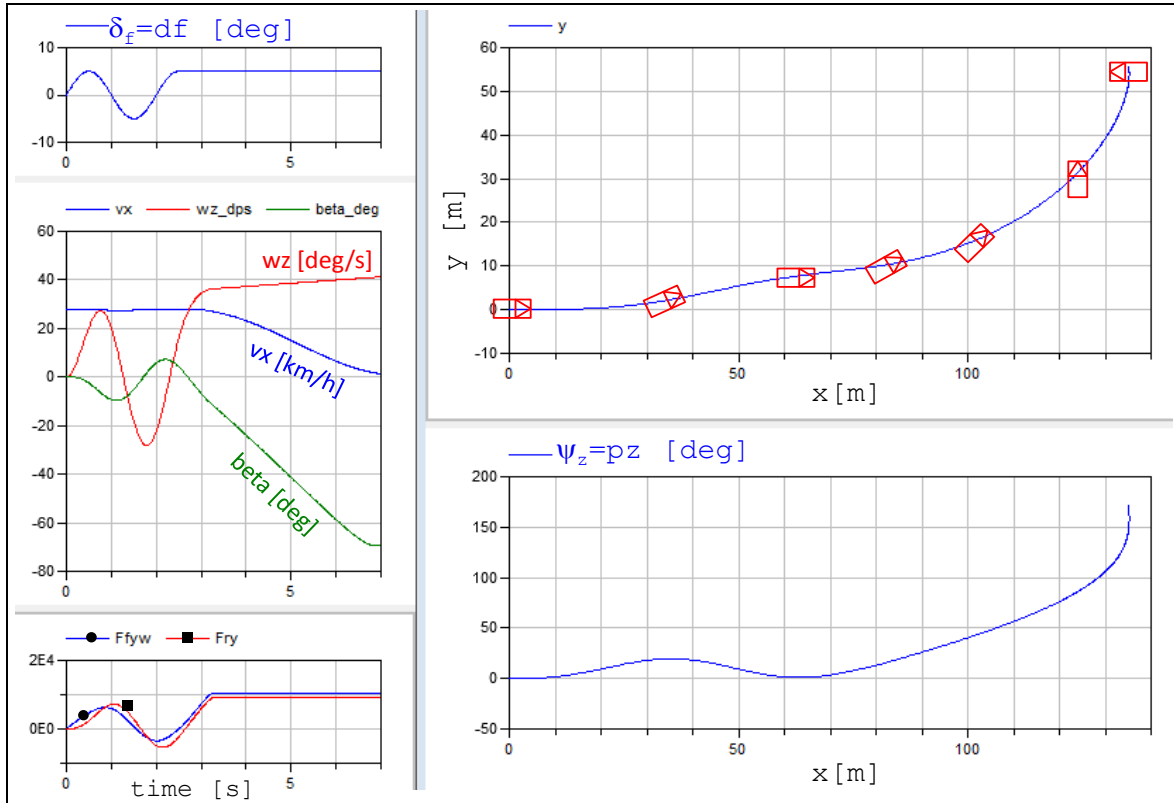
Figure 4-61: Simulation results of one-track model for transient dynamics. The vehicle drawn in the path plot is not in proper scale, but the orientation is approximately correct.

A simplified version of the mathematical model in Eq [4.69] follows in Eq [4.71]; assuming constant v_x and small angles and small propulsion force and no $M_{act,z}$.

Equilibrium in road plane (lateral, yaw):

$$m \cdot (\dot{v}_y + \omega_z \cdot v_x) = F_{fy} + F_{ry};$$
$$J \cdot \dot{\omega}_z = F_{fy} \cdot l_f - F_{ry} \cdot l_r;$$

Equilibrium out of road plane (vertical, pitch):

$$F_{fz} + F_{rz} - m \cdot g = 0;$$
$$-F_{fz} \cdot l_f + F_{rz} \cdot l_r = 0;$$

Constitution:

$$F_{fy} = -\text{sign}(s_{fy}) \cdot \min(C_f \cdot |s_{fy}|; \mu \cdot F_{fz});$$
$$F_{ry} = -\text{sign}(s_{ry}) \cdot \min(C_r \cdot |s_{ry}|; \mu \cdot F_{rz});$$

Compatibility:

$$\delta_f + s_{fy} = \frac{v_y + l_f \cdot \omega_z}{v_x}; \quad and \quad s_{ry} = \frac{v_y - l_r \cdot \omega_z}{v_x};$$

[4.71]

4.5.2.2 Transient models for articulated vehicles

A disclaimer to readers which only read the compendium, without following the course: This section might appear incomplete, while the course lectures and hand-out of model (Modelica model at course public web page) is more complete. Still, the description in compendium is regarded as relevant to give general feeling for the modelling challenges with articulated vehicles.

A model for a combination vehicle will now be derived. It is the simplest possible model; same type as in Equation [4.57] and Figure 4-52. It is drawn as car with trailer or rigid truck with centre-axle trailer, but with $l_{1c} < L_1$ it becomes a model of a tractor with semitrailer, which is a very common vehicle on our roads.
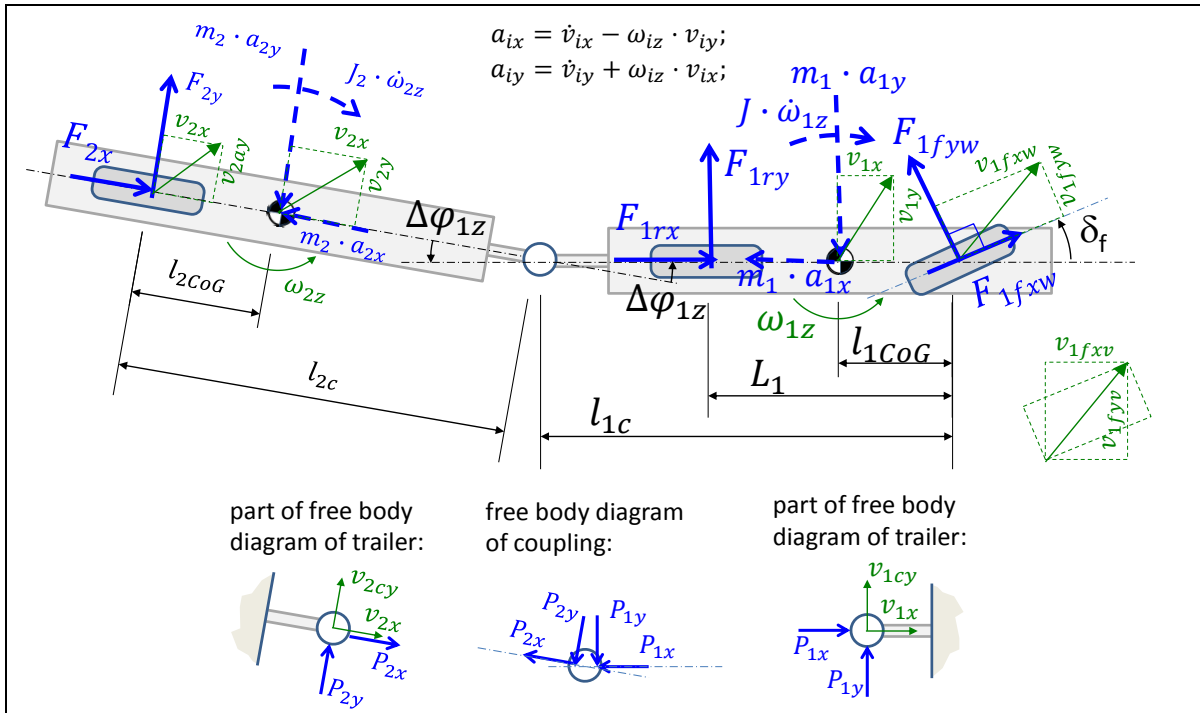
Figure 4-64: Model of two-unit articulated vehicle.

Model equations for the 1st unit:

In-road-plane Equilibrium of 1st unit (x,y,rotz):

$$m_1 \cdot (\dot{v}_{1x} - \omega_{1z} \cdot v_{1y}) = \cos(\delta_f) \cdot F_{1fxw} - \sin(\delta_f) \cdot F_{1fyw} + F_{1rx} + P_{1x};$$

$$m_1 \cdot (\dot{v}_{1y} + \omega_{1z} \cdot v_{1x}) = \sin(\delta_f) \cdot F_{1fxw} + \cos(\delta_f) \cdot F_{1fyw} + F_{1ry} + P_{1y};$$

$$J_1 \cdot \dot{\omega}_{1z} = (\sin(\delta_f) \cdot F_{1fxw} + \cos(\delta_f) \cdot F_{1fyw}) \cdot l_{1CoG} - F_{1ry} \cdot (L_1 - l_{1CoG}) - P_{1y} \cdot (l_{1c} - l_{1CoG});$$

Compatibility, within 1st unit:

$$v_{1fyw} = -\sin(\delta_f) \cdot v_{1x} + \cos(\delta_f) \cdot v_{1fyv};$$

$$v_{1fyv} = v_{1y} + \omega_{1z} \cdot l_{1CoG};$$

$$v_{1ry} = v_{1y} - \omega_{1z} \cdot (L_1 - l_{1CoG});$$

$$v_{1cy} = v_{1y} - \omega_{1z} \cdot (l_{1c} - l_{1CoG});$$

Constitution for axles on 1st unit:

$$F_{1fyw} = -C_{1f} \cdot s_{1fy}; \quad s_{1fy} = \frac{v_{1fyw}}{v_{1x}};$$

$$F_{1ry} = -C_{1r} \cdot s_{1ry}; \quad s_{1ry} = \frac{v_{1ry}}{v_{1x}};$$

[4.73]

Model equations for the 2nd unit:

Equilibrium of 2nd unit (x,y,rotz):

$$m_2 \cdot (\dot{v}_{2x} - \omega_{2z} \cdot v_{2y}) = F_{2x} + P_{2x};$$

$$m_2 \cdot (\dot{v}_{2y} + \omega_{2z} \cdot v_{2x}) = F_{2y} + P_{2y};$$

$$J_2 \cdot \dot{\omega}_{2z} = -F_{2y} \cdot l_{2CoG} + P_{2y} \cdot (l_{2c} - l_{2CoG});$$

Compatibility, within 2nd unit:

$$v_{2ay} = v_{2y} - \omega_{2z} \cdot l_{2CoG};$$

$$v_{2cy} = v_{2y} + \omega_{2z} \cdot (l_{2c} - l_{2CoG});$$

Constitution for axles on 2nd unit:

$$F_{2y} = -C_2 \cdot s_{2y}; \quad s_{2y} = \frac{v_{2ay}}{v_{2x}};$$

[4.74]

Model equations for the coupling:

Equilibrium of coupling (x,y in 1st unit's coordinates):

$$P_{1x} + \cos(\Delta\varphi_{1z}) \cdot P_{2x} + \sin(\Delta\varphi_{1z}) \cdot P_{2y} = 0;$$

$$P_{1y} - \sin(\Delta\varphi_{1z}) \cdot P_{2x} + \cos(\Delta\varphi_{1z}) \cdot P_{2y} = 0;$$

Compatibility of coupling:

$$v_{1x} = +\cos(\Delta\varphi_{1z}) \cdot v_{2x} + \sin(\Delta\varphi_{1z}) \cdot v_{2cy};$$

$$v_{1cy} = -\sin(\Delta\varphi_{1z}) \cdot v_{2x} + \cos(\Delta\varphi_{1z}) \cdot v_{2cy};$$

$$\Delta\dot{\varphi}_{1z} = \omega_{1z} - \omega_{2z};$$

[4.75]

Let us assume $\delta_f; F_{1fxw}; F_{1rxw}; F_{2x}$ are known inputs. The above is then a DAE system in Equations [4.73].. [4.75] with 19 equations and 19 unknowns: $v_{1x}; v_{1y}; \omega_{1z}; v_{2x}; v_{2y}; \omega_{2z}; \Delta\varphi_{1z}; F_{1fyw}; F_{1ry}; F_{2y}; s_{1fy}; s_{1ry}; s_{2y}; v_{1cy}; v_{2cy}; P_{1x}; P_{1y}; P_{2x}; P_{2y}$. The equations can be written directly into a Modelica tool, which will find the explicit form and simulations can be done. The use of a Modelica tool is much more motivated here, compared to a non-articulated vehicle, since the articulation points makes the DAE system of equation to be of "higher index", meaning that some equations needs to be differentiated, cf. Section 3.3.2.

4.5.2.2.1 Model library for articulated vehicles

The first model (Eqs [4.73].. [4.75]) for articulated vehicle is written so that each equation belongs to either a unit or a coupling. This opens up for systematic treatment of combination vehicles with more than one articulation point. There are basically two conceptual ways:

- Vectorised formulation, see Reference (Sundström, o.a., 2014).
- Modular library from which parts can be graphically dragged, dropped and connected. This is briefly visualized as implemented in the Modelica-tool Dymola in Figure 4-66.

4.5.2.2.1.1 Modular library

A modular library is shown in Figure 4-66. Eq [4.73] is declared in "Unit" and Eq [4.75] in "Coupling".
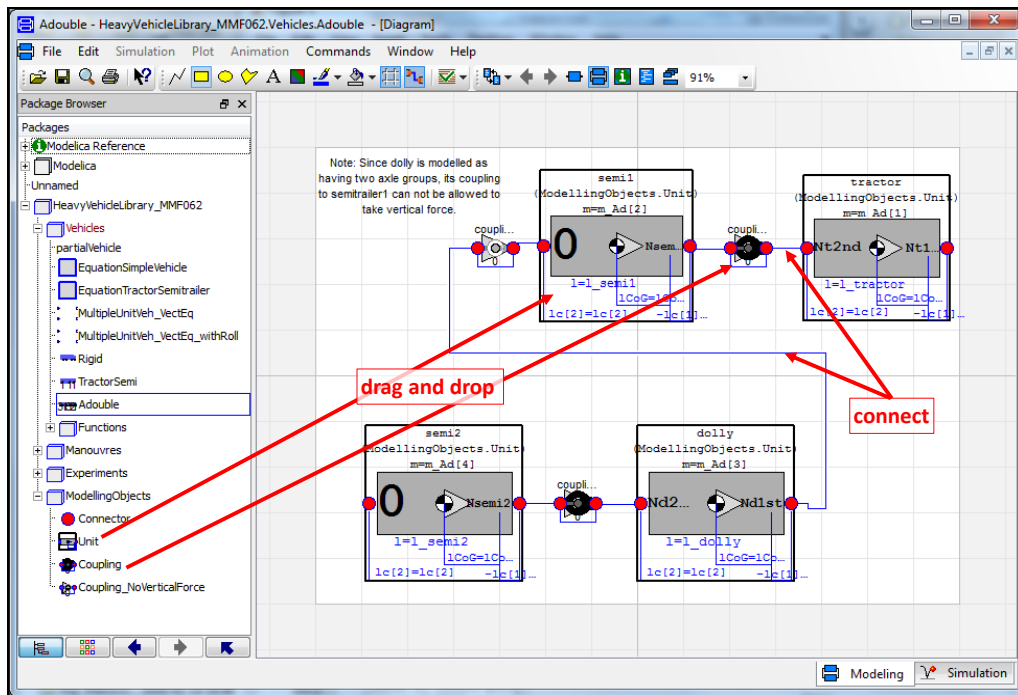
Figure 4-66: Drag, drop and connect library for heavy combination vehicles. The model example show a so called A-double, Tractor+Semitrailer+Dolly+Semitrailer.

An example of lane change manoeuvre, defined as lateral acceleration on 1st axle follows a single sine-wave, is shown in Figure 4-67. The natural input would be steering angle ($\delta_f = \sin(time)$;), but since modelled in Modelica, it is as easy to prescribe lateral acceleration ($a_{f1y} = \sin(time)$;). The Modelica tool will find the inverse model and the required steering angle, δ_f, will be an output.
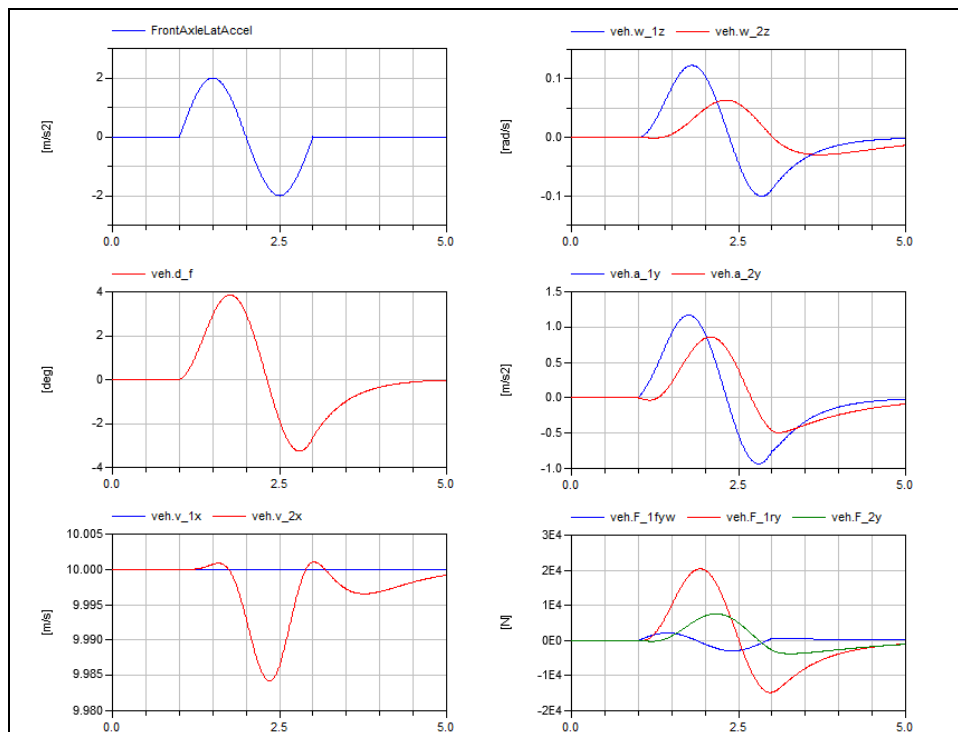
Figure 4-67: One period sinus test of a Tractor+Semitrailer.

4.5.2.3 Cambering vehicle model

The model below shows how a cambering vehicle can be modelled. The model is mainly made for lateral dynamics, but it allows also longitudinal acceleration. The drawing shows a two-wheeler, but any or both of the axles could have two wheels, as long as the suspension linkage is such that the axle does not take any roll moment. The model is shown in Eq [4.78] in Modelica format. It is not modelled that driver moves within the vehicle, which is why the inertial data is constant. Also, the chassis (frame) is modelled as stiff and steering system as massless. The model lacks two equations, which is logical since a driver model can add prescribed steering angle and prescribed F_{rx}.
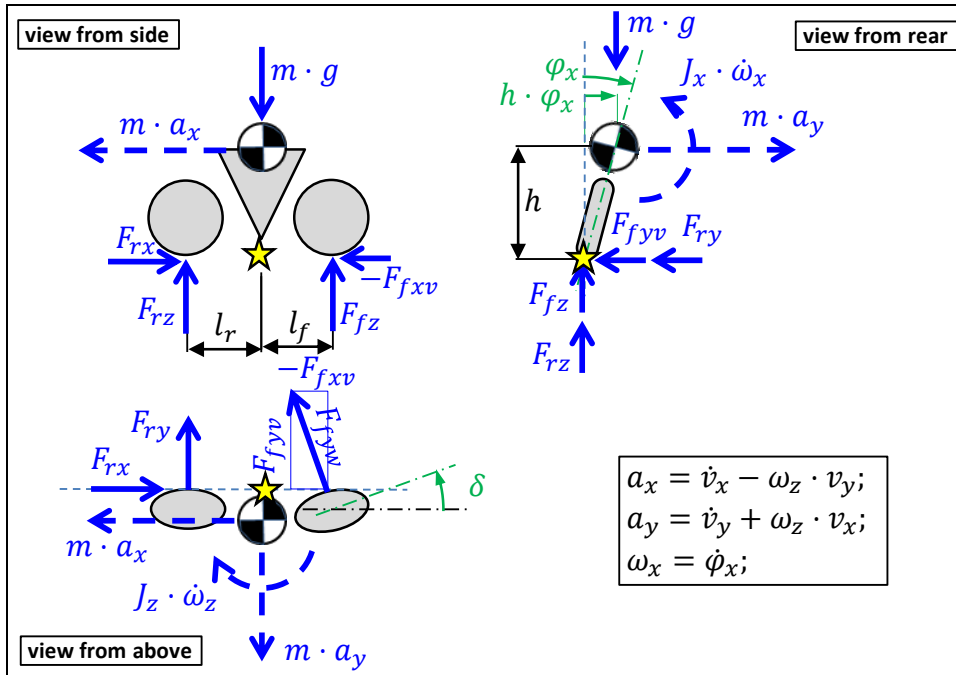
Figure 4-68: Model of cambering vehicle. (The stars marks point of moment equilibria in the "mathematical model" derived from this "physical model".)

```
//Equilibrium in road plane (x,y,rotz):
m*ax = Ffxv + Frx;
m*ay = Ffyv + Fry;
Jz*der(wz) = Ffyv*lf - Fry*lr - m*ax*h*px;
ax = der(vx) - wz*vy;
ay = der(vy) + wz*vx;

//Equilibrium out of road plane (z, rotx, roty):
m*g = Ffz + Frz;
Jx*der(wx) = m*g*h*px + m*ay*h;
0 = -Ffz*lf + Frz*lr - m*ax*h;
wx = der(px);

//Constitution:
Ffyw = -CC*Ffz*sfy;
Fry = -CC*Frz*sry;

//Compatibility, slip definition:
atan(sfy) = atan2(vy + lf*wz + h*wx, vx - h*px*wz) - d;
atan(sry) = atan2(vy - lr*wz + h*wx, vx - h*px*wz) - 0;

//Force coordinate transformation:
Ffxv = -Ffyw*sin(d);
Ffyv = +Ffyw*cos(d);
```

[4.78]

When entering a constant radius curve from straight driving one has to first steer out of the curve to tilt the vehicle a suitable amount for the coming path curvature, R_p. The suitable amount is hence

$\varphi_{x,suitable} = -a_y/g = -\omega_z \cdot v_x/g = -v_x^2/(R_p \cdot g)$;. Then one steers with the turn and balances (closed loop controls) to the desired roll angle. Systems like this, which has to be operated in opposite direction initially is called "Non-minimum phase systems". It is generally difficult to design a controller for such systems. The two simulations shown in Figure 4-85 are done with the above model. Initial speed is $v_x = 10\ m/s$ and $F_{rx} = 0$. Path radius, $R_p(t) = step\ function\ at\ t = 0.1$, representing a suddenly curving road or path.

- One simulation (veh_driver) uses a closed loop driver model which first steers outwards ($\delta < 0$) and then continuously calculates the steering angle as a closed loop controller: $\delta = Gain \cdot (\varphi_{x,req} - \varphi_x)$;. It is not claimed that the driver model is representative for real drivers.
- In the other simulation (veh_inverse), the roll angle is prescribed as $\varphi_x = -v_x^2/(R_p \cdot g)$;. To prescribe the roll angle, instead of steering angle, is a way to avoid the "Non-minimum phase" difficulties. The system becomes a normal Minimum phase system if actuated with roll angle instead of steering angle. The price one have to pay for this is that the model equations has to go through a more advanced symbolic manipulation, e.g. differentiation, to solve for all variables, including the steering angle δ. However, with a Modelica tool the symbolic manipulation is done automatically. One can see this as a way to avoid a controller design and instead use an optimal driver; optimal in the sense that it follows the path curvature with optimal yaw agility. The road path curvature is a step function, but has to be filtered twice (time constant 0.1 s is used in Figure 4-85) to become differentiable.

The latter, optimal driver, negotiates the turn without overshot in yaw rate, so it follows a suddenly curving path better.
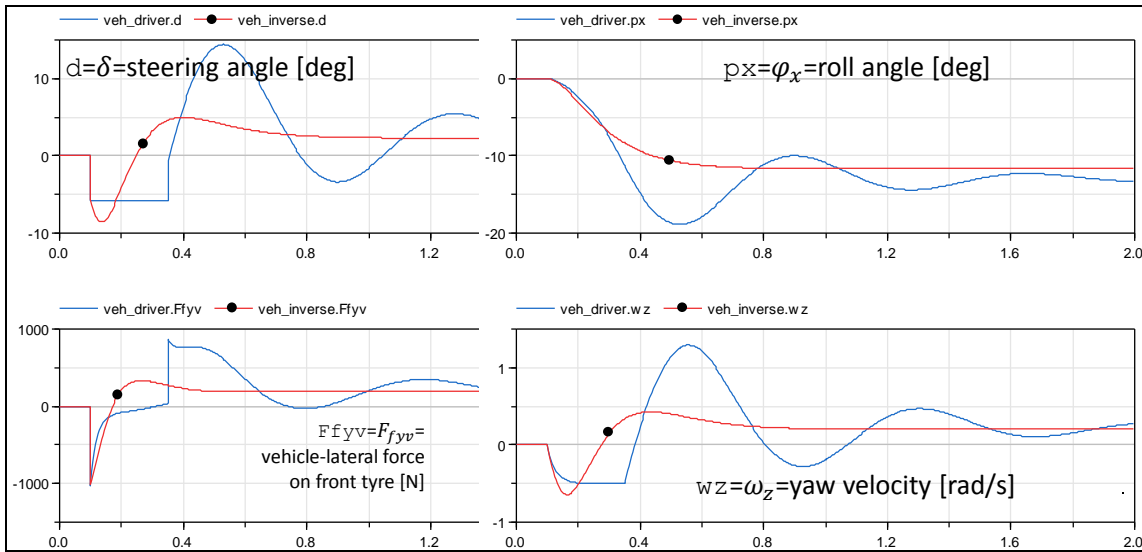
Figure 4-69: Simulations of entering a curve with a cambering vehicle. Blue solid curves without dot-marker show a closed-loop driver model which actuates δ. Red curves with dot-marker shows an optimal/inverse driver model which actuates φ$_x$.

Both driver models above only exemplifies the low-level, roll-balancing, part of a driver. To run the model in an environment with obstacles, one would also need a high-level, path selecting, part which outputs desired, e.g., δ or φ_x. Additional driver model for longitudinal actuation is also needed.

It can be noted that the roll influences in two ways, compared to the non-cambering (roll-stiff) vehicles previously modelled in the compendium:

- The roll motion itself is a dynamic motion, where the roll velocity becomes a state variable carrying kinetic energy.
- The roll influences the tyre slip, e.g. rear: $s_{ry} = (v_y - l_r \cdot \omega_z + h \cdot \omega_x)/(v_x - h \cdot \varphi_x \cdot \omega_z)$;. The term $h \cdot \omega_x$ can generally be neglected for non-cambering vehicles, but for a cambering vehicle,

such as a bike, it is essential. The term $h \cdot \varphi_x \cdot \omega_z$ is only important at large roll angles, it is for instance used as lever for longitudinal wheel forces in ESC-like control systems for motorbikes.

4.5.3 Transient model, with Lateral load transfer

In model of longitudinal load transfer in Section 3.3.9, we assumed instantaneous load transfer. In present chapter we aim to capture the transients better.

4.5.3.1 (Example of) Mathematical model; two-axle vehicle

Compared to the model presented in Figure 4-40 and Equations [4.39]..[4.45], we add the following:

- Inertial term for roll rotation, i.e. $J_{sx} \cdot \dot{\omega}_x$. Note that sprung body roll inertia ($J_{s,x}$), not whole vehicle roll inertia (J_x), is used in roll equilibrium because the unsprung parts does not participate in roll motion.
- Damping forces in parallel to each spring force, i.e. adding F_{dfl}, F_{dfr}, F_{drl}, and F_{drr}.

Due to the axle roll centre model, as opposed to wheel pivot point model, the heave acceleration is zero. Hence, no inertial force $m \cdot a_z$ needs to be introduced.

The free-body diagrams are given in Figure 4-70, which should be compared to Figure 4-40.
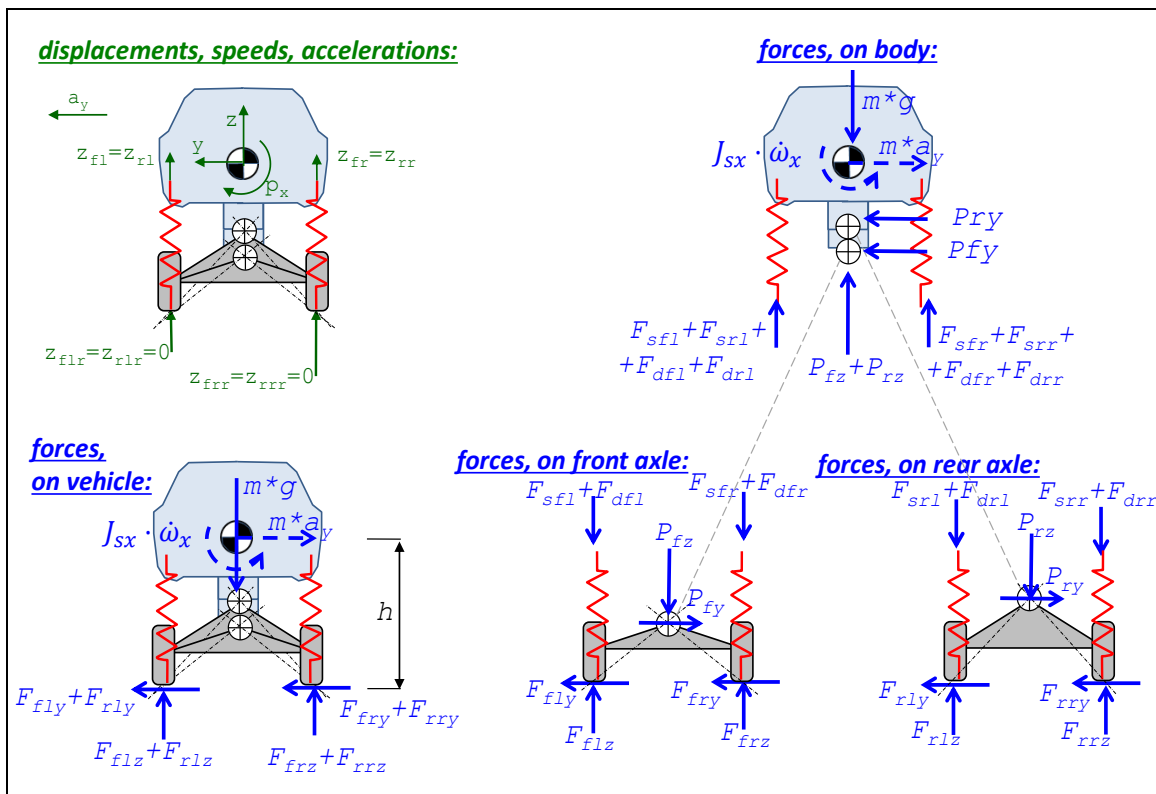
Figure 4-70: Model for transient load transfer due to lateral acceleration, using axle roll centres.

The constitutive equations for the compliances (or springs) are as follows, see Equation [4.38]. Note that the anti-roll bars are not modelled. Note also that we differentiate, since we will later use the spring forces as state variables in a simulation.

$$F_{sfl} = F_{sfl0} + c_{fw} \cdot (z_{flr} - z_{fl}); \Rightarrow \dot{F}_{sfl} = -c_{fw} \cdot \dot{z}_{fl} = -c_{fw} \cdot v_{flz};$$
$$F_{sfr} = F_{sfr0} + c_{fw} \cdot (z_{frr} - z_{fr}); \Rightarrow \dot{F}_{sfr} = -c_{fw} \cdot \dot{z}_{fr} = -c_{fw} \cdot v_{frz};$$
$$F_{srl} = F_{srl0} + c_{rw} \cdot (z_{rlr} - z_{rl}); \Rightarrow \dot{F}_{srl} = -c_{rw} \cdot \dot{z}_{rl} = -c_{rw} \cdot v_{rlz};$$
$$F_{srr} = F_{srr0} + c_{rw} \cdot (z_{rrr} - z_{rr}); \Rightarrow \dot{F}_{srr} = -c_{rw} \cdot \dot{z}_{rr} = -c_{rw} \cdot v_{rrz};$$
$$where\ F_{sfl0} = F_{sfr0} = \frac{m \cdot g \cdot l_r}{2 \cdot L};\ and\ F_{srl0} = F_{srr0} = \frac{m \cdot g \cdot l_f}{2 \cdot L};$$

[4.79]

The constitutive equations for the dampers have to be added:

$$F_{dfl} = -d_{fw} \cdot v_{flz};$$
$$F_{dfr} = -d_{fw} \cdot v_{frz};$$
$$F_{drl} = -d_{rw} \cdot v_{rlz};$$
$$F_{drr} = -d_{rw} \cdot v_{rrz};$$

[4.80]

As comparable with Equation [4.39], we get the next equation to fulfil the equilibrium. The change compared to Equation [4.39] is that we also have a roll and lateral inertia terms and 4 damper forces, acting in parallel to each of the 4 spring forces. Actually, when setting up equations, we also understand that a model for longitudinal load transfer is needed, which is why the simplest possible such, which is the stiff suspension on in Equation [3.20].

In-road-plane: Equilibrium for vehicle (longitudinal, lateral, yaw):

$$m \cdot a_x = m \cdot (\dot{v}_x - \omega_z \cdot v_y) = F_{fx} + F_{rx};$$
$$m \cdot a_y = m \cdot (\dot{v}_y + \omega_z \cdot v_x) = F_{fy} + F_{ry};$$
$$J_z \cdot \dot{\omega}_z = F_{fy} \cdot l_f - F_{ry} \cdot l_r;$$

Out-of-road-plane: Equilibrium for vehicle (vertical, pitch, roll):

$$F_{flz} + F_{frz} + F_{rlz} + F_{rrz} - m \cdot g = 0;$$
$$-(F_{flz} + F_{frz}) \cdot l_f + (F_{rlz} + F_{rrz}) \cdot l_r - (F_{fx} + F_{rx}) \cdot h = 0;$$
$$J_{s,x} \cdot \dot{\omega}_x = (F_{flz} + F_{rlz}) \cdot \frac{w}{2} - (F_{frz} + F_{rrz}) \cdot \frac{w}{2} + (F_{fy} + F_{ry}) \cdot h;$$

Equilibrium for each axle (pitch, around roll centre):

$$\left(F_{flz} - (F_{sfl} + F_{dfl})\right) \cdot \frac{w}{2} - \left(F_{frz} - (F_{sfr} + F_{dfr})\right) \cdot \frac{w}{2} + F_{fy} \cdot h_{RCf} = 0;$$
$$\left(F_{rlz} - (F_{srl} + F_{drl})\right) \cdot \frac{w}{2} - \left(F_{rrz} - (F_{srr} + F_{drr})\right) \cdot \frac{w}{2} + F_{ry} \cdot h_{RCr} = 0;$$

[4.81]

Compatibility gives, keeping in mind that ω_x is the only non-zero out-of road plane velocity (i.e. $\dot{z} = \omega_y = 0$):

$$\dot{z}_{fl} = v_{flz} = +\frac{w}{2} \cdot \omega_x;\ and\ \dot{z}_{fr} = v_{frz} = -\frac{w}{2} \cdot \omega_x;$$
$$\dot{z}_{rl} = v_{rlz} = +\frac{w}{2} \cdot \omega_x;\ and\ \dot{z}_{rr} = v_{rrz} = -\frac{w}{2} \cdot \omega_x;$$

[4.82]

Constitution for tyre forces versus slip in ground plane becomes per wheel, as opposed to per axle in previous model:

$$F_{fyw} = -\text{sign}(s_{fy}) \cdot \left(\min\left(\frac{C_f}{2} \cdot |s_{fy}|; \mu \cdot F_{flz}\right) + \min\left(\frac{C_f}{2} \cdot |s_{fy}|; \mu \cdot F_{frz}\right)\right);$$
$$F_{ry} = -\text{sign}(s_{ry}) \cdot \left(\min\left(\frac{C_r}{2} \cdot |s_{ry}|; \mu \cdot F_{rlz}\right) + \min\left(\frac{C_r}{2} \cdot |s_{ry}|; \mu \cdot F_{rrz}\right)\right);$$

[4.83]

Equations [4.79]..[4.83] give a model very similar to the one in Equation [4.70]. Only the additional equations from this new model are shown in Equation [4.84]. Note especially the new lateral tyre force model equations, which now have one term per wheel, because one wheel on an axle can saturate independent of the other on the same axle.

```
//Equilibrium, roll
  Jsx*der(wx) = (Fflz + Frlz)*w/2 - (Ffrz + Frrz)*w/2 + (Ffyv + Fry)*h;
//Equilibrium for each axle (pitch, around roll centre):
  (Fflz - (Fsfl + Fdfl))*w/2 - (Ffrz - (Fsfr + Fdfr))*w/2 + Ffy*hRCf = 0;
  (Frlz - (Fsrl + Fdrl))*w/2 - (Frrz - (Fsrr + Fdrr))*w/2 + Fry*hRCr = 0;

//Constitutive relation for tyres (Lateral tyre force model):
  Ffyw = -
sign(sfy)*(min((Cf/2)*abs(sfy), mu*Fflz) + min((Cf/2)*abs(sfy), mu*Ffrz));
  Fry  = -
sign(sry)*(min((Cr/2)*abs(sry), mu*Frlz) + min((Cr/2)*abs(sry), mu*Frrz));
  sfy = vfyw/vfxw;
  sry = vry/vrx;
//Constitution for springs:
  der(Fsfl) = -cfw*vflz;
  der(Fsfr) = -cfw*vfrz;
  der(Fsrl) = -crw*vrlz;
  der(Fsrr) = -crw*vrrz;
//Constitution for dampers:
  Fdfl = -dfw*vflz;
  Fdfr = -dfw*vfrz;
  Fdrl = -drw*vrlz;
  Fdrr = -drw*vrrz;

//Compatibility, out of road plane:
  vflz = +w/2*wx;
  vfrz = -w/2*wx;
  vrlz = +w/2*wx;
  vrrz = -w/2*wx;
```

[4.84]

A simulation of this model should be compared with the simulation in Figure 4-51. When comparing these, we see a slight difference, which is that the axles saturate gradually during 3<time<3.5, instead of both at once at time=3.25.

Even if the load transfer model does not influence the vehicle path a lot in this case, it may be important to include it to validity check the model through checking wheel lift. Wheel lift can be identified as negative vertical wheel forces, which are why we plot some vertical wheel forces, see Figure 4-72. In this case we see that we have no wheel lift (which would disqualify the simulation). In the right part of the figure we can also see the separate contribution from spring (F_{srr}), damper (F_{drr}) and linkage ($F_{link}, f_{l,z} = F_{flz} - F_{sfl} - F_{dfl}$).

4.5.3.1.1 Additional phenomena

It is relevant to point out the following, which are not modelled in this compendium:

- Same as pointed out as missing for longitudinal load transfer, see Section 3.4.9.5.
- Additionally, anti-roll arrangements (elastic connections between left and right wheel on one axle, often built as torsion bar) are not modelled in this compendium. With same modelling concept as used above, each such would be treated as a separate spring with one state variable, e.g. F_{af} (Force-antiroll-front). This force will act in parallel with F_{sf} and F_{df} on each side. Note that it will be added on one side and subtracted on the other.
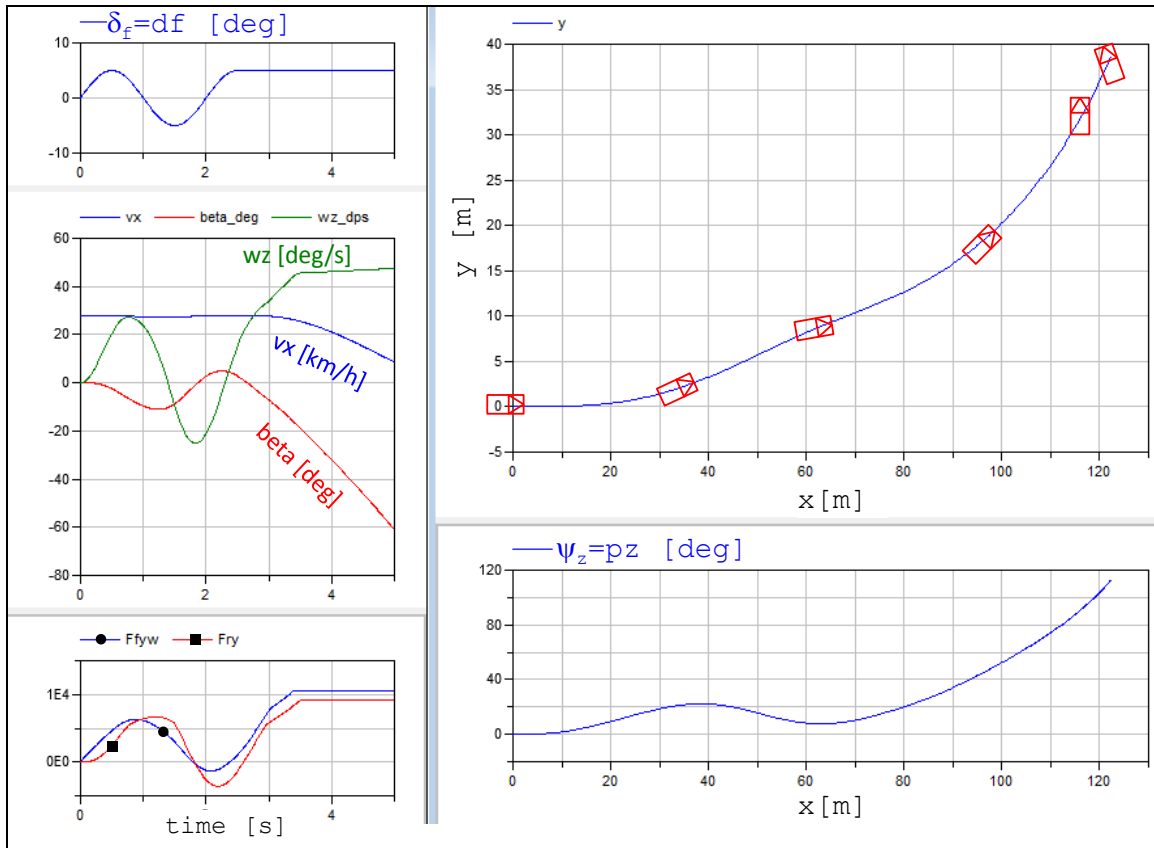
Figure 4-71: Simulation results of one-track model for transient dynamics with lateral load transfer dynamics. The vehicle drawn in the path plot is not in proper scale, but the orientation is approximately correct.
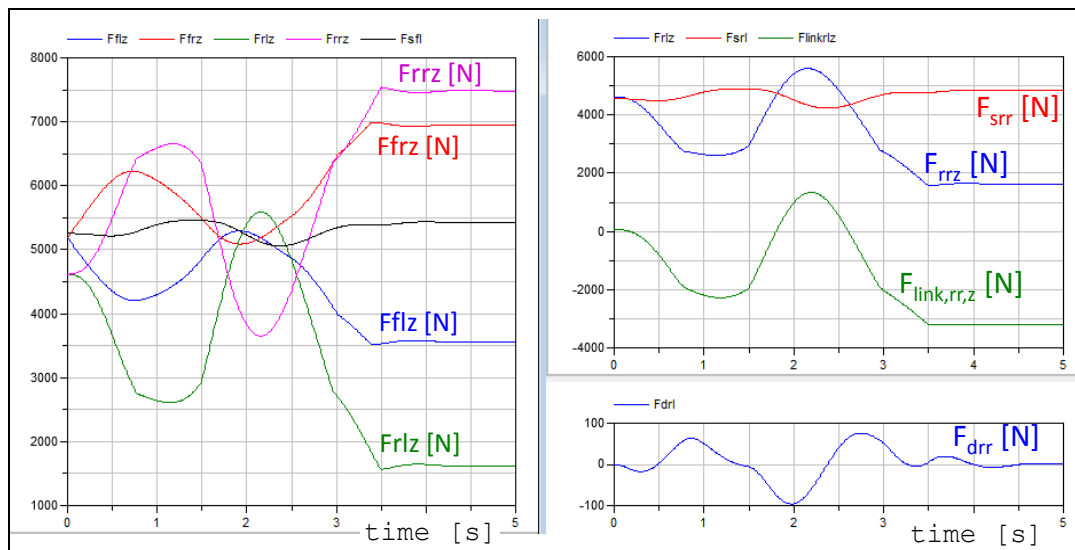
Figure 4-72: Suspension vertical force plots from simulation with one-track model for transient dynamics with lateral load transfer dynamics (same simulation as in Figure 4-71). Left: Road contact forces for all wheels. Right: Different forces for one wheel, rear left.

4.5.3.2   (Example of) Explicit form model; two-axle vehicle, driver and environment

A disclaimer to readers which only read the compendium, without following the course: This section might appear incomplete, while the course lectures and hand-out of model (Simulink model at course public web page) is more complete. Still, the description in compendium is regarded as relevant to give general feeling for an Explicit form model.

The implementation of the model in Section 4.5.2.3 is done in Modelica. A Modelica tool (such as Dymola) automatically transforms the model to explicit form and automatically generates simulation code, which is very efficient. But, as mentioned in Section 1.5.7.5, explicit form models can sometimes facilitate the understanding of the vehicle's dynamics. This is why the following model is presented. It is implemented in the data flow diagram tool Simulink. This section explains how the **states** (or state variables) together with **inputs** (or input variables), influence the **derivatives** (or state derivatives).

The example model in this section is similar, but not identical, to the model in Section 4.5.2.3. The aim is to model in-road-plane motion, due to transient actuation (wheel torques and wheel steering angles). Limitations in this example model are:

- Influence from vertically uneven road is NOT modelled.
- Influence from varying road friction is NOT modelled.
- Wheel lift from ground is NOT modelled
- Hitting bump stop is NOT modelled
- Control functions (such as ABS, TC and ESC) are NOT modelled
- The pendulum effect is NOT modelled
- Wheel camber angle change with suspension travel is NOT modelled (Camber ≡ 0).
- Wheel steering angle change with suspension travel is NOT modelled (change ≡ 0).

The model is a typical two axle vehicle with interface to driver and environment, see Figure 4-73. The driver interface is the normal, 2 pedals and one steering wheel. The additional discrete request from driver, `LongDir` (=-1 or +1), is also needed to reflect whether driver requests forward or reverse longitudinal actuation. The interface to environment is motion (variable position) in surrounding world. To try out the vehicle model, driver and environment is also modelled. This includes also the interface between them, which is motion of obstacles in environment, relative to subject vehicle. The suspension is exemplified with wheel-individual suspension on both axles.
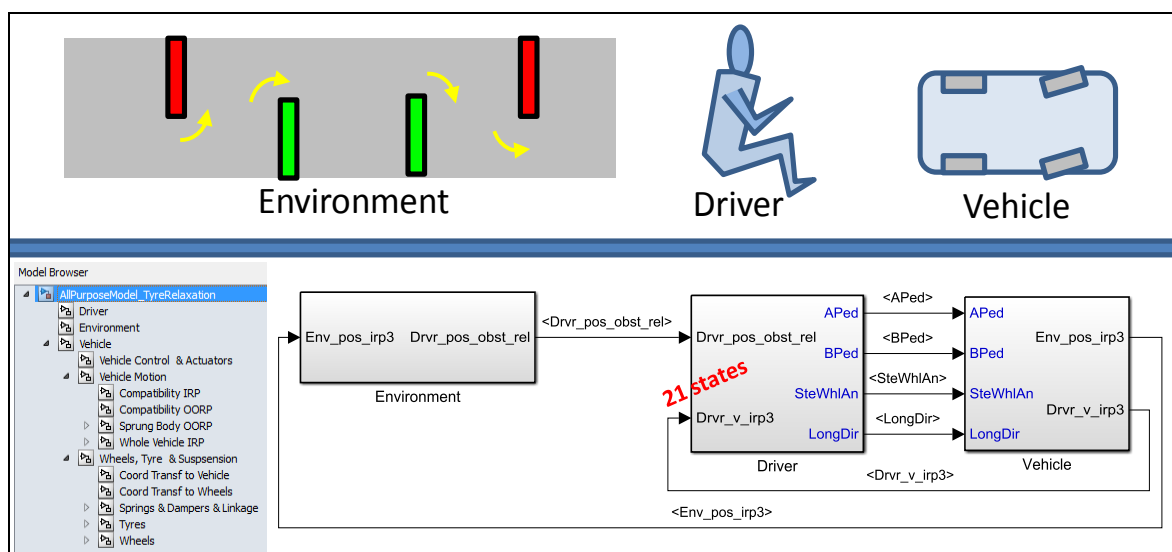
Figure 4-73: Top level of model with model tree structure. The Environment is a track test with cone walls to go left and right around. Notation "irp" and "oorp" refers to in-road-plane and out-of-road-plane, respectively.

As an initial overview, the states are presented. There are **21 states** in total, and distributed:

- <u>Driver</u>: 0 states
- <u>Vehicle</u>:
  - Vehicle Control & Actuation: 0 states
  - **Wheels, Tyres & Suspension: 12 states** (4 wheel rotational speed, 4 Elastic part of vertical wheel forces, 4 Longitudinal tyre forces, 4 Lateral tyre force)
  - **Vehicle Motion: 9 states** (6 velocities and 3 positions)
- <u>Environment</u>: 0 states

The 4+4 tyre force states arise from modelled tyre relaxation, see Section 2.6.5.

4.5.3.2.1 Submodel Environment

Generally, the environment model is where the surrounding to the driver and the vehicle should be defined: road/road network, obstacles, other road users and the "driving task"/"driving instructions". In this example, it is very small and simple; it only captures stand-still point obstacles, each with instructions whether to be passed as obstacle left or right of the vehicle. Inputs to environment model is the (subject) vehicles position, including orientation in global coordinates. Outputs are the relative position (x,y) to each obstacle, in (subject) vehicle coordinate system.

4.5.3.2.2 Submodel Driver

In this example, the driver model is very small and simple. Briefly described, it treats the longitudinal dynamics very simple, as closed loop control towards a constant desired speed forward. The lateral dynamics is divided into two parts:

- Driver planning: Based on how driver perceives the obstacles relative to the vehicle, one of the objects is selected to mind for, which leads to where to be aim. Basically, the nearest obstacle ahead of vehicle is selected as mind for and aim is, in principle, either half a vehicle width left (or right) of this obstacle.
- Driver operation: Based on the driver's motorics, the steering wheel angle is calculated. In the example, it is simply an inverse model of an ideally tracking two-axle vehicle which calculates which constant steering wheel angle that would be needed to make front axle run over the aim obstacle.

It can be noted that a Driver model would also be a logical model part where to include calculation of driver's perception, such as steering effort and perceived safety during manoeuvre, etc. It can also be noted that the border between Environment and Driver is sometimes not obvious, especially when it comes to modelling the "driving task" in the Environment model, which can also be seen as a "driver high-level decision" and then be a logical part of the Driver model. If Environment model includes surrounding vehicles (object vehicles), it also includes driver models for those. For automatic functionality, anything from cruise control to autonomous driving, there should also be a "button HMI output" from Driver model, not only pedals and steering wheel. Such interface would turn on/off such functionality in the Vehicle model.

4.5.3.2.3 Submodel Vehicle
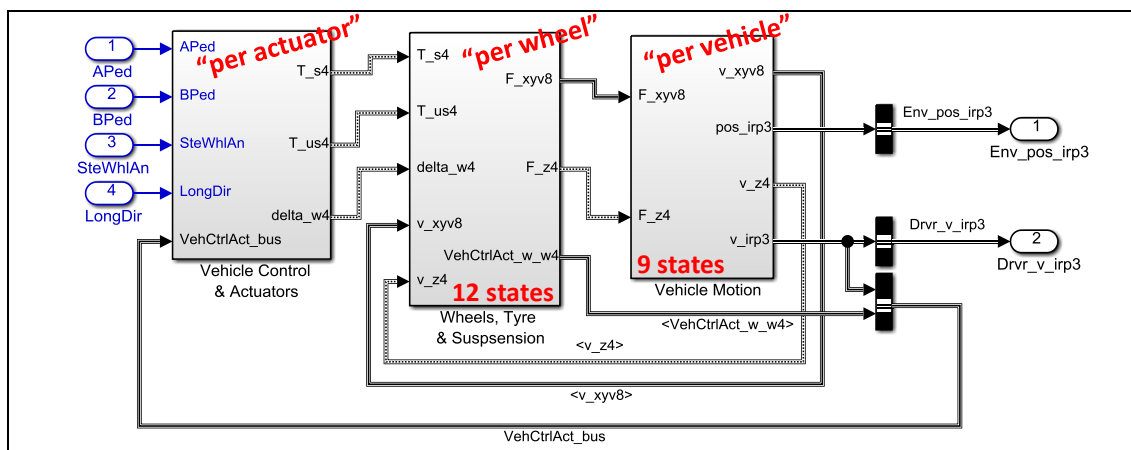
Figure 4-74: Vehicle submodel.

The figure shows the decomposition of the vehicle into 3 parts:

- Submodel **"Vehicle Control & Actuation"** models the actuators (Propulsion system, Brake system and Steering system, including "control functions") that respond on requests from the driver with wheel torques (`T_s` and `T_us`) and wheel steering angles (`delta_w`). The

notation ending "4" refers to that the quantities are vectors with 4 components, one per wheel. `T_s` is shaft torque and `T_us` is torque applied from unsprung parts, e.g. friction brake torque from brake calliper. One can think of very advanced models of these actuator systems, including e.g. propulsion system dynamics and control functions (ABS, ESC, TC, …). However, in this example model it is only modelled very simple:

- o Propulsion system outputs a fraction (determined by `APed`) of a certain maximum power, distributed equally on front left and front right wheel. If brake pedal is applied, the propulsion system outputs zero torque.
- o Brake system outputs a fraction (determined by `BPed`) of a maximum brake torque ($\mu \cdot m \cdot g / R_w$), distributed in a certain fix fraction between front and rear axle (70/30). The distribution within each axle is equal on left and right wheel.
- o There are **no states** modelled in the vehicle Control & Actuator submodel.

- Submodel **"Wheels, Tyre & Suspension"** models the part which pushes the tyres towards the ground and consequently transforms the wheel torques and wheel steering angles, via the tyre, to forces on the whole vehicle. `F_xyv8` is the x and y forces in each of the 4 wheels, 2x4=8. `F_z4` is the 4 vertical forces under each wheel. Submodel "Wheels, Tyre & Suspension" is **further explained** in Section 4.5.3.2.4.

- Submodel "**Vehicle Motion**" models motion of whole vehicle in-road-plane and motion of sprung body out-of-road-plane. The inertial effects (mass·acceleration) of the unsprung parts are taken into account for in-road-plane but not for out-of-road-plane. This submodel includes integrators for the 3+3+3=9 **states**:
  - o Velocities in-road-plane, v_x, v_y, ω_z: **`v_irp3`** (which is transformed to x- and y-velocities of each wheel and then fed back as `v_irpv8`)
  - o Position in-road-plane, x, y, φ_z: **`pos_irp3`** (which is only fed forward to "Environment")
  - o Velocities out-of-road-plane, v_z, ω_x, ω_y: **`v_oorp3`** (which is transformed to z-velocities of sprung body over each wheel and then fed back as `v_z4`)

4.5.3.2.4 Submodel Wheels, Tyres & Suspension
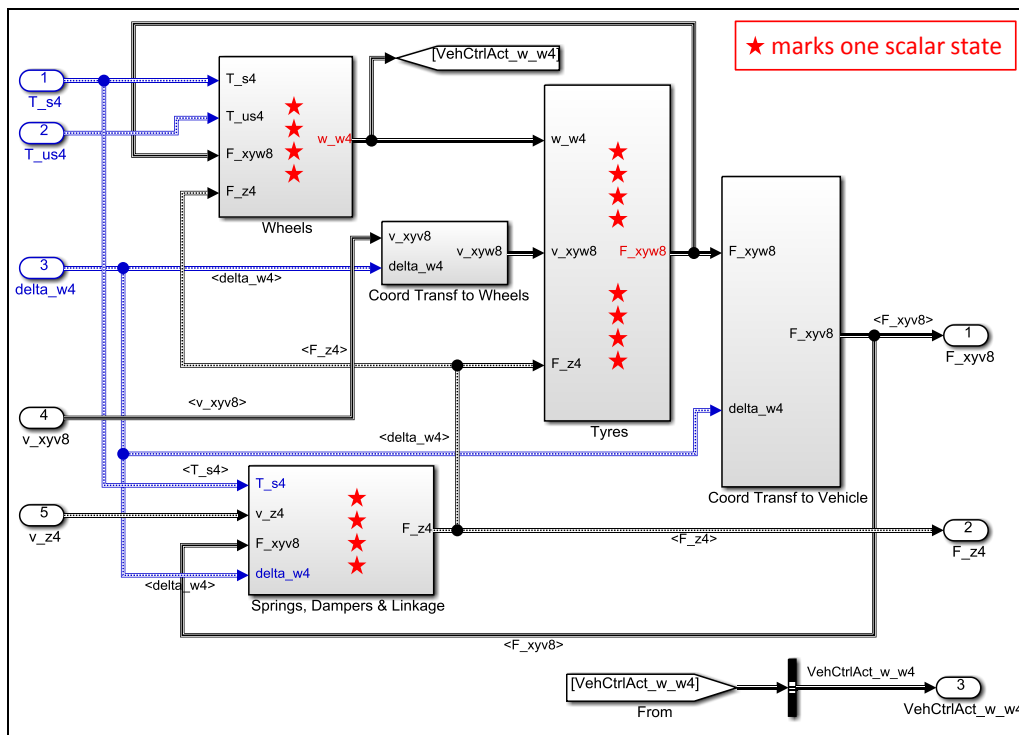
Figure 4-75: Wheels, Tyres & Suspension sub-model.

- The two sub-models "**Coord Transf …**" are straight-forward coordinate transformations, using Eq [4.3].
- The sub-model "**Wheels**" is also relatively straight-forward. For each wheel, the rotational equilibrium is used as model: $J \cdot \dot{\omega} = T_{us} + T_s - F_x \cdot R_w - \text{sign}(\omega) \cdot RRC \cdot F_z \cdot R_w$; where R_w is wheel radius and RRC is rolling resistance coeeficient. The submodel will hence contain the 4 **states**:
  - Rotational speeds of each wheel: **w_w4.**
- The sub-model "**Springs, Dampers & Linkage**" models the springs (incl. anti-roll-bars) and dampers and the linkage. For each wheel:
  - Four **states**: Elastic part of vertical tyre force under each wheel: **F_s4**
  - The derivatives are governed by the differentiated constitution of the springs: Conceptually $\dot{F}_s = -c \cdot v_z$; but involving both wheel spring and anti-roll-bar.
  - The force in damper is governed by the dampers constitutive relation: $F_d = -d \cdot v_z$;
  - The contact forces F_z are calculated in submodel "Suspension Equilibrium" in Figure 4-77. They are calculated from moment equilibrium of unsprung parts around a 3-dimensional pivot axis. The pivot axis is defined by two points, the pivot point in longitudinal load transfer (see Figure 3-45) and the pivot point in longitudinal load transfer (see Figure 4-39). The scalar equilibrium equation for one wheel can be expressed, with vector (cross) and scalar (dot) products, in $F_{xv}, F_{yv}, F_s, F_d, T_s, F_z$ and point coordinates. From this, F_z can be solved.
- The sub-model "**Tyres**" models the tyre mechanics, very much like the combined slip model in Equation [2.42] and the relaxation model in Equation [2.49]. For each wheel:
  - Four **states**: Magnitudes of tyre forces in ground plane (F_{xy}) for each wheel: **F_xyw4**
  - Unfortunately, the tyre forces F_x and F_y depend on F_z. This could easily create algebraic loops. However, since we also model relaxation, the tyre forces becomes state variables which breaks such algebraic loops. Another way of getting rid of the algebraic loops could have been to use "memory blocks". "Memories" are such that value from last time instant is used to calculate derivatives in present time instant. This is generally NOT a recommended way of modelling.
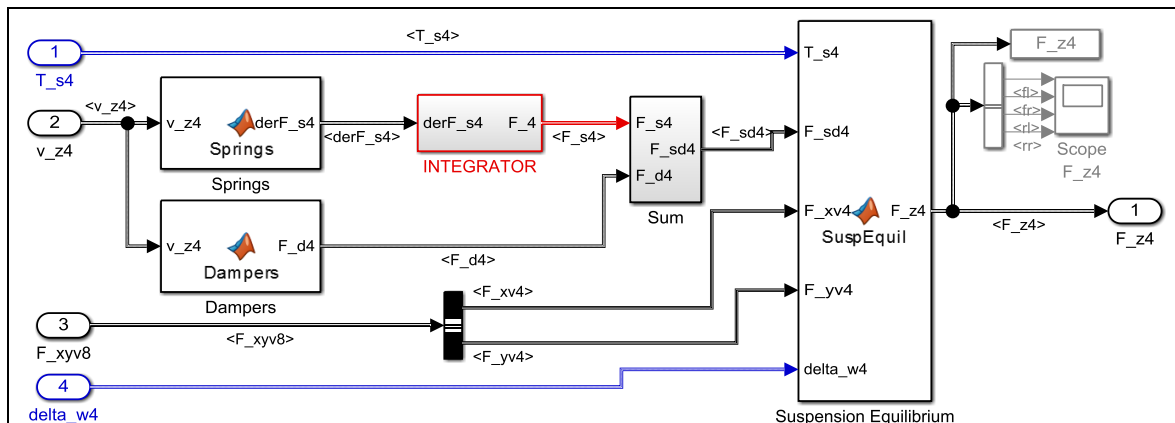
Figure 4-76: Sub-model "Springs, Dampers & Linkage" below.
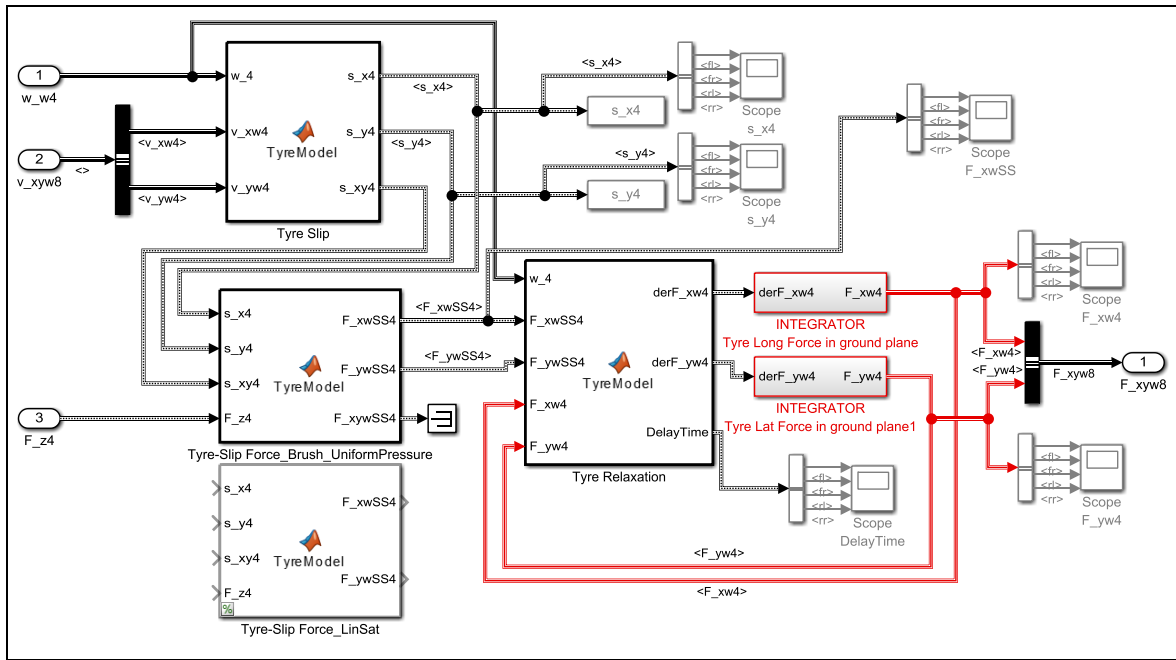
Figure 4-77: Sub-model "Tyres".

4.5.3.2.5 Sub-model Vehicle Motion

The sub-model is shown in Figure 4-78. It is divided in upper part in-road-plane (irp) and lower part out-of-road-plane (oorp). The velocities in road plane (v_irp3= $[v_x, v_y, \omega_z]$) is needed also in Sprung body OORP because of the centripetal term, $\omega_y \cdot v_x$, identified in Section 3.4.7 and used in 3.4.13.
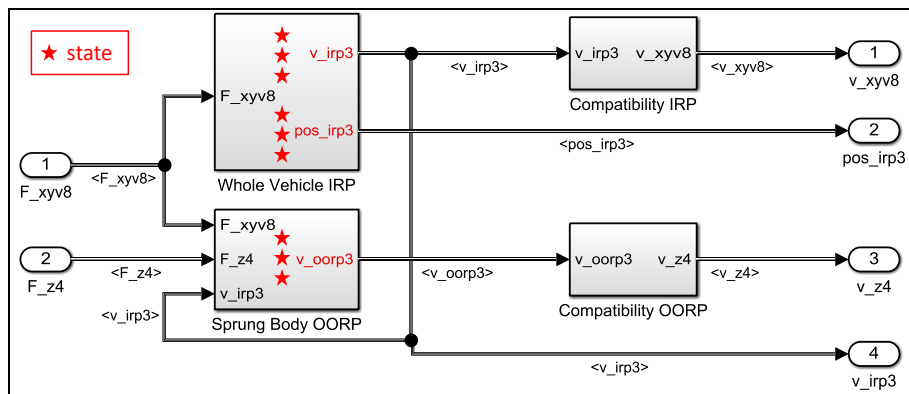
Figure 4-78: Vehicle Motion.

4.5.3.2.6 Simulation example Double Lane Change

A double lane change between cones is used as simulation example, see Figure 4-79. The cones are run over and even passed on the wrong side because the driver model is very simple.
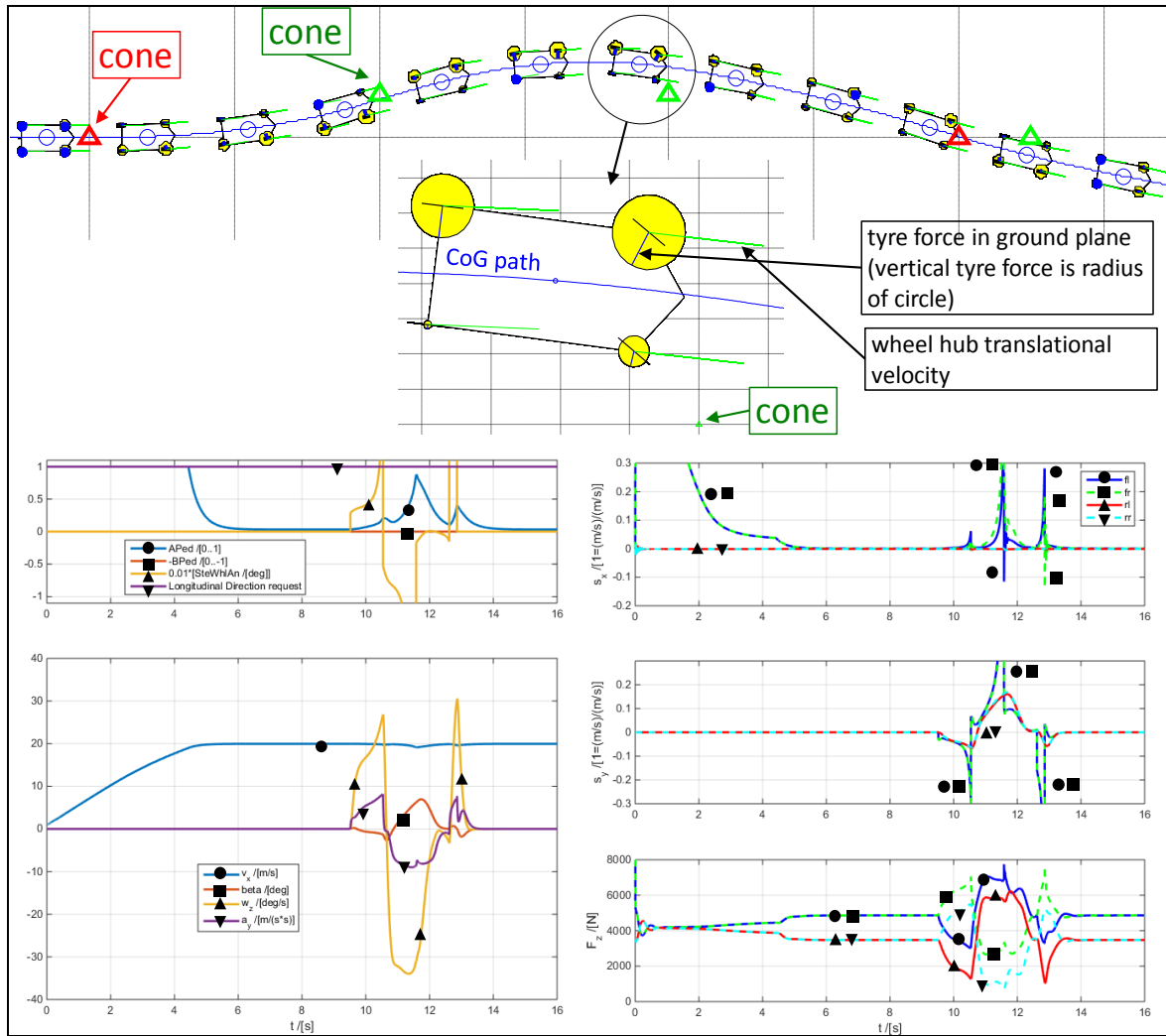
Figure 4-79: Simulation results of a double lane change between cones.

4.5.3.3   Transient roll-over *

Function definition: **Transient roll-over resistance** *is the most severe measure of a certain transient manoeuvre that the vehicle can manage without lifting all wheels on one side. The manoeuvre is typically on level ground with high road friction and certain payload, loaded high.*

The manoeuvre can typically be a double lane change, since the double triggers roll oscillations. The severity measure of the manoeuvre can be the peak lateral acceleration or a lane change width or longitudinal speed for given lane width.

4.5.4   Step steering response *

Function definition: **Step steering response** *is the response to a step in steering wheel angle measured in certain vehicle measures. The step is made from a certain steady state cornering condition to a certain steering wheel angle. The response can be the time history or certain measures on the time history, such as delay time and overshoot.*

4.5.4.1   Mild step steering response

This section is to be compared with section 4.5.4.2, which uses a more advanced model. In present section a less advanced model will be used, which is enough for small steering steps.

The model used for single frequency stationary oscillating steering can also be used for other purposes, as long as limited lateral accelerations. Most common interpretation is to make the steering step from an initial straight line driving. In reality, the step will be a quick ramp. Equation [4.60] allows an explicit solution prediction of stationary oscillating steering, but also for step response:

Start from **Equation [4.60]**: $\begin{bmatrix} \dot{v}_y \\ \dot{\omega}_z \end{bmatrix} = \mathbf{A} \cdot \begin{bmatrix} v_y \\ \omega_z \end{bmatrix} + \mathbf{B} \cdot \delta_f$;

With **initial conditions**: $\begin{bmatrix} v_y(0) \\ \omega_z(0) \end{bmatrix} = \begin{bmatrix} v_{y0} \\ \omega_{z0} \end{bmatrix}$; or $\begin{bmatrix} v_{y0} \\ \omega_{z0} \end{bmatrix} = -\mathbf{A}^{-1} \cdot \mathbf{B} \cdot \delta_{f0}$; where δ_{f0} is before step.

Assume: $\begin{bmatrix} v_y \\ \omega_z \end{bmatrix} = \begin{bmatrix} v_{y\infty} \\ \omega_{z\infty} \end{bmatrix} + \begin{bmatrix} \begin{bmatrix} \hat{v}_{y1} \\ \hat{\omega}_{z1} \end{bmatrix} & \begin{bmatrix} \hat{v}_{y2} \\ \hat{\omega}_{z2} \end{bmatrix} \end{bmatrix} \cdot \begin{bmatrix} e^{\lambda_1 \cdot t} & 0 \\ 0 & e^{\lambda_2 \cdot t} \end{bmatrix} \cdot \begin{bmatrix} a_1 \\ a_2 \end{bmatrix}$; $\Rightarrow$

$$\Rightarrow \begin{bmatrix} \dot{v}_y \\ \dot{\omega}_z \end{bmatrix} = \begin{bmatrix} \begin{bmatrix} \hat{v}_{y1} \\ \hat{\omega}_{z1} \end{bmatrix} & \begin{bmatrix} \hat{v}_{y2} \\ \hat{\omega}_{z2} \end{bmatrix} \end{bmatrix} \cdot \begin{bmatrix} \lambda_1 \cdot e^{\lambda_1 \cdot t} & 0 \\ 0 & \lambda_2 \cdot e^{\lambda_2 \cdot t} \end{bmatrix} \cdot \begin{bmatrix} a_1 \\ a_2 \end{bmatrix};$$

Insert: $\begin{bmatrix} \begin{bmatrix} \hat{v}_{y1} \\ \hat{\omega}_{z1} \end{bmatrix} & \begin{bmatrix} \hat{v}_{y2} \\ \hat{\omega}_{z2} \end{bmatrix} \end{bmatrix} \cdot \begin{bmatrix} \lambda_1 \cdot e^{\lambda_1 \cdot t} & 0 \\ 0 & \lambda_2 \cdot e^{\lambda_2 \cdot t} \end{bmatrix} \cdot \begin{bmatrix} a_1 \\ a_2 \end{bmatrix} =$

$$= \mathbf{A} \cdot \left(\begin{bmatrix} v_{y\infty} \\ \omega_{z\infty} \end{bmatrix} + \begin{bmatrix} \begin{bmatrix} \hat{v}_{y1} \\ \hat{\omega}_{z1} \end{bmatrix} & \begin{bmatrix} \hat{v}_{y2} \\ \hat{\omega}_{z2} \end{bmatrix} \end{bmatrix} \cdot \begin{bmatrix} e^{\lambda_1 \cdot t} & 0 \\ 0 & e^{\lambda_2 \cdot t} \end{bmatrix} \cdot \begin{bmatrix} a_1 \\ a_2 \end{bmatrix} \right) + \mathbf{B} \cdot \delta_f;$$

Solve for each time function term (constant, $e^{\lambda_1 \cdot t}$ and $e^{\lambda_2 \cdot t}$ terms):

$$\begin{bmatrix} v_{y\infty} \\ \omega_{z\infty} \end{bmatrix} = -\mathbf{A}^{-1} \cdot \mathbf{B} \cdot \delta_f; \quad and \quad \begin{bmatrix} \begin{bmatrix} \hat{v}_{y1} \\ \hat{\omega}_{z1} \end{bmatrix} & \begin{bmatrix} \hat{v}_{y2} \\ \hat{\omega}_{z2} \end{bmatrix} \end{bmatrix}, \begin{bmatrix} \lambda_1 & 0 \\ 0 & \lambda_2 \end{bmatrix} = \mathrm{eig}(\mathbf{A});$$

The function "eig" is identical to function "eig" in Matlab. It is defined as eigenvalues and eigenvectors for the matrix input argument.

Initial conditions: $\begin{bmatrix} v_{y0} \\ \omega_{z0} \end{bmatrix} = \begin{bmatrix} v_{y\infty} \\ \omega_{z\infty} \end{bmatrix} + \begin{bmatrix} \begin{bmatrix} \hat{v}_{y1} \\ \hat{\omega}_{z1} \end{bmatrix} & \begin{bmatrix} \hat{v}_{y2} \\ \hat{\omega}_{z2} \end{bmatrix} \end{bmatrix} \cdot \begin{bmatrix} a_1 \\ a_2 \end{bmatrix}$; $\Rightarrow$

$$\Rightarrow \begin{bmatrix} a_1 \\ a_2 \end{bmatrix} = \begin{bmatrix} \begin{bmatrix} \hat{v}_{y1} \\ \hat{\omega}_{z1} \end{bmatrix} & \begin{bmatrix} \hat{v}_{y2} \\ \hat{\omega}_{z2} \end{bmatrix} \end{bmatrix}^{-1} \cdot \left(\begin{bmatrix} v_{y0} \\ \omega_{z0} \end{bmatrix} - \begin{bmatrix} v_{y\infty} \\ \omega_{z\infty} \end{bmatrix} \right);$$

The solution in summary:

$$\begin{cases} \begin{bmatrix} v_y \\ \omega_z \end{bmatrix} = \begin{bmatrix} v_{y\infty} \\ \omega_{z\infty} \end{bmatrix} + \begin{bmatrix} \begin{bmatrix} \hat{v}_{y1} \\ \hat{\omega}_{z1} \end{bmatrix} & \begin{bmatrix} \hat{v}_{y2} \\ \hat{\omega}_{z2} \end{bmatrix} \end{bmatrix} \cdot \begin{bmatrix} e^{\lambda_1 \cdot t} & 0 \\ 0 & e^{\lambda_2 \cdot t} \end{bmatrix} \cdot \begin{bmatrix} a_1 \\ a_2 \end{bmatrix}; \\ a_y = \dot{v}_y + v_x \cdot \omega_z = \lambda_1 \cdot \hat{v}_{y1} \cdot e^{\lambda_1 \cdot t} \cdot a_1 + \lambda_2 \cdot \hat{v}_{y2} \cdot e^{\lambda_2 \cdot t} \cdot a_2 + v_x \cdot \omega_z; \end{cases}$$

where: $\begin{bmatrix} v_{y\infty} \\ \omega_{z\infty} \end{bmatrix} = -\mathbf{A}^{-1} \cdot \mathbf{B} \cdot \delta_f$;

and $\begin{bmatrix} \begin{bmatrix} \hat{v}_{y1} \\ \hat{\omega}_{z1} \end{bmatrix} & \begin{bmatrix} \hat{v}_{y2} \\ \hat{\omega}_{z2} \end{bmatrix} \end{bmatrix}, \begin{bmatrix} \lambda_1 & 0 \\ 0 & \lambda_2 \end{bmatrix} = \mathrm{eig}(\mathbf{A})$;

and $\begin{bmatrix} a_1 \\ a_2 \end{bmatrix} = \begin{bmatrix} \begin{bmatrix} \hat{v}_{y1} \\ \hat{\omega}_{z1} \end{bmatrix} & \begin{bmatrix} \hat{v}_{y2} \\ \hat{\omega}_{z2} \end{bmatrix} \end{bmatrix}^{-1} \cdot \left(\begin{bmatrix} v_{y0} \\ \omega_{z0} \end{bmatrix} - \begin{bmatrix} v_{y\infty} \\ \omega_{z\infty} \end{bmatrix} \right)$;

[4.85]

Results from this model for step steer to +3 deg are shown in Figure 4-80. Left diagram shows step steer from straight line driving, while right diagram shows a step from steady state cornering with -3 deg steering angle.

4.5.4.2 Violent step steering response

This section is to be compared with section 4.5.4.1 Mild step steering response, which uses a model with linear tyre models without saturation. In present section a more advanced model will be used, which might be needed when the step steering is more violent.
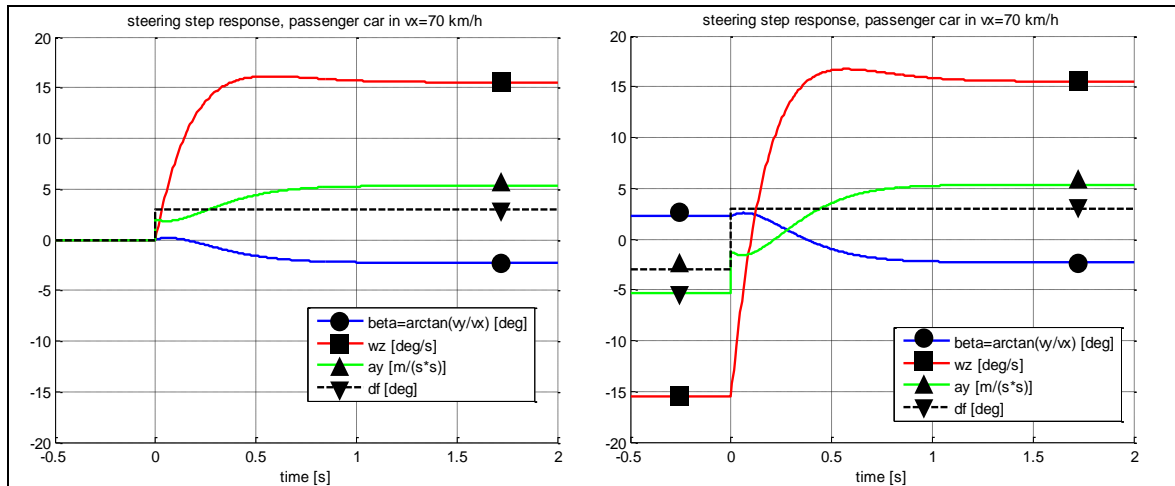
Figure 4-80: Steering step response. Simulation with model from Equation [4.85].

Most common interpretation is to make the steering step from an initial straight line driving. In reality, the step will be a quick ramp. In simulations an ideal step can be used.

The transients can easily be that violent that a model as Equations [4.79]..[4.84] is needed. If ESC is to be simulated, even more detailed models are needed (full two-track models, which are not presented in this compendium). Anyway, if we apply a step steer to the model in Equations [4.79]..[4.84], we can simulate as in Figure 4-81.
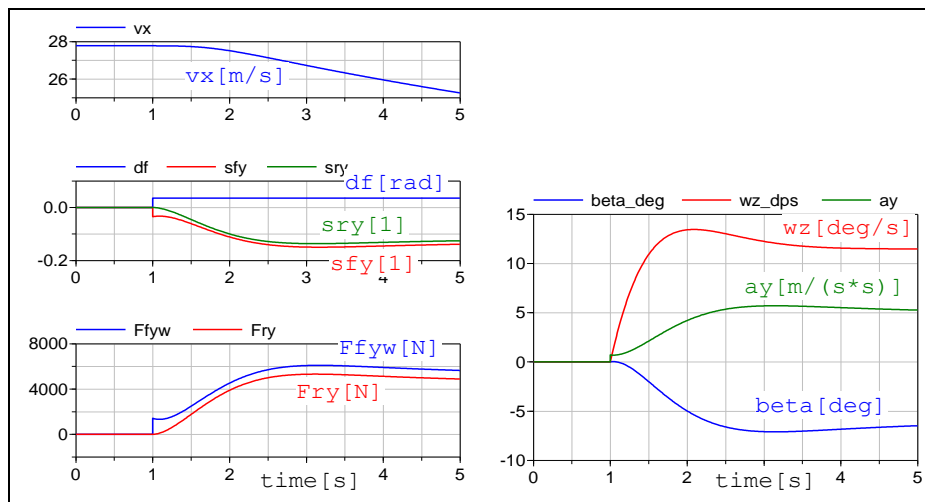
Figure 4-81: Step steer with 2 deg on road wheels at $v_x = 100$ km/h. Simulation using model from Eq [4.79]..[4.84].

4.5.4.3 Phase portrait

The transient from one steady state to another is seen after the steps in Figure 4-80 and Figure 4-81. Plotting several such transients as trajectories in a β, ω_z-diagram gives a phase portrait, which is a good graphical representation to understand how a vehicle stabilize itself, or gets instable. For transients that stays within unsaturated tyre slip, the linear one-track model can be used and the trajectories can then be explicit time expressions using Eq[4.85]. This is exemplified in left part of Figure 4-82. Some states can be confirmed stable already from this simple model. Simulations with higher fidelity model is exemplified in right part of Figure 4-82. With that one can confirm some more stable areas.
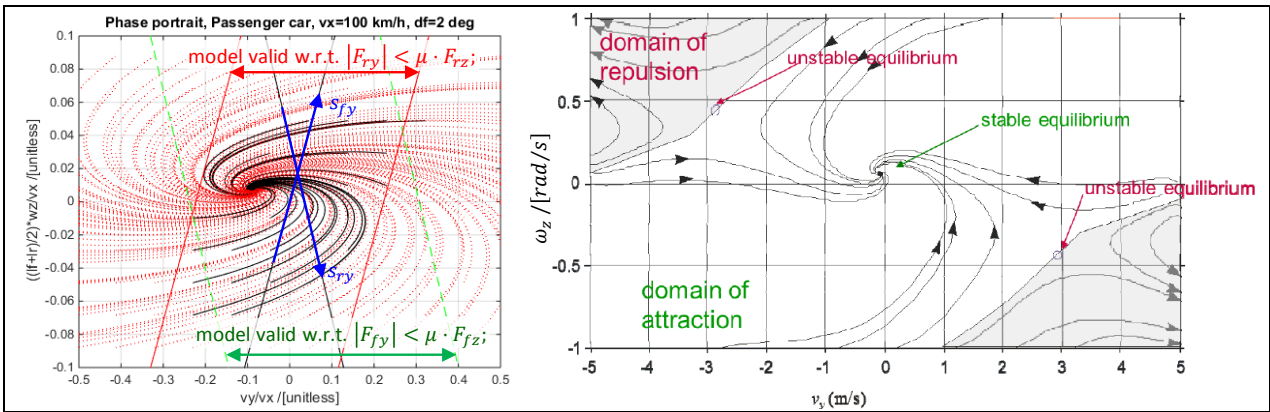
Figure 4-82: Phase portrait for constant v_x and constant steering angle δ_f. Left: Using simple model in Eq [4.60]. Only black solid trajectories credible, since they are completely within model validity. Right: Using a model with larger validity. From Mats Jonasson, VCC.

4.5.5 Long heavy vehicle combinations manoeuvrability measures

It is sometimes irrelevant (or difficult) to apply functions/measures from two axle vehicles on combinations of units. This can be the case for passenger cars with a trailer, but it is even more obvious for long combinations of heavy vehicles.

Some typical measures for multi-unit vehicle combination are given in Figure 4-83, Figure 4-84 and Figure 4-85.

4.5.5.1 Rearward Amplification *

Function definition: **Rearward Amplification for long heavy vehicle combinations** *is the ratio of the maximum value of the motion variable of interest (e.g. yaw rate or lateral acceleration of the centre of gravity) of the worst excited following vehicle unit to that of the first vehicle unit during a specified manoeuvre at a certain friction level and constant speed. From Reference [(Kati, 2013)].*

Figure 4-83 illustrates Rearward Amplification, RWA. RWA is defined for a special manoeuvre, e.g. a certain lane change or step steer. RWA is the ratio of the peak value of yaw rate or lateral acceleration for the rearmost unit to that of the lead unit. This performance measure indicates the increased risk for a swing out or rollover of the last unit compared to what the driver is experiencing in the lead unit.
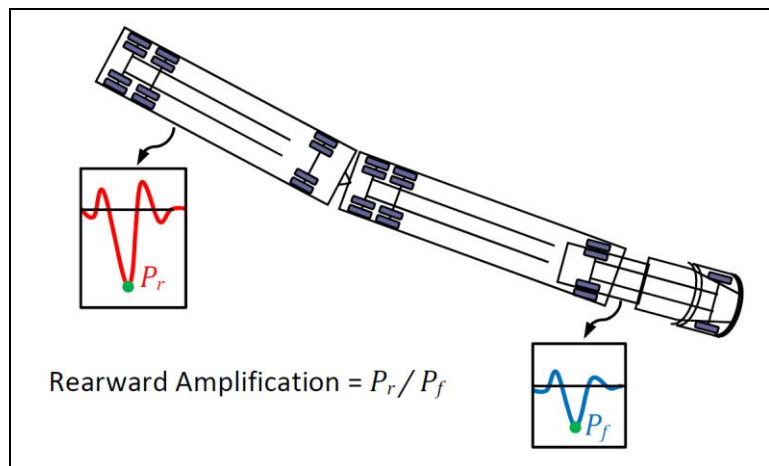
Figure 4-83: Illustration of rearward amplification, P denotes peak value of the motion variable of interest. From (Kharrazi , 2012).

4.5.5.2   Off-tracking *

Function definition: **High speed transient off-tracking for long heavy vehicle combinations** *is the overshoot in the lateral distance between the paths of the centre of the front axle and the centre of the most severely off-tracking axle of any unit in a specified manoeuvre at a certain friction level and a certain constant longitudinal speed. From Reference [(Kati, 2013)].*

Function definition: **High speed steady-state off-tracking for long heavy vehicle combinations** *is the lateral offset between the paths of the centre of the front axle and the centre of the most severely off-tracking axle of any unit in a steady turn at a certain friction level and a certain constant longitudinal speed. From Reference [(Kati, 2013)].*

Figure 4-84 illustrates Off-tracking. Off-tracking was also mentioned in Section 4.2. The measure is, as RWA, a comparison between the lead and last unit, but in terms of the additional road space required for the last unit manoeuvring. High speed Off-tracking, which is an outboard off-tracking, can be either determined in a steady state turn or in a transient manoeuvre such as lane change; the latter is termed as high speed transient off-tracking.
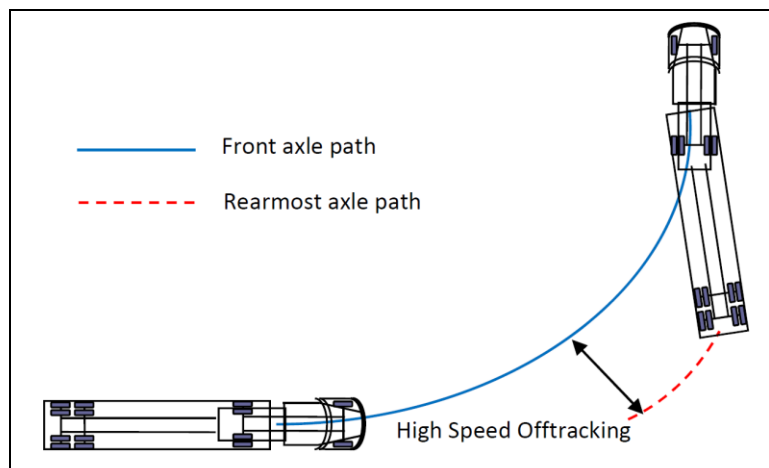
Figure 4-84: Illustration of high speed steady-state off-tracking. From (Kharrazi , 2012).

4.5.5.3   Yaw Damping *

Function definition: Yaw Damping for long heavy vehicle combinations is the damping ratio of the least damped articulation joint's angle of the vehicle combination during free oscillations excited by actuating the steering wheel with a certain pulse or a certain sine-wave steer input at a certain friction level. From Reference [(Kati, 2013)].

Figure 4-85 illustrates Yaw Damping. It is the damping ratio of the least damped articulation joint of the vehicle combination during free oscillations. Yaw damping ratio of an articulation joint is determined from the amplitudes of the articulation angle of subsequent oscillations.
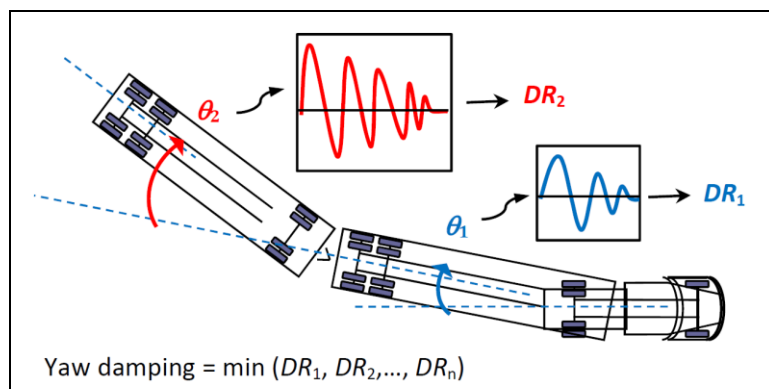
Figure 4-85: Illustration of yaw damping for multi-unit vehicle combination, DR denotes damping ratio of the articulation joint. From (Kharrazi , 2012).

4.5.5.4 Zero-damping speed

Function definition: Zero-damping speed for long heavy combination vehicles is the longitudinal speed at which a yaw disturbance leads to undamped response.

The measure can be calculated from a linear model as the longitudinal speed when the damping coefficient, for any mode involving yaw velocity, equals zero. If the measure is applied on a two-axle vehicle it is same as critical speed.

4.6 Lateral Control Functions

Some control functions involving lateral vehicle dynamics will be presented briefly. There are more, but the following are among the most well-established ones. But initially, some general aspects of lateral control is given.

4.6.1 Lateral Control Design

Sensors available in production vehicles and used for lateral control are, generally those mentioned as available for Longitudinal Control, see Section 3.5 plus some more:

Steering wheel sensors gives at least steering wheel angle, if the vehicle is equipped with ESC (which is a legal requirement on many markets). Additionally, if the steering assistance is electrical, the steering wheel torque can be sensed.

High specification modern vehicles also have environment sensors (camera, radar, etc) that can give laterally interesting information, such as: Subject vehicle lateral position versus lane markers ahead and other vehicles to the side or rear of subject vehicle.

As general considerations for actuators, one can mention that interventions with friction brake normally have to have thresholds, because interventions are noticed by driver and also generate energy loss. Interventions with steering are less sensitive, and can be designed without thresholds.

4.6.2 Lateral Control Functions

4.6.2.1 Lane Keeping Aid, LKA *

*Function definition: **Lane Keeping Aid** steers the vehicle without driver having to steer, when probability for lane departure is predicted as high. It is normally actuated as an additional steering wheel torque. Conceptually, it can also be actuated as a steering wheel angle offset.*

Lane Keeping Aid (or *Lane Departure Prevention*) has the purpose to guide the driver to keep in the lane. Given the lane position from a camera, the function detects whether vehicle tends to leave the lane. If so, the function requests a mild steering wheel torque (typically 1..2 Nm) in appropriate direction. Driver can easily overcome the additional torque. Function does not intervene if too low speed or turning indicator (blinker) is used. There are different concepts whether the function continuously should aim at keeping the vehicle in centre of lane, or just intervene when close to leaving the lane, see Figure 4-86.
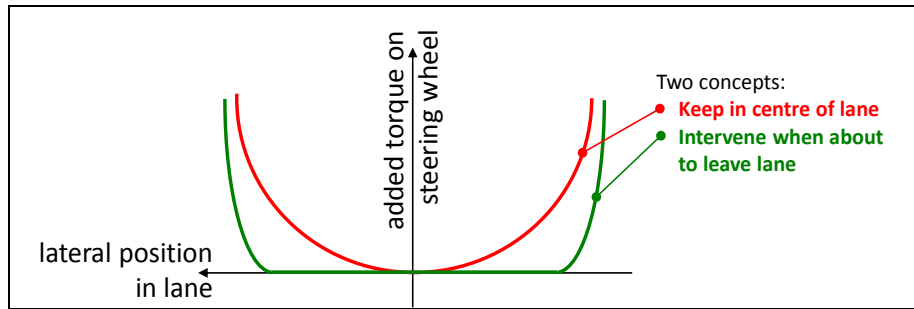
Figure 4-86: Two concepts for Lane Keeping Aid.

4.6.2.2 Electronic Stability Control, ESC *

Function definition: **Electronic Stability Control** *directs the vehicle to match a desired yaw behaviour, when the deviation from desired behaviour becomes above certain thresholds. ESC typically monitors vehicle speed, steering angle and yaw rate to calculate a yaw rate error and uses friction brakes as actuator to reduce it.*

There are 3 conceptual parts of ESC: Over-steer control, Under-steer control, Over-speed control. The actual control error that the vehicle reacts on is typically the yaw rate error between sensed yaw rate and desired yaw rate. Desired yaw rate is calculated from a so called reference model. Some of today's advanced ESC also intervenes on sensed/estimated side slip.

Desired yaw rate (and side-slip) is calculated using a reference model. The reference model requires at least steering angle and longitudinal velocity as input. The reference model can be either of steady state type (approximately as Equation [4.28]) or transient (approximately as Equation [4.57]). The vehicle modelled by the reference model should rather be the desired vehicle than the actually controlled vehicle. But, in order to avoid too much friction brake interventions; the reference model cannot be too different. Also, in order to avoid that vehicle yaws more than its path curvature; the reference model has to be almost as understeered as the controlled vehicle, which typically can be fixed by saturating lateral tyre forces on the front axle of the reference model. This requires some kind of friction estimation, especially for low-mu driving.

When controlling yaw via wheel torques, one can identify some different concepts such as direct and in-direct yaw moment, see Section 4.3.5.8. For ESC there is also a "pre-cautious yaw control" which aims at reducing speed, see Section 4.6.2.2.3.

4.6.2.2.1 Over-steer Control

Over-steer control was the first and most efficient concept in ESC. When a vehicle over-steers, ESC will brake the outer front wheel. It can brake to deep slip levels (typically -50%) since losing side grip on front axle is positive in an over-steer situation. More advanced ESC variants also brakes outer rear, but less and not to same deep slip level.

For multi-unit vehicle combinations with trailers that have controllable brakes, also the trailer is braked to avoid jack-knife effect, see Figure 4-84, or swing-out of the towed units.

4.6.2.2.2 Under-steer Control

Under-steer control means that inner rear is braked when vehicle under-steers. This helps the vehicle turn-in. This intervention is most efficient on low mu, because on high mu the inner rear wheel normally has very little normal load. Also, the slip levels are not usually as deep as corresponding over-steer intervention, but rather -10%. This is because there is always a danger in braking too much on rear axle, since it can cause over-steering. More advanced ESC variants also brakes inner front, which makes the function very similar to the function in Section 4.6.2.2.3.
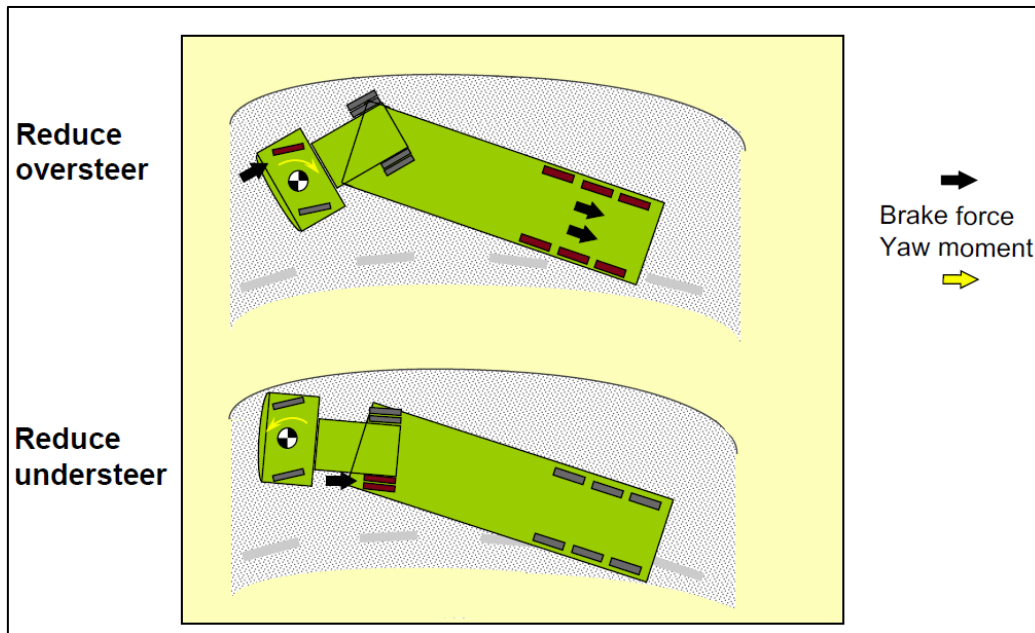
Figure 4-87: ESC when over-steer and understeer, on a truck with trailer

4.6.2.2.3 Over-speed Control

Over-speed control is not always recognised as a separate concept, but a part of under-steer control. It means that more than just inner rear wheels are braked. In this text, we identify this as done to decrease speed, which has a positive effect later in the curve.

4.6.2.2.4 Wheel-level control

A pre-requisite for all controls mentioned above in Section 4.6.2.2 is that the wheel torque actuator respond to a torque request, but it is a normal design that it is also responding to a longitudinal slip request. The slip request is generally used as a sort of "safety net" to not lock-up the wheel more than 10-20%, but at RSC interventions (see Section 4.6.2.3) the lateral grip should be braked away, so a deeper slip request is then used, typically 50-70%.
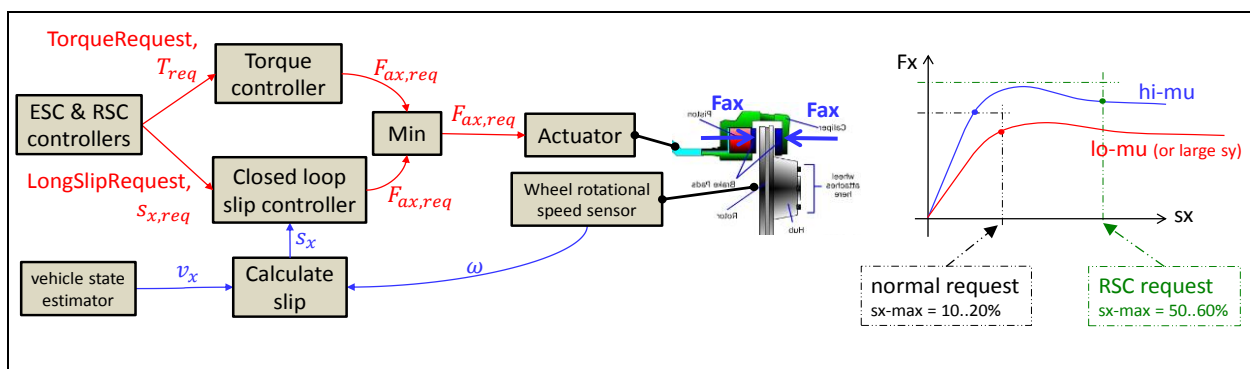
Figure 4-88: Individual wheel control by friction brakes for ESC-type functions

4.6.2.2.5 Other intervention than individual wheel brakes

4.6.2.2.5.1 Balancing with Propulsion per axle

For vehicles with controllable distribution of propulsion torque between the axles, ESC can intervene also with a request for redistribution of the propulsion torque. If over-steering, the propulsion should be redistributed towards front and opposite for understeering.

4.6.2.2.5.2 Torque Vectoring

For vehicles with controllable distribution of propulsion torque between the left and right, ESC can intervene also with a request for redistribution of the propulsion torque. If over-steering, the propulsion should be redistributed towards inner side and opposite for understeering.

4.6.2.2.5.3 Steering guidance

For vehicles with controllable steering wheel torque, ESC can intervene also with a request for additional steering wheel torque. The most obvious functions is to guide driver to open up steering (counter-steer) when the vehicle over-steers. Such functions are on market in passenger cars today. Less obvious is how to guide the driver when vehicle is under-steering.

4.6.2.2.6 Environment-information-based-ESC and/or ESC-for-the-virtual-driver

A prognosis of the future development of ESC like functions is that environment sensors can be used to better predict what driver tries to do; presently ESC can only look at steering wheel angle.

Related to this, but still somewhat different, would be to utilize the autonomous driving development by utilizing that a "virtual driver" can be much better predicted than a "manual driver". So, a predictive ESC control is more possible.

4.6.2.3   Roll Stability Control, RSC *

Function definition: **Roll Stability Control, RSC**, *prohibits vehicle to roll-over due to lateral wheel forces from road friction. RSC uses friction brake as actuator.*

The purpose of RSC is to avoid un-tripped roll-overs. The actuator used is the friction brake system. When roll-over risk is detected, via lateral acceleration sensor (or in some advanced RSC implementations, also roll rate sensor), the outer front wheel is braked. RSC can brake to deep slip levels (typically -70%..-50%) since losing side grip on front axle is positive in this situation. To lock the wheels (slip= $-\infty$) is undesired since wheel rotational inertia makes it difficult to quickly regain lateral grip when needed after the intervention.

On heavy vehicles, RSC intervenes earlier and similar to function described in Section 4.6.2.2.3 Over-speed Control.

In future, RSC could be developed towards also using steering.

4.6.2.4   Lateral Collision Avoidance, LCA *

Function definition: **Lateral Collision Avoidance** *support the driver when he has to do late lateral obstacle avoidance, when probability for forward collision is predicted as high.*

There are systems on the market for Automatic Emergency Brake, see Section 3.5. If these are seen as Longitudinal Collision Avoidance, one could also think of Lateral Collision Avoidance functions, which would automatically steer away laterally from an obstacle ahead of subject vehicle. There are not yet any such functions on market. One possible first market introduction could be that triggering requires driver to initiate steering. Another would be to trigger on a first collision impact, see Reference (Yang, 2013).

4.6.2.5   Autonomous Driving (AD)

Combining longitudinal control (such as ACC, in Section 3.5.2.2) with a lateral control (such as LKA, see Section 4.6.2.1) results in functionality which clearly approaches autonomous driving (AD). AD is a very general expression but are sometimes interpreted as more specific, but specific in different ways depending on context. In a way, AD is already reality since there are vehicles on the road which can be driven (or drive themselves) with ACC and LKA active at the same time. On the other hand, AD can be seen as very futuristic, since completely driverless vehicle which can operate in all situations is far from produced and sold.

5 VERTICAL DYNAMICS

5.1 Introduction

The vertical dynamics are needed since vehicles are operated on real roads, and real roads are not perfectly smooth. Also, vehicle scan be operated off-road, where the ground unevenness is even larger.

The irregularities of the road can be categorized. A **transient** disturbance, such as a pothole or object on the road, can be represented as a step input. Undulating surfaces like grooves across the road may be a type of sinusoidal or other **stationary** (or periodic) input. More natural input like the random surface texture of the road may be a **random** noise distribution. In all cases, the same mechanical system must react when the vehicle travels over the road at varying speeds including doing manoeuvres in longitudinal and lateral directions.

The chapter is organised around the 3 complete vehicle functions: 5.6 Ride comfort, 5.7 Fatigue life, and 5.8 Road grip. It is, to a larger extent than Chapters 3 and 4, organised so that all theory (knowledge) comes first and the vehicle functions comes after. In Figure 5-1 shows the 3 main functions, Ride comfort, Fatigue life and Road grip. It is supposed to explain the importance of the vehicle's dynamic structure. The vehicle's dynamic structure calls for a pretty extensive theory base, described mainly in Section 5.3.

Models in this chapter focus the disturbance from vertical irregularities from the road, i.e. only the vertical forces on the tyre from the road and **not** the forces in road plane. This enables the use of simple models which are independent of exact wheel and axle suspension, such as pivot axes and roll centres. Only the wheel stiffness rate (effective stiffness) and wheel damping rate (effective damping), see Figure 3-43, has to be given. This has the benefit that the chapter becomes relatively independent of previous chapters, but it has the drawback that the presented models are **not** really suitable for studies of steep road irregularities (which have longitudinal components) and sudden changes in wheel torque or tyre side forces. Also noise is not covered in this compendium.

5.1.1   References for this chapter

- *"Chapter 21 Suspension Systems" in Reference* (Ploechl, 2013)*.*
- *"Chapter 29 Ride Comfort and Road Holding" in Reference* (Ploechl, 2013)*.*
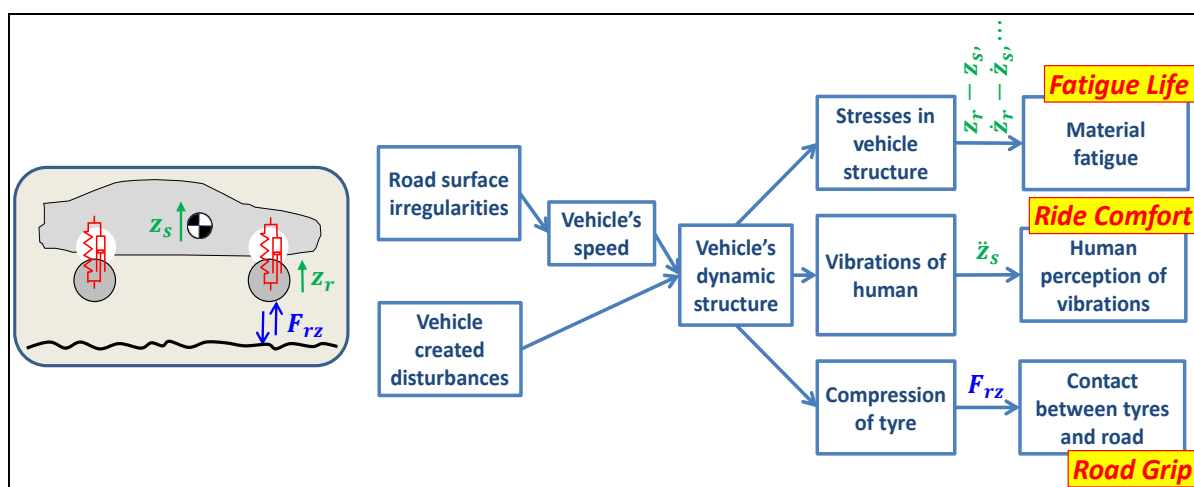
Figure 5-1: Different types of knowledge and functions in the area of vertical vehicle dynamics, organised around the vehicle's dynamic structure.

5.2 Suspension System

Suspension design is briefly discussed at these places in this compendium: Section 3.4.7, Section 4.3.9.4 and Section 5.2.

Suspension design influence ride comfort, load on suspension and road grip through how **vertical forces** and **camber and steering angles** on each wheel changes with **body motion** (heave, roll, pitch), **road unevenness** (bumps, potholes, waviness) and **wheel forces in ground plane** (from Propulsion, Braking and Steering subsystems).

Suspension in a vehicle may refer to suspension wheels (or axles), suspension of sub-frame and drivetrain and suspension of cabin (for heavy trucks). In present section, only wheel (or axle) suspension is considered.

A wheel suspension has the purpose to constrain the wheel from 6 degrees of freedom, dofs, relative the body, to 2 or 3 dofs. A steered wheel needs 3 dofs (pitch rotation, vertical translation and yaw rotation). For an un-steered wheel, also the yaw rotation should be constrained. For most steering, left and right wheels on an axle have dependent steering angles, which could be seen as 2.5 dofs/wheel.
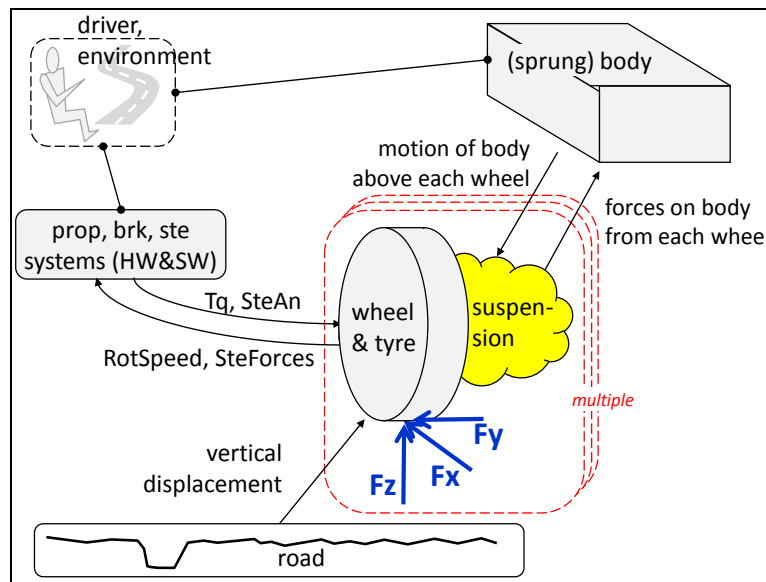
Figure 5-2: Individual wheel suspension described as one modular sub-model per wheel. It may be noted that a both wheel model (main geometry such as wheel radius) and tyre model (how F_x and F_y vary with tyre slip and F_z) is a part of each such sub-model.

An (axle) suspension system mainly consists of:

- **Linkage**, which has the purpose to constrain the relative motion between wheel and body via kinematics. An alternative way to express this is that the linkage defines how longitudinal and lateral wheel forces are brought into the body (body = sprung mass). Effective pivot points and roll/pitch centres, mentioned earlier in this compendium, are defined through the linkage. In the real pivot points in the linkage, there are **bushings** with stiffness and damping. The bushings stiffness is much larger than the stiffness of the compliances mentioned below. For steered wheels, the linkage also has the purpose to allow steering.
There are two main concepts: Individual wheel suspension and rigid axle suspension.
- **Compliances** (or springs), which has the purpose to allow temporary vertical displacement of the wheels relative to the body. There are often one spring per wheel but also a spring per axle. The second is called anti-roll bar and connects left and right wheel to each other to reduce body roll. Compliances often have a rather linear relation between the vertical displacement and force of each wheel, but there are exceptions:

- o **Anti-roll bars** make two wheels dependent of each other (still linear). Anti-roll bars can be used on both individual wheel suspensions and rigid axle suspensions.
  - o The compliances can be intentionally designed to be non-linear in the outer end of the stroke, e.g. **bump stops.**
  - o The compliances can be non-linear during the whole stroke, e.g. **air-springs** and **leaf-springs**.
  - o The compliances can be intentionally designed to be **controllable** during operation of the vehicle. This can be to change the pre-load level to adjust for varying roads or varying weight of vehicle cargo or to be controllable in a shorter time scale for compensating in each oscillation cycle. The latter is very energy consuming and no such "active suspension" is available on market.
- **Dampers**, which has the purpose to dissipate energy from any oscillations of the vertical displacement of the wheel relative to the body. Dampers often has a rather linear relation between the vertical deformation speed and force of each wheel, but there are exceptions:
  - o The dampers can be intentionally designed to be different in different deformation direction. This is actually the normal design for dampers of **hydraulic piston type**, and it means that damping coefficient is different in compression and rebound. Typical values are about 3 times more damping in rebound (extension) than compression (bump). This can be motivated from that driving over a steep bump requires low damping to reduce upward jerk in vehicle, especially since there is a hard bump stop in the end of the spring stroke. In the other direction, driving over equally steep hole the downward jerk is limited by that the wheel cannot develop pulling forces on the ground; instead it lifts from ground if hole is too steep. So larger damping can be allowed in rebound. A reflection here is that high damping damps oscillations, but high damping also increases the shock transmittance (with this reasoning, the name "shock-absorber" is misleading).
  - o Damping in **leaf springs** is non-linear since they work with dry friction.
  - o Damping in **air-springs** is non-linear due to the nature of compressing gas.
  - o The dampers can be intentionally designed to be **controllable** during operation of the vehicle. This can be to change the damping characteristics to adjust for varying roads or varying weight of vehicle cargo or to be controllable in a shorter time scale for compensating in each oscillation cycle. The latter is called "semi-active suspension" and is available on some high-end vehicles on market.

The simplest view we can have of a suspension system is that there is an individual suspension between the vehicle body and each wheel. Each such suspension is a parallel arrangement of one linear spring and one linear damper. Chapter 5 uses this simple view for analysis models, because it facilitates understanding and it is enough for a first order evaluation of the functions studied (comfort, road grip and fatigue load) during normal driving on normal roads.

5.3 Stationary oscillations theory

Many vehicle functions in this chapter will be studied using stationary oscillations (cyclic repeating), as opposed to transiently varying. An example of transiently varying quantity is a single step function or single square pulse. A stationary oscillation can always be expressed as a sum of several harmonic terms, a so called multiple frequency harmonic stationary oscillation. The special case that only one frequency is contained can be called single frequency harmonic stationary oscillation. See Figure 5-3 and Equation [5.1].
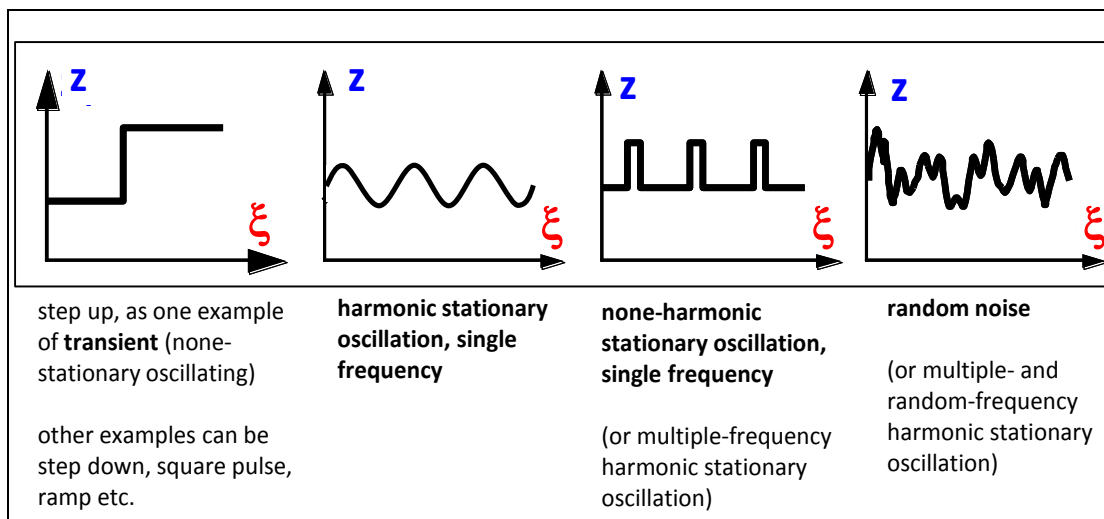
Figure 5-3: Different types of variables, both transient and stationary oscillating. The independent variable ξ can, typically, be either time or distance.

Harmonic stationary oscillations:

$Single\ frequency: z(\xi) = \hat{z} \cdot \cos(\omega \cdot \xi + \varphi);$

$Multiple\ frequencies: z(\xi) = \sum_{i=1}^{N} \hat{z}_i \cdot \cos(\omega_i \cdot \xi + \varphi_i);$

$where\ \xi\ is\ the\ independent\ variable.$

[5.1]

The most intuitive is probably to think of time as the independent variable, i.e. that the variation takes place as function of time. This would mean that $\xi = t$ in Equation [5.1]. However, for one specific road, the vertical displacement varies with longitudinal position, rather than with time. This is why we can either do analysis in **time domain** ($\xi = t$) and **space domain** ($\xi = x$).

Since the same oscillation can be described either as a function of ξ ($z = z(\xi)$) or as a function of frequency ω ($\hat{z} = \hat{z}(\omega)$), we can do analysis either in the **independent variable domain** (ξ) or in **frequency domain** (ω).

The four combinations of domains are shown in Figure 5-4.
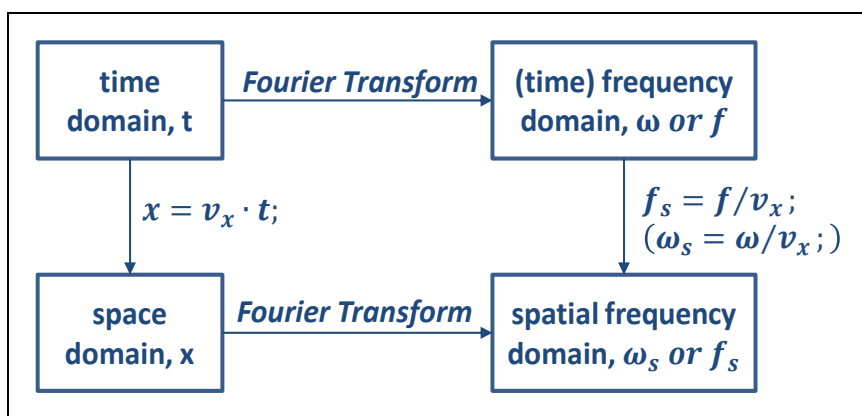
Figure 5-4: Four combinations of domains

Time and space domains are treated in section 5.3.1 and 0. In addition to the domains, we also need to differ between discrete and continuous representations in the frequency domains, see 5.3.1.2 and 5.3.2.2.

5.3.1 Time as independent variable

With time as independent variable, the frequency has the common understanding of "how often per time". Even so, there are two relevant ways to measure frequency: angular (time) frequency, and (time) frequency.

$$
\begin{aligned}
\omega &= 2 \cdot \pi \cdot f; \\
where \quad \omega \left[\frac{rad}{s}\right] &= angular \ (time) \ frequency; \\
and \quad f \left[\frac{1}{s} = \frac{oscillations}{s}\right] &= (time) \ frequency;
\end{aligned}
$$

[5.2]

The time for one oscillation is called the period time. It is denoted T:

$$
T = \frac{1}{f} = \frac{2 \cdot \pi}{\omega};
$$

[5.3]

5.3.1.1 Mean Square (MS) and Root Mean Square (RMS) of variable

For a variable, z, we can define MS and RMS values as follows:

$$
\begin{aligned}
Variable&: & z &= z(t); \\
MeanSquare&: & MS(z) &= \frac{\int_0^{t_{end}} z^2 \cdot dt}{t_{end}}; \\
RootMeanSquare&: & RMS(z) &= \sqrt{\frac{\int_0^{t_{end}} z^2 \cdot dt}{t_{end}}};
\end{aligned}
$$

[5.4]

If the variable is written as a single frequency harmonic stationary oscillation, these values becomes as follows:

$$
\begin{aligned}
Variable&: & z &= \hat{z} \cdot \cos(\omega \cdot t + \varphi); \\
MeanSquare&: & MS(z) &= \frac{\int_0^{t_{end}} z^2 \cdot dt}{t_{end}} = \frac{\int_0^{t_{end}} (\hat{z} \cdot \cos(\omega \cdot t + \varphi))^2 \cdot dt}{t_{end}} = \\
& & &= \frac{\hat{z}^2 \cdot \left[\frac{t}{2} + \frac{\sin(2 \cdot \omega \cdot t)}{4 \cdot \omega}\right]_{t=0}^{t=t_{end}}}{t_{end}} = \frac{\hat{z}^2 \cdot \left(\frac{t_{end}}{2} + \frac{\sin(2 \cdot \omega \cdot t_{end})}{4 \cdot \omega}\right)}{t_{end}} \xrightarrow[t_{end} \to \infty]{} \frac{\hat{z}^2}{2}; \\
RootMeanSquare&: & RMS(z) &= \sqrt{\frac{\int_0^{t_{end}} z^2 \cdot dt}{t_{end}}} = \sqrt{MS(z)} = \frac{|\hat{z}|}{\sqrt{2}};
\end{aligned}
$$

[5.5]

If the variable is written as a multiple frequency harmonic stationary oscillation, these values becomes as follows:

$$Variable: \qquad z \qquad = \sum_{i=1}^{N} z_i = \sum_{i=1}^{N} \hat{z}_i \cdot \cos(\omega_i \cdot t + \varphi_i);$$

$$MeanSquare: \qquad MS(z) \quad = \frac{\int_0^{t_{end}} z^2 \cdot dt}{t_{end}} = \frac{\int_0^{t_{end}} \left(\sum_{i=1}^{N} z_i\right)^2 \cdot dt}{t_{end}} =$$

$$= \frac{\int_0^{t_{end}} \left(\sum_{i=1}^{N} \hat{z}_i \cdot \cos(\omega_i \cdot t + \varphi_i)\right)^2 \cdot dt}{t_{end}} \xrightarrow{t_{end} \to \infty}$$

$$\xrightarrow{t_{end} \to \infty} \frac{\int_0^{t_{end}} \sum_{i=1}^{N} \hat{z}_i{}^2 \cdot (\cos(\omega_i \cdot t + \varphi_i))^2 \cdot dt}{t_{end}} = \sum_{i=1}^{N} MS(z_i) = \sum_{i=1}^{N} \frac{\hat{z}_i{}^2}{2};$$

$$RootMeanSquare: \quad RMS(z) = \sqrt{MS(z)} = \sqrt{\sum_{i=1}^{N} \frac{\hat{z}_i{}^2}{2}} = \sqrt{\sum_{i=1}^{N} MS(z_i)} =$$

$$= \sqrt{\sum_{i=1}^{N} \left(RMS(z_i)\right)^2};$$

[5.6]

5.3.1.2 Power Spectral Density and Frequency bands

So far, the frequency has been a discrete number of frequencies, $\omega_1, \omega_2, \cdots, \omega_N$. There are reasons to treat the frequency as a continuous variable instead. The discrete amplitudes, $\hat{z}_1, \hat{z}_2, \cdots, \hat{z}_N$, should then be thought of as integrals of a "continuous amplitude curve", $\hat{z}_c$, where the integration is done over a small frequency interval, centred around a each mid frequency, ω_i:

$$\hat{z}_i = \int_{\omega = \frac{\omega_{i-1} + \omega_i}{2}}^{\frac{\omega_i + \omega_{i+1}}{2}} \hat{z}_c \cdot d\omega = \hat{z}_c(\omega_i) \cdot \frac{\omega_{i+1} - \omega_{i-1}}{2} = \hat{z}_c(\omega_i) \cdot \Delta\omega_i; \Rightarrow \hat{z}_c(\omega_i) = \frac{\hat{z}_i}{\Delta\omega_i};$$

[5.7]

We realize that the unit of $\hat{z}_c$ has to be same as for z, but per [rad/s]. So, if z is a displacement in [m], $\hat{z}_c$ has the unit [m/(rad/s)]. Now, $\hat{z}_c$ is a way to understand the concept of a spectral density. A similar value, but more used, is the Power Spectral Density, PSD (also called Mean Square Spectral Density).

$PSD(\omega)$ is a continuous function, while $\hat{z}_i$ is a discrete function. That means that $PSD(\omega)$ is fully determined by a certain measured or calculated variable $z(t)$, while $\hat{z}_i$ depends on which discretization (which ω_i or which $\Delta\omega$) that is chosen.

$$PSD(z(t), \omega, \Delta\omega) = \frac{MS\big(filter(z(t), \omega, \Delta\omega)\big)}{\Delta\omega} = G(\omega);$$
$$where \text{ filter} is \ a \ bandpass \ filter \ centered \ around \ \omega \ and \ with \ band \ width \ \Delta\omega;$$

[5.8]

PSD can also be defined with band width in time frequency instead of angular frequency. The Equation [5.8] is the same but replacing $\Delta\omega$ with Δf.

When the variable to study (z) is known and the band width is known, one often write simply $PSD(\omega)$ or $G(\omega)$. G has the same unit as z^2, but per [rad/s] or per [oscillations/s]. So, if z is a displacement in [m], G has the unit $[\frac{m^2}{rad/s}]$ or $[\frac{m^2}{1/s} = m^2 \cdot s]$.

The usage of the PSD is, primarily, to easily obtain the RMS via integration:

$$RMS(z) = \sqrt{\sum_{i=1}^{N} MS(z_i)} = \sqrt{\sum_{i=1}^{N} G(\omega_i) \cdot \Delta\omega_i} = \sqrt{\int_{\omega=0}^{\infty} G(\omega) \cdot d\omega} \; ; \qquad [5.9]$$

RMS is square root of the area under the PSD curve.

5.3.1.2.1 Differentiation of PSD

Knowing the PSD of a variable, we can easily obtain the PSD for the derivative of the same variable:

$$G_{\dot{z}}(\omega) = \omega^2 \cdot G_z(\omega); \qquad [5.10]$$

5.3.1.3   Transfer function

In a minimum model for vertical dynamics there is at least one excitation, often road vertical displacement, z_r, and one response, e.g. vertical displacement of sprung mass (=vehicle body), z_s. A Transfer function, $H = H(j \cdot \omega)$, is the function which we can use to find the response, given the excitation:

$$Z_s(\omega) = H(\omega) \cdot Z_r(\omega); \quad \Leftrightarrow \quad \mathcal{F}\big(z_s(t)\big) = H(\omega) \cdot \mathcal{F}\big(z_r(t)\big);$$
$$where \; \mathcal{F} \; is \; the \; Fourier \; operator: Z(\omega) = \mathcal{F}\big(z(t)\big) = \int_{0}^{\infty} e^{-j\cdot\omega\cdot t} \cdot z(t) \cdot dt \; ; \qquad [5.11]$$

H is complex, which is why it has a magnitude, $|H| = \sqrt{(\text{Re}(H))^2 + (\text{Im}(H))^2}$, and phase, $\arg\big(H(\omega)\big) = \arctan(\text{Im}(H)/\text{Re}(H))$.

$$Amplitude: \; \hat{z}_s(\omega) = |H(\omega)| \cdot \hat{z}_r(\omega);$$
$$Phase: \; \varphi_s(\omega) - \varphi_r(\omega) = \arg\big(H(\omega)\big);$$
$$where \; z = \sum_{i=1}^{N} \hat{z}(\omega_i) \cdot \cos(\omega_i \cdot t + \varphi_i); \qquad [5.12]$$

Since there can be different excitations and responses in a system, there are several transfer functions. To distinguish between those, a subscripting of H is often used: $H_{excitation \rightarrow response}$, which would be $H_{z_r \rightarrow z_s} = H_{road \; displacement \rightarrow sprung \; mass \; displacement}$ in the example above. Other examples of relevant transfer functions in vertical vehicle dynamics are:

* $H_{road \; displacement \rightarrow sprung \; mass \; acceleration} \; [(m/s^2)/m]$, see Section 5.6
* $H_{road \; displacement \rightarrow suspension \; deformation} \; [m/m]$, see Section 5.7
* $H_{road \; displacement \rightarrow tyre \; force} \; [N/m]$, see Section 5.8

When transfer function for one derivative is found, it is often easy to convert it to another:

$$H_{z_1 \rightarrow \dot{z}_2} = j \cdot \omega \cdot H_{z_1 \rightarrow z_2};$$
$$H_{z_1 \rightarrow \ddot{z}_2} = j \cdot \omega \cdot j \cdot \omega \cdot H_{z_1 \rightarrow z_2} = -\omega^2 \cdot H_{z_1 \rightarrow z_2}; \qquad [5.13]$$
$$H_{z_1 \rightarrow z_2 - z_3} = H_{z_1 \rightarrow z_2} - H_{z_1 \rightarrow z_3};$$

Note that these relations are valid for the complex transfer function. They corresponding relations can be used with $|H|$ replacing H, in cases where the phase is same for all involve variables, which often can be the case when damping is neglected.

The usage of the transfer function is, primarily, to easily obtain the response from the excitation, as shown in Equation [5.12]. Also, the transfer function can operate on the Power Spectral Density, PSD=G, as shown in the following:

$$G_{z_s}(\omega) = \frac{MS(z_s(t), \omega)}{\Delta\omega} = \frac{\left(\hat{z}_s(\omega)\right)^2/2}{\Delta\omega} = \frac{\left(|H(\omega)| \cdot \hat{z}_r(\omega)\right)^2/2}{\Delta\omega} =$$
$$= \left|H_{z_r \to z_s}(\omega)\right|^2 \cdot \frac{\left(\hat{z}_r(\omega)\right)^2/2}{\Delta\omega} = \left|H_{z_r \to z_s}(\omega)\right|^2 \cdot G_{z_r}(\omega);$$

[5.14]

Using Equation [5.9], we can then calculate $RMS(z_s)$ from $G_{z_s}(\omega)$.

5.3.2   Space as independent variable

All transformations, in this compendium, between time domain and space domain requires a constant longitudinal speed, v_x, so that:

$$x = v_x \cdot t + x_0;$$

[5.15]

The offset (x_0) is the phase (spatial) offset (x_0) is the correspondence to the phase angle (φ).

The corresponding formulas as given in Equations [5.2]..[5.13] can be formulated when changing to space domain, or spatial domain. It is generally a good idea to use a separate set of notations for the spatial domain. Hence the formulas are repeated with new notations, which is basically what will be done in present section.

There are not relevant to define transfer functions for the spatial domain before a road model is given, see Section 5.4.2.1.

In space domain, the frequency has the common understanding of "how often per **distance**". Even so, there are two relevant ways to measure frequency: spatial angular frequency and spatial frequency.

$$\Omega = 2 \cdot \pi \cdot f_s;$$
$$where \quad \Omega \left[\frac{rad}{m}\right] = angular\ spatial\ frequency;$$
$$and \quad f_s \left[\frac{1}{m} = \frac{oscillations}{m}\right] = spatial\ frequency;$$

[5.16]

The correspondence to period time is wave length, denoted λ:

$$\lambda[m] = \frac{1}{f_s} = \frac{2 \cdot \pi}{\Omega};$$

[5.17]

Now, the basic assumption in Equation [5.15] and definitions of frequencies gives:

$$\omega = v_x \cdot \Omega; \quad and \quad f = v_x \cdot f_s;$$

[5.18]

The relation between the phase (spatial) offset (x_0) and the phase angle (φ) is:

$$x_0 = \frac{\lambda \cdot \varphi}{2 \cdot \pi};$$

[5.19]

5.3.2.1 Spatial Mean Square (MS) and spatial Root Mean Square (RMS) of variable

In space domain, a variable, z, varies with distance, x. We can define Mean Square and Root Mean Square values also in space domain. We subscript these with s for space.

$$
\begin{aligned}
Variable: \quad & z && = z(x); \\
MeanSquare: \quad & MS_s(z) && = \frac{\int_0^{x_{end}} z^2 \cdot dx}{x_{end}}; \\
RootMeanSquare: \quad & RMS_s(z) && = \sqrt{\frac{\int_0^{x_{end}} z^2 \cdot dx}{x_{end}}};
\end{aligned}
$$

[5.20]

Because v_x is constant, the Mean Square and Root Mean Square will be the same in time and space domain. If the variable is written as a single frequency harmonic stationary oscillation, these values becomes as follows:

$$
\begin{aligned}
Variable: \quad & z && = \hat{z} \cdot \cos(\Omega \cdot x + x_0); \\
MeanSquare: \quad & MS_s(z) && = \cdots = \frac{\hat{z}^2}{2} = MS(z); \\
RootMeanSquare: \quad & RMS_s(z) && = \cdots = \frac{|\hat{z}|}{\sqrt{2}} = RMS(z);
\end{aligned}
$$

[5.21]

If the variable is written as a multiple frequency harmonic stationary oscillation, these values becomes as follows:

$$
\begin{aligned}
Variable: \quad & z && = \sum_{i=1}^{N} z_i = \sum_{i=1}^{N} \hat{z}_i \cdot \cos(\Omega_i \cdot x + x_{0i}); \\
MeanSquare: \quad & MS_s(z) && = \sum_{i=1}^{N} \frac{\hat{z}_i^2}{2} = MS(z); \\
RootMeanSquare: \quad & RMS_s(z) && = \sqrt{MS_s(z)} = \sqrt{\sum_{i=1}^{N} \left(RMS(z_i)\right)^2} = RMS(z);
\end{aligned}
$$

[5.22]

5.3.2.2 Spatial Power Spectral Density and Frequency bands

A correspondence to Power Spectral Density in space domain is denoted PSD_s in the following:

$$PSD_s(z(x), \Omega, \Delta\lambda) = \frac{MS(filter(z(x),\Omega,\Delta\lambda))}{\Delta\lambda} = \Phi(\Omega);$$

where "filter" is a band pass filter centred around ω and with band width Δf;

[5.23]

When the variable to study (z) is known and the band width is known, one often write simply $PSD_s(\Omega)$ or $\Phi(\Omega)$. Φ has the same unit as z^2, but per [rad/m] or per [oscillations/m]. So, if z is a displacement in [m], Φ has the unit $[\frac{m^2}{rad/m} = \frac{m^3}{rad}]$ or $[\frac{m^2}{1/m} = m^3]$.

5.4 Road models

In general, a road model can include ground properties such as coefficient of friction, damping/elasticity of ground and vertical position. The independent variable is either one, along an assumed path, or generally two, x and y in ground plane. In vertical dynamics in this compendium, we

only assume vertical displacement as function of a path. We use x as independent variable along the path, meaning that the road model is: $z_r = z_r(x)$. The function $z_r(x)$ can be either of the types in

Figure 5-3. We will concentrate on stationary oscillations, which by Fourier series, always can be expressed as multiple (spatial) frequency harmonic stationary oscillation. This can be specialized to either single (spatial) frequency or random (spatial) frequency. Hence, the general form of the road model is multiple (spatial) frequencies:

$$z_r = z_r(x) = \sum_{i=1}^{N} \hat{z}_i \cdot \cos(\Omega_i \cdot x + x_{0i}) ; \qquad \text{[5.24]}$$

5.4.1   One frequency road model

For certain roads, such as roads built with concrete blocks, a single (spatial) frequency can be a relevant approximation to study a certain single wave length. Also, the single (spatial) frequency road model is good for learning the different concepts. A single (spatial) frequency model is the same as a single wave length model ($\lambda = 2 \cdot \pi / \Omega$, from Equation [5.16]) and it can be described as:

$$z_r = z_r(x) = \hat{z} \cdot \cos(\Omega \cdot x + x_0) ; \qquad \text{[5.25]}$$

5.4.2   Multiple frequency road models

Based on the general format in Equation [5.24], we will now specialise to models for different road qualities. In Figure 5-5, there are 4 types of road types defined. Approximately, the 3 upper of those are roads and they are also defined as PSD-plots in Figure 5-6. The mathematical formula is given in Equation [5.26] and numerical parameter values are given in Equation [5.27].

$$\Phi = \Phi(\Omega) = \Phi_0 \cdot \left(\frac{\Omega}{\Omega_0}\right)^{-w} = \frac{MS_s(z_r, \Omega)}{\Delta\Omega} ;$$

where Φ_0 = road severity $\left[\frac{\text{m}^2}{\text{rad/m}}\right]$;

w = road waviness [1];
Ω = spatial angular frequency [rad/m];
Ω_0 = 1 [rad/m];

[5.26]

Typical values are

Very good road: $\Phi_0 = 1 \cdot 10^{-6} \left[\frac{\text{m}^2}{\text{rad/m}}\right]$;

Bad road : $\Phi_0 = 10 \cdot 10^{-6} \left[\frac{\text{m}^2}{\text{rad/m}}\right]$;

Very bad road : $\Phi_0 = 100 \cdot 10^{-6} \left[\frac{\text{m}^2}{\text{rad/m}}\right]$;

The waviness is normally in the range of $w = 2..3$ *[1],*
where smooth roads have larger waviness than bad roads.

[5.27]

The decreasing amplitude for higher (spatial) frequencies (i.e. for smaller wave length) can be explained by that height variation over a short distance requires large gradients. On micro-level, in the granular level in the asphalt, there can of course be steep slopes on the each small stone in the asphalt.

These are of less interest for vehicle vertical dynamics, since the wheel dimensions filter out wave length << tyre contact length, see Figure 2-43.

A certain road can be described with:

- $\Omega_1, \cdots, \Omega_N$
- $\hat{z}_1, \cdots, \hat{z}_N$
- $x_{01}, \cdots, x_{0N}$

Figure 5-5: Four typical road types, whereof the upper 3 can be considered as road types. From (AB Volvo, 2011).
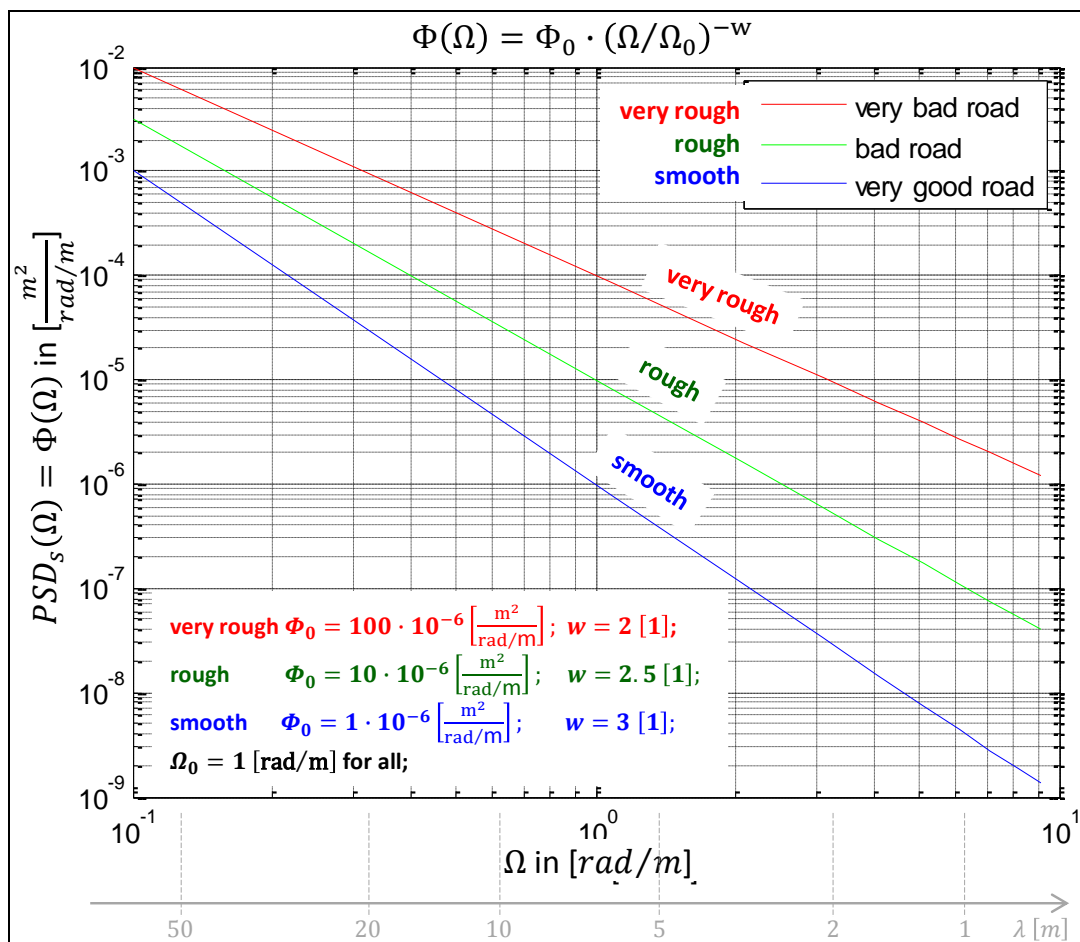
Figure 5-6: PSD spectra for the three typical roads in Figure 5-5.

Number of frequency components, N, to select is a matter of accuracy or experience. The offsets, $x_{01}, \cdots, x_{0N}$, can often be assumed to be zero. If phase is to be studied, as in Figure 5-6, a random generation of offsets is suitable. See also Reference (ISO 8608).

If we generate the actual $z_r(x)$ curves for the 3 road types in Figure 5-6, we can plot as shown in Figure 5-7. To generate those plots, we have to assume different number of harmonic components (N in Equation [5.24]) and also randomly generate the phase for each component (each x_{0i}) .
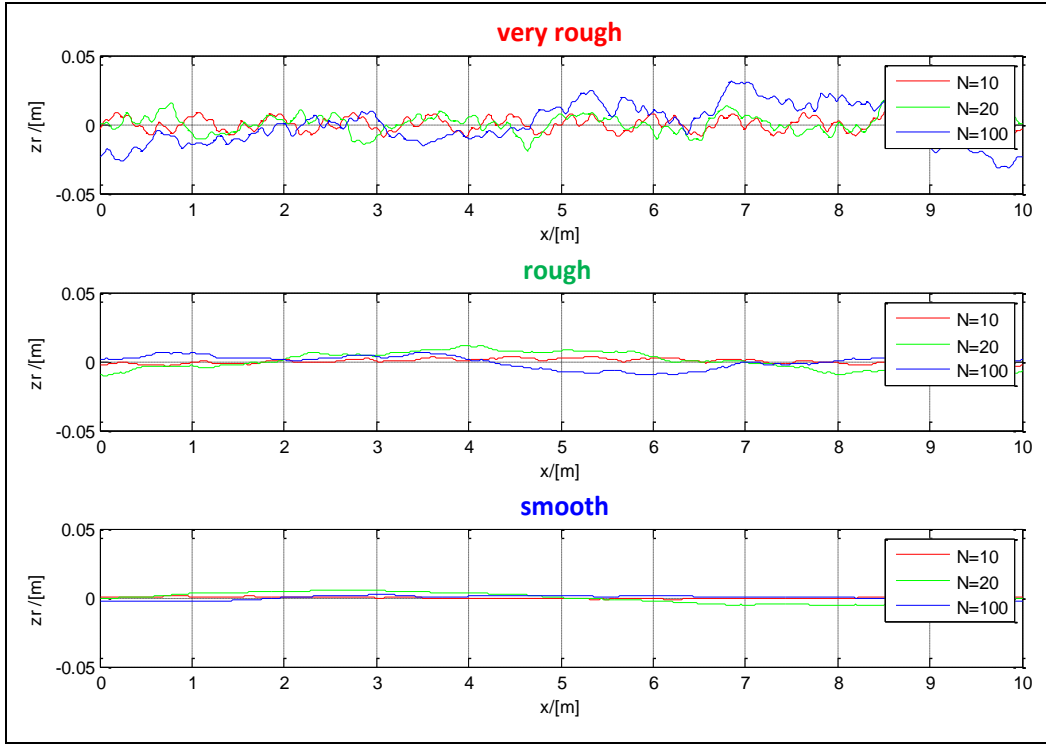
Figure 5-7: Road profiles, $z_r(x)$, for the three typical roads in Figure 5-5.

5.4.2.1 Transfer function from road spectrum in spatial domain to system response in time domain

Since we assume constant longitudinal velocity, v_x, the road spectrum can be transformed to the time-frequency domain:

$$G_{z_r}(\omega) = \frac{MS(z_r, \omega)}{\Delta\omega} = \{use: \omega = v_x \cdot \Omega\} = \frac{MS_s(z_r, \Omega)}{v_x \cdot \Delta\Omega} =$$

$$= \left\{use: \Phi_0 \cdot \left(\frac{\Omega}{\Omega_0}\right)^{-w} = \frac{MS_s(z_r, \Omega)}{\Delta\Omega}\right\} = \frac{\Phi_0 \cdot \left(\frac{\Omega}{\Omega_0}\right)^{-w}}{v_x} =$$

$$= \frac{\Phi_0 \cdot \Omega^{-w}}{\Omega_0^{-w} \cdot v_x} = \frac{\Phi_0}{\Omega_0^{-w}} \cdot \frac{\left(\frac{\omega}{v_x}\right)^{-w}}{v_x} = \frac{\Phi_0}{\Omega_0^{-w}} \cdot v_x^{w-1} \cdot \omega^{-w};$$

[5.28]

Then, we can use Equation [5.14] to obtain the response z_s:

$$G_{z_s}(\omega) = \left|H_{z_r \to z_s}(\omega)\right|^2 \cdot G_{z_r}(\omega) = \left|H_{z_r \to z_s}(\omega)\right|^2 \cdot \frac{\Phi_0}{\Omega_0^{-w}} \cdot v_x^{w-1} \cdot \omega^{-w};$$

[5.29]

Then we can use Equation [5.9] to obtain the RMS of the response z_s:

$$RMS(z_s) = \sqrt{\sum_{i=1}^{N} G_{z_s}(\omega_i) \cdot \Delta\omega} = \sqrt{\frac{\Phi_0}{\Omega_0^{-w}} \cdot v_x^{w-1} \cdot \sum_{i=1}^{N} \left|H_{z_r \to z_s}(\omega_i)\right|^2 \cdot \omega_i^{-w} \cdot \Delta\omega} \; ;$$

or

$$RMS(z_s) = \sqrt{\int_{\omega=0}^{\infty} G_{z_s}(\omega) \cdot d\omega} = \sqrt{\frac{\Phi_0}{\Omega_0^{-w}} \cdot v_x^{w-1} \cdot \int_{\omega=0}^{\infty} \left|H_{z_r \to z_s}(\omega)\right|^2 \cdot \omega^{-w} \cdot d\omega} \; ;$$

[5.30]

5.5 One-dimensional vehicle models

"One-dimensional" refers to pure vertical motion, i.e. that the vehicle heaves without pitch and without roll. The tyre is stiff and massless.

This can be seen as that the whole vehicle mass, m, is modelled as suspended by the sum of all wheels' vertical forces, $F_z = F_{flz} + F_{frz} + F_{rlz} + F_{rrz}$. However, the model can sometimes be referred to as a "quarter-car-model". That is because one can see the model as a quarter of the vehicle mass, $m/4$, which is suspended by one of the wheel's vertical force, F_{ijz}. The exact physical interpolation of a quarter car is less obvious, since one can argue whether the fraction ¼ of the vehicle mass is the proper fraction or from which point of view it is proper. Using the fraction ¼ is as least debatable if the vehicle is completely symmetrical, both left/right and front/rear.

5.5.1 One-dimensional model without dynamic degree of freedom

"Without dynamic degree of freedom" refers to that the (axle) suspension is modelled as ideally stiff. The model can be visualised as in Figure 5-8.
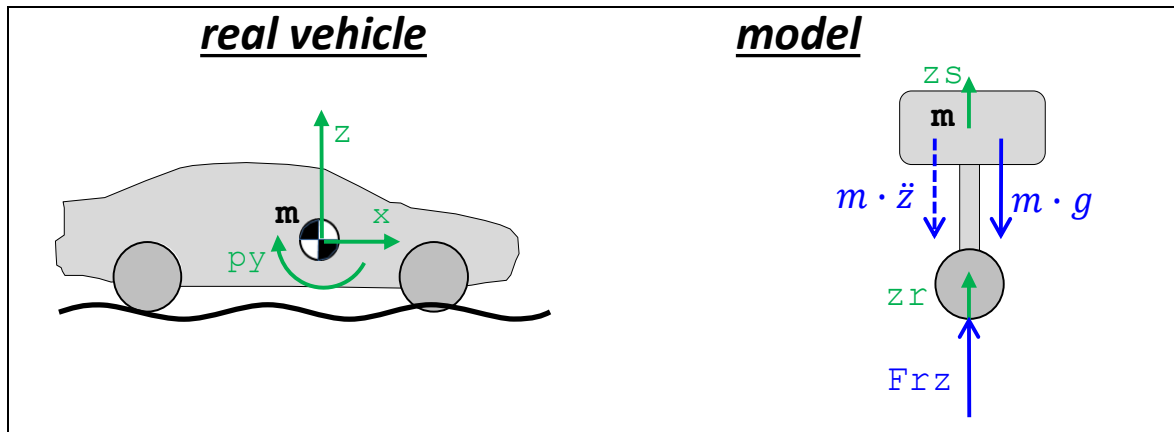
Figure 5-8: One-dimensional model without dynamic degree of freedom

Probably, we could find the equations without very much formalism ($m \cdot \ddot{z}_s = F_{rz}$; and $z_s = z_r(t)$;), but the following equations exemplifies a formalism which will be useful when we expand the model later.

$$\begin{aligned} &\textbf{\textit{Equilibrium}}: && m \cdot \ddot{z} + m \cdot g = F_{rz}; \\ &\textbf{\textit{Compatibility}}: && z_r = z; \\ &\textbf{\textit{Excitation}}: && z_r = z_r(t); \end{aligned}$$

[5.31]

5.5.1.1 Response to a single frequency excitation

Assume that the road has only one (spatial) frequency, i.e. one wave length. Then the excitation is as follows:

$$\begin{cases} z_r = z_r(x) = \hat{z}_r \cdot \cos(\Omega \cdot x + x_0) = \hat{z}_r \cdot \cos\left(\frac{2 \cdot \pi}{\lambda} \cdot x + x_0\right); \\ x = v_x \cdot t; \\ \text{Assume } x_0 = 0; \end{cases} \Rightarrow$$

$$\Rightarrow z_r(t) = \hat{z}_r \cdot \cos\left(\frac{2 \cdot \pi \cdot v_x}{\lambda} \cdot t\right) = \hat{z}_r \cdot \cos(\omega \cdot t); \Rightarrow$$

$$\Rightarrow \dot{z}_r(t) = -\frac{2 \cdot \pi \cdot v_x}{\lambda} \cdot \hat{z}_r \cdot \sin\left(\frac{2 \cdot \pi \cdot v_x}{\lambda} \cdot t\right) = -\omega \cdot \hat{z}_r \cdot \sin(\omega \cdot t); \Rightarrow$$

$$\Rightarrow \ddot{z}_r(t) = -\left(\frac{2 \cdot \pi \cdot v_x}{\lambda}\right)^2 \cdot \hat{z}_r \cdot \cos\left(\frac{2 \cdot \pi \cdot v_x}{\lambda} \cdot t\right) = -\omega^2 \cdot \hat{z}_r \cdot \cos(\omega \cdot t);$$

[5.32]

Insertion in the model in Equation [5.31] gives directly the solution:

$$\begin{cases} F_{rz}(t) = m \cdot g + \Delta F(t) = m \cdot g + \hat{F}_{rz} \cdot \cos(\omega \cdot t); \\ z_r(t) = z_s(t) = \hat{z}_r \cdot \cos(\omega \cdot t); \\ \ddot{z}_r(t) = \ddot{z}_s(t) = \hat{a} \cdot \cos(\omega \cdot t); \end{cases}$$

$$where \begin{cases} \hat{F}_{rz} = -m \cdot \omega^2 \cdot \hat{z}_r; \\ \hat{a} = -\omega^2 \cdot \hat{z}_r; \end{cases}$$

[5.33]

5.5.1.1.1 Analysis of solution

We can identify the magnitude of the transfer functions. The negative sign in Equation [5.33] means 180 degrees phase shift:

$$H_{z_r \to z_s} = \left\{ H_{z_r \to z_s} = \frac{\mathcal{F}(z_s)}{\mathcal{F}(z_r)} \right\} = 1 + j \cdot 0;$$

$$H_{z_r \to z_r - z_s} = \left\{ H_{z_r \to z_r - z_s} = H_{z_r \to z_s} - H_{z_s \to z_s} = H_{z_r \to z_s} - 1 \right\} = 0 + j \cdot 0;$$

$$H_{z_r \to \ddot{z}_s} = \left\{ H_{z_r \to \ddot{z}_s} = (j \cdot \omega)^2 \cdot H_{z_r \to z_s} = -\omega^2 \cdot H_{z_r \to z_s} \right\} = -\omega^2 + j \cdot 0;$$

$$H_{z_r \to \Delta F_{rz}} = \left\{ H_{z_r \to \Delta F_{rz}} = m \cdot H_{z_r \to \ddot{z}_s} \right\} = -m \cdot \omega^2 + j \cdot 0;$$

[5.34]

The motivation to choose exactly those transfer functions is revealed later, in Section 5.6, 5.7 and 5.8. For now, we simply conclude that various transfer functions can be identified and plotted. The plots are found in Figure 5-9. Numerical values for m and λ has been chosen.

So, for example, we can use the transfer function diagram as follows: If we have a road displacement amplitude of 1 cm ($\hat{z}_r = 0.01\ m$) and a speed of 50 km/h ($v_x \approx 14\ m/s \,\hat{=}\approx 2.8 Hz$), we can read out, e.g.:

- $\left|H_{z_r \to \ddot{z}_s}(v_x)\right| \approx 305; \Rightarrow |\hat{a}| = 310 \cdot \hat{z}_r = 305 \cdot 0.01 = 3.05\ m/s^2;$. From this we can calculate $RMS(\ddot{z}_s) = |3.05|/\sqrt{2} \approx 2.16\ m/s^2$. The RMS value of acceleration will later be related to ride comfort, see Section 5.6.
- $\left|H_{z_r \to z_r - z_s}(v_x)\right| = 0;$, i.e. no deformation, which is not strange, since model is stiff. The deformation of suspension will later be related to fatigue life, see Section 5.7.
- $\left|H_{z_r \to \Delta F_{rz}}(v_x)\right| \approx 487000; \Rightarrow |\hat{F}| = 487000 \cdot \hat{z}_r = 487000 \cdot 0.01 = 4870\ N;$. If $|\hat{F}|$ had been $> m \cdot g \approx 16000\ N$, the model would have been outside its validity region, because it would require pulling forces between tyre and road, which is not possible. The variation in tyre road contact force will be related to road grip, see Section 5.8.

The phases for the studied variables can be found in Equation [5.34]. With this model, the phases becomes constant and $\pm 90 \, deg$.
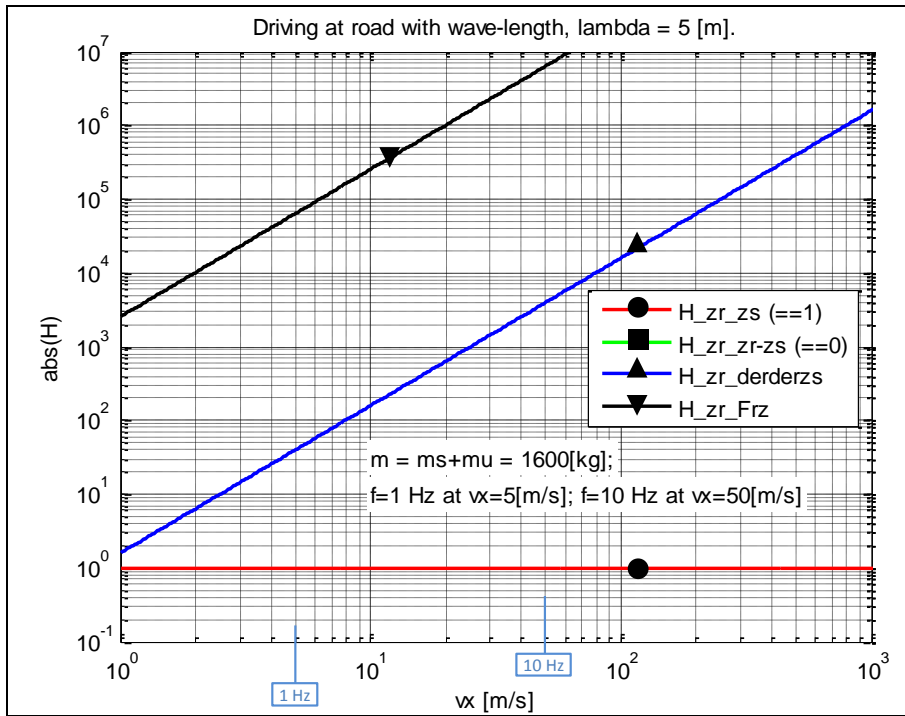
Figure 5-9: Transfer functions from model in Figure 5-8, excited with single frequencies.

5.5.1.2 Response to a multiple frequency excitation

Using Equation [5.30], Equation [5.44] and values for road type "rough" in Figure 5-6, we can conclude:

$$RMS(z_s) = \sqrt{\frac{\Phi_0}{\Omega_0^{-w}} \cdot v_x^{\, w-1} \cdot \int_{\omega=0}^{\infty} \left| H_{z_r \to z_s}(\omega) \right|^2 \cdot \omega^{-w} \cdot d\omega} =$$

$$= \sqrt{\frac{10 \cdot 10^{-6}}{1} \cdot v_x^{\, 2.5-1} \cdot \int_{\omega=0}^{\infty} \left| H_{z_r \to z_s}(\omega) \right|^2 \cdot \omega^{-2.5} \cdot d\omega} \; ; \qquad [5.35]$$

For now, we simply note that it is possible to calculate this (scalar) RMS value for each vehicle speed over the assumed road. In corresponding way, an RMS value can be calculated for any of the oscillating variables, such as $\ddot{z}_s$, $z_r - z_s$ and F_{rz}. We will come back to Equation [5.35] in Section 5.6.2.

5.5.2 One dimensional model with one dynamic degree of freedom

"With one dynamic degree of freedom" refers to that the axle suspension is modelled as a linear spring and linear (viscous) damper in parallel. The tyre is still stiff and massless as in model in Section 5.5.1. The model can be visualised as in Figure 5-10.
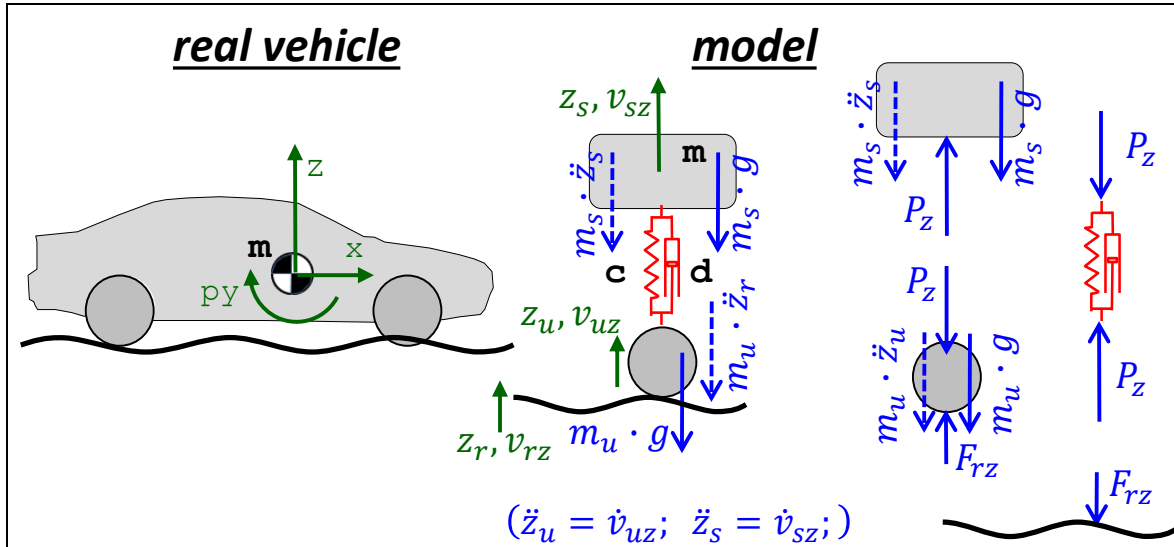
Figure 5-10: One-dimensional model with one dynamic degree of freedom

Note that the mass is now divided into sprung and unsprung mass, m_s and m_u. The mathematical model becomes as follows:.

Equilibrium sprung mass: $P_z - m_s \cdot \ddot{z}_s - m_s \cdot g = 0$;

Equilibrium unsprung mass: $F_{rz} - P_z - m_u \cdot \ddot{z}_r - m_u \cdot g = 0$;

Constitution: $P_z = c \cdot (z_r - z_s) + d \cdot (\dot{z}_r - \dot{z}_s) + m_s \cdot g$;

Excitation: $z_r = z_r(t)$;

[5.36]

5.5.2.1 Response to a single frequency excitation

Eliminating P_z and z_r gives:

$m_s \cdot \ddot{z}_s = c \cdot (z_r(t) - z_s) + d \cdot (\dot{z}_r(t) - \dot{z}_s)$;

$\Delta F_{rz} = c \cdot (z_r(t) - z_s) + d \cdot (\dot{z}_r(t) - \dot{z}_s) + m_u \cdot \ddot{z}_r(t)$;

$where\ F_{rz} = \Delta F_{rz} + (m_s + m_u) \cdot g$;

[5.37]

Note that since we measure z_u and z_s from the static equilibrium, the static load, $m_s \cdot g$, disappears when constitution is inserted in equilibrium.

Assume that the road has only one (spatial) frequency, i.e. one wave length. Then the excitation is as in Equation [5.25], in which we assume $x_0 = 0$. So, we can insert $z_r(t) = \hat{z}_r \cdot \cos(\omega \cdot t) \Rightarrow \dot{z}_r(t) = -\omega \cdot \hat{z}_r \cdot \sin(\omega \cdot t) \Rightarrow \ddot{z}_r(t) = -\omega^2 \cdot \hat{z}_r \cdot \cos(\omega \cdot t)$; in Equation [5.37] and solve it for $z_s(t)$ and $\Delta F_{rz}(t)$ with trigonometry or Fourier transform.

5.5.2.1.1 Solution with Fourier transform

Fourier transform of Equation [5.37] yields:

$m_s \cdot \left(-\omega^2 \cdot \mathcal{F}(z_s)\right) = c \cdot \left(\mathcal{F}(z_r) - \mathcal{F}(z_s)\right) + d \cdot \left(j \cdot \omega \cdot \mathcal{F}(z_r) - j \cdot \omega \cdot \mathcal{F}(z_s)\right)$;

$\mathcal{F}(\Delta F_{rz}) = c \cdot \left(\mathcal{F}(z_r) - \mathcal{F}(z_s)\right) + d \cdot \left(j \cdot \omega \cdot \mathcal{F}(z_r) - j \cdot \omega \cdot \mathcal{F}(z_s)\right) - m_u \cdot \omega^2 \cdot \mathcal{F}(z_r)$;

[5.38]

From this, we can then solve the transfer functions:

$$H_{z_r \to z_s} = \frac{\mathcal{F}(z_s)}{\mathcal{F}(z_r)} = \frac{c + j \cdot d \cdot \omega}{c + j \cdot d \cdot \omega - m_s \cdot \omega^2};$$

$$H_{z_r \to \Delta F_{rz}} = \frac{\mathcal{F}(\Delta F_{rz})}{\mathcal{F}(z_r)} = (-c - j \cdot \omega \cdot d) \cdot H_{z_r \to z_s} + c + j \cdot \omega \cdot d - m_u \cdot \omega^2 =$$

$$= \frac{c^2 - \omega^2 \cdot d^2}{c + j \cdot \omega \cdot d - m_s \cdot \omega^2} + c + j \cdot \omega \cdot d - m_u \cdot \omega^2;$$

[5.39]

5.5.2.1.2 Solution with trigonometry

One way to solve the mathematical model in Equation [5.36] is to assume a real solution, insert the assumption and find expressions for the coefficients in the assumption. Assume such solution (and that $x_0 = 0$ in Equation [5.25]):

$$m \cdot \ddot{z}_s + d \cdot \dot{z}_s + c \cdot z_s = \hat{z}_r \cdot (c \cdot \cos(\omega \cdot t) - d \cdot \omega \cdot \sin(\omega \cdot t));$$

[5.40]

Assumed solution:

$$z_s = \hat{z}_s \cdot \cos(\omega \cdot t - \varphi); \Rightarrow$$
$$\Rightarrow \{use: \cos(a - b) = \cos a \cdot \cos b + \sin a \cdot \sin b\} \Rightarrow$$
$$\Rightarrow z_s = \hat{z}_s \cdot [\cos(\omega \cdot t) \cdot \cos \varphi + \sin(\omega \cdot t) \cdot \sin \varphi]; \Rightarrow$$
$$\Rightarrow \dot{z}_s = \hat{z}_s \cdot \omega \cdot [-\sin(\omega \cdot t) \cdot \cos \varphi + \cos(\omega \cdot t) \cdot \sin \varphi]; \Rightarrow$$
$$\Rightarrow \ddot{z}_s = -\hat{z}_s \cdot \omega^2 \cdot [\cos(\omega \cdot t) \cdot \cos \varphi + \sin(\omega \cdot t) \cdot \sin \varphi];$$

[5.41]

Insertion:

$$-m \cdot \hat{z}_s \cdot \omega^2 \cdot [\cos(\omega \cdot t) \cdot \cos \varphi + \sin(\omega \cdot t) \cdot \sin \varphi] +$$
$$+d \cdot \hat{z}_s \cdot \omega \cdot [-\sin(\omega \cdot t) \cdot \cos \varphi + \cos(\omega \cdot t) \cdot \sin \varphi] +$$
$$+c \cdot \hat{z}_s \cdot [\cos(\omega \cdot t) \cdot \cos \varphi + \sin(\omega \cdot t) \cdot \sin \varphi] =$$
$$= \hat{z}_r \cdot (c \cdot \cos(\omega \cdot t) - d \cdot \omega \cdot \sin(\omega \cdot t)); \Rightarrow$$
$$\Rightarrow \begin{cases} \pmb{cos\ terms}: -m \cdot \hat{z}_s \cdot \omega^2 \cdot \cos \varphi + d \cdot \hat{z}_s \cdot \omega \cdot \sin \varphi + c \cdot \hat{z}_s \cdot \cos \varphi = \hat{z}_r \cdot c; \\ \pmb{sin\ terms}: -m \cdot \hat{z}_s \cdot \omega^2 \cdot \sin \varphi - d \cdot \hat{z}_s \cdot \omega \cdot \cos \varphi + c \cdot \hat{z}_s \cdot \sin \varphi = -\hat{z}_r \cdot d \cdot \omega; \end{cases} \Rightarrow$$
$$\Rightarrow \begin{cases} \varphi = \arctan\left(\dfrac{m \cdot d \cdot \omega^3}{c^2 - m \cdot c \cdot \omega^2 + d^2 \cdot \omega^2}\right); \\ \dfrac{\hat{z}_s}{\hat{z}_r} = \dfrac{d \cdot \omega}{(m \cdot \omega^2 - c) \cdot \sin \varphi + d \cdot \omega \cdot \cos \varphi} = |H_{z_r \to z_s}|; \end{cases}$$
$$where\ \omega = \frac{2 \cdot \pi \cdot v_x}{\lambda};$$

[5.42]

We have identified $|H_{z_r \to z_s}(v_x)|$, which can be compared to $|H_{z_r \to z_s}(v_x)|$ in Equation [5.34]. The other transfer functions in Equation [5.34] are more difficult to express using the method with real algebra. We leave them to next section.

5.5.2.1.3 Analysis of solution

We can elaborate further with Equation [5.39]:

Amplitude:

$$\left|H_{z_r \to z_s}\right| = \frac{\hat{z}_s}{\hat{z}_r} = \left|\frac{c + j \cdot d \cdot \omega}{(c - m \cdot \omega^2) + j \cdot d \cdot \omega}\right| =$$

$$= \left\{ \begin{array}{c} \text{Assume } \frac{c + j \cdot d \cdot \omega}{(c - m \cdot \omega^2) + j \cdot d \cdot \omega} = ReH + j \cdot ImH; \\ \text{Solve for ReH and ImH;} \\ \left|H_{z_r \to z_s}\right| = \sqrt{ReH^2 + ImH^2}; \end{array} \right\} = \cdots = \sqrt{\frac{c^2 + d^2 \cdot \omega^2}{\left(c - m \cdot \omega^2\right)^2 + d^2 \cdot \omega^2}};$$

Phase:

$$\varphi_s(\omega) - \varphi_r(\omega) = \arg\left(\frac{c + j \cdot d \cdot \omega}{-m \cdot \omega^2 + c + j \cdot d \cdot \omega}\right) =$$

$$= \left\{ \begin{array}{c} \text{Assume } \frac{c + j \cdot d \cdot \omega}{(c - m \cdot \omega^2) + j \cdot d \cdot \omega} = ReH + j \cdot ImH; \\ \text{Solve for ReH and ImH;} \\ \tan(\arg(H_{z_r \to z_s})) = ImH/ReH; \end{array} \right\} = \cdots =$$

$$= \arctan\left(\frac{m \cdot d \cdot \omega^3}{c^2 - m \cdot c \cdot \omega^2 + d^2 \cdot \omega^2}\right); \quad \text{where } \omega = \frac{2 \cdot \pi \cdot v_x}{\lambda};$$

[5.43]

Equation [5.13] now allows us to get the magnitudes of the other transfer functions as well:

$$H_{z_r \to z_s} = \text{from Equation [5.39]};$$
$$H_{z_r \to z_r - z_s} = H_{z_r \to z_r} - H_{z_r \to z_s} = 1 - H_{z_r \to z_s};$$
$$H_{z_r \to \ddot{z}_s} = -\omega^2 \cdot H_{z_r \to z_s};$$
$$H_{z_r \to \Delta F_{rz}} = \{\Delta F_{rz} = c \cdot (z_r - z_s) + d \cdot (\dot{z}_r - \dot{z}_s)\} =$$
$$= c \cdot \left(H_{z_r \to z_r} - H_{z_r \to z_s}\right) + d \cdot \left(H_{z_r \to \dot{z}_r} - H_{z_r \to \dot{z}_s}\right) =$$
$$= (c + j \cdot d \cdot \omega) \cdot \left(H_{z_r \to z_r} - H_{z_r \to z_s}\right) =$$
$$= (c + j \cdot d \cdot \omega) \cdot \left(1 - H_{z_r \to z_s}\right);$$

[5.44]

The motivation to choose exactly those transfer functions is revealed later, in Section5.6, 5.7 and 5.8. Some of those magnitudes are easily expressed in reel (non-complex) mathematics using Equation [5.43]:

$$\left|H_{z_r \to z_s}\right| = \sqrt{\frac{c^2 + d^2 \cdot \omega^2}{(c - m \cdot \omega^2)^2 + d^2 \cdot \omega^2}};$$

$$\left|H_{z_r \to \ddot{z}_s}\right| = \omega^2 \cdot \sqrt{\frac{c^2 + d^2 \cdot \omega^2}{(c - m \cdot \omega^2)^2 + d^2 \cdot \omega^2}};$$

[5.45]

The transfer functions in Equation [5.43] are plotted in Figure 5-11 and Figure 5-12. Numerical values for m and λ has been chosen.

For example, we can use Figure 5-11 as follows, cf. end of Section 5.5.1.1.1: If we have a certain road, with displacement amplitude of 1 cm ($\hat{z}_r = 0.01\ m$) and the vehicle should drive on it at a speed of 50 km/h ($v_x \approx 14\ m/s \triangleq\approx 2.8Hz$), we can read out, e.g.:

- Ride comfort related: $\left|H_{z_r \to \ddot{z}_s}(v_x)\right| \approx 120;\ \Rightarrow\ |\hat{a}| = 120 \cdot \hat{z}_r = 120 \cdot 0.01 = 1.20\ m/s^2$;. From this we can calculate $RMS(\ddot{z}_s) = |1.20|/\sqrt{2} \approx 0.8485\ m/s^2$.
- Fatigue life related: $\left|H_{z_r \to z_r - z_s}(v_x)\right| \approx 1.11;\ \Rightarrow\ |\hat{z}_r - \hat{z}_s| = 1.11 \cdot \hat{z}_r = 1.11 \cdot 0.01 = 0.0111\ m = 1.11\ cm;.$
- Road grip related: $\left|H_{z_r \to \Delta F_{rz}}(v_x)\right| \approx 59795;\ \Rightarrow\ |\hat{F}_{rz}| = 59795 \cdot \hat{z}_r = 59795 \cdot 0.01 = 598\ N;.$
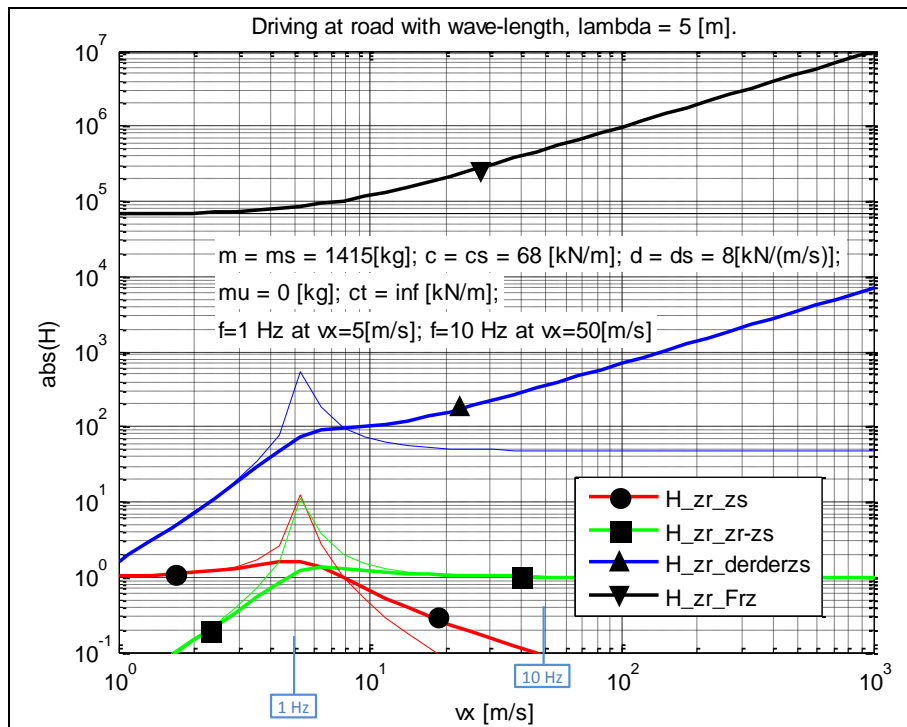
Figure 5-11: Transfer functions for amplitudes from model in Figure 5-10, excited with single frequencies. Thin lines are without damping. Notation: $H_{a\rightarrow b}$ is denoted `H_a_b`.
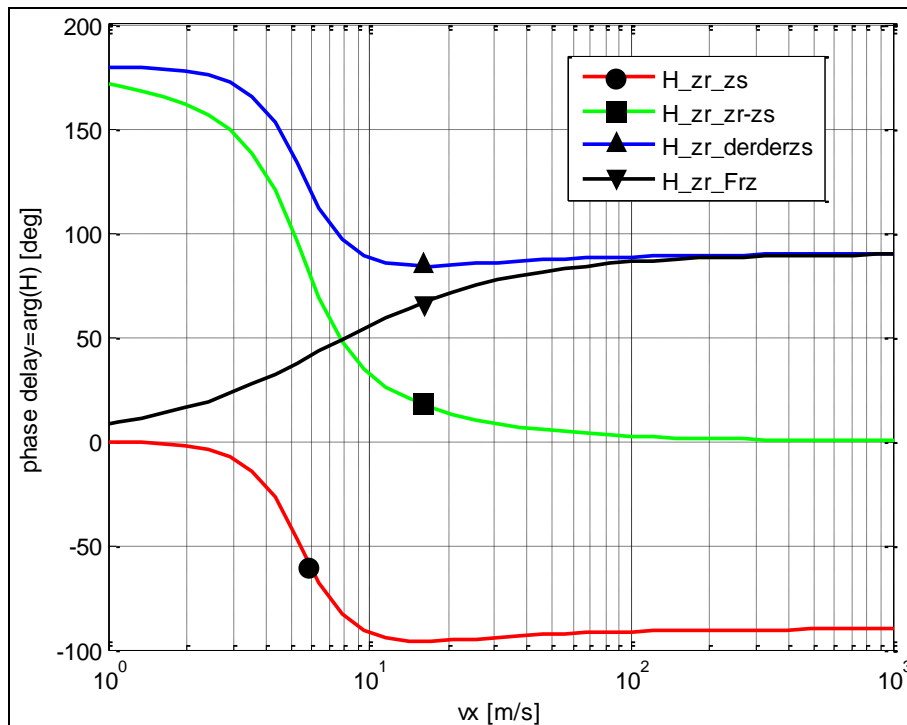
Figure 5-12: Transfer functions for phase delays from model in Figure 5-10, excited with single frequencies.

We compare these numbers with the corresponding numbers for the simpler model, see Sections 5.5.1.1.1. The comfort is has been better. The fatigue life and road grip have become more realistic.

Figure 5-11 also shows the curves for the undamped system (d=0). The highest peaks appear at approximately $v_x = 5..6$ m/s. This corresponds to the speed where the natural (=undamped) eigen frequency appears ($v_{x,crit} = \lambda \cdot f_{crit} = \lambda \cdot \omega_{crit}/(2 \cdot \pi) = \lambda \cdot \sqrt{c/m}/(2 \cdot \pi) \approx 5.5\ m/s$).

Figure 5-12 shows the phase angles for the different responses.

5.5.3 One dimensional model with two degrees of freedom

The expression "two dynamic degree of freedom" in section the heading refers to that both elasticity between road and wheel as well as between wheel and sprung mass is modelled. Alternatively, one can describe the two degrees of freedom as the suspension spring deformation and the tyre spring deformation.

The model can be visualised as in Figure 5-13. No damping is modelled in tyre (in parallel with elasticity c_t) because it is generally relatively low.
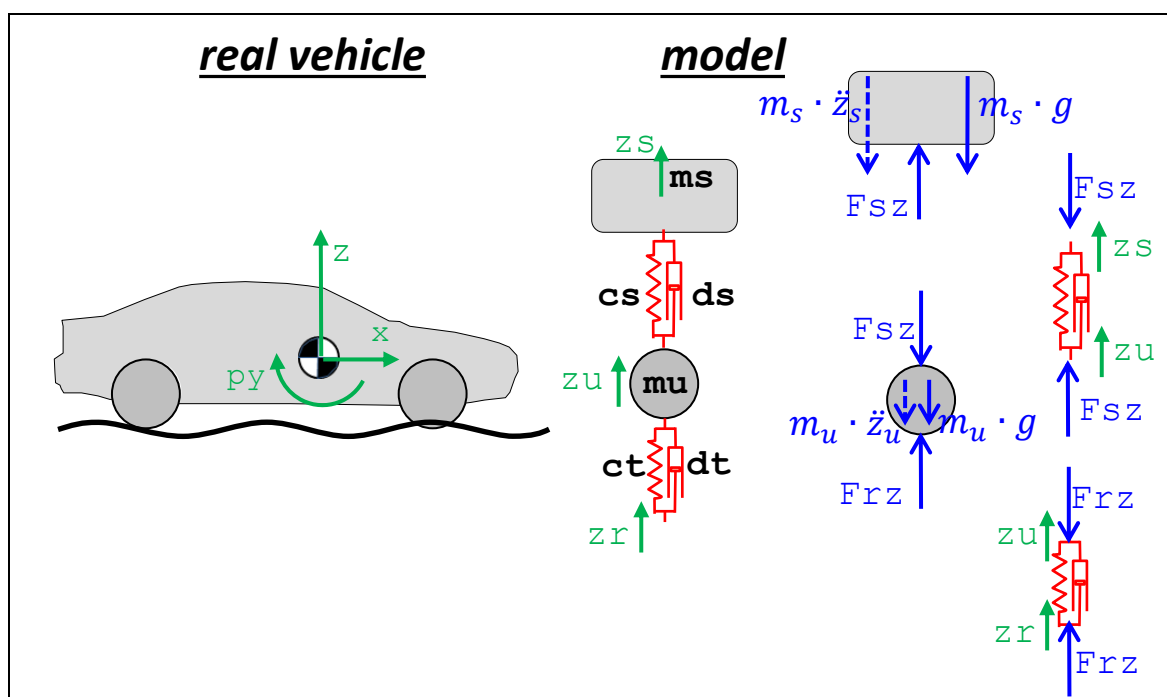
Figure 5-13: One-dimensional model with two dynamic degrees of freedom

The corresponding mathematical model becomes as follows:

Equilibrium:

$$m_s \cdot \ddot{z}_s = F_{sz} - m_s \cdot g;$$
$$m_u \cdot \ddot{z}_u = F_{rz} - F_{sz} - m_u \cdot g;$$

Constitution (displacements counted from static equilibrium):

$$F_{sz} = c_s \cdot (z_u - z_s) + d_s \cdot (\dot{z}_u - \dot{z}_s) + m_s \cdot g;$$
$$F_{rz} = c_t \cdot (z_r - z_u) + d_t \cdot (\dot{z}_r - \dot{z}_u) + (m_s + m_u) \cdot g;$$

Excitation:

$$z_r = z_r(t);$$

[5.46]

The same can be formulated with matrices and Fourier transforms:

$$\begin{bmatrix} m_s & 0 \\ 0 & m_u \end{bmatrix} \cdot \begin{bmatrix} \ddot{z}_s \\ \ddot{z}_u \end{bmatrix} + \begin{bmatrix} d_s & -d_s \\ -d_s & d_s + d_t \end{bmatrix} \cdot \begin{bmatrix} \dot{z}_s \\ \dot{z}_u \end{bmatrix} + \begin{bmatrix} c_s & -c_s \\ -c_s & c_s + c_t \end{bmatrix} \cdot \begin{bmatrix} z_s \\ z_u \end{bmatrix} = \begin{bmatrix} 0 \\ d_t \end{bmatrix} \cdot \dot{z}_r + \begin{bmatrix} 0 \\ c_t \end{bmatrix} \cdot z_r;$$

$$\Rightarrow \boldsymbol{M} \cdot \begin{bmatrix} \ddot{z}_s \\ \ddot{z}_u \end{bmatrix} + \boldsymbol{D} \cdot \begin{bmatrix} \dot{z}_s \\ \dot{z}_u \end{bmatrix} + \boldsymbol{C} \cdot \begin{bmatrix} z_s \\ z_u \end{bmatrix} = \boldsymbol{D_r} \cdot \dot{z}_r + \boldsymbol{C_r} \cdot z_r; \Rightarrow$$

$$\Rightarrow \boldsymbol{M} \cdot (-\omega^2 \cdot Z_{su}) + \boldsymbol{D} \cdot (j \cdot \omega \cdot Z_{su}) + \boldsymbol{C} \cdot Z_{su} = \boldsymbol{D_r} \cdot (j \cdot \omega \cdot Z_r) + \boldsymbol{C_r} \cdot Z_r; \Rightarrow$$

$$\Rightarrow (-\omega^2 \cdot \boldsymbol{M} + j \cdot \omega \cdot \boldsymbol{D} + \boldsymbol{C}) \cdot Z_{su} = (j \cdot \omega \cdot \boldsymbol{D_r} + \boldsymbol{C_r}) \cdot Z_r;$$

$$where\ Z_{su} = \begin{bmatrix} Z_s \\ Z_u \end{bmatrix} = \begin{bmatrix} \mathcal{F}(z_s) \\ \mathcal{F}(z_u) \end{bmatrix};\ and\ Z_r = \mathcal{F}(z_r);$$

[5.47]

The matrix $\boldsymbol{D_r}$ is zero, but marks a more general form, typical for modelling damping also in the tyre.

5.5.3.1 Response to a single frequency excitation

5.5.3.1.1 Solution with Fourier transform

We can find the transfer functions via Fourier transform, starting from Equation [4.63]:

$$\begin{bmatrix} H_{z_r \to z_s} \\ H_{z_r \to z_u} \end{bmatrix} = \begin{bmatrix} Z_s \\ Z_u \end{bmatrix} \cdot \frac{1}{Z_r} = Z_{su} \cdot \frac{1}{Z_r} = (-\omega^2 \cdot \boldsymbol{M} + j \cdot \omega \cdot \boldsymbol{D} + \boldsymbol{C})^{-1} \cdot (j \cdot \omega \cdot \boldsymbol{D_r} + \boldsymbol{C_r});$$

[5.48]

This format is very compact, since it includes both transfer functions for amplitude and phase. For numerical analyses, the expression in Equation [5.51] is explicit enough, since there are tools, e.g. Matlab, which supports matrix inversion and complex mathematics.

For analytic solution one would need symbolic tools, e.g. Mathematica or Matlab with symbolic toolbox, or careful manual algebraic operations. With $d_t = 0$, the explicit forms becomes as follows:

$$H_{z_r \to z_s} = \frac{Z_s}{Z_r} = \frac{\dfrac{(-m_u \cdot \omega^2 + j \cdot d_s \cdot \omega + c_t + c_s) \cdot c_t}{-m_u \cdot \omega^2 + j \cdot d_s \cdot \omega + c_t + c_s - \dfrac{(c_s + j \cdot d_s \cdot \omega)^2}{-m_s \cdot \omega^2 + j \cdot d_s \cdot \omega + c_s}} - c_t}{c_s + j \cdot d_s \cdot \omega};$$

$$H_{z_r \to z_u} = \frac{Z_u}{Z_r} = \frac{c_t}{-m_u \cdot \omega^2 + j \cdot d_s \cdot \omega + c_t + c_s - \dfrac{(c_s + j \cdot d_s \cdot \omega)^2}{-m_s \cdot \omega^2 + j \cdot d_s \cdot \omega + c_s}};$$

where $\omega = \dfrac{2 \cdot \pi \cdot v_x}{\lambda};$

[5.49]

5.5.3.1.2 Analysis of solution

Equation [5.13] now allows us to get the magnitudes of the other transfer functions as well:

$$H_{z_r \to z_s} = see\ Equation\ [5.49];$$
$$H_{z_r \to z_u} = see\ Equation\ [5.49];$$
$$H_{z_r \to z_r - z_u} = H_{z_r \to z_r} - H_{z_r \to z_u} = 1 - H_{z_r \to z_u};$$
$$H_{z_r \to z_u - z_s} = H_{z_r \to z_u} - H_{z_r \to z_s};$$
$$H_{z_r \to \ddot{z}_s} = -\omega^2 \cdot H_{z_r \to z_s};$$
$$H_{z_r \to \Delta F_{sz}} = \{\Delta F_{sz} = c_s \cdot (z_u - z_s) + d_s \cdot (\dot{z}_u - \dot{z}_s)\} =$$
$$= c_s \cdot (H_{z_r \to z_u} - H_{z_r \to z_s}) + d_s \cdot j \cdot \omega \cdot (H_{z_r \to z_u} - H_{z_r \to z_s}) =$$
$$= (c_s + j \cdot d_s \cdot \omega) \cdot (H_{z_r \to z_u} - H_{z_r \to z_s});$$
$$H_{z_r \to \Delta F_{rz}} = \{\Delta F_{rz} = c_t \cdot (z_r - z_u)\} = c_t \cdot (H_{z_r \to z_r} - H_{z_r \to z_u}) = c_t \cdot (1 - H_{z_r \to z_u});$$

[5.50]

Expression in real can be derived, see Equation [5.51]. Note that it is more general than Equation [5.50], having a tyre damper modelled, $d_t \neq 0$. The derivation is not documented in present compendium.

$$\left|H_{z_r \to \ddot{z}_s}\right| = \omega^2 \cdot \frac{\sqrt{(c_s \cdot c_t - d_s \cdot d_t \cdot \omega^2)^2 + \left(\omega \cdot (d_s \cdot c_t + d_t \cdot c_s)\right)^2}}{\sqrt{A^2 + B^2}};$$

$$\left|H_{z_r \to z_u - z_s}\right| = \frac{m_s \cdot \sqrt{(c_t \cdot \omega^2)^2 + (d_t \cdot \omega^3)^2}}{\sqrt{A^2 + B^2}};$$

$$\left|H_{z_r \to z_r - z_u}\right| = \frac{\sqrt{(-m_s \cdot m_u \cdot \omega^4 + \omega^2 \cdot (m_s + m_u) \cdot c_s)^2 + (\omega^3 \cdot (m_s + m_u) \cdot d_s)^2}}{\sqrt{A^2 + B^2}};$$

$$A = \omega^4 \cdot m_s \cdot m_u - \omega^2 \cdot (m_s \cdot c_t + m_s \cdot c_s + d_s \cdot d_t + c_s \cdot m_u) + c_s \cdot c_t;$$

$$B = \omega^3 \cdot (m_s \cdot d_t + m_s \cdot d_s + m_u \cdot d_s) - \omega \cdot (d_s \cdot c_t + d_t \cdot c_s);$$

[5.51]

The transfer functions in Equation [5.50] are plotted in Figure 5-14. If we have a certain road, with displacement amplitude of 1 cm ($\hat{z}_r = 0.01\ m$) and the vehicle should drive on it at a speed of 50 km/h ($v_x \approx 14 \frac{m}{s} \cong \approx 2.8 Hz$), we can read out, e.g.:

- Ride comfort related: $\left|H_{z_r \to \ddot{z}_s}(v_x)\right| \approx 123;\ \Rightarrow |\hat{a}| = 123 \cdot \hat{z}_r = 123 \cdot 0.01 = 1.23\ m/s^2$;. From this we can calculate $RMS(\ddot{z}_s) = |1.23|/\sqrt{2} \approx 0.8697\ m/s^2$.
- Fatigue life related: $\left|H_{z_r \to z_u - z_s}(v_x)\right| \approx 1.14;\ \Rightarrow\ |\hat{z}_u - \hat{z}_s| = 1.14 \cdot \hat{z}_r = 1.14 \cdot 0.01 = 0.0114\ m = 1.14\ cm$;.
- Road grip related: $\left|H_{z_r \to \Delta F_{rz}}(v_x)\right| \approx 177470;\ \Rightarrow\ |\hat{F}_{rz}| = 177470 \cdot \hat{z}_r = 177470 \cdot 0.01 = 1775\ N$;.

This analysis can be compared with the analysis in Section 5.5.2.1.3. Ride comfort and fatigue does not change a lot, but road grip does. This indicates that the more advanced model is only needed for road grip evaluation.

Figure 5-15 shows the phase angles for the different responses.

Figure 5-16, shows the amplitude gains for the corresponding un-damped system. We identify natural frequencies at around 5 m/s and 50 m/s. These two speeds correspond to frequencies $v_{x,crit}/\lambda$, i.e. approximately 1 Hz and 10 Hz. The lower frequency is an oscillation mode where the both masses move in phase with each other, the so called "bounce mode". The higher frequency comes from the mode where the masses are in counter-phase to each other, the so called "wheel hop mode". In the wheel hop mode, the sprung mass is almost not moving at all. We will come back to these modes in Section 5.5.3.2.
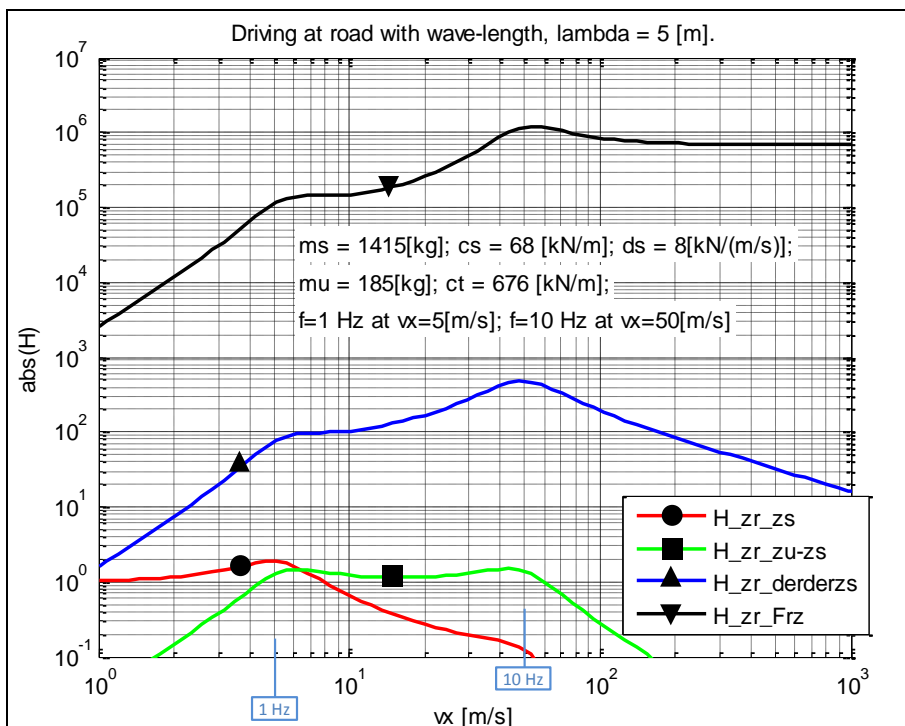
Figure 5-14: Transfer functions for amplitudes from model in Figure 5-13, excited with single frequencies. Notation: $H_{a\rightarrow b}$ is denoted H_a_b.
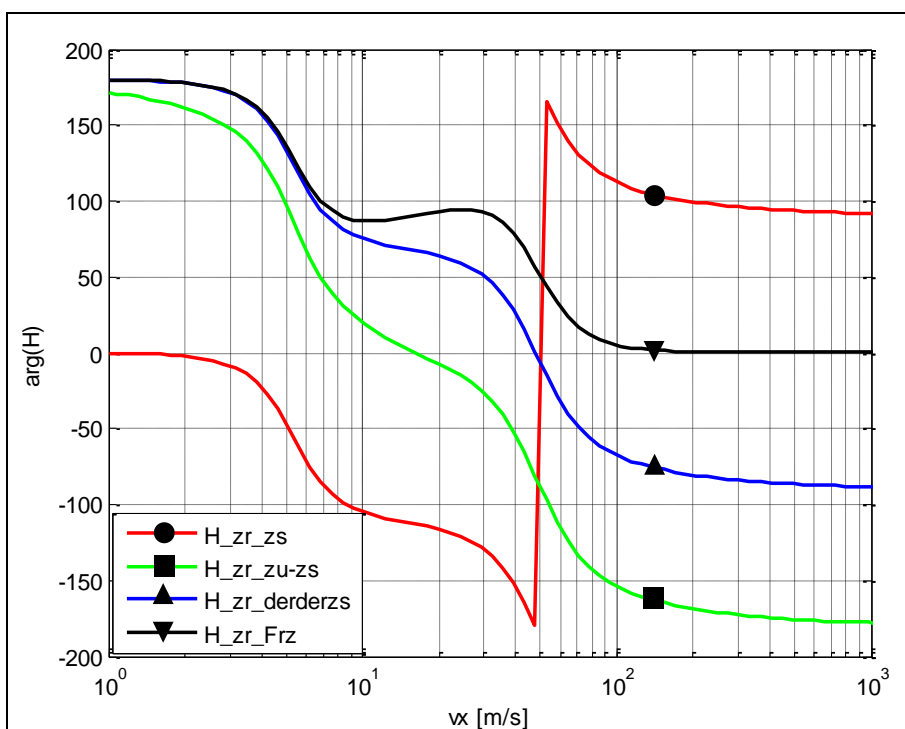
Figure 5-15: Transfer functions for phase delays. Same model and data as in Figure 5-14.
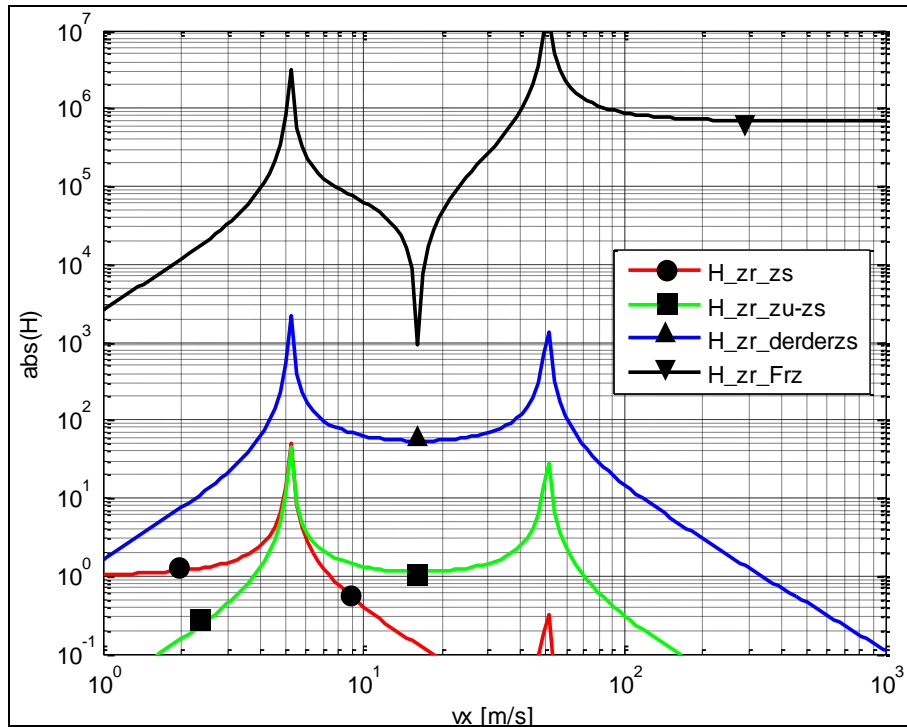
Figure 5-16: Un-damped transfer functions for amplitudes. Same model and data as in Figure 5-14, except $c_s = 0$.

5.5.3.2   Simplified model

A more practical way to approach the system is to consider the properties of the system. The sprung mass is typically an order of magnitude greater than the unsprung mass and the suspension spring is usually an order of magnitude lower than the tyre stiffness. Then, one can split the model in to models, which explains one mode each, see Figure 5-17. The modes were identified already in Section 5.5.3.1.1.
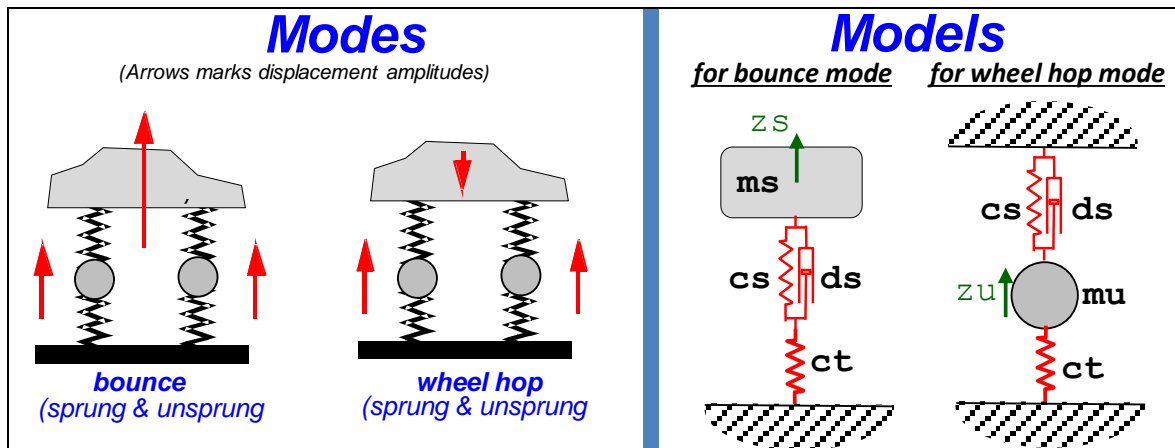
Figure 5-17: Modes and approximate models.

We will now derive the natural frequencies for the two models, and compared with the natural frequencies ($d_s = 0$) found for the combined model, in Figure 5-16. Both models are one degree of freedom models with mass and spring, why the Eigen frequency is $\sqrt{\text{stiffness/mass}}$.

For the bounce model, the mass is m_s. Stiffnesses c_s and c_t are series connected, which means that the total stiffness$= 1/\big((1/c_s) + (1/c_t)\big)$.

For the wheel hop model, the mass is m_u. Stiffnesses c_s and c_t are parallel connected, which means that the total stiffness$= c_s + c_t$.

$$\omega_{Bounce} = \sqrt{\frac{1/\left(\frac{1}{c_s} + \frac{1}{c_t}\right)}{m_s}} = 15.3\frac{rad}{s};$$

$$\omega_{WheelHop} = \sqrt{\frac{c_s + c_t}{m_u}} = 86.0\frac{rad}{s};$$

[5.52]

We see that the numbers match well with the more advanced model, which gave 15.2 rad/s and 86.7 rad/s, respectively.

Bounce refers to the mode where the sprung mass has the greatest amplitude and wheel hop is related to the case when the unsprung mass exhibits the greatest amplitude. For a passenger car, the spring mass has the lowest frequency, typically around 1 Hz while tyre hop is more prevalent at frequencies around 10 Hz.

5.6 Ride comfort *

Function definition: **(Stationary) Ride comfort** *is the comfort that vehicle occupants experience from stationary oscillations when the vehicle travels over a road with certain vertical irregularity in a certain speed. The measure is defined at least including driver (or driver seat) vertical acceleration amplitudes.*

Ride comfort is sometimes divided into:

* **Primary Ride** – the vehicle body on its suspension. Bounce(Heave), Pitch and Roll ≈0..4 Hz

* **Secondary Ride** – same but above body natural frequencies, i.e. ≈4..25 Hz

5.6.1 Single frequency

It is generally accepted for stationary vibrations, that humans are sensitive to the RMS value of the acceleration. However, the sensitivity is frequency dependent, so that highest discomfort appears for a certain range of frequencies. Some human tolerance curves are shown in Figure 5-18 and Figure 5-19.

The curves can be considered a threshold for acceptance where everything above the line is unacceptable and points below the curve are acceptable. Discomfort is a subjective measure, and this is why the different diagrams cannot be directly compared to each other. The SAE has suggested that frequencies from 4 to 8 Hz are the most sensitive and the accepted accelerations for these are no higher than 0.025 g (RMS).

The curves in Figure 5-18 mostly represent an extended exposure to the vibration. As one can expect, a human can endure exposure to more severe conditions for short periods of time. The SAE limits presented are indicative of 8 hours of continuous exposure. Curves for different exposure times can also be obtained from ISO, (ISO2631). The ISO curves are from the first version of ISO 2631 and were later modified, see Figure 5-19.
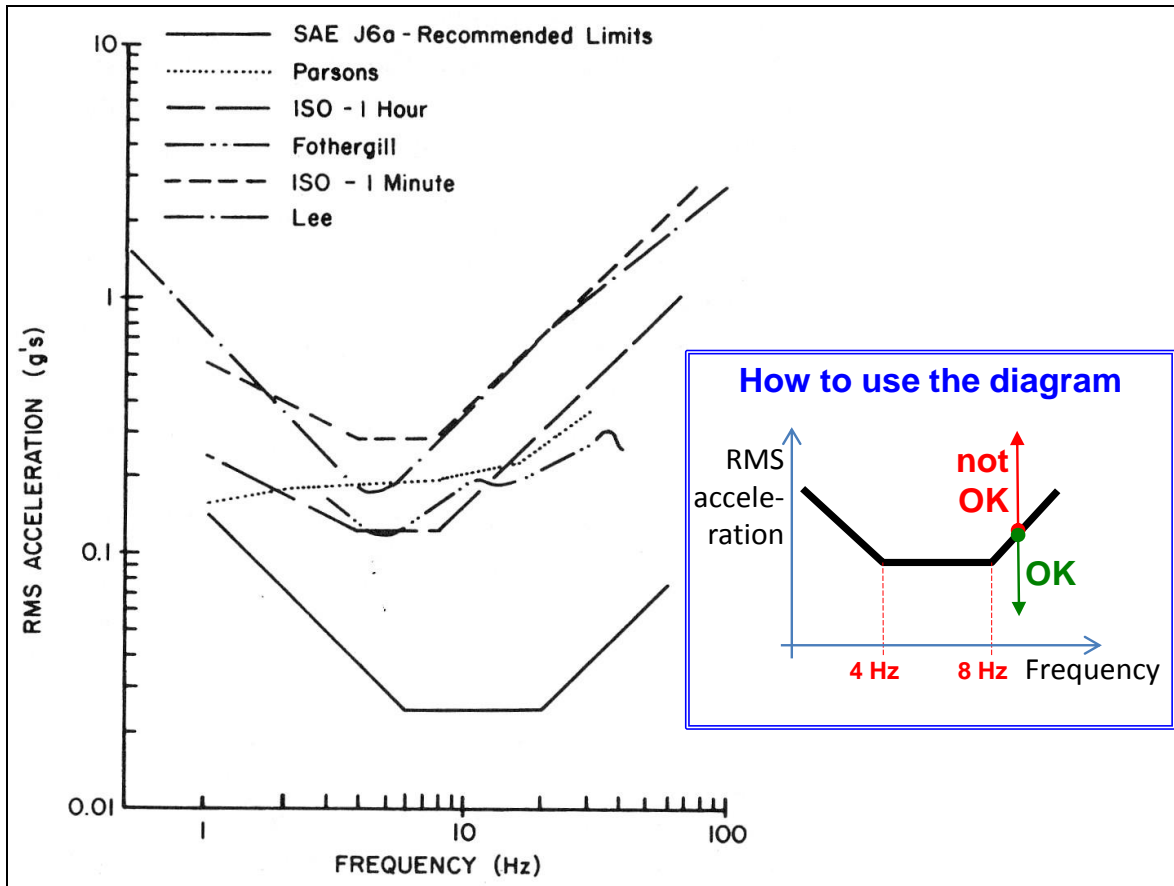
Figure 5-18: Various Human Sensitivity Curves to Vertical Vibration, (Gillespie, 1992)
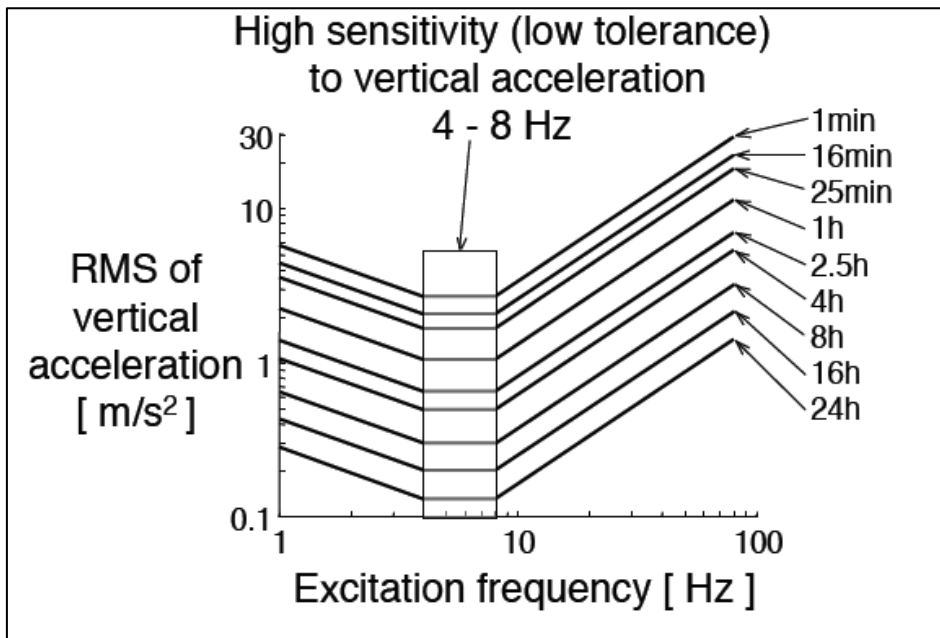
Figure 5-19: ISO 2631 Tolerance Curves

5.6.2 Multiple frequencies

The curves in Figure 5-18 and Figure 5-19 can be interpreted as a filter, where the response of the human is influenced by the frequencies they are exposed to. This leads to the concept of a Human Filter Function $W_k(f)$. (W_k refers to vertical whole human body vibration sensitivity, while there are other for sensitivities for other directions and human parts.) This approach uses the concept of a

transfer function from driver seat to somewhere inside the drivers brain, where discomfort is perceived.
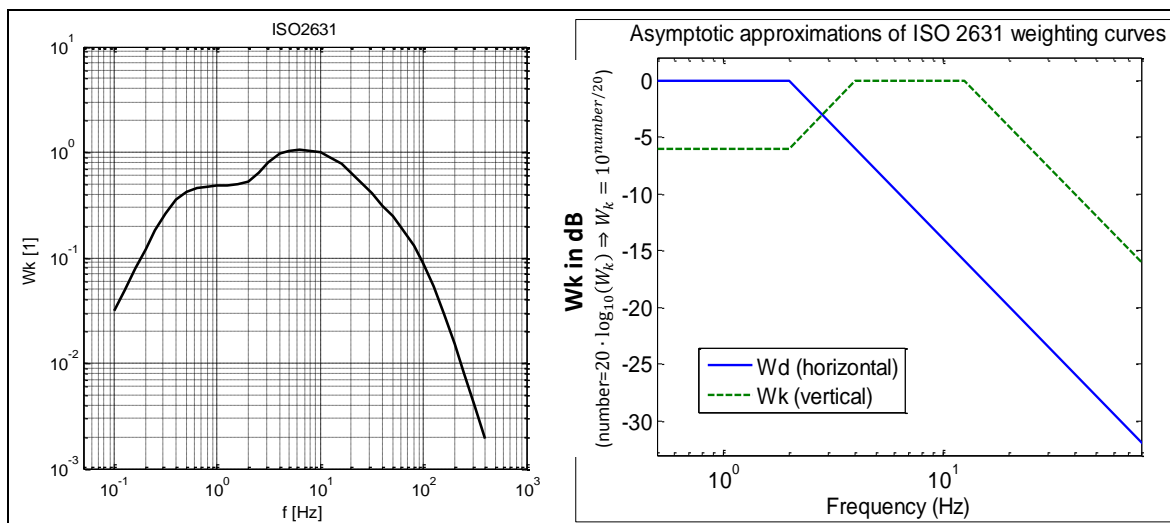
Figure 5-20: Human Filter Function. From (ISO2631). <u>Right</u>: Asymptotic approximation

Figure 5-21: Human Filter Function for vertical vibrations. Table from (ISO2631).

With formulas from earlier in this chapter we can calculate an RMS value of a signal with multiple frequencies, see Equation [5.6]. Consequently, we can calculate RMS of multiple frequency acceleration. Since humans are sensitive to acceleration, it would give one measure of human discomfort. However, to get a measure which is useful for comparing accelerations with different frequency content, the measure have to take the human filter function into account. The Weighted RMS Acceleration, a_w, in the following formula is such measure:

$$a_w = a_w\big(\ddot{z}(t)\big) = \left\{use: RMS\big(\ddot{z}(t)\big) = \sqrt{\sum_{i=1}^{N} \frac{\hat{\ddot{z}}_i^{\,2}}{2}}\right\} = \sqrt{\sum_{i=1}^{N} \frac{\big(W_k(\omega_i) \cdot \hat{\ddot{z}}_i\big)^2}{2}}\,;$$

or

$$a_w = a_w\big(\ddot{z}(t)\big) = \left\{use: RMS\big(\ddot{z}(t)\big) = \sqrt{\int_{\omega=0}^{\infty} G_{\ddot{z}}(\omega) \cdot d\omega}\right\} =$$

$$= \sqrt{\int_{\omega=0}^{\infty} \big(W_k(\omega)\big)^2 \cdot G_{\ddot{z}}(\omega) \cdot d\omega}\,;$$

[5.53]

Equation [5.53] is written for a case with only vertical vibrations, hence W_k and $G_{\ddot{z}}$. If vibrations in several directions, a total a_w can still be calculated, see (ISO2631).

In (ISO2631) one can also find the following equation, which weights together several time periods, with different vibrations spectra. Time averaged whole-body vibration exposure value is denoted a_w.

$$a_w = \sqrt{\frac{\sum_i a_{wi}^{\,2} \cdot T_i}{\sum_i T_i}}\,;$$

[5.54]

The a_w in Eq [5.54] is used both for vehicle customer requirement setting at OEMs and governmental legislation. One example of legislation is (DIRECTIVE 2002/44/EC, 2002). This directive stipulates that a_w in Eq [5.54] in any direction, normalized to 8 hours, may not exceed 1.15 m/s², and if the value exceeds 0.5 m/s² action must be taken.

5.6.2.1   Certain combination of road, vehicle and speed

Now we can use Equation [5.35] without assuming road type. However, we have to identify $\hat{\ddot{z}}_s$ and multiply it with $W_k(\omega)$, according to Equation [5.53]. Then we get [5.55].

Using Equation [5.55], we can calculate the weighted RMS value for the different models in Sections 5.5.1, 5.5.2 and 5.5.3. For each model, it will vary with speed, vx. A plot, assuming a certain road type ("Rough" from Figure 5-6) is shown in Figure 5-28. We can see that the simplest model "*stiff tyre, no unsprung mass*" gives much different comfort value than the two other, so the simplest is not goof to estimate comfort. However, the two other models give approximately same result, which indicates that the medium model, "*stiff tyre, no unsprung mass*", is enough for comfort evaluation. This is no general truth but an indication that the most advanced model, "*two masses, elastic tyre*", is not needed for comfort on normal roads. The advanced model is more needed for road grip.

We can also see that the comfort decreases, the faster the vehicle drives. If we read out at which speed we reach $a_w = 1\ m/s^2$ (which is a reasonable value for long time exposure) we get around $v_x \approx 70\ m/s \approx 250\ km/h$ on this road type ("Rough") with the medium (and advanced) model. With the simplest model we get $v_x \approx 1\ m/s \approx 3..4\ km/h$.

$$RMS(\ddot{z}_s) = \sqrt{\frac{\Phi_0}{\Omega_0^{-w}} \cdot v_x^{w-1} \cdot \int_{\omega=0}^{\infty} \left|H_{z_r \to \ddot{z}_s}(\omega)\right|^2 \cdot \omega^{-w} \cdot d\omega} = \left\{\begin{matrix} use: H_{z_r \to \ddot{z}_s} = \\ = -\omega^2 \cdot H_{z_r \to z_s} \end{matrix}\right\} =$$

$$= \sqrt{\frac{\Phi_0}{\Omega_0^{-w}} \cdot v_x^{w-1} \cdot \int_{\omega=0}^{\infty} \left|\omega^2 \cdot H_{z_r \to z_s}(\omega)\right|^2 \cdot \omega^{-w} \cdot d\omega} =$$

$$= \sqrt{\frac{\Phi_0}{\Omega_0^{-w}} \cdot v_x^{w-1} \cdot \int_{\omega=0}^{\infty} \left|H_{z_r \to z_s}(\omega)\right|^2 \cdot \omega^{4-w} \cdot d\omega} ; \Rightarrow \left\{\begin{matrix} use: \\ Equation \\ [5.53] \end{matrix}\right\} \Rightarrow \qquad [5.55]$$

$$\Rightarrow a_w = \sqrt{\frac{\Phi_0}{\Omega_0^{-w}} \cdot v_x^{w-1} \cdot \int_{\omega=0}^{\infty} \left(W_k(\omega)\right)^2 \cdot \left|H_{z_r \to z_s}(\omega)\right|^2 \cdot \omega^{4-w} \cdot d\omega} =$$

$$= \sqrt{\frac{\Phi_0}{\Omega_0^{-w}} \cdot v_x^{w-1} \cdot \int_{\omega=0}^{\infty} \left(W_k(\omega)\right)^2 \cdot \left|H_{z_r \to z_s}(\omega)\right|^2 \cdot \omega^{4-w} \cdot d\omega} ;$$
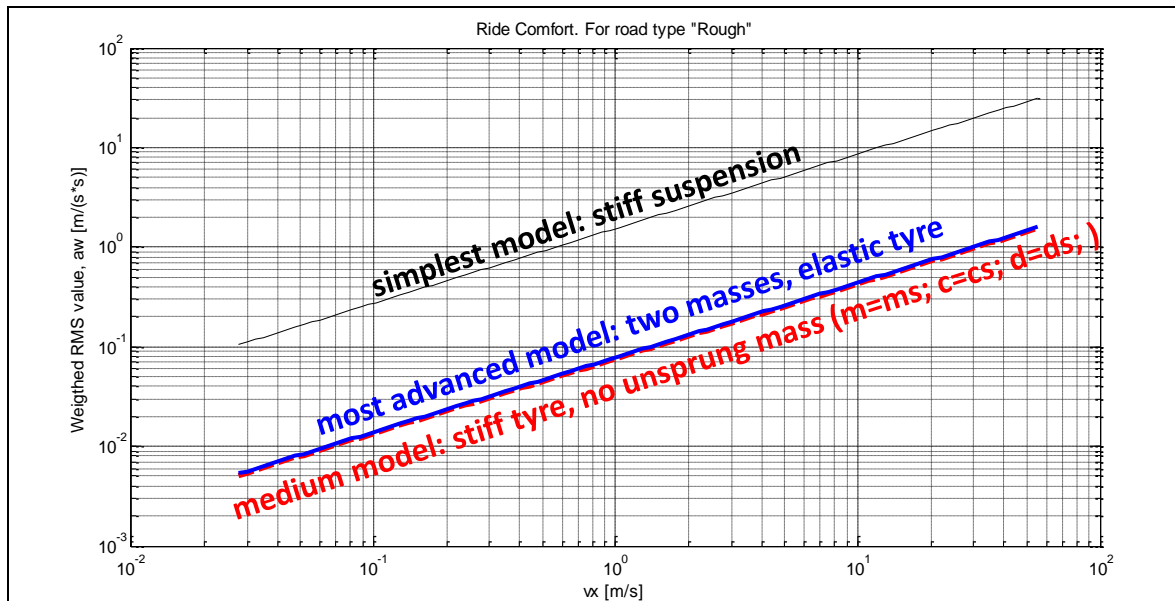
Figure 5-22: Weighted RMS values for road type "Smooth" from Figure 5-6. The 3 curves show 3 different models: Simplest (from Sections 1.5.1), Medium (from Section 1.5.2) and Most advanced (from Section 1.5.3).

5.6.3   Other excitation sources

Present chapter focuses on the influence of excitation from vertical displacement of the road. Examples of other, but often co-operating, excitation sources are:

- Powertrain vibrations, non-uniform rotation in engine. Frequencies will be proportional to engine speed
- Wheel vibrations, e.g. due to non-round wheels or otherwise unbalanced wheels. Frequencies will be proportional to vehicle speed.
- Special machineries mounted on vehicles (e.g. climate systems or concrete mixers)

5.7 Fatigue life *

*Function definition: **(Vehicle) Fatigue life** is the life that the vehicle, mainly suspension, can reach due to stationary oscillations when vehicle travels over a road with certain vertical irregularity in a certain speed. The measure is defined at least including suspension vertical deformation amplitudes.*

Beside human comfort, the fatigue of the vehicle structure itself is one issue to consider in vertical vehicle dynamics.

5.7.1 Single frequency

5.7.1.1 Loads on suspension spring

In particular, the suspension spring may be subject to fatigue. The variation in spring material stress is dimensioning, which is why the force variation or amplitude in the springs should be under observation. Since spring force is proportional to deformation, the suspension deformation amplitude is proposed as a good measure. This is the explanation to why the amplitude of $z_u - z_s$ is plotted in Figure 5-11.

Beside fatigue loads, $z_u - z_s$ is also relevant for judging whether suspension bump-stops become engaged or not. At normal driving, that limit should be far from reached, except possibly at high loads (many persons/much payload).

It can be noted that $z_u - z_s$ represents the variation in material stress only if spring is not changed. So, if different spring designs are compared, it is not sufficient to study only $z_u - z_s$.

5.7.1.2 Fatigue of other components

Fatigue of other parts may require other amplitudes.

One other relevant example can be the damper fatigue. Damper fatigue would be more relevant to judge from amplitude of $\dot{z}_u - \dot{z}_s$, which determines the force level and hence the stress level.

Another example is the load of the road itself. For heavy trucks it is important to consider how much they wear the road. At some roads with legislated maximum (static) axle load, one can be allowed to exceed that limit if the vehicle has especially road friendly suspensions. For these judgements, it is the contact force between tyre and road, $\hat{F}_{rz}$, which is the most relevant variable to study.

5.7.2 Multiple frequencies

If the excitation is of one single frequency, the stress amplitude can be used when comparing two designs. However, for spectra of multiple frequencies, one cannot look at amplitudes solely, $[\hat{z}_1, \hat{z}_2, \cdots, \hat{z}_N]$, because the amplitudes will depend on how the discretization is done, i.e. the number N. Some kind of integral of a spectral density is more reasonable. In this compendium it is proposed that a very approximate measure of fatigue load is calculated as follows, exemplified for the case of fatigue of the spring:

$$Measure\ for\ spring\ fatigue\ life = RMS\big(z_u(t) - z_s(t)\big) =$$

$$= \sqrt{\frac{\Phi_0}{\Omega_0^{-w}} \cdot v_x^{w-1} \cdot \int_{\omega=0}^{\infty} \left|H_{z_r \to z_u - z_s}(\omega)\right|^2 \cdot \omega^{-w} \cdot d\omega} = \left\{ \begin{array}{l} use: H_{z_r \to z_u - z_s} = \\ = H_{z_r \to z_u} - H_{z_r \to z_s} \end{array} \right\} =$$

$$= \sqrt{\frac{\Phi_0}{\Omega_0^{-w}} \cdot v_x^{w-1} \cdot \int_{\omega=0}^{\infty} \left|H_{z_r \to z_u}(\omega) - H_{z_r \to z_s}(\omega)\right|^2 \cdot \omega^{-w} \cdot d\omega}\ ;$$

[5.56]

Equation is written for application to a known road spectra (Φ_0, w) and vehicle dynamic structure ($H_{z_r \to z_u}, H_{z_r \to z_s}$), but the first expression ($RMS\big(z_u(t) - z_s(t)\big)$) is applicable on a measured or simulated time domain solution.

Road grip *

Function definition: **Road grip (on undulated roads)** *is how well the longitudinal and lateral grip between tyres and road is retained due to stationary oscillations when the vehicle travels over a road with certain vertical irregularity in a certain speed.*

Sections **3.3** and **3.4** show the brush model explain how the tyre forces in the ground plane appears. It is a physical model where the contact length influences how stiff the tyre is for longitudinal and lateral slip. There is also a brief description of relaxation models for tyres. This together motivates that a tyre have more difficult to build up forces in ground plane if the vertical force varies. We can understand it as when contact length varies, the shear stress build up has to start all over again. As an average effect, the tyre will lose more and more grip, the more the vertical force varies.

5.8.1   Multiple frequencies

If the excitation is of one single frequency, the stress amplitude can be used when comparing two designs. However, for spectra of multiple frequencies, one cannot look at amplitudes solely, $[\hat{z}_1, \hat{z}_2, \cdots, \hat{z}_N]$, because the amplitudes will depend on how the discretization is done, i.e. the number N. Some kind of integral of a spectral density is more reasonable. In this compendium it is proposed that a very approximate measure of road grip is calculated as follows:

$$Measure\ for\ (bad)road\ grip = RMS\big(\Delta F_{rz}(t)\big) =$$

$$= \sqrt{\frac{\Phi_0}{\Omega_0^{-w}} \cdot v_x^{w-1} \cdot \int_{\omega=0}^{\infty} \left|H_{z_r \to \Delta F_{rz}}(\omega)\right|^2 \cdot \omega^{-w} \cdot d\omega} =$$

$$= \left\{ use: H_{z_r \to z_u - z_s} = c_t \cdot \left(1 - H_{z_r \to z_u}\right) \right\} =$$

$$= \sqrt{\frac{\Phi_0}{\Omega_0^{-w}} \cdot v_x^{w-1} \cdot \int_{\omega=0}^{\infty} \left|c_t \cdot \left(1 - H_{z_r \to z_u}\right)\right|^2 \cdot \omega^{-w} \cdot d\omega}\ ;$$

[5.57]

Equation is written for application to a known road spectra (Φ_0, w) and vehicle dynamic structure ($H_{z_r \to z_u}$), but the first expression ($RMS\big(\Delta F_{rz}(t)\big)$) is applicable on a measured or simulated time domain solution.

5.9 Other functions

Present chapter focuses on the functions, (vertical) ride comfort, fatigue and road grip. Examples of others functions are:

- An area of functions that encompasses the vertical dynamics is **Noise, Vibration, and Harshness – NVH**. It is similar to ride comfort, but the frequencies are higher, stretching up to sound which is heard by humans.
- **Ground clearance** (static and dynamic) between vehicle body and ground. Typically important for off-road situations.
- **Longitudinal comfort**, due to drive line oscillations and/or vertical road displacements. Especially critical when driver cabin is separately suspended to the body. This is the case for heavy trucks.
- **Disturbances in steering wheel feel**, due to one-sided bumps. Especially critical for rigid steered axles. This is often the design of the front axle in heavy trucks.
- There are of course an infinite amount of combined manoeuvres, in which functions with requirements can be found. Examples can be **bump during strong cornering** (possibly destabilizing vehicle) or **one-sided bump** (exciting both bounce, pitch and roll modes). When studying such transients, the vertical dynamics is not enough to capture the comfort, but one often need to involve also **longitudinal** dynamics; the linkage with ant-dive/anti-squat geometry from Chapter 3 becomes important as well as tyre vertical (radial) deflection characteristics.
- Energy is dissipated in suspension dampers, which influence **energy consumption** for the vehicle. This energy loss is much related, but not same as, to (tyre) rolling resistance. Suspension characteristics do influence this energy loss, but it is normally negligible, unless driving very fast on very uneven road.

5.10 Variation of suspension design

The influence of design parameters on vehicle functions Ride comfort, Suspension fatigue and Road grip can now be made. E.g., it is important to not only use the transfer function, but also take the road and human sensitivity into account, which calls for different weighting for different frequencies.

Transfer function for the model in Section 5.5.3 is shown as dashed lines in

Figure 5-23. Same figure also shows the Road- and Human-weighted versions. Studying how these curves change with design parameters gives a quantitative understanding of how different suspension design parameters influence. Such variations will be done in Sections 5.10.1 to 5.10.4.

There are two particular frequency intervals of the graphs to observe. These are the 2 peaks around the two the natural frequencies of the sprung and unsprung masses, the peak at lower frequency is mainly a resonance in bounce mode, while the higher one is in wheel hop mode.
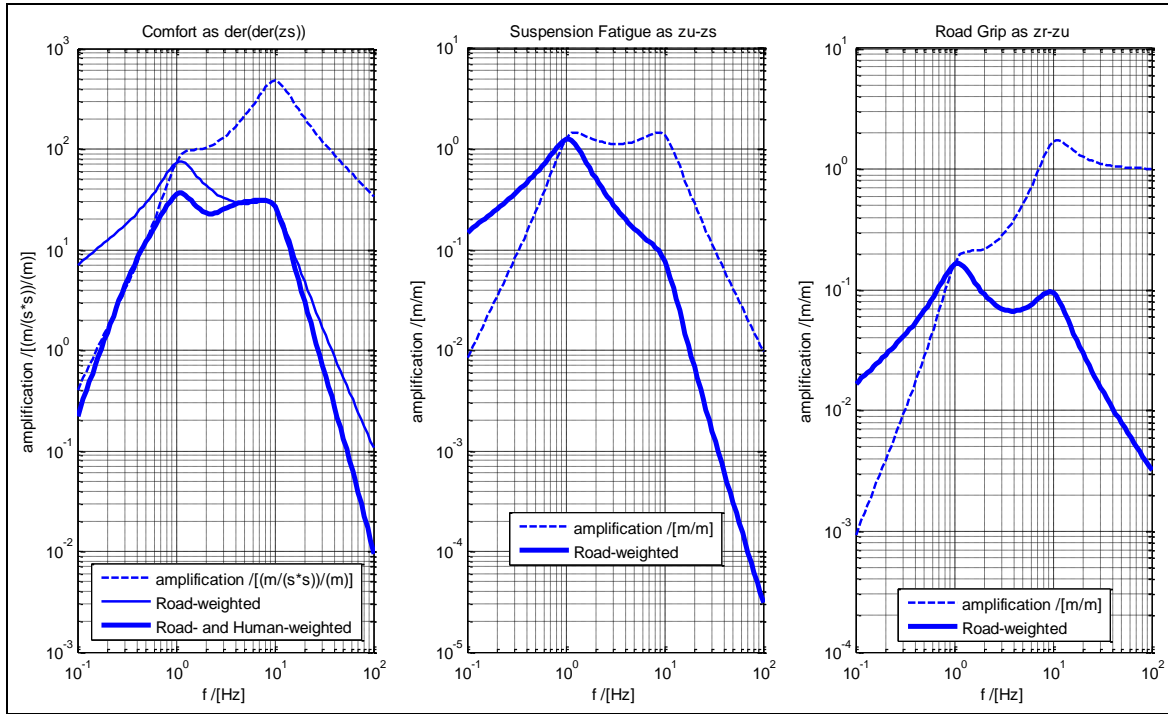
Figure 5-23: For a passenger car with $m_s = 1600 [kg], m_u = 200 [kg], c_s = 76 [kN/m], d_s = 9 [kN/(m/s)], c_t = 764 [kN/m], d_t = 0$. Left is vertical acceleration (amplitude) of sprung mass for Ride Comfort. Middle is relative displacement (amplitude) between sprung and unsprung mass for Suspension Fatigue. Right is deformation (amplitude) of tyre spring for Road Grip. Weightings for typical road and for human sensitivity is shown.

5.10.1 Varying suspension stiffness

In Figure 5-24 the benefits of the low suspension stiffness (1 Hz) is seen for suspension travel and comfort without much change in the road grip performance.
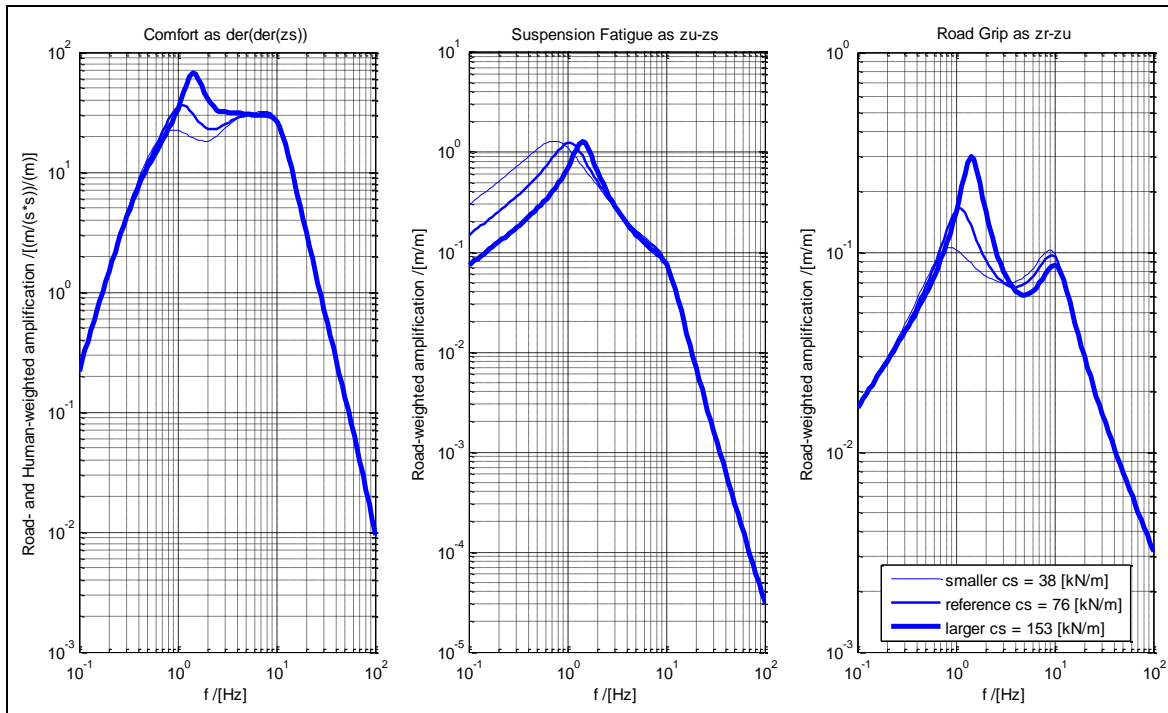
Figure 5-24: Result from varying suspension stiffness, c_s

Regarding Figure 5-24 and Figure 5-25 we see that there is a large influence of the acceleration gain at low frequencies with little change at the wheel hop and higher frequencies. The suspension stiffness and damping was seen to have little influence on the ride comfort / road grip response around 10 Hz.

5.10.2   Varying suspension damping

In Figure 5-25, we see that the changes in suspension damping have opposite effects for the bounce and wheel hop frequency responses. High damping is good for reducing bounce, but not so effective for wheel hop.
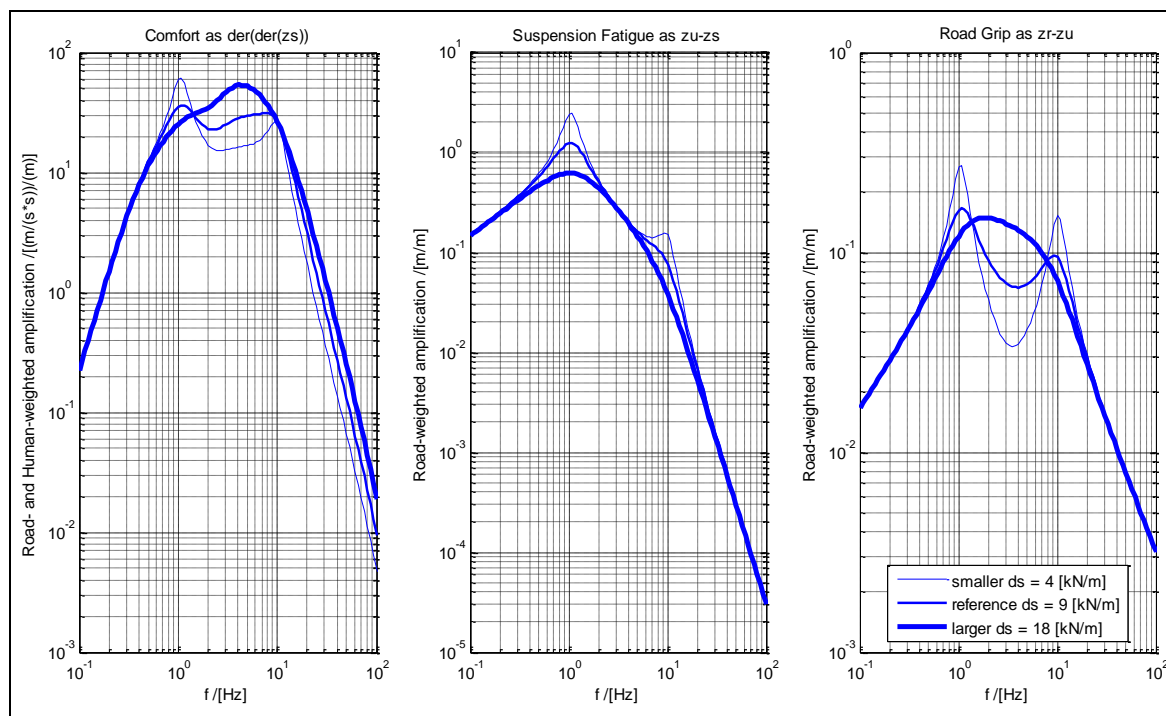
Figure 5-25: Result from varying suspension damping, d_s

5.10.3   Varying unsprung mass

In Figure 5-26, we see that if the response around the wheel hop frequency is to be changed, the unsprung mass is one of the most influential parameters. The unsprung mass is usually in the range of 10% of the sprung mass. Opposite to the suspension parameters, the unsprung mass influences frequencies around the wheel hop frequency with little influence around the bounce frequency.

In Figure 5-26, the case with $m_u = 0$ is added. This is to demonstrate what a model with neglected mass gives and can be nearly compared with the model in Section 5.5.2.

5.10.4   Varying tyre stiffness

In Figure 5-27 a general observation is that low sprung mass natural frequencies are preferred for comfort considerations. Another parameter that has a strong affect near the wheel hop frequency is the tyre stiffness. The strongest response is noticed for the road grip function. (Note that, since c_t is now varying, we have to express road grip as $c_t \cdot (z_r - z_u)$; only $z_r - z_u$ does not give a fair comparison.)
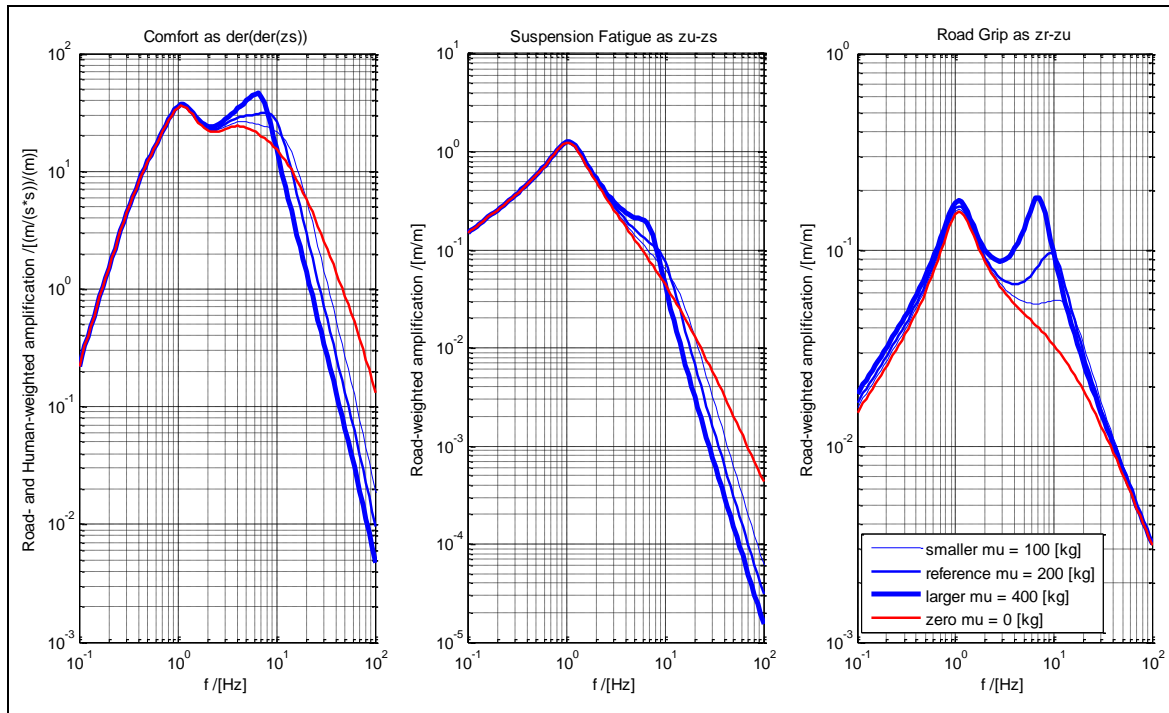
Figure 5-26: Result from varying unsprung mass, m_u
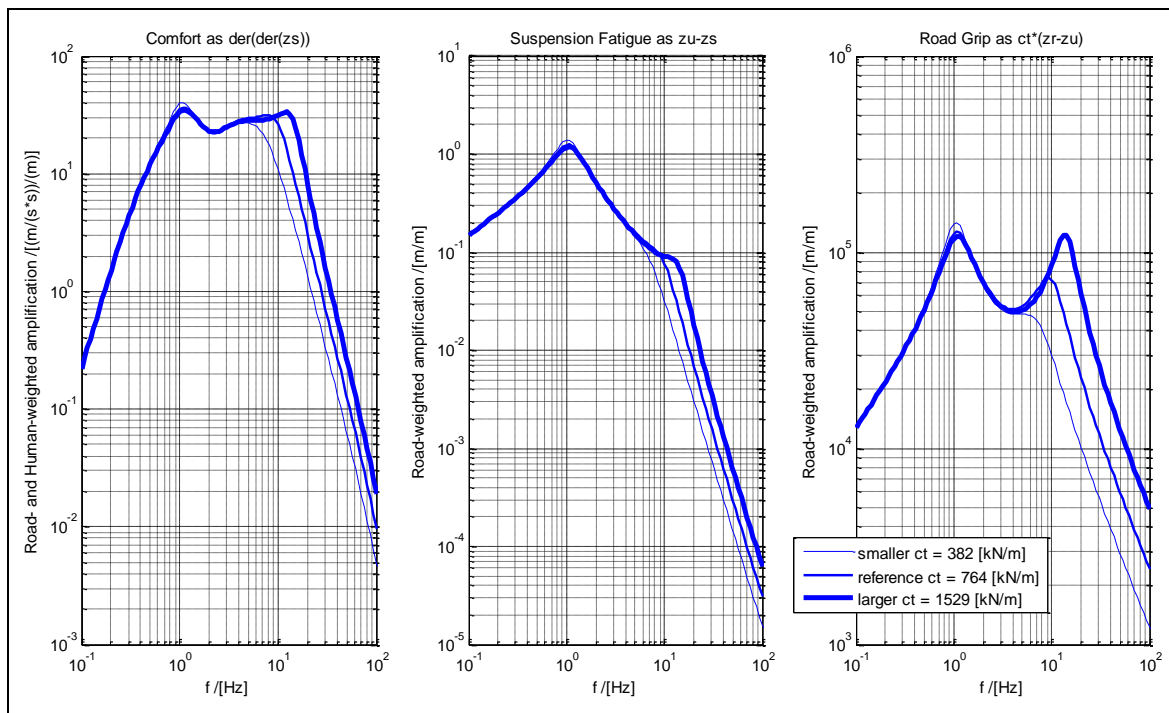
Figure 5-27: Result from varying Tyre Stiffness, c_t

5.11 Two dimensional oscillations

The one-dimensional model is useful for analysing the response of one wheel/suspension assembly. Some phenomena do connect other vehicle body motions than the vertical translation, especially pitch and roll. Here, other models are needed, such as Figure 5-28 and Figure 5-32.

5.11.1 Bounce (heave) and pitch

A model like in Figure 5-28 is proposed. We have been studying bounce and pitch before, in Section 3.4.9. Hence compare with corresponding model in Figure 3-46. In Chapter 3, the excitation was longitudinal tyre forces, while the vertical displacement of the road was assumed to be zero. In vertical vehicle dynamics, it is the opposite. The importance of model with linkage geometry (pitch centre or axle pivot points above ground level) is that tyre forces are transferred correctly to the body. That means that the linkage geometry is not so relevant for vertical vehicle dynamics in Chapter 5. So the model can be somewhat simpler.
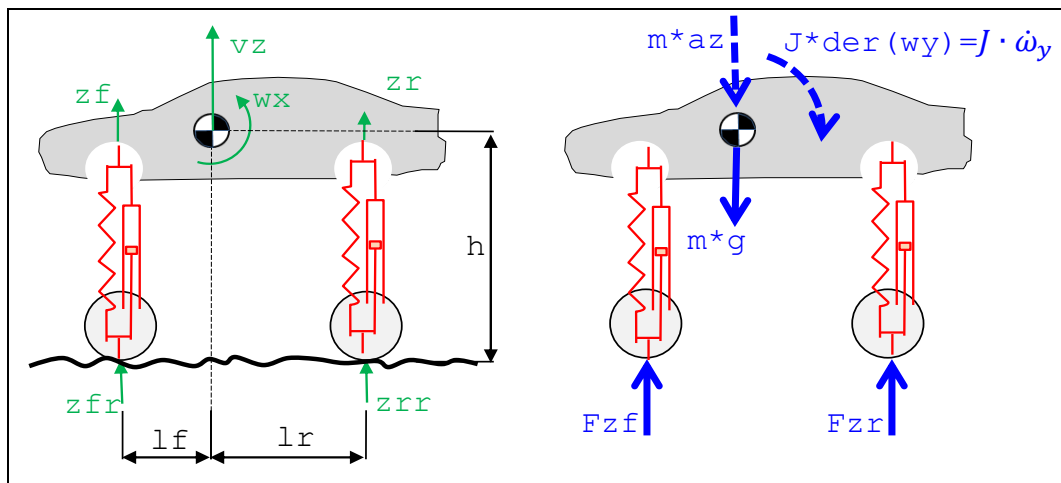
Figure 5-28: Bounce (heave) and pitch model.

No equations will be formulated for this model. The model would typically show two different modes, see Figure 5-29. The bounce eigen-frequency is typically 1-1.5 Hz for a passenger car. The pitch frequency is somewhat higher.

We should reflect on that if we are analysis the same vehicle with the models in Section 5.5 and 5.11.1, we are actually talking about the same bounce mode. But the models will most likely give different numbers of, e.g. Eigen frequency. A total model, with all motion degrees of freedom, would align those values, but the larger a model is the more data it produces which often leads to less easy design decisions.
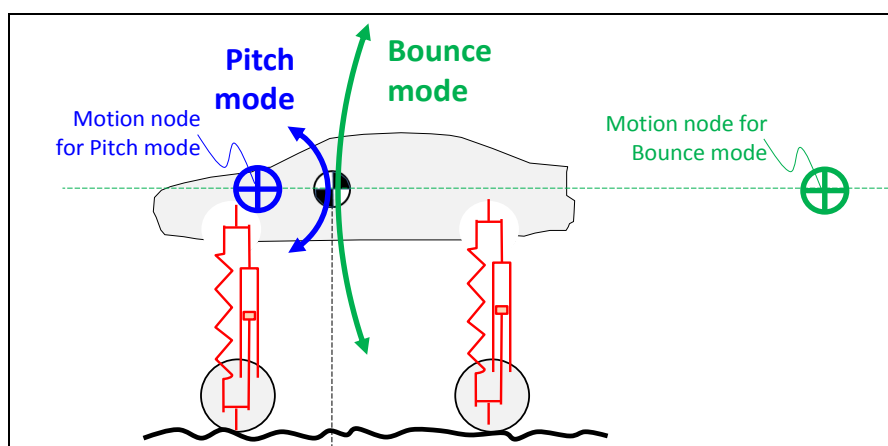
Figure 5-29: Oscillation modes of a Bounce and Pitch model.

5.11.1.1 Wheel base filtering

The response of the vehicle to road irregularities can be envisioned as in Figure 5-30. The vehicle can be excited in a pure bounce motion if the road wavelength is exciting each axle identically. In a similar

analysis, the pure pitch motion can be excited with the road displacing the axles out of phase with each other. So, at some frequencies, one mode is not excited at all, which is called "wheel base filtering".

Figure 5-31 gives an example of spectrum for vertical and pitch accelerations. It compares the accelerations for the correlated and uncorrelated excitation.
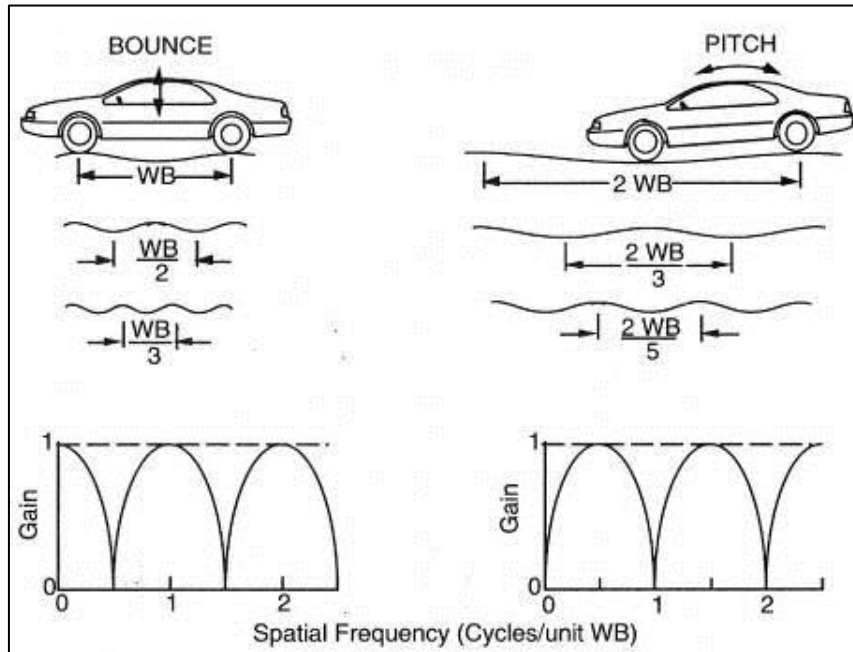
Figure 5-30: Response of the Vehicle to Different Road Wavelengths. (Gillespie, 1992)
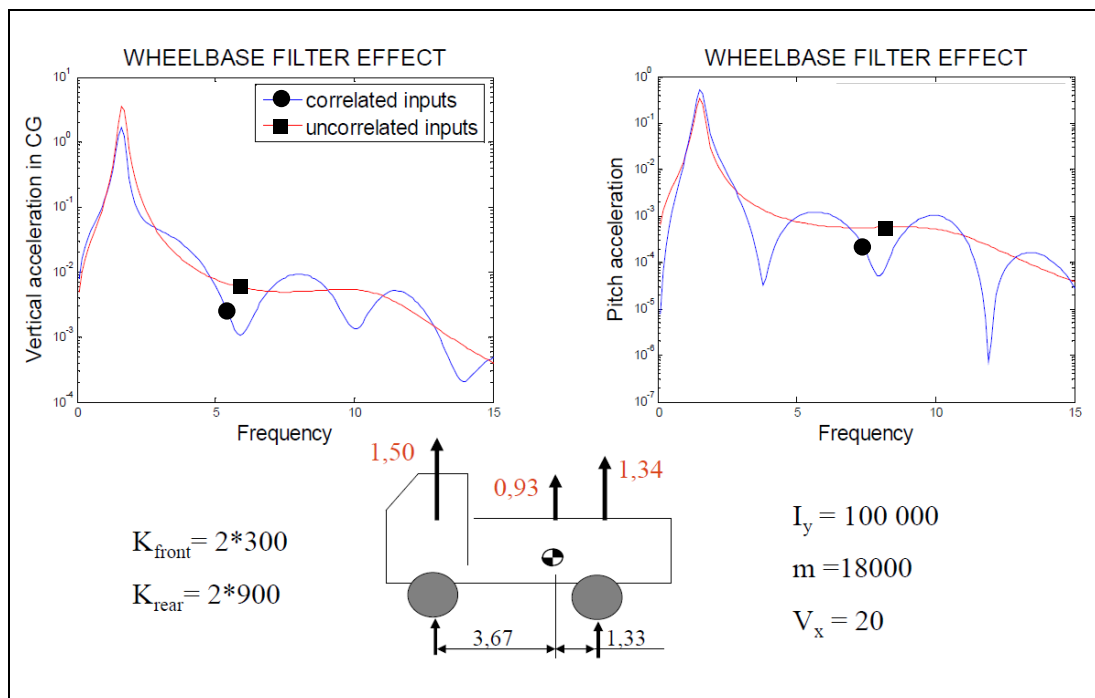
Figure 5-31: Example of wheelbase filter effect

5.11.2   Bounce (heave) and roll

A model like in Figure 5-32 is proposed. We have been studying bounce and pitch before, in Sections 4.3.9 and 4.5.2.3. Hence compare with corresponding model in Figure 4-70. In Chapter **4**, the excitation was lateral tyre/axle forces, while the vertical displacement of the road was assumed to be zero. In

vertical vehicle dynamics, it is the opposite. That means that the linkage geometry (roll centre or wheel pivot points) is not so relevant here. So the model can be somewhat simpler.
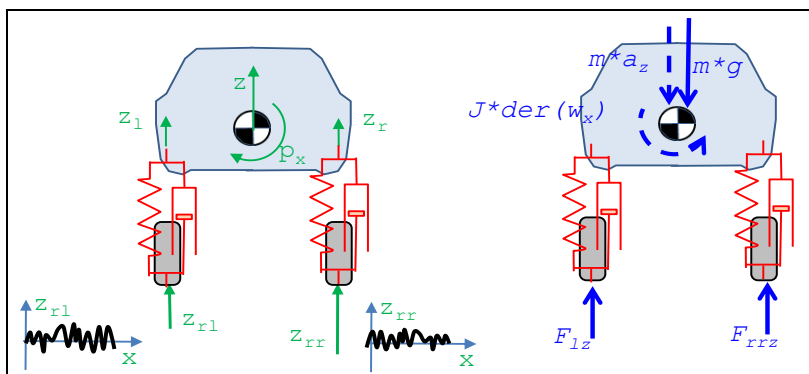
Figure 5-32: Bounce (heave) and roll model.

No equations is formulated for this model in this compendium, but a model will typically show two different modes, the bounce and roll. Bounce Eigen frequency is typically 1-1.5 Hz for a passenger car, as mentioned before. The roll frequency is similar or somewhat higher.

5.12 Transient vertical dynamics

The majority of the chapter you read now, considers normal driving which is how the vehicle is driven for during long time periods. Functions are then suitably analysed using theory for stationary oscillations.

Vertical vehicle dynamics also have transient disturbances to consider. Test cases can be one-sided or two sides road bumps or pot-holes. Two sided bump is envisioned in

Figure 5-33. It can represent driving over a speed bump or an object/low animal on a road.

Models from earlier in this chapter are all relevant for two-sided bumps/pot-holes, but one might need to consider non-linearities such as bump stops or wheel lift as well as different damping in compression and rebound. For one-sided bumps/potholes, the models from earlier in this chapter are generally not enough. The evaluation criteria should be shifted somewhat:

- Human **comfort** for transients are often better described as time derivative of acceleration (called "jerk").
- The material **loads** are more of maximum load type than fatigue life dimensioning, i.e. higher material stress but fewer load cycles during vehicle life time.
- **Road grip** studies over road bumps and pot-holes are challenging. Qualitatively, the tyre models have to include relaxation, because that is the mechanism which reduces road grip when vertical load shifts. To get quantitatively correct tyre models is beyond the goal of the compendium you presently read.
- **Roll-over** can be tripped by large one sided bumps. This kind of roll-overs is unusual and requires complex models.
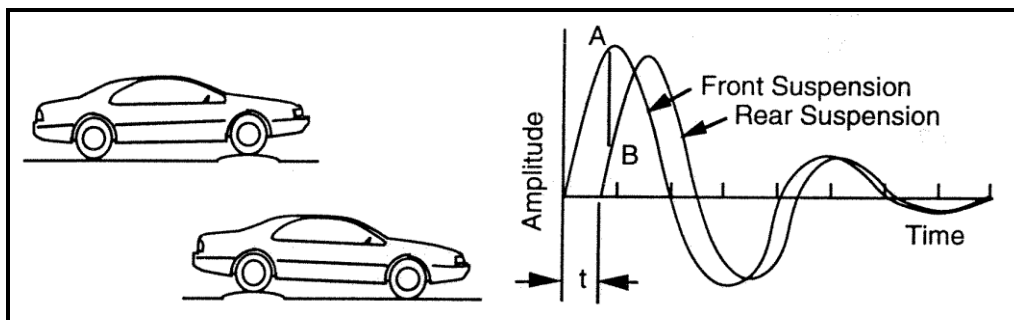
Figure 5-33: Response of Vehicle for Front and Rear Axle Impulses, (Gillespie, 1992)

Bibliography

AB Volvo. 2011. *Global Transport Application.* 2011.

Andreasson, Johan. 2007. *On Generic Road Vehicle Motion Modelling and Control.* Stockholm : KTH, 2007. Dissertation.

Bakker, E., Nyborg, L., Pacejka, H.B. 1987. *Tyre Modelling for use in Vehicle Dynamics Studies.* 1987. SAE Paper No.870495.

Barnard, R. H. *Road Vehicle Aerodynamic Design.* u.o. : Mechaero Publishing. ISBN 0954073479.

—. 2010. *Road Vehicle Aerodynamic Design.* u.o. : Mechaero Publishing, 2010.

Boerboom, Max. 2012. *Electric Vehicle Blended Braking maximizing energy recovery while maintaining vehicle stability and maneuverability.* Göteborg, Sweden : Chalmers University of Technology, 2012. Diploma work - Department of Applied Mechanics. ISSN 1652-8557; no 2012:01.

Clark, S, (ed). 1971. *Mechanics of Pneumatic Tires, Monograph 122.* u.o. : National Bureau of Standards, USA, 1971.

Cooper Tire & Rubber Co. 2007. Passenger radial tire cutaway. Online Art. [Online] Cooper Tire & Rubber Co., den 16 September 2007. http://deantires.com/us/en/information/info-construction.asp.

DIRECTIVE 2002/44/EC. 2002. *DIRECTIVE 2002/44/EC OF THE EUROPEAN PARLIAMENT AND OF THE COUNCIL.* 2002. http://europa.eu/legislation_summaries/employment_and_social_policy/health_hygiene_safety_at_work/c11145_en.htm.

Drenth, Edo F. 1993. *Brake Stability of Front Wheel Driven Cars at High Speed.* Delft, Netherlands : Delft University of Technology., 1993. Master thesis.

Encyclopædia Britannica Online. 2007. belted tire: tire designs." Online Art. Encyclopædia Britannica Online. [Online] 16 September 2007. http://www.britannica.com/eb/art-7786.

Gillespie, T. 1992. *Fundamentals of Vehicle Dynamics.* s.l. : Society of Automotive Engineers, 1992.

Grosch, K.A. and Schallamach, A. 1961. Tyre wear at controlled slip. *Wear.* September–October 1961, Vol. Volume 4, Issue 5, pp. Pages 356–371.

Happian-Smith, Julian. 2002. *An Introduction to Modern Vehicle Design.* u.o. : Butterwoth-Heinemann, ISBN 0-7506-5044-3, 2002.

Hirschberg, W., Rill, G. and Weinfurter, H. 2007. Tire model TMeasy. *Vehicle System Dynamics.* 2007, Vol. 45:1, pp. 101 — 119.

Hucho, Wolf-Heinric. 1998. *Aerodynamics of Road Vehicles.* u.o. : SAE International, 1998. R-177.

ISO 11026. *ISO 11026 Heavy commercial vehicles and buses - Test method for roll stability - Closing-curve test.* u.o. : ISO.

ISO 14791. *ISO 14791 Road vehicles - Heavy commercial vehicle combinations and articulated buses - Lateral stability test methods.* u.o. : ISO.

ISO 14792. *ISO14792 Road vehicles - Heavy commercial vehicles and buses - Steady-state circular tests.* u.o. : ISO. ISO14792.

ISO 14793. *ISO 14793 Road vehicles – Heavy commercial vehicles and buses – Lateral transient response test methods.* u.o. : ISO.

ISO 14794. 2011. *ISO 14794 Heavy commercial vehicles and buses - Braking in a turn - Open-loop test methods.* u.o. : ISO, 2011. ISO 14794.

ISO 3888. *ISO 3888 Passenenger Cars -- Test track for severe lane change manouvre -- Part 2: Obstacle Avoidance.* u.o. : ISO. ISO 3888.

ISO 4138. *ISO 4138 Passenger cars – Steady-state circular driving behaviour - Open-loop test methods.* u.o. : ISO. ISO 4138.

ISO 7401. *ISO 7401 Lateral transient response test methods - Open-loop test methods.* u.o. : ISO.

ISO 7975. 2006. *Passenger cars – Braking in a turn – Open-loop test method.* u.o. : ISO, 2006. ISO 7975.

ISO 8608. *ISO 8608 Mechanical vibration - Road surface profiles - Reporting of measured data.* u.o. : ISO.

ISO. 2011. *ISO 14794 Heavy commercial vehicles and buses - Braking in a turn - Open-loop test methods.* u.o. : ISO, 2011. ISO 14794.

—. 2006. *Passenger cars – Braking in a turn – Open-loop test method.* u.o. : ISO, 2006. ISO 7975.

ISO2631. *ISO 2631 – Evaluation of Human Exposure to Whole-Body Vibration.* Genève, Switzerland : International Organization for Standardization.

ISO8855. *ISO 8855 – Road vehicle – Vehicle dynamics and road holding ability – Vocabulary.* s.l. : International Organization for Standardization, Genève, Switzerland.

Kati, Maliheh Sadeghi. 2013. *Definitions of Performance Based Characteristics for Long Heavy Vehicle Combinations.* Signals and Systems. u.o. : Chalmers University of Technology, 2013. ISSN 1403-266x.

Kharrazi , Sogol. 2012. *Steering Based Lateral Performance Control of Long Heavy Vehicle Combinations.* Göteborg, Sweden : Chalmers University of Technology, 2012. ISBN/ISSN: 978-91-7385-724-6.

Kiencke, U. and Nielsen, L. 2005 . *Automotive Control Systems.* 2005 .

Lex, Cornelia. 2015. *Estimation of the Maximum Coefficient of Friction between Tire and Road based on Vehicle State measurements.* Graz : Graz University of Technology, 2015. Doctoral thesis.

Michelin. 2003. *The tyre Rolling resistance and fuel savings.* u.o. : Michelin, 2003.

NHTSA. *Electronic Stability Control Systems.* u.o. : NHTSA. FMVSS 126.

Pacejka, H. 2005. *Tyre and Vehicle Dynamics, 2nd ed.* u.o. : Elsevier, 2005.

Ploechl, Manfred, [red.]. 2013. *Road and Off-Road Vehicle System Dynamics Handbook.* u.o. : CRC Press, 2013. Print ISBN: 978-0-8493-3322-4; eBook ISBN: 978-1-4200-0490-8; http://www.crcnetbase.com/isbn/9781420004908.

Rajamani, Rajesh. 2012. *Vehicle Dynamics and Control.* u.o. : Springer, 2012. ISSN 0941-5122.

Rill, Georg. 2006. *FIRST ORDER TIRE DYNAMICS.* Lisbon, Portugal : III European Conference on Computational Mechanics Solids, Structures and Coupled Problems in Engineering, 5–8 June 2006, 2006.

Robert Bosch GmbH. 2004. *Bosch Automotive Handbook 6th Edition.* s.l. : Bentley Publishes, 2004.

Rösth, Markus. 2007. *Hydraulic Power Steering System Design in Road Vehicles: Analysis, Testing and Enhanced Functionality.* Linköping : Linköping Univeristy, Department of Management and Engineering, Fluid and Mechatronic Systems, 2007. Dissertation. Dissertations, ISSN 0345-7524; 1068.

SAEJ670. *SAE J670e - Vehicle Dynamics Terminology.* u.o. : Society of Automotive Engineers, Warrendale, PA, USA.

Sundström, Peter, Jacobson, Bengt och Laine, Leo. 2014. Vectorized single-track model in Modelica for articulated vehicles with arbitrary number of units and axles. Lund, Sweden : Modelica conference 2014, March 10-12, 2014, 2014.

Svendenius, Jacob. 2007. *Tire Modeling and Friction Estimation.* Lund, Sweden : Department of Automatic Control, Lund University, 2007. Dissertation.

UN ECE 111. 2001. *UNIFORM PROVISIONS CONCERNING THE APPROVAL OF TANK VEHICLES OF CATEGORIES N AND O WITH REGARD TO ROLLOVER STABILITY.* u.o. : UNITED NATIONS, 2001. Regulation No. 111.

Wipke, Keith B, Cuddy, Matthew R. och Burch, Steven D. 1999. ADVISOR 2.1: A User-Friendly Advanced Powertrain Simulation Using a Combined Backward/Forward Approach. *IEEE TRANSACTIONS ON VEHICULAR TECHNOLOGY.* 1999, Vol. 48, 6, ss. 1751-1761.

Wong, J.Y. 2001. *Theory of Ground Vehicles (3rd ed.).* s.l. : John Wiley and Sons, Inc., New York, 2001.

Yang, Derong. 2013. *Vehicle Dynamics Control after Impacts in Multiple-Event Accidents.* Göteborg : Chalmers University of Technology, 2013. PhD thesis. ISBN 978-91-7385-887-8.

Index